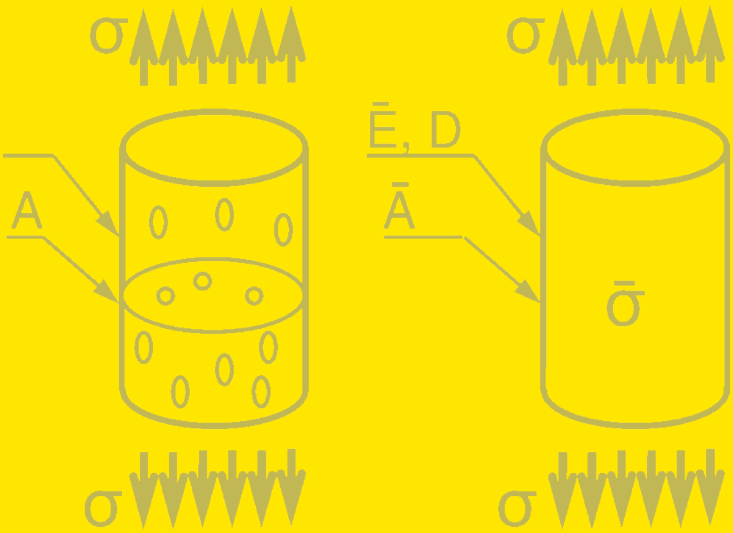

SECOND EDITION

FINITE ELEMENT ANALYSIS OF COMPOSITE MATERIALS USING ANSYS®

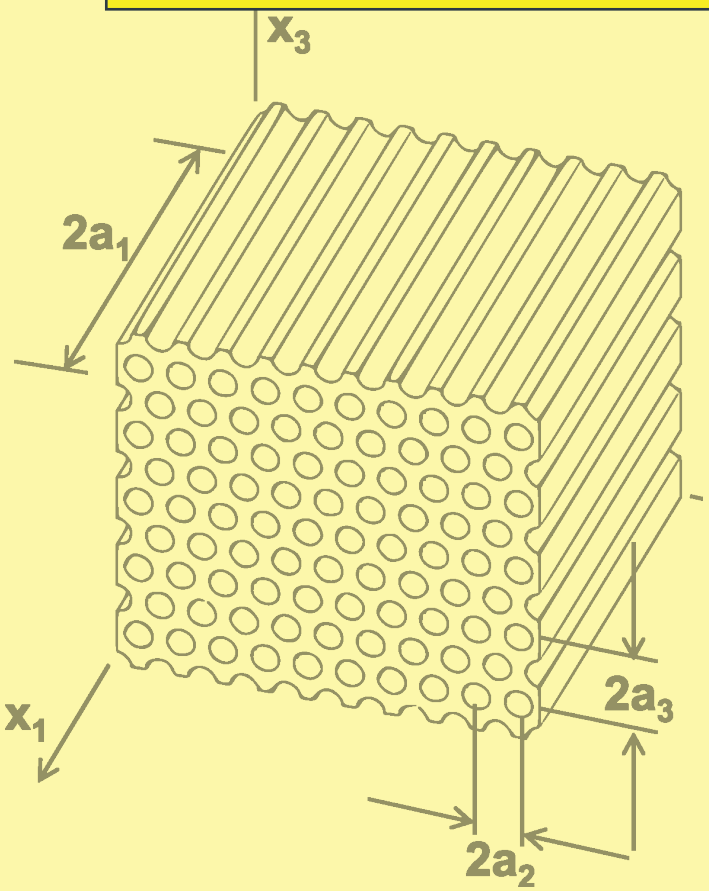

Ever J. Barbero

CRC Press
Taylor & Francis Group

FINITE ELEMENT ANALYSIS OF COMPOSITE MATERIALS USING ANSYS®

SECOND EDITION

Composite Materials: Analysis and Design

Series Editor

Ever J. Barbero

PUBLISHED

Finite Element Analysis of Composite Materials Using ANSYS,® Second Edition, *Ever J. Barbero*

Smart Composites: Mechanics and Design, *Rani El-Hajjar, Valeria La Saponara, and Anastasia Muliana*

Finite Element Analysis of Composite Materials with Abaqus, *Ever J. Barbero*

FRP Deck and Steel Girder Bridge Systems: Analysis and Design, *Julio F. Davalos, An Chen, Bin Zou, and Pizhong Qiao*

Introduction to Composite Materials Design, Second Edition, *Ever J. Barbero*

Finite Element Analysis of Composite Materials, *Ever J. Barbero*

FINITE ELEMENT ANALYSIS OF COMPOSITE MATERIALS USING ANSYS®

SECOND EDITION

Ever J. Barbero

CRC Press
Taylor & Francis Group
6000 Broken Sound Parkway NW, Suite 300
Boca Raton, FL 33487-2742

Version Date: 20131219

International Standard Book Number-13: 978-1-4665-1690-8 (eBook - PDF)

Dedicado a la memoria de mi padre, Ever Francisco Barbero (1928–2007).

Contents

Series Preface xiii

Preface xv

Acknowledgments xix

List of Symbols xxi

List of Examples xxix

Errata xxxi

1 Mechanics of Orthotropic Materials 1

1.1 Lamina Coordinate System 1
1.2 Displacements 1
1.3 Strain 2
1.4 Stress 4
1.5 Contracted Notation 5
1.5.1 Alternate Contracted Notation 5
1.6 Equilibrium and Virtual Work 6
1.7 Boundary Conditions 8
1.7.1 Traction Boundary Conditions 8
1.7.2 Free Surface Boundary Conditions 8
1.8 Continuity Conditions 9
1.8.1 Traction Continuity 9
1.8.2 Displacement Continuity 9
1.9 Compatibility 10
1.10 Coordinate Transformations 10
1.10.1 Stress Transformation 13
1.10.2 Strain Transformation 15
1.11 Transformation of Constitutive Equations 16
1.12 3D Constitutive Equations 17
1.12.1 Anisotropic Material 18
1.12.2 Monoclinic Material 19

1.12.3 Orthotropic Material 20
1.12.4 Transversely Isotropic Material 22
1.12.5 Isotropic Material 23
1.13 Engineering Constants 24
1.13.1 Restrictions on Engineering Constants 28
1.14 From 3D to Plane Stress Equations 29
1.15 Apparent Laminate Properties 31
Suggested Problems 33

2 Introduction to Finite Element Analysis **37**
2.1 Basic FEM Procedure 37
2.1.1 Discretization 38
2.1.2 Element Equations 38
2.1.3 Approximation over an Element 39
2.1.4 Interpolation Functions 40
2.1.5 Element Equations for a Specific Problem 42
2.1.6 Assembly of Element Equations 43
2.1.7 Boundary Conditions 44
2.1.8 Solution of the Equations 44
2.1.9 Solution Inside the Elements 44
2.1.10 Derived Results 45
2.2 General Finite Element Procedure 45
2.3 Solid Modeling, Analysis, and Visualization 49
2.3.1 Model Geometry 49
2.3.2 Material and Section Properties 52
2.3.3 Assembly 53
2.3.4 Solution Steps 54
2.3.5 Loads 54
2.3.6 Boundary Conditions 54
2.3.7 Meshing and Element Type 56
2.3.8 Solution Phase 56
2.3.9 Post-Processing and Visualization 56
Suggested Problems 61

3 Elasticity and Strength of Laminates **63**
3.1 Kinematics of Shells 64
3.1.1 First-Order Shear Deformation Theory 65
3.1.2 Kirchhoff Theory 69
3.2 Finite Element Analysis of Laminates 71
3.2.1 Element Types 73
3.2.2 Sandwich Shells 74
3.2.3 Nodes and Curvature 74
3.2.4 Drilling Rotation 74
3.2.5 A-B-D-H Input Data for Laminate FEA 74
3.2.6 Equivalent Orthotropic Input for Laminate FEA 77

3.2.7 LSS for Multidirectional Laminate FEA . . . 82
3.2.8 FEA of Ply Drop-Off Laminates . . . 83
3.2.9 FEA of Sandwich Shells . . . 87
3.2.10 Element Coordinate System . . . 88
3.2.11 Constraints . . . 94
3.3 Failure Criteria . . . 100
3.3.1 2D Failure Criteria . . . 101
3.3.2 3D Failure Criteria . . . 103
Suggested Problems . . . 110

4 Buckling 113
4.1 Eigenvalue Buckling Analysis . . . 113
4.1.1 Imperfection Sensitivity . . . 120
4.1.2 Asymmetric Bifurcation . . . 121
4.1.3 Post-Critical Path . . . 121
4.2 Continuation Methods . . . 126
Suggested Problems . . . 130

5 Free Edge Stresses 133
5.1 Poisson's Mismatch . . . 134
5.1.1 Interlaminar Force . . . 134
5.1.2 Interlaminar Moment . . . 135
5.2 Coefficient of Mutual Influence . . . 141
5.2.1 Interlaminar Stress due to Mutual Influence . . . 143
Suggested Problems . . . 147

6 Computational Micromechanics 151
6.1 Analytical Homogenization . . . 152
6.1.1 Reuss Model . . . 152
6.1.2 Voigt Model . . . 153
6.1.3 Periodic Microstructure Model . . . 153
6.1.4 Transversely Isotropic Averaging . . . 154
6.2 Numerical Homogenization . . . 157
6.3 Global-Local Analysis . . . 172
6.4 Laminated RVE . . . 175
Suggested Problems . . . 178

7 Viscoelasticity 179
7.1 Viscoelastic Models . . . 181
7.1.1 Maxwell Model . . . 181
7.1.2 Kelvin Model . . . 182
7.1.3 Standard Linear Solid . . . 183
7.1.4 Maxwell-Kelvin Model . . . 183
7.1.5 Power Law . . . 184
7.1.6 Prony Series . . . 184

7.1.7 Standard Nonlinear Solid . . . 185
7.1.8 Nonlinear Power Law . . . 186
7.2 Boltzmann Superposition . . . 187
7.2.1 Linear Viscoelastic Material . . . 187
7.2.2 Unaging Viscoelastic Material . . . 189
7.3 Correspondence Principle . . . 190
7.4 Frequency Domain . . . 191
7.5 Spectrum Representation . . . 192
7.6 Micromechanics of Viscoelastic Composites . . . 192
7.6.1 One-Dimensional Case . . . 192
7.6.2 Three-Dimensional Case . . . 193
7.7 Macromechanics of Viscoelastic Composites . . . 197
7.7.1 Balanced Symmetric Laminates . . . 197
7.7.2 General Laminates . . . 197
7.8 FEA of Viscoelastic Composites . . . 198
Suggested Problems . . . 204

8 Continuum Damage Mechanics 207
8.1 One-Dimensional Damage Mechanics . . . 208
8.1.1 Damage Variable . . . 208
8.1.2 Damage Threshold and Activation Function . . . 210
8.1.3 Kinetic Equation . . . 211
8.1.4 Statistical Interpretation of the Kinetic Equation . . . 212
8.1.5 One-Dimensional Random-Strength Model . . . 213
8.1.6 Fiber Direction, Tension Damage . . . 218
8.1.7 Fiber Direction, Compression Damage . . . 222
8.2 Multidimensional Damage and Effective Spaces . . . 226
8.3 Thermodynamics Formulation . . . 228
8.3.1 First Law . . . 228
8.3.2 Second Law . . . 230
8.4 Kinetic Law in Three-Dimensional Space . . . 235
8.4.1 Return-Mapping Algorithm . . . 238
8.5 Damage and Plasticity . . . 244
Suggested Problems . . . 245

9 Discrete Damage Mechanics 249
9.1 Overview . . . 250
9.2 Approximations . . . 254
9.3 Lamina Constitutive Equation . . . 256
9.4 Displacement Field . . . 256
9.4.1 Boundary Conditions for $\Delta T = 0$ . . . 258
9.4.2 Boundary Conditions for $\Delta T \neq 0$ . . . 259
9.5 Degraded Laminate Stiffness and CTE . . . 260
9.6 Degraded Lamina Stiffness . . . 261
9.7 Fracture Energy . . . 262

9.8 Solution Algorithm . . . 263
9.8.1 Lamina Iterations . . . 263
9.8.2 Laminate Iterations . . . 264
Suggested Problems . . . 271

10 Delaminations **273**
10.1 Cohesive Zone Method . . . 276
10.1.1 Single Mode Cohesive Model . . . 278
10.1.2 Mixed Mode Cohesive Model . . . 281
10.2 Virtual Crack Closure Technique . . . 290
Suggested Problems . . . 295

A Tensor Algebra **297**
A.1 Principal Directions of Stress and Strain . . . 297
A.2 Tensor Symmetry . . . 297
A.3 Matrix Representation of a Tensor . . . 298
A.4 Double Contraction . . . 299
A.5 Tensor Inversion . . . 299
A.6 Tensor Differentiation . . . 300
A.6.1 Derivative of a Tensor . . . 300
A.6.2 Derivative of the Inverse of a Tensor . . . 301

B Second-Order Diagonal Damage Models **303**
B.1 Effective and Damaged Spaces . . . 303
B.2 Thermodynamic Force **Y** . . . 304
B.3 Damage Surface . . . 306
B.4 Unrecoverable-Strain Surface . . . 307

C Software Used **309**
C.1 ANSYS Mechanical APDL . . . 309
C.1.1 ANSYS USERMAT, Compilation and Execution . . . 311
C.2 BMI3 . . . 314
C.2.1 Stand-Alone BMI3 . . . 314
C.2.2 BMI3 within ANSYS . . . 314

References **317**

Series Preface

Half a century after their commercial introduction, composite materials are of widespread use in many industries. Applications such as aerospace, windmill blades, highway bridge retrofit, and many more require designs that assure safe and reliable operation for twenty years or more. Using composite materials, virtually any property, such as stiffness, strength, thermal conductivity, and fire resistance, can be tailored to the users needs by selecting the constituent material, their proportion and geometrical arrangement, and so on. In other words, the engineer is able to design the material concurrently with the structure. Also, modes of failure are much more complex in composites than in classical materials. Such demands for performance, safety, and reliability require that engineers consider a variety of phenomena during the design. Therefore, the aim of the *Composite Materials: Analysis and Design* book series is to bring to the design engineer a collection of works written by experts on every aspect of composite materials that is relevant to their design.

Variety and sophistication of material systems and processing techniques has grown exponentially in response to an ever-increasing number and type of applications. Given the variety of composite materials available as well as their continuous change and improvement, understanding of composite materials is by no means complete. Therefore, this book series serves not only the practicing engineer but also the researcher and student who are looking to advance the state-of-the-art in understanding material and structural response and developing new engineering tools for modeling and predicting such responses.

Thus, the series is focused on bringing to the public existing and developing knowledge about the material-property relationships, processing-property relationships, and structural response of composite materials and structures. The series scope includes analytical, experimental, and numerical methods that have a clear impact on the design of composite structures.

Ever Barbero, book series editor
West Virginia University, Morgantown, WV

Preface

Finite Element Analysis of Composite Materials Using ANSYS® deals with the analysis of structures made of composite materials, also called *composites*. The analysis of composites treated in this textbook includes the analysis of the material itself, at the microlevel, and the analysis of structures made of composite materials. This textbook evolved from the class notes of *MAE 646 Advanced Mechanics of Composite Materials* that I teach as a graduate course at West Virginia University. Although this is a textbook on advanced mechanics of composite materials, the use of the finite element method is essential for the solution of the complex boundary value problems encountered in the advanced analysis of composites, and thus the title of the book.

There are a number of good textbooks on advanced mechanics of composite materials, but none carries the theory to a practical level by actually solving problems, as it is done in this textbook. Some books devoted exclusively to finite element analysis include some examples about modeling composites but fall quite short of dealing with the actual analysis and design issues of composite materials and composite structures. This textbook includes an explanation of the concepts involved in the detailed analysis of composites, a sound explanation of the mechanics needed to translate those concepts into a mathematical representation of the physical reality, and a detailed explanation of the solution of the resulting boundary value problems by using commercial Finite Element Analysis software such as ANSYS *Mechanical APDL*. Furthermore, this textbook includes more than fifty fully developed examples interspersed with the theory, as well as more than seventy-five exercises at the end of chapters, and more than fifty separate pieces of ANSYS APDL code used to explain in detail the solution of example problems. The reader will be able to reproduce the examples and complete the exercises. When a finite element analysis is called for, the reader will be able to do it with commercially or otherwise available software. A Web site is set up with links to download the necessary software unless it is easily available from Finite Element Analysis software vendors. ANSYS and MATLAB® code is explained in the examples, and the code can be downloaded from the Web site as well. Furthermore, the reader will be able to extend the capabilities of ANSYS by user material subroutines, as demonstrated in the examples included in this textbook.

Chapters 1 through 7 can be covered in a one-semester graduate course. Chapter 2 contains a brief introduction intended for those readers who have not had a formal course or prior knowledge about the finite element method. Chapter 4

(Buckling) is not referenced in the remainder of the textbook and thus it could be omitted in favor of more exhaustive coverage of content in later chapters. Chapters 7 (Viscoelasticity) and 8 (Continuum Damage Mechanics) are placed consecutively to emphasize hereditary phenomena. However, Chapter 7 can be skipped if more emphasis on damage and/or delaminations is desired in a one-semester course. The foundations for the analysis of damage is laid out in Chapter 8 followed by a chapter on Discrete Damage Mechanics (Chapter 9). Either or both chapters could be omitted for the sake of time, for example if the instructor desires to cover Chapter 10 (Delaminations) as part of a one-semester course.

The *inductive method* is applied as much as possible in this textbook. That is, topics are introduced with examples of increasing complexity, until sufficient physical understanding is reached to introduce the general theory without difficulty. This method will sometimes require that, at earlier stages of the presentation, certain facts, models, and relationships be accepted as fact, until they are completely proven later on. For example, in Chapter 7, viscoelastic models are introduced early to aid the reader in gaining an appreciation for the response of viscoelastic materials. This is done simultaneously with a cursory introduction to the superposition principle and the Laplace transform, which are formally introduced only later in the chapter. For those readers accustomed to the *deductive method*, this may seem odd, but many years of teaching have convinced me that students acquire and retain knowledge more efficiently in this way.

It is assumed that the reader is familiar with basic mechanics of composites as covered in introductory level textbooks such as my previous textbook *Introduction to Composite Material Design–Second Edition*. Furthermore, it is assumed that the reader masters a body of knowledge that is commonly acquired as part of a bachelor of science degree in any of the following disciplines: Aerospace, Mechanical, Civil, or similar. References to books and to other sections in this textbook, as well as footnotes, are used to assist the reader in refreshing those concepts and to clarify the notation used. Prior knowledge of continuum mechanics, tensor analysis, and the finite element method would enhance the learning experience but are not necessary for studying with this textbook. The finite element method is used as a tool to solve practical problems. For the most part, ANSYS is used throughout the book. Computing programming using Fortran and MATLAB is limited to programming material models and post-processing algorithms. Basic knowledge of these programming languages is useful but not essential.

Only three software packages are used throughout the book. ANSYS is needed for the finite element solution of numerous examples and suggested problems. MATLAB is needed for both symbolic and numerical solution of examples and suggested problems. Additionally, BMI3©, which is available free of charge on the book's Web site, is used in Chapter 4. Several other programs such as *Abaqus*™, LS-DYNA®, MSC-MARC®, and *SolidWorks*™ are cited, but not used in the examples. All the APDL code for the examples in this textbook is available on the book's Web site `http://barbero.cadec-online.com/feacm-ansys/`.

Composite materials are now ubiquitous in the marketplace, including extensive applications in aerospace, automotive, civil infrastructure, sporting goods, and so

on. Their design is especially challenging because, unlike conventional materials such as metals, the composite material itself is designed concurrently with the composite structure. Preliminary design of composites is based on the assumption of a state of plane stress in the laminate. Furthermore, rough approximations are made about the geometry of the part, as well as the loading and support conditions. In this way, relatively simple analysis methods exist and computations can be carried out simply using algebra. However, preliminary analysis methods have a number of shortcomings that are remedied with advanced mechanics and finite element analysis, as explained in this textbook. Recent advances in commercial finite element analysis packages, with user friendly pre- and post-processing, as well as powerful user-programmable features, have made detailed analysis of composites quite accessible to the designer. This textbook bridges the gap between powerful finite element tools and practical problems in structural analysis of composites. I expect that many graduate students, practicing engineers, and instructors will find this to be a useful and practical textbook on finite element analysis of composite materials based on sound understanding of advanced mechanics of composite materials.

Ever J. Barbero, 2013

Acknowledgments

I wish to thank Raimondo Luciano and Elio Sacco for their contributions to Chapter 6 and to Tom Damiani, Joan Andreu Mayugo Majo, and Xavier Martinez, who taught the course in 2004, 2006, and 2009, making many corrections and additions to the course notes on which this textbook is based. Also, I wish to recognize Adi Adumitroaie, who taught invited lectures on progressive damage analysis and cohesive zone models, thus providing the basis for Chapter 10. I am also grateful to those who reviewed parts of the manuscript including Enrique Barbero, Grama Bhashyam, Guillermo Creus, Fabrizio Greco, Luis Godoy, Paolo Lonetti, Severino Marques, Pizhong Qiao, Timothy Norman, Sonia Sanchez, and Eduardo Sosa. Furthermore, recognition is due to those who helped me compile the solutions manual, including Hermann Alcazar, John Sandro Rivas, and Rajiv Dastane. Also, I wish to thank Ruth Roman for helping me update the examples to Release 14 of ANSYS and to my colleagues and students for their valuable suggestions and contributions to this textbook. Finally, my gratitude goes to my wife, Ana Maria, and to my children, Margaret and Daniel, who gave up many opportunities to bond with their dad so that I might write this book.

List of Symbols

Symbols Related to Mechanics of Orthotropic Materials

$\boldsymbol{\epsilon}$	Strain tensor
ε_{ij}	Strain components in tensor notation
ϵ_α	Strain components in contracted notation
ϵ_α^e	Elastic strain
ϵ_α^p	Plastic strain
λ	Lame constant
ν	Poisson's ratio
ν_{12}	In-plane Poisson's ratio
ν_{23}, ν_{13}	Interlaminar Poisson's ratios
ν_{xy}	Apparent laminate Poisson's ratio x-y
$\boldsymbol{\sigma}$	Stress tensor
σ_{ij}	Stress components in tensor notation
σ_α	Stress components in contracted notation
$[a]$	Transformation matrix for vectors
e_i	Unit vector components in global coordinates
e_i'	Unit vector components in materials coordinates
f_i, f_{ij}	Tsai-Wu coefficients
l, m, n	Direction cosines
$\widetilde{u}(\varepsilon_{ij})$	Strain energy per unit volume
u_i	Displacement vector components
x_i	Global directions or axes
x_i'	Materials directions or axes
$\mathbf{C}$	Stiffness tensor
C_{ijkl}	Stiffness in index notation
$C_{\alpha,\beta}$	Stiffness in contracted notation
E	Young's modulus
E_1	Longitudinal modulus
E_2	Transverse modulus
E_2	Transverse-thickness modulus
E_x	Apparent laminate modulus in the global x-direction
$G = \mu$	Shear modulus
G_{12}	In-plane shear modulus
G_{23}, G_{13}	Interlaminar shear moduli
G_{xy}	Apparent laminate shear modulus x-y

I_{ij}	Second-order identity tensor
I_{ijkl}	Fourth-order identity tensor
K	Bulk modulus
Q'_{ij}	Lamina stiffness components in lamina coordinates
$[R]$	Reuter matrix
$\mathbf{S}$	Compliance tensor
S_{ijkl}	Compliance in index notation
$S_{\alpha,\beta}$	Compliance in contracted notation
$[T]$	Coordinate transformation matrix for stress
$[\overline{T}]$	Coordinate transformation matrix for strain

Symbols Related to Finite Element Analysis

$\underline{\underline{\partial}}$	Strain-displacement equations in matrix form
$\underline{\epsilon}$	Six-element array of strain components
$\theta_x, \theta_y, \theta_z$	Rotation angles following the right-hand rule (Figure 2.8)
$\underline{\sigma}$	Six-element array of stress components
ϕ_x, ϕ_y	Rotation angles used in plate and shell theory
$\underline{a}$	Nodal displacement array
u_j^e	Unknown parameters in the discretization
$\underline{\underline{B}}$	Strain-displacement matrix
$\underline{\underline{C}}$	Stiffness matrix
$\underline{\underline{K}}$	Assembled global stiffness matrix
$\underline{\underline{K}}^e$	Element stiffness matrix
$\underline{N}$	Interpolation function array
N_j^e	Interpolation functions in the discretization
$\underline{P}^e$	Element force array
$\underline{P}$	Assembled global force array

Symbols Related to Elasticity and Strength of Laminates

γ_{xy}^0	In-plane shear strain
γ_{4u}	Ultimate interlaminar shear strain in the 2-3 plane
γ_{5u}	Ultimate interlaminar shear strain in the 1-3 plane
γ_{6u}	Ultimate in-plane shear strain
$\epsilon_x^0, \epsilon_y^0$	In-plane strains
ϵ_{1t}	Ultimate longitudinal tensile strain
ϵ_{2t}	Ultimate transverse tensile strain
ϵ_{3t}	Ultimate transverse-thickness tensile strain
ϵ_{1c}	Ultimate longitudinal compressive strain
ϵ_{2c}	Ultimate transverse compressive strain
ϵ_{3c}	Ultimate transverse-thickness compressive strain
κ_x, κ_y	Bending curvatures
κ_{xy}	Twisting curvature

ϕ_x, ϕ_y	Rotations of the middle surface of the shell (Figure 2.8)
c_4, c_5, c_6	Tsai-Wu coupling coefficients
t_k	Lamina thickness
u_0, v_0, w_0	Displacements of the middle surface of the shell
z	Distance from the middle surface of the shell
A_{ij}	Components of the extensional stiffness matrix $[A]$
B_{ij}	Components of the bending-extension coupling matrix $[B]$
D_{ij}	Components of the bending stiffness matrix $[D]$
$[E_0]$	Extensional stiffness matrix $[A]$, in ANSYS notation
$[E_1]$	Bending-extension matrix $[B]$, in ANSYS notation
$[E_2]$	Bending stiffness matrix $[D]$, in ANSYS notation
F_{1t}	Longitudinal tensile strength
F_{2t}	Transverse tensile strength
F_{3t}	Transverse-thickness tensile strength
F_{1c}	Longitudinal compressive strength
F_{2c}	Transverse compressive strength
F_{3c}	Transverse-thickness compressive strength
F_4	Interlaminar shear strength in the 2-3 plane
F_5	Interlaminar shear strength in the 1-3 plane
F_6	In-plane shear strength
H_{ij}	Components of the interlaminar shear matrix $[H]$
I_F	Failure index
M_x, M_y, M_xy	Moments per unit length (Figure 3.3)
$\widehat{M}_n$	Applied bending moment per unit length
N_x, N_y, N_xy	In-plane forces per unit length (Figure 3.3)
$\widehat{N}_n$	Applied in-plane force per unit length, normal to the edge
$\widehat{N}_{ns}$	Applied in-plane shear force per unit length, tangential
$\left(\overline{Q}_{ij}\right)_k$	Lamina stiffness components in laminate coordinates, layer k
V_x, V_y	Shear forces per unit length (Figure 3.3)

Symbols Related to Buckling

λ, λ_i	Eigenvalues
s	Perturbation parameter
Λ	Load multiplier
$\Lambda^{(cr)}$	Bifurcation multiplier or critical load multiplier
$\Lambda^{(1)}$	Slope of the post-critical path
$\Lambda^{(2)}$	Curvature of the post-critical path
v	Eigenvectors (buckling modes)
$[K]$	Stiffness matrix
$[K_s]$	Stress stiffness matrix
P_{CR}	Critical load

Symbols Related to Free Edge Stresses

$\eta_{xy,x}, \eta_{xy,y}$	Coefficients of mutual influence
$\eta_{x,xy}, \eta_{y,xy}$	Alternate coefficients of mutual influence
F_{yz}	Interlaminar shear force y-z
F_{xz}	Interlaminar shear force x-z
M_z	Interlaminar moment

Symbols Related to Micromechanics

$\overline{\epsilon}_\alpha$	Average engineering strain components
$\overline{\varepsilon}_{ij}$	Average tensor strain components
$\epsilon^0_\alpha, \varepsilon^0_{ij}$	Far-field applied strain components
$\overline{\sigma}_\alpha$	Average stress components
$\mathbf{A}^i$	Strain concentration tensor, i-th phase, contracted notation
$2a_1, 2a_2, 2a_3$	Dimensions of the representative volume element (RVE)
A_{ijkl}	Components of the strain concentration tensor
$\mathbf{B}^i$	Stress concentration tensor, i-th phase, contracted notation
B_{ijkl}	Components of the stress concentration tensor
I	6×6 identity matrix
P_{ijkl}	Eshelby tensor
V_f	Fiber volume fraction
V_m	Matrix volume fraction

Symbols Related to Viscoelasticity

$\dot{\varepsilon}$	Stress rate
η	Viscosity
θ	Age or aging time
$\dot{\sigma}$	Stress rate
τ	Time constant of the material or system
Γ	Gamma function
s	Laplace variable
t	Time
$C_{\alpha,\beta}(t)$	Stiffness tensor in the time domain
$C_{\alpha,\beta}(s)$	Stiffness tensor in the Laplace domain
$\widehat{C}_{\alpha,\beta}(s)$	Stiffness tensor in the Carson domain
$D(t)$	Compliance
$D_0, (D_i)_0$	Initial compliance values
$D_c(t)$	Creep component of the total compliance $D(t)$
D', D''	Storage and loss compliances
$E_0, (E_i)_0$	Initial moduli
E_∞	Equilibrium modulus
E, E_0, E_1, E_2	Parameters in the viscoelastic models (Figure 7.1)
$E(t)$	Relaxation

E', E''	Storage and loss moduli
$F[]$	Fourier transform
$(G_{ij})_0$	Initial shear moduli
$H(t-t_0)$	Heaviside step function
$H(\theta)$	Relaxation spectrum
$L[]$	Laplace transform
$L[]^{-1}$	Inverse Laplace transform

Symbols Related to Damage

α	Laminate coefficient of thermal expansion (CTE)
$\alpha^{(k)}$	CTE of lamina k
α_{cr}	Critical misalignment angle at longitudinal compression failure
α_σ	Standard deviation of fiber misalignment
$\gamma(\delta)$	Damage hardening function
γ_0	Damage threshold
δ_{ij}	Kronecker delta
δ	Damage hardening variable
ε	Effective strain
$\overline{\varepsilon}$	Undamaged strain
ε^p	Plastic strain
$\dot{\gamma}$	Heat dissipation rate per unit volume
$\dot{\gamma}_s$	Internal entropy production rate
λ	Crack density
λ_{lim}	Saturation crack density
$\dot{\lambda}, \dot{\lambda}^d$	Damage multiplier
$\dot{\lambda}^p$	Yield multiplier
ρ	Density
σ	Effective stress
$\overline{\sigma}$	Undamaged stress
τ_{13}, τ_{23}	Intralaminar shear stress components
φ, φ^*	Strain energy density, and complementary SED
χ	Gibbs energy density
ψ	Helmholtz free energy density
ΔT	Change in temperature
$\mathbf{\Omega} = \Omega_{ij}$	Integrity tensor
$2a_0$	Representative crack size
d_i	Eigenvalues of the damage tensor
f^d	Damage flow surface
f^p	Yield flow surface
$f(x), F(x)$	Probability density, and its cumulative probability
g	Damage activation function
g^d	Damage surface
g^p	Yield surface
h	Laminate thickness

h_k	Thickness of lamina k
m	Weibull modulus
p	Yield hardening variable
$\widehat{p}$	Thickness average of quantity p
$\widetilde{p}$	Virgin value of quantity p
$\overline{p}$	Volume average of quantity p
$\mathbf{q}$	Hear flow vector per unit area
r	Radiation heat per unit mass
s	Specific entropy
$u(\varepsilon_{ij})$	Internal energy density
A	Crack area
$[A]$	Laminate in-plane stiffness matrix
A_{ijkl}	Tension-compression damage constitutive tensor
B_{ijkl}	Shear damage constitutive tensor
B_a	Dimensionless number (8.57)
$\overline{C}_{\alpha,\beta}$	Stiffness matrix in the undamaged configuration
$\mathbf{C}^{ed}$	Tangent stiffness tensor
D_{ij}	Damage tensor
D_{1t}^{cr}	Critical damage at longitudinal tensile failure
D_{1c}^{cr}	Critical damage at longitudinal compression failure
D_{2t}^{cr}	Critical damage at transverse tensile failure
D_2, D_6	Damage variables
$E(D)$	Effective modulus
$\overline{E}$	Undamaged (virgin) modulus
$G_c = 2\gamma_c$	Surface energy
G_{Ic}, G_{IIc}	Critical energy release rate in modes I and II
J_{ijkl}	Normal damage constitutive tensor
M_{ijkl}	Damage effect tensor
N	Number of laminas in the laminate
$\{N\}$	Membrane stress resultant array
Q	Degraded 3x3 stiffness matrix of the laminate
$R(p)$	Yield hardening function
R_0	Yield threshold
S	Entropy or Laminate complinace matrix, depending on context
T	Temperature
U	Strain energy
V	Volume of the RVE
Y_{ij}	Thermodynamic force tensor

Symbols Related to Delaminations

α	Mixed mode crack propagation exponent
β_δ, β_G	Mixed mode ratios
δ	Separation of the interface in the cohesive zone model (CZM)
δ_m	Mixed mode separation

δ_m^0	Mixed mode separation at damage onset
δ_m^0	Mixed mode separation at fracture
σ^0	CZM critical separation at damage onset
ℓ	Delamination length for 2D delaminations
σ^0	CZM strength of the interface
ψ_{xi}, ψ_{yi}	Rotation of normals to the middle surface of the plate
Ω	Volume of the body
Ω_D	Delaminated region
Π_e	Potential energy, elastic
Π^r	Potential energy, total
$\dot{\Gamma}$	Dissipation rate
Λ	Interface strain energy density per unit area
$\partial\Omega$	Boundary of the body
d	One-dimensional damage state variable
k_{xy}, k_z	Displacement continuity parameters
$[A_i], [B_i], [D_i]$	Laminate stiffness submatrices
D_I, D_{II}, D_{III}	Damage variables for modes I, II, and III of CZM
$G(\ell)$	Energy release rate (ERR), total, in 2D
G	Energy release rate (ERR), total, in 3D
G_I, G_{II}, G_{III}	Energy release rate (ERR) of modes I, II, and III
G_c	Critical energy release rate (ERR), total, in 3D
G_I^c	Critical energy release rate mode I
$[H_i]$	Laminate interlaminar shear stiffness matrix
K	Penalty stiffness
$\tilde{K}$	Virgin penalty stiffness
K_I, K_{II}, K_{III}	Stress intensity factors (SIF) of modes I, II, and III
N_i, M_i, T_i	Stress resultants
U	Internal energy
W	Work done by the body on its surroundings
$W_{closure}$	Crack closure work

List of Examples

Example 1.1, *7*
Example 1.2, *11*
Example 1.3, *12*
Example 1.4, *28*
Example 1.5, *30*
Example 1.6, *31*
Example 2.1, *48*
Example 2.2, *50*
Example 2.3, *51*
Example 2.4, *57*
Example 2.5, *57*
Example 2.6, *59*
Example 3.1, *75*
Example 3.2, *77*
Example 3.3, *79*
Example 3.4, *82*
Example 3.5, *84*
Example 3.6, *86*
Example 3.7, *87*
Example 3.8, *90*
Example 3.9, *91*
Example 3.10, *92*
Example 3.11, *96*
Example 3.12, *104*
Example 3.13, *106*
Example 3.14, *108*
Example 4.1, *115*
Example 4.2, *122*
Example 4.3, *127*
Example 4.4, *129*
Example 5.1, *137*
Example 5.2, *137*
Example 5.3, *144*
Example 5.4, *144*
Example 6.1, *155*
Example 6.2, *162*
Example 6.3, *170*
Example 6.4, *174*
Example 6.5, *176*
Example 7.1, *186*
Example 7.2, *189*
Example 7.3, *192*
Example 7.4, *197*
Example 7.5, *198*
Example 7.6, *201*
Example 8.1, *212*
Example 8.2, *216*
Example 8.3, *220*
Example 8.4, *234*
Example 8.5, *240*
Example 9.1, *264*
Example 10.1, *284*
Example 10.2, *287*
Example 10.3, *292*

Errata

For the most current errata, go to
`http://forum.cadec-online.com/viewforum.php?f=6`

Chapter 1

Mechanics of Orthotropic Materials

This chapter provides the foundation for the rest of the book. Basic concepts of mechanics, tailored for composite materials, are presented, including coordinate transformations, constitutive equations, and so on. Continuum mechanics is used to describe deformation and stress in an orthotropic material. The basic equations are reviewed in Sections 1.2 to 1.9. Tensor operations are reviewed in Section 1.10 because they are used in the rest of the chapter. Coordinate transformations are required to express quantities such as stress, strain, and stiffness in lamina coordinates, in laminate coordinates, and so on. They are reviewed in Sections 1.10 to 1.11. This chapter is heavily referenced in the rest of the book, and thus readers who are already versed in continuum mechanics may choose to come back to review this material as needed.

1.1 Lamina Coordinate System

A single lamina of fiber reinforced composite behaves as an orthotropic material. That is, the material has three mutually perpendicular planes of symmetry. The intersection of these three planes defines three axes that coincide with the fiber direction (x_1'), the thickness coordinate (x_3'), and a third direction $x_2' = x_3' \times x_1'$ perpendicular to the other two [1].[1]

1.2 Displacements

Under the action of forces, every point in a body may translate and rotate as a rigid body as well as deform to occupy a new region. The displacements u_i of any point P in the body (Figure 1.1) are defined in terms of the three components of the vector u_i (in a rectangular Cartesian coordinate system) as $u_i = (u_{1,}u_{2,}u_3)$. An

[1] $\times$ denotes vector cross product.

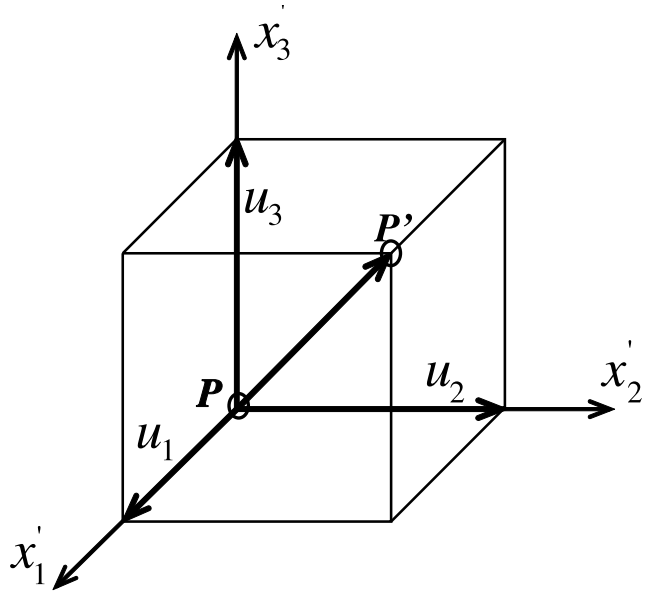

Figure 1.1: Notation for displacement components.

alternate notation for displacements is $u_i = (u, v, w)$. Displacement is a vector or first-order tensor quantity

$$\mathbf{u} = u_i = (u_1, u_2, u_3) \; ; \; i = 1...3 \tag{1.1}$$

where boldface (e.g., $\mathbf{u}$) indicates a *tensor* written in tensor notation, in this case a vector (or first-order tensor). In this book, all tensors are boldfaced (e.g., $\boldsymbol{\sigma}$), but their components are not (e.g., σ_{ij}). The order of the tensor (i.e., first, second, fourth, etc.) must be inferred from context, or as in (1.1), by looking at the number of subscripts of the same entity written in index notation (e.g., u_i).

1.3 Strain

For geometric nonlinear analysis, the components of the Lagrangian strain tensor are [2]

$$L_{ij} = \frac{1}{2}(u_{i,j} + u_{j,i} + u_{r,i}u_{r,j}) \tag{1.2}$$

where

$$u_{i,j} = \frac{\partial u_i}{\partial x_j} \tag{1.3}$$

If the gradients of the displacements are so small that products of partial derivatives of u_i are negligible compared with linear (first-order) derivative terms, then the (infinitesimal) strain tensor ε_{ij} is given by [2]

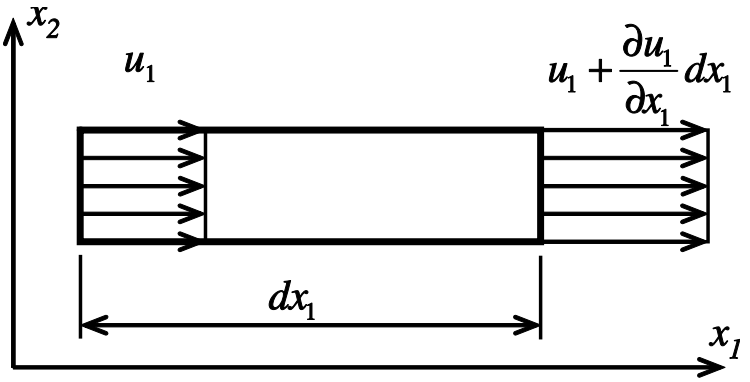

Figure 1.2: Normal strain.

$$\boldsymbol{\varepsilon} = \varepsilon_{ij} = \frac{1}{2}(u_{i,j} + u_{j,i}) \tag{1.4}$$

Again, boldface indicates a tensor, the order of which is implied from the context. For example ε is a one-dimensional strain and $\boldsymbol{\varepsilon}$ is the second-order tensor of strain. Index notation (e.g., $= \varepsilon_{ij}$) is used most of the time and the tensor character of variables (scalar, vector, second order, and so on) is easily understood from context.

From the definition (1.4), strain is a second-order, symmetric tensor (i.e., $\varepsilon_{ij} = \varepsilon_{ji}$). In expanded form the strains are defined by

$$\begin{aligned}
\varepsilon_{11} &= \frac{\partial u_1}{\partial x_1} = \epsilon_1 \ ; \quad 2\varepsilon_{12} = 2\varepsilon_{21} = \left(\frac{\partial u_1}{\partial x_2} + \frac{\partial u_2}{\partial x_1}\right) = \gamma_6 = \epsilon_6 \\
\varepsilon_{22} &= \frac{\partial u_2}{\partial x_2} = \epsilon_2 \ ; \quad 2\varepsilon_{13} = 2\varepsilon_{31} = \left(\frac{\partial u_1}{\partial x_3} + \frac{\partial u_3}{\partial x_1}\right) = \gamma_5 = \epsilon_5 \\
\varepsilon_{33} &= \frac{\partial u_3}{\partial x_3} = \epsilon_3 \ ; \quad 2\varepsilon_{23} = 2\varepsilon_{32} = \left(\frac{\partial u_2}{\partial x_3} + \frac{\partial u_3}{\partial x_2}\right) = \gamma_4 = \epsilon_4
\end{aligned} \tag{1.5}$$

where ϵ_α with $\alpha = 1..6$ are defined in Section 1.5. The normal components of strain ($i = j$) represent the change in length per unit length (Figure 1.2). The shear components of strain ($i \neq j$) represent one-half the change in an original right angle (Figure 1.3). The engineering shear strain $\gamma_\alpha = 2\varepsilon_{ij}$, for $i \neq j$ is often used instead of the tensor shear strain because the shear modulus G is defined by $\tau = G\gamma$ in mechanics of materials [3]. The strain tensor, being a second order tensor, can be displayed as a matrix

$$[\varepsilon] = \begin{bmatrix} \varepsilon_{11} & \varepsilon_{12} & \varepsilon_{13} \\ \varepsilon_{12} & \varepsilon_{22} & \varepsilon_{23} \\ \varepsilon_{13} & \varepsilon_{23} & \varepsilon_{33} \end{bmatrix} = \begin{bmatrix} \epsilon_1 & \epsilon_6/2 & \epsilon_5/2 \\ \epsilon_6/2 & \epsilon_2 & \epsilon_4/2 \\ \epsilon_5/2 & \epsilon_4/2 & \epsilon_3 \end{bmatrix} \tag{1.6}$$

where [ ] is used to denote matrices.

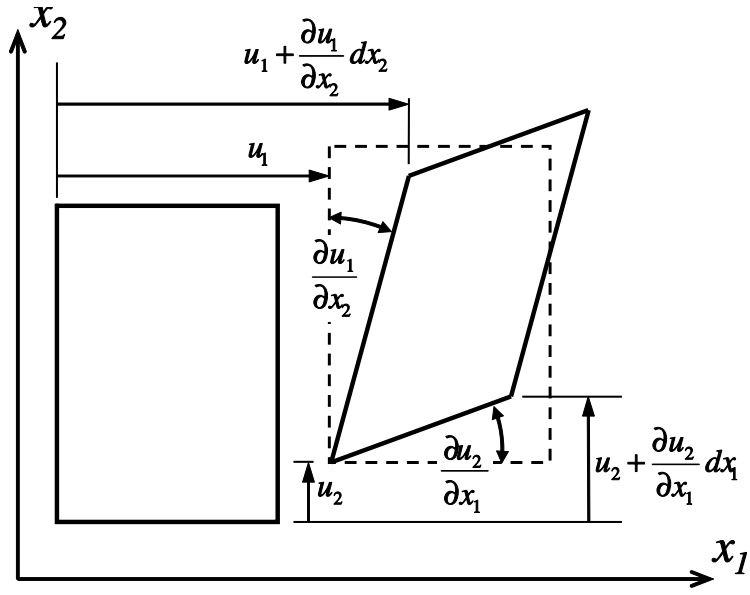

Figure 1.3: Engineering shear strain.

1.4 Stress

The stress vector associated to a plane passing through a point is the force per unit area acting on the plane passing through the point. A second-order tensor, called the stress tensor, completely describes the state of stress at a point. The stress tensor can be expressed in terms of the components acting on three mutually perpendicular planes aligned with the orthogonal coordinate directions as indicated in Figure 1.4. The tensor notation for stress is σ_{ij} with $(i, j = 1, 2, 3)$, where the first subscript corresponds to the direction of the normal to the plane of interest and the second subscript corresponds to the direction of the stress. Tensile normal stresses $(i = j)$ are defined to be positive when the normal to the plane and the stress component directions are either both positive or both negative. All components of stress depicted in Figure 1.4 have a positive sense. Force and moment equilibrium of the element in Figure 1.4 requires that the stress tensor be symmetric (i.e., $\sigma_{ij} = \sigma_{ji}$) [3]. The stress tensor, being a second order tensor, can be displayed as a matrix

$$[\sigma] = \begin{bmatrix} \sigma_{11} & \sigma_{12} & \sigma_{13} \\ \sigma_{12} & \sigma_{22} & \sigma_{23} \\ \sigma_{13} & \sigma_{23} & \sigma_{33} \end{bmatrix} = \begin{bmatrix} \sigma_1 & \sigma_6 & \sigma_5 \\ \sigma_6 & \sigma_2 & \sigma_4 \\ \sigma_5 & \sigma_4 & \sigma_3 \end{bmatrix} \tag{1.7}$$

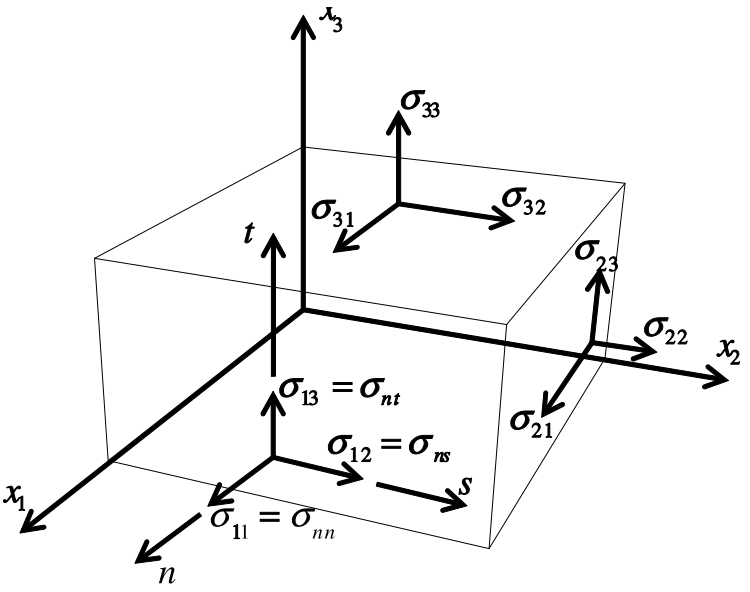

Figure 1.4: Stress components.

1.5 Contracted Notation

Since the stress is symmetric, it can be written in Voigt contracted notation as

$$\sigma_\alpha = \sigma_{ij} = \sigma_{ji} \tag{1.8}$$

with the contraction rule defined as follows

$$\begin{aligned} &\alpha = i && if \quad i = j \\ &\alpha = 9 - i - j && if \quad i \neq j \end{aligned} \tag{1.9}$$

resulting in the contracted version of stress components shown in (1.7). The same applies to the strain tensor, resulting in the contracted version of strain shown in (1.6). Note that the six components of stress σ_α with $\alpha = 1 \ldots 6$ can be arranged into a column array, denoted by curly brackets { } as in (1.10), but $\{\sigma\}$ is not a vector, but just a convenient way to arrange the six unique components of a symmetric second-order tensor.

1.5.1 Alternate Contracted Notation

Some finite element analysis (FEA) packages use different contracted notations, as shown in Table 1.1. For example, to transform stresses or strains from standard notation to *Abaqus*$^{\text{TM}}$ notation, a transformation matrix can be used as follows

$$\{\sigma_A\} = [T]\{\sigma\} \tag{1.10}$$

where the subscript $()_A$ denotes a quantity in *Abaqus* notation. Also note that { } denotes a column array, in this case of six elements, and [ ] denotes a matrix, in this case the 6×6 rotation matrix given by

Table 1.1: Contracted notation convention used by various FEA software packages

Standard convention	*Abaqus*/Standard	LS-DYNA and *Abaqus*/Explicit	ANSYS/Mechanical
$11 \longrightarrow 1$	$11 \longrightarrow 1$	$11 \longrightarrow 1$	$11 \longrightarrow 1$
$22 \longrightarrow 2$	$22 \longrightarrow 2$	$22 \longrightarrow 2$	$22 \longrightarrow 2$
$33 \longrightarrow 3$	$33 \longrightarrow 3$	$33 \longrightarrow 3$	$33 \longrightarrow 3$
$23 \longrightarrow 4$	$12 \longrightarrow 4$	$12 \longrightarrow 4$	$12 \longrightarrow 4$
$13 \longrightarrow 5$	$13 \longrightarrow 5$	$23 \longrightarrow 5$	$23 \longrightarrow 5$
$12 \longrightarrow 6$	$23 \longrightarrow 6$	$13 \longrightarrow 6$	$13 \longrightarrow 6$

$$[T] = \begin{bmatrix} 1 & 0 & 0 & 0 & 0 & 0 \\ 0 & 1 & 0 & 0 & 0 & 0 \\ 0 & 0 & 1 & 0 & 0 & 0 \\ 0 & 0 & 0 & 0 & 0 & 1 \\ 0 & 0 & 0 & 0 & 1 & 0 \\ 0 & 0 & 0 & 1 & 0 & 0 \end{bmatrix} \tag{1.11}$$

The stiffness matrix transforms as follows

$$[C_A] = [T]^T [C][T] \tag{1.12}$$

For LS-DYNA® and ANSYS®, the transformation matrix is

$$[T] = \begin{bmatrix} 1 & 0 & 0 & 0 & 0 & 0 \\ 0 & 1 & 0 & 0 & 0 & 0 \\ 0 & 0 & 1 & 0 & 0 & 0 \\ 0 & 0 & 0 & 0 & 0 & 1 \\ 0 & 0 & 0 & 1 & 0 & 0 \\ 0 & 0 & 0 & 0 & 1 & 0 \end{bmatrix} \tag{1.13}$$

1.6 Equilibrium and Virtual Work

The three equations of equilibrium at every point in a body are written in tensor notation as

$$\sigma_{ij,j} + f_i = 0 \tag{1.14}$$

where f_i is the body force per unit volume and $(\ )_{,j} = \dfrac{\partial}{\partial x_j}$. When body forces are negligible, the expanded form of the equilibrium equations, written in the laminate coordinate system x-y-z, is

$$\begin{aligned}\frac{\partial \sigma_{xx}}{\partial x}+\frac{\partial \sigma_{xy}}{\partial y}+\frac{\partial \sigma_{xz}}{\partial z}&=0\\ \frac{\partial \sigma_{xy}}{\partial x}+\frac{\partial \sigma_{yy}}{\partial y}+\frac{\partial \sigma_{yz}}{\partial z}&=0\\ \frac{\partial \sigma_{xz}}{\partial x}+\frac{\partial \sigma_{yz}}{\partial y}+\frac{\partial \sigma_{zz}}{\partial z}&=0\end{aligned} \tag{1.15}$$

The principle of virtual work (PVW) provides an alternative to the equations of equilibrium [4]. Since the PVW is an integral expression, it is more convenient than (1.14) for finite element formulation. The PVW reads

$$\int_V \sigma_{ij}\delta\epsilon_{ij}dV-\int_S t_i\delta u_i dS-\int_V f_i\delta u_i dV=0 \tag{1.16}$$

where t_i are the surface tractions per unit area acting on the surface S. The negative sign means that work is done by external forces (t_i, f_i) on the body. The forces and the displacements follow the same sign convention; that is, a component is positive when it points in the positive direction of the respective axis. The first term in (1.16) is the virtual work performed by the internal stresses and it is positive following the same sign convention.

Example 1.1 *Find the displacement function $u(x)$ for a slender rod of cross-sectional area A, length L, modulus E and density ρ, hanging from the top end and subjected to its own weight. Use a coordinate x pointing downward with the origin at the top end.*

Solution to Example 1.1 *We assume a quadratic displacement function*

$$u(x)=C_0+C_1x+C_2x^2$$

Using the boundary condition (BC) at the top yields $C_0=0$. The PVW (1.16) simplifies because the only nonzero strain is ϵ_x and there is no surface traction. Using Hooke's law

$$\int_0^L E\epsilon_x\delta\epsilon_x A dx-\int_0^L \rho g\delta u A dx=0$$

From the assumed displacement

$$\begin{aligned}\delta u&=x\delta C_1+x^2\delta C_2\\ \epsilon_x&=\frac{du}{dx}=C_1+2xC_2\\ \delta\epsilon_x&=\delta C_1+2x\delta C_2\end{aligned}$$

Substituting

$$EA\int_o^L(C_1+2xC_2)(\delta C_1+2x\delta C_2)dx-\rho gA\int_0^L(x\delta C_1+x^2\delta C_2)dx=0$$

Integrating and collecting terms in δC_1 and δC_2 separately

$$(EC_2L^2 + EC_1L - \frac{\rho g L^2}{2})\delta C_1 + (\frac{4}{3}EC_2L^3 + EC_1L^2 - \frac{\rho g L^3}{3})\delta C_2 = 0$$

Since δC_1 and δC_2 have arbitrary (virtual) values, two equations in two unknowns are obtained, one inside each parenthesis. Solving them we get

$$C_1 = \frac{L\rho g}{E} \; ; \; C_2 = -\frac{\rho g}{2E}$$

Substituting back into $u(x)$

$$u(x) = \frac{\rho g}{2E}(2L - x)x$$

which coincides with the exact solution from mechanics of materials.

1.7 Boundary Conditions

1.7.1 Traction Boundary Conditions

The solution of problems in solid mechanics requires that boundary conditions be specified. The boundary conditions may be specified in terms of components of displacement, stress, or a combination of both. For any point on an arbitrary surface, the traction T_i is defined as the vector consisting of the three components of stress acting on the surface at the point of interest. As indicated in Figure 1.4 the traction vector consists of one component of normal stress, σ_{nn}, and two components of shear stress, σ_{nt} and σ_{ns}. The traction vector can be written using Cauchy's law

$$T_i = \sigma_{ji} n_j = \sum_{j}^{3} \sigma_{ji} n_j \tag{1.17}$$

where n_j is the unit normal to the surface at the point under consideration.[2] For a plane perpendicular to the x_1 axis $n_i = (1, 0, 0)$ and the components of the traction are $T_1 = \sigma_{11}$, $T_2 = \sigma_{12}$, and $T_3 = \sigma_{13}$.

1.7.2 Free Surface Boundary Conditions

The condition that a surface be free of stress is equivalent to all components of traction being zero, i.e., $T_n = \sigma_{nn} = 0$, $T_t = \sigma_{nt} = 0$, and $T_s = \sigma_{ns} = 0$. It is possible that only selected components of the traction be zero while others are not zero. For example, pure pressure loading corresponds to nonzero normal stress and zero shear stresses.

[2]Einstein's summation convention can be introduced with (1.17) as an example. Any pair of repeated indices implies a summation over all the values of the index in question. Furthermore, each pair of repeated indices represents a *contraction*. That is, the order of resulting tensor, in this case order one for T_i, is two less than the sum of the orders of the tensors involved in the operation. The resulting tensor keeps only the *free* indices that are not involved in the contraction–in this case only i remains.

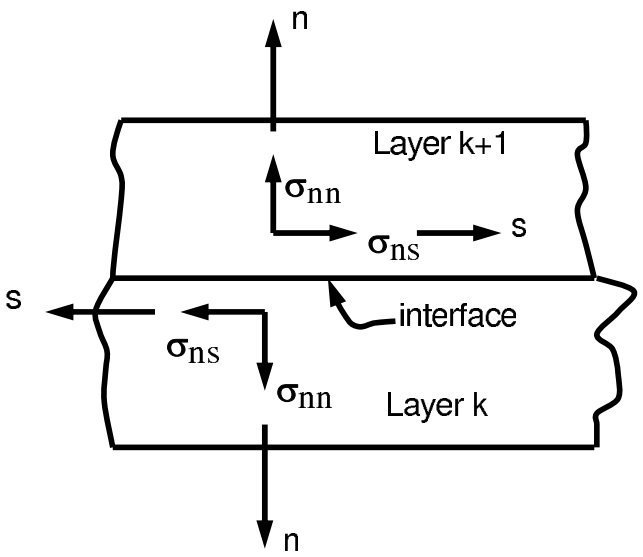

Figure 1.5: Traction continuity across an interface.

1.8 Continuity Conditions

1.8.1 Traction Continuity

Equilibrium (action and reaction) requires that the traction components T_i must be continuous across any surface. Mathematically this is stated as $T_i^+ - T_i^- = 0$. Using (1.17), $T_i^+ = \sigma_{ji}^+ n_j$. Since $n_j^+ = -n_j^-$, we have $\sigma_{ji}^+ = \sigma_{ji}^-$. In terms of individual stress components, $\sigma_{nn}^+ = \sigma_{nn}^-$, $\sigma_{nt}^+ = \sigma_{nt}^-$, and $\sigma_{ns}^+ = \sigma_{ns}^-$ (Figure 1.5). Thus, the normal and shear components of stress acting on a surface must be continuous across that surface. There are no continuity requirements on the other three components of stress. That is, it is possible that $\sigma_{tt}^+ \neq \sigma_{tt}^-$, $\sigma_{ss}^+ \neq \sigma_{ss}^-$, and $\sigma_{ts}^+ \neq \sigma_{ts}^-$. Lack of continuity of the two normal and one shear components of stress is very common because the material properties are discontinuous across lamina boundaries.

1.8.2 Displacement Continuity

Certain conditions on displacements must be satisfied along any surface in a perfectly bonded continuum. Consider for example buckling of a cylinder under external pressure (Figure 1.6). The displacements associated with the material from either side of the line A-A must be identical $u_i^+ = u_i^-$. The continuity conditions must be satisfied at every point in a perfectly bonded continuum. However, continuity is not required in the presence of debonding or sliding between regions or phases of a material. For the example shown, continuity of slope must be satisfied also $(\dfrac{\partial w^+}{\partial \theta} = \dfrac{\partial w^-}{\partial \theta})$, where w is the radial displacement.

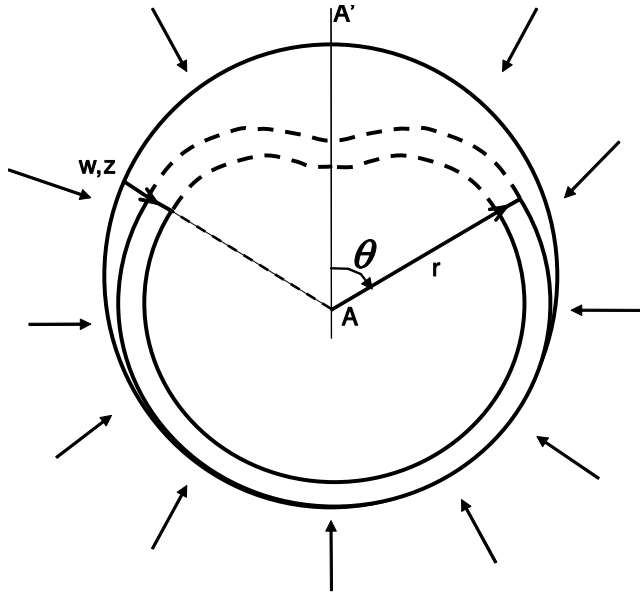

Figure 1.6: Buckling of an encased cylindrical pipe under external pressure.

1.9 Compatibility

The strain displacement equations (1.5) provide six equations for only three unknown displacements u_i. Thus, integration of equations (1.5) to determine the unknown displacements will not have a single-valued solution unless the strains ε_{ij} satisfy certain conditions. Arbitrary specification of the ε_{ij} could result in discontinuities in the material, including gaps and/or overlapping regions.

The necessary conditions for single-valued displacements are the *compatibility conditions.* Although these six equations are available [2], they are not used here because the displacement method, which is used throughout this book, does not require them. That is, in solving problems, the form of displacements u_i is always assumed a priori. Then, the strains are computed with (1.5), and the stress with (1.46). Finally, equilibrium is enforced by using the PVW (1.16).

1.10 Coordinate Transformations

The coordinates of point P in the prime coordinate system can be found from its coordinates in the unprimed system. From Figure 1.7, the coordinates of point P are

$$\begin{aligned} x_1' &= x_1 \cos\theta + x_2 \sin\theta \\ x_2' &= -x_1 \sin\theta + x_2 \cos\theta \\ x_3' &= x_3 \end{aligned} \tag{1.18}$$

or

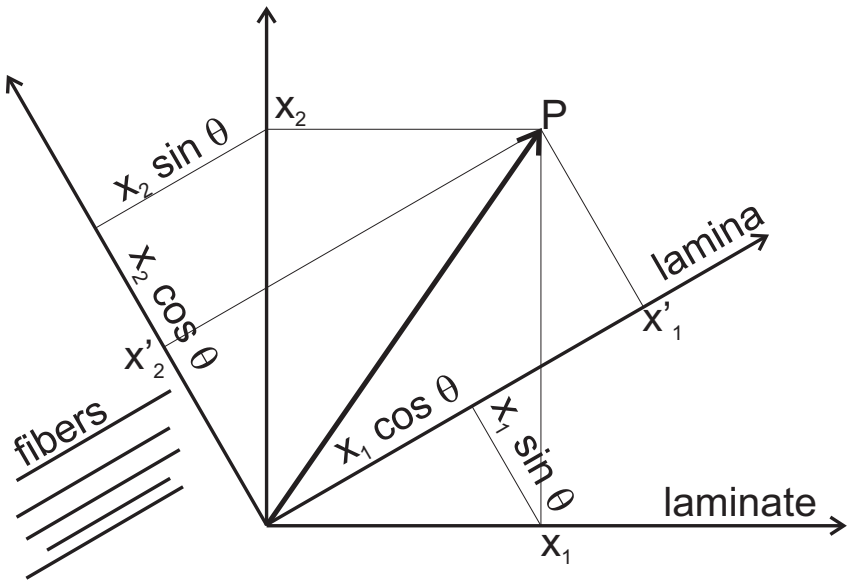

Figure 1.7: Coordinate transformation.

$$x_i' = a_{ij} x_j \tag{1.19}$$

or in matrix notation

$$\{x'\} = [a]\,\{x\} \tag{1.20}$$

where a_{ij} are the components of the unit vectors of the primed system e_i' on the unprimed system e_j, by rows [2]

$$a_{ij} = \cos(e_i', e_j) = \begin{array}{c|ccc} & e_1 & e_2 & e_3 \\ \hline e_1' & a_{11} & a_{12} & a_{13} \\ e_2' & a_{21} & a_{22} & a_{23} \\ e_3' & a_{31} & a_{32} & a_{33} \end{array} \tag{1.21}$$

If primed coordinates denote the lamina coordinates and unprimed denote the laminate coordinates, then (1.19) transforms vectors from laminate to lamina coordinates. The inverse transformation simply uses the transpose matrix

$$\{x\} = [a]^T \left\{x'\right\} \tag{1.22}$$

Example 1.2 *A composite lamina has fiber orientation $\theta = 30°$. Construct the [a] matrix by calculating the direction cosines of the lamina system, i.e., the components of the unit vectors of the lamina system (x_i') on the laminate system (x_j).*

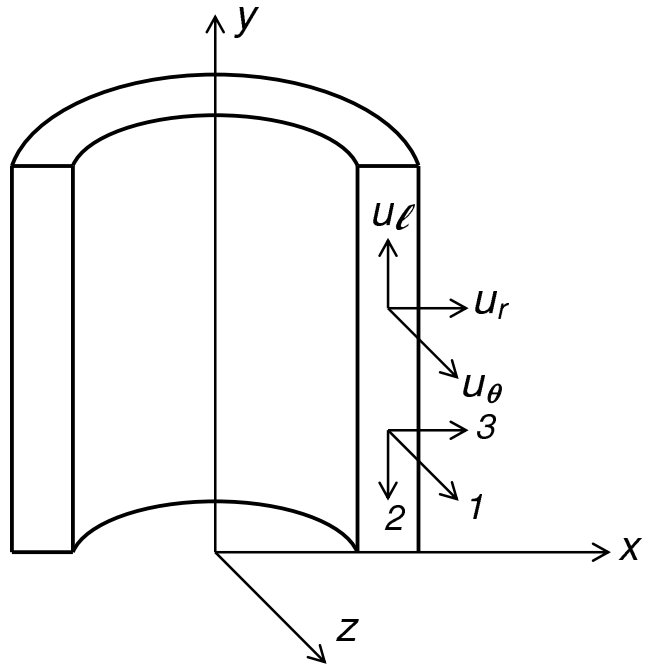

Figure 1.8: Coordinate transformation for axial-symmetric analysis.

Solution to Example 1.2 *From Figure 1.7 and (1.19) we have*

$$
\begin{aligned}
a_{11} &= \cos\theta = \frac{\sqrt{3}}{2} \\
a_{12} &= \sin\theta = \frac{1}{2} \\
a_{13} &= 0 \\
a_{21} &= -\sin\theta = -\frac{1}{2} \\
a_{22} &= \cos\theta = \frac{\sqrt{3}}{2} \\
a_{23} &= 0 \\
a_{31} &= 0 \\
a_{32} &= 0 \\
a_{33} &= 1
\end{aligned}
$$

Example 1.3 *A fiber reinforced composite tube is wound in the hoop direction (1-direction). Formulas for the stiffness values (E_1, E_2, etc.) are given in that system. However, when analyzing the cross-section of this material with generalized plane strain elements (CAX4 in* Abaqus*), the model is typically constructed in the structural X, Y, Z system. It is therefore necessary to provide the stiffness values in the structural system as E_x, E_y, etc. Construct the transformation matrix $[a]^T$ to go from lamina coordinates (1-2-3) to structural coordinates in Figure 1.8.*

Solution to Example 1.3 *First, construct* $[a]$ *using the definition (1.21). Taking each unit vector (1-2-3) at a time we construct the matrix* $[a]$ *by rows. The i-th row contains the components of* ($i = 1, 2, 3$) *along (X-Y-Z).*

$[a]$	X	Y	Z
1	0	0	1
2	0	-1	0
3	1	0	0

The required transformation is just the transpose of the matrix above.

1.10.1 Stress Transformation

A second-order tensor σ_{pq} can be thought as the (uncontracted) outer product[3] of two vectors V_p and V_q

$$\sigma_{pq} = V_p \otimes V_q \tag{1.23}$$

each of which transforms as (1.19)

$$\sigma'_{ij} = a_{ip} V_p \otimes a_{jq} V_q \tag{1.24}$$

Therefore,

$$\sigma'_{ij} = a_{ip} a_{jq} \sigma_{pq} \tag{1.25}$$

or, in matrix notation

$$\{\sigma'\} = [a]\{\sigma\}[a]^T \tag{1.26}$$

For example, expand σ'_{11} in contracted notation

$$\sigma'_1 = a_{11}^2\sigma_1 + a_{12}^2\sigma_2 + a_{13}^2\sigma_3 + 2a_{11}a_{12}\sigma_6 + 2a_{11}a_{13}\sigma_5 + 2a_{12}a_{13}\sigma_4 \tag{1.27}$$

Expanding σ'_{12} in contracted notation yields

$$\begin{aligned}\sigma'_6 = {} & a_{11}a_{21}\sigma_1 + a_{12}a_{22}\sigma_2 + a_{13}a_{23}\sigma_3 + (a_{11}a_{22} + a_{12}a_{21})\sigma_6 \\ & + (a_{11}a_{23} + a_{13}a_{21})\sigma_5 + (a_{12}a_{23} + a_{13}a_{22})\sigma_4\end{aligned} \tag{1.28}$$

The following algorithm is used to obtain a 6×6 coordinate transformation matrix [T] such that (1.25) is rewritten in contracted notation as

$$\sigma'_\alpha = T_{\alpha\beta}\sigma_\beta \tag{1.29}$$

If $\alpha \leq 3$ and $\beta \leq 3$ then $i = j$ and $p = q$, so

$$T_{\alpha\beta} = a_{ip}a_{ip} = a_{ip}^2 \quad \text{no sum on } i, p \tag{1.30}$$

If $\alpha \leq 3$ and $\beta > 3$ then $i = j$ but $p \neq q$, and taking into account that switching p by q yields the same value of $\beta = 9 - p - q$ as per (1.9) we have

[3]The outer product preserves all indices of the entities involved, thus creating a tensor of order equal to the sum of the order of the entities involved.

$$T_{\alpha\beta} = a_{ip}a_{iq} + a_{iq}a_{ip} = 2a_{ip}a_{iq} \quad \text{no sum on } i, p \tag{1.31}$$

If $\alpha > 3$, then $i \neq j$, but we want only one stress, say σ_{ij}, not σ_{ji} because they are numerically equal. In fact $\sigma_\alpha = \sigma_{ij} = \sigma_{ji}$ with $\alpha = 9 - i - j$. If in addition $\beta \leq 3$ then $p = q$ and we get

$$T_{\alpha\beta} = a_{ip}a_{jp} \quad \text{no sum on } i, p \tag{1.32}$$

When $\alpha > 3$ and $\beta > 3$, $i \neq j$ and $p \neq q$ so we get

$$T_{\alpha\beta} = a_{ip}a_{jq} + a_{iq}a_{jp} \tag{1.33}$$

which completes the derivation of $T_{\alpha\beta}$. Expanding (1.30–1.33) and using (1.21) we get

$$[T] = \begin{bmatrix} a_{11}^2 & a_{12}^2 & a_{13}^2 & 2\,a_{12}\,a_{13} & 2\,a_{11}\,a_{13} & 2\,a_{11}\,a_{12} \\ a_{21}^2 & a_{22}^2 & a_{23}^2 & 2\,a_{22}\,a_{23} & 2\,a_{21}\,a_{23} & 2\,a_{21}\,a_{22} \\ a_{31}^2 & a_{32}^2 & a_{33}^2 & 2\,a_{32}\,a_{33} & 2\,a_{31}\,a_{33} & 2\,a_{31}\,a_{32} \\ a_{21}\,a_{31} & a_{22}\,a_{32} & a_{23}\,a_{33} & a_{22}\,a_{33} + a_{23}\,a_{32} & a_{21}\,a_{33} + a_{23}\,a_{31} & a_{21}\,a_{32} + a_{22}\,a_{31} \\ a_{11}\,a_{31} & a_{12}\,a_{32} & a_{13}\,a_{33} & a_{12}\,a_{33} + a_{13}\,a_{32} & a_{11}\,a_{33} + a_{13}\,a_{31} & a_{11}\,a_{32} + a_{12}\,a_{31} \\ a_{11}\,a_{21} & a_{12}\,a_{22} & a_{13}\,a_{23} & a_{12}\,a_{23} + a_{13}\,a_{22} & a_{11}\,a_{23} + a_{13}\,a_{21} & a_{11}\,a_{22} + a_{12}\,a_{21} \end{bmatrix} \tag{1.34}$$

A MATLAB® program that can be used to generate (1.34) is shown next (also available in [5]).

```
% Derivation of the transformation matrix [T]
clear all;
syms T alpha R
syms a a11 a12 a13 a21 a22 a23 a31 a32 a33
a = [a11,a12,a13;
     a21,a22,a23;
     a31,a32,a33];
T(1:6,1:6) = 0;
for i=1:1:3
for j=1:1:3
 if i==j; alpha = j; else alpha = 9-i-j; end
 for p=1:1:3
 for q=1:1:3
  if p==q beta = p; else beta = 9-p-q; end
  T(alpha,beta) = 0;
  if alpha<=3 & beta<= 3; T(alpha,beta)=a(i,p)*a(i,p); end
  if alpha> 3 & beta<= 3; T(alpha,beta)=a(i,p)*a(j,p); end
  if alpha<=3 & beta>3; T(alpha,beta)=a(i,q)*a(i,p)+a(i,p)*a(i,q);end
  if alpha>3 & beta>3; T(alpha,beta)=a(i,p)*a(j,q)+a(i,q)*a(j,p);end
 end
 end
end
end
```

```
T
R = eye(6,6); R(4,4)=2; R(5,5)=2; R(6,6)=2; % Reuter matrix
Tbar = R*T*R^(-1)
```

1.10.2 Strain Transformation

The tensor components of strain ε_{ij} transform in the same way as the stress components

$$\varepsilon'_{ij} = a_{ip} a_{jq} \varepsilon_{pq} \tag{1.35}$$

or

$$\varepsilon'_{\alpha} = T_{\alpha\beta} \varepsilon_{\beta} \tag{1.36}$$

with $T_{\alpha\beta}$ given by (1.34). However, the three engineering shear strains $\gamma_{xz}, \gamma_{yz}, \gamma_{xy}$ are normally used instead of tensor shear strains $\varepsilon_{xz}, \varepsilon_{yz}, \varepsilon_{xy}$. The engineering strains (ϵ instead of ε) are defined in (1.5). They can be obtained from the tensor components by the following relationship

$$\epsilon_{\delta} = R_{\delta\gamma} \varepsilon_{\gamma} \tag{1.37}$$

with the Reuter matrix given by

$$[R] = \begin{bmatrix} 1 & 0 & 0 & 0 & 0 & 0 \\ 0 & 1 & 0 & 0 & 0 & 0 \\ 0 & 0 & 1 & 0 & 0 & 0 \\ 0 & 0 & 0 & 2 & 0 & 0 \\ 0 & 0 & 0 & 0 & 2 & 0 \\ 0 & 0 & 0 & 0 & 0 & 2 \end{bmatrix} \tag{1.38}$$

Then, the coordinate transformation of engineering strain results from (1.36) and (1.37) as

$$\epsilon'_{\alpha} = \overline{T}_{\alpha\beta} \epsilon_{\beta} \tag{1.39}$$

with

$$\left[\overline{T} \right] = [R][T][R]^{-1} \tag{1.40}$$

used only to transform engineering strains. Explicitly we have

$$\left[\overline{T} \right] = \begin{bmatrix} a_{11}^2 & a_{12}^2 & a_{13}^2 & a_{12}\,a_{13} & a_{11}\,a_{13} & a_{11}\,a_{12} \\ a_{21}^2 & a_{22}^2 & a_{23}^2 & a_{22}\,a_{23} & a_{21}\,a_{23} & a_{21}\,a_{22} \\ a_{31}^2 & a_{32}^2 & a_{33}^2 & a_{32}\,a_{33} & a_{31}\,a_{33} & a_{31}\,a_{32} \\ 2\,a_{21}\,a_{31} & 2\,a_{22}\,a_{32} & 2\,a_{23}\,a_{33} & a_{22}\,a_{33} + a_{23}\,a_{32} & a_{21}\,a_{33} + a_{23}\,a_{31} & a_{21}\,a_{32} + a_{22}\,a_{31} \\ 2\,a_{11}\,a_{31} & 2\,a_{12}\,a_{32} & 2\,a_{13}\,a_{33} & a_{12}\,a_{33} + a_{13}\,a_{32} & a_{11}\,a_{33} + a_{13}\,a_{31} & a_{11}\,a_{32} + a_{12}\,a_{31} \\ 2\,a_{11}\,a_{21} & 2\,a_{12}\,a_{22} & 2\,a_{13}\,a_{23} & a_{12}\,a_{23} + a_{13}\,a_{22} & a_{11}\,a_{23} + a_{13}\,a_{21} & a_{11}\,a_{22} + a_{12}\,a_{21} \end{bmatrix} \tag{1.41}$$

1.11 Transformation of Constitutive Equations

The constitutive equations that relate stress $\boldsymbol{\sigma}$ to strain $\boldsymbol{\varepsilon}$ are defined using tensor strains ($\boldsymbol{\varepsilon}$, not $\boldsymbol{\epsilon}$), as

$$\begin{aligned} \boldsymbol{\sigma}' &= \mathbf{C}' : \boldsymbol{\varepsilon}' \\ \sigma'_{ij} &= C'_{ijkl}\varepsilon'_{kl} \end{aligned} \tag{1.42}$$

where both *tensor* and *index* notations have been used.[4]

For simplicity consider an orthotropic material (Section 1.12.3). Then, it is possible to write σ'_{11}, and σ'_{12} as

$$\begin{aligned} \sigma'_{11} &= C'_{1111}\varepsilon'_{11} + C'_{1122}\varepsilon'_{22} + C'_{1133}\varepsilon'_{33} \\ \sigma'_{12} &= C'_{1212}\varepsilon'_{12} + C'_{1221}\varepsilon'_{21} = 2C'_{1212}\varepsilon'_{12} \end{aligned} \tag{1.43}$$

Rewriting (1.43) in contracted notation, it is clear that in contracted notation all the shear strains appear twice, as follows

$$\begin{aligned} \sigma'_1 &= C'_{11}\varepsilon'_1 + C'_{12}\varepsilon'_2 + C'_{13}\varepsilon'_3 \\ \sigma'_6 &= 2C'_{66}\varepsilon'_6 \end{aligned} \tag{1.44}$$

The factor 2 in front of the tensor shear strains is caused by two facts, the minor symmetry of the tensors C and ε (see (1.5,1.55,1.56) and the contraction of the last two indices of C_{ijkl} with the strain ε_{kl} in (1.43). Therefore, *any double contraction of tensors with minor symmetry needs to be corrected by a Reuter matrix (1.38) when written in the contracted notation.* Next, (1.42) can be written as

$$\sigma'_\alpha = C'_{\alpha\beta}R_{\beta\delta}\varepsilon'_\delta \tag{1.45}$$

Note that the Reuter matrix in (1.45) can be combined with the tensor strains using (1.37), to write

$$\sigma'_\alpha = C'_{\alpha\beta}\epsilon'_\beta \tag{1.46}$$

in terms of engineering strains. To obtain the stiffness matrix $[C]$ in the laminate coordinate system, introduce (1.29) and (1.39) into (1.46) so that

$$T_{\alpha\delta}\sigma_\delta = C'_{\alpha\beta}\overline{T}_{\beta\gamma}\epsilon_\gamma \tag{1.47}$$

It can be shown that

$$[T]^{-1} = [\overline{T}]^T \tag{1.48}$$

Therefore

$$\{\sigma\} = [C]\{\epsilon\} \tag{1.49}$$

[4] A double contraction involves contraction of two indices, in this case k and l, and it is denoted by : in tensor notation. Also note the use of boldface to indicate tensors in tensor notation.

with

$$[C] = [\overline{T}]^T [C'][\overline{T}] \tag{1.50}$$

and

$$[C'] = [\overline{T}]^{-T} [C][\overline{T}]^{-1} = [T][C][T]^T \tag{1.51}$$

The compliance matrix is the inverse of the stiffness matrix, not the inverse of the fourth-order tensor C_{ijkl}. Therefore,

$$[S'] = [C']^{-1} \tag{1.52}$$

Taking into account (1.48) and (1.50), the compliance matrix transforms as

$$[S] = [T]^T [S'][T] \tag{1.53}$$

$$[S'] = [T]^{-T} [S][T]^{-1} = [\overline{T}][S][\overline{T}]^T \tag{1.54}$$

1.12 3D Constitutive Equations

Hooke's law in three dimensions (3D) takes the form of (1.42). The 3D stiffness tensor C_{ijkl} is a fourth-order tensor with 81 components. For anisotropic materials only 21 components are independent. That is, the remaining 60 components can be written in terms of the other 21. The one dimensional case (1D), studied in mechanics of materials, is recovered when all the stress components are zero except σ_{11}. Only for the 1D case, $\sigma_{11} = \sigma$,$\varepsilon_{11} = \epsilon$,$C_{1111} = E$, and $\sigma = E\epsilon$. All the derivations in this section are carried out in lamina coordinates *but for simplicity the prime symbol* ($'$) *is omitted, in this section only.*

In (1.42), exchanging the dummy indexes i by j, and k by l we have

$$\sigma_{ji} = C_{jilk}\varepsilon_{lk} \tag{1.55}$$

Since the stress and strain tensors are symmetric, i.e., $\sigma_{ij} = \sigma_{ji}$ and $\varepsilon_{kl} = \varepsilon_{kl}$, it follows that

$$C_{ijkl} = C_{jikl} = C_{ijlk} = C_{jilk} \tag{1.56}$$

which effectively reduces the number of independent components from 81 to 36. For example, $C_{1213} = C_{2131}$ and so on. Then, the 36 independent components can be written as a 6×6 matrix.

Furthermore, an elastic material does not dissipate energy. All elastic energy stored during loading is recovered during unloading. Therefore, the elastic energy at any point on the stress-strain curve is independent on the path that was followed to arrive at that point. A path independent function is called a potential function. In this case, the potential is the strain energy density $\widetilde{u}(\varepsilon_{ij})$. Expanding the strain energy density in a Taylor power series

$$\widetilde{u} = \widetilde{u}_0 + \left.\frac{\partial \widetilde{u}}{\partial \varepsilon_{ij}}\right|_0 \varepsilon_{ij} + \frac{1}{2} \left.\frac{\partial^2 \widetilde{u}}{\partial \varepsilon_{ij} \partial \varepsilon_{kl}}\right|_0 \varepsilon_{ij}\, \varepsilon_{kl} + ... \tag{1.57}$$

Now take a derivative with respect to ε_{ij}

$$\frac{\partial \widetilde{u}}{\partial \varepsilon_{ij}} = 0 + \beta_{ij} + \frac{1}{2} \left(\alpha_{ijkl}\, \varepsilon_{kl} + \alpha_{klij}\, \varepsilon_{ij}\right) \tag{1.58}$$

where β_{ij} and α_{ijkl} are constants. From here, one can write

$$\sigma_{ij} - \sigma^0_{ij} = C_{ijkl}\, \varepsilon_{kl} \tag{1.59}$$

where $\sigma^0_{ij} = \beta_{ij}$ is the residual stress and $\alpha_{ijkl} = 1/2(C_{ijkl} + C_{klik}) = C_{ijkl}$ is the symmetric stiffness tensor (see (1.56)). Equation (1.59) is a generalization of (1.55) including residual stresses.

Using contracted notation, the generalized Hooke's law becomes

$$\left\{\begin{array}{c} \sigma_1 \\ \sigma_2 \\ \sigma_3 \\ \sigma_4 \\ \sigma_5 \\ \sigma_6 \end{array}\right\} = \left[\begin{array}{cccccc} C_{11} & C_{12} & C_{13} & C_{14} & C_{15} & C_{16} \\ C_{12} & C_{22} & C_{23} & C_{24} & C_{25} & C_{26} \\ C_{13} & C_{23} & C_{33} & C_{34} & C_{35} & C_{36} \\ C_{14} & C_{24} & C_{34} & C_{44} & C_{45} & C_{46} \\ C_{15} & C_{25} & C_{35} & C_{45} & C_{55} & C_{56} \\ C_{16} & C_{26} & C_{36} & C_{46} & C_{56} & C_{66} \end{array}\right] \left\{\begin{array}{c} \epsilon_1 \\ \epsilon_2 \\ \epsilon_3 \\ \gamma_4 \\ \gamma_5 \\ \gamma_6 \end{array}\right\} \tag{1.60}$$

Once again, the 1D case is covered when $\sigma_\alpha = 0$ if $\alpha \neq 1$. Then, $\sigma_1 = \sigma, \epsilon_1 = \epsilon, C_{11} = E$.

1.12.1 Anisotropic Material

Equation (1.60) represents a fully anisotropic material. Such a material has properties that change with the orientation. For example, the material body depicted in Figure 1.9 deforms differently in the directions P, T, and Q, even if the forces applied along the directions P, T, and Q are equal. The number of constants required to describe anisotropic materials is 21.

The inverse of the stiffness matrix is the compliance matrix $[S] = [C]^{-1}$. The constitutive equation (3D Hooke's law) is written in terms of compliances as follows

$$\left\{\begin{array}{c} \epsilon_1 \\ \epsilon_2 \\ \epsilon_3 \\ \gamma_4 \\ \gamma_5 \\ \gamma_6 \end{array}\right\} = \left[\begin{array}{cccccc} S_{11} & S_{12} & S_{13} & S_{14} & S_{15} & S_{16} \\ S_{12} & S_{22} & S_{23} & S_{24} & S_{25} & S_{26} \\ S_{13} & S_{23} & S_{33} & S_{34} & S_{35} & S_{36} \\ S_{14} & S_{24} & S_{34} & S_{44} & S_{45} & S_{46} \\ S_{15} & S_{25} & S_{35} & S_{45} & S_{55} & S_{56} \\ S_{16} & S_{26} & S_{36} & S_{46} & S_{56} & S_{66} \end{array}\right] \left\{\begin{array}{c} \sigma_1 \\ \sigma_2 \\ \sigma_3 \\ \sigma_4 \\ \sigma_5 \\ \sigma_6 \end{array}\right\} \tag{1.61}$$

The $[S]$ matrix is also symmetric and it has 21 independent constants. For the 1D case, $\sigma = 0$ if $p \neq 1$. Then, $\sigma_1 = \sigma, \epsilon_1 = \epsilon, S_{11} = 1/E$.

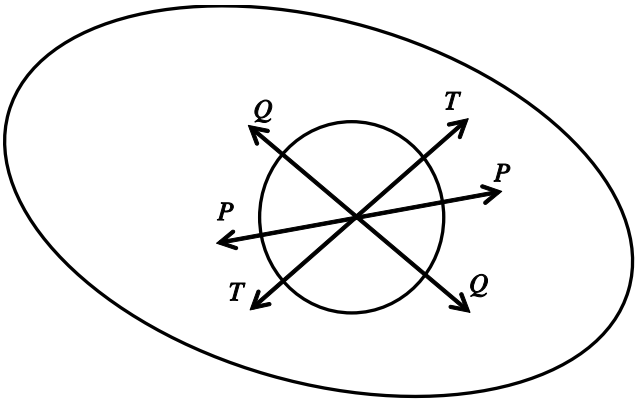

Figure 1.9: Anisotropic material.

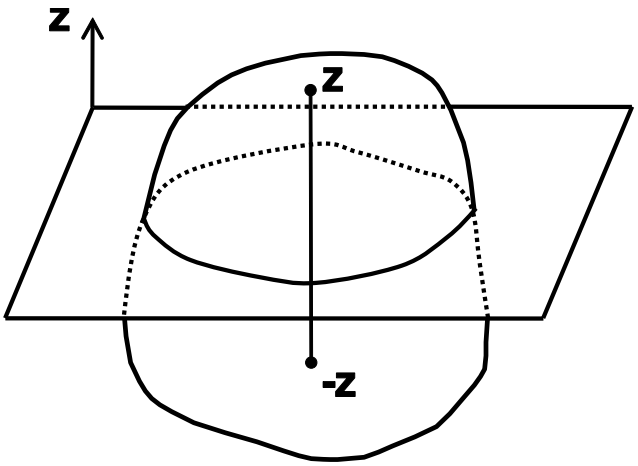

Figure 1.10: Monoclinic material.

1.12.2 Monoclinic Material

If a material has one plane of symmetry (Figure 1.10) it is called monoclinic and 13 constants are required to describe it. One plane of symmetry means that the properties are the same at symmetric points (z and $-z$ as in Figure 1.10).

When the material is symmetric about the 1-2 plane, the material properties are identical upon reflection with respect to the 1-2 plane. For such reflection the a-matrix (1.21) is

$$\begin{array}{c} \\ e_1'' \\ e_2'' \\ e_3'' \end{array} \begin{array}{c} \begin{array}{ccc} x_1 & x_2 & x_3 \end{array} \\ \begin{bmatrix} 1 & 0 & 0 \\ 0 & 1 & 0 \\ 0 & 0 & -1 \end{bmatrix} \end{array} \tag{1.62}$$

where $''$ has been used to avoid confusion with the lamina coordinate system that is denoted without $'$ in this section but with $'$ elsewhere in this book. From (1.40) we get

$$\left[\overline{T}\right] = \begin{bmatrix} 1 & 0 & 0 & 0 & 0 & 0 \\ 0 & 1 & 0 & 0 & 0 & 0 \\ 0 & 0 & 1 & 0 & 0 & 0 \\ 0 & 0 & 0 & -1 & 0 & 0 \\ 0 & 0 & 0 & 0 & -1 & 0 \\ 0 & 0 & 0 & 0 & 0 & 1 \end{bmatrix} \tag{1.63}$$

The effect of $\left[\overline{T}\right]$ is to multiply rows and columns 4 and 5 in $[C]$ by -1. The diagonal terms C_{44} and C_{55} remain positive because they are multiplied twice. Therefore, $C''_{i4} = -C_{i4}$ with $i \neq 4, 5$, $C''_{i5} = -C_{i5}$ with $i \neq 4, 5$, with everything else unchanged. Since the material properties in a monoclinic material cannot change by a reflection, it must be $C_{4i} = C_{i4} = 0$ with $i \neq 4, 5$, $C_{5i} = C_{i5} = 0$ with $i \neq 4, 5$. That is, 3D Hooke's law reduces to

$$\begin{Bmatrix} \sigma_1 \\ \sigma_2 \\ \sigma_3 \\ \sigma_4 \\ \sigma_5 \\ \sigma_6 \end{Bmatrix} = \begin{bmatrix} C_{11} & C_{12} & C_{13} & 0 & 0 & C_{16} \\ C_{12} & C_{22} & C_{23} & 0 & 0 & C_{26} \\ C_{13} & C_{23} & C_{33} & 0 & 0 & C_{36} \\ 0 & 0 & 0 & C_{44} & C_{45} & 0 \\ 0 & 0 & 0 & C_{45} & C_{55} & 0 \\ C_{16} & C_{26} & C_{36} & 0 & 0 & C_{66} \end{bmatrix} \begin{Bmatrix} \epsilon_1 \\ \epsilon_2 \\ \epsilon_3 \\ \gamma_4 \\ \gamma_5 \\ \gamma_6 \end{Bmatrix} \tag{1.64}$$

and in terms of the compliances to

$$\begin{Bmatrix} \epsilon_1 \\ \epsilon_2 \\ \epsilon_3 \\ \gamma_4 \\ \gamma_5 \\ \gamma_6 \end{Bmatrix} = \begin{bmatrix} S_{11} & S_{12} & S_{13} & 0 & 0 & S_{16} \\ S_{12} & S_{22} & S_{23} & 0 & 0 & S_{26} \\ S_{13} & S_{23} & S_{33} & 0 & 0 & S_{36} \\ 0 & 0 & 0 & S_{44} & S_{45} & 0 \\ 0 & 0 & 0 & S_{45} & S_{55} & 0 \\ S_{16} & S_{26} & S_{36} & 0 & 0 & S_{66} \end{bmatrix} \begin{Bmatrix} \sigma_1 \\ \sigma_2 \\ \sigma_3 \\ \sigma_4 \\ \sigma_5 \\ \sigma_6 \end{Bmatrix} \tag{1.65}$$

1.12.3 Orthotropic Material

An orthotropic material has three planes of symmetry that coincide with the coordinate planes. It can be shown that if two orthogonal planes of symmetry exist, there is always a third orthogonal plane of symmetry. Nine constants are required to describe this type of material.

The symmetry planes can be Cartesian, as depicted in Figure 1.11, or they may correspond to any other coordinate representation (cylindrical, spherical, etc.). For example, the trunk of a tree has cylindrical orthotropy because of the growth rings. However, most practical materials exhibit Cartesian orthotropy. A unidirectional fiber reinforced composite may be considered to be orthotropic. One plane of symmetry is perpendicular to the fiber direction, and the other two are parallel to the fiber direction and orthogonal among themselves.

In addition to the reflection about the 1-2 plane discussed in Section 1.12.2, a second reflection about the 1-3 plane should not affect the properties of the orthotropic materials. In this case the a-matrix is

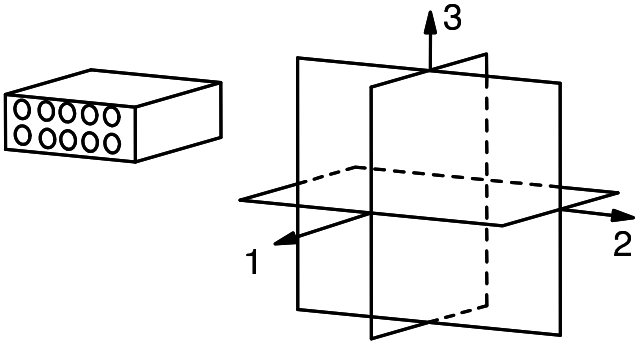

Figure 1.11: Orthotropic material.

$$[a] = \begin{bmatrix} 1 & 0 & 0 \\ 0 & -1 & 0 \\ 0 & 0 & 1 \end{bmatrix} \tag{1.66}$$

The $\overline{T}$-matrix from (1.40) is

$$[\overline{T}] = \begin{bmatrix} 1 & 0 & 0 & 0 & 0 & 0 \\ 0 & 1 & 0 & 0 & 0 & 0 \\ 0 & 0 & 1 & 0 & 0 & 0 \\ 0 & 0 & 0 & -1 & 0 & 0 \\ 0 & 0 & 0 & 0 & 1 & 0 \\ 0 & 0 & 0 & 0 & 0 & -1 \end{bmatrix} \tag{1.67}$$

This will make $C_{i6} = -C_{i6}$, $i \neq 4, 6$ and $C_{i4} = -C_{i4}$, $i \neq 4, 6$. Since the material has symmetry about the 1-3 plane, this means that $C_{i6} = C_{6i} = 0$, $i \neq 6$. In this case, 3D Hooke's law reduces to

$$\begin{Bmatrix} \sigma_1 \\ \sigma_2 \\ \sigma_3 \\ \sigma_4 \\ \sigma_5 \\ \sigma_6 \end{Bmatrix} = \begin{bmatrix} C_{11} & C_{12} & C_{13} & 0 & 0 & 0 \\ C_{12} & C_{22} & C_{23} & 0 & 0 & 0 \\ C_{13} & C_{23} & C_{33} & 0 & 0 & 0 \\ 0 & 0 & 0 & C_{44} & 0 & 0 \\ 0 & 0 & 0 & 0 & C_{55} & 0 \\ 0 & 0 & 0 & 0 & 0 & C_{66} \end{bmatrix} \begin{Bmatrix} \epsilon_1 \\ \epsilon_2 \\ \epsilon_3 \\ \gamma_4 \\ \gamma_5 \\ \gamma_6 \end{Bmatrix} \tag{1.68}$$

and in terms of the compliances to

$$\begin{Bmatrix} \epsilon_1 \\ \epsilon_2 \\ \epsilon_3 \\ \gamma_4 \\ \gamma_5 \\ \gamma_6 \end{Bmatrix} = \begin{bmatrix} S_{11} & S_{12} & S_{13} & 0 & 0 & 0 \\ S_{12} & S_{22} & S_{23} & 0 & 0 & 0 \\ S_{13} & S_{23} & S_{33} & 0 & 0 & 0 \\ 0 & 0 & 0 & S_{44} & 0 & 0 \\ 0 & 0 & 0 & 0 & S_{55} & 0 \\ 0 & 0 & 0 & 0 & 0 & S_{66} \end{bmatrix} \begin{Bmatrix} \sigma_1 \\ \sigma_2 \\ \sigma_3 \\ \sigma_4 \\ \sigma_5 \\ \sigma_6 \end{Bmatrix} \tag{1.69}$$

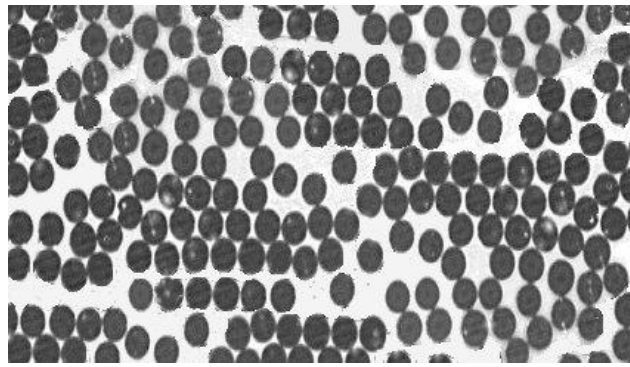

Figure 1.12: Randomly distributed E-glass fibers with 200X magnification.

Note that if the material has two planes of symmetry, it automatically has three because applying the procedure once more for a third plane (the 2-3 plane) will not change (1.68–1.69).

1.12.4 Transversely Isotropic Material

A transversely isotropic material has one axis of symmetry. For example, the fiber direction of a unidirectional fiber reinforced composite can be considered an axis of symmetry if the fibers are randomly distributed in the cross-section (Figure 1.12). In this case, any plane containing the fiber direction is a plane of symmetry. A transversely isotropic material is described by five constants. When the axis of symmetry is the fiber direction (1-direction), 3D Hooke's law reduces to

$$\begin{Bmatrix} \sigma_1 \\ \sigma_2 \\ \sigma_3 \\ \sigma_4 \\ \sigma_5 \\ \sigma_6 \end{Bmatrix} = \begin{bmatrix} C_{11} & C_{12} & C_{12} & 0 & 0 & 0 \\ C_{12} & C_{22} & C_{23} & 0 & 0 & 0 \\ C_{12} & C_{23} & C_{22} & 0 & 0 & 0 \\ 0 & 0 & 0 & (C_{22}-C_{23})/2 & 0 & 0 \\ 0 & 0 & 0 & 0 & C_{66} & 0 \\ 0 & 0 & 0 & 0 & 0 & C_{66} \end{bmatrix} \begin{Bmatrix} \epsilon_1 \\ \epsilon_2 \\ \epsilon_3 \\ \gamma_4 \\ \gamma_5 \\ \gamma_6 \end{Bmatrix} \tag{1.70}$$

and in terms of the compliances to

$$\begin{Bmatrix} \epsilon_1 \\ \epsilon_2 \\ \epsilon_3 \\ \gamma_4 \\ \gamma_5 \\ \gamma_6 \end{Bmatrix} = \begin{bmatrix} S_{11} & S_{12} & S_{12} & 0 & 0 & 0 \\ S_{12} & S_{22} & S_{23} & 0 & 0 & 0 \\ S_{12} & S_{23} & S_{22} & 0 & 0 & 0 \\ 0 & 0 & 0 & 2(S_{22}-S_{23}) & 0 & 0 \\ 0 & 0 & 0 & 0 & S_{66} & 0 \\ 0 & 0 & 0 & 0 & 0 & S_{66} \end{bmatrix} \begin{Bmatrix} \sigma_1 \\ \sigma_2 \\ \sigma_3 \\ \sigma_4 \\ \sigma_5 \\ \sigma_6 \end{Bmatrix} \tag{1.71}$$

Note the equations would be different if the axis of symmetry is not the 1-direction. In terms of engineering properties (Section 1.13), and taking into account

that the directions 2 and 3 are indistinguishable, the following relations apply for a transversely isotropic material:

$$\begin{aligned} E_2 &= E_3 \\ \nu_{12} &= \nu_{13} \\ G_{12} &= G_{13} \end{aligned} \tag{1.72}$$

In addition, any two perpendicular directions on the plane 2-3 can be taken as axes. In other words, the plane 2-3 is isotropic. Therefore, the following holds in the 2-3 plane

$$G_{23} = \frac{E_2}{2(1+\nu_{23})} \tag{1.73}$$

just as it holds for isotropic materials (see Problem 1.14).

1.12.5 Isotropic Material

The most common materials of industrial use are isotropic, like aluminium, steel, etc. Isotropic materials have an infinite number of planes of symmetry, meaning that the properties are independent of the orientation. Only two constants are needed to represent the elastic properties. These two properties can be the Young's modulus E and the Poisson's ratio ν, but several other pairs of constants are used whenever it is convenient. However, any pair of properties has to be related to any other pair. For example, you could describe isotropic materials by E and G, but the shear modulus of isotropic materials is related to E and ν by

$$G = \frac{E}{2(1+\nu)} \tag{1.74}$$

Also, the Lamé constants are sometimes used for convenience, in this case the two constants are

$$\begin{aligned} \lambda &= \frac{E\,\nu}{(1+\nu)(1-2\nu)} \\ \mu &= G \end{aligned} \tag{1.75}$$

To form yet another pair, any of the above properties could be substituted by the bulk modulus K, as follows

$$K = \frac{E}{3(1-2\nu)} \tag{1.76}$$

which relates the hydrostatic pressure p to the volumetric strain as

$$p = K\ (\epsilon_{1+}\epsilon_{2+}\epsilon_3) \tag{1.77}$$

For isotropic materials, the 3D Hooke's law is written in terms of only two constants C_{11} and C_{12} as

$$\begin{Bmatrix} \sigma_1 \\ \sigma_2 \\ \sigma_3 \\ \sigma_4 \\ \sigma_5 \\ \sigma_6 \end{Bmatrix} = \begin{bmatrix} C_{11} & C_{12} & C_{12} & 0 & 0 & 0 \\ C_{12} & C_{11} & C_{12} & 0 & 0 & 0 \\ C_{12} & C_{12} & C_{11} & 0 & 0 & 0 \\ 0 & 0 & 0 & \frac{(C_{11}-C_{12})}{2} & 0 & 0 \\ 0 & 0 & 0 & 0 & \frac{(C_{11}-C_{12})}{2} & 0 \\ 0 & 0 & 0 & 0 & 0 & \frac{(C_{11}-C_{12})}{2} \end{bmatrix} \begin{Bmatrix} \epsilon_1 \\ \epsilon_2 \\ \epsilon_3 \\ \gamma_4 \\ \gamma_5 \\ \gamma_6 \end{Bmatrix} \tag{1.78}$$

In terms of compliances, once again, two constants are used, S_{11} and S_{12} as follows

$$\begin{Bmatrix} \epsilon_1 \\ \epsilon_2 \\ \epsilon_3 \\ \gamma_4 \\ \gamma_5 \\ \gamma_6 \end{Bmatrix} = \begin{bmatrix} S_{11} & S_{12} & S_{12} & 0 & 0 & 0 \\ S_{12} & S_{11} & S_{12} & 0 & 0 & 0 \\ S_{12} & S_{12} & S_{11} & 0 & 0 & 0 \\ 0 & 0 & 0 & 2s & 0 & 0 \\ 0 & 0 & 0 & 0 & 2s & 0 \\ 0 & 0 & 0 & 0 & 0 & 2s \end{bmatrix} \begin{Bmatrix} \sigma_1 \\ \sigma_2 \\ \sigma_3 \\ \sigma_4 \\ \sigma_5 \\ \sigma_6 \end{Bmatrix} \tag{1.79}$$

$$s = S_{11} - S_{12}$$

Not only are the various constants related in pairs, but also certain restrictions apply on the values that these constants may have for real materials. Since the Young and shear moduli must always be positive, the Poisson's ratio must be $\nu > -1$. Furthermore, since the bulk modulus must be positive, we have $\nu < \frac{1}{2}$. Finally, the Poisson's ratio of isotropic materials is constrained by $-1 < \nu < \frac{1}{2}$.

1.13 Engineering Constants

Please note from here forward $'$ denotes the lamina coordinate system. Our next task is to write the components of the stiffness and compliance matrices in terms of engineering constants for orthotropic materials. For this purpose it is easier to work with the compliance matrix, which is defined as the inverse of the stiffness matrix. In *lamina coordinates* $[S'] = [C']^{-1}$. The compliance matrix is used to write the relationship between strains and stresses (1.69) for an orthotropic material. Let's rewrite the first of (1.69), which corresponds to the strain in the 1-direction (fiber direction)

$$\epsilon'_1 = S'_{11}\sigma'_1 + S'_{12}\sigma'_2 + S'_{13}\sigma'_3 \tag{1.80}$$

and let's perform a thought experiment. Note that $[S']$ is used to emphasize the fact that we are working in the lamina coordinate system. First, apply a tensile stress along the 1-direction (fiber direction) as in Figure 1.13, with all the other stresses equal to zero, and compute the strain produced in the 1-direction, which is

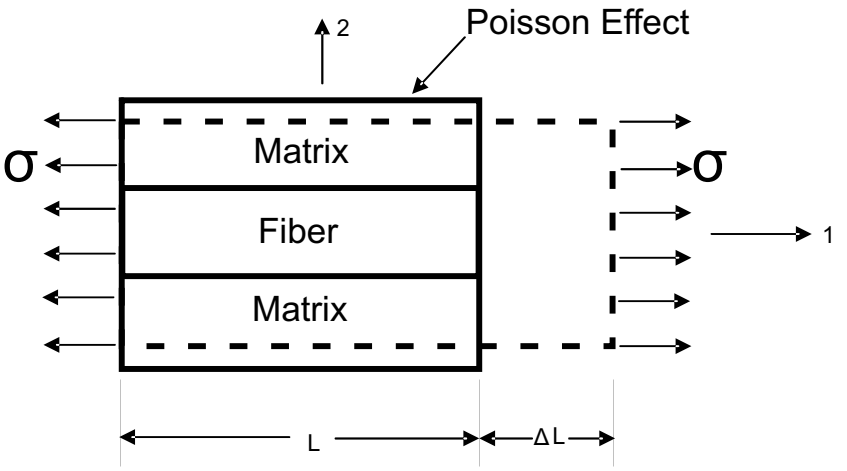

Figure 1.13: Longitudinal loading.

$$\epsilon_1' = \frac{{\sigma_1}'}{E_1} \tag{1.81}$$

Then, apply a stress in the 2-direction only, and compute the strain in the 1-direction using the appropriate Poisson's ratio [1]

$$\epsilon_1' = -\nu_{21}\frac{\sigma_2'}{E_2} \tag{1.82}$$

Now, apply a stress in the 3-direction only, and compute the strain in the 1-direction using the appropriate Poisson's ratio,

$$\epsilon_1' = -\nu_{31}\frac{\sigma_3'}{E_3} \tag{1.83}$$

The total strain ϵ_1' is the sum of equations (1.81), (1.82), and (1.83)

$$\epsilon_1' = \frac{1}{E_1}\sigma_1' - \frac{\nu_{21}}{E_2}\sigma_2' - \frac{\nu_{31}}{E_3}\sigma_3' \tag{1.84}$$

Comparing (1.84) with (1.80) we conclude that

$$S_{11}' = \frac{1}{E_1}; S_{12}' = -\frac{\nu_{21}}{E_2}; S_{13}' = -\frac{\nu_{31}}{E_3} \tag{1.85}$$

Repeat the same procedure for the equations corresponding to ϵ_2' and ϵ_3' to obtain the coefficients in the second and third rows of the compliance matrix (1.69).

For the shear terms use the 4th, 5th, and 6th rows of the compliance matrix (1.69). For example, from Figure 1.14 we write

$$\sigma_6' = \epsilon_6' G_{12} = 2\varepsilon_6' G_{12} \tag{1.86}$$

which compared to the 6th row of (1.69) leads to $S_{66} = 1/G_{12}$.

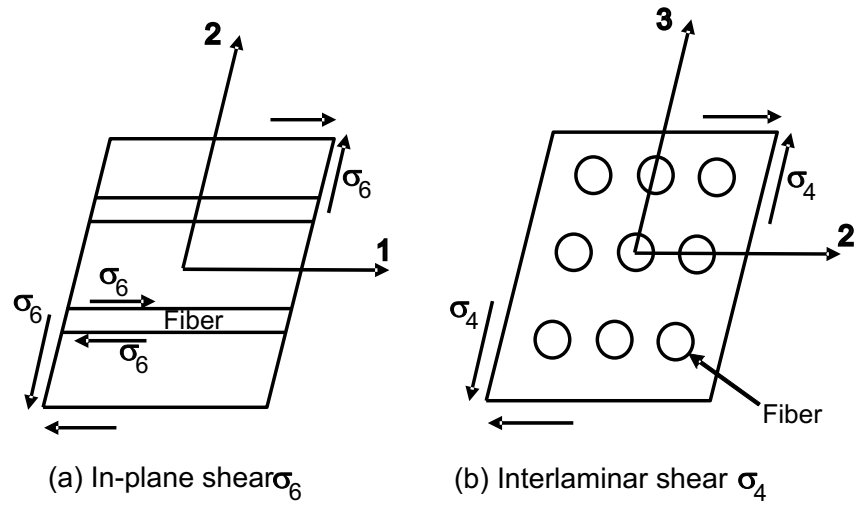

Figure 1.14: Shear loading.

For an orthotropic material, the compliance matrix $[S']$ is defined in the lamina coordinate system as

$$[S'] = \begin{bmatrix} \frac{1}{E_1} & \frac{-\nu_{21}}{E_2} & \frac{-\nu_{31}}{E_3} & 0 & 0 & 0 \\ \frac{-\nu_{12}}{E_1} & \frac{1}{E_2} & \frac{-\nu_{32}}{E_3} & 0 & 0 & 0 \\ \frac{-\nu_{13}}{E_1} & \frac{-\nu_{23}}{E_2} & \frac{1}{E_3} & 0 & 0 & 0 \\ 0 & 0 & 0 & \frac{1}{G_{23}} & 0 & 0 \\ 0 & 0 & 0 & 0 & \frac{1}{G_{13}} & 0 \\ 0 & 0 & 0 & 0 & 0 & \frac{1}{G_{12}} \end{bmatrix} \tag{1.87}$$

where E_i, G_{ij}, and ν_{ij}, are the elastic moduli, shear moduli, and Poisson's ratios, respectively. Furthermore, the subscripts indicate lamina coordinates, i.e.,

$$\nu_{ij} = \nu_{x'_i x'_j} \text{ and } E_{ii} = E_{x'_i} \tag{1.88}$$

Since $[S']$ is symmetric, the following must be satisfied

$$\frac{\nu_{ij}}{E_{ii}} = \frac{\nu_{ji}}{E_{jj}} \ , \ i, j = 1..3 \tag{1.89}$$

Furthermore, Poisson's ratios are defined so that the lateral strain is given by

$$\nu_j = -\nu_{ij}\epsilon_i \tag{1.90}$$

In ANSYS, the Poisson's ratios are defined differently that in this textbook. In fact, $\nu_{xy}, \nu_{xz}, \nu_{yz}$ are denoted PRXY, PRXZ, and PRYZ, while $\nu_{yx}, \nu_{zx}, \nu_{zy}$ are

denoted by NUXY, NUXZ, and NUYZ. On the contrary, *Abaqus* uses the standard notation also used in this textbook. That is, the symbols NU12, NU13, NU23, follow the convention described by (1.90).

After computing S_{ij}, the components of stress are obtained by using (1.46) or (1.49). This formulation predicts realistic behavior for finite displacement and rotations as long as the strains are small. This formulation is expensive to use since it needs 18 state variables: 12 components of the strain displacement matrix computed in the initial configuration ($u_{i,j}$ and $u_{r,i}u_{r,j}$) plus 6 direction cosines $[a]$ to account for finite rotations.

However, in (1.87) only nine constants are independent because the matrix $[S']$ must be symmetric (see 1.93), so

$$[S'] = \begin{bmatrix} \frac{1}{E_1} & -\frac{\nu_{12}}{E_1} & -\frac{\nu_{13}}{E_1} & 0 & 0 & 0 \\ -\frac{\nu_{12}}{E_1} & \frac{1}{E_2} & -\frac{\nu_{23}}{E_2} & 0 & 0 & 0 \\ -\frac{\nu_{13}}{E_1} & -\frac{\nu_{23}}{E_2} & \frac{1}{E_3} & 0 & 0 & 0 \\ 0 & 0 & 0 & \frac{1}{G_{23}} & 0 & 0 \\ 0 & 0 & 0 & 0 & \frac{1}{G_{13}} & 0 \\ 0 & 0 & 0 & 0 & 0 & \frac{1}{G_{12}} \end{bmatrix} \tag{1.91}$$

The stiffness matrix can be computed also in terms of engineering constants by inverting the above equation so that $[C'] = [S']^{-1}$, with components given in terms of engineering constants as

$$\begin{aligned} C'_{11} &= \frac{1-\nu_{23}\nu_{32}}{E_2E_3\Delta} \\ C'_{12} &= \frac{\nu_{21}+\nu_{31}\nu_{23}}{E_2E_3\Delta} = \frac{\nu_{12}+\nu_{32}\nu_{13}}{E_1E_3\Delta} \\ C'_{13} &= \frac{\nu_{31}+\nu_{21}\nu_{32}}{E_2E_3\Delta} = \frac{\nu_{13}+\nu_{12}\nu_{23}}{E_1E_2\Delta} \\ C'_{22} &= \frac{1-\nu_{13}\nu_{31}}{E_1E_3\Delta} \\ C'_{23} &= \frac{\nu_{32}+\nu_{12}\nu_{31}}{E_1E_3\Delta} = \frac{\nu_{23}+\nu_{21}\nu_{13}}{E_1E_2\Delta} \\ C'_{33} &= \frac{1-\nu_{12}\nu_{21}}{E_1E_2\Delta} \\ C'_{44} &= G_{23} \\ C'_{55} &= G_{13} \\ C'_{66} &= G_{12} \\ \Delta &= \frac{1-\nu_{12}\nu_{21}-\nu_{23}\nu_{32}-\nu_{31}\nu_{13}-2\nu_{21}\nu_{32}\nu_{13}}{E_1E_2E_3} \end{aligned} \tag{1.92}$$

So far both $[S']$ and $[C']$ are 6×6 matrices with 9 independent constants for the case of orthotropic materials. If the material is transversely isotropic $G_{13} = G_{12}, \nu_{13} = \nu_{12}, E_3 = E_2$.

1.13.1 Restrictions on Engineering Constants

It is important to note that because of the symmetry of the compliance matrix (1.91), the following restrictions on engineering constants apply

$$\frac{\nu_{ij}}{E_i} = \frac{\nu_{ji}}{E_j}; \quad i, j = 1..3; \quad i \neq j \tag{1.93}$$

Further restrictions on the values of the elastic constants can be derived from the fact that all diagonal terms in both the compliance and stiffness matrices must be positive. Since all the engineering elastic constants must be positive $(E_1, E_2, E_3, G_{12}, G_{23}, G_{31} > 0)$, all the diagonal terms of the stiffness matrix (1.92) will be positive if the following two conditions are met. The first condition is that $(1 - \nu_{ij}\nu_{ji}) > 0$ for $i, j = 1..3$ and $i \neq j$, which leads to the following restriction on the values of the engineering constants

$$0 < \nu_{ij} < \sqrt{\frac{E_i}{E_j}}; \; i, j = 1..3; \; i \neq j \tag{1.94}$$

The second condition is that

$$\Delta = 1 - \nu_{12}\nu_{21} - \nu_{23}\nu_{32} - \nu_{31}\nu_{13} - 2\nu_{21}\nu_{32}\nu_{13} > 0 \tag{1.95}$$

These restrictions can be used to check experimental data. For example, consider an experimental program in which if E_1 and ν_{12} are measured in a longitudinal test (fibers in the direction of loading) by using two strain gauges, one longitudinal and one transverse, and E_2 and ν_{21} are measured in the transverse tensile tests (fibers perpendicular to loading). For the test procedure to be valid, all the four data values, E_1, E_2, ν_{12} and ν_{21} must conform to (1.93–1.95) within the margin allowed by experimental errors.

Example 1.4 *Sonti et al. [6] performed a series of tests on pultruded glass-fiber reinforced composites. From tensile tests along the longitudinal axis, the average of eight tests gives* $E_1 = 19.981$ *GPa and* $\nu_{12} = 0.274$. *The average of eight tests in the transverse direction gives* $E_2 = 11.389$ *GPa and* $\nu_{21} = 0.192$. *Does this data fall within the constraints on elastic constants?*

Solution to Example 1.4 *First compute both sides of (1.93) for* $i, j = 1, 2$ *as*

$$\frac{E_1}{\nu_{12}} = \frac{19.981}{0.274} = 72.9 \; GPa$$
$$\frac{E_2}{\nu_{21}} = \frac{11.389}{0.192} = 59.3 \; GPa$$

The transverse result is 23% lower than expected. Either E_2 measured is too low or ν_{21} measured is 23% higher than what it should be. In any case a 23% difference deserves some scrutiny.

Next check (1.94)

$$abs(\nu_{12}) < \sqrt{\frac{E_1}{E_2}}$$
$$0.274 < 1.32$$
$$abs(\nu_{21}) < \sqrt{\frac{E_2}{E_1}}$$
$$0.192 < 0.75$$

Finally, there is insufficient data to evaluate the last of the restrictions on elastic constants from (1.95).

1.14 From 3D to Plane Stress Equations

Setting $\sigma_3 = 0$ in the compliance equations (1.69) of an orthotropic material implies that the third row and column of the compliance matrix are not used

$$\begin{Bmatrix} \epsilon'_1 \\ \epsilon'_2 \\ \epsilon'_3 \\ \gamma'_4 \\ \gamma'_5 \\ \gamma'_6 \end{Bmatrix} = \begin{bmatrix} S'_{11} & S'_{12} & S'_{13} & 0 & 0 & 0 \\ S'_{12} & S'_{22} & S'_{23} & 0 & 0 & 0 \\ S'_{13} & S'_{23} & S'_{33} & 0 & 0 & 0 \\ 0 & 0 & 0 & S'_{44} & 0 & 0 \\ 0 & 0 & 0 & 0 & S'_{55} & 0 \\ 0 & 0 & 0 & 0 & 0 & S'_{66} \end{bmatrix} \begin{Bmatrix} \sigma'_1 \\ \sigma'_2 \\ \sigma'_3 = 0 \\ \sigma'_4 \\ \sigma'_5 \\ \sigma'_6 \end{Bmatrix} \tag{1.96}$$

so, the first two equations plus the last one can be written separately of the remaining, in terms of a 3×3 reduced compliance matrix $[S]$ and using $\gamma = 2\epsilon$, we have

$$\begin{Bmatrix} \epsilon'_1 \\ \epsilon'_2 \\ \gamma'_6 \end{Bmatrix} = \begin{bmatrix} S'_{11} & S'_{12} & 0 \\ S'_{12} & S'_{22} & 0 \\ 0 & 0 & S'_{66} \end{bmatrix} \begin{Bmatrix} \sigma'_1 \\ \sigma'_2 \\ \sigma'_6 \end{Bmatrix} \tag{1.97}$$

The third equation is seldom used

$$\epsilon'_3 = S'_{13}\sigma'_1 + S'_{23}\sigma'_2 \tag{1.98}$$

and the remaining two equations can be written separately as

$$\begin{Bmatrix} \gamma'_4 \\ \gamma'_5 \end{Bmatrix} = \begin{bmatrix} S'_{44} & 0 \\ 0 & S'_{55} \end{bmatrix} \begin{Bmatrix} \sigma'_4 \\ \sigma'_5 \end{Bmatrix} \tag{1.99}$$

To compute stress components from strains, (1.97) can be inverted to get $\{\sigma\} = [Q]\{\epsilon\}$ or

$$\begin{Bmatrix} \sigma'_1 \\ \sigma'_2 \\ \sigma'_6 \end{Bmatrix} = \begin{bmatrix} Q'_{11} & Q'_{12} & 0 \\ Q'_{12} & Q'_{22} & 0 \\ 0 & 0 & Q'_{66} \end{bmatrix} \begin{Bmatrix} \epsilon'_1 \\ \epsilon'_2 \\ \gamma'_6 \end{Bmatrix} \tag{1.100}$$

where the matrix $[Q'] = [S'_{3\times3}]^{-1}$ is the reduced stiffness matrix for plane stress. Note that while the components of the reduced compliance matrix $[S'_{3\times3}]$ are numerically identical to the corresponding entries in the 6×6 compliance matrix, the components of the reduced stiffness matrix $[Q']$ are not numerically equal to the corresponding entries on the 6×6 stiffness matrix $[C']$, thus the change in name. This is because the inverse of a 3×3 matrix produces different values than the inverse of a 6×6 matrix. The set of equations is completed by writing

$$\left\{ \begin{array}{c} \sigma'_4 \\ \sigma'_5 \end{array} \right\} = \left[\begin{array}{cc} C'_{44} & 0 \\ 0 & C'_{55} \end{array} \right] \left\{ \begin{array}{c} \gamma'_4 \\ \gamma'_6 \end{array} \right\} \tag{1.101}$$

where the coefficient C'_{44} and C'_{55} are numerically equal to the corresponding entries in the 6×6 stiffness matrix because the 2×2 matrix in (1.101) is diagonal.

Example 1.5 *Show that the change in the thickness $t\epsilon_3$ of a plate is negligible when compared to the in-plane elongations $a\epsilon_1$ and $b\epsilon_2$. Use the data from a composite plate with thickness $t = 0.635\ mm$, and dimensions $a = 279\ mm$ and $b = 203\ mm$. Take $E_1 = 19.981\ GPa$, $E_2 = 11.389\ GPa$, $\nu_{12} = 0.274$.*

Solution to Example 1.5 *Assuming that the 0.635 mm thick glass-reinforced Polyester plate is transversely isotropic, take $E_3 = E_2 = 11.389\ GPa$, $\nu_{13} = \nu_{12} = 0.274$, $G_{31} = G_{12}$. Sonti et al. [6] report the average of eight torsion tests as $G_{12} = 3.789\ GPa$. Lacking experimental data, assume $\nu_{23} \approx \nu_m = 0.3$, $G_{23} \approx G_m = 0.385\ GPa$, with the properties of the Polyester matrix taken from [1]. The remaining properties in (1.91) can be obtained, using (1.93), as*

$$\begin{aligned} \nu_{21} &= \nu_{12}\frac{E_2}{E_1} = 0.274\left(\frac{11.389}{19.981}\right) = 0.156 \\ \nu_{31} &= \nu_{13}\frac{E_3}{E_1} = 0.274\left(\frac{11.389}{19.981}\right) = 0.156 \\ \nu_{32} &= \nu_{23}\frac{E_3}{E_2} = 0.3\left(\frac{11.389}{11.389}\right) = 0.3 \end{aligned}$$

Because transverse isotropy $G_{13} = G_{12} = 3.789\ GPa$. Now, assume a state of stress $\sigma'_1 = \sigma'_2 = 0.1\ GPa, \sigma'_4 = \sigma'_5 = \sigma'_6 = 0$ and $\sigma'_3 = 0$ because of the assumption of plane stress. Using (1.97) we get

$$\begin{aligned} \epsilon'_1 &= S'_{11}\sigma'_1 + S'_{12}\sigma'_2 = \frac{0.1}{19.981} - \frac{0.1(0.156)}{11.389} = 3.635\ 10^{-3} \\ \epsilon'_2 &= S'_{12}\sigma'_1 + S'_{22}\sigma'_2 = -\frac{0.1(0.156)}{11.389} + \frac{0.1}{11.389} = 7.411\ 10^{-3} \\ \epsilon'_3 &= S'_{13}\sigma'_1 + S'_{23}\sigma'_2 = -\frac{0.274(0.1)}{19.981} - \frac{0.3(0.1)}{11.389} = -4.005\ 10^{-3} \end{aligned}$$

Finally

$$\begin{aligned} t\epsilon'_3 &= -0.635(4.005\ 10^{-3}) = -2.543\ 10^{-3}\ mm \\ a\epsilon'_1 &= 279(3.635\ 10^{-3}) = 1.014\ mm \\ b\epsilon'_2 &= 203(7.411\ 10^{-3}) = 1.504\ mm \end{aligned}$$

Since the elongation in the transverse direction is so small, it is neglected in the derivation of the plate equations in [1, Section 6.1].

1.15 Apparent Laminate Properties

The stiffness matrix $[C]$ of a balanced, symmetric laminate with N laminas is built by adding the lamina matrices in laminate coordinate system multiplied by the thickness ratio t_k/t of each lamina, where t is the laminate thickness and t_k denotes the thickness of the k-th lamina

$$[C] = \sum_{k=1}^{N} \frac{t_k}{t}[C_k] \tag{1.102}$$

Note that compliances cannot be added nor averaged. The laminate compliance is obtained inverting the 6×6 stiffness matrix, as

$$[S] = [C]^{-1} \tag{1.103}$$

A laminate is called balanced if the total thickness of laminas oriented with respect to the laminate direction at $+\theta$ and $-\theta$ are the same. Such a laminate has orthotropic stiffness $[C]$ and compliance $[S]$. In terms of the apparent engineering properties of the laminate, the compliance is

$$[S] = \begin{bmatrix} \frac{1}{E_x} & -\frac{\nu_{yx}}{E_y} & -\frac{\nu_{zx}}{E_z} & 0 & 0 & 0 \\ -\frac{\nu_{xy}}{E_x} & \frac{1}{E_y} & -\frac{\nu_{zy}}{E_z} & 0 & 0 & 0 \\ -\frac{\nu_{xz}}{E_x} & -\frac{\nu_{yz}}{E_y} & \frac{1}{E_z} & 0 & 0 & 0 \\ 0 & 0 & 0 & \frac{1}{G_{yz}} & 0 & 0 \\ 0 & 0 & 0 & 0 & \frac{1}{G_{xz}} & 0 \\ 0 & 0 & 0 & 0 & 0 & \frac{1}{G_{xy}} \end{bmatrix} \tag{1.104}$$

Since the compliance must be symmetric, it must satisfy (1.93) with $i, j = x, y, z$. Therefore, it is possible to compute the apparent engineering properties of a laminate in terms of the laminate compliance, as follows

$$\begin{aligned} E_x &= 1/S_{11} & \nu_{xy} &= -S_{21}/S_{11} \\ E_y &= 1/S_{22} & \nu_{xz} &= -S_{31}/S_{11} \\ E_z &= 1/S_{33} & \nu_{yz} &= -S_{32}/S_{22} \\ G_{yz} &= 1/S_{44} \\ G_{xz} &= 1/S_{55} \\ G_{xy} &= 1/S_{66} \end{aligned} \tag{1.105}$$

Example 1.6 *Compute the laminate properties of* $[0/90/\pm 30]_S$ *with* $t_k = 1.5$ *mm,* $E_f = 241$ *GPa,* $\nu_f = 0.2$*,* $E_m = 3.12$ *GPa,* $\nu_m = 0.38$*, fiber volume fraction* $V_f = 0.6$*, where f,m, denote fiber and matrix, respectively.*

Solution to Example 1.6 *First use periodic microstructure micromechanics (6.8) to obtain the lamina properties (in MPa).*

$$\begin{array}{lll} E_1 = 145,880 & G_{12} = 4,386 & \nu_{12} = \nu_{13} = 0.263 \\ E_2 = 11,590 & G_{23} = 3,767 & \nu_{23} = 0.538 \end{array}$$

Then, compute the compliance matrix $[S']$ *using (1.91), the rotation matrix* $[T]$ *using (1.34), the compliance* $[S]$ *in laminate coordinate system using (1.53), and the stiffness* $[C] = [S]^{-1}$ *in the laminate coordinate system for each lamina. Then, average them using (1.102), invert the average, and finally using (1.105) get*

$$\begin{array}{lll} E_x = 75,924 & G_{xy} = 38,048 & \nu_{xy} = 0.370 \\ E_y = 44,913 & G_{yz} = 3,999 & \nu_{yz} = 0.394 \\ E_z = 15,119 & G_{xz} = 4,154 & \nu_{xz} = 0.276 \end{array}$$

This example can be solved with the following MATLAB code:

```
function Ex106
    % Example 1.6 laminate stiffness as per section 1.15
    clc
    % Lamina properties calculated with PMM in cadec-online
    % Cprime (1.92) calculated with
    % http://www.cadec-online.com/Chapters/Chapter5/3DConstitutiveEquations
    % /StiffnessMatrix.aspx
    Cprime = [
    149395.9113 6754.740801 6754.740801 0 0 0;
    6754.740801 16627.00749 9093.208855 0 0 0;
    6754.740801 9093.208855 16627.00749 0 0 0;
    0 0 0 3766.899318 0 0;
    0 0 0 0 4385.907534 0;
    0 0 0 0 0 4385.907534;
    ]

    theta = [0,90,30,-30];
    thickness = [1,1,1,1]*1.5;  % mm
    laminateThickness = sum(thickness);
    C = zeros(6);
    for i=1:length(theta)
        [T,Tbar] = RotationMatrix3D(theta(i));
        C = C + Tbar*Cprime*Tbar*thickness(i)/laminateThickness; % (1.102)
    end
    S = C^-1;       % (1.103)
    display(S);
    Ex  =1/S(1,1)   % (1.105)
    Ey  =1/S(2,2)
    Ez  =1/S(3,3)
    Gxy =1/S(6,6)
    Gyz =1/S(4,4)
    Gxz =1/S(5,5)
    PRxy=-S(2,1)/S(1,1)
    PRyz=-S(3,2)/S(2,2)
    PRxz=-S(3,1)/S(1,1)
end
```

which uses the following code for coordinate transformation in 3D:

```
function [T,Tbar] = RotationMatrix3D(t);
    R = eye(6,6); R(4,4)=2; R(5,5)=2; R(6,6)=2; % Reuter matrix
    a = [cosd(t), sind(t), 0;sind(t), cosd(t), 0; 0, 0, 1];
    T(1:6,1:6) = 0;
    for i=1:1:3
    for j=1:1:3
    if i==j; alpha = j; else alpha = 9-i-j; end
    for p=1:1:3
    for q=1:1:3
    if p==q beta = p; else beta = 9-p-q; end
    T(alpha,beta) = 0;
    if alpha<=3 & beta<= 3; T(alpha,beta)=a(i,p)*a(i,p); end
    if alpha> 3 & beta<= 3; T(alpha,beta)=a(i,p)*a(j,p); end
    if alpha<=3 & beta>3; T(alpha,beta)=a(i,q)*a(i,p)+a(i,p)*a(i,q);end
    if alpha>3 & beta>3; T(alpha,beta)=a(i,p)*a(j,q)+a(i,q)*a(j,p);end
    end
    end
    end
    end
    Tbar = R*T*R^(-1);
end
```

Suggested Problems

Problem 1.1 *Using the principle of virtual work (PVW), find a quadratic displacement function $u(x)$ in $0 < x < L$ of a tapered slender rod of length L, fixed at the origin and loaded axially in tension at the free end. The cross-section area changes linearly and the areas are $A_1 > A_2$ at the fixed and free ends, respectively. The material is homogeneous and isotropic with modulus E.*

Problem 1.2 *Using the principle of virtual work (PVW), find a quadratic rotation angle function $\theta(x)$ in $0 < x < L$ of a tapered slender shaft of circular cross-section and length L, fixed at the origin and loaded by a torque T at the free end. The cross-section area changes linearly and the areas are $A_1 > A_2$ at the fixed and free ends, respectively. The material is homogeneous and isotropic with shear modulus G.*

Problem 1.3 *Construct a rotation matrix $[a]$ resulting from three consecutive reflections about (a) the x-y plane, (b) the x-z plane, (c) the y-z plane. The resulting system does not follow the right-hand rule.*

Problem 1.4 *Construct three rotation matrices $[a]$ for rotations $\theta = \pi$ about (a) the x-axis, (b) the y-axis, (c) the z-axis.*

Problem 1.5 *Using*

$$\sigma = \begin{bmatrix} 10 & 2 & 1 \\ 2 & 5 & 1 \\ 1 & 1 & 3 \end{bmatrix}$$

and $[a]$ of Example 1.2, verify that (1.29) yields the same result as (1.26).

Problem 1.6 *Write a computer program to evaluate the compliance and stiffness matrices in terms of engineering properties. Take the input from a file and the output to another file. Validate the program with your own examples. You may use material properties from [1, Tables 1.3–1.4] and assume the material is transversely isotropic as per Section 1.12.4. Show all work in a report.*

Problem 1.7 *Write a computer program to transform the stiffness and compliance matrix from lamina coordinates C', S', to another coordinate system C, S, by a rotation $-\theta$ around the z-axis (Figure 1.7). The data C', S', θ, should be read from a file. The output C, S should be written to another file. Validate your program with your own examples. You may use material properties from [1, Tables 1.3–1.4] and assume the material is transversely isotropic as per Section 1.12.4. Show all work in a report.*

Problem 1.8 *Verify numerically (1.92) against $[S]^{-1}$ for the material of your choice. You may use material properties from [1, Tables 1.3–1.4] and assume the material is transversely isotropic as per Section 1.12.4.*

Problem 1.9 *The following data has been obtained experimentally for a composite based on a unidirectional carbon-epoxy prepreg (MR50 carbon fiber at 63% by volume in LTM25 Epoxy). Determine if the restrictions on elastic constants are satisfied.*

$$
\begin{aligned}
E_1 &= 156.403\ GPa, & E_2 &= 7.786\ GPa \\
\nu_{12} &= 0.352, & \nu_{21} &= 0.016 \\
G_{12} &= 3.762\ GPa & & \\
\sigma^u_{1t} &= 1.826\ GPa, & \sigma^u_{1c} &= 1.134\ GPa \\
\sigma^u_{2t} &= 19\ MPa, & \sigma^u_{2c} &= 131\ MPa \\
\sigma^u_{6} &= 75\ MPa & & \\
\epsilon^u_{1t} &= 11,900\ 10^{-6}, & \epsilon^u_{1c} &= 8,180\ 10^{-6} \\
\epsilon^u_{2t} &= 2,480\ 10^{-6}, & \epsilon^u_{2c} &= 22,100\ 10^{-6} \\
\gamma^u_{12} &= 20,000\ 10^{-6} & &
\end{aligned}
$$

Problem 1.10 *Explain contracted notation for stresses and strains.*

Problem 1.11 *What is an orthotropic material and how many constants are needed to describe it?*

Problem 1.12 *What is a transversely isotropic material and how many constants are needed to describe it?*

Problem 1.13 *Use the three rotations matrices in Problem 1.4 to verify (1.48) numerically.*

Problem 1.14 *Prove (1.73) using (1.71) and (1.91).*

Problem 1.15 *Demonstrate that a material having two perpendicular planes of symmetry also has a third. Apply a reflection about the 2-3 plane to (1.68) using the procedure in Section 1.12.3.*

Problem 1.16 *What is a plane stress assumption?*

Problem 1.17 *Write a computer program to evaluate the laminate engineering properties for symmetric balanced laminates. All laminas are of the same material. Input data consists of all the engineering constants for a transversely isotropic material, number of laminas N, thickness and angle for all the laminas t_k, θ_k with $k = 1...N$. Use Sections 1.15, 1.12.4, and 1.13.*

Chapter 2

Introduction to Finite Element Analysis

In this textbook, the finite element method (FEM) is used as a tool to solve practical problems. For the most part, commercial packages, mainly ANSYS®, are used in the examples. Computer programming is limited to implementing material models and post-processing algorithms. When commercial codes lack needed features, other codes are used, which are provided in [5]. A basic understanding of the finite element method is necessary for effective use of any finite element software. Therefore, this chapter contains a brief introduction intended for those readers who have not had a formal course or prior knowledge about the finite element method. Furthermore, an introduction to ANSYS *Mechanical APDL* is presented to familiarize the reader with the typical procedures used for finite element modeling using commercial software.

2.1 Basic FEM Procedure

Consider the axial deformation of a rod. The ordinary differential equation (ODE) describing the deformation of the rod is

$$-\frac{d}{dx}\left(EA\frac{du}{dx}\right) - f = 0 \quad ; \quad 0 \le x \le L \tag{2.1}$$

where E, A are the modulus and cross-section area of the rod, respectively, and f is the distributed force. The boundary conditions for the case illustrated in Figure 2.1 are

$$\begin{aligned} u(0) &= 0 \\ \left[\left(EA\frac{du}{dx}\right)\right]_{x=L} &= P \end{aligned} \tag{2.2}$$

As it is customary in mechanics of materials textbooks, the real rod shown in Figure 2.1(a) is mathematically modeled as a line in Figure 2.1(b). The rod occupies the domain $[0, L]$ along the real axis x.

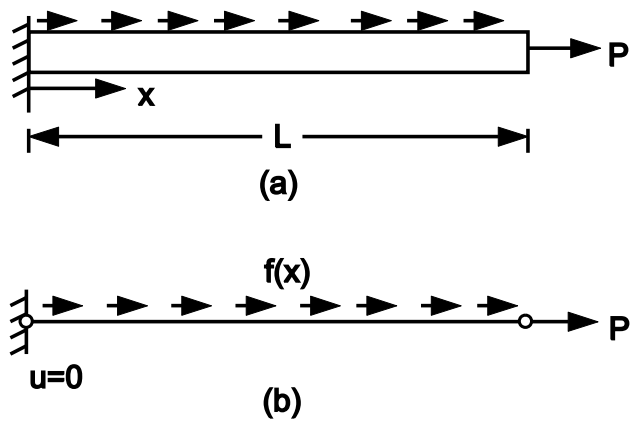

Figure 2.1: Physical and mathematical (idealization) model.

2.1.1 Discretization

The next step is to divide the domain into discrete elements, as shown in Figure 2.2.

2.1.2 Element Equations

To derive the element equations, an integral form of the ordinary differential equation (ODE) is used, which is obtained by integrating the product of the ODE times a weight function v as follows

$$0 = \int_{x_A}^{x_B} v \left[-\frac{d}{dx}\left(EA\frac{du}{dx} \right) - f \right] dx \tag{2.3}$$

This is called a weak form because the solution $u(x)$ does not have to satisfy the ODE (2.1) for all and every one of the infinite values of x in $[0, L]$, in a strong sense. Instead, the solution $u(x)$ only has to satisfy the ODE in (2.3) in a weighted average sense. It is therefore easier to find a weak solution than a strong one. Although for the case of the rod, the strong (exact) solution is known, most problems of composite mechanics do not have an exact solution. The governing equation is obtained by integrating (2.3) by parts as follows

$$0 = \int_{x_A}^{x_B} EA\frac{dv}{dx}\frac{du}{dx}dx - \int_{x_A}^{x_B} vf dx - \left[v\left(EA\frac{du}{dx} \right) \right]_{x_A}^{x_B} \tag{2.4}$$

where $v(x)$ is a weight function, which is usually set equal to the primary variable $u(x)$. From the boundary term, it is concluded that

- specifying $v(x)$ at x_A *or* x_B is an essential boundary condition
- specifying $\left(EA\frac{du}{dx}\right)$ at either end is the natural boundary condition

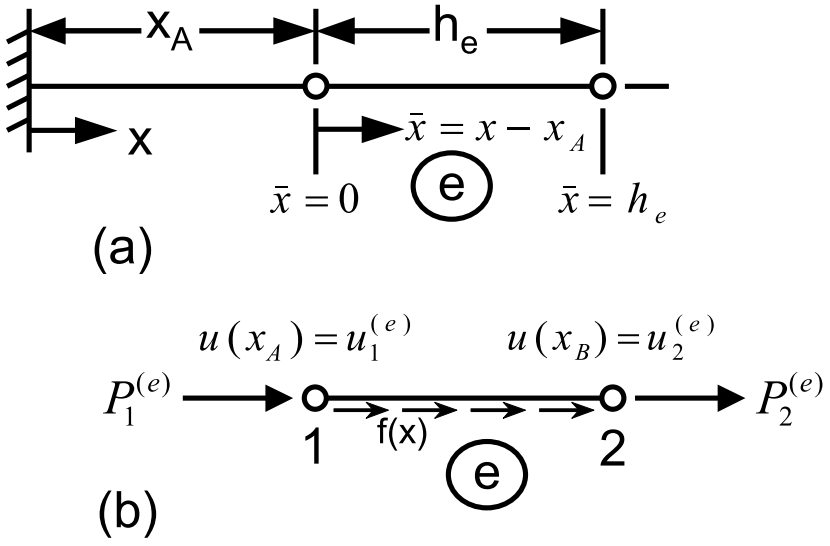

Figure 2.2: Discretization into elements.

While $u(x)$ is the *primary variable*, $\left(EA\frac{du}{dx}\right) = EA\epsilon_x = A\sigma_x$ is the *secondary variable*. Let

$$\begin{aligned} u(x_A) &= u_1^e \\ u(x_B) &= u_2^e \\ -\left[\left(EA\frac{du}{dx}\right)\right]_{x_A} &= P_1^e \\ \left[\left(EA\frac{du}{dx}\right)\right]_{x_B} &= P_2^e \end{aligned} \tag{2.5}$$

Then, the governing equation becomes

$$0 = \int_{x_A}^{x_B} \left(EA\frac{dv}{dx}\frac{du}{dx} - vf\right) dx - P_1^e v(x_A) - P_2^e v(x_B) = B(v,u) - l(v) \tag{2.6}$$

with

$$\begin{aligned} B(u,v) &= \int_{x_A}^{x_B} EA\frac{dv}{dx}\frac{du}{dx}dx \\ l(v) &= \int_{x_A}^{x_B} vf dx + P_1^e v(x_A) + P_2^e v(x_B) \end{aligned} \tag{2.7}$$

2.1.3 Approximation over an Element

Now, the unknown $u(x)$ is approximated as a linear combination (series expansion) of known functions $N_i^e(x)$ and unknown coefficients a_j^e, as

$$u_e(x) = \sum_{j=1}^{n} a_j^e N_j^e(x)$$

where a_j^e are the coefficients to be found and $N_j^e(x)$ are the interpolation functions. For the weight function $v(x)$, the Ritz method can be used [4], in which $v(x) = N_j^e(x)$. Substituting in the governing equation (2.6) we get

$$\sum_{j=1}^{n} \left(\int_{x_A}^{x_B} EA \frac{dN_i^e}{dx} \frac{dN_j^e}{dx} dx \right) a_j^e = \int_{x_A}^{x_B} N_i^e f dx + P_1^e N_i^e(x_A) + P_2^e N_i^e(x_B) \tag{2.8}$$

which can be written as

$$\sum_{j=1}^{n} K_{ij}^e a_j^e = F_i^e \tag{2.9}$$

or in matrix form

$$[K^e]\{a^e\} = \{F^e\} \tag{2.10}$$

where $[K^e]$ is the element stiffness matrix, $\{F^e\}$ is the element vector equivalent force, and $\{a^e\}$ are the element unknown parameters.

2.1.4 Interpolation Functions

Although any complete set of linearly independent functions could be used as interpolation functions, it is convenient to choose the function in such a way that the unknown coefficients represent the nodal displacements, that is $a_i = u_i$. For a two-node element spanning the interval $x_e \leq x \leq x_{e+1}$, the following linear interpolation functions (Figure 2.3) can be used

$$\begin{aligned} N_1^e &= \frac{x_{e+1} - x}{h_e} \\ N_2^e &= \frac{x - x_e}{h_e} \end{aligned} \tag{2.11}$$

where $h_e = x_{e+1} - x_e$ is the element length. These interpolation functions satisfy the following conditions

$$N_i^e(x_j) = \begin{Bmatrix} 0 & if & i \neq j \\ 1 & if & i = j \end{Bmatrix} \tag{2.12}$$

$$\sum_{i=1}^{2} N_i^e(x) = 1 \tag{2.13}$$

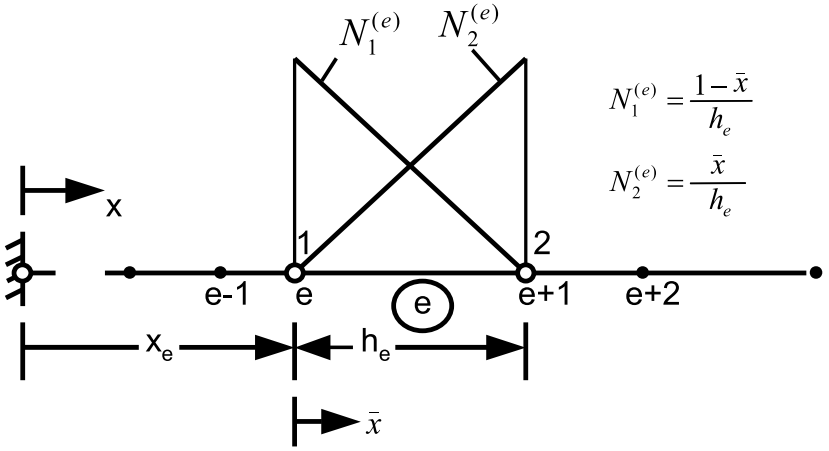

Figure 2.3: Linear interpolation functions for a two-node element rod.

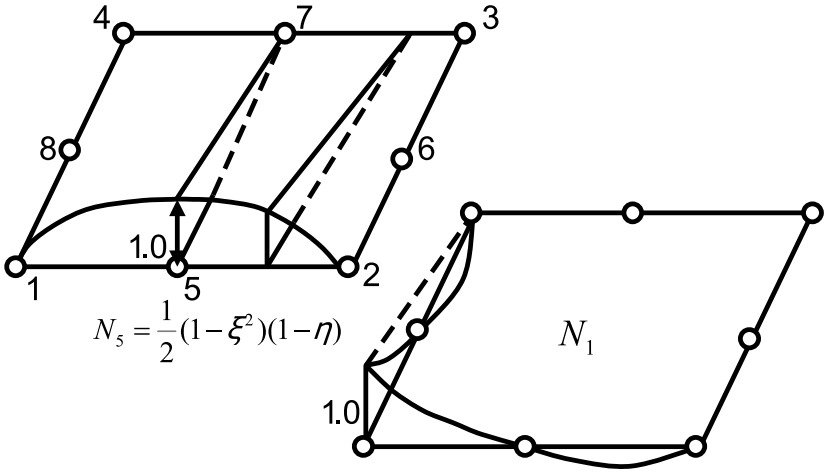

Figure 2.4: Two-dimensional interpolation functions.

which guarantees that the unknown coefficients represent the nodal displacements, i.e., $a_i = u_i$.

Many other interpolation functions can be used, each one with some advantages and disadvantages. The interpolation functions are intimately related to the number of nodes of the element. Figure 2.4 illustrates the shape of the interpolation functions N_1 and N_5 (corresponding to nodes 1 and 5) in an eight-node shell element.

Broadly speaking, more nodes per element imply more accuracy and less need for a fine mesh, but also imply higher cost in terms of computer time. Figure 2.5 illustrates how the approximate solution converges to the exact one as the number of elements increases from 2 to 4 or as the number of nodes in the element increases from 2 for the linear element to 3 for the quadratic element.

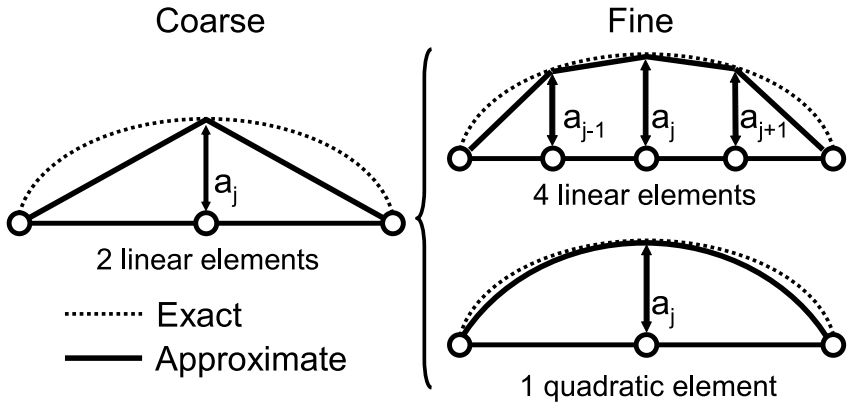

Figure 2.5: Discretization error.

2.1.5 Element Equations for a Specific Problem

With interpolation functions that satisfy the conditions in (2.12–2.13), it is possible to rewrite (2.10) as

$$[K^e]\{u^e\} = \{F^e\} \tag{2.14}$$

where $\{u^e\}$ are the nodal displacements, $[K^e]$ is the element stiffness matrix given by

$$[K^e] = \begin{bmatrix} \int_{x_A}^{x_B} EA\frac{dN_1^e}{dx}\frac{dN_1^e}{dx}dx & \int_{x_A}^{x_B} EA\frac{dN_1^e}{dx}\frac{dN_2^e}{dx}dx \\ \int_{x_A}^{x_B} EA\frac{dN_2^e}{dx}\frac{dN_1^e}{dx}dx & \int_{x_A}^{x_B} EA\frac{dN_2^e}{dx}\frac{dN_2^e}{dx}dx \end{bmatrix} \tag{2.15}$$

and $\{F^e\}$ is the element force vector

$$\{F_i^e\} = \begin{Bmatrix} \int_{x_A}^{x_B} N_1^e f dx + P_1^e \\ \int_{x_A}^{x_B} N_2^e f dx + P_2^e \end{Bmatrix} \tag{2.16}$$

For a two-node rod element number e, the constant cross-section area A_e, the element length h_e, and the modulus E are fixed. These values define the tensile-compression element stiffness as

$$k^e = \frac{EA_e}{h_e} \tag{2.17}$$

The external loads on the element are the distributed force f_e, the force at end number 1, P_1^e, and the force at end number 2, P_2^e. Using these values, the linear interpolation functions (2.11), as well as (2.15) and (2.16), the element matrix stiffness and the equivalent nodal forces become

$$[K^e] = \begin{bmatrix} k^e & -k^e \\ -k^e & k^e \end{bmatrix} = \frac{EA_e}{h_e}\begin{bmatrix} 1 & -1 \\ -1 & 1 \end{bmatrix} \tag{2.18}$$

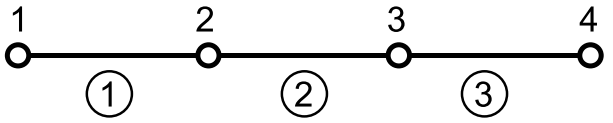

Figure 2.6: Connectivity between three two-node elements.

$$\{F^e\} = \frac{f_e h_e}{2} \left\{ \begin{array}{c} 1 \\ 1 \end{array} \right\} + \left\{ \begin{array}{c} P_1^e \\ P_2^e \end{array} \right\} \tag{2.19}$$

2.1.6 Assembly of Element Equations

The element unknown parameters correspond to displacements at the element nodes. Since a node must have the same displacement on both adjacent elements, the value is unique. For example, using the connectivity of elements shown in Figure 2.6, unique labels are assigned to the displacements, using capital letters. While a superscript denotes an element number, a subscript indicates a nodal number, as follows

$$\begin{aligned} u_1^1 &= U_1 \\ u_2^1 &= U_2 = u_1^2 \\ u_1^2 &= U_3 = u_1^3 \\ u_2^3 &= U_4 \end{aligned} \tag{2.20}$$

Now, the element equations can be assembled into the global system. First, the contribution of element #1 is

$$\left[\begin{array}{cccc} k^1 & -k^1 & 0 & 0 \\ -k^1 & k^1 & 0 & 0 \\ 0 & 0 & 0 & 0 \\ 0 & 0 & 0 & 0 \end{array} \right] \left\{ \begin{array}{c} U_1 \\ U_2 \\ U_3 \\ U_4 \end{array} \right\} = \left\{ \begin{array}{c} f_1 h_1/2 \\ f_1 h_1/2 \\ 0 \\ 0 \end{array} \right\} + \left\{ \begin{array}{c} P_1^1 \\ P_2^1 \\ 0 \\ 0 \end{array} \right\} \tag{2.21}$$

Add the contribution of element #2, as follows

$$\left[\begin{array}{cccc} k^1 & -k^1 & 0 & 0 \\ -k^1 & k^1 + k^2 & -k^2 & 0 \\ 0 & -k^2 & k^2 & 0 \\ 0 & 0 & 0 & 0 \end{array} \right] \left\{ \begin{array}{c} U_1 \\ U_2 \\ U_3 \\ U_4 \end{array} \right\} = \left\{ \begin{array}{c} f_1 h_1/2 \\ f_1 h_1/2 + f_2 h_2/2 \\ f_2 h_2/2 \\ 0 \end{array} \right\} + \left\{ \begin{array}{c} P_1^1 \\ P_2^1 + P_1^2 \\ P_2^2 \\ 0 \end{array} \right\} \tag{2.22}$$

Finally, add element #3 to obtain the fully assembled system, as follows

$$\begin{bmatrix} k^1 & -k^1 & 0 & 0 \\ -k^1 & k^1+k^2 & -k^2 & 0 \\ 0 & -k^2 & k^2+k^3 & -k^3 \\ 0 & 0 & -k^3 & k^3 \end{bmatrix} \begin{Bmatrix} U_1 \\ U_2 \\ U_3 \\ U_4 \end{Bmatrix} = \begin{Bmatrix} f_1 h_1/2 \\ f_1 h_1/2 + f_2 h_2/2 \\ f_2 h_2/2 + f_3 h_3/2 \\ f_3 h_3/2 \end{Bmatrix} + \begin{Bmatrix} P_1^1 \\ P_2^1 + P_1^2 \\ P_2^2 + P_1^3 \\ P_2^3 \end{Bmatrix} \tag{2.23}$$

2.1.7 Boundary Conditions

By equilibrium (see Figure 2.2), the internal loads cancel whenever two elements share a node, or

$$\begin{aligned} P_2^1 + P_1^2 &= 0 \\ P_2^2 + P_1^3 &= 0 \end{aligned} \tag{2.24}$$

The remaining P_1^1 and P_3^2 are the forces at the end of the rod. If either end of the rod is fixed, then the displacement must be set to zero at that end. Say the end at $x = 0$ is fixed, then $U_1 = 0$. If the end at $x = L$ is free, then P_3^2 must be specified, since $U_4 \neq 0$. If it is not specified, then it is assumed that the force is zero.

2.1.8 Solution of the Equations

Since $U_1 = 0$, eliminating the first row and column of the stiffness matrix, a 3×3 system of algebraic equations is obtained, and solved for 3 unknowns: U_2, U_3, U_4. Once a solution for U_2 is found, the reaction P_1^1 is computed from the first equation of (2.23), as follows

$$-k^1 U_2 = \frac{f_1 h_1}{2} + P_1^1 \tag{2.25}$$

2.1.9 Solution Inside the Elements

Now, the solution U_i at 4 points along the rod is available. Next, the solution at any location x can be computed by interpolating with the interpolation functions, as follows

$$U^e(x) = \sum_{j=1}^{2} U_j^e N_j^e(x) \tag{2.26}$$

or

$$u(x) = \begin{cases} U_1 N_1^1(x) + U_2 N_2^1(x) & if \quad 0 \leq x \leq h_1 \\ U_2 N_1^2(x) + U_3 N_2^2(x) & if \quad h_1 \leq x \leq h_1 + h_2 \\ U_3 N_1^3(x) + U_4 N_2^3(x) & if \quad h_1 + h_2 \leq x \leq h_1 + h_2 + h_3 \end{cases} \tag{2.27}$$

2.1.10 Derived Results

Strains

Strains are computed using (1.5) directly from the known displacements inside the element. For example,

$$\epsilon_x = \frac{du}{dx} = \sum_{j=1}^{2} U_j^e \frac{dN_j^e}{dx} \tag{2.28}$$

Note that if $N_j^e(x)$ are linear functions, the strains are constant over the element. In general the quality of the strains is one order of magnitude poorer than the primary variable (displacements).

Stresses

Stress values are usually computed from strains through the constitutive equations. In this example, with one-dimensional stress-strain behavior

$$\sigma_x = E\ \epsilon_x \tag{2.29}$$

Note that the quality of stresses is the same as that of the strains.

2.2 General Finite Element Procedure

The derivation of the element equations, assembly, and solution for any type of elements is similar to that of the one-dimensional rod element described in Section 2.1, with the exception that the principle of virtual work (PVW, 1.16) is used instead of the governing equation (2.1). The PVW provides a weak form similar to that in (2.4). Expanding (1.16) for a full 3D state of deformation, the internal virtual work is

$$\begin{aligned} \delta W_I &= \int \left(\sigma_{xx}\delta\epsilon_{xx} + \sigma_{yy}\delta\epsilon_{yy} + \sigma_{zz}\delta\epsilon_{zz} + \sigma_{yz}\delta\gamma_{yz} + \sigma_{xz}\delta\gamma_{xz} + \sigma_{xy}\delta\gamma_{xy}\right) dV \\ &= \int_V \underline{\sigma}^T \underline{\delta\epsilon}\ dV \end{aligned} \tag{2.30}$$

where

$$\begin{aligned} \underline{\sigma}^T &= [\sigma_{xx}, \sigma_{yy}, \sigma_{zz}, \sigma_{yz}, \sigma_{xz}, \sigma_{xy}] \\ \underline{\delta\epsilon}^T &= [\delta\epsilon_{xx}, \delta\epsilon_{yy}, \delta\epsilon_{zz}, \delta\gamma_{yz}, \delta\gamma_{xz}, \delta\gamma_{xy}] \end{aligned} \tag{2.31}$$

Next, the external work is

$$\delta W_E = \int_V \underline{f}^T \underline{\delta u}\ dV + \int_S \underline{t}^T \underline{\delta u}\ dS \tag{2.32}$$

where the volume forces per unit volume and surface forces per unit area are

$$\begin{aligned} \underline{f}^T &= [f_x, f_y, f_z] \\ \underline{t}^T &= [t_x, t_y, t_z] \end{aligned} \tag{2.33}$$

Here, underline (_) denotes a one-dimensional array, not necessarily a vector. For example, $\underline{u}$ is a vector but $\underline{\sigma}$ are the six components of stress arranged in a six-element array. The virtual strains are strains that would be produced by virtual displacements $\underline{\delta u}$ ($\underline{x}$). Therefore, virtual strains are computed from virtual displacements using the strain-displacement equations (1.5). In matrix notation

$$\begin{aligned} \underline{\epsilon} &= \underline{\underline{\partial}}\, \underline{u} \\ \underline{\delta\epsilon} &= \underline{\underline{\partial}}\, \underline{\delta u} \end{aligned} \tag{2.34}$$

where

$$\underline{\underline{\partial}} = \begin{bmatrix} \dfrac{\partial}{\partial x} & 0 & 0 & \dfrac{\partial}{\partial y} & 0 & \dfrac{\partial}{\partial z} \\ 0 & \dfrac{\partial}{\partial y} & 0 & \dfrac{\partial}{\partial x} & \dfrac{\partial}{\partial z} & 0 \\ 0 & 0 & \dfrac{\partial}{\partial z} & 0 & \dfrac{\partial}{\partial y} & \dfrac{\partial}{\partial x} \end{bmatrix} \tag{2.35}$$

Then, the PVW is written in matrix notation as

$$\int_V \underline{\sigma}^T \underline{\underline{\partial}}\, \underline{\delta u}\, dV = \int_V \underline{f}^T \underline{\delta u}\, dV + \int_S \underline{t}^T \underline{\delta u}\, dS \tag{2.36}$$

The integrals over the volume V and surface S of the body can be broken element by element over m elements, as

$$\sum_{e=1}^{m} \left[\int_{V_e} \underline{\sigma}^T \underline{\underline{\partial}}\, \underline{\delta u}\, dV \right] = \sum_{e=1}^{m} \left[\int_{V_e} \underline{f}^T \underline{\delta u}\, dV + \int_{S_e} \underline{t}^T \underline{\delta u}\, dS \right] \tag{2.37}$$

Whenever two elements share a surface, the contributions of the second integral cancel out, just as the internal loads canceled in Section 2.1.7. The stress components are given by the constitutive equations. For a linear material

$$\underline{\sigma} = \underline{\underline{C}}\, \underline{\epsilon} \tag{2.38}$$

with $\underline{\underline{C}}$ given by (1.68). The internal virtual work over each element becomes

$$\delta W_I^e = \int_{V_e} \underline{\sigma}^T \underline{\delta\epsilon}\, dV = \int_{V_e} \underline{\epsilon}^T \underline{\underline{C}}\, \underline{\delta\epsilon}\, dV \tag{2.39}$$

The expansion of the displacements can be written in matrix form as

$$\underline{u} = \underline{N}\, \underline{a} \tag{2.40}$$

where $\underline{N}$ contains the element interpolation functions and $\underline{a}$ the nodal displacements of the element, just as in Section 2.1.4. Therefore, the strains are

$$\underline{\epsilon} = \underline{\underline{\partial}}\, \underline{u} = \underline{\underline{\partial}}\, \underline{N}\, \underline{a} = \underline{\underline{B}}\, \underline{a} \tag{2.41}$$

where $\underline{\underline{B}} = \underline{\underline{\partial}}\, \underline{N}$ is the strain-displacement matrix. Now, the discretized form of the internal virtual work over an element can be computed as

$$\delta W_I^e = \int_{V_e} \underline{a}^T \underline{\underline{B}}^T \underline{\underline{C}}\, \underline{\underline{B}}\, \underline{\delta a}\, dV = \underline{a}^T \int_{V_e} \underline{\underline{B}}^T \underline{\underline{C}}\, \underline{\underline{B}}\, dV\, \underline{\delta a} = \underline{a}^T \underline{\underline{K^e}}\, \underline{\delta a} \tag{2.42}$$

where the element stiffness matrix K^e is

$$\underline{\underline{K^e}} = \int_{V_e} \underline{\underline{B}}^T \underline{\underline{C}}\, \underline{\underline{B}}\, dV \tag{2.43}$$

The external virtual work becomes

$$\begin{aligned} \delta W_E^e &= \int_{V_e} \underline{f}^T \delta \underline{u}\, dV + \int_{S_e} \underline{t}^T \delta \underline{u}\, dS \\ &= \left(\int_{V_e} \underline{f}^T \underline{N}\, dV + \int_{S_e} \underline{t}^T \underline{N}\, dS \right) \delta \underline{a} = (\underline{P^e})^T\, \delta \underline{a} \end{aligned} \tag{2.44}$$

where the element force vector is

$$\underline{P^e} = \int_{V_e} \underline{N}^T \underline{f}\, dV + \int_{S_e} \underline{N}^T \underline{t}\, dS \tag{2.45}$$

The integrals over the element volume V_e and element surface S_e are usually evaluated numerically by the Gauss integration procedure. For the volume integral, such a procedure needs evaluation of the integrand at a few points inside the volume. Such points, which are called Gauss points, are important for two reasons. First, the constitutive matrix C is evaluated at those locations. Second, the most accurate values of strains (and stresses) are obtained at those locations too.

The assembly of the element equations δW_I^e and δW_E^e into the PVW for the whole body is done similarly to the process in Section 2.1.6. Obviously the process is more complicated than for rod elements. The details of such process and its computer programming are part of finite element technology, which is outside the scope of this textbook. Eventually all the element stiffness matrices K^e and element force vectors P^e are assembled into a global system for the whole body

$$\underline{\underline{K}}\, \underline{a} = \underline{P} \tag{2.46}$$

Next, boundary conditions are applied on the system (2.46) in a systematic way resembling the procedure in Section 2.1.6. Next, the algebraic system of equations (2.46) is solved to find the nodal displacement array $\underline{a}$ over the whole body. Since the nodal displacements results for every element can be found somewhere in $\underline{a}$, it is possible to go back to (2.34) and to (2.38) to compute the strains and stresses anywhere inside the elements.

Example 2.1 *Compute the element stiffness matrix (2.43) and the equivalent force vector (2.45) of a rod discretized with one element. Use linear interpolation functions such as (2.11). Compare the result with (2.18-2.19).*

Solution to Example 2.1 *Let A_e be the transverse area of the rod and h_e the element length, with $x_e = 0$ and $x_{e+1} = h_e$. Substituting these values in the linear interpolation functions from equation (2.11), the interpolation functions arrays are obtained as follows*

$$\underline{N^T} = \begin{bmatrix} N_1^e \\ N_2^e \end{bmatrix} = \begin{bmatrix} \dfrac{x_{e+1} - x}{h_e} \\ \dfrac{x - x_e}{h_e} \end{bmatrix} = \begin{bmatrix} 1 - x/h_e \\ x/h_e \end{bmatrix}$$

The strain-displacement array is obtained as

$$\underline{\underline{B^T}} = \underline{\underline{\partial}}\ \underline{N^T} = \begin{bmatrix} \partial N_1^e/\partial x \\ \partial N_2^e/\partial x \end{bmatrix} = \begin{bmatrix} -1/h_e \\ 1/h_e \end{bmatrix}$$

The rod element has a one-dimensional strain-stress state with linear elastic behavior. Therefore

$$\underline{\underline{C}} = E$$

Then, using equation (2.43) we can write

$$\underline{\underline{K^e}} = \int_{V_e} \underline{\underline{B}}^T \underline{\underline{C}}\ \underline{\underline{B}}\, dV = \int_0^{h_e} \begin{bmatrix} -1/h_e & 1/h_e \end{bmatrix} E \begin{bmatrix} -1/h_e \\ 1/h_e \end{bmatrix} A_e dx$$

The element stiffness matrix is obtained by integration

$$[K^e] = \frac{EA_e}{h_e} \begin{bmatrix} 1 & -1 \\ -1 & 1 \end{bmatrix}$$

To calculate the equivalent vector force, f_e is defined as the distributed force on element, P_1^e is the force at end $x = 0$, and P_2^e is the force at end $x = h_e$. Substituting into equation (2.45) we obtain

$$\underline{P^e} = \int_{V_e} \underline{N}^T \underline{f}\, dV + \int_{S_e} \underline{N}^T \underline{t}\, dS = \int_0^{h_e} \begin{bmatrix} 1 - x/h_e \\ x/h_e \end{bmatrix} f_e dx + \begin{bmatrix} P_1^e \\ P_2^e \end{bmatrix}$$

The element equivalent force vector is obtained by integration

$$\underline{P^e} = \frac{f_e h_e}{2} \begin{bmatrix} 1 \\ 1 \end{bmatrix} + \begin{bmatrix} P_1^e \\ P_2^e \end{bmatrix}$$

Using MATLAB®

```
% FEACM solution Example 2.1
clear all
syms x x1 x2 h E A f real
% shape functions (linear Lagrange polynomial)
N(1)=(x-x2)/(x1-x2)
N(2)=(x-x1)/(x2-x1)
N=subs(N,{x1,x2},{0,h})
% Strain-displacement matrix B
B=diff(N,x)
```

```
% Stiffness matrix
K_e = int(B'*E*B,x,0,h)*A
% Equivalent nodal force vector
P_e=int(f*N,0,h)
```

2.3 Solid Modeling, Analysis, and Visualization

Many commercial programs exist with finite element analysis capabilities for different engineering disciplines. They help solve a variety of problems from simple linear static analysis to nonlinear transient analysis. A few of these codes, such as ANSYS® and *Abaqus*™, have special capabilities to analyze composite materials and they accept custom, user-programmed constitutive equations and element formulations. Since these software packages not only provide analysis tools, geometric modeling, and visualization of results, but also they can be integrated in the larger design, production, and product life-cycle process, they are often called complete analysis environments or computer aided engineering (CAE) systems.

Modern finite element analysis (FEA) software are commonly organized into three blocks: the pre-processor, the processor, and the post-processor. In the pre-processor, the model is built defining the geometry, material properties, and element type. Also, loads and boundary conditions are entered in the pre-processor, but they may also be entered during the solution phase. With this information, the processor can compute the stiffness matrix and the force vector. Next, the algebraic equations (2.46) are solved and the solution is obtained in the form of displacement values. In the last block–the post-processor–derived results, such as stress, strain, and failure ratios, are computed. The solution can be reviewed using graphic tools.

In the remainder of this chapter, a general description of the procedures and the specific steps for a basic FEA are presented using examples executed with ANSYS. Although the emphasis of the textbook is on the mechanics of composite materials, concepts are illustrated with examples that are solved using ANSYS. Solutions to similar examples using *Abaqus* are available in [7].

The first requirement of the model is the geometry. Then, material properties are given for the various parts that make up the geometry. Next, loads and boundary conditions are applied on the geometry. Next, the geometry is discretized into elements, which are defined in terms of the nodes and element connectivity. The element type is chosen to represent the type of problem to be solved. Next, the model is solved. Finally, derived results are computed and visualized.

2.3.1 Model Geometry

The model geometry is obtained specifying all nodes, their position, and the element connectivity. The connectivity information allows the program to assemble the element stiffness matrix and the element equivalent force vector to obtain the global equilibrium equations, as shown in Section 2.1.6.

There are two ways to generate the model. The first is to manually create a mesh. The second is to use solid modeling, and then mesh the solid to get the node

and element distribution.

Manual Meshing

Manual mesh generation was the only method before solid modeling became widespread among commercial packages. It is still the only option with some older and custom software, although in those cases it is always possible to use a general purpose, solid modeling pre-processor to generate the mesh. With manual meshing, the user creates nodes, then connects the nodes into elements. Afterward, the user applies boundary conditions and loads directly on nodes and/or elements. Manual meshing is used in Example 2.2.

Example 2.2 *Use ANSYS to model the curved beam shown in Figure 2.7. Use manual meshing for generating the mesh geometry. Since the thickness is small and constant, use planar solid elements with plane stress analysis. Add the boundary conditions and loads shown in the figure. Solve the problem and visualize a contour plot of von Mises stress on the deformed shape. The thickness of the part is* 4.0 *mm. The material properties are* $E = 195,000\ MPa$, $\nu = 0.3$.

Solution to Example 2.2 *The commands listed below, which are available on the Web site [5], define the model geometry by using* manual meshing. *The characters after* (!) *are comments. These commands can be typed one line at a time in the ANSYS command window (see Appendix C). Alternatively, in the ANSYS command window, read the text file by entering* `/input,file,ext`, *where* `file` *is the name of the file, and* `ext` *is the file extension.*

```
/TITLE, Ex. 2.2 Bending curved beam (manual meshing)
/PREP7                  ! Start pre-processor module
ET,1,PLANE182           ! Element type #1: PLANE182
KEYOPT,1,3,3            ! Key option #3 = 3, plane stress with thickness input
R,1,4                   ! Real constant #1: Th = 4 mm
MP,EX,1,195000          ! Material #1: E=195000 MPa
MP,NUXY,1,0.3           ! Material #1: Poisson coefficient 0.3
! Nodes and elements
CSYS,1                  ! Activate polar coordinate system
N,1,20,180              ! Define node #1: radius=20mm, angle=180
N,10,20,90              ! Define node #10: radius=20mm, angle=90
FILL,1,10               ! Fill nodes between node 1 and 10
NGEN,9,20,1,10,,2.5     ! Generate new node rows increasing radius 2.5 mm
CSYS,0                  ! Activate Cartesian coordinate system
N,15,20,20              ! Define node #15: x=20mm, y=20mm
FILL,10,15              ! Fill nodes between node 10 and 15
NGEN,9,20,11,15,,,2.5   ! Generate new node rows increasing y 2.5 mm
E,1,2,22,21             ! Define element #1,joining nodes 1,2,22,21
EGEN,8,20,1             ! Generate a row of elements
EGEN,14,1,ALL           ! Generate the rest of elements
FINISH                  ! Exit pre-processor module
/SOLU                   ! Solution module
ANTYPE,STATIC           ! Set static analysis
D,1,ALL,0,0,161,20      ! Impose Clamped BC
```

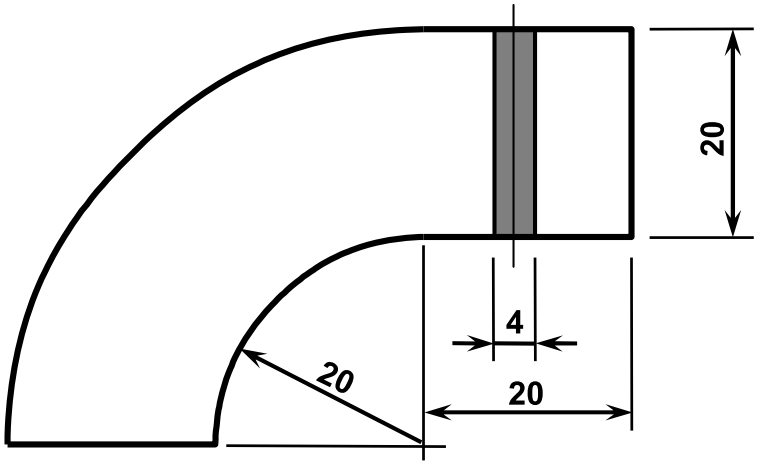

Figure 2.7: Curved beam.

```
ESEL,S,ELEM,,105,112    ! Select a subset of elements
SFE,ALL,2,PRES,0,-9.5   ! Apply pressure on subset
ESEL,ALL                ! Reselect all elements
SOLVE                   ! Solve the current load state
FINISH                  ! Exit solution module
/POST1                  ! Start Post-processor module
PLNSOL,S,EQV,2,1        ! Contour plot Von Mises equivalent stress
FINISH                  ! Exit post-processor module
```

The maximum value of von Mises stress is 108.124 MPa*, but this value is sensitive to mesh density, so the value will vary if you use a different mesh.*

Solid Modeling

With solid modeling, the user creates a geometric representation of the geometry using solid model constructs, such as volumes, areas, lines, and points. Boundary conditions, loads, and material properties can be assigned to parts of the solid model before meshing. In this way, re-meshing can be done without losing, or having to remove, the loads and boundary conditions. The models are meshed just prior to the solution. Solid modeling is used in Example 2.3.

Example 2.3 *Use ANSYS to generate the same model in Example 2.2, but this time use Solid Modeling commands for generating the mesh geometry.*

Solution to Example 2.3 *The commands listed below generate the geometry using Solid Modeling [5].*

```
/TITLE, Ex. 2.3 Bending curved beam (Solid Modeling)
/PREP7                  ! Start pre-processor module
ET,1,PLANE182           ! Element type #1: PLANE182
KEYOPT,1,3,3            ! Key option #3 = 3, plane stress
```

```
R,1,4                   ! Real constant #1: Th = 4 mm
MP,EX,1,195000          ! Material #1: E=195000 MPa
MP,NUXY,1,0.3           ! Material #1: Poisson coefficient 0.3
! Geometry
CYL4,0,0,40,90,20,180   ! Generate curved area
BLC4,0,20,20,20         ! Generate rectangular area
AGLUE,all               ! Glue both areas
LESIZE,2,,,8            ! Define divisions of elements by lines
LESIZE,4,,,8
LESIZE,6,,,8
LESIZE,1,,,10
LESIZE,3,,,10
LESIZE,9,,,5
LESIZE,10,,,5
MSHKEY,1                ! Force meshing by quadrilateral elements
AMESH,all               ! Mesh all areas
FINISH                  ! Exit pre-processor module
/SOLU                   ! Solution module
ANTYPE,STATIC           ! Set static analysis
DL,2,1,all,0            ! Impose Clamped BC
SFL,6,PRES,-9.5         ! Apply pressure
SOLVE                   ! Solve the current load state
FINISH                  ! Exit solution module
/POST1                  ! Start Post-processor module
PLNSOL,S,EQV,2,1        ! Contour plot Von Mises equivalent stress
FINISH                  ! Exit post-processor module
```

The maximum value of von Mises stress 109.238 MPa*, but this value is sensitive to mesh density, so the value will vary if you use a different mesh.*

2.3.2 Material and Section Properties

Parts must be associated to materials. Depending on the analysis, material properties can be linear (linear elastic analysis) or nonlinear (e.g., damage mechanics analysis), isotropic or orthotropic, constant or temperature-dependent. Entering the correct materials properties is one of the most important aspects of a successful analysis of composite materials. A great deal of attention is devoted to material properties in the rest of the textbook. For now it will suffice to illustrate the process using a linear elastic, isotropic material. For structural analysis, elastic properties must be defined according to Section (1.12). Other mechanical properties, such as strength, density, and thermal expansion coefficients are optional and their definition depends on the objectives of the analysis.

All elements need material properties, but structural elements need additional parameters that vary with the type of element. These parameters result from analytical integration of the 3D governing equations while formulating the element. For example, the cross-section area A appears in (2.1) because the 3D partial differential equations have been integrated over the cross-section of the rod to arrive at the ordinary differential equation (2.1). Beam elements require the cross-section area and the moment of inertia to be specified. Laminated shell elements require

Table 2.1: Some of the elements available in *Abaqus* and ANSYS

Abaqus	**ANSYS**	**nodes**	**DOF**	**Element Description**
Structural elements				
T2D2	-	2	$u_X\ u_Y$	line bar/truss, 2D space
T3D2	LINK180	2	$u_X\ u_Y\ u_Z$	line bar/truss, 3D space
-	COMBIN14	2	$u_X\ u_Y\ u_Z$	spring/damper, 3D space
B21	-	2	$u_X\ u_Y$ $\theta_X\ \theta_Y$	line beam in 2D space
B31	BEAM188	2	$u_X\ u_Y\ u_Z$ $\theta_X\ \theta_Y\ \theta_Z$	line beam in 3D space
CPE4R	PLANE182	4	$u_X\ u_Y$	solid quadrilateral in 2D space
CPE8R	PLANE183	8	$u_X\ u_Y$	solid quadrilateral in 2D space
S4R	SHELL181	4	$u_X\ u_Y\ u_Z$ $\theta_X\ \theta_Y\ \theta_Z$	shell quadrilateral in 3D space (conventional)
S8R	SHELL281	8	$u_X\ u_Y\ u_Z$ $\theta_X\ \theta_Y\ \theta_Z$	shell quadrilateral in 3D space (conventional)
S8R5	-	4	$u_X\ u_Y\ u_Z$ $\theta_X\ \theta_Y$	thin shell quadrilateral in 3D space (conventional)
SAX1	SHELL208	2	$u_X\ u_Y\ \theta_Z$	axisymmetric
SAX2	SHELL209	3	$u_X\ u_Y\ \theta_Z$	axisymmetric
Continuum elements[1]				
C3D8	SOLID185	8	$u_X\ u_Y\ u_Z$	solid hexahedra in 3D space
C3D20	SOLID186	20	$u_X\ u_Y\ u_Z$	solid hexahedra in 3D space
SC8R	SOLSH190	8	$u_X\ u_Y\ u_Z$	shell hexahedra in 3D space (continuum)

the laminate stacking sequence (LSS). Continuum elements (see Table 2.1) do not require additional parameters, only material properties, because the geometry is fully described by the mesh. However, continuum elements representing laminated composites still require the LSS.

2.3.3 Assembly

If more than one part exists, assembly is necessary to put the parts together into what is called an *assembly*, which represents the physical object you are trying to

[1] *Continuum* means that the 3D volume is discretized with and no section properties are required. *Structural* means that the volume is discretized as 2D or 1D and section properties, such as shell thickness, are required to complete the description of the volume. 3D solid elements are typical continuum elements. Conventional shells and beams are typical structural elements. Continuum shells are continuum elements with kinematic constrains to represent shell behavior.

analyze.

2.3.4 Solution Steps

Next, the analysis process is normally broken down into several *steps*, each representing different loading and constraint conditions. The minimum number of steps is two: an initial step and at least one additional step. No loads can be applied on the initial step, only boundary conditions.

2.3.5 Loads

In structural analysis, loads are defined by forces, pressures, inertial forces (as gravity), and specified displacements, all applied to the model. Specification of different kinds of loads for the finite element model are explained in the following sections. The reactions obtained by fixing a nodal degree of freedom (displacements and rotations) are discussed in Section 2.3.6.

Loads can be applied on nodes by means of concentrated forces and moments, as shown in Example 2.4. Also, loads can be distributed over the elements as: surface loads, body loads, inertia loads, or other coupled-field loads (for example, thermal strains). Surface loads are used in Example 2.5.

A surface load is a distributed load applied over a surface, for example a pressure. A body load is a volumetric load, for example expansion of material by temperature increase in structural analysis. Inertia loads are those attributable to the inertia of a body, such as gravitational acceleration, angular velocity, and acceleration.

A concentrated load applied on a node is directly added to the force vector. However, the element interpolation functions are used to compute the equivalent forces vector due to distributed loads.

2.3.6 Boundary Conditions

The boundary conditions are the known values of the degrees of freedom (DOF) on the boundary. In structural analysis, the DOF are displacements and rotations. With this information, the software knows which values of $\underline{a}$ in (2.46) are known or unknown.

Constrained Displacements and Rotations

In general, a node can have more than one degree of freedom. For example, if the finite element model uses beam elements in 2D space, there are three DOF: the horizontal displacement, the vertical displacement, and the rotation around an axis perpendicular to the plane. Constraining different sets of DOF results in different boundary conditions being applied. In the 2D beam element case, constraining only the horizontal and vertical displacements results in a simple support, but constraining all the DOF results in a clamped condition.

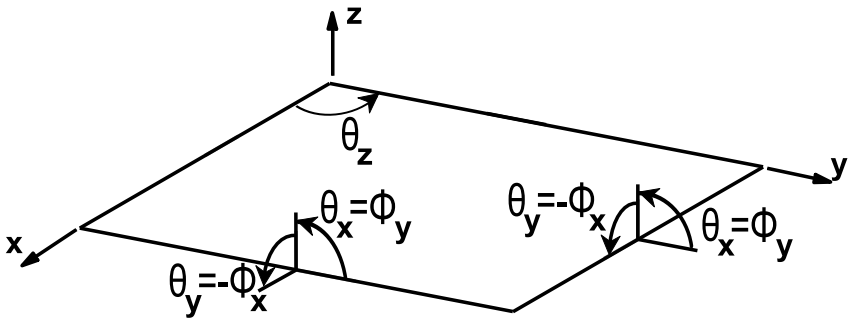

Figure 2.8: Convention for rotations of a plate or shell.

Symmetry Conditions

Symmetry conditions can be applied to reduce the size of the model without loss of accuracy. Four types of symmetry must exist concurrently: symmetry of geometry, boundary conditions, material, and loads. Under these conditions the solution will also be symmetric. For example, symmetry with respect to the $y-z$ plane means that the nodes on the symmetry plane have the following constraints

$$u_x = 0 \quad ; \quad \theta_y = 0 \quad ; \quad \theta_z = 0 \tag{2.47}$$

where u_x is the displacement along the x-direction, θ_y and θ_z are the rotations around the y and z axis, respectively (Figure 2.8). Note that the definition of rotations used in shell theory (ϕ_i, see Section 3.1) is different than the usual definition of rotations θ_i that follows the right-hand rule. Rotations in ANSYS are described using right-hand-rule rotations θ_i. Symmetry boundary conditions on nodes in the symmetry plane involve the restriction of DOF translations out-of-plane with respect to the symmetry plane and restriction of the DOF rotations in-plane with respect to the symmetry plane. Symmetry boundary conditions are used in Example 2.5.

Antisymmetry Conditions

Antisymmetry conditions are similar to the symmetry conditions. They can be applied when the model exhibits antisymmetry of loads but otherwise the model exhibits symmetry of geometry, symmetry of boundary conditions, and symmetry of material. Antisymmetry boundary conditions on nodes in the antisymmetry plane involve restriction of DOF translations in the antisymmetry plane and restriction of DOF rotations out-of-plane with respect to the antisymmetry plane.

Periodicity Conditions

When the material, load, boundary conditions, and geometry are periodic with period $(x, y, z) = (2a_i, 2b_i, 2c_i)$, only a portion of the structure needs to be modeled, with dimensions $(2a_i, 2b_i, 2c_i)$. The fact that the structure repeats itself periodically means that the solution will also be periodic. Periodicity conditions can be

imposed by different means. One possibility involves using constrained equations (CE) between DOF (see Section 6.2) or using Lagrange multipliers.

2.3.7 Meshing and Element Type

Next, the assembly needs to be meshed. Before meshing, the element type needs to be chosen. Finite Element Analysis (FEA) programs have an *element library* that contains many different element types. The element type determines the element formulation used. For example, the degree of freedom set, the interpolation functions, whether the element is for 2D or 3D space, etc. The element type identifies the element category: bar/rod tensile-compression, beam bending, solid, shell, laminate shell, etc. Each commercial code identifies element formulations with different labels. Identification labels and basic characteristics of a few element formulations are shown in Table 2.1. Also, each element type has different options. For example, on a planar solid element, an option allows one to choose between plane strain and plane stress analysis.

2.3.8 Solution Phase

In the solution phase of the analysis, the solver subroutine included in the finite element program solves the simultaneous set of equations (2.46) that the finite element method generates. Usually, the primary solution is obtained by solving for the nodal degree of freedom values, i.e., displacements and rotations. Then, derived results, such as stresses and strains, are calculated at the integration points. In ANSYS, primary results are called *nodal solutions* and derived results are called *element solutions*.

Several methods of solving the system of simultaneous equations are available. Some methods are better for larger models, others are faster for nonlinear analysis, others allow one to distribute the solution by parallel computation. Commercial finite element programs solve these equations in batch mode. The frontal direct solution method is commonly used because it is rather efficient for FEA. When the analysis is nonlinear, the equations must be solved repeatedly, thus increasing the computational time significantly.

2.3.9 Post-Processing and Visualization

Once the solution has been calculated, the post-processor can be used to review and to analyze the results. Results can be reviewed graphically or by listing the values numerically. Since a model usually contains a considerable amount of results, it may be better to use graphical tools. Post-processors of commercial codes produce contour plots of stress and strain distributions, deformed shapes, etc. The software usually includes derived calculations such as error estimation, load case combinations, or path operations. Examples 2.4 and 2.5 include commands to review the results by listing and by graphic output, respectively.

Example 2.4 *Use ANSYS to find the axial displacement at the axially loaded end of a bar clamped at the other end. The bar is made of steel $E = 200,000\ MPa$, diameter $d = 9\ mm$, length $L = 750\ mm$, and load $P = 100,000\ N$. Also find the stress and strain. Use three two-node (linear) link elements.*

Solution to Example 2.4 *The ANSYS command sequence for this example is listed below. You can either type these commands on the command window, or you can type them on a text file [5], then, on the command window enter* `/input,file,ext`*, where* `file` *is the name of the file, and* `ext` *is the file extension (see Appendix C).*

```
/TITLE, Ex. 2.4 Axially loaded bar
/PREP7                  ! Start pre-processor module
ET,1,LINK180            ! Define element type #1 LINK180 - 3D bar
R,1,63.6173             ! Define real constant A=63.6173 mm^2
MP,EX,1,200E3           ! Define elastic modulus E=200,000 MPa
N,1                     ! Define node 1, coordinates=0,0,0
NGEN,4,1,1,,,250        ! Generate 3 additional nodes
                        ! distance between adjacent nodes 250 mm
E,1,2                   ! Generate element 1 by node 1 to 2
EGEN,3,1,1              ! Generate element 2,3
FINISH                  ! Exit pre-processor module
/SOLU                   ! Start Solution module
OUTPR,ALL,LAST,
D,1,all                 ! Define b.c. in node 1, totally fixed
F,4,FX,100E3            ! Define horizontal force in node 4
SOLVE                   ! Solve the current load state
/STAT,SOLU              ! Provides a solution status summary
FINISH                  ! Exit solution module
```

To see the printout you need to execute the following commands manually by typing them in the ANSYS command window or using the graphical user interface (GUI):

```
/POST1                  ! Start Post-processor module
PRNSOL,U,X              ! Print in a list the horizonal disp.
PRESOL,ELEM             ! Print all line element results
PRRSOL,FX               ! Print horizontal reactions
FINISH                  ! Exit post-processor module
```

A convenient combination of units for this case is Newton, mm, and MPa. The analysis results can be easily verified by strength of material calculations, as follows

$$U_x = \frac{PL}{AE} = \frac{(750)(100000)}{(63.617)(200000)} = 5.894\ mm$$

$$\sigma = \frac{P}{A} = \frac{100000}{63.617} = 1571.9\ MPa$$

$$\epsilon = \frac{\sigma}{E} = 7.859 \cdot 10^{-3}$$

Example 2.5 *Use ANSYS to find the stress concentration factor of a rectangular notched strap. The dimensions and the load state are defined in Figure 2.9. Use eight-node (quadratic) quadrilateral plane stress elements.*

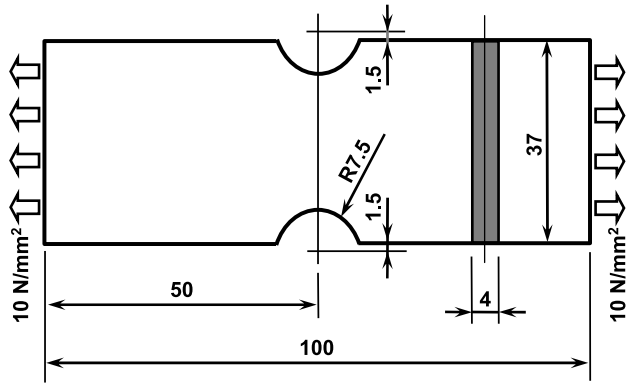

Figure 2.9: Rectangular notched strap analyzed in Example 2.5.

Solution to Example 2.5 *The ANSYS command sequence for this example is listed below. These commands can be typed on the command window or in a text file [5], then, on the command window enter* `/input,file,ext`*, where* `file` *is the name of the file, and* `ext` *is the file extension (see Appendix C).*

```
/TITLE, Ex. 2.5 Stress concentration
/PREP7                  ! Start pre-processor module
ET,1,PLANE183           ! Define element type #1 PLANE183 8-noded 2-D
KEYOPT,1,3,3            ! Key option #3 = 3, plane stress
R,1,4                   ! Define real constant th=4 mm
MP,EX,1,190E3           ! Define elastic modulus E=190,000 MPa
MP,PRXY,1,0.3           ! Define Poisson coefficient 0.3
BLC4,0,0,50,18.5        ! Define squared area 18.5x50 mm
CYL4,0,20,7.5           ! Define circular area radius 7,5 mm
ASBA,1,2                ! Subtract previous areas
ESIZE,1.5,0,            ! Define element size
MSHKEY,0                ! Free mesh
AMESH,all               ! Mesh
FINISH                  ! Exit pre-processor module
/SOLU                   ! Start Solution module
DL, 1, ,SYMM            ! Define symmetry b. conditions in line 1
DL, 9, ,SYMM            ! Define symmetry b. conditions in line 9
SFL,2,PRES,-10          ! Apply pressure on line 2
SOLVE                   ! Solve the current load state
FINISH                  ! Exit solution module
/POST1                  ! Start Post-processor module
PLNSOL,S,X,2,1          ! Contour plot horizontal stress
PLNSOL,S,EQV,2,1        ! Contour plot Von Mises equivalent stress
PLVECT,S                ! Vector plot principal stress
FINISH                  ! Exit post-processor module
```

The stress in the net area without stress concentration is

$$\sigma_o = \frac{P}{A} = \frac{10 \cdot 37 \cdot 4}{25 \cdot 4} = 14.8 \ MPa$$

The maximum horizontal stress close to the notch is 28 MPa obtained from the finite element model (`PLNSOL,S,X,2,1`). Therefore, the concentration factor is

$$k = \frac{\sigma_{max}}{\sigma_o} = 1.89$$

Example 2.6 *Using ANSYS generate a model for a dome (Figure 2.10) with different types of elements (shell and beam elements), using two materials, and different section data. Use solid modeling to generate the mesh geometry. Report the minimum and maximum values of von Mises stress, and the maximum displacement.*

Solution to Example 2.6 *The element types in ANSYS are defined by the ET command [8]. The element types can be defined by their library names (see Table 2.1) and given reference numbers to be used later. For example, the commands shown below define two element types, BEAM188 and SHELL181, and assign them type reference numbers 1 and 2, respectively.*

```
ET,1,BEAM188                    ! Define element type #1 BEAM188
ET,2,SHELL181                   ! Define element type #2 SHELL181
```

For material definition, MP can be used along with the appropriate property label; e.g., EX for Young's modulus, NUXY for Poisson's ratio, etc. For isotropic material, only the X-direction properties need to be defined. The remaining properties in the other directions default to the X-direction values. Also a reference number is used for each material. For example, the following code defines two materials

```
MP,EX,1,200E3                   ! Define material #1 E=200000MPa
MP,NUXY,1,0.29                  ! Define material #1 Poisson ratio
MP,EX,2,190E3                   ! Define material #2 E=190000MPa
MP,NUXY,2,0.27                  ! Define material #2 Poisson ratio
```

Section properties are required for all elements where one or more dimensions have been integrated a priori, e.g., beam and shell elements. That is, beam elements require the area, and shell elements the thickness. In previous versions of ANSYS, section properties were introduced via REAL constants but that is changing to using SECTION data. For this example,

```
SECTYPE,1,BEAM,RECT             ! Define SECTION 1
SECDATA,10.,10.                 ! Assign cross-section 10x10 squared
SECTYPE,2,SHELL                 ! Define SECTION 2
SECDATA,6.                      ! Assign Th = 6 mm
SECTYPE,3,SHELL                 ! Define SECTION 3
SECDATA,4.                      ! Assign Th = 4 mm
```

The commands shown above define a database with a table of elements type, another with materials, and lastly another with section data. The reference number of each table can be selected by using the commands TYPE, MAT, and SECNUM before defining the mesh, as shown in the ANSYS command sequence listed below. These commands can be typed on the command window, or in a text file [5], then, on the command window enter `/input,file,ext`, where `file` is the name of the file, and `ext` is the file extension (see Appendix C).

```
/TITLE, Ex. 2.6 Dome
/PREP7                          ! Start pre-processor module
! Define element types
ET,1,BEAM188                    ! Define element type #1 BEAM188
ET,2,SHELL181                   ! Define element type #2 SHELL181
! Define materials
MP,EX,1,200E3                   ! Define material #1 E=200,000 MPa
MP,NUXY,1,0.29                  ! Define material #1 Poisson ratio
MP,EX,2,190E3                   ! Define material #2 E=190,000 MPa
MP,NUXY,2,0.27                  ! Define material #2 Poisson ratio
! Define sections
SECTYPE,1,BEAM,RECT             ! Define SECTION 1
SECDATA,10.,10.                 ! Assign cross-section 10x10 squared
SECTYPE,2,SHELL                 ! Define SECTION 2
SECDATA,6.                      ! Assign Th = 6 mm
SECTYPE,3,SHELL                 ! Define SECTION 3
SECDATA,4.                      ! Assign Th = 4 mm
! Create geometry by solid modelling
SPH4, , ,500                    ! Define sphere radius 500 mm
BLOCK,-600,600,-600,600,-600,0  ! Define blocks for substract ...
BLOCK, 300,600,-600,600,0,600   ! ...to sphere
BLOCK,-300,-600,-600,600,0,600
BLOCK,-600,600,300,600,0,600
BLOCK,-600,600,-300,-600,0,600
VADD,2,3,4,5,6                  ! Add all blocks
VSBV,1,7                        ! Substract blocks to the shephere
WPAVE,0,0,200                   ! Offset working plane z=+200 mm
VSBW,ALL                        ! Divide Volume by working plane
! Mesh geometry
ESIZE,20                        ! Define element size
TYPE,2                          ! Assign SHELL to elements defined next
MAT,2                           ! Assign material #2 to elements defined next
SECNUM,2                        ! Assign section #2 to elements defined next
AMESH,8,9                       ! Mesh areas 8 and 9 (top surface dome).
SECNUM,3                        ! Assign section #3 to elements defined next
AMESH,12,15                     ! Mesh areas 12,13,14 and 15 (side surface dome)
TYPE,1                          ! Assign BEAM to elements defined next
MAT,1                           ! Assign material #1 to elements defined next
SECNUM,1                        ! Assign section #1 to elements defined next
LMESH,1,2                       ! Mesh lines 1 and 2 (columns)
LMESH,4,5                       ! Mesh lines 4 and 5 (columns)
FINISH                          ! Exit pre-processor module
/SOLU                           ! Solution module
ANTYPE,STATIC                   ! Set static analysis
D,2007,ALL,0,0,2037,10          ! Impose Clamped BC-lower-end of the columns
LSEL,S,LINE,,13,16,1            ! Select a subset of lines
DL,ALL,,UX,0,0                  ! Impose BC-vertical edges of the side walls
DL,ALL,,UY,0,0                  ! Impose BC-vertical edges of the side walls
LSEL,ALL                        ! Reselect all lines
ESEL,S,SEC,,2                   ! Select a subset of elements
SFE,ALL,2,PRES,0,-100           ! Apply pressure on subset
```

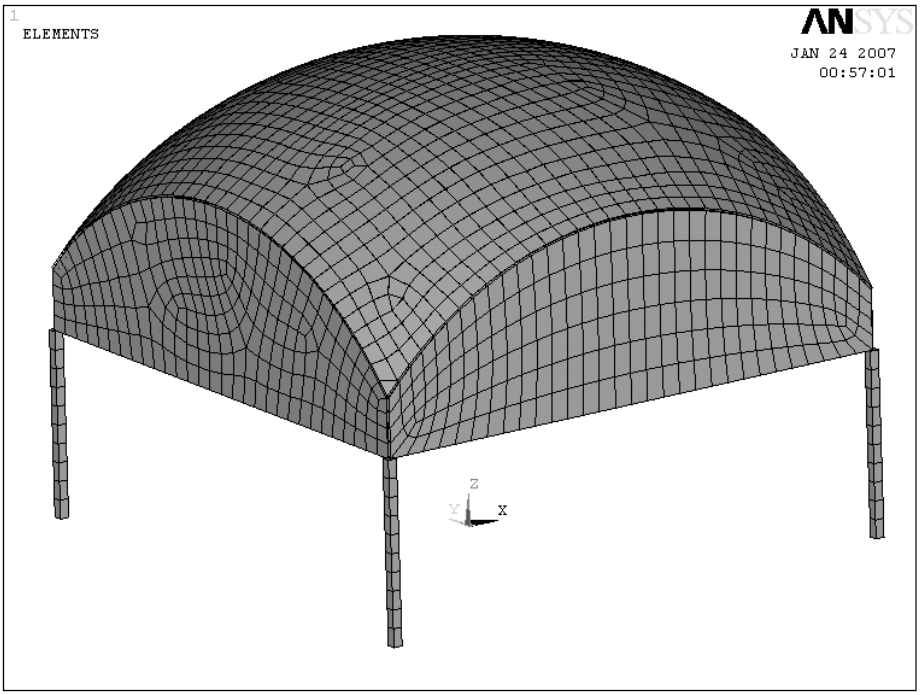

Figure 2.10: Mesh obtained by the command sequence used to generate a dome.

```
ESEL,ALL                        ! Reselect all elements
SOLVE                           ! Solve the current load state
FINISH                          ! Exit solution module
/POST1                          ! Start Post-processor module
PLNSOL,S,EQV,2,1                ! Contour plot Von Mises equivalent stress
!FINISH                         ! Exit post-processor module
```

Using `PLNSOL,S,EQV,2,1`*, the maximum value of von Mises stress* $83,513\ MPa$ *at the attachment to the columns. The minimum value of von Mises stress* $255\ MPa$ *on the shell body. The maximum displacement is* $155\ mm$.

Suggested Problems

Problem 2.1 *Solve Example 2.4 explicitly as it is done in Section 2.1, using only two elements. Show all work.*

Problem 2.2 *From the solution of Problem 2.1, compute the axial displacement at (a)* $x = 500\ mm$*, (b)* $x = 700\ mm$.

Problem 2.3 *Using the same procedure in Example 2.1 calculate the element stiffness matrix and the equivalent force vector of a three-node element rod with quadratic interpolation functions. The interpolation functions are*

$$N_1^e = \frac{x - x_2}{x_1 - x_2}\frac{x - x_3}{x_1 - x_3} \quad N_2^e = \frac{x - x_3}{x_2 - x_3}\frac{x - x_1}{x_2 - x_1} \quad N_3^e = \frac{x - x_1}{x_3 - x_1}\frac{x - x_2}{x_3 - x_2}$$

where x_1, x_2 and x_3 are the coordinate positions of node 1, 2, and 3 respectively. Use $x_1 = 0$, $x_2 = h/2$ and $x_3 = h$, where h is the element length. Show all work.

Problem 2.4 *Program a finite element code using the element formulation obtained in Example 2.1 and the assembly procedure shown in Section 2.1.6. With this code, solve Example 2.4. Show all work in a report.*

Problem 2.5 *Program a finite element code using the element formulation obtained in Problem 2.3 and the assembly procedure shown in Section 2.1.6. With this code, solve Example 2.4. Show all work in a report.*

Chapter 3

Elasticity and Strength of Laminates

Most composite structures are built as assemblies of plates and shells. This is because the structure is more efficient when it carries membrane loads. Another important reason is that thick laminates are difficult to produce.

For example, consider a beam made of an homogeneous material with tensile and compressive strength σ_u subjected to bending moment M. Further, consider a solid beam of square cross-section (Figure 3.1), equal width and depth $2c$, with area A, inertia I, and section modulus S given by

$$\begin{aligned} A &= 4c^2 \\ I &= \frac{4}{3}c^4 \\ S &= \frac{I}{c} = \frac{4}{3}c^3 \end{aligned} \tag{3.1}$$

When the stress on the surface of the beam reaches the failure stress σ_u, the bending moment per unit area is

$$m_u = \frac{M_u}{A} = \frac{S\sigma_u}{A} = \frac{1}{3}c\sigma_u \tag{3.2}$$

Now consider a square hollow tube (Figure 3.1) of dimensions $2c \times 2c$ and wall thickness t, with $2c >> t$, so that the following approximations are valid

$$\begin{aligned} A &= 4(2c)t = 8ct \\ I &= 2\left[\frac{t(2c)^3}{12} + c^2(2ct)\right] = \frac{16}{3}tc^3 \\ S &= \frac{I}{c} = \frac{16}{3}tc^2 \end{aligned} \tag{3.3}$$

Then

$$m_u = \frac{M_u}{A} = \frac{S\sigma_u}{A} = \frac{\frac{16}{3}tc^2\sigma_u}{8ct} = \frac{2}{3}c\sigma_u \tag{3.4}$$

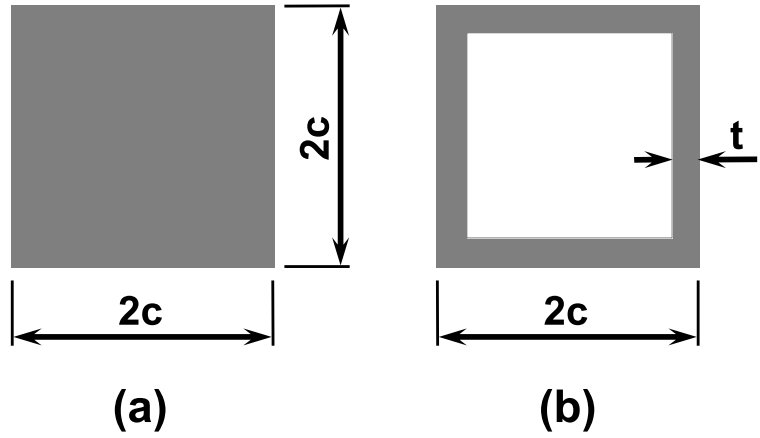

Figure 3.1: Solid section (a) and hollow square tube (b).

The failure moment per unit area m_u is twice as large for a hollow square tube with thin walls than for a solid section.

Of course, the failure moment is limited by buckling of the thin walls (see Chapter 4). This is the reason buckling analysis is so important for composites. Most composite structures are designed under buckling constraints because the thicknesses are small and the material is very strong, so normally one does not encounter material failure as in metallic structures (e.g., yield stress) but structural failure such as buckling.

Plates are a particular case of shells, having no initial curvature. Therefore, only shells will be mentioned in the sequel. Shells are modeled as two-dimensional structures because two dimensions (length and width) are much larger than thickness. The thickness coordinate is eliminated from the governing equations so that the 3D problem simplifies to 2D. In the process, the thickness becomes a parameter that is known and supplied to the analysis model.

Modeling of laminated composites differs from modeling conventional materials in three aspects. First, the constitutive equations of each lamina are orthotropic (Section 1.12.3). Second, the constitutive equations of the element depend on the kinematic assumptions of the shell theory used and their implementation into the element. Finally, material symmetry is as important as geometric and load symmetry when trying to use symmetry conditions in the models.

3.1 Kinematics of Shells

Shell elements are based on various shell theories which in turn are based on kinematic assumptions. That is, there are some underlying assumptions about the likely type of deformation of the material through the thickness of the shell. These assumptions are needed to reduce the 3D governing equations to 2D. Such assumptions are more or less appropriate for various situations, as discussed next.

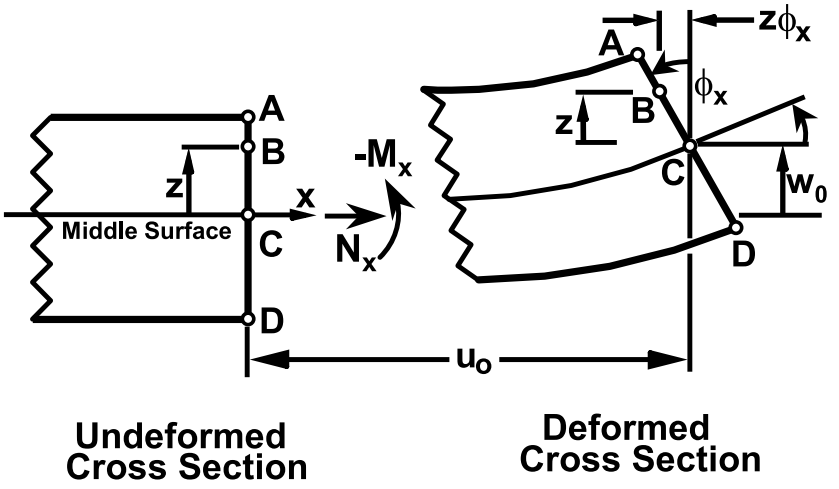

Figure 3.2: Assumed deformation in FSDT.[1]

3.1.1 First-Order Shear Deformation Theory

The most popular composite shell theory is the first-order shear deformation theory (FSDT). It is based on the following assumptions:

i. A straight line drawn through the thickness of the shell in the undeformed configuration may rotate but it will remain straight when the shell deforms. The angles it forms (if any) with the normal to the undeformed mid-surface are denoted by ϕ_x and ϕ_y when measured in the $x-z$ and $y-z$ planes, respectively (Figures 2.8 and 3.2).

ii. As the shell deforms, the change in thickness of the shell is negligible.

These assumptions are verified by experimental observation in most laminated shells when the following are true:

– The aspect ratio $r = a/t$, defined as the ratio between the shortest surface dimension a and the thickness t, is larger than 10.

– The stiffness of the laminas in shell coordinates (x, y, z) do not differ by more than two orders of magnitude. This restriction effectively rules out sandwich shells, where the core is much softer than the faces.

Based on the assumptions above, the displacement of a generic point B anywhere in the shell can be written in terms of the displacement and rotations at the mid-surface C as

[1]Reprinted from *Introduction to Composite Materials Design*, E. J. Barbero, Figure 6.2, copyright (1999), with permission from Taylor & Francis.

$$\begin{aligned} u(x,y,z) &= u_0(x,y) - z\phi_x(x,y) \\ v(x,y,z) &= v_0(x,y) - z\phi_y(x,y) \\ w(x,y,z) &= w_0(x,y) \end{aligned} \tag{3.5}$$

The mid-surface variables on the right-hand side of (3.5) are functions of only two coordinates (x and y), thus the shell theory is 2D. On the left-hand side, the displacements are functions of three coordinates, and thus correspond to the 3D representation of the material. At the 3D level, we use the 3D constitutive equations (1.68) and the 3D strain-displacement equations (1.5), which now can be written in terms of 2D quantities as

$$\begin{aligned} \epsilon_x(x,y,z) &= \frac{\partial u_0}{\partial x} - z\frac{\partial \phi_x}{\partial x} = \epsilon_x^0 + z\kappa_x \\ \epsilon_y(x,y,z) &= \frac{\partial v_0}{\partial y} - z\frac{\partial \phi_y}{\partial y} = \epsilon_y^0 + z\kappa_y \\ \gamma_{xy}(x,y,z) &= \frac{\partial u_0}{\partial y} + \frac{\partial v_0}{\partial x} - z\left(\frac{\partial \phi_x}{\partial y} + \frac{\partial \phi_y}{\partial x}\right) = \gamma_{xy}^0 + z\kappa_{xy} \\ \gamma_{yz}(x,y) &= -\phi_y + \frac{\partial w_0}{\partial y} \\ \gamma_{xz}(x,y) &= -\phi_x + \frac{\partial w_0}{\partial x} \\ \epsilon_z &= 0 \end{aligned} \tag{3.6}$$

where

- The mid-surface strains ϵ_x^0, ϵ_y^0 , γ_{xy}^0, also called membrane strains, represent stretching and in-plane shear of the mid-surface.
- The change in curvature κ_x, κ_y, κ_{xy}, which are close but not exactly the same as the geometric curvatures of the mid-surface. They are exactly that for the Kirchhoff theory discussed in Section 3.1.2.
- The intralaminar shear strains γ_{xz}, γ_{yz}, which are through-the-thickness shear deformations. These are small but not negligible for laminated composites because the intralaminar shear moduli G_{23}, G_{13} are small when compared with the in-plane modulus E_1. Metals are relatively stiff in shear ($G = E/2(1+\nu)$), and thus the intralaminar strains are negligible. In addition, the intralaminar shear strength of composites F_4, F_5 are relatively small when compared to the in-plane strength values F_{1t}, F_{1c}, thus making evaluation of intralaminar strains (and possibly stresses) a necessity. On the other hand, the shear strength of metals is comparable to their tensile strength, and since the intralaminar stress is always smaller than the in-plane stress, it is not necessary to check for intralaminar failure of metallic homogeneous shells. That is not the case for laminated metallic shells since the adhesive is not quite strong and it may fail by intralaminar shear.

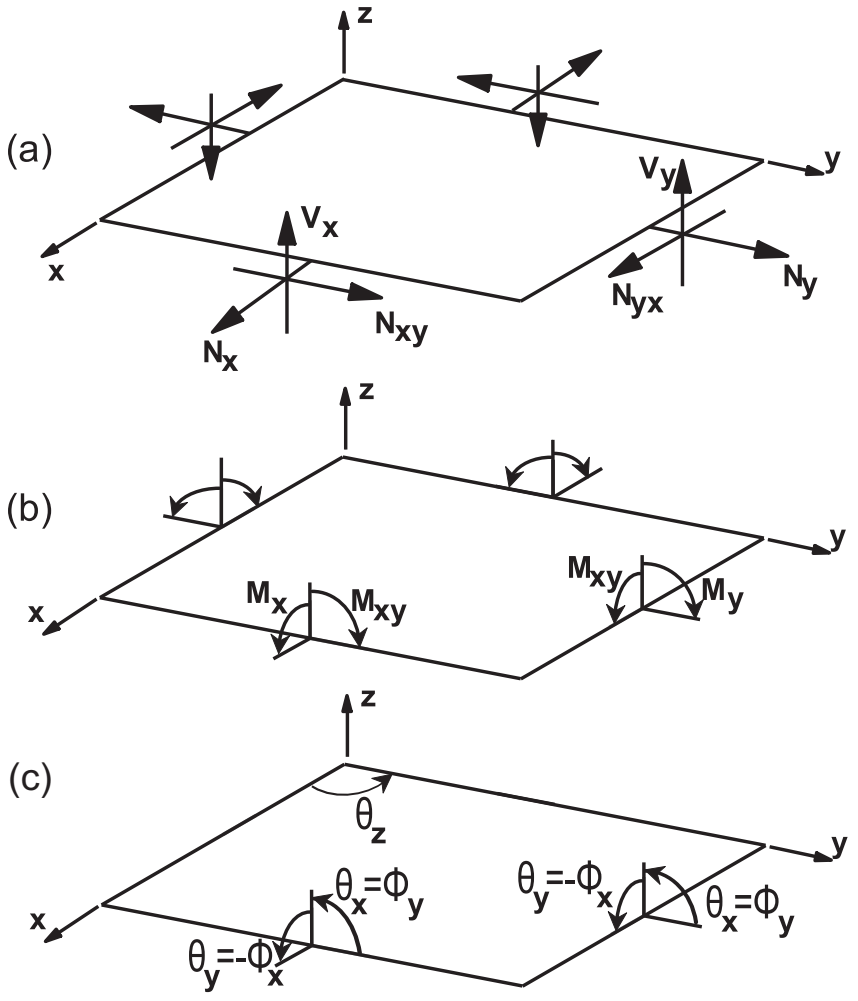

Figure 3.3: Stress resultants acting on a plate or shell element: (a) forces per unit length, and (b) moments per unit length, and (c) definition of shell theory rotations ϕ compared to mathematical angles θ.

While the 3D constitutive equations relate strains to stress, the laminate constitutive equations relate mid-surface strains and curvatures. The laminate constitutive equations are obtained by using the definition of stress resultants. While in 3D elasticity every material point is under stress, a shell is loaded by stress resultants (Figure 3.3), which are simply integrals of the stress components through the thickness of the shell, as follows

$$\begin{aligned}
\left\{ \begin{array}{c} N_x \\ N_y \\ N_{xy} \end{array} \right\} &= \sum_{k=1}^{N} \int_{z_{k-1}}^{z_k} \left\{ \begin{array}{c} \sigma_x \\ \sigma_y \\ \sigma_{xy} \end{array} \right\}^k dz \\
\left\{ \begin{array}{c} V_y \\ V_x \end{array} \right\} &= \sum_{k=1}^{N} \int_{z_{k-1}}^{z_k} \left\{ \begin{array}{c} \sigma_{yz} \\ \sigma_{xz} \end{array} \right\}^k dz \\
\left\{ \begin{array}{c} M_x \\ M_y \\ M_{xy} \end{array} \right\} &= \sum_{k=1}^{N} \int_{z_{k-1}}^{z_k} \left\{ \begin{array}{c} \sigma_x \\ \sigma_y \\ \sigma_{xy} \end{array} \right\}^k z \; dz
\end{aligned} \tag{3.7}$$

where N is the number of laminas, z_{k-1} and z_k are the coordinates at the bottom and top surfaces of the k-th lamina, respectively. Replacing the plane stress version of the 3D constitutive equations in shell local coordinates (1.100–1.101) at each lamina and performing the integration we get

$$\begin{aligned}
\left\{ \begin{array}{c} N_x \\ N_y \\ N_{xy} \\ M_x \\ M_y \\ M_{xy} \end{array} \right\} &= \left[\begin{array}{cccccc} A_{11} & A_{12} & A_{16} & B_{11} & B_{12} & B_{16} \\ A_{12} & A_{22} & A_{26} & B_{12} & B_{22} & B_{26} \\ A_{16} & A_{26} & A_{66} & B_{16} & B_{26} & B_{66} \\ B_{11} & B_{12} & B_{16} & D_{11} & D_{12} & D_{16} \\ B_{12} & B_{22} & B_{26} & D_{12} & D_{22} & D_{26} \\ B_{16} & B_{26} & B_{66} & D_{16} & D_{26} & D_{66} \end{array} \right] \left\{ \begin{array}{c} \epsilon_x^0 \\ \epsilon_y^0 \\ \gamma_{xy}^0 \\ \kappa_x \\ \kappa_y \\ \kappa_{xy} \end{array} \right\} \\
\left\{ \begin{array}{c} V_y \\ V_x \end{array} \right\} &= \left[\begin{array}{cc} H_{44} & H_{45} \\ H_{45} & H_{55} \end{array} \right] \left\{ \begin{array}{c} \gamma_{yz} \\ \gamma_{xz} \end{array} \right\}
\end{aligned} \tag{3.8}$$

where

$$\begin{aligned}
A_{ij} &= \sum_{k=1}^{N} \left(\overline{Q}_{ij}\right)_k t_k; \qquad i,j = 1,2,6 \\
B_{ij} &= \sum_{k=1}^{N} \left(\overline{Q}_{ij}\right)_k t_k \bar{z}_k; \qquad i,j = 1,2,6 \\
D_{ij} &= \sum_{k=1}^{N} \left(\overline{Q}_{ij}\right)_k \left(t_k \bar{z}_k^2 + \frac{t_k^3}{12} \right); \qquad i,j = 1,2,6 \\
H_{ij} &= \frac{5}{4} \sum_{k=1}^{N} \left(\overline{Q}_{ij}^*\right)_k \left[t_k - \frac{4}{t^2} \left(t_k \bar{z}_k^2 + \frac{t_k^3}{12} \right) \right]; \qquad i,j = 4,5
\end{aligned} \tag{3.9}$$

where $\left(\overline{Q}_{ij}\right)_k$ are the coefficients in laminate coordinates of the plane-stress stiffness matrix for lamina number k, t_k is the thickness of lamina k, and $\bar{z}_k$ is the coordinate of the middle surface of the k-th lamina. For an in-depth discussion of the meaning of various terms see [1]. In summary, the A_{ij} coefficients represent in-plane stiffness of the laminate, the D_{ij} coefficients represent bending stiffness, the B_{ij} represent bending-extension coupling, and the H_{ij} represent intralaminar shear stiffness. All these coefficients can be calculated by (3.9) and are implemented in widely available software packages such as CADEC [9].

When membrane and bending deformations are uncoupled (e.g., symmetric laminates), the governing equations of FSDT involve three variables for solving the bending problem (w^0, ϕ_x, ϕ_y) and two to solve the membrane problem (u^0, v^0). Bending-extension coupling means that all five variables will have to be found simultaneously, which is what finite element analysis (FEA) software codes do for every case, whether the problem is coupled or not.

The equilibrium equations of plates can be derived by using the principle of virtual work (PVW, see (1.16)). Furthermore, the governing equations can be derived by substituting the constitutive equations (3.8) into the equilibrium equations.

Simply Supported Boundary Conditions in Plates

Composite plates with coupling effects may have bending, shear, and membrane deformations coupled even if loaded by pure bending, pure shear, or pure in-plane loads (see p. 141 in [1]). While the term *simply supported* always means to restrict the transverse deflection $w(x, y)$, it does not uniquely define the boundary conditions on the in-plane displacements u_n and u_s, normal and tangent to the boundary, respectively. In the context of analytical solutions, it is customary to restrict either u_n or u_s. Therefore, the following possibilities exist

- SS-1: $w = u_s = \phi_s = 0; N_n = \widehat{N}_n; M_n = \widehat{M}_n$
- SS-2: $w = u_n = \phi_s = 0; N_{ns} = \widehat{N}_{ns}; M_n = \widehat{M_n}$

In type SS-1, a normal force and a moment are specified. In SS-2, a shear force and a moment are specified. If the laminate does not have bending-extension coupling, and the analysis is geometrically linear, transverse loads will not induce u_n. The naming convention for the rotations is the same as that used for moment resultants in Figure 3.3, where a subscript $_n$ indicates the direction normal to the edge of the shell, and a subscript $_s$ indicates the direction tangent to the edge (see also [10, Figure 6.2.1]). Furthermore $\widehat{\ }$ represents a fixed known value that may or may not be zero.

3.1.2 Kirchhoff Theory

Historically, Kirchhoff theory was preferred because the governing equations can be written in terms of only one variable, the transverse deflection of the shell w_0. In the pre-information age, it was easier to obtain analytical solutions in terms of only one variable rather than in terms of the three variables needed in FSDT. This means

that a wealth of closed form design equations and approximate solutions exist in engineering design manuals which are based on Kirchhoff theory [11]. Such simple design formulas can still be used for preliminary design of composite shells if we are careful and we understand their limitations. Metallic shells were and still are commonly modeled with Kirchhoff theory. The FSDT governing equations can be reduced to Kirchhoff governing equations, and closed form solutions can be found, as shown in [10].

In Kirchhoff theory the intralaminar shear strain is assumed to be zero. From the last two equations in (3.6) we get

$$\begin{aligned} \phi_x &= \frac{\partial w_0}{\partial x} \\ \phi_y &= \frac{\partial w_0}{\partial y} \end{aligned} \tag{3.10}$$

and introducing them into the first three equations in (3.6) we get

$$\begin{aligned} \epsilon_x(x,y,z) &= \frac{\partial u_0}{\partial x} - z\frac{\partial^2 w_0}{\partial x^2} = \epsilon_x^0 + z\kappa_x \\ \epsilon_y(x,y,z) &= \frac{\partial v_0}{\partial y} - z\frac{\partial^2 w_0}{\partial y^2} = \epsilon_y^0 + z\kappa_y \\ \gamma_{xy}(x,y,z) &= \frac{\partial u_0}{\partial y} + \frac{\partial v_0}{\partial x} - 2z\frac{\partial^2 w_0}{\partial x \partial y} = \gamma_{xy}^0 + z\kappa_{xy} \end{aligned} \tag{3.11}$$

Notice that the variables ϕ_x, ϕ_y have been eliminated and Kirchhoff theory only uses three variables $u_0(x,y)$, $v_0(x,y)$, and $w_0(x,y)$. This makes analytical solutions easier to find, but numerically Kirchhoff theory is more complex to implement. Since second derivatives of w_0 are needed to write the strains, the weak form (2.30) will have second derivatives of w_0. This will require that the interpolation functions (see Section 2.1.4) have C^1 continuity. That is, the interpolation functions must be such that not only the displacements but also the slopes be continuous across element boundaries. In other words, both the displacement w_0 and the slopes $\partial w_0/\partial x$, $\partial w_0/\partial y$ will have to be identical at the boundary between elements when calculated from either element sharing the boundary. This is difficult to implement.

Consider the case of beam bending. The ordinary differential equation (ODE) with an applied distributed load $\widehat{q}(x)$ is

$$EI\frac{d^4 w_0}{dx^4} = \widehat{q}(x) \tag{3.12}$$

The weak form is obtained as in (2.3)

$$0 = \int_{x_A}^{x_B} v\left[-EI\frac{d^4 w_0}{dx^4} + \widehat{q}(x)\right] dx \tag{3.13}$$

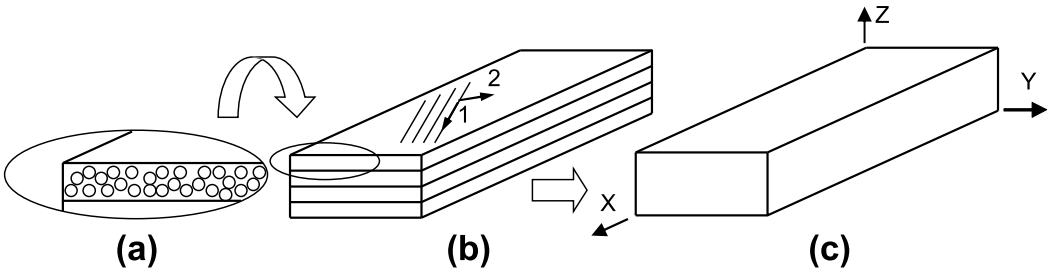

Figure 3.4: (a) Micromechanics, (b) lamina level, and (c) laminate level approach.

Integrating by parts twice

$$
\begin{aligned}
0 &= \int_{x_A}^{x_B} \frac{d^2v}{dx^2} EI \frac{d^2w_0}{dx^2} dx + vEI\frac{d^3w_0}{dx^3} - \frac{dv}{dx} EI \frac{d^2w_0}{dx^2} - \int_{x_A}^{x_B} v\widehat{q}(x)dx \\
0 &= B(v, w_0) + [vQ_x]_{x_A}^{x_B} - \left[\frac{dv}{dx} M_x\right]_{x_A}^{x_B} - \int_{x_A}^{x_B} v\widehat{M}(x)dx \\
0 &= B(v, w_0) + L(v)
\end{aligned} \tag{3.14}
$$

When the elements are assembled as in Section 2.1.6, it turns out that adjacent elements i and $i+1$ that share a node have identical deflection but opposite shear force Q_x and bending moment M_x at their common node, as follows

$$
\begin{aligned}
w^i &= w^{i+1} \\
Q^i &= -Q^{i+1} \\
M^i &= -M^{i+1}
\end{aligned} \tag{3.15}
$$

For the shear forces to cancel as in (2.24), it is only required to have $v^i = v^{i+1}$, which is satisfied by C^0 continuity elements having $w^i = w^{i+1}$ at the common node. For the bending moments to cancel as in (2.24), it is required that $dw^i/dx = dw^{i+1}/dx$. This can only be done if the elements have C^1 continuity. That is, the slopes $dw^i/dx = dw^{i+1}/dx$ must be identical at the common node. Such elements are difficult to work with ([12, page 276]).

In FSDT theory, only first derivatives are used in the strains (3.6). So, the weak form (2.30) has only first derivatives and, like (2.24), all the internal generalized forces cancel at common nodes with only C^0 element continuity.

3.2 Finite Element Analysis of Laminates

Deformation and stress analysis of laminated composites can be done at different levels (Figure 3.4). The level of detail necessary for description of the material depends on the level of post-processing desired.

When a great level of detail is necessary (Figure 3.4.a), the strain and stress are computed at the constituent level, i.e., fiber and matrix. In this case, it is

necessary to describe the microstructure, including the fiber shape and geometrical distribution, and the material properties of the constituents. More details are given in Chapter 6 where micromechanical modeling is used to generate properties for any combination of fibers and matrix. Also, when the composite material is a woven fabric, or the laminate is very thick, or when studying localized phenomena such as free edges effects (Chapter 5), the composite should be analyzed as solid, as shown in Chapter 5. However, it must be noted that most of the laminated structures can be analyzed using the plates and shell simplifications explained in Section 3.1.

At the other end of the spectrum (Figure 3.4.c), the composite material can be considered as a homogeneous equivalent material. In this case, its structural behavior can be analyzed by using orthotropic properties shown in Chapter 1. If the whole laminate is analyzed as a homogeneous equivalent shell, using the macroscale level approach (Figure 3.4.c), the stress distribution in the laminate cannot be obtained. However, this very simple description of the laminate is sufficient when only displacements, buckling loads and modes, or vibration frequencies and modes are required. In these cases, only the laminate stiffness (3.8) is needed (see Section 3.2.5). In certain cases, even a simpler material description will suffice. For example, when the laminate is only unidirectional, or if the laminate is balanced and symmetric (see [1, Section 6.3]), the laminate can be modeled as a single lamina of orthotropic material (Section 3.2.6).

In most cases, stress and strains need to be calculated for every lamina in the laminate. Then, the actual laminate stacking sequence (LSS) must be input to the program (Section 3.2.7). In this case, the elastic properties of each lamina, as well as thickness and fiber orientation of every lamina must be given. This method is usually called the mesoscale level approach (Figure 3.4.b).

A unidirectional lamina can be satisfactorily approximated as being transversely isotropic. Then, it suffices to use $E_3 = E_2$, and $G_{23} = E_3/2(1 + \nu_{23})$ in the equations for an orthotropic material. The elastic properties of a unidirectional lamina can be computed using micromechanics (Chapter 6) or with experimental data of unidirectional laminates. Material properties of some unidirectional composites are shown in Table 3.1.

In the analysis of most composite structures, it is usual to avoid the micromechanics approach and to obtain experimentally the properties of the unidirectional lamina, or even the whole laminate. However, the experimental approach is not ideal because a change of constituents or fiber volume fraction during the design process invalidates all the material data and requires a new experimental program for the new material. It is better to calculate the elastic properties of the lamina using micromechanics formulas, using software such as [9] (see also Section 6.1). Unfortunately, micromechanics formulas are not accurate to predict strength, so experimental work cannot be ruled out completely.

In summary, laminate properties can be specified in two ways:

- by the constitutive matrices A, B, D, and H, or
- by specifying the laminate stacking sequence (LSS) and properties for every lamina.

Table 3.1: Material properties of unidirectional carbon/epoxy composites

Property[2]	**Unit**	**AS4D/9310**	**T300/5208**
E_1	[GPa]	133.86	136.00
$E_2 = E_3$	[GPa]	7.706	9.80
$G_{12} = G_{13}$	[GPa]	4.306	4.70
G_{23}	[GPa]	2.76	4.261
$\nu_{12} = \nu_{13}$		0.301	0.280
ν_{23}		0.396	0.150
V_f		0.55	
ρ	[g/cm^3]	1.52	1.54
α_1	[$10^{-6}/°C$]	0.32	
α_2	[$10^{-6}/°C$]	25.89	
F_{1t}	[MPa]	1830	1550
F_{1c}	[MPa]	1096	1090
$F_{2t} = F_{3t}$	[MPa]	57	59
$F_{2c} = F_{3c}$	[MPa]	228	207
F_4	[MPa]	141	128
F_6	[MPa]	71	75

When the constitutive matrices A, B, D, H, of the laminate are used to define the laminate, the shell element cannot distinguish between different laminas. It can only relate generalized forces and moments to generalized strains and curvatures. On the other hand, laminated shell elements have the capability to compute the laminate properties using the Laminate Stacking Sequence (LSS) and the laminas properties.

3.2.1 Element Types

In commercial finite element codes, various plates and shells theories are implemented and differentiated by element types, called shell elements [13, 14]. The main shell elements available in ANSYS® for the analysis of composite materials/structures are shown in Table 2.1.

Shell elements allow one to model thin to moderately thick shells, down to a side-to-thickness ratio of 10. While some of them have 3 or 4 nodes, others have 8 nodes, thus using interpolation functions of higher degree. Shell elements are defined in 3D space and have 5 or 6 degrees of freedom (DOF) at each node (translations in the nodal x, y, and z directions and rotations about the nodal x, y, and z axis). The 6th DOF (rotation about the z axis) is included in the shell formulation to allow modeling of folded plates, but it would not be necessary if the shell surface is smooth.

Modeling of different types of laminates with various levels of detail is explained in the next few sections.

[2] F_4 was calculated with [1, Eq. 4.109] assuming the angle of the fracture plane to be $\alpha_0 = 54°$.

3.2.2 Sandwich Shells

For a sandwich shell, the core is much softer that the faces, and the transverse shear deformations are significant regardless of the total thickness of the shell. Conventional shell elements may not have the shear flexibility required. In ANSYS, elements SHELL181 and SHELL281 model the transverse shear deflection using an energy equivalence method, which is recommended for sandwich shells. See Example 3.7.

3.2.3 Nodes and Curvature

Typically, four node elements are flat, but since R14.0, ANSYS SHELL181 is capable of recovering the initial shell curvature from the mesh. For curved shells, it is better to use eight node elements such as SHELL281. The degenerate triangular option of SHELL181 is not recommended but can be used if needed as filler elements if the mesh generation algorithm requires it. However, SHELL281 is acceptable when used as a triangle.

3.2.4 Drilling Rotation

Conventional shell elements are based on shell theory, which constrains the 3D continuum deformations according to some kinematic assumptions, such as Kirchhoff, FSDT, or one of many others. In continuum theory, the deformation of a point in 3D can be described in terms of the relative displacements of two points, thus requiring six degrees of freedom (three per point). Both Kirchhoff and FSDT theories formally reduce the requirement to three displacements and two in-plane rotations at a single point. The two rotations ϕ_x, ϕ_y, are rotations of the normal to the reference surface. These are called in-plane rotations because the rotation vectors lie on the surface of the shell. For a smoothly curved or flat shell, there is no need of tracking the rotation of the normal around itself ϕ_z. This last rotation is called drilling rotation. However, if the shell has a fold, an in-plane rotation on one side of the fold corresponds to a drilling rotation on the other side (Figure 3.5). Thus, to enforce compatibility of displacements, the drilling rotations become necessary. Since elements having 5 DOF do not have drilling rotation, they are suited to model smoothly curved shells but not folded shells.

3.2.5 A-B-D-H Input Data for Laminate FEA

As previously mentioned, macroscale level (laminate level) analysis is adequate if only deflections, modal analysis, or buckling analysis are to be performed, with no requirement for detailed stress analysis. Then it is not necessary to specify the laminate stacking sequence (LSS), the thickness, and the elastic properties of each lamina of the laminate. Only the elastic laminate properties (A, B, D, H, matrices) defined in (3.9) are required. This is convenient because it allows one to input the aggregate composite material behavior with few parameters. The reduction of

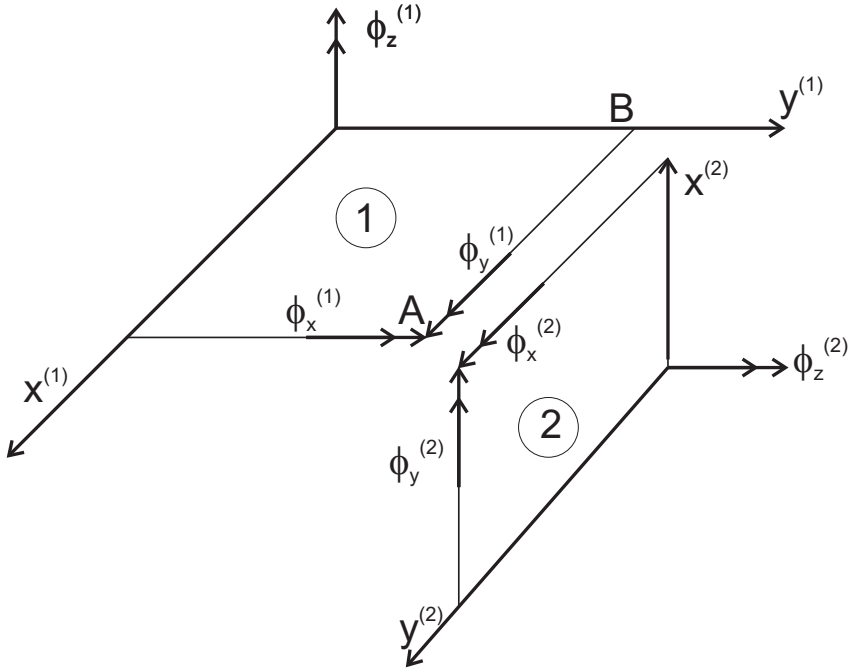

Figure 3.5: Exploded view of a plate folded along AB. Drilling rotations $\phi_z^{(1)}$ and $\phi_z^{(2)}$ associated to elements 1 and 2, respectively.

the complexity of the input data allows modeling of laminates with an unlimited number of laminas, using only four matrices.

When the $A, B, D, H,$ matrices are used to define the finite element analysis, the computer model knows the correct stiffness but it does not know the LSS. Therefore, the software can compute the deformation response (including buckling and vibrations) and even the strain distribution through the thickness of the shell, but it cannot compute the stress components because it does not know where the lamina material properties change from lamina to lamina.

The A, B, D, H input data can be found by using (3.9) or [9]. Then, these are input into the finite element software, as illustrated in Example 3.1.

Example 3.1 *Consider a simply supported square plate* $a_x = a_y = 2000$ *mm, thickness* $t = 10$ *mm laminated with AS4D/9310 (Table 3.1) in a* $[0/90]_n$ *configuration. Tabulate the center deflection perpendicular to the plate surface when the number of laminas is* $n = 1, 5, 10, 15, 20$. *The plate is loaded in compression with and edge load* $N_x = -1$ *N/mm and* $(N_y = N_{xy} = M_x = M_y = M_{xy} = 0)$. *Use symmetry to model 1/4 of the plate. Generate the* $A, B, D,$ *and* H *matrices and enter them into ANSYS.*

Solution to Example 3.1 *Due to the symmetry of the plate, only 1/4 of it will be modeled. The matrices* $A, B, D, H,$ *are calculated using (3.9), which are implemented in CADEC [9]. In ANSYS, SHELL181 and SHELL281 allow data input in the form of* $A, B, D, H,$ *matrices using preintegrated general shell section via* `SECTYPE,1,GENS`. *Then, the laminate stiffness matrices must be placed in the input file using four matrices called* $A, B, D, E,$ *as follows*

```
SSPA,711563,23328.8,0,711563,0,43600                ! A11,A21,A31,A22,A32,A33
SSPB,-1.58515e+006,0,0,1.58515e+006,0,0             ! B11,B21,B31,B22,B32,B33
SSPD,5.92969e+006,194407,0,5.92969e+006,0,363333    ! D11,D21,D31,D22,D32,D33
SSPE,29666.7,0,29666.7                              ! H11,H21,H22
SLIST                                               ! List A,B,D,H submatrices
```

In this case the input data does not need material properties. The complete input file, which is available on the Web site [5], is listed below for $n = 1$. See Appendix C for an introduction to the software interface.

Note that in ANSYS a ***pressure*** *applied on the boundary acts* ***on*** *the element; that is, opposite to the outside normal to the boundary and thus a compressive edge load in this case is applied as* `SFL,2,PRES,1.0`.

```
/TITLE,Simply Supported [0/90] Plate Nx=1 N/mm - SHELL281
! Material is AS4D/9310 - laminate [0/90]n, n=1
/UNITS,MPA              ! Units are in mm, MPa, and Newtons
/PREP7                  ! Pre-processor module
! This input data does not need material properties

ET,1,SHELL281          ! Chooses SHELL281 element for analysis
SECTYPE,1,GENS         ! Use preintegrated general shell section (ABDH matrix)

! ABDH matrix definition
SSPA,711563,23328.8,0,711563,0,43600                ! A11,A21,A31,A22,A32,A33
SSPB,-1.58515e+006,0,0,1.58515e+006,0,0             ! B11,B21,B31,B22,B32,B33
SSPD,5.92969e+006,194407,0,5.92969e+006,0,363333    ! D11,D21,D31,D22,D32,D33
SSPE,29666.7,0,29666.7                              ! H11,H21,H22
SLIST                                               ! List A,B,D,H submatrices

! Geometry and mesh
RECTNG,0,1000,0,1000    ! Creates a rectangle with x=1 m and y=1 m
ESIZE,100               ! Element size 100 mm
AMESH,all               ! Mesh the area
FINISH                  ! Exit pre-processor module

/SOLU                   ! Solution module
ANTYPE,STATIC           ! Set static analysis
DL,2,1,uz,0             ! Impose Simple Supported BC
DL,3,1,uz,0
DL,1,1,symm             ! Impose Symmetry BC
DL,4,1,symm
!d,all,rotz             ! Constraint rotations about z axes (optional)

SFL,2,PRES,1.0          ! Apply uniform pressure in N/mm

SOLVE                   ! Solve current load state
FINISH                  ! Exit solution module

/POST1                  ! Post-processor module
PLDISP                  ! Display deformed shape
PLNSOL,u,z              ! Display contour of displacements z
```

```
!plesol,s,x              ! Notice this cannot be done, try it
FINISH                   ! Exit post-processor module
```

The solution is tabulated in Table 3.2, using `PLDISP`*. Bending extension coupling produces a lateral deflection, which diminishes as the number of laminas grow.*

Table 3.2: Lateral deflection vs. number of laminas in Example 3.1

n	δ [mm]
1	0.2191
5	0.0211
10	0.0104
15	0.0069
20	0.0052

3.2.6 Equivalent Orthotropic Input for Laminate FEA

Some FEA codes do not have laminated elements and do not accept the A, B, D, and H matrices as explained in Section 3.2.5. However, if they have orthotropic elements, it is still possible to perform deformation, vibration, and buckling analysis for laminated composites, as it is shown in this section.

Unidirectional Laminate FEA

Standard shell elements, even if they are not laminated, can be used to model a unidirectional laminate and still obtain correct results of displacements, strains, and stress. The geometry of shells is a surface that represents the mid-surface of the real shell, located halfway through the thickness. The positive thickness coordinate points along a normal to the shell mid-surface (local z-direction which coincides with the 3-direction). This is the normal definition of shells and it is used in shell elements, as shown in Example 3.2.

Example 3.2 *Use ANSYS to model a simply supported rectangular plate with dimensions $a_x = 4000\ mm$, $a_y = 2000\ mm$, thickness $t = 10\ mm$. Apply a uniform transverse load $q_0 = 0.12 \times 10^{-3}\ MPa$. The material is a unidirectional laminate AS4D/9310 (Table 3.1), with the fibers oriented in the x-direction. Determine the deflection of the center point of the plate. This example is continued in Example 3.8.*

Solution to Example 3.2 *The thickness coordinate is eliminated from the governing equations so that the 3D problem simplifies to 2D. In the process, the thickness becomes a parameter, which is known and supplied to the modeling software. Most software packages differentiate between material properties and parameters but both are supplied as known input data. For example, the shell thickness is supplied to ANSYS as section data (*`SECDATA`*), while material properties are entered separately with* `UIMP`*.*

SHELL281, an 8-node shell element, is used in this example. Symmetry with respect to the x-z and y-z planes is used to model 1/4 of the plate. The APDL file commands, also available in [5, FEAcomp_Ex302.inp], are shown below

```
/TITLE,Simply Supported Plate under q=0.12e-3 MPa - SHELL281
! Material is UD AS4D/3100 Carbon/Epoxy - 8 laminas 1.25 mm thick
/UNITS,MPA              ! Units are in mm, MPa, and Newtons

/PREP7                  ! Pre-processor module
! Material properties FOR AS4D/9110 orthotropic laminate
UIMP,1,EX,EY,EZ,133.86E3,7.706E3,7.706E3
UIMP,1,GXY,GYZ,GXZ,4.306E3,2.76E3,4.306E3
UIMP,1,PRXY,PRYZ,PRXZ,0.301,0.396,0.301

ET,1,SHELL281            ! Chooses SHELL281 element for analysis
SECTYPE,1,SHELL
SECDATA,10,1,0           ! Thickness=10mm, Material 1, Layer 0 deg

! Geometry and mesh
RECTNG,0,2000,0,1000    ! Creates a rectangle with x=2 m and y=1 m
ESIZE,250               ! Element size 250 mm
AMESH,ALL               ! Mesh the area

FINISH                  ! Exit pre-processor module

/SOLU                   ! Solution module
ANTYPE,STATIC           ! Set static analysis
DL,2,1,uz,0             ! Impose Simple Supported BC
DL,3,1,uz,0
DL,1,1,symm             ! Impose Symmetry BC
DL,4,1,symm
!d,all,rotz             ! Constraint rotations about z axes (optional)

SFA,ALL,2,PRES,1.2E-4,  ! Apply uniform pressure in MPa

SOLVE                   ! Solve current load state
FINISH                  ! Exit solution module

/POST1                  ! Post-processor module
PLDISP,1                ! plots displaced plate
PLNSOL,u,z              ! contour plot of z direction displacements
PLESOL,s,x              ! contour plot of x direction stress
FINISH                  ! Exit post-processor module
```

The maximum deflection is 17.47 *mm at the center of the plate, using* `PLDISP,1`.

Symmetric Laminate FEA

If a multidirectional laminate is balanced and symmetric, the apparent laminate orthotropic properties can be found as explained in Section 1.15. The apparent laminate properties represent the stiffness of an equivalent (fictitious) orthotropic plate that behaves like the actual laminate under in-plane loads. These apparent properties should not be used to predict bending response. When the only important response is bending, e.g., a thick cantilever plate under bending, the formulation

shown in [1, (6.33)] should be used to obtain the apparent laminate properties. However, in most structural designs using composite shells, the laminate works under in-plane loads and the formulation in Section 1.15 should be used.

If the laminate is symmetric but not balanced, the axes of orthotropy are rotated with respect to the laminate coordinate system, but still the laminate is equivalent to an orthotropic material as per Section 1.15. For example, a unidirectional laminate oriented at an angle θ with respect to global axes, should be modeled on a coordinate system oriented along the fiber direction (see Section 3.2.10).

Example 3.3 *Use ANSYS to model a simply supported rectangular plate with dimensions* $a_x = 2{,}000\ mm$, $a_y = 2{,}000\ mm$, *for a laminate* $[\pm 45/0]_S$. *Apply a tensile edge load* $N_x = 200\ N/mm$. *Find the maximum horizontal displacement. Each lamina is* 1 *mm thick with the following properties*

$$E_1 = 37.88\ GPa \quad G_{12} = 3.405\ GPa \quad \nu_{12} = 0.299$$
$$E_2 = 9.407\ GPa \quad G_{23} = 3.308\ GPa \quad \nu_{23} = 0.422$$

Solution to Example 3.3 *Since the laminate is balanced symmetric, compute the averaged laminate properties* E_x, E_y, *and so on using Section 1.15, for example using the following MATLAB® code (available in [5, Ex_3_3.m])*

```
function Ex33
    % Example 3.3 laminate stiffness as per section 1.15
    clc
    % G23 = E2/2/(1+nu23)
    % Cprime (1.92) calculated with
    % http://www.cadec-online.com/Chapters/Chapter5/3DConstitutiveEquations
    % /StiffnessMatrix.aspx
    E1  = 37.88E3;
    E2  =  9.407E3;     E3  = E2;
    G12 =  3.405E3;     G13 =  G12;
    nu12=  0.299;       nu13=  nu12;
    nu23=  0.422;
    G23 = E2/2/(1+nu23);

    % (1.104)
    Sprime = [
        1/E1, -nu12/E1, -nu13/E1,0,0,0;
        -nu12/E1, 1/E2, -nu23/E2,0,0,0;
        -nu13/E1, -nu23/E2, 1/E3,0,0,0;
        0,0,0,1/G23,0,0;
        0,0,0,0,1/G13,0;
        0,0,0,0,0,1/G12];

    Cprime = Sprime^-1;

    theta = [45,-45,0];
    thickness = [1,1,1];
    laminateThickness = sum(thickness);
    C = zeros(6);
    for i=1:length(theta);
```

```
        [T,Tbar] = RotationMatrix3D(theta(i));
        C = C + Tbar*Cprime*Tbar*thickness(i)/laminateThickness; % (1.102)
    end
    S = C^-1;       % (1.103)
    Ex  =1/S(1,1)   % (1.105)
    Ey  =1/S(2,2)
    Ez  =1/S(3,3)
    Gxy =1/S(6,6)
    Gyz =1/S(4,4)
    Gxz =1/S(5,5)
    PRxy=-S(2,1)/S(1,1)
    PRyz=-S(3,2)/S(2,2)
    PRxz=-S(3,1)/S(1,1)
end
```

The function RotationMatrix3D is given in Example 1.6. Then, the MATLAB code yields

$$\begin{array}{lll} E_x = 13.825\ GPa & G_{xy} = 24.637\ GPa & \nu_{xy} = 0.832 \\ E_y = 8.007\ GPa & G_{yz} = 3.340\ GPa & \nu_{yz} = 0.235 \\ E_z = 10.220\ GPa & G_{xz} = 3.372\ GPa & \nu_{xz} = 0.069 \end{array}$$

The APDL command file is shown below and also available in [5, FEAcomp_Ex303]. Note that in ANSYS a pressure applied on the boundary acts on the element; that is, opposite to the outside normal to the boundary and thus a tensile load in this case is applied as `SFL,2,PRES,-200.0`.

```
/TITLE,Simply Supported Plate Nx=200 N/mm - equivalent [45/-45/0]s
! [45/-45/0]s laminate of E-Glass/Vinyl, vf=0.5 and th=1*6 mm
! quarter plate with symmetry conditions
/UNITS,MPA              ! Units are in mm, MPa, and Newtons

/PREP7                  ! Pre-processor module
! Equivalent orthotropic material properties for the LAMINATE
UIMP,1, EX, EY, EZ, 13.825E3, 8.007E3, 10.220E3
UIMP,1, GXY, GYZ, GXZ, 24.636E3, 3.340E3, 3.372E3
UIMP,1, PRXY, PRYZ, PRXZ, 0.832, 0.232, 0.069

ET,1,SHELL281           ! Chooses Shell 281 element for analysis
SECTYPE,1,SHELL         ! Section shell set #1
SECDATA,1,1,45          ! 1st layer: mat. #1,   45 deg, Th=1.0 mm
SECDATA,1,1,-45         ! 2nd layer: mat. #1,   -45 deg, Th=1.0 mm
SECDATA,1,1,0           ! 3rd layer: mat. #1,   0 deg, Th=1.0 mm
SECDATA,1,1,0           ! Same layers in symmetrical order
SECDATA,1,1,-45
SECDATA,1,1,45

! Geometry and mesh
RECTNG,0,1000,0,1000    ! Creates a rectangle with x=1 m and y=1 m
ESIZE,100               ! Element size 100 mm
AMESH,all               ! Mesh the area
/PNUM,LINE,1
```

```
LPLOT
FINISH                  ! Exit pre-processor module

/SOLU                   ! Solution module
ANTYPE,STATIC           ! Set static analysis
DL,2,1,uz,0             ! Impose Simple Supported BC
DL,3,1,uz,0
DL,1,1,symm             ! Impose Symmetry BC
DL,4,1,symm
!D,ALL,ROTZ             ! Constraint rotations about z axes (optional)

SFL,2,PRES,-200         ! Apply uniform linear load in N/mm

SOLVE                   ! Solve current load state
FINISH                  ! Exit solution module

/POST1                  ! Post-processor module
/VIEW,,1,1,1
!PLDISP,2               ! Plots displaced plate
PLNSOL,u,x              ! Contour plot of x direction displacements
!plesol,s,x             ! Notice the stress results are incorrect
FINISH                  ! Exit post-processor module
```

The resulting maximum horizontal displacement on a quarter-plate model is $0.996\ mm$ *at the edge of the plate. The planes* $x = 0$ *and* $y = 0$ *are not symmetry planes for a* $[\pm 45/0]_S$ *but once the laminate is represented by equivalent orthotropic properties, as is done in this example, the lack of symmetry at the lamina level is lost and it does not have any effect on the mid-surface displacements. Therefore, one-quarter of the plate represents well the entire plate as long as no stress analysis is performed. Furthermore, displacement and mid-surface strain analysis can be done with the laminate replaced by an equivalent orthotropic material. However, even if the full plate were to be modeled, the stress values in the equivalent orthotropic material are not the actual stress values of the laminate. While the material analyzed in this example is not homogeneous, but laminated, the material in Example 3.2 is a homogeneous unidirectional material. Therefore, the stress values are not correct in this example but they are correct in Example 3.2.*

Asymmetric Laminate FEA

If the laminate is not symmetric, bending-extension coupling must be considered. Strictly speaking, such material is not orthotropic and should not be modeled with an equivalent laminate material. Even then, if only orthotropic shell elements are available and the bending-extension coupling effects are not severe, the material could be approximated by an orthotropic material by neglecting the matrices B and D. The ratios defined in [1, (6.37)–(6.38)] can be used to assess the quality of the approximation obtained using apparent elastic properties. Care must be taken for unbalanced laminates that the A and H matrix are formulated in a coordinate system coinciding with the axes of orthotropy of the laminate.

3.2.7 LSS for Multidirectional Laminate FEA

For computation of strain and stress at the mesoscale (lamina level), it is necessary to know the description of the laminate and the properties of each lamina. The description of the multidirectional laminate includes the LSS, which specifies the angle of each lamina with respect to the x-axis of the laminate, the thickness, and the elastic material properties of each lamina. Then, the software computes the matrices A, B, D, and H internally. In this way, the software can compute the stress components in each lamina. This approach is illustrated in the following example.

Example 3.4 *Consider a simply supported square plate $a_x = a_y = 2000\ mm$, $t = 10\ mm$ thick, laminated with AS4D/9310 (Table 3.1) in a $[0/90/\pm 45]_S$ symmetric laminate configuration. The plate is loaded with a tensile load $N_x = 100\ N/mm$ and ($N_y = N_{xy} = M_x = M_y = M_{xy} = 0$). Compute maximum displacement at the edge of the plate.*

Solution to Example 3.4 *The problem can be solved using shell elements SHELL181 or SHELL281. Other than the element selection, the models are identical. Note the LSS is given starting at lamina #1 at the bottom. Although a quarter model with symmetry could be used, a full plate is modeled to show how to constrain the model from experiencing rigid body motion.*

```
/TITLE,Simply Supported [0/90/45/-45]s - uniform load - SHELL181
! Material is AS4D/9310 - [0/90/45/-45]s, Th=1.25 mm per lamina
/UNITS,MPA              ! Units are in mm, MPa, and Newtons

/PREP7                  ! Pre-processor module
! Material properties FOR AS4D/9310 orthotropic laminate
UIMP,1,EX,EY,EZ,133.86E3,7.706E3,7.706E3
UIMP,1,GXY,GYZ,GXZ,4.306E3,2.76E3,4.306E3
UIMP,1,PRXY,PRYZ,PRXZ,0.301,0.396,0.301

ET,1,SHELL181           ! Chooses SHELL181 element for analysis
KEYOPT,1,3,2            ! Set KEYOPT(3)=2, Full integration
                        ! (recommended for SHELL 181/composites)
KEYOPT,1,8,1            ! Set KEYOPT(8)=1, Store data for all laminas
SECTYPE,1,SHELL,,La1    ! Section shell set #1, [0/90/45/-45]s, label=La1
SECDATA, 1.25,1,0.0,3   ! 1st lamina: mat. #1,   0 deg, Th=1.25 mm
SECDATA, 1.25,1,90,3    ! 2nd lamina: mat. #1,  90 deg, Th=1.25 mm
SECDATA, 1.25,1,45,3    ! 3nd lamina: mat. #1, +45 deg, Th=1.25 mm
SECDATA, 1.25,1,-45,3   ! 4rt lamina: mat. #1, -45 deg, Th=1.25 mm
SECDATA, 1.25,1,-45,3   ! Same laminas in symmetrical order
SECDATA, 1.25,1,45,3
SECDATA, 1.25,1,90,3
SECDATA, 1.25,1,0.0,3
SECOFFSET,MID           ! Nodes on the laminate middle thickness

! Geometry and mesh
RECTNG,-1000,1000,-1000,1000    ! Creates a rectangle with x=2 m and y=2 m
ESIZE,250               ! Element size 250 mm
```

```
AMESH,all               ! Mesh the area
FINISH                  ! Exit pre-processor module

/SOLU                   ! Solution module
ANTYPE,STATIC           ! Set static analysis
DL,2,1,uz,0             ! Impose Simple Supported BC
DL,3,1,uz,0
DL,1,1,uz,0
DL,4,1,uz,0
!D,ALL,ROTZ             ! Constraint rotations about z axes (optional)
CEN_NODE=NODE(0,0,0)    ! Center node
D,CEN_NODE,UX ! Constraint nodes to avoid rigid body motion
LEFT_NODE=NODE(-1000,0,0)  ! Middle node in left edge
D,LEFT_NODE,UY
RIGH_NODE=NODE(1000,0,0) ! Middle node in right edge
D,RIGH_NODE,UY

SFL,2,PRES,-100         ! Apply uniform edge pressure in N/mm
SFL,4,PRES,-100
SOLVE                   ! Solve current load state
FINISH                  ! Exit solution module

/POST1                  ! Post-processor module
PLDISP,1                ! Display the deformed plate
FINISH                  ! Exit post-processor module
```

The maximum displacement at the edge of the plate is 0.206 *mm.*

Note that `SECOFFSET,MID` *is used to place the nodes on the mid-surface. The deformation of the lamina is in-plane only because the laminate is symmetric, balanced, and in-plane loaded. The distributed edge load is applied at the mid-surface. However, the same model is re-executed with* `SECOFFSET,BOT` *(nodes on bottom face) or with* `SECOFFSET,TOP` *(nodes on top face), the edge load will be applied on the bottom edge or on the top edge of the laminate. In these cases, out-plane deformations will appear.*

Other model definition aspects that can be controlled include: the position of the bottom and top surfaces of the laminate (i.e., the direction of the vector normal to the surface of the shell), the relative position of the shell surface through the real laminate thickness (at the bottom, at the middle, or at the top), the orientation of laminate reference axis (as is shown in Section 3.2.10), and so on.

3.2.8 FEA of Ply Drop-Off Laminates

Sometimes it is convenient to set the reference surface at the bottom (or top) of the shell. One such case is when the laminate has ply drop-offs, as shown in Figure 3.6. When the design calls for a reduction of laminate thickness, plies can be gradually terminated from the thick to the thin part of the shell. As a rule of thumb, ply drop-off should be limited to a 1:16 to 1:20 ratio ($Th : L$ ratio in Figure 3.6) unless detailed analysis and/or testing supports a steeper drop-off ratio. For this case, it is convenient to specify the geometry of the smooth surface, or tool surface.

Then, every time a ply or set of plies is dropped, the material and thickness for those elements is changed. This is illustrated in the next examples. Not all software

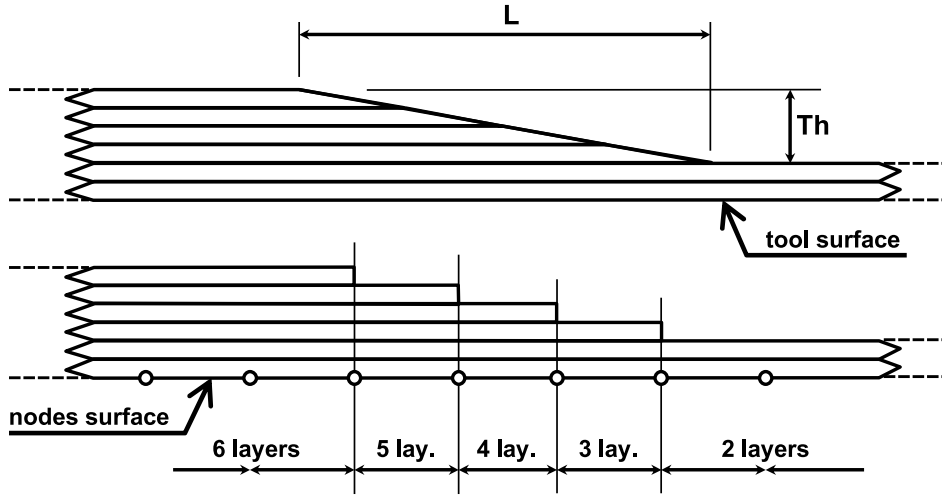

Figure 3.6: Ply drop-off of length (L) and thickness (Th) and finite element model simplifications.

has this capability and it may be necessary to assume that the mid-surface is smooth while in reality only the tool surface is smooth. As long as the thickness is small compared to the other two dimensions of the structure, such assumption is unlikely to have a dramatic effect in the results of a global analysis, such as deformation, buckling, and even membrane stress analysis. The exact description of the thickness geometry begins to play a role when detailed 3D stress analysis of the ply drop-off region is required, but at that point, a 3D local model is more adequate.

Example 3.5 *A ply drop-off is defined between the laminate A,* $[90/0]_S$*, and the laminate B,* $[90/0]$*. The ply drop-off ratio is 1:20 The lamina thickness is* 0.75 *mm. Consider a composite strip* 120 *mm long and* 100 *mm wide under tension* $N = 10$ *N/mm applied to the bottom edges on the strip. Use symmetry to model 1/2 of the tape. Visualize and report the maximum transverse deflection.*

Solution to Example 3.5 *Using shell elements SHELL181, three different sections are defined, one for A, one for B, and one section to model the ply drop-off between them.*

The thickness of the drop-off is $0.75 \times 2 = 1.5$ *mm. With a ply drop-off ratio 1:20, the length of the ply drop-off is* $1.5 \times 20 = 30$ *mm. Every* 30 *mm there is a section change.*

The bottom lamina is designated as lamina #1, and additional laminas are stacked from bottom to top in the positive normal direction of the element coordinate system. The APDL code is shown below and also available in [5, FEAcomp_Ex305.inp].

```
/TITLE,Tape with Ply Drop-off between [90/0]s and [90/0]
! Material is AS4D/9310 - Th=0.75 mm per lamina - SHELL181
/UNITS,MPA              ! Units are in mm, MPa, and Newtons

/PREP7                  ! Pre-processor module
! Material properties FOR AS4D/9310 orthotropic laminate
UIMP,1,EX,EY,EZ,133.86E3,7.706E3,7.706E3
UIMP,1,GXY,GYZ,GXZ,4.306E3,2.76E3,4.306E3
```

```
UIMP,1,PRXY,PRYZ,PRXZ,0.301,0.396,0.301

ET,1,SHELL181           ! Chooses SHELL181 element for analysis

KEYOPT,1,3,2            ! Set KEYOPT(3)=2, Full integration
                        ! (recommended for SHELL181/composites)
SECTYPE,1,SHELL,,A      ! Section shell set #1, [90/0]s, A
SECDATA, 0.75,1,90,3    ! 1st lamina: mat. #1, 90 deg, Th=0.75 mm
SECDATA, 0.75,1,0,3     ! 2nd lamina: mat. #1,  0 deg, Th=0.75 mm
SECDATA, 0.75,1,0,3     ! 3rd lamina: mat. #1,  0 deg, Th=0.75 mm
SECDATA, 0.75,1,90,3    ! 4th lamina: mat. #1, 90 deg, Th=0.75 mm
SECOFFSET,BOT           ! Nodes on the laminate BOTTOM thickness

SECTYPE,2,SHELL,,DROP   ! Section shell set #2, [90/0/0], DROP
SECDATA, 0.75,1,90,3    ! 1st lamina: mat. #1, 90 deg, Th=0.75 mm
SECDATA, 0.75,1,0,3     ! 2nd lamina: mat. #1,  0 deg, Th=0.75 mm
SECDATA, 0.75,1,0,3     ! 3rd lamina: mat. #1,  0 deg, Th=0.75 mm
SECOFFSET,BOT           ! Nodes on the laminate BOTTOM thickness

SECTYPE,3,SHELL,,B      ! Section shell set #2, [90/0], B
SECDATA, 0.75,1,90,3    ! 1st lamina: mat. #1, 90 deg, Th=0.75 mm
SECDATA, 0.75,1,0,3     ! 2nd lamina: mat. #1,  0 deg, Th=0.75 mm
SECOFFSET,BOT           ! Nodes on the laminate BOTTOM thickness

! Geometry and mesh
RECTNG,0,60,0,50              ! Laminate A x=60 mm and y=50 mm
RECTNG,60,(60+30),0,50        ! Laminate Drop x=15 mm and y=50 mm
RECTNG,(60+30),(120),0,50     ! Laminate B x=60 m and y=50 mm
AGLUE,all               ! Glue all areas
ESIZE,5                 ! Element size 5 mm
SECNUM,1
AMESH,1                 ! Mesh the area number 1
SECNUM,2
AMESH,4                 ! Mesh the area number 2
SECNUM,3
AMESH,5                 ! Mesh the area number 3
FINISH                  ! Exit pre-processor module

/SOLU                   ! Solution module
ANTYPE,STATIC           ! Set static analysis
DL,4,1,all,0            ! Impose clamped BC
DL,1,1,symm             ! Impose Symmetry BC
DL,13,4,symm
DL,15,5,symm
SFL,10,PRES,-10         ! Apply uniform pressure in N/mm
SOLVE                   ! Solve current load state
FINISH                  ! Exit solution module

/POST1                  ! Post-processor module
PLDISP,1                ! Display the deformed plate
FINISH                  ! Exit post-processor module
```

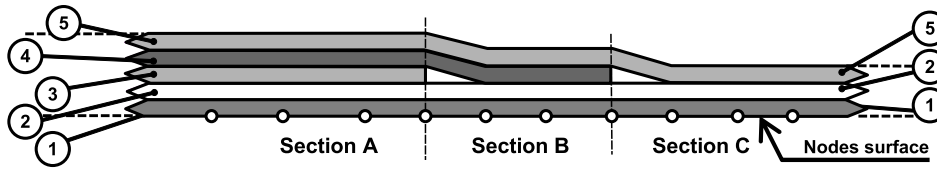

Figure 3.7: Laminate with dropped laminas.

The maximum transverse deflection is 2.579 mm.

When an inner lamina extends over only part of the geometry, it is convenient that the remaining laminas maintain their numbering through the entire model. Otherwise, if the continuity in numbering of laminas is lost, the post-processing and result visualization will be extremely difficult. A model with a few laminas, some of which are dropped over part of the laminate, is shown in Figure 3.7.

Example 3.6 *Define the three different sections of the laminate shown in Figure 3.7. The laminate in section A is a* $[+45/-45/0/90/0]$. *The thickness of each lamina is* 1.2 mm.

Solution to Example 3.6 *Using shell elements SHELL181, the different sections are defined as shown in the APDL code shown below [5, FEAcomp_Ex306]. The bottom lamina is designated as lamina #1, and additional laminas are stacked from bottom to top in the positive normal direction of the element coordinate system. The dropped laminas are modeled using zero thickness in order to maintain continuous numbering of the remaining laminas.*

```
! Material is AS4D/9310 - [+45/-45/0/90/0]s, Th=1.2 mm per lamina
/UNITS,MPa              ! Units are in mm, MPa, and Newtons

/PREP7                  ! Pre-processor module
! Material properties FOR AS4D/9310 orthotropic laminate
UIMP,1,EX,EY,EZ,133.86E3,7.706E3,7.706E3
UIMP,1,GXY,GYZ,GXZ,4.306E3,2.76E3,4.306E3
UIMP,1,PRXY,PRYZ,PRXZ,0.301,0.396,0.301

ET,1,SHELL181           ! Chooses SHELL181 element for analysis

KEYOPT,1,3,2            ! Set KEYOPT(3)=2, Full integration
                        ! (recommended for SHELL181/composites)
SECTYPE,1,SHELL,,A      ! Section shell set #1, section A
SECDATA, 1.2,1,45,3     ! 1st lamina: mat. #1, +45 deg, Th=1.2 mm
SECDATA, 1.2,1,-45,3    ! 2nd lamina: mat. #1, -45 deg, Th=1.2 mm
SECDATA, 1.2,1,0,3      ! 3rd lamina: mat. #1, 0   deg, Th=1.2 mm
SECDATA, 1.2,1,90,3     ! 4th lamina: mat. #1, 90  deg, Th=1.2 mm
SECDATA, 1.2,1,0,3      ! 5th lamina: mat. #1, 0   deg, Th=1.2 mm
SECOFFSET,BOT           ! Nodes on the laminate bottom thickness

SECTYPE,1,SHELL,,B      ! Section shell set #1, section B
SECDATA, 1.2,1,45,3     ! 1st lamina: mat. #1, +45 deg, Th=1.2 mm
SECDATA, 1.2,1,-45,3    ! 2nd lamina: mat. #1, -45 deg, Th=1.2 mm
SECDATA, 0  ,1,0,3      ! 3rd lamina: Thk=0 mm, do not compute
```

```
SECDATA, 1.2,1,90,3     ! 4th lamina: mat. #1, 90  deg, Th=1.2 mm
SECDATA, 1.2,1,0,3      ! 5th lamina: mat. #1,  0  deg, Th=1.2 mm
SECOFFSET,BOT           ! Nodes on the laminate bottom thickness

SECTYPE,1,SHELL,,C      ! Section shell set #1, section C
SECDATA, 1.2,1,45,3     ! 1st lamina: mat. #1, +45 deg, Th=1.2 mm
SECDATA, 1.2,1,-45,3    ! 2nd lamina: mat. #1, -45 deg, Th=1.2 mm
SECDATA, 0  ,1,0,3      ! 3rd lamina: Thk=0 mm, do not compute
SECDATA, 0  ,1,90,3     ! 4th lamina: Thk=0 mm, do not compute
SECDATA, 1.2,1,0,3      ! 5th lamina: mat. #1,  0  deg, Th=1.2 mm
SECOFFSET,BOT           ! Nodes on the laminate bottom thickness
```

3.2.9 FEA of Sandwich Shells

Some laminates can be considered *sandwich* when specifically designed for sandwich construction with thin faceplates and a thick, relatively weak, core. The faceplates are intended to carry all, or almost all, of the bending and in-plane normal load. Conversely, the core is assumed to carry all of the transverse shear. Example 3.7 shows how to define and calculate a sandwich cantilever beam.

The following assumptions are customarily made for a sandwich shell:

- The terms H_{ij} in (3.9) depend only on the middle lamina (core) and they can be calculated as
$$H_{ij} = \left(\overline{Q}^*_{ij}\right)_{core} t_{core}; i, j = 4, 5 \tag{3.16}$$
- The transverse shear moduli (G_{23} and G_{13}) are set to zero for the top and bottom laminas (face laminas).
- The transverse shear strains and stresses in the face laminas are neglected or assumed to be zero.
- The transverse shear strains and shear stresses in the core are assumed constant through the thickness.

Example 3.7 *Calculate the maximum deflection of a sandwich cantilever beam subject to an end load $F_z = -100$. The beam is made of a sandwich of two outer aluminum plates (with thickness 1 mm each, $E = 69\ GPa, \nu = 0.3$) and an inner core of foam (with thickness 50 mm, $E = 300\ MPa, \nu = 0.1$).*

Solution to Example 3.7 *ANSYS element SHELL281 is used in this example. Another element with capabilities to analyze sandwich structures is SHELL181. Both elements model the transverse shear deflection using an energy equivalence method, which is recommended for sandwich shells. The APDL code is shown below and in [5, FEAcomp_Ex307].*

```
/TITLE, Cantilever Beam with Sandwich [Al/foam/Al] material
! Material is Aluminium (Th=1mm) and FOAM (Th=50 mm) - SHELL281
/UNITS,MPa              ! Units are in mm, MPa, and Newtons

/PREP7                  ! Pre-processor module
! Material definition
```

```
MP,EX,1,69e3            ! Aluminium Young's modulus
MP,NUXY,1,0.3           ! Aluminium Poisson ratio
MP,EX,2,300             ! Foam Young's modulus
MP,NUXY,2,0.1           ! Foam Poisson ratio

ET,1,SHELL281           ! Chooses SHELL281 element for analysis
KEYOPT,1,8,1            ! Set KEYOPT(8)=1, Store data for all laminas
SECTYPE,1,SHELL         ! Section shell set #1
SECDATA,1,1,0           ! 1st lamina: mat. #1,   0 deg, Th=1.0 mm
SECDATA,50,2,0          ! 2nd lamina: mat. #2,   0 deg, Th=50.0 mm
SECDATA,1,1,0           ! 3rd lamina: mat. #1,   0 deg, Th=1.0 mm

! Geometry and mesh
RECTNG,0,3e3,0,600      ! Creates a rectangle with x=3 m and y=600 mm
ESIZE,200               ! Element size 200 mm
AMESH,all               ! Mesh the area
FINISH                  ! Exit pre-processor module

/SOLU                   ! Solution module
ANTYPE,STATIC           ! Set static analysis
DL,4,1,all,0            ! Impose Clamped BC
NSEL,S,LOC,x,3e3
CP,1,UZ,ALL             ! Coupling DOF set, vertical displacement
NSEL,R,LOC,y,300
F,all,FZ,-100           ! Apply force in a end line node
NSEL,all
SOLVE                   ! Solve current load state
FINISH                  ! Exit solution module

/POST1                  ! Post-processor module
PLDISP,1
FINISH                  ! Exit post-processor module
```

The maximum displacement is 16.0 mm.

3.2.10 Element Coordinate System

In the pre-processor, during the definition of the laminate, it is very important to know the orientation of the laminate coordinate system. Material properties, the relative lamina orientation with respect to the laminate axis, and other parameters and properties are defined in the laminate coordinate system, unless specified otherwise. Also, it can be used to obtain the derived results (strains and stress) in these directions. In FEA, the laminate coordinate system is associated to the element coordinate system, with a unique right-handed orthogonal system associated to each element.

The element coordinate system orientation is associated with the element type. For bar or beam elements the orientation of the x-axis is generally along the line defined by the end nodes of the element. For solid elements in two and three dimensions, the orientation is typically defined parallel to the global coordinate

system. For shell elements this is not useful. Axes x and y need to be defined on the element surface, with the z-axis always normal to the surface. The default orientation of x and y axes depends on the commercial code and the element type.

There are various ways to define the default orientation of x and y in shell elements (see Figure 3.8).

In Figure 3.8.(a) the x-axis is aligned with the edge defined by the first and second nodes of each element, the z-axis normal to the shell surface (with the outward direction determined by the right-hand rule), and the y-axis perpendicular to the x- and z-axis.

MSC-MARC$^{\text{TM}}$ calculates the orientation of the x-axis from the lines defined by the middle points of the edges as shown in Figure 3.8(b).

In ANSYS, Figure 3.8.(b), the orientation of the x_e axis is aligned with the shell surface coordinate at the center of the element, connecting the mid-sides of edges $i-l$ and $j-k$, and formally defined as

$$\begin{aligned} x_e &= \frac{\partial\{x\}/\partial s}{|\partial\{x\}/\partial s|} \\ \{x\} &= \sum_{i=1}^{n} h_i(s,r)\{x\}_i \end{aligned} \tag{3.17}$$

where $\{x\}$ are the nodal coordinates in the global coordinate system; s, r, are the coordinates of the isoparametric master element, and h_i are the shape functions [12].

In *Abaqus*$^{\text{TM}}$, Figure 3.8.(c), the local x-direction is calculated projecting the global X-direction onto the surface of the element, i.e.,

$$\begin{aligned} \hat{i} &= (\hat{I} - \hat{i}^*)/\|\hat{I} - \hat{i}^*\| \\ \hat{k} &= \hat{n} \\ \hat{j} &= \hat{k} \times \hat{i} \end{aligned} \tag{3.18}$$

with $\hat{i}^* = (\hat{I} \cdot \hat{n})\hat{n}$ being the projection of the global x-direction, $\hat{I}$, along the normal of the element, $\hat{n}$. If the global X-direction, $\hat{I}$, is within 0.1° of the normal to the element, $\hat{n}$, i.e., they are almost parallel, the local x-direction is calculated using the global z-direction, $\hat{K}$, instead of $\hat{I}$. The local coordinate system can be redefined using the procedures described in the *Abaqus* documentation [14, Section 2.2.5].

If no additional rotation is specified, the *laminate coordinate system* coincides with the element coordinate system. Additional rotations are specified by `ESYS` in ANSYS and `CSYS` in *Abaqus*, as shown in Examples 3.8 and 3.9.

In Examples 3.2–3.7, only rectangular plates with rectangular elements are analyzed. All of them have the first and the second node aligned with the global X-axis. Therefore, the material axes have been chosen parallel to the global axis. But this doesn't need to be the case. Most commercial codes have utilities to change the element coordinate system. Example 3.8 illustrates how to change the element coordinate system orientation in a plate. Example 3.9 illustrates how it can be done in a shell with curvature. Example 3.10 illustrates how different orientations can be used in different locations of the structure.

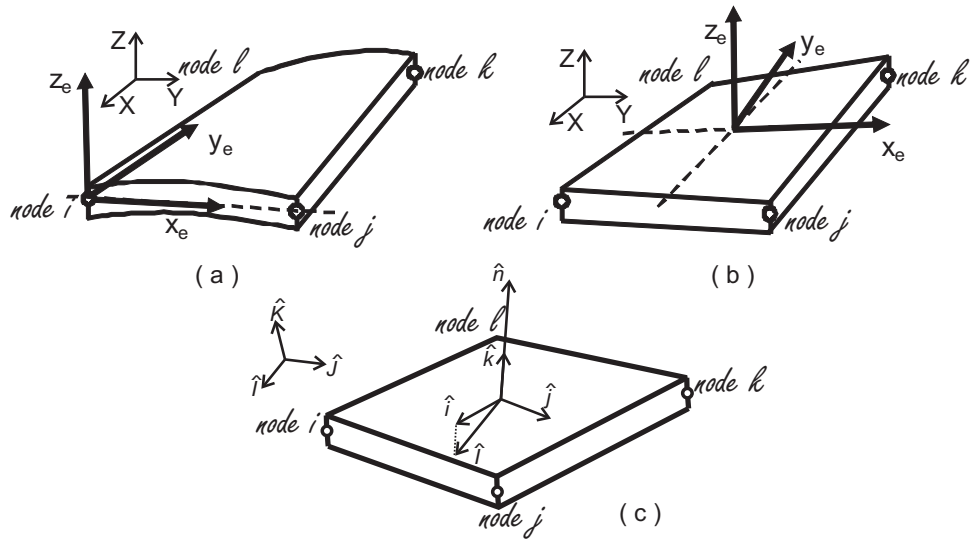

Figure 3.8: Default orientations of element coordinate systems in shell elements: (a) Along side 1, (b) ANSYS, (c) *Abaqus*.

Example 3.8 *Use a local coordinate system to model the plate of Example 3.2 if the orthotropic material is rotated* $+30$ *degrees with respect the* x*-direction. This example continues in Example 3.14.*

Solution to Example 3.8 *This example illustrates the use of local coordinate system in a rectangular plate. In ANSYS a local coordinate system is defined using* `LOCAL` *commands, which can be Cartesian, cylindrical, or spherical. Then, each element is linked to a previously defined local coordinate system using the element property* `ESYS`*. The objective is to orient the* x*-axis element coordinate system parallel to the* x*-axis laminate coordinate system. Also, it is possible to define element coordinate system orientations by user written subroutines [15]. Element coordinate systems may be displayed as a triad with the* `/PSYMB` *command or as an* `ESYS` *number (if specified) with the* `/PNUM` *command.*

Although this example is a continuation of Example 3.2, the material is no longer symmetric so we cannot reuse `FEAcomp_Ex302.inp` *and we must construct a new full model. The APDL file commands, also available in [5, FEAcomp_Ex308_full_plate.inp], are shown below*

```
/TITLE,SIMPLY SUPPORTED PLATE UNDER UNIFORM LOAD Q=1.2E-4 MPA - SHELL281
! FULL PLATE
/UNITS,MPA              ! UNITS ARE IN MM, MPA, AND NEWTONS
/PREP7                  ! PRE-PROCESSOR MODULE
! MATERIAL PROPERTIES FOR AS4D/9310 ORTHOTROPIC LAMINATE
UIMP,1,EX,EY,EZ,133.86E3,7.706E3,7.706E3
UIMP,1,GXY,GYZ,GXZ,4.306E3,2.76E3,4.306E3
UIMP,1,PRXY,PRYZ,PRXZ,0.301,0.396,0.301

ET,1,SHELL281           ! CHOOSES SHELL281 ELEMENT FOR ANALYSIS

SECTYPE,1,SHELL         ! SECTION SHELL SET #1
```

```
SECDATA,10,1,0          ! THICKNESS=10MM, MATERIAL 1, 0-DEG LAYER

! GEOMETRY AND MESH
LOCAL,11,0,,,,30,0,0    ! DEFINE LOCAL COORD. SYSTEM, XYROT=30 DEG
ESYS,11                 ! SET COORD. SYSTEM FOR ELEMENTS MESHED
RECTNG,-2000,2000,-1000,1000    ! RECTANGLE WITH X=4 M AND Y=2 M
ESIZE,250               ! ELEMENT SIZE 250 MM
AMESH,ALL               ! MESH THE AREA
CSYS,0                  ! GO BACK TO DEFAULT COORD. SYSTEM
/PSYMB,ESYS,1           ! SET ON DISPLAY LAMINATE ORIENTATION
EPLOT                   ! DISPLAY ELEMENTS
FINISH                  ! EXIT PRE-PROCESSOR MODULE

/SOLU                   ! SOLUTION MODULE
DL,2,1,UZ,0             ! IMPOSE SIMPLE SUPPORTED BC, SS1
DL,2,1,UY,0
DL,2,1,ROTX,0
DL,4,1,UZ,0             ! IMPOSE SIMPLE SUPPORTED BC, SS1
DL,4,1,UY,0
DL,4,1,ROTX,0
DL,1,1,UZ,0             ! IMPOSE SIMPLE SUPPORTED BC, SS1
DL,1,1,UX,0
DL,1,1,ROTY,0
DL,3,1,UZ,0             ! IMPOSE SIMPLE SUPPORTED BC, SS1
DL,3,1,UX,0
DL,3,1,ROTY,0
D,ALL,ROTZ              ! CONSTRAINT ROTATIONS ABOUT Z AXES (OPTIONAL)
SFA,ALL,2,PRES,1.2E-4   ! APPLY UNIFORM PRESSURE IN MPA
SOLVE                   ! SOLVE CURRENT LOAD STATE
FINISH                  ! EXIT SOLUTION MODULE

/POST1                  ! POST-PROCESSOR MODULE
PLDISP,1                ! PLOTS DEFORMED PLATE
RSYS,SOLU               ! ACTIVATE RESULTS IN SOLUTION COOD. SYSTEM
PLESOL,S,X              ! CONTOUR PLOT STRESS 1(FIBER), LAYER2, TOP FACE
FINISH                  ! EXIT POST-PROCESSOR MODULE
```

The maximum deflection of the model is 8.448 *mm.*

Example 3.9 *Align the laminate coordinate system with the global* Y*-axis of a 3D curved shell.*

Solution to Example 3.9 *For the analysis of laminated composite shells, it is very important to define clearly a reference direction with respect to which one can specify the fiber direction of each lamina. One way of doing it, is to force the laminate coordinate system (c.s.) to be aligned with the projection of one of the global axes on the surface of the shell.*

For shells defined in 3D, the ESYS orientation uses the projection of the local system on the shell surface. The element x*-axis is determined from the projection of the local* x*-axis on the shell surface. The* z*-axis is determined normal to the shell surface (with the outward direction determined by the right-hand rule), and the* y*-axis perpendicular to the* x*- and* z*-axis. For elements without mid-side nodes (linear interpolation functions), the projection*

is evaluated at the element centroid and it is assumed constant in direction throughout the element. For elements with mid-side nodes (quadratic interpolation functions), the projection is evaluated at each integration point and may vary in direction throughout the element. See the APDL file listed below (available in [5, FEAcomp_Ex309]) to align the element x*-axis with the global* Y*-axis. See Figure 3.9.*

```
/TITLE,Curved surface - SHELL281
!Material is AS4D/9310 Carbon/Epoxy [90/45/-45]T - Th=1.05mm per lamina
!units are in mm, MPa, and Newtons

/PREP7                  ! Pre-processor module
! Material properties FOR AS4D/9310 orthotropic laminate
UIMP,1,EX,EY,EZ,133.86E3,7.706E3,7.706E3
UIMP,1,GXY,GYZ,GXZ,4.306E3,2.76E3,4.306E3
UIMP,1,PRXY,PRYZ,PRXZ,0.301,0.396,0.301

ET,1,SHELL281           ! Chooses SHELL281 element for analysis
SECTYPE,1,SHELL         ! Section shell set #1
SECDATA, 1.05,1,90      ! 1st lamina: mat. #1,  90 deg, Th=1.05 mm
SECDATA, 1.05,1,45      ! 2nd lamina: mat. #1,  45 deg, Th=1.05 mm
SECDATA, 1.05,1,-45     ! 3nd lamina: mat. #1, -45 deg, Th=1.05 mm

! Create geometry by solid modeling
K,1,300,0,135
K,2,0,0,235
K,3,-300,0,135
K,4,200,200,0
K,5,0,200,135
K,6,-200,200,0
L,1,4
L,3,6
BSPLIN,1,2,3
BSPLIN,4,5,6
AL,ALL
! Mesh geometry
LOCAL,11,0,,,,90,0,0    ! Define local coord. system, XYrot=90 deg
ESYS,11                 ! Set coord. system for elements meshed
ESIZE,50                ! Define element size
AMESH,1                 ! Mesh the area
CSYS,0                  ! Go back to default coord. system
/PSYMB,esys,1           ! Set on display laminate orientation
/TYPE,1,0               ! Not hidden surfaces
EPLOT                   ! Display elements
FINISH                  ! Exit pre-processor module
```

Example 3.10 *Model in ANSYS a flanged tube with axial and radial laminate orientation. In the cylindrical part, the reference axis will be in the longitudinal direction. In the flange, the reference axis will be radial (see Figure 3.10).*

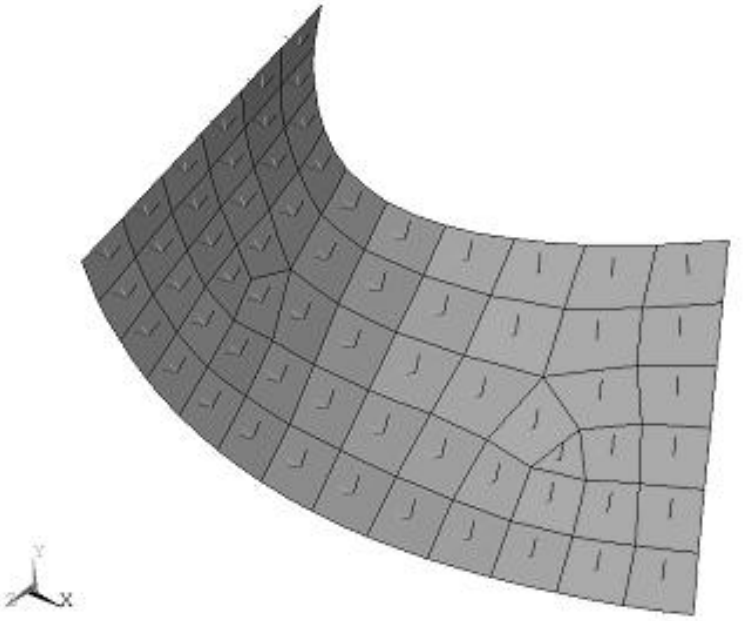

Figure 3.9: Curved shell in Example 3.9.

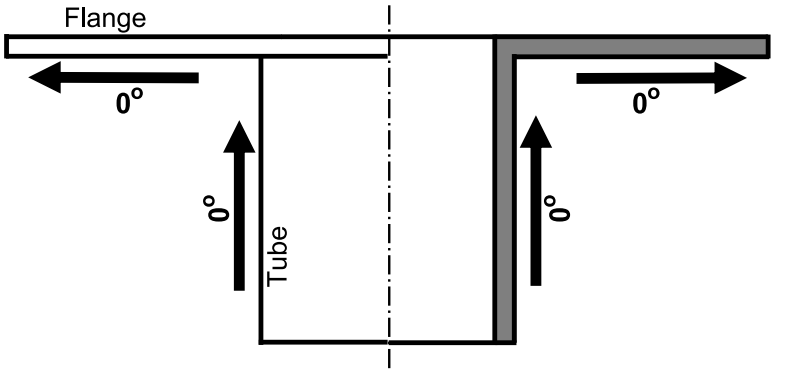

Figure 3.10: Reference axis in a flange tube.

Solution to Example 3.10 *Different orientation systems are needed for different model locations. Therefore, two local reference axes are defined and activated using the* ESYS *command. The APDL file listed below aligns the elements on the cylinder in the axial direction and aligns the elements on the flange in the radial direction [5, FEAcomp_Ex310]. See Figure 3.11.*

```
/TITLE,Flange tube with axial and radial laminate orientation - SHELL 281
! Material is AS4D/3100 Carbon/Epoxy [0/45/45] - Th=1.05 mm per lamina
! Units are in mm, MPa, and Newtons

/PREP7                  ! Pre-processor module
! Material properties FOR AS4D/9110 orthotropic laminate
UIMP,1,EX,EY,EZ,133.86E3,7.706E3,7.706E3
UIMP,1,GXY,GYZ,GXZ,4.306E3,2.76E3,4.306E3
UIMP,1,PRXY,PRYZ,PRXZ,0.301,0.396,0.301

ET,1,SHELL281           ! Chooses SHELL281 element for analysis
SECTYPE,1,SHELL         ! Section shell set #1
SECDATA,1.05,1,0        ! 1st lamina: mat. #1,   0 deg, Th=1.05 mm
SECDATA,1.05,1,45       ! 2nd lamina: mat. #1,  45 deg, Th=1.05 mm
SECDATA,1.05,1,-45      ! 3rd lamina: mat. #1, -45 deg, Th=1.05 mm

! Create geometry by solid modeling
CYL4,0,0,350,,,,300
CYL4,0,0,350,,550
AGLUE,3,4,5             ! Glue areas, area 5 become area 6

! Mesh geometry
LOCAL,11,0,,,,0,0,90    ! Define rotation=90 deg around Y (cylinder)
LOCAL,12,1,,,,0,0,0     ! Define polar coordinate system (flange)
ESIZE,50                ! Define element size
ESYS,11                 ! Set coord. system for elements meshed
AMESH,3,4               ! Mesh the cylindrical areas (areas 3 and 4)
ESYS,12                 ! Set coord. system for elements meshed
AMESH,6                 ! Mesh the flange area (area 6)
CSYS,0                  ! Go back to default coord. system
/PSYMB,esys,1           ! Set on display laminate orientation
/TYPE,1,0               ! Not hidden surfaces
EPLOT                   ! Display elements
FINISH                  ! Exit pre-processor module
```

3.2.11 Constraints

Constraints are used to restrict the motion of portions of a model in a variety of ways, as summarized below:

Tie Constraint tie two regions regardless of the meshes on the two regions being identical or not. See Example 6.3.

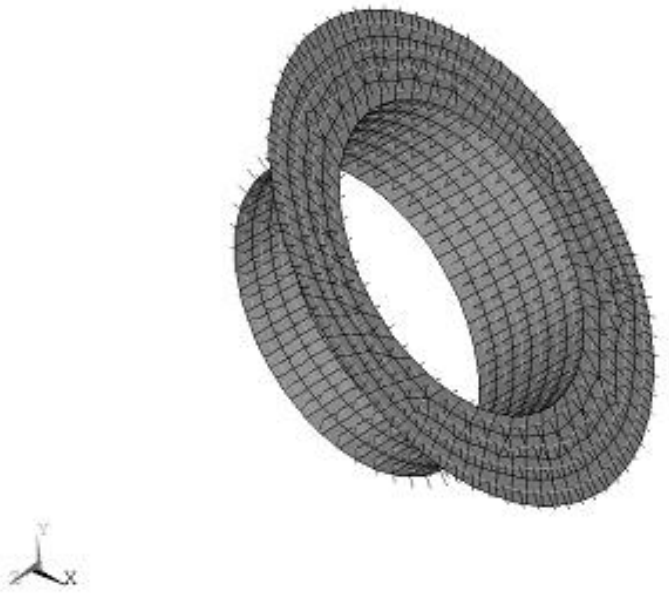

Figure 3.11: Flange in Example 3.10.

Rigid Body Constraint couples the motion of regions in an assembly to the motion of a reference point. *Relative positions* of regions that make up the rigid body will remain unchanged during the analysis. With a rigid body constraint, `pin nodes` makes all displacements equal to those of the reference point, and `tie nodes` makes all displacements *and rotations* equal to those of the reference point. Rigid body constraints are very useful to force pinned boundary conditions as in Example 3.11.

Coupling Constraint couples the motion of a surface to the motion of a single point. Although a mesh of 3D solids has only 3 DOF per node, the reference point will have 6 DOF. Therefore, it will be necessary to constraint the rotations of the reference point (RP) if the intent is to have the coupled surface translate but not rotate as a rigid surface.

Multipoint Constraint (MPC) couples the motion of selected slave nodes to the motion of a single point.

Shell-to-Solid Coupling Constraint couples the motion of a shell edge to the motion of an adjacent solid face. This is useful for detailed modeling of small regions using solid elements while large portions of the model are idealized with shell elements.

Embedded Region Constraint embeds a (small) region of a model within a host region of a (larger) model. This is useful for global-local analysis, multiscale analysis, and multiphysics analysis.

Example 3.11 *Create a finite element model for a pultruded composite column under axial compression load $P = 11,452\ N$ [16] and calculate the end axial displacement $u(L/2)$, where $x = 0$ is located at the half-length of the column. The column is simply supported (pinned) at both ends $x = (-L/2, L2)$. Its length is $L = 1.816\ m$. The cross-section of the column is that of a wide-flange I-beam (also called H-beam) with equal outside height and width, $H = W = 304.8\ mm$. The thickness of both the flange and the web is $t_f = t_w = 12.7\ mm$. The material properties are given by the A, B, D, and H matrices, with units [mm MPa], [mm^2 MPa], [mm^3 MPa], and [mm MPa], respectively. For the flange:*

$$[A] = \begin{bmatrix} 335{,}053 & 47{,}658 & 0 \\ 47{,}658 & 146{,}155 & 0 \\ 0 & 0 & 49{,}984 \end{bmatrix} \quad ; \quad [B] = \begin{bmatrix} -29{,}251 & -1{,}154 & 0 \\ -1{,}154 & -5{,}262 & 0 \\ 0 & 0 & -2{,}274 \end{bmatrix}$$

$$[D] = \begin{bmatrix} 4{,}261{,}183 & 686{,}071 & 0 \\ 686{,}071 & 2{,}023{,}742 & 0 \\ 0 & 0 & 677{,}544 \end{bmatrix} \quad ; \quad [H] = \begin{bmatrix} 34{,}216 & 0 \\ 0 & 31{,}190 \end{bmatrix}$$

For the web:

$$[A] = \begin{bmatrix} 338{,}016 & 44{,}127 & 0 \\ 44{,}127 & 143{,}646 & 0 \\ 0 & 0 & 49{,}997 \end{bmatrix} \quad ; \quad [B] = \begin{bmatrix} -6{,}088 & -14{,}698 & 0 \\ -14{,}698 & -6{,}088 & 0 \\ 0 & 0 & 0 \end{bmatrix}$$

$$[D] = \begin{bmatrix} 4{,}769{,}538 & 650{,}127 & 0 \\ 650{,}127 & 2{,}155{,}470 & 0 \\ 0 & 0 & 739{,}467 \end{bmatrix} \quad ; \quad [H] = \begin{bmatrix} 34{,}654 & 0 \\ 0 & 31{,}623 \end{bmatrix}$$

This example continues in Example 4.4.

Solution to Example 3.11 *The APDL file is shown next [5, FEAcomp_Ex311.inp]. A number of modeling techniques are illustrated, which are very useful for FEA of composite structures. Solid modeling is based on areas, and the use of lines to effectively impose boundary conditions and to control the mesh refinement is illustrated. Only one-half of the length of the column is modeled using symmetry boundary conditions. The loaded end is constrained to move as a rigid body using* `CERIG` *so that the pinned boundary condition is properly simulated.*

The model is set up parametrically so that all the geometric parameters of the column, such as the length, as well as mesh refinement can be easily changed. Only displacements can be displayed because the model is set up with A-B-D-H matrices, but the `.inp` *file can be easily modified to enter the LSS along with lamina material properties as in Example 3.4.* `LOCAL` *and* `ESYS` *coordinate systems are used so that all the local and the element coordinate systems are oriented similarly; this is necessary to facilitate the specification of directionally dependent materials properties and also interpretation of stress and strain results.*

```
/TITLE, H-COLUMN, Ref: CST 58 (1998) 1335-1341 SHELL181 - ANSYS R14
!Ref: COMPOSITE SCIENCE AND TECHNOLOGY 58 (1998) 1335-1341
/UNITS,MPA              !UNITS ARE mm, MPa, Newtons
WPSTYLE,,,,,,,,1        !WORKPLANE VISIBLE
/VSCALE,1,2.5,0 !2.5 LARGER ARROWS
                !ARROW & TRIAD COLORS: WHITE=X, GREEN=Y, BLUE=Z
```

```
/TRIAD,LBOT     !MOVE COORDINATE LABELS TO LEFT-BOTTOM
/VIEW,,1,2,3    !OBLIQUE VIEW
/PNUM,KP,0      !THESE ARE ALL THE NUMBERING OPTIONS
/PNUM,LINE,0    !ENTITY NUMBERING OFF=0, ON=1
/PNUM,AREA,1
/PNUM,VOLU,0
/PNUM,NODE,0
/PNUM,TABN,0
/PNUM,SVAL,0
/NUMBER,0

/PBC,ALL,,1     !THESE ARE ALL THE BC DISPLAY OPTIONS
/PBC,NFOR,,0    !DISPLAY ALL APPLIED BC, OFF=0, ON=1
/PBC,NMOM,,0
/PBC,RFOR,,0
/PBC,RMOM,,0
/PBC,PATH,,0

/PSYMB,CS,1     !THESE ARE ALL THE SYMBOL DISPLAY OPTIONS
/PSYMB,NDIR,0
/PSYMB,ESYS,0
/PSYMB,LDIV,1   !SHOW LESIZE ON LINES
/PSYMB,LDIR,1   !SHOW LDIR TO DECIDE ON LESIZE BIAS
/PSYMB,ADIR,0
/PSYMB,ECON,0
/PSYMB,XNODE,0
/PSYMB,DOT,1
/PSYMB,PCONV,
/PSYMB,LAYR,0
/PSYMB,FBCS,0

/PREP7          !ENTER THE PREPROCESSOR
!DEFINE PARAMETRIC VALUES==================
LOAD=11452      !APPLIED LOAD           [N]
L2=1816/2       !COLUMN HALF LENGTH  [mm]
WW=304.8        !OUTER WEB WIDHT [mm]
FW=WW           !OUTER FLANGE WIDTH
WT=12.7         !WEB THICKNESS [mm]
FT=WT           !FLANGE THICKNESS
WW1=WW-FT       !MID-PLANE WEB WIDTH
FW1=FW          !MID-PLANE FLANGE WIDTH
WW2=WW1/2
FW2=FW1/2
CSAREA=2*FW*FT+(WW-FT)*WT       !CROSS-SECTION AREA
NELEN=10        !NUMBER OF ELEMENTS ALONG THE LENGTH
NEWEB=4         !NUMBER OF ELEMENTS ON THE WEB
NEFLA=2         !NUMBER OF ELEMENTS ON 1/2 FLANGE
!
ET,1,SHELL181           ! Chooses SHELL181 element for analysis
KEYOPT,1,3,2            ! Set KEYOPT(3)=2, Full integration
                        ! (recommended in SHELL181/composites)
```

```
!=====================================================================
! Commands for Preintegrated Shell Section Data (A-B-D-H MATRICES)
! SSPA,a11,A21,A31,A22,A32,A33,Temperature    Membrane stiffness
! SSPB,B11,B21,B31,B22,B32,B33,Temperature    Coupling stiffness
! SSPD,D11,D21,D31,D22,D32,D33,Temperature    Bending stiffness
! SSPE,H11,H21,H22,Temperature       Transverse shear stiffness
!
!FLANGE [mm,Mpa,Newton]
SECTYPE,1,GENS                            ! Define SECTION 1 (FLANGE)
SSPA,335053,47658,0,146155,0,49984        ! A11,A21,A31,A22,A32,A33
SSPB,-29251,-1154,0,-5262,0,-2274         ! B11,B21,B31,B22,B32,B33
SSPD,4261183,686071,0,2023742,0,677544    ! D11,D21,D31,D22,D32,D33
SSPE,34216,0,31190                        ! H11,H21,H22
!
! WEB [mm, Mpa, Newton]
SECTYPE,2,GENS                            ! Define SECTION 2 (WEB)
SSPA,338016,44127,0,143646,0,49997        ! A11,A21,A31,A22,A32,A33
SSPB,-6088,-14698,0,-6088,0,0             ! B11,B21,B31,B22,B32,B33
SSPD,4769538,650127,0,21554700,739467     ! D11,D21,D31,D22,D32,D33
SSPE,34654,0,31623                        ! H11,H21,H22
!
!DEFINE SOLID MODEL USING AREAS======================
RECTNG,0,L2,-WW2,WW2,    !WEB
WPAVE,0,WW2,0            !MOVE WORKPLANE TO TOP FLANGE
WPRO,,-90.000000,        !ROTATE WORKPLANE AS FLANGE
RECTNG,0,L2,-FW2,FW2,    !TOP FLANGE
WPAVE,0,-WW2,0
RECTNG,0,L2,-FW2,FW2,    !BOTTOM FLANGE
AOVLAP,all      !JOINS AREAS CREATING INTERSECTIONS IF NEEDED
NUMCMP,AREA     !COMPRESS AREA NUMBERS
/REPLOT
WPSTYLE,,,,,,,,0         !HIDE WORKPLANE
!
LPLOT           !PLOT LINES
LSEL,S,LOC,X,0  !SELECT SYMMETRY END
/REPLOT
/PBC,ALL,,1     !DISPLAY ALL APPLIED BC, OFF=0, ON=1
DL,ALL, ,SYMM   !APPLY SYMMETRY BC
!NOTE SYMM DISPLAYED AS S ON LINES, BUT WILL NOT SHOW ON NODES LATER
ALLSEL,ALL      !RESELECT ALL ENTITIES
/REPLOT
!
!MESHING=============================================================
LOCAL,11,0,,,, , ,0     !DEFINE LOCAL COORD SYS TO ALIGN W/MAT PROPS
ESYS,11                 !USE IT FOR ALL ELEMS
/VSCALE,1,2.5,0         !2.5 LARGER ARROWS
/PSYMB,ESYS,1           !DISPLAY IT
/PSYMB,ESYS,0           !DO NOT DISPLAY IT
/VSCALE,1,1.0,0         !RESET TO DEFAULT ARROW LENGTH
MSHAPE,0,2D             !QUADRILATERAL 0, MESHING 2D
MSHKEY,1                !MAPPED MESHING 1 (FREE WOULD BE 0)
```

```
!
LESIZE,ALL,,,NEFLA      !ALL LINES DIVIDED IN NEFLA ELEMENTS
LESIZE, 2,,,NEWEB,0     !LINE 2, DIV NEWEB, NO BIAS, OVERRIDES PREVIOUS
LESIZE, 4,,,NEWEB
LESIZE, 1,,,NELEN,1/2   !LINE 1, DIV 10, BIAS 1/2 TOWARDS LINE END
LESIZE, 3,,,NELEN,2     !LINE 3, DIV 10, BIAS 2 TOWARDS LINE ORIGIN
LESIZE, 5,,,NELEN,1/2
LESIZE, 7,,,NELEN,2
LESIZE, 9,,,NELEN,1/2
LESIZE,11,,,NELEN,2
/PNUM,REAL,1    !COLOR AND NUMBER ELEMENTS BY REAL SET
ASEL,ALL        !SELECT ALL AREAS
ASEL,S,,,1      !SELECT AREA 1 (WEB)
AATT,,2,        !USE SECTION 2 FOR THE WEB
AMESH,ALL       !MESH ALL AREAS CURRENTLY SELECTED (I.E., WEB)
ASEL,S,,,ALL    !SELECT ALL
ASEL,U,,,1      !UNSELECT AREA 1 TO KEEP THE FLANGES
AATT,,1         !USE SECTION 1 FOR THE FLANGE
AMESH,ALL       !MESH ALL AREAS CURRENTLY SELECTED (I.E., FLANGE)
ASEL,ALL
/PNUM,REAL,0    !SUPRESS NUMBERING
CSYS,0          !RETURN TO GLOBAL COORD SYSTEM TO DISPLAY STRESSES
!
NSEL,S,LOC,X,0  !PREVENT RIGID BODY TRANSLATION
NSEL,R,LOC,Y,0
D,ALL,UY,0
D,ALL,UZ,0
D,ALL,ROTX,0    !PREVENT RIGIT BODY TWIST
NSEL,ALL
!
NSEL,S,LOC,X,L2 !SELECT LOAD END
NSEL,R,LOC,Y,0  !SELECT CENTER NODE ONLY
/PNUM,NODE,1
NPLOT
*GET,MYNODE,NODE,,NUM,MIN       !GET LABEL OF CENTER NODE
NSEL,S,LOC,X,L2 !SELECT LOAD END AGAIN
/PNUM,NODE,0 !TURN OFF NODE NUMBER DISPLAY
/REPLOT
! APPLY RIGID BC AT LOADED END
CERIG,MYNODE,ALL,UXYZ, , , ,    !MYNODE MASTER, ALL OTHER SLAVES
F,MYNODE,FX,-LOAD               !APPLY COMPRESSION LOAD
!
ALLSEL,ALL      !RESELECT EVERYTHING
FINISH          !EXIT PREPROCESSOR
!
/SOLU                   !ENTER SOLUTION MODULE
ANTYPE,STATIC           !STATIC ANALYSIS
RESCONTROL,LINEAR       !CONTROL FILE WRITING FOR MULTIFRAME RESTARTS
SOLVE
FINISH                  !EXIT SOLUTION MODULE
!
```

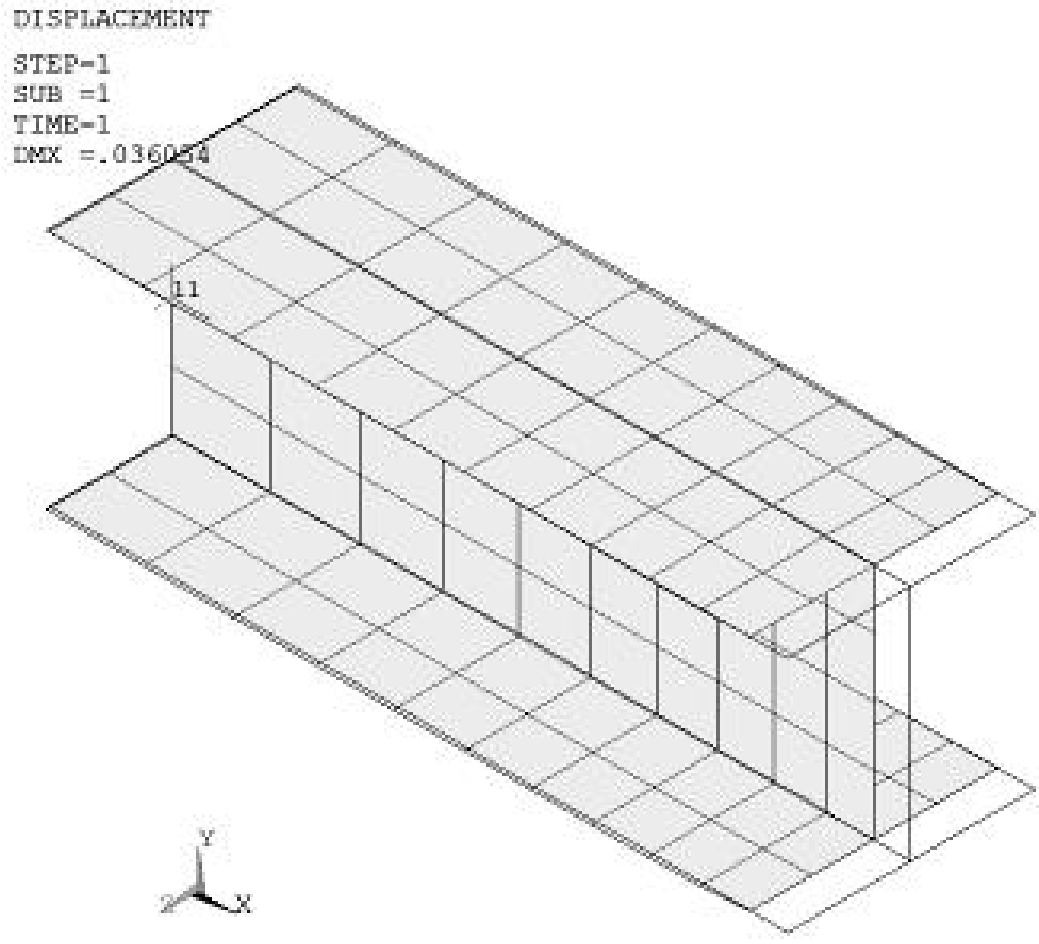

Figure 3.12: Deformed and undeformed shapes of the H column in Example 3.11.

```
/POST1          !ENTER POSTPROCESSOR MODULE
/VIEW,,1,1,1    !ISOMETRIC VIEW
PLDISP,2        !PLOT DEFORMED SHAPE AND UNDEF OUTLINE
!FINISH
```

The axial displacement at the loaded end of the column is 0.036 *mm. See Figure 3.12. This example continues in Example 4.4.*

3.3 Failure Criteria

Failure criteria are curve fits of experimental data that attempt to predict failure under multiaxial stress based on experimental data obtained under uniaxial stress. All failure criteria described in this section predict the first occurrence of failure in one of the laminas but are unable to track failure propagation until complete laminate failure. Damage mechanics is used in Chapters 8 and 9 to track damage evolution

up to laminate failure. The truncated-maximum-strain criterion estimates laminate failure without tracking damage evolution by making certain approximations and assumptions about the behavior of the laminate [1].

In this section, failure criteria are presented using the notion of failure index, which is used for several FEA packages, and it is defined as

$$I_F = \frac{stress}{strength} \tag{3.19}$$

Failure is predicted when $I_F \geq 1$. The strength ratio [1, Section 7.1.1] is the inverse of the failure index

$$R = \frac{1}{I_F} = \frac{strength}{stress} \tag{3.20}$$

Failure is predicted when $R \leq 1$.

3.3.1 2D Failure Criteria

Strength-based failure criteria are commonly used in FEA to predict failure events in composite structures. Numerous criteria exist for unidirectional (UD) laminas subjected to a state of plane stress ($\sigma_3 = 0$). The most commonly used are described in [1]. They are:

- Maximum stress criterion
- Maximum strain criterion
- Truncated maximum strain criterion, and
- Interacting failure criterion

A few additional criteria are presented in this section.

Hashin Failure Criterion

The Hashin failure criterion (HFC) proposes four separate modes of failure:

- Fiber tension
- Fiber compression
- Matrix tension
- Matrix compression

that are predicted by four separate equations, as follows[3]:

[3]The Hashin failure equations on the right-hand side of (3.21–3.24) yield squares of failure indexes I_F. Compare to the Maximum Stress Criterion (i.e., $I_{Fft} = \sigma_1/F_{1T}$) and so on.

$$I_{Fft}^2 = \left(\frac{\sigma_1}{F_{1t}}\right)^2 + \alpha\left(\frac{\sigma_6}{F_6}\right)^2 \qquad \text{if } \sigma_1 \geq 0 \tag{3.21}$$

$$I_{Ffc}^2 = \left(\frac{\sigma_1}{F_{1c}}\right)^2 \qquad \text{if } \sigma_1 < 0 \tag{3.22}$$

$$I_{Fmt}^2 = \left(\frac{\sigma_2}{F_{2t}}\right)^2 + \left(\frac{\sigma_6}{F_6}\right)^2 \qquad \text{if } \sigma_2 \geq 0 \tag{3.23}$$

$$I_{Fmc}^2 = \left(\frac{\sigma_2}{2F_4}\right)^2 + \left[\left(\frac{F_{2c}}{2F_4}\right)^2 - 1\right]\frac{\sigma_2}{F_{2c}} + \left(\frac{\sigma_6}{F_6}\right)^2 \qquad \text{if } \sigma_2 < 0 \tag{3.24}$$

where α is a weight factor to give more or less emphasis to the influence of shear on fiber failure. With $\alpha = 0$, Hashin failure criterion (FC) and Maximum Stress FC would predict longitudinal tensile failure of the unidirectional lamina at the same stress σ_1. Note (3.22) predicts longitudinal compressive failure without influence of the shear stress, although it is well known that the state of shear has a strong influence on the longitudinal compression failure [17].

Equations (3.21–3.24) define the *square* of failure indexes according to Hashin FC. The values of F_{1c} and F_{2c} are considered positive throughout this textbook and most of the literature. The Tsai-Hill, Azzi-Tsai-Hill, and Tsai-Wu failure criteria are not recommended because they over emphasize the interaction between fiber (σ_1) and transverse matrix (σ_2) damage modes.

Puck Failure Criterion

The Puck failure criterion [18] distinguishes between fiber failure (FF) and matrix failure (MF). In the case of plane stress, the MF criteria discriminates three different modes. Mode A is when transverse cracks appear in the lamina under transverse tensile stress with or without in-plane shear stress. Mode B also denotes transverse cracks, but in this case they appear under in-plane shear stress with small transverse compression stress. Mode C indicates the onset of oblique cracks (typically with an angle of 53° in carbon epoxy laminates) when the material is under significant transverse compression.

The FF and the three MF modes yield separate failure indexes. The Puck criterion assumes that FF only depends on longitudinal tension. Therefore, the failure index for FF is defined as

$$I_{FF} = \begin{cases} \sigma_1/F_{1t} & \text{if } \sigma_1 > 0 \\ -\sigma_1/F_{1c} & \text{if } \sigma_1 < 0 \end{cases} \tag{3.25}$$

The MF failure indexes have different expressions depending on the mode that becomes active. With positive transverse stress, mode A is active. In this case, the failure index for matrix dominated tensile failure (mode A) is

$$I_{MF,A} = \sqrt{\left(\frac{\sigma_6}{F_6}\right)^2 + \left(1 - p_{6t}\frac{F_{2t}}{F_6}\right)^2\left(\frac{\sigma_2}{F_{2t}}\right)^2} + p_{6t}\frac{\sigma_2}{F_6} \quad \text{if } \sigma_2 \geq 0 \tag{3.26}$$

where p_{6t} is a fitting parameter. Lacking experimental values, it is assumed that $p_{6t} = 0.3$ [18].

Under negative transverse stress, either mode B or mode C is active, depending on the relationship between in-plane shear stress and transverse shear stress. The limit between mode B and C is defined by the relation F_{2A}/F_{6A}, where

$$F_{2A} = \frac{F_6}{2p_{6c}} \left[\sqrt{1 + 2p_{6c}\frac{F_{2c}}{F_6}} - 1 \right] \tag{3.27}$$

$$F_{6A} = F_6\sqrt{1 + 2p_{2c}} \tag{3.28}$$

and p_{2c} is defined as

$$p_{2c} = p_{6c}\frac{F_{2A}}{F_6} \tag{3.29}$$

and p_{6c} is another fitting parameter. Lacking experimental values, it is assumed that $p_{6c} = 0.2$ [18].

Finally, the failure index for matrix dominated shear (mode B) is

$$I_{MF,B} = \frac{1}{F_6}\left[\sqrt{\sigma_6^2 + (p_{6c}\sigma_2)^2} + p_{6c}\sigma_2\right] \quad \text{if} \begin{cases} \sigma_2 < 0 \\ \left|\frac{\sigma_2}{\sigma_6}\right| \leq \frac{F_{2A}}{F_{6A}} \end{cases} \tag{3.30}$$

and for matrix dominated compression (mode C) is

$$I_{MF,C} = -\frac{F_{2c}}{\sigma_2}\left[\left(\frac{\sigma_6}{2(1+p_{2c})F_6}\right)^2 + \left(\frac{\sigma_2}{F_{2c}}\right)^2\right] \quad \text{if} \begin{cases} \sigma_2 < 0 \\ \left|\frac{\sigma_2}{\sigma_6}\right| \geq \frac{F_{2A}}{F_{6A}} \end{cases} \tag{3.31}$$

3.3.2 3D Failure Criteria

Failure criteria presented here are 3D generalizations of the ones presented in [1, Section 7.1]. The user of FEA packages should be careful because some packages use only the in-plane stress components for the computation of the failure index (e.g., *Abaqus*), even though all six stress components may be available from the analysis. In those cases the intralaminar and thickness components of stress should be evaluated separately to see if they lead to failure.

In this section, the numerical subscript denotes the directions of (1) fiber, (2) in-plane transverse to the fibers, and (3) through the thickness of the lamina. The letter subscript denotes (t) tensile and (c) compressive. Contracted notation is used for the shear components as described in Section 1.5.

Maximum Strain Criterion

The failure index is defined as

$$I_F = \max \begin{cases} \epsilon_1/\epsilon_{1t} & \text{if } \epsilon_1 > 0 \text{ or } -\epsilon_1/\epsilon_{1c} \text{ if } \epsilon_1 < 0 \\ \epsilon_2/\epsilon_{2t} & \text{if } \epsilon_2 > 0 \text{ or } -\epsilon_2/\epsilon_{2c} \text{ if } \epsilon_2 < 0 \\ \epsilon_3/\epsilon_{3t} & \text{if } \epsilon_3 > 0 \text{ or } -\epsilon_3/\epsilon_{3c} \text{ if } \epsilon_3 < 0 \\ abs(\gamma_4)/\gamma_{4u} \\ abs(\gamma_5)/\gamma_{5u} \\ abs(\gamma_6)/\gamma_{6u} \end{cases} \tag{3.32}$$

The quantities in the denominator are the ultimate strains of the unidirectional lamina. Note that compression ultimate strains in (3.32) are positive numbers.

Maximum Stress Criterion

The failure index is defined as

$$I_F = \max \begin{cases} \sigma_1/F_{1t} & \text{if } \sigma_1 > 0 \text{ or } -\sigma_1/F_{1c} \text{ if } \sigma_1 < 0 \\ \sigma_2/F_{2t} & \text{if } \sigma_2 > 0 \text{ or } -\sigma_2/F_{2c} \text{ if } \sigma_2 < 0 \\ \sigma_3/F_{3t} & \text{if } \sigma_3 > 0 \text{ or } -\sigma_3/F_{3c} \text{ if } \sigma_3 < 0 \\ abs(\sigma_4)/F_4 \\ abs(\sigma_5)/F_5 \\ abs(\sigma_6)/F_6 \end{cases} \tag{3.33}$$

The letter F is used here to denote a strength value for a unidirectional lamina as in [19]. Note that compression strength in (3.33) are positive numbers.

Tsai-Wu Criterion

Using the Tsai-Wu criterion the failure index is defined as

$$I_F = \frac{1}{R} = \left[-\frac{B}{2A} + \sqrt{\left(\frac{B}{2A}\right)^2 + \frac{1}{A}} \right]^{-1} \tag{3.34}$$

with

$$\begin{aligned} A = {} & \frac{\sigma_1^2}{F_{1t}F_{1c}} + \frac{\sigma_2^2}{F_{2t}F_{2c}} + \frac{\sigma_3^2}{F_{3t}F_{3c}} + \frac{\sigma_4^2}{F_4^2} + \frac{\sigma_5^2}{F_5^2} + \frac{\sigma_6^2}{F_6^2} \\ & + c_4 \frac{\sigma_2\sigma_3}{\sqrt{F_{2t}F_{2c}F_{3t}F_{3c}}} + c_5 \frac{\sigma_1\sigma_3}{\sqrt{F_{1t}F_{1c}F_{3t}F_{3c}}} + c_6 \frac{\sigma_1\sigma_2}{\sqrt{F_{1t}F_{1c}F_{2t}F_{2c}}} \end{aligned} \tag{3.35}$$

and

$$B = \left(F_{1t}^{-1} - F_{1c}^{-1}\right)\sigma_1 + \left(F_{2t}^{-1} - F_{2c}^{-1}\right)\sigma_2 + \left(F_{3t}^{-1} - F_{3c}^{-1}\right)\sigma_3 \tag{3.36}$$

where c_i, $i = 4..6$, are the Tsai-Wu coupling coefficients, that by default are taken to be -1. Note that compression strength in (3.35) and (3.36) are here positive numbers.

The through-the-thickness strength values F_{3t} and F_{3c} are seldom available in the open literature, so it is common practice to use the corresponding in-plane transverse values of strength. Also, the intralaminar strength F_5 is commonly assumed to be equal to the in-plane shear strength. Lacking experimental data for the remaining intralaminar strength F_4, it can be estimated as the shear strength of the matrix.

Example 3.12 *Compute the failure index I_F in each lamina of Example 3.4 using the maximum stress failure criterion and the Tsai-Wu criterion. The lamina strength values are given in Table 3.1, p. 73. Determine the strength ratio of the laminate using both criteria.*

Solution to Example 3.12 *Once the model is solved, inside /POST1 module, the FC commands (FC, FCDELE, FCLIST, etc.) can be used to define the failure criteria parameters. Before defining the failure criteria parameters, ANSYS must show the solution in "results" coordinate system using RSYS, SOLU command. The LAYER command is used to select the lamina where the failure criterion is to be calculated.*

After Example 3.4, include the commands below to compute the I_F of each lamina. Note that in ANSYS compression strength must be introduced using negative numbers. If the compression strength value is not given, ANSYS takes the compression strength equal to the negative value of the tensile strength. Also note that ANSYS uses x, y, z to denote the lamina coordinates that are denoted as $1, 2, 3$, in this textbook.

```
/TITLE,Simply Supported [0/90/45/-45]s - uniform load - SHELL281
! Material is AS4D/9310 - [0/90/45/-45]s, Th=1.25 mm per lamina
/UNITS,MPA              ! Units are in mm, MPa, and Newtons

/PREP7                  ! Pre-processor module
! Material properties FOR AS4D/9310 orthotropic laminate
uimp,1,ex,ey,ez,133.86E3,7.706E3,7.706E3
uimp,1,gxy,gyz,gxz,4.306E3,2.76E3,4.306E3
uimp,1,prxy,pryz,prxz,0.301,0.396,0.301

ET,1,SHELL281           ! Chooses SHELL281 element for analysis
KEYOPT,1,8,1            ! Set KEYOPT(8)=1, Store data for all layers
SECTYPE,1,SHELL         ! Section shell set #1
SECDATA, 1.25,1,0       ! 1st layer: mat. #1,   0 deg, Th=1.25 mm
SECDATA, 1.25,1,90      ! 2nd layer: mat. #1,  90 deg, Th=1.25 mm
SECDATA, 1.25,1,45      ! 3nd layer: mat. #1, +45 deg, Th=1.25 mm
SECDATA, 1.25,1,-45     ! 4rt layer: mat. #1, -45 deg, Th=1.25 mm
SECDATA, 1.25,1,-45     ! Same layers in symmetrical order
SECDATA, 1.25,1,45
SECDATA, 1.25,1,90
SECDATA, 1.25,1,0
SECOFFSET,MID           ! NODES ON THE LAMINATE MIDLLE THICKNESS

! Geometry and mesh
RECTNG,0,1000,0,1000    ! Creates a rectangle with x=1 m and y=1 m
ESIZE,250               ! Element size 250 mm
AMESH,all               ! Mesh the area
FINISH                  ! Exit pre-processor module

/SOLU                   ! Solution module
ANTYPE,STATIC           ! Set static analysis
DL,2,1,uz,0             ! Impose Simple Supported BC
DL,3,1,uz,0
DL,1,1,symm             ! Impose Symmetry BC
DL,4,1,symm
!d,all,rotz             ! Constraint rotations about z axes (optional)
SFL,2,PRES,-100         ! Apply uniform pressure in N/mm
SOLVE                   ! Solve current load state
FINISH                  ! Exit solution module
```

```
/post1                  ! Post-processor module
PLDISP,1                ! Display the deformed plate
RSYS,SOLU               ! Activate the ESYS

!Failure criteria definition
FC,1,s,xten, 1830   ! F1t strength
FC,1,s,xcmp,-1096   ! F1c strength
FC,1,s,yten, 57     ! F2t strength
FC,1,s,ycmp,-228    ! F2c strength
FC,1,s,zten, 1e6    ! F3c=-F3t strength (large value so it does not compute)
FC,1,s,xy,71        ! F6 strength
FC,1,s,yz,1e6       ! F4 strength (large value, not compute)
FC,1,s,xz,1e6       ! F5 strength (large value, not compute)
FC,1,s,XYCP,-1      ! c6 coefficient. Defaults to -1.0
FC,1,s,YZCP,-1      ! c4 coefficient. Defaults to -1.0
FC,1,s,XZCP,-1      ! c5 coefficient. Defaults to -1.0

LAYER, 1            ! Select layer #1
PRNSOL,S,FAIL       ! Print table with FAIL index, where:
                    ! MAXF is index failure for Maximum Stress
                    ! TWSI is index failure for Tsai-Wu criteria

! Repeat this with the others layers
!LAYER, 2            ! Select layer #2
!PRNSOL,S,FAIL       ! Print table with FAIL index
!LAYER, 3            ! Select layer #3
!PRNSOL,S,FAIL       ! Print table with FAIL index
!LAYER, 4            ! Select layer #4
!PRNSOL,S,FAIL       ! Print table with FAIL index
!FINISH              ! End Post-process module
```

The `MAXF` and the `TWSR` are the failure index defined in Eqs. (3.33) and (3.34) respectively. The `TWSI`, called Tsai-Wu "strength index," is the addition of the value A in Eq. (3.35) and value B in Eq. (3.36), i.e., $TWSI = A + B$. This "index" does not have engineering interpretation and we recommend not to use it.

The solution is tabulated in Table 3.3, showing the failure indexes and the strength ratios obtained for maximum stress criterion and Tsai-Wu criterion in each lamina.

Table 3.3: Failure indexes and strength ratios for each lamina in Example 3.12

Layer		**Maximum Stress**		**Tsai-Wu**	
		I_F	R	I_F	R
#1,	0^o	0.0144	69.34	0.0144	69.38
#2,	90^o	0.0243	41.16	0.0294	34.04
#3,	$+45^o$	0.0157	63.84	0.0199	50.18
#4,	-45^o	0.0157	63.84	0.0199	50.18

Example 3.13 *Compute the 2D Tsai-Wu failure index I_F in each lamina of Example 3.4 using APDL language. The lamina strength values are given in Table 3.1.*

Solution to Example 3.13 *First, run* `FEAcomp_Ex304_shell181.inp` *to calculate displacements, strain, and stress in all laminas. Then, the computation of Tsai-Wu failure index* I_F *is achieved by running* `TSAIWU2D.mac`. *Both are avaliable in [5, FEAcomp_Ex313].*

Using the APDL scripting language of ANSYS [20], it is possible to automate common tasks (macros) or build parametric models. To create macros, a set of commands can be saved in a text file using extension `.mac` *in the ANSYS working directory. Then, these commands can be executed by using the name of the* `.mac` *file.*

After executing `FEAcomp_Ex304_shell181.inp`*, you should manually enter the following APDL commands at the ANSYS Command Prompt located at the top of the graphical user interface (GUI), immediately below the Menu Bar (File Select List...).*

```
/POST1      ! POST-PROCESSOR MODULE
RSYS,SOLU   ! activate the solution reference axes
! REPEAT FOR ALL LAYERS
LAYER,1     ! select the lamina
TSAIWU2D    ! execute the macro
PRNSOL,EPSW ! PRINT FAILURE INDEX IN A LIST
```

When you are done, exit the post-processor:

```
FINISH
```

In this example, the commands to compute, print, and plot the 2D Tsai-Wu failure index are saved in a file named `TSAIWU2D.mac`*, reproduced below:*

```
! Macro: Tsai-Wu failure criterion using APDL macro language
! Tested with SHELL181 (2013)

! Define parameters
F1t= 1830   ! F1t strength
F1c= 1096   ! F1c strength
F2t= 57     ! F2t strength
F2c= 228    ! F2c strength
F6 = 71     ! F6 strength
c6 = -1     ! Tsai-Wu coefficient

! initialize arrays
*get,nelem,elem,,num,max    ! get number of elements
*get,nnode,node,,num,max    ! get number of nodes

*set,I_F,                   ! delete array if already used
*set,sel,                   ! delete array if already used
*dim,I_F,,nnode             ! set up array for element nodes
*dim,sel,,nnode             ! set up array for select vector

nsle,s,corner       ! select only nodes at element corners
*vget,sel(1),node,1,nsel    ! mask for compute only corners

! compute Tsai-Wu failure criterion
*do,in,1,nnode
    *if,sel(in),gt,0,then       ! read only selected nodes
        *get,s_1,node,in,s,x    ! get stress each node
```

```
        *get,s_2,node,in,s,y
        *get,s_6,node,in,s,xy
        A1= s_1**2/(F1t*F1c)
        A2= s_2**2/(F2t*F2c)
        A6= s_6**2/(F6)**2
        A12= c6*s_1*s_2/(F1t*F1c*F2t*F2c)**0.5
        A = A1+A2+A6+A12
        B= (1/F1t-1/F1c)*s_1+(1/F2t-1/F2c)*s_2
        R_tw=-B/(2*A)+((B/2/A)**2+1/A)**0.5
        If_tw=1/R_tw
        I_F(in)=If_tw
    *endif
*enddo

*vput,I_F,node,1,epsw, ! write failure index in results database
! end macro
```

The solution is tabulated in Table 3.4, showing the failure indexes obtained by using the Tsai-Wu criterion in each lamina.

Table 3.4: Failure indexes and strength ratios for each lamina in Example 3.13

Layer		I_F	R
#1,	0^o	0.0144	69.44
#2,	90^o	0.0294	34.01
#3,	$+45^o$	0.0200	50.00
#4,	-45^o	0.0200	50.00

Example 3.14 *Compute the Tsai-Wu failure index I_F on each lamina of a quasi-isotropic laminate $[0/90/\pm 45]_S$, otherwise identical to Example 3.8, using a USERMAT subroutine (`usermatps_314.f90` for shell elements). The lamina strength values are given in Table 3.1, p. 73.*

Solution to Example 3.14 *See user material subroutine `usermatps_314.f90` and model file `FEAcomp_Ex314.inp` on the Web site [5]. Refer to Appendix C for program compilation and execution details.*

First, follow the instructions in Appendix C.1.1 to create a `USERMATLib.DLL`. For this particular example, copy `usermatps_314.f90` to `c:\Ansys\User\usermatps.f90`. Note the change of file name. At this stage, probably you are overwriting a `usermatps.f90` that was in your work directory. If so, make sure you keep a backup.

Next, double click on `AnsUserMatEjb.bat` to create the DLL.

Next, open ANSYS/Mechanical, then `File>Read Input from>FEAcomp\Ex314.inp` available in [5] and shown next.

```
/TITLE, SS FULL PLATE, UNIFORM LOAD Q=1.2E-4 MPA, SHELL181/281
! FULL PLATE
/UNITS,MPA          ! UNITS ARE IN MM, MPA, AND NEWTONS
/PREP7              ! PRE-PROCESSOR MODULE
!FROM EX.3.8: MATERIAL PROPERTIES FOR AS4D/9310 ORTHOTROPIC LAMINATE
!UIMP,1,EX,EY,EZ,133.86E3,7.706E3,7.706E3
```

```
!UIMP,1,GXY,GYZ,GXZ,4.306E3,2.76E3,4.306E3
!UIMP,1,PRXY,PRYZ,PRXZ,0.301,0.396,0.301

! 12 PROPERTIES AS FOLLOWS
! E1  E2  NU12    NU23    G12     G23
! F1T F1C F2T     F2C     F6      C6
TBDELETE,USER,1,,,  ! DELETE USER PROPERTIES IN CASE WERE DEFINED BEFORE
! A TB,USER, CARD IMMEDIATELY FORCES ANSYS TO LOOK FOR A USERMAT
TB,USER,1,1,12,     ! 12 PROPERTIES FOR MATERIAL 1, 1 TEMPERATURE
TBTEMP,0.           ! ZERO TEMPERATURE
TBDATA,,133.86E3,7.706E3,0.301,0.396,4.306E3,2.76E3
TBDATA,,1830,1096,57,228,71,-1
TB,STAT,1,,2,       ! 2 STATE VARIABLES FOR MATERIAL 1
TBDATA,1,0.,0.,,,,  ! INITIALIZE THE STATE VARIABLES TO ZERO

ET,1,SHELL181,,,2   ! FOR SHELL 181 SET KEYOPT(3)=2, FULL INTEGRATION
!CHOICE !ET,1,SHELL281,,,    ! FOR SHELL 281 DEFAULT REDUCED INTEGRATION
KEYOPT,1,8,1            ! SET KEYOPT(8)=1, STORAGE DATA: ALL LAYERS
SECTYPE,1,SHELL         ! SECTION SHELL SET #1
SECDATA, 1.25,1,0.0,3   ! 1ST LAYER: MAT. #1,   0 DEG, TH=1.25 MM
SECDATA, 1.25,1,90,3    ! 2ND LAYER: MAT. #1,  90 DEG, TH=1.25 MM
SECDATA, 1.25,1,45,3    ! 3ND LAYER: MAT. #1, +45 DEG, TH=1.25 MM
SECDATA, 1.25,1,-45,3   ! 4RT LAYER: MAT. #1, -45 DEG, TH=1.25 MM
SECDATA, 1.25,1,-45,3   ! SAME LAYERS IN SYMMETRICAL ORDER
SECDATA, 1.25,1,45,3
SECDATA, 1.25,1,90,3
SECDATA, 1.25,1,0.0,3
SECOFFSET,MID           ! NODES ON THE LAMINATE MIDDLE THICKNESS

! GEOMETRY AND MESH
LOCAL,11,0,,,,30,0,0    ! DEFINE LOCAL COORD. SYSTEM, XYROT=30 DEG
ESYS,11                 ! SET COORD. SYSTEM FOR ELEMENTS MESHED
RECTNG,-2000,2000,-1000,1000    ! RECTANGLE WITH X=4 M AND Y=2 M
ESIZE,250               ! ELEMENT SIZE 250 MM
AMESH,ALL               ! MESH THE AREA
CSYS,0                  ! GO BACK TO DEFAULT COORD. SYSTEM
/PSYMB,ESYS,1           ! SET ON DISPLAY LAMINATE ORIENTATION
EPLOT                   ! DISPLAY ELEMENTS
FINISH                  ! EXIT PRE-PROCESSOR MODULE

/SOLU                   ! SOLUTION MODULE
DL,2,1,UZ,0             ! IMPOSE SIMPLE SUPPORTED BC, SS1
DL,2,1,UY,0
DL,2,1,ROTX,0
DL,4,1,UZ,0             ! IMPOSE SIMPLE SUPPORTED BC, SS1
DL,4,1,UY,0
DL,4,1,ROTX,0
DL,1,1,UZ,0             ! IMPOSE SIMPLE SUPPORTED BC, SS1
DL,1,1,UX,0
DL,1,1,ROTY,0
DL,3,1,UZ,0             ! IMPOSE SIMPLE SUPPORTED BC, SS1
```

```
DL,3,1,UX,0
DL,3,1,ROTY,0
D,ALL,ROTZ              ! CONSTRAINT ROTATIONS ABOUT Z AXES (OPTIONAL)
SFA,ALL,2,PRES,1.2E-4   ! APPLY UNIFORM PRESSURE IN MPA

ANTYPE,STATIC           ! SET STATIC ANALYSIS
OUTRES,SVAR,1           ! STORE STATE VARIABLES
SOLVE                   ! SOLVE CURRENT LOAD STATE
FINISH                  ! EXIT SOLUTION MODULE

/POST1                  ! POST-PROCESSOR MODULE
PLDISP,1                ! PLOTS DISPLACED PLATE
/GRA,FULL
RSYS,SOLU               ! ACTIVATE RESULTS IN SOLUTION COOD. SYSTEM
LAYER,2
PLESOL,SVAR,1           ! CONTOUR PLOT STRESS STATE VARIABLE 1
FINISH                  ! EXIT POST-PROCESSOR MODULE
```

Suggested Problems

Problem 3.1 *Compute the maximum bending moment per unit cross-sectional area m_u that can be applied to a beam of circular hollow cross-section of outside radius r_o and inner radius r_i. The loading is pure bending, no shear. The material is homogeneous and failure occurs when the maximum stress reaches the strength σ_u of the material. The hollow section is filled with foam to prevent buckling. Derive an expression for the efficiency of the cross-section as the ratio of m_u of the hollow beam by m_u of a solid rod of same outside radius. Faced with the problem of using a strong and relatively expensive material, would you recommend a small or large radius?*

Problem 3.2 *Compute the maximum outside radius for a cantilever beam of length L, loaded by a tip load P, otherwise similar to the beam in Problem 3.1 but subjected to pure shear loading. The shear strength is $\tau_u = \sigma_u/2$. Consider only shear. Buckling of the thin wall is likely to limit further the practical thickness of the wall.*

Problem 3.3 *Compute the maximum deflection per unit volume δ_V that can be applied to a beam of circular hollow cross-section of outside radius r_o and inner radius r_i. This is a cantilever beam of length L, loaded by a tip load P. The hollow section is made of an homogeneous material with moduli E and $G = E/2.5$, filled with foam to prevent buckling. Derive an expression for the efficiency of the cross-section as the ratio of δ_V between the hollow cross-section and a solid rod of the same outside radius. Faced with the problem of using a relatively expensive and not quite stiff material, would you recommend a small or large radius?*

Problem 3.4 *Write a computer program to evaluate (3.9). The program data input is the LSS, the thickness of the laminas, and the material elastic properties. The output should be written in a file. Show all work in a report.*

Problem 3.5 *Using the program of Problem 3.4 compute the A, B, D, and H matrices for the following laminates. The material is AS4D/9310 and all laminas are 0.85 mm thick. Comment on the coupling of the constitutive equations for each case: (a) one lamina $[0]$, (b) one lamina $[30]$, (c) $[0/90]_2$, (d) $[0/90]_s$, (e) $[0/90]_8$, (f) $[\pm 45]_2 = [+45/-45/+45/-45]$, (g) $[\pm 45]_s = [+45/-45/-45/+45]$, (h) $[\pm 45/0/90/\pm 30]$. Show all work in a report.*

Problem 3.6 *(FEA) Compute the value and location of the absolute maximum transverse shear strain γ_{23} in Example 3.2. At that location plot the distribution of γ_{23} through the thickness of the plate. Is that distribution a reasonable answer?*

Problem 3.7 *(FEA) Recompute Example 3.2 with a doubly sinusoidal load*

$$q(x,y) = q_0 \sin(\pi x/2a)\sin(\pi x/2b)$$

where $2a, 2b$ are the plate dimensions in x and y, respectively. Compare the result with the exact solution at the center of the plate, that is

$$w_0 = 16q_0b^4/[\pi^4(D_{11}s^4 + 2(D_{12} + 2D_{66})s^2 + D_{22})]$$

where $s = b/a$ [10, (5.2.8–5.2.10)].

Problem 3.8 *(FEA) Calculate the first vibration frequency ϖ_{11} of the plate with the analytical solution $\varpi_{mn}^2 = \pi^4[D_{11}m^4s^4 + 2(D_{12} + 2D_{66})m^2n^2s^2 + D_{22}n^4]/(16\rho hb^4)$, where ρ, h are the density and thickness of the plate, respectively ([10, (5.7.8)]).*

Problem 3.9 *(FEA) Using ANSYS finite element code, generate a rectangular plate with $a_x = 1000$ mm and $b_y = 100$ mm. The laminas are made of AS4D/9310 (Table 3.1) 1.2 mm thick. Look up four different LSS laminates where appear: (a) bending extension coupling effect, (b) thermal expansion coupling effect, (c) torsion extension coupling effect, and (d) shear extension (these coupling effects are shown in [1, Figure 6.7]). Model (i) one half of the plate, 500×100 mm, and (ii) one quarter of the plate, 500×50 mm, applying symmetry conditions and report when it is correct or not to use each of these reduced models. Show all work in a report.*

Problem 3.10 *Using a program (e.g., MATLAB) to plot the failure limits (with $I_f = 1$) of maximum stress, Tsai-Wu, and Puck failure criteria in the plane $\sigma_1 - \sigma_2$, and in the plane $\sigma_2 - \sigma_6$.*

Problem 3.11 *(FEA) Compute the failure index I_F at the center point on each lamina of Example 3.12 using the maximum stress failure criterion and the Tsai-Wu failure criterion. The lamina strength values are given in Table 3.1. (a) Calculate the failure indexes using the `FC` commands in ANSYS, (b) Write the nodal stress results at the top and bottom of each lamina in a file. Then, using an external program (e.g., MATLAB) compute the same failure indexes as in part (a) and compare them at the center of the plate. Show all work in a report.*

Problem 3.12 *Compute the failure index I_F on each lamina of Example 3.12 using the Puck failure criterion. The lamina strength values are given in Table 3.1. Calculate the failure indexes using: (a) APDL script in ANSYS and (b) a USERMAT subroutine (for shell elements `usermatps.f`). Show all work in a report.*

Problem 3.13 *Visualize and report the maximum value of transverse deflection U_3 for the ply drop-off Example 3.6 with a ply drop-off ratio 1:10. The strip is 120 mm long and 100 mm, loaded by tension $N_x = 10$ N/mm applied to the bottom edges on the strip. Use symmetry to model 1/2 of the tape. The material is AS4D/9310 (Table 3.1).*

Problem 3.14 *Perform a modal analysis using ANSYS for a 1×1 m plate with all edges fixed using the same laminate layup properties of Example 3.3. Compare the 10 lower eigenvalues obtained with "layered shell" (Example 3.4) and "equivalent orthotropic" (Example 3.3) approaches.*

Chapter 4

Buckling

Most composite structures are thin walled. This is a natural consequence of the following facts:

- Composites are stronger than conventional materials. Then, it is possible to carry very high loads with a small area, and thus small thickness in most components.

- Composites are expensive when compared to conventional materials. Therefore, there is a strong motivation to reduce the volume, and thus the thickness as much as possible.

- The cost of polymer matrix composites increases with their stiffness. The stiffness in the fiber direction can be estimated by using the fiber-dominated rule of mixtures, $E_1 = E_f V_f$. For example, when glass fibers are combined with a polymer matrix, the resulting composite stiffness is lower than that of aluminum. Using Aramid yields a stiffness comparable to aluminum. Carbon fibers yield composite stiffness lower than steel. Therefore, there is strong motivation to increase the moment of inertia of beams and stiffeners without increasing the cross-sectional area. The best option is to increase the moment of inertia by enlarging the cross-section dimensions and reducing the thickness.

All the above factors often lead to the design of composite structures with larger, thin-walled cross-sections, with modes of failure likely to be controlled by buckling.

4.1 Eigenvalue Buckling Analysis

Buckling is loss of stability due to geometric effects rather than material failure. But it can lead to material failure and collapse if the ensuing deformations are not restrained. Most structures can operate in a linear elastic range. That is, they return to the undeformed configuration upon removal of the load. Permanent deformations result if the elastic range is exceeded, as when matrix cracking occurs in a composite.

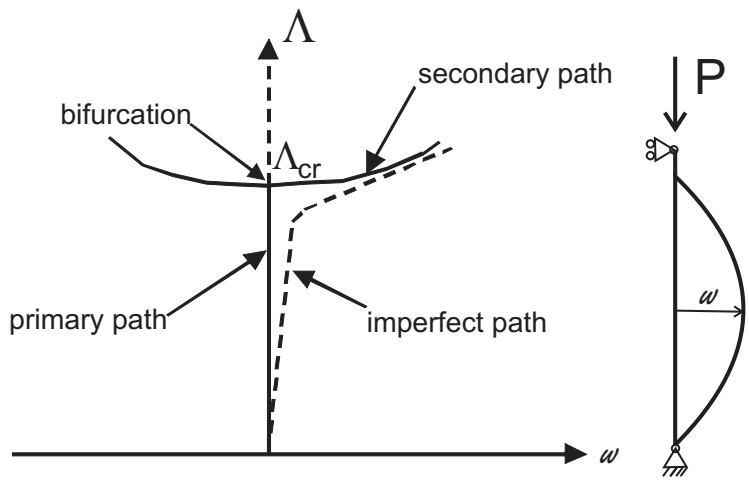

Figure 4.1: Equilibrium paths for the perfect column.

Consider a simply supported column of area A, length L, and moment of inertia I, made of homogeneous material with modulus E and strength F along the length of the column. The column is loaded by a compressive load P acting on the centroid of the cross-section [3]. If the column geometry, loading, and material have no imperfections, the axial deformation is

$$u = PL/EA \tag{4.1}$$

with no lateral deformation $w = 0$. The deformation of the structure (u, v, w) before buckling occurs is called the *primary path* (Figure 4.1). The slightest imperfection will make the column buckle when

$$P_{cr} = \pi^2(EI)/L^2 \tag{4.2}$$

The load capacity for long slender columns will be controlled by buckling, as opposed to the crushing strength of the material. What happens after the column reaches its critical load depends largely on the support conditions. For the simply supported column, the lateral deflection[1]

$$w = A\sin(\pi x/L) \tag{4.3}$$

will grow indefinitely ($A \to \infty$) when the load just barely exceeds P_{CR}. Such large lateral deflections will cause the material to fail and the column will collapse. The behavior of the structure after buckling has occurred is called *post-buckling*.

The simply supported column in Figure 4.1 experiences no deformations in the shape of the buckling mode (4.3) before buckling actually happens. In this case, it is said that the structure has a *trivial* primary path. This is a consequence of having a perfect structure with perfectly aligned loading. For these type of structures,

[1]With x measured from one end of the column.

buckling occurs at a bifurcation point. A bifurcation point is the intersection of the primary path with the secondary path, i.e., the post-buckling path [21].

The bifurcation loads, one for every possible mode of buckling, are fairly easy to obtain using commercial software. The geometry of the structure is that of the perfect undeformed configuration, loaded with the nominal loads, and the material is elastic. Such analysis requires a minimum of effort on the part of the analyst. Commercial programs refer to this analysis as an *eigenvalue buckling analysis* because the critical loads are the eigenvalues λ_i of the discretized system of equations

$$([K] - \lambda[K_s])\{v\} = 0 \tag{4.4}$$

where K and K_s are the stiffness and stress stiffness matrix, respectively, and v is the column of eigenvectors (buckling modes) [21].

Example 4.1 *Consider a simple supported plate, with side dimensions $a_x = 1000$ mm, $a_y = 500$ mm, edgewise loaded in compression with $N_x = N_y = 1$ N/mm. The plate is made of $[(0/90)_3]_S$, AS4/9310 (Table 4.1) composite with fiber volume fraction 0.6 and total thickness $t_T = 10.2$ mm. Compute the critical load of the lowest four modes using eigenvalue analysis. Visualize the lower four modes.*

Table 4.1: Lamina elastic properties. AS4/9310, $V_f = 0.6$

Young's Moduli	**Shear Moduli**	**Poisson's Ratio**
$E_1 = 145880$ MPa	$G_{12} = G_{13} = 4386$ MPa	$\nu_{12} = \nu_{13} = 0.263$
$E_2 = E_3 = 13312$ MPa	$G_{23} = 4529$ MPa	$\nu_{23} = 0.470$

Solution to Example 4.1 *Since the laminate is symmetric, and stress computation lamina by lamina is not required, the critical loads can be obtained using three different approaches. This example continues in Example 4.3.*

First approach: Equivalent Laminate Moduli. *The equivalent laminate moduli are calculated and used along with an orthotropic shell element. In this case, laminate moduli represent the stiffness of an equivalent orthotropic plate that behaves likes the actual laminate under in-plane loads, neglecting the bending loads (see Section 3.2.6). Laminate moduli can be found as explained in Section 1.15. Introduce the lamina properties (Table 4.1) into (1.91), rotate each lamina (1.53), add then according to (1.102) get the laminate moduli (1.105) listed in Table 4.2. Note that in some cases bending laminate moduli E_x^b, etc. [1, (6.36)] may give more accurate results than in-plane laminate moduli E_x, etc. [1, (6.35)].*

The portion of the ANSYS® input file used to enter the laminate moduli is listed below and available on the Web site [5, FEAComp_Ex401_orthotropic]. Element type `SHELL281` *is used.*

Table 4.2: Equivalent laminate moduli for $[0/90_3]_S$

Young's Moduli	**Shear Moduli**	**Poisson's Ratio**
$E_x = 79985$ MPa	$G_{xy} = 4386$ MPa	$\nu_{xy} = 0.044$
$E_y = 79985$ MPa	$G_{yz} = 4458$ MPa	$\nu_{yz} = 0.415$
$E_z = 16128$ MPa	$G_{xz} = 4458$ MPa	$\nu_{xz} = 0.415$

```
/TITLE, Bifurcation, Orthotropic, FEACM with ANSYS (c) Barbero (2012)
/UNITS,MPA              ! Units are in mm, MPa, and Newtons

/PREP7                  ! Pre-processor module
! Equivalent Laminate Properties
UIMP,1,EX,EY,EZ,79985,79985,16128
UIMP,1,GXY,GYZ,GXZ,4386,4458,4458
UIMP,1,PRXY,PRYZ,PRXZ,0.044,0.415,0.415

ET,1,SHELL281           ! Chooses SHELL281 element for analysis
SECTYPE,1,SHELL         ! Section shell set #1
SECDATA,10.2,1          ! Laminate section: Th=10.2 mm, Mat. #1

! Geometry and mesh
RECTNG,0,500,0,250      ! Creates a rectangle with x=1 m and y=1 m
ESIZE,,25               ! 25 divisions for edge
AMESH,all               ! Mesh the area

FINISH                  ! Exit pre-processor module

/SOLU                   ! Solution module, (i) STATIC ANALYSIS
ANTYPE,STATIC           ! Set static analysis
PSTRESS,ON              ! Calculate the stress stiffness matrix
DL,2,1,uz,0             ! Impose Simple Supported BC
DL,3,1,uz,0
DL,1,1,symm             ! Impose Symmetry BC
DL,4,1,symm
!d,all,rotz             ! Constraint rotations about z axes (optional)
!Load application
SFL,2,PRES,1            ! Apply uniform pressure in x=500 mm
SFL,3,PRES,1            ! Apply uniform pressure in y=250 mm
SOLVE                   ! Solve current load state
FINISH                  ! Exit solution module

/SOLU                   ! Solution module, (ii) find the BIFURCATION LOADS
ANTYPE,BUCK
BUCOPT,SUBSP,10         ! Find the first 10 bifurcations loads
SOLVE                   ! Solve
FINISH                  ! Exit solution module

/SOLU                   ! Solution module, (ii) find the BUCKLING MODES
EXPASS
MXPAND
SOLVE                   ! Solve
FINISH                  ! Exit solution module

/POST1                  ! Post-processor module
SET,LIST                ! List the critical loads
SET,1,2                 ! Set mode number 2 shape
PLDISP,1                ! Display the mode 2 shape displacements
FINISH                  ! Exit post-processor module
```

The buckling loads are shown in Table 4.3.

Second approach: Using A, B, D, H, matrices*. To calculate the $A, B, D, H,$ matrices, introduce the lamina properties (Table 4.1) into (3.9). The resulting laminate matrices are*

$$\begin{bmatrix} A & B \\ B & D \end{bmatrix} = \begin{bmatrix} 817036 & 35937.6 & 0 & 0 & 0 & 0 \\ 35937.6 & 817036 & 0 & 0 & 0 & 0 \\ 0 & 0 & 44737.2 & 0 & 0 & 0 \\ 0 & 0 & 0 & 8.55845\ 10^6 & 311579 & 0 \\ 0 & 0 & 0 & 311579 & 5.60896\ 10^6 & 0 \\ 0 & 0 & 0 & 0 & 0 & 387872 \end{bmatrix}$$

$$[H] = \begin{bmatrix} 37812.8 & 0 \\ 0 & 37964.7 \end{bmatrix}$$

The ANSYS input file used to define the laminate using `SHELL281` *elements and $A, B, C, H,$ matrices is listed below.*

```
/TITLE, Bifurcation, ABDH input, FEACM with ANSYS (c) Barbero (2012)
/UNITS,MPA              ! Units are in mm, MPa, and Newtons

/PREP7                  ! Pre-processor module
! This example does not need material properties

ET,1,SHELL281           ! Chooses SHELL281 element for analysis
SECTYPE,1,GENS          ! Use preintegrated general shell section (ABDH matrix)

! ABDH matrix definition
SSPA,817036,35937.6,0,817036,0,44737.2            ! A11,A21,A31,A22,A32,A33
SSPB,0,0,0,0,0,0                                  ! B11,B21,B31,B22,B32,B33
SSPD,8.55845e+006,311579,0,5.60896e+006,0,387872  ! D11,D21,D31,D22,D32,D33
SSPE,37812.8,0,37964.7                            ! H11,H21,H22

! Geometry and mesh
RECTNG,0,500,0,250      ! Creates a rectangle with x=1 m and y=1 m
ESIZE,,25               ! 25 divisions for edge
AMESH,all               ! Mesh the area

FINISH                  ! Exit pre-processor module

/SOLU                   ! Solution module, (i) STATIC ANALYSIS
ANTYPE,STATIC           ! Set static analysis
PSTRESS,ON              ! Calculate the stress stiffness matrix
DL,2,1,uz,0             ! Impose Simple Supported BC
DL,3,1,uz,0
DL,1,1,symm             ! Impose Symmetry BC
DL,4,1,symm
!D,ALL,ROTZ             ! Constrain rotations about z axes (optional)

!Load application
```

```
SFL,2,PRES,1            ! Apply uniform pressure in x=500 mm
SFL,3,PRES,1            ! Apply uniform pressure in y=250 mm
SOLVE                   ! Solve current load state
FINISH                  ! Exit solution module

/SOLU                   ! Solution module, (ii) find the BIFURCATION LOADS
ANTYPE,BUCK
BUCOPT,SUBSP,10         ! Find the first 10 bifurcations loads
SOLVE                   ! Solve
FINISH                  ! Exit solution module

/SOLU                   ! Solution module, (ii) find the BUCKLING MODES
EXPASS
MXPAND
SOLVE                   ! Solve
FINISH                  ! Exit solution module

/POST1                  ! Post-processor module
SET,LIST                ! List the critical loads
SET,1,2                 ! Set mode number 2 shape
PLDISP,1                ! Display the mode 2 shape displacements
FINISH                  ! Exit post-processor module
```

The buckling loads are shown in Table 4.3.

Third approach: Using LLS*. The laminate stacking sequence (LSS) and the lamina properties (Table 4.1) are entered. The ANSYS input file commands to define the laminate are listed below. Element type* `SHELL281` *is used.*

```
/TITLE, Bifurcation, LSS input, FEACM with ANSYS (c) Barbero (2012)
/UNITS,MPA              ! Units are in mm, MPa, and Newtons

/PREP7                  ! Pre-processor module
! Material properties for a lamina
UIMP,1,EX,EY,EZ,145880,13312,13312
UIMP,1,GXY,GYZ,GXZ,4386,4529,4386
UIMP,1,PRXY,PRYZ,PRXZ,0.263,0.470,0.263

ET,1,SHELL281           ! Chooses Shell281 element for analysis
SECTYPE,1,SHELL         ! Section shell set #1
SECDATA,0.85,1,0        ! 1st lamina: mat. #1,  0 deg, Th=0.85 mm
SECDATA,0.85,1,90       ! 2nd lamina: mat. #1, 90 deg, Th=0.85 mm
SECDATA,0.85,1,0        ! Repeat the pattern
SECDATA,0.85,1,90
SECDATA,0.85,1,0
SECDATA,0.85,1,90       ! Same laminas in symmetrical order
SECDATA,0.85,1,90
SECDATA,0.85,1,0
SECDATA,0.85,1,90
SECDATA,0.85,1,0
SECDATA,0.85,1,90
```

```
SECDATA,0.85,1,0

! Geometry and mesh
RECTNG,0,500,0,250      ! Creates a rectangle with x=1 m and y=1 m
ESIZE,,25               ! 25 divisions for edge
AMESH,all               ! Mesh the area

FINISH                  ! Exit pre-processor module

/SOLU                   ! Solution module, (i) STATIC ANALYSIS
ANTYPE,STATIC           ! Set static analysis
PSTRESS,ON              ! Calculate the stress stiffness matrix
DL,2,1,UZ,0             ! Impose Simple Supported BC
DL,3,1,UZ,0
DL,1,1,SYMM             ! Impose Symmetry BC
DL,4,1,SYMM
!D,ALL,ROTZ             ! Constrain rotations about z axes (optional)
!Load application
SFL,2,PRES,1            ! Apply uniform pressure in x=500 mm
SFL,3,PRES,1            ! Apply uniform pressure in y=250 mm
SOLVE                   ! Solve current load state
FINISH                  ! Exit solution module

/SOLU                   ! Solution module, (ii) find the BIFURCATION LOADS
ANTYPE,BUCK
BUCOPT,SUBSP,10         ! Find the first 10 bifurcations loads
SOLVE                   ! Solve
FINISH                  ! Exit solution module

/SOLU                   ! Solution module, (ii) find the BUCKLING MODES
EXPASS
MXPAND
SOLVE                   ! Solve
FINISH                  ! Exit solution module

/POST1                  ! Post-processor module
SET,LIST                ! List the critical loads
SET,1,2                 ! Set mode number 2 shape
PLDISP,1                ! Display the mode 2 shape displacements
FINISH                  ! Exit post-processor module
```

The procedure for obtaining the solution of "Eigenvalue Buckling Analysis" in ANSYS has three steps: (i) solve the static solution using the `PSTRESS,ON` *command to obtain the stress stiffness matrix, (ii) obtain the bifurcation loads using the eigenvalue buckling solution, and (iii) expand the solution if the buckled mode shapes are needed. By running the code listed below, the critical load and buckling mode shape for every mode are obtained.*

```
/SOLU                   ! Solution module, (i) STATIC ANALYSIS
ANTYPE,STATIC           ! Set static analysis
PSTRESS,ON              ! Calculate the stress stiffness matrix
DL,2,1,UZ,0             ! Impose Simple Supported BC
```

```
DL,3,1,UZ,0
DL,1,1,SYMM             ! Impose Symmetry BC
DL,4,1,SYMM
!D,ALL,ROTZ             ! Constrain rotations about z axes (optional)
!Load application
SFL,2,PRES,1            ! Apply uniform pressure in x=500 mm
SFL,3,PRES,1            ! Apply uniform pressure in y=250 mm
SOLVE                   ! Solve current load state
FINISH                  ! Exit solution module

/SOLU                   ! Solution module, (ii) find the BIFURCATION LOADS
ANTYPE,BUCK
BUCOPT,SUBSP,10         ! Find the first 10 bifurcations loads
SOLVE                   ! Solve
FINISH                  ! Exit solution module

/SOLU                   ! Solution module, (ii) find the BUCKLING MODES
EXPASS
MXPAND
SOLVE                   ! Solve
FINISH                  ! Exit solution module
```

Using the command `SET,LIST` *in the post-processor, a list with the critical buckling loads is obtained. With* `SET,1,n`*, where n is the mode number, it is possible to select different solutions corresponding to different mode shapes, which can be plotted using* `PLDISP,1` *command, as indicated in the listing below.*

```
/POST1                  ! Post-processor module
SET,LIST                ! List the critical loads
SET,1,2                 ! Set mode number 2 shape
PLDISP,1                ! Display the mode 2 shape displacements
FINISH                  ! Exit post-processor module
```

The results of the first five modes are summarized in Table 4.3 for the equivalent lamina, A, B, D, H, matrix input, as well as for LSS. Values are shown for only five modes because lack of accuracy of results for modes above 1/2 the number of iteration vectors used in the subspace method.

Table 4.3: Bifurcation loads [N/mm]

Mode	1	2	3	4	5
Orthotropic Equivalent	252.70	570.55	1547.40	2150.80	2318.20
ABDH Input	209.53	639.98	1802.80	1822.50	1863.40
LSS Input	209.42	640.43	1794.93	1826.86	1854.23

4.1.1 Imperfection Sensitivity

To illustrate the influence of imperfections in buckling, let us consider the solid lines in Figure 4.1. The lateral deflection is zero for any load below the bifurcation load P_{CR}, that is on the primary path of the perfect structure. The primary path

intersects the secondary path at the bifurcation point, for which the load is P_{CR}. The post-critical behavior of the column is indifferent and slightly stable. Indifferent means that the column can deflect right or left. Stable post-critical path means that the column can take a slightly higher load once it has buckled. For a column, this stiffening behavior is so small that one cannot rely upon it to carry any load beyond P_{CR}. In fact, the column will deform laterally so much that the material will fail and the system will collapse. Unlike columns, simply supported plates experience significant stiffening on the secondary path.

4.1.2 Asymmetric Bifurcation

Consider the frame illustrated in Figure 4.2. An eigenvalue analysis using one finite element per bar [21, Sections 5.9 and 7.8] reveals the bifurcation load

$$P_{CR} = 8.932(10^{-6})AE \tag{4.5}$$

but gives no indication about the nature of the critical state: whether it is stable or not, whether the post-critical path is symmetric or not, and so on. We shall see later on that the frame has an asymmetric, and thus unstable post-critical path, as represented in Figure 4.2. That is, the post-critical path has a slope

$$P^{(1)} = 18.73(10^{-9})AE \text{ (1/rad)} \tag{4.6}$$

in the force-rotation diagram in Figure 4.2, where θ is the rotation of the joint at the load point.

In general, the problem with eigenvalue analysis is that it provides no indication as to the nature of the post-critical path. If the post-critical path is stiffening and symmetric as in Figure 4.1, the real structure may have a load capacity close to the bifurcation load. But if the post-critical path is unstable and/or asymmetric, as in Figure 4.2 or if there is mode interaction [16, 22–26], the real structure may have a load capacity much smaller than the bifurcation load. In order to use the information provided by eigenvalue analysis, it is necessary to understand and quantify the post-buckling behavior.

4.1.3 Post-Critical Path

One way to investigate the post-buckling behavior is to perform a continuation analysis of the imperfect structure, as presented in Section 4.2. This is perfectly possible, but complicated and time consuming, as it will be seen later in this chapter. A more expedient solution can be obtained using software capable of predicting the nature of the post-critical path, including symmetry, curvature, and mode interaction. If the secondary path is stable and symmetric, the bifurcation load can be used as a good estimate of the load capacity of the structure. The curvature of the post-critical path gives a good indication of the post-buckling stiffening and it can be used to a certain extent to predict post-buckling deformations.

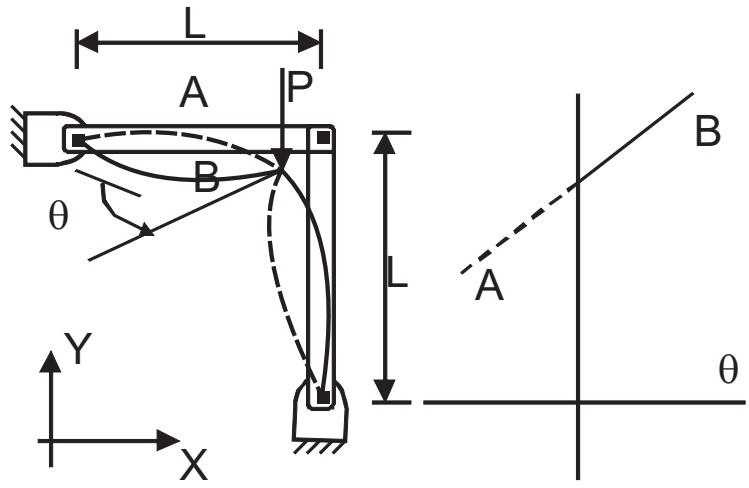

Figure 4.2: Two-bar frame.

The bifurcation load, slope, and curvature of the post-critical path emerging from the bifurcation (4.1) can be computed with BMI3 [23–25] available in [5]. The post-buckling behavior is represented by the following formula

$$\Lambda = \Lambda^{(cr)} + \Lambda^{(1)} s + \frac{1}{2}\,\Lambda^{(2)} s^2 + \dots \tag{4.7}$$

where s is the perturbation parameter, which is chosen as one component of the displacement of one node, $\Lambda^{(cr)}$ is the bifurcation multiplier, $\Lambda^{(1)}$ is the slope, and $\Lambda^{(2)}$ is the curvature of the post-critical path [22, (43)], [16,23–26]. When the slope is zero, the post-critical path is symmetric. Therefore, buckling is indifferent, and the real structure will buckle to either side. There is no way to predict which way it is going to buckle, unless of course one knows the shape of the imperfections on the real plate, which is seldom the case. A positive curvature denotes stiffening during post-buckling, and a negative one indicates that the stiffness decreases.

Example 4.2 *Consider the simple supported plate of Example 4.1. Compute the bifurcation multiplier Λ_{CR}, the critical load N_{CR}, the slope $\Lambda^{(1)}$, and the curvature $\Lambda^{(2)}$ of the post-critical path. Estimate the load when the maximum lateral deflection is equal to the thickness of the plate. As perturbation parameter, use the largest displacement component of the buckling mode with lowest buckling load.*

Solution to Example 4.2 *The program BMI3 [22], available in [5], is used in this case to compute the bifurcation multiplier Λ_{CR}, the slope $\Lambda^{(1)}$, and the curvature $\Lambda^{(2)}$ of the post-critical path. Refer to Appendix C for a description of the software interface and operation procedure. BMI3© is used from within the ANSYS graphical user interface (GUI) in this example. Since BMI3 requires the A-B-D-H matrices, the ANSYS input file is a slightly modified version of that used for the* ***second approach*** *in Example 4.1, as follows [5, FEAcomp_Ex402_ABDH.inp]*

```
/TITLE, ORTHOTROPIC PLATE WITH EDGE LOAD, BIFURCATION ANALYSIS
/UNITS,MPA              ! UNITS ARE IN MM, MPA, AND NEWTONS
```

```
/PREP7                  ! PRE-PROCESSOR MODULE
! THIS INPUT DATA DOES NOT NEED MATERIAL PROPERTIES

ET,1,SHELL99,,2         ! CHOOSES SHELL99 ELEMENT FOR ANALYSIS
                        ! SET KEYOPT(2)=2, THEN SUPPLY ABDH MATRIX
KEYOPT,1,10,2           ! SET KEYOPT(10)=2, PRINT ABDH MATRIX FILE.ABD

! REAL CONSTANT SET #1, ABDH MATRIX DEFINITION
R,1,817036,35937.6,0,0,0,0              ! REAL SET #1, A11,A12,0,A16,0,0
RMODIF,1,7,817036,0,0,0,0               ! REAL SET #1, A22,0,A26,0,0
RMODIF,1,16,44737.2,0,0                 ! REAL SET #1, A66,0,0
RMODIF,1,19,37812.8,0                   ! REAL SET #1, H44,H45
RMODIF,1,21,37964.7                     ! REAL SET #1, H55
RMODIF,1,43,8.55845E+006,311579,0,0,0,0 ! REAL SET #1, D11,D12,0,D16,0,0
RMODIF,1,49,5.60896E+006,0,0,0,0        ! REAL SET #1, D22,0,D26,0,0
RMODIF,1,58,387872,0,0                  ! REAL SET #1, D66,0,0
RMODIF,1,76,,10.2           ! REAL SET #1, AVERAGE DENSITY AND THICKNESS

! GEOMETRY AND MESH
RECTNG,0,500,0,250      ! CREATES A RECTANGLE WITH X=1 M AND Y=1 M
ESIZE,50                ! 50 SIZE ELEMENT EDGE
AMESH,ALL               ! MESH THE AREA

FINISH                  ! EXIT PRE-PROCESSOR MODULE

/SOLU                   ! SOLUTION MODULE, (I) STATIC ANALYSIS
ANTYPE,STATIC           ! SET STATIC ANALYSIS
PSTRESS,ON              ! CALCULATE THE STRESS STIFFNESS MATRIX
DL,2,1,UZ,0             ! IMPOSE SIMPLE SUPPORTED BC
DL,3,1,UZ,0
DL,1,1,SYMM             ! IMPOSE SYMMETRY BC
DL,4,1,SYMM
!D,ALL,ROTZ             ! CONSTRAINT ROTATIONS ABOUT Z AXES (OPTIONAL)

!LOAD APPLICATION
!SFL,2,PRES,1           ! APPLY UNIFORM PRESSURE IN X=500 MM
LSEL,S,LOC,X,500
NSLL,S,1
*GET,NNOD,NODE,,COUNT
F,ALL,FX,-(1*250)/NNOD

!SFL,3,PRES,1            ! APPLY UNIFORM PRESSURE IN Y=250 MM
LSEL,S,LOC,Y,250
NSLL,S,1
*GET,NNOD,NODE,,COUNT
F,ALL,FY,-(1*500)/NNOD
ALLSEL

SOLVE                   ! SOLVE CURRENT LOAD STATE
FINISH                  ! EXIT SOLUTION MODULE
```

```
/SOLU                   ! SOLUTION MODULE, (II) FIND THE BIFURCATION LOADS
ANTYPE,BUCK
BUCOPT,SUBSP,10         ! FIND THE FIRST 10 BIFURCATIONS LOADS
SOLVE                   ! SOLVE
FINISH                  ! EXIT SOLUTION MODULE

/SOLU                   ! SOLUTION MODULE, (II) FIND THE BUCKLING MODES
EXPASS
MXPAND
SOLVE                   ! SOLVE
FINISH                  ! EXIT SOLUTION MODULE

/POST1                  ! POST-PROCESSOR MODULE
SET,LIST                ! LIST THE CRITICAL LOADS
SET,1,1                 ! SET MODE NUMBER 1 SHAPE
/VIEW,,1,1,1
PLDISP,2                ! DISPLAY THE MODE SHAPE
FINISH                  ! EXIT POST-PROCESSOR MODULE
```

The model in ANSYS and solved by using the "Eigenvalue buckling analysis" procedure for obtaining the bifurcation loads $\Lambda^{(cr)}$. *The critical lowest load is displayed on the ANSYS GUI as* `FREQ=210.2` *for* `STEP=1`, `SUB=1`. *Since the buckling mode is scaled to a maximum amplitude of 1.0, we get* `DMX=1`. *A list of buckling loads can be recalled by the command* `SET,LIST`.

Next, details about how to run BMI3 from within ANSYS are given in Appendix C.2.2. Within the ANSYS GUI, Run the APDL macro `ans2i` *(available in [5]) simply by entering* `ans2i` *in the ANSYS command line to calculate parameters of the post-critical path. BMI3 will be executed.*

Find the `ANSYS Output Window` *minimized in your Taskbar and open it up. Then, manually introduce the following responses to the prompts:*

- *...sort (0 = none, 1 =* x*, 2 =* y*, 3 =* z*):* `1`. *To minimize the bandwidth, usually it is best to sort along the direction that has more elements and/or nodes.*
- *...for perturbation analysis (y/n)?:* `n`. *In this way, BMI3 chooses as perturbation parameter the largest displacement component of the buckling mode with lowest buckling load. In this case, that corresponds to the first buckling mode, the node in the middle of the plate, and the deflection direction* δ.

The following results are obtained:

$$\Lambda^{(cr)} = -209.0418; \quad \Lambda^{(1)} \approx 0; \quad \Lambda^{(2)} = -0.2308$$

Since BMI3 solves the problem using reversed loads (see Appendix C), then (4.7) becomes

$$\begin{aligned} -N = &\quad \Lambda^{(cr)} + \Lambda^{(1)} s + \tfrac{1}{2}\, \Lambda^{(2)} s^2 \\ N = &\quad -\Lambda^{(cr)} - \Lambda^{(1)} s - \tfrac{1}{2}\, \Lambda^{(2)} s^2 \end{aligned}$$

and, in this case the perturbation direction is $s = -\delta$, *so*

$$\begin{aligned} N = &\quad -\Lambda^{(cr)} - \Lambda^{(1)}(-\delta) - \tfrac{1}{2}\, \Lambda^{(2)}(-\delta)^2 \\ N = &\quad -\Lambda^{(cr)} + \Lambda^{(1)} \delta - \tfrac{1}{2}\, \Lambda^{(2)} \delta^2 \end{aligned}$$

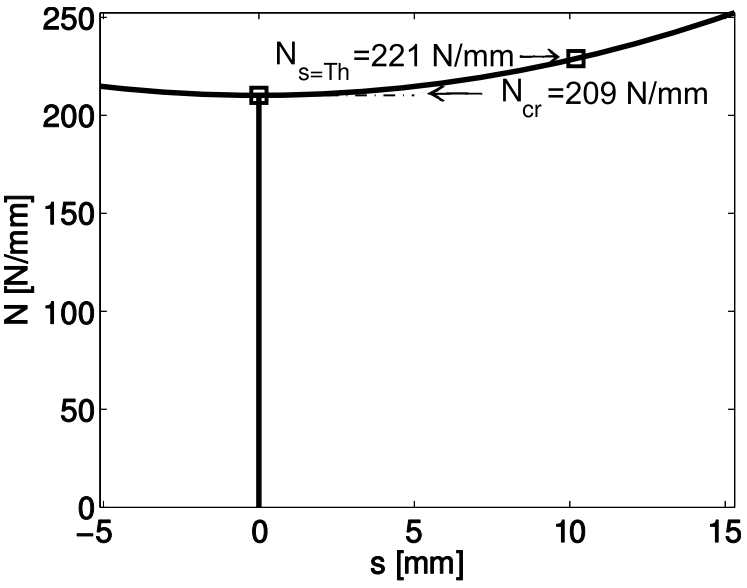

Figure 4.3: Equilibrium paths for a perfect plate.

Therefore, using the results from BMI3, the secondary path of bifurcation analysis is

$$N = -(-209.0418) + (0)\ \delta - (-0.1154)\ \delta^2 = 209.0418 + 0.1154\ \delta^2$$

Since the slope $\Lambda(1)$ *is zero, the post-critical path is symmetric. The post-buckling load when the lateral deflection (w) is equal to the thickness* ($s = Th = 10.2$ *mm) is equal to* 221 *N/mm, as shown in Figure 4.3.*

Figure 4.3 can be drawn based on the results from BMI3 by using the MATLAB® code shown next.

```
% plot Figure~4.3, FEA of Comp Mater Using ANSYS--Second Ed.
% Ever J. Barbero (c) 2007, 2013
clear all; close all;
Th=0.85*12 %10.8
lambda0= +(-209.04) %216.66%  210.7879
lambda1= -(-0)      %-0.24389% 2.063125
lambda2= +(-0.2308) %0.3602 %0.36291%  0.368516
s_ini=-0.5*Th;
s_fin=1.5*Th;
s_inc = [s_ini:0.1:s_fin];
P_inc = lambda0 + lambda1 .* s_inc + lambda2.*s_inc.^2;
s = 1*Th;
P = lambda0 + lambda1*s + lambda2*s^2;
Po= lambda0;
s1_inc = [0,0]; %[0.2,0.2];
P1_inc = [0,Po];
so_inc = [0:1:Th/2];
Po_inc = lambda0 .* so_inc./so_inc;
```

```
% Ansys results OPEN I/O FILES
n_file = 'FEAcomp_Ex402_conti_225' % series name
fidinp = fopen([n_file,'.txt'],'r');
results = (fscanf(fidinp,'%g %g',[2 inf]));
fclose(fidinp);
results(1,:)=(results(1,:)-1)*(225)
linetxt1 = ['N_{s=Th}=' num2str(-int32(P)) ' N/mm  \rightarrow  ']
linetxt2 = [' \leftarrow N_{cr}=' num2str(-int32(Po)) ' N/mm']
linewth  = 2.8
figure1 = figure
plot(s_inc,-P_inc,'k','LineWidth',linewth)
xlabel('s [mm]','Fontsize',16);ylabel('N [N/mm]','Fontsize',16);
hold on
plot(s1_inc,-P1_inc,'k','LineWidth',linewth)
plot(so_inc,-Po_inc,'k-.','LineWidth',1)
text(s,-P,linetxt1,'HorizontalAlignment','right','Fontsize',16)
text(Th/2,-Po,linetxt2,'HorizontalAlignment','left','Fontsize',16)
axis([s_ini s_fin 0 -min(P_inc)])
set(gca,'Fontsize',16);
plot(s,-P,'ks','MarkerSize',10,'LineWidth',2)
plot(0,-Po,'ks','MarkerSize',10,'LineWidth',2)
hold off
saveas(figure1,['Fig4_3'],'pdf');
```

4.2 Continuation Methods

The strain to failure of polymer matrix composites (PMC) is high. Compare 1.29% for AS4/3501 and 2.9% for S-glass/epoxy with only 0.2% for steel and 0.4% for aluminum. That means that buckling deformations can go into the post-buckling regime while the material remains elastic. However, great care must be taken that no matrix dominated degradation mode takes place, in which case the material will not remain elastic (see Chapter 8). Eigenvalue buckling analysis is relatively simple as long as the material remains elastic because classical theory of elastic stability can be used, as was done in Section 4.1. Material nonlinearity is one reason that motivates an incremental analysis. Another reason is to evaluate the magnitude of the buckling load for an *imperfection sensitive* structure.

In an incremental analysis, also called continuation analysis, the load is increased gradually step by step. At each step, the deformation, and possibly the changing material properties, are evaluated. Incremental analysis must include some type of imperfection, in the geometry, material, or alignment of loads. Lacking any imperfection, incremental analysis will track the linear solution, revealing no bifurcations or limit points.

Continuation methods are a form of geometrically nonlinear analysis. The system must have a nontrivial fundamental path, such as a flat plate with asymmetric laminate stacking sequence (LSS) under edge loads.

If the system has a trivial fundamental path, such a flat plate with symmetric LSS under edge load, the nontrivial fundamental path can be forced by introducing

an imperfection. Several types of imperfections are possible, including material imperfections (e.g., unsymmetrical LSS), geometric imperfections, or load eccentricity are used.

Since the real geometric imperfections are seldom known, the preferred artificial geometric imperfection is in the form of the bifurcation mode having the lowest bifurcation load. This is true in most cases; however, in some cases, a second mode that is associated to imperfections that are more damaging to the structure should be used [27]. Also, if the structure has an asymmetric post-buckling path, as the two-bar example in Figure 4.2, care must be taken not to force the structure along the stiffening path.

Finite element analysis (FEA) codes allow the user to modify a mesh by superposing an imperfection in the shape of any mode from a previous bifurcation analysis onto the perfect geometry (see Example 4.3).

Example 4.3 *Using ANSYS, apply a geometric imperfection $w_p(x,y) = \delta_0\ \phi(x,y)$ to Example 4.1 and plot the load-multiplier vs. maximum lateral deflection for an imperfection magnitude $\delta_0 = Th/10$ and $\delta_0 = Th/100$, where Th is the total laminate thickness, and $\phi(x,y)$ is the buckling mode corresponding to the lowest bifurcation load found in Example 4.1.*

Solution to Example 4.3 *First the buckling modes are found using the bifurcation method (execute the commands shown in Example 4.1).*

Then the nodal positions are updated using the `UPGEOM` *command. Using this command the displacements from a previous analysis can be added in order to update the geometry of the finite element model to that of the deformed configuration.*

Since the displacements have been obtained from a mode shape, the maximum displacement in the results file is 1.0. *The* `UPGEOM` *allows the user to define a multiplier for displacements being added to the nodal coordinates. In this case, the multiplier factors chosen are $\delta_0 = Th/10$ and $\delta_0 = Th/100$. Therefore, an initial deflection equal to the first mode of buckling with a central deflection δ_0 is forced on the structure.*

Using a continuation method with this imperfect geometry, the continuation equilibrium paths shown in Figure 4.4 are obtained. It can be seen that eventually the continuation solution approaches the secondary path of the perfect structure, shown by dashed lines in Figure 4.4. For smaller imperfections, the continuation solution follows more closely the primary path, then the secondary path. A structure with large imperfections deviates more from the behavior of the perfect structure, as show by the solution corresponding to an imperfection $\delta_0 = Th/10$.

```
/TITLE, Geometric imperfection, FEACM with ANSYS (c) Barbero (2012)
/UNITS,MPa              ! Units are in mm, MPa, and Newtons

/PREP7                  ! Pre-processor module
! Material properties for lamina
UIMP,1,EX,EY,EZ,145880,13312,13312
UIMP,1,GXY,GYZ,GXZ,4386,4529,4386
UIMP,1,PRXY,PRYZ,PRXZ,0.263,0.470,0.263

ET,1,SHELL281           ! Chooses Shell281 element for analysis
SECTYPE,1,SHELL         ! Section shell set #1
```

```
SECDATA,0.85,1,0        ! 1st lamina: mat. #1,  0 deg, Th=0.85 mm
SECDATA,0.85,1,90       ! 2nd lamina: mat. #1, 90 deg, Th=0.85 mm
SECDATA,0.85,1,0        ! Repeat the pattern
SECDATA,0.85,1,90
SECDATA,0.85,1,0
SECDATA,0.85,1,90       ! Same laminas in symmetrical order
SECDATA,0.85,1,90
SECDATA,0.85,1,0
SECDATA,0.85,1,90
SECDATA,0.85,1,0
SECDATA,0.85,1,90
SECDATA,0.85,1,0

! Geometry and mesh
RECTNG,0,500,0,250      ! Creates a rectangle with x=1 m and y=1 m
ESIZE,50                ! 50 size element edge
AMESH,all               ! Mesh the area

FINISH                  ! Exit pre-processor module

/SOLU                   ! Solution module, (i) STATIC ANALYSIS
ANTYPE,STATIC           ! Set static analysis
PSTRESS,ON              ! Calculate the stress stiffness matrix
DL,2,1,uz,0             ! Impose Simple Supported BC
DL,3,1,uz,0
DL,1,1,symm             ! Impose Symmetry BC
DL,4,1,symm
!D,ALL,ROTZ             ! Constraint rotations about z axes (optional)

!Load application
SFL,2,PRES,1            ! Apply uniform pressure in x=500 mm
SFL,3,PRES,1            ! Apply uniform pressure in y=250 mm
SOLVE                   ! Solve current load state
FINISH                  ! Exit solution module

/SOLU                   ! Solution module, (ii) find the BIFURCATION LOADS
ANTYPE,BUCK
BUCOPT,SUBSP,10         ! Find the first 10 bifurcations loads
SOLVE                   ! Solve
FINISH                  ! Exit solution module

/SOLU                   ! Solution module, (ii) find the BUCKLING MODES
EXPASS
MXPAND
SOLVE                   ! Solve
FINISH                  ! Exit solution module

/PREP7                  ! Pre-processor module
ftr=(10.8/10)           ! Multiplicator shape factor (Th/10)
UPGEOM,ftr,1,1,file,rst
    ! ftr: Multiplier for displacements added to coordinates
```

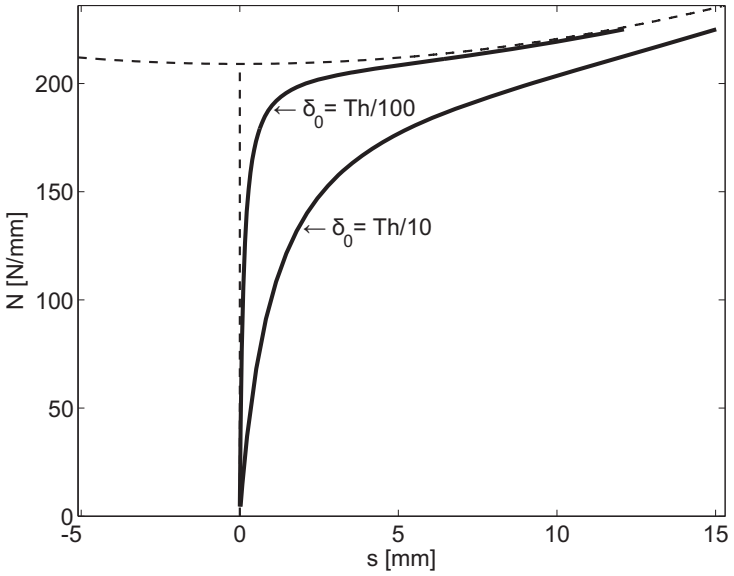

Figure 4.4: Equilibrium paths for a $[(0/90)_3]_S$ plate, with $\delta_0 = Th/10$ and $\delta_0 = Th/100$.

```
    ! 1,1 : Load step 1, substep=1, equivalent to mode =1
    ! file,rst: results file to obtain displacements
FINISH                  ! Exit pre-processor module

/SOLU                   ! Solution module, Continuation loads
ANTYPE,STATIC           ! Set static analysis
NLGEOM,1                ! Use large displacements analysis
OUTRES,ALL,ALL          ! Keep results of each substep

mult=225                ! Apply loads until N = 225 N/mm
SFL,2,PRES,1*mult       ! Apply uniform pressure in x=500 mm
SFL,3,PRES,1*mult       ! Apply uniform pressure in y=250 mm

ARCLEN,1,10,0.1         ! Use ARCLENG method to obtain solution
NSUBST,50,0,0           ! #Substeps
SOLVE                   ! Solve current load state
FINISH                  ! Exit solution module

/POST26                 ! Post-processor module
LINES,1000              ! List without breaks between pages
NSOL,2,1,U,Z,UZ_node1   ! Load deflexion in central plate node
PLVAR,2                 ! DISPLAY VARIABLES evolution
PRVAR,2                 ! PRINT VARIABLES evolution
FINISH
```

Example 4.4 *Find the buckling load multiplier and the first mode shape for Example 3.11.*

Solution to Example 4.4 *The solution is found by first executing the APDL code for Example 3.11, available in [5, FEAComp_Ex_311.inp]. Then, execute the APDL shown next.*

```
!Buckling analysis for H-COLUMN CST 58 (1998) 1335-1341 - ANSYS R14
/SOLU                          !ENTER SOLUTION MODULE
!FIRST PHASE
ANTYPE,STATIC,RESTART,,,PERTURB !RESTART THE LINEAR BASE ANALYSIS
PERTURB,BUCKLE,,,ALLKEEP     !LINEAR PERTURBATION EIGENVALUE BUCKLING
                               !KEEP ALL THE BOUNDARY CONDITIONS
SOLVE,ELFORM                   !REGENERATE ELEMENT MATRICES
!SECOND PHASE
BUCOPT,SUBSP,1                 !SUBSPACE ITERATION EIGENSOLVER
                               !EXTRACT 1 BUCKLING MODE
MXPAND,1                       !NUMBER OF MODES TO EXPAND AND WRITE
SOLVE
FINISH                         !EXIT SOLUTION MODULE

/POST1           !POSTPROCESSOR MODULE
FILE,,RSTP       !*.RSTP FILE TO REVIEW RESULTS FROM LINEAR PERTURBATION
SET,1,1          !SELECT 1ST LOAD CASE, 1ST EIGENVALUE
*GET,LCR,TIME    !GET THE EIGENVALUE IN USER DEFINED VARIABLE LCR
PLDISP,2         !PLOT MODE SHAPE AND OUTLINE OF UNDEFORMED SHAPE
```

The load multiplier Λ^{cr} can be read from the GUI as `FREQ=54.288` on the same screen that shows the mode shape for mode one (`STEP=1, SUB=1`). The buckling load is simply the product of the load multiplier by the applied load $P^{cr} = 54.142 \times 11,452 = 597,130\ N$. The buckling mode shape can be seen in Figure 4.5. The value of DMX is irrelevant because in eigenvalue analysis the amplitude of the deformed shape of the buckling modes is undetermined.

Suggested Problems

Problem 4.1 *Compute the bifurcation load P^c of the two-bar frame in Figure 4.2 using one quadratic beam element per bar. Each bar has length $L = 580\ mm$, area $A = 41\ mm^2$, inertia $I = 8.5\ mm^4$, height $H = 10\ mm$, and modulus $E = 200\ GPa$. The connection between the two bars is rigid.*

Problem 4.2 *Perform a convergence study on the bifurcation load P^c of the two-bar frame in Problem 4.1 by increasing the number of elements per bar N until the bifurcation load converges within 2%. Plot P^c vs. N.*

Problem 4.3 *Recalculate Example 4.2 when the LSS changes to $[(0/90)_6]_T$, thus becoming asymmetric. Do not introduce any imperfection but rather analyze the perfect system, which in this case is asymmetric.*

Problem 4.4 *Recalculate Example 4.2 with $[(0/90)_6]_T$, and $N_x = 1, N_y = N_{xy} = 0$. Do not introduce any imperfection but rather analyze the perfect system, which in this case is asymmetric.*

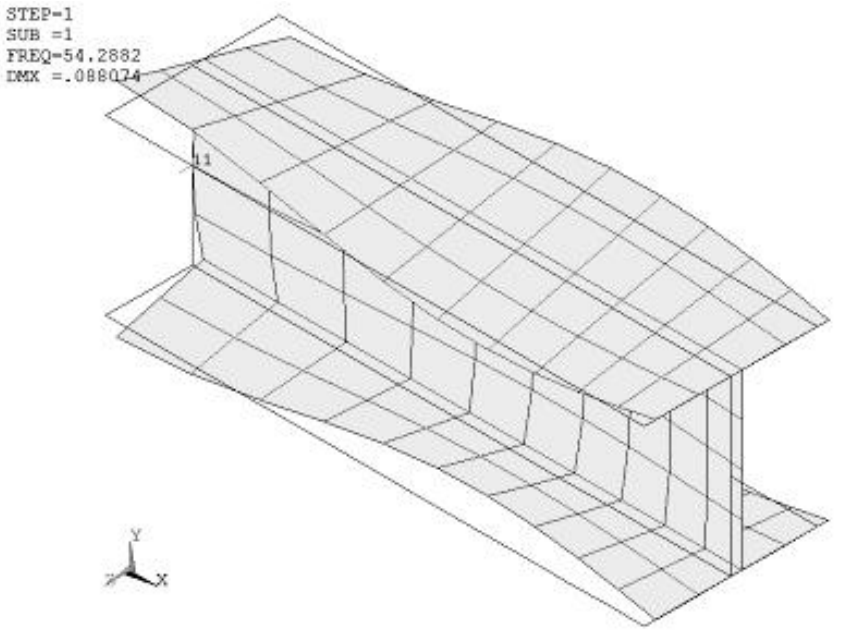

Figure 4.5: Buckling mode shape, Example 4.4.

Problem 4.5 *Using a FEA code, plot the continuation solution for* $\delta_0 = Th/100$ *as in Figure 4.4, for a cylindrical shell with distributed axial compression on the edges. The cylinder has a length of* $L = 965$ *mm and a mid-surface radius of* $a = 242$ *mm. The LSS is* $[(0/90)_6]_S$*, with lamina thickness* $t = 0.127$ *mm. The laminas are of E-glass/epoxy with* E_1*=54 GPa,* E_2*=18 GPa,* $G_{12} = 9$ *GPa,* $\nu_{12} = 0.25$*, and* $\nu_{23} = 0.38$*.*

Problem 4.6 *Compute the maximum stress failure index* I_f *of Problem 4.5 at* $P = \Lambda^{(cr)}$*. The strength values are* $F_{1t} = 1034$ *MPa,* $F_{1c} = 1034$ *MPa,* $F_{2t} = 31$ *MPa,* $F_{2c} = 138$ *MPa, and* $F_{6t} = 41$ *MPa.*

Problem 4.7 *Plot the imperfection sensitivity of the cylindrical shell of Problem 4.5, for imperfections in the range* $(Th/200) < s < Th$*.*

Chapter 5

Free Edge Stresses

In-plane loading N_x, N_y, N_{xy}, of symmetric laminates induces only in-plane stress σ_x, σ_y, σ_{xy}, in the interior of the laminate. Near the free edges, interlaminar stresses σ_z, σ_{yz}, σ_{xz}, are induced due to the imbalance of the in-plane stress components at the free edge.

For illustration, consider a long laminated strip of length $2L$, width $2b << 2L$, and thickness $2H < 2b$ (Figure 5.1). The strip is loaded by an axial force N_x only. For a balanced, symmetric laminate the mid-plane strains and curvatures (see (3.6)) are uniform over the entire cross-section and given by

$$\begin{aligned} \epsilon_x^0 &= \alpha_{11} N_x \\ \epsilon_y^0 &= \alpha_{12} N_x \\ \gamma_{xy}^0 &= 0 \\ k_x = k_y = k_{xy} &= 0 \end{aligned} \tag{5.1}$$

where α_{11}, α_{12}, are in-plane laminate compliances, which are obtained by inverting (3.8); see also [1, (6.21)]. From the constitutive equation [1, (6.24)] for lamina k, we get

$$\begin{aligned} \sigma_x^k &= \left(\overline{Q}_{11}^k \alpha_{11} + \overline{Q}_{12}^k \alpha_{12}\right) N_x \\ \sigma_y^k &= \left(\overline{Q}_{12}^k \alpha_{11} + \overline{Q}_{22}^k \alpha_{12}\right) N_x \\ \sigma_{xy}^k &= \left(\overline{Q}_{16}^k \alpha_{11} + \overline{Q}_{26}^k \alpha_{12}\right) N_x \\ \sigma_z^k = \sigma_{xz}^k &= \sigma_{yz}^k = 0 \end{aligned} \tag{5.2}$$

A piece of laminate taken out of the interior of the laminate will have balanced σ_y and σ_{xy} on opposite faces; the free body diagram (FBD) is in equilibrium without the need for any additional forces. In this case we say the stress components are self-equilibrating. At the free edge in Figure 5.1, σ_y=σ_{xy}=σ_{yz}=0. If σ_y and σ_{xy} are not zero in the interior of the laminate, but are zero at the free edge, then some other stresses must equilibrate them.

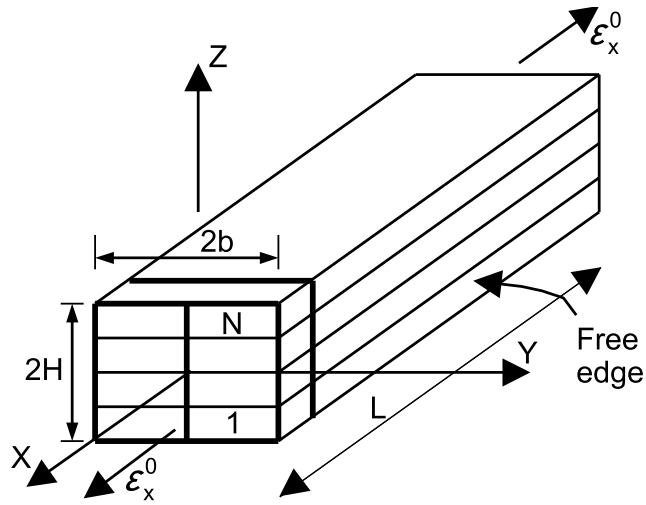

Figure 5.1: Tensile coupon.[1]

5.1 Poisson's Mismatch

A lamina subjected to tensile loading in one direction will contract in the direction perpendicular to the load. If two or more laminas with different Poisson's ratios are bonded together, interlaminar stress will be induced to force all laminas to deform equally at the interfaces (Figure 5.2). Over the entire laminate thickness, these stresses add up to zero since there is no transverse loading N_y applied. In other words, they are self-equilibrating in such a way that

$$\int_{z_0}^{z_N} \sigma_y dz = 0 \tag{5.3}$$

where z_0 and z_N are the coordinates of the bottom and top surfaces, respectively.

5.1.1 Interlaminar Force

As noted in (5.3), the in-plane stress σ_y calculated with classical lamination theory (CLT) is self-equilibrating when added through the whole thickness of the laminate [1, Chapter 6]. But on a portion of the laminate (above z_k in Figure 5.3), the stresses σ_y may not be self-equilibrating. Therefore, the contraction or expansion of one or more laminas must be equilibrated by interlaminar shear stress σ_{yz}. Since there is no shear loading on the laminate, the integral of σ_{yz} over the entire width of the sample must vanish. Over half the width of the laminate, however, an interlaminar shear force exists if the stress σ_y above or below the surface is not self-equilibrating. The magnitude of these per unit length forces can be estimated by integrating the interlaminar shear stress σ_{yz} over half the width of the laminate ($0 < y < b$). By

[1]Reprinted from *Mechanics of Fibrous Composites*, C. T. Herakovich, Figure 8.1, copyright (1998), with permission from John Wiley & Sons, Inc.

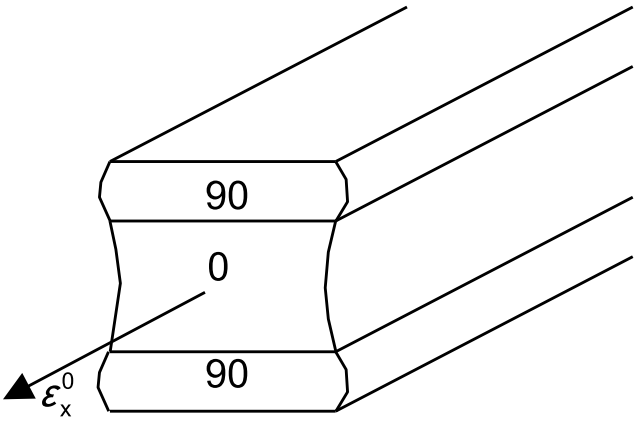

Figure 5.2: Poisson's effect.[2]

equilibrium

$$F_{yz}(z_k) = \int_0^b \sigma_{yz_{(z=z_k)}} dy = -\int_{z_k}^{z_N} \sigma_y dz \tag{5.4}$$

The interlaminar shear stress σ_{yz} is not available from classical lamination theory but the transverse stress σ_y is. Therefore, the magnitude of the interlaminar shear force can be computed anywhere through the thickness of a laminate in terms of the known transverse stress distribution σ_y.

The in-plane stress σ_y in a balanced, symmetric laminate under tensile load is constant in each lamina. Therefore, when the interlaminar force is evaluated at an interface (located at $z = z_k$), the integration above reduces to

$$F_{yz}(z_k) = -\sum_{i=k}^{N} \sigma_y^i t_i \tag{5.5}$$

where t_i are the thicknesses of the laminas.

The magnitude of the interlaminar shear force F_{yz} can be used to compare different stacking sequences in an effort to minimize the free-edge interlaminar shear stress σ_{yz}. However, the force does not indicate how large the actual stress is. Therefore, it can be used to compare different laminate stacking sequence (LSS) but not as a failure criterion.

5.1.2 Interlaminar Moment

The interlaminar shear stress σ_{yz} produces shear strain γ_{yz}, which must vanish at the center line of the sample because of symmetry. Therefore, $\sigma_{yz} = 0$ at the center line. Also, at the free edge, σ_{yz} must vanish because σ_{zy} vanishes there. But for any position z_k above which σ_y is not self-equilibrating, σ_{yz} must be different from zero somewhere between the edge and the center line. A numerical solution of σ_{yz}

[2]Reprinted from *Mechanics of Fibrous Composites*, C. T. Herakovich, Figure 8.14, copyright (1998), with permission from John Wiley & Sons, Inc.

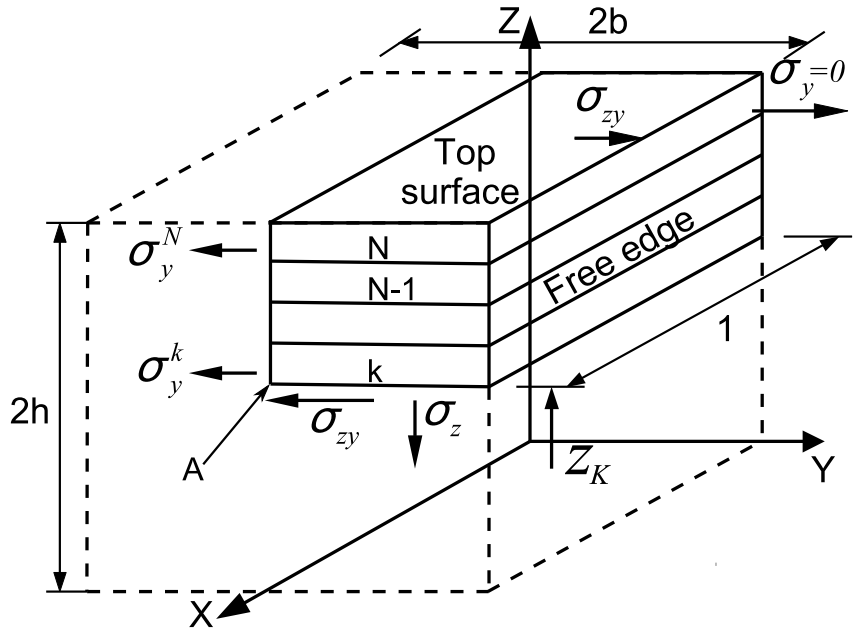

Figure 5.3: Free body diagram of sublaminate used for computation of Poisson-induced forces F_{yz} and moments M_z.

is plotted in Figure 5.5 in terms of the distance y/b from the free edge. It reveals that σ_{yz} grows rapidly near the free edge and then tapers out at the interior of the laminate.

A not self-equilibrating distribution of stress yields both a force F_{yz} (5.5) and a moment. To compute the moment M_z, take moments of the stress σ_y with respect to point A in Figure 5.3. A non-vanishing moment produced by σ_y can only be equilibrated by a moment produced by transverse stress σ_z. Therefore, the moment M_z is defined as

$$M_z(z_k) = \int_0^b \sigma_{z_{(z=z_k)}} y dy = \int_{z_k}^{z_N} (z - z_k)\sigma_y dz \tag{5.6}$$

where z_k is the coordinate of the top surface of lamina k, and z_N is the coordinate of the top surface of the laminate (see [1, Figure 6.6] for the definition of the coordinate system through the thickness of the laminate).

The existence of σ_z is corroborated by free-edge delamination during a tensile test, at a much lower load than the failure load of the laminate. The magnitude of the moment can be used to compare different stacking sequences in an effort to minimize the thickness stress σ_z. However, the moment does not indicate how large the actual stress is, and thus it cannot be used as a failure criterion.

The in-plane stress σ_y in a balanced laminate under tensile load is constant in each lamina. Therefore, when the interlaminar moment is evaluated at an interface (located at $z = z_k$), the integration above reduces to

$$M_z(z_k) = \sum_{i=k}^{N} \sigma_y^i (z_i t_i + \frac{t_i^2}{2} - z_k t_i) \tag{5.7}$$

Since σ_z is a by-product of σ_{yz}, which vanishes at $y = 0$ due to symmetry, then σ_z must vanish at the center line of the specimen ($y = 0$) but it is large near the edge. Since no vertical load is applied, the integral of σ_z must be zero. Therefore, it must be tensile (positive) on some regions and compressive (negative) at others. A numerical solution reveals that σ_z grows rapidly near the free edge, dips to negative values, and then tapers out at the interior of the laminate. A numerical solution of σ_z is plotted in Figure 5.5 in terms of the distance y/b from the free edge. However, $\sigma_z \to \infty$ as $y \to b$. This is a singularity that is not handled well by finite element analysis (FEA). Therefore the results, even for $y < b$, will be very dependent on the mesh refinement. Furthermore, since $\sigma_z \to \infty$, the results cannot be used in a failure criterion without further consideration.

Example 5.1 *Compute F_{yz} and M_z at all interfaces of a balanced $[0_2/90_2]_s$ symmetric laminate (Figure 5.1) loaded with $N_x = 175$ KN/m. Use unidirectional lamina carbon/epoxy properties E_1=139 GPa, E_2=14.5 GPa, $G_{12} = G_{13} = 5.86$ GPa, $G_{23} = 5.25$ GPa, $\nu_{12} = \nu_{13} = 0.21$, $\nu_{23} = 0.38$. The lamina thickness is $t_k = 0.127$ mm.*

Solution to Example 5.1 *The in-plane stress distribution σ_y through the thickness can be obtained by the procedure described in [1, Section 6.2], which is implemented in CADEC [9]. The stress values are shown in Table 5.1.*

To calculate F_{yz}, compute the contribution of all laminas above a given interface using (5.5). The in-plane stress σ_y in a balanced laminate under in-plane load is constant in each lamina, so (5.5) applies. For other cases, (5.4) can be integrated exactly since σ_y is linear in z, or F_{yz} can be approximated by (5.5) using the average σ_y in each lamina.

Since the laminate is balanced and loaded with in-plane loads only, M_z can be computed using (5.7). Otherwise, use (5.6) or approximate M_z by using the average σ_z in each lamina into (5.7).

The results are shown Table 5.1 and Figure 5.4.

Example 5.2 *Plot σ_{yz} and σ_z vs y for $0 < y < b$ at the 90/0 interface above the middle surface of a $[0/90]_s$ laminate with properties $E_1 = 139$ GPa, $E_2 = 14.5$ GPa, $G_{12} = G_{13} = 5.86$ GPa, $G_{23} = 5.25$ GPa, $\nu_{12} = \nu_{13} = 0.21$, $\nu_{23} = 0.38$. Take $2b = 20$ mm, length of the sample $2L = 80$ mm, thickness of each lamina $t_k = 1.25$ mm. Load the sample with a uniform strain $\epsilon_x = 0.01$ by applying a uniform displacement at $x = L$. Use orthotropic solid elements on each lamina. Refine the mesh towards the free edge. Use at least two quadratic elements through the thickness of each lamina and an element aspect ratio approximately one near the free edge.*

Solution to Example 5.2 *Note that it is not necessary to model the whole geometry. Symmetry can be used to model only the quadrant with $x > 0, y > 0, z > 0$; that is one-eighth of the plate, as shown in Figure 5.3. Since any cross-section $y - z$ has the same behavior, only a short segment between $x = 0$ and $x = L\star$ needs to be modeled. Since free edge effects also occur at $x = 0$ and $x = L\star$, take $L\star = 8h$ and plot the results at $x = L\star/2$ to avoid free edge effects at the two loaded ends of the model. The solution is shown in Figure 5.5.*

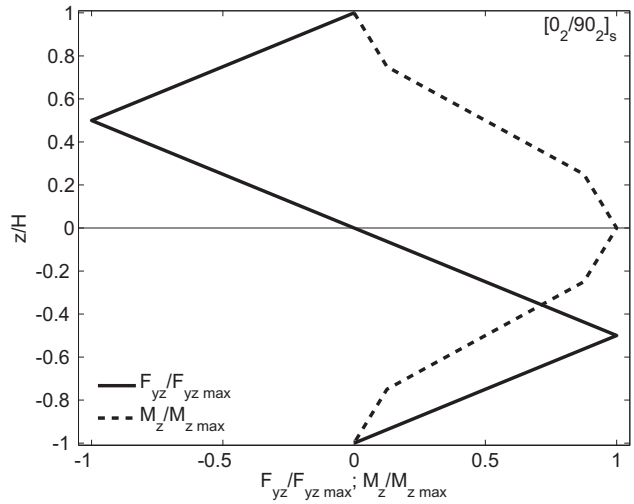

Figure 5.4: Interlaminar force F_{yz} and moment M_z due to Poisson's effect.

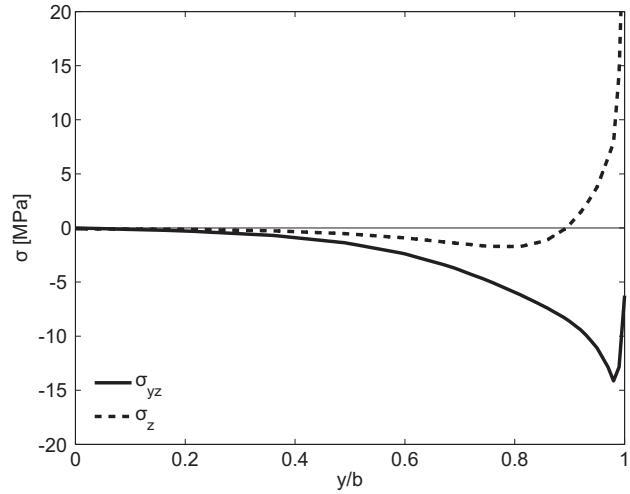

Figure 5.5: Interlaminar stress σ_{yz} and σ_z at the 90/0 interface of a carbon/epoxy $[0/90]_S$ laminate (FEA).

Table 5.1: Poisson's interlaminar force F_{yz}

k	Pos	σ_y [MPa]	t_k [mm]	z [mm]	F_{yz} [kN/m]	M_z [N m/m]
8	TOP	$5.55\ 10^{-3}$		0.508	0.000	
8	BOT	$5.55\ 10^{-3}$	0.127	0.381	-0.705	0.045
7	TOP	$5.55\ 10^{-3}$		0.381	-0.705	
7	BOT	$5.55\ 10^{-3}$	0.127	0.254	-1.410	0.179
6	TOP	$-5.55\ 10^{-3}$		0.254	-1.410	
6	BOT	$-5.55\ 10^{-3}$	0.127	0.127	-0.705	0.313
5	TOP	$-5.55\ 10^{-3}$		0.127	-0.705	
5	BOT	$-5.55\ 10^{-3}$	0.127	0.000	0.000	0.358
4	TOP	$-5.55\ 10^{-3}$		0.000	0.000	
4	BOT	$-5.55\ 10^{-3}$	0.127	-0.127	0.705	0.313
3	TOP	$-5.55\ 10^{-3}$		-0.127	0.705	
3	BOT	$-5.55\ 10^{-3}$	0.127	-0.254	1.410	0.179
2	TOP	$5.55\ 10^{-3}$		-0.254	1.410	
2	BOT	$5.55\ 10^{-3}$	0.127	-0.381	0.705	0.045
1	TOP	$5.55\ 10^{-3}$		-0.381	0.705	
1	BOT	$5.55\ 10^{-3}$	0.127	-0.508	0.000	0.000

See the command input file below. The `PATH` *commands define, plot, and print the stress values shown in Figure 5.5.*

```
/TITLE,Free Edge Analysis [0/90]s laminate
/PREP7                  ! Pre-processor module
*SET,THZ,1.25           ! thickness of lamina in mm
*SET,LX,8*THZ           ! 1/2 length of laminate in mm
*SET,BY,10.0            ! 1/2 width of laminate in mm
*SET,NEX,8              ! number of elements in x/z direction
*SET,NEY,14             ! number of elements in y direction
*SET,EPSX,0.01          ! uniform strain in x direction

! Equivalent Material properties
UIMP,1,EX,EY,EZ,139E3,14.5E3,14.5E3
UIMP,1,GXY,GYZ,GXZ,5.86E3,5.25E3,5.86E3
UIMP,1,PRXY,PRYZ,PRXZ,0.21,0.38,0.21

ET,1,SOLID186               ! Chooses SOLID186 element for analysis
KEYOPT,1,2,1                ! KEYOPT(2) = 1 Enables Full Integration

! Define material orientation by local Coordinate
LOCAL,11,,0,0,0,90          ! defines 90 degree local cs
LOCAL,12,,0,0,0,0           ! defines 0 degree local cs
CSYS,0                      ! set active cs to cart. system

! Generate Geometry
BLOCK,0,LX,0,BY,0,THZ       ! 90 degrees lamina
BLOCK,0,LX,0,BY,THZ,2*THZ   ! 0 degress lamina
VGLUE,ALL                   ! Glue volumes
```

```
! Mesh Control and Mesh
LESIZE,ALL,,,NEX            ! line number divisions = nex
LSEL,S,LOC,Z,0              ! selects lines z=0
LSEL,A,LOC,Z,THZ            ! add lines z=thz to selection
LSEL,A,LOC,Z,2*THZ          ! add lines z=2thz to selection
LSEL,R,LOC,X,0              ! reselects lines x=0
LESIZE,ALL,,,NEY,15,1,,,1   ! define element size in selected lines
LSEL,S,LOC,Z,0              ! selects lines z=0
LSEL,A,LOC,Z,THZ            ! add lines z=thz to selection
LSEL,A,LOC,Z,2*THZ          ! add lines z=2thz to selection
LSEL,R,LOC,X,LX             ! reselects lines x=lx
LESIZE,ALL,,,NEY,(1/15),1,,,1  ! define ele. size selected lines
LSEL,ALL                    ! select all lines
MSHKEY,1                    ! Specifies mapped meshing
ESYS,11                     ! Selects 90 degrees material orientation
VMESH,1                     ! Meshes 90 degrees lamina
ESYS,12                     ! Selects 0 degrees material orientation
VMESH,3                     ! Meshes 0 degree lamina
FINISH                      ! Exit pre-processor module

/SOLU                       ! Solution module,
ANTYPE,STATIC               ! Set static analysis
ASEL,S,LOC,X,0
ASEL,A,LOC,Y,0
ASEL,A,LOC,Z,0
DA,ALL,SYMM                 ! Impose Symmetry BC
ASEL,S,LOC,X,LX
DA,ALL,UX,(EPSX*LX)         ! Impose displacement on the end
ALLSEL,ALL              ! Selects all areas
SOLVE                   ! Solve current load state
FINISH                  ! Exit solution module

/POST1                  ! Post-processor module
RSYS,0                  ! Set results in global coordinates system
PATH,INTERFACE,2,,100   ! Define a path between two points, 100 values
PPATH,1,0,0,0,THZ,0     ! 1st point of the path location
PPATH,2,0,0,bY,THZ,0    ! 2nd point of the path location
PDEF,zero,EPSW,,AVG     ! Compute zero axis (optional)
PLPATH,SZ,SXZ,SYZ,ZERO  ! Plot Sz,Sxz,Syz
/PAGE,1000,,1000        ! Define print list without skips between pages
FINISH                  ! Exit post-processor module

/POST1                  ! Post-processor module
RSYS,0                  ! Set results in global coordinates system
PATH,INTERFACE,2,,100   ! path between two points, compute 100 values
PPATH,1,0,LX/2,0,THZ,0  ! 1st point of the path location
PPATH,2,0,LX/2,BY,THZ,0 ! 2nd point of the path location
PDEF,Sz ,S,Z,AVG        ! Compute Sz
PDEF,Syz,S,YZ,AVG       ! Compute Syz
PDEF,zero,EPSW,,!AVG    ! Compute zero axis (optional)
PLPATH,SZ,SYZ,ZERO      ! Plot Sz,Syz
```

```
/PAGE,1000,,1000        ! Define print list without skips between pages
PRPATH,SZ,SYZ           ! Print Sz,Syz
FINISH                  ! Exit post-processor module
```

5.2 Coefficient of Mutual Influence

In classical lamination theory, it is assumed that the portion of the laminate being analyzed is far from the edges of the laminate. Stress resultants N and M are then applied to a portion of the laminate and these induce in-plane stress σ_x, σ_y, σ_{xy}, on each lamina. In the interior of the laminate, interlaminar stress σ_{xz}, σ_{yz}, are induced only if shear forces are applied.

For uniaxial loading N_x, the transverse stresses generated in each lamina as a result of Poisson's effect must cancel out to yield a null laminate force N_y. Also, the in-plane shear stress on off-axis laminas must cancel out with those of other laminas to yield zero shear force N_{xy} for the laminate. The situation is more complex near the edges as the various components of in-plane stress do not cancel each out other across the lamina interfaces. For the time being, let us revisit the concept of laminate engineering properties. In material axes, the plane stress compliance equations are

$$\begin{Bmatrix} \epsilon_1 \\ \epsilon_2 \\ \gamma_6 \end{Bmatrix} = \begin{bmatrix} S_{11} & S_{12} & 0 \\ S_{12} & S_{22} & 0 \\ 0 & 0 & S_{66} \end{bmatrix} \begin{Bmatrix} \sigma_1 \\ \sigma_2 \\ \sigma_6 \end{Bmatrix} \tag{5.8}$$

It is also known that the compliance coefficients can be written in terms of engineering properties as

$$[S] = \begin{bmatrix} 1/E_1 & -\nu_{12}/E_1 & 0 \\ -\nu_{12}/E_1 & 1/E_2 & 0 \\ 0 & 0 & 1/G_{12} \end{bmatrix} \tag{5.9}$$

For an off-axis lamina (oriented arbitrarily with respect to the global axes), we have

$$\begin{Bmatrix} \epsilon_x \\ \epsilon_y \\ \gamma_{xy} \end{Bmatrix} = \begin{bmatrix} \overline{S}_{11} & \overline{S}_{12} & \overline{S}_{16} \\ \overline{S}_{12} & \overline{S}_{22} & \overline{S}_{26} \\ \overline{S}_{16} & \overline{S}_{26} & \overline{S}_{66} \end{bmatrix} \begin{Bmatrix} \sigma_x \\ \sigma_y \\ \sigma_{xy} \end{Bmatrix} \tag{5.10}$$

Here it can be seen that uniaxial load ($\sigma_y = \sigma_{xy} = 0$) yields shear strain as a result of the shear-extension coupling

$$\gamma_{xy} = \overline{S}_{16}\sigma_x \tag{5.11}$$

where

$$\begin{aligned} \overline{S}_{16} = {} & (2S_{11} - 2S_{12} - S_{66}) \sin\theta \cos^3\theta \\ & - (2S_{22} - 2S_{12} - S_{66}) \sin^3\theta \cos\theta \end{aligned} \tag{5.12}$$

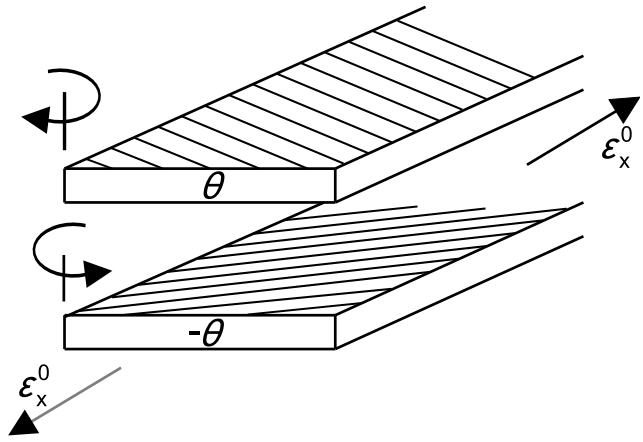

Figure 5.6: Deformation caused by mutual influence.[3]

Now, the coefficients of $[\overline{S}]$ can be defined in term of the engineering properties for the off-axis lamina as

$$\begin{aligned} &\overline{S}_{11} = 1/E_x \ ; \ \overline{S}_{12} = -\nu_{xy}/E_x = -\nu_{yx}/E_y \\ &\overline{S}_{22} = 1/E_y \ ; \ \overline{S}_{66} = 1/G_{xy} \end{aligned} \tag{5.13}$$

To complete the definition of $[\overline{S}]$ in (5.10), two new engineering properties describing shear-extension coupling, $\eta_{xy,x}$ and $\eta_{xy,y}$, are defined as

$$\overline{S}_{16} = \frac{\eta_{xy,x}}{E_x} \quad ; \quad \overline{S}_{26} = \frac{\eta_{xy,y}}{E_x} \tag{5.14}$$

The engineering properties $\eta_{xy,x}$ and $\eta_{xy,y}$ are called coefficients of mutual influence and they represent the shear caused by stretching. Their formal definition is obtained by imposing an axial stress and measuring the resulting shear strain

$$\eta_{ij,i} = \frac{\gamma_{ij}}{\epsilon_i} \tag{5.15}$$

Alternatively, two other coefficients of mutual influence could be defined to represent the stretching caused by shear

$$\overline{S}_{16} = \frac{\eta_{x,xy}}{G_{xy}} \ ; \ \overline{S}_{26} = \frac{\eta_{y,xy}}{G_{xy}} \tag{5.16}$$

These are defined by imposing a shear stress and measuring the axial strain

$$\eta_{i,ij} = \frac{\epsilon_i}{\gamma_{ij}} \tag{5.17}$$

[3]Reprinted from *Mechanics of Fibrous Composites*, C. T. Herakovich, Figure 8.14, copyright (1998), with permission from John Wiley & Sons, Inc.

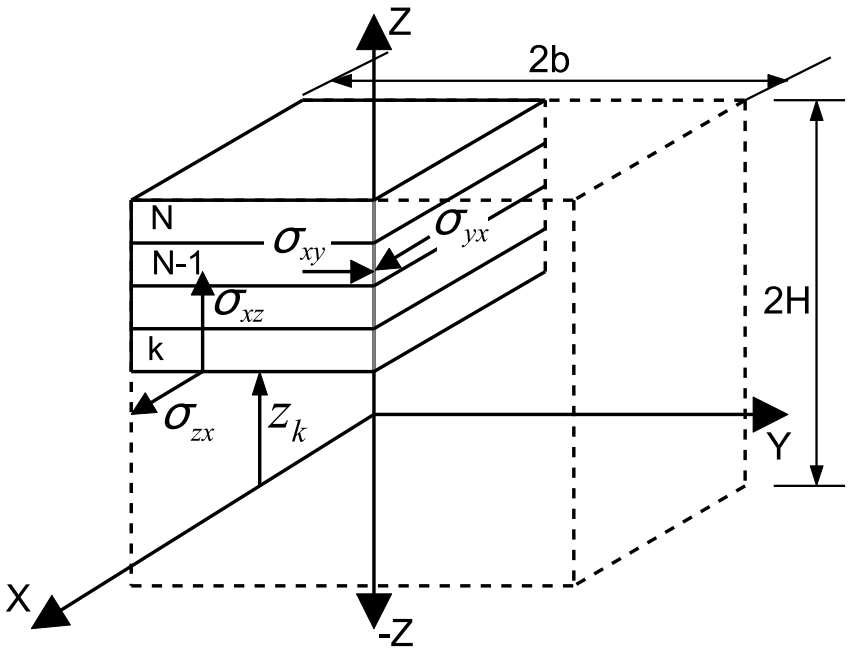

Figure 5.7: Free body diagram of sublaminate to compute the interlaminar force F_{xz} due to mutual influence.

5.2.1 Interlaminar Stress due to Mutual Influence

Off-axis laminas induce in-plane shear stress when subject to axial loading because the natural shear deformations that would occur on an isolated lamina (Figure 5.6) are constrained by the other laminas. Through the whole thickness of the laminate, these stresses cancel out, but over unbalanced sublaminates (e.g., the top lamina in Figure 5.6), they amount to a net shear.

That shear can only be balanced by interlaminar stress σ_{zx} at the bottom of the sublaminate (Figure 5.7). Then, summation of forces along x leads to a net force

$$F_{xz}(z_k) = \int_0^b \sigma_{zx_{(z=z_k)}} dy = -\int_{z_k}^{z_N} \sigma_{xy} dz \tag{5.18}$$

Once again, the in-plane shear stress calculated with classical lamination theory (CLT) [1, Chapter 6] can be used to compute the interlaminar force per unit length F_{xz}. For in-plane loading, CLT yields constant shear stress in each lamina. When the interlaminar force is evaluated at an interface (located at $z = z_k$), the integration above reduces to

$$F_{xz}(z_k) = -\sum_{i=k}^{N} \sigma_{xy}^i t_i \tag{5.19}$$

The force F_{xz}, as well as the values of the coefficients of mutual influence can be used to qualitatively select the LSS with the least interlaminar stress. Actual values

of interlaminar stresses can be found by numerical analysis. However, $\sigma_z \to \infty$ as $y \to b$. This is a singularity that is not handled well by FEA. Therefore the results, even for $y < b$, are very dependent on mesh refinement. Furthermore, since $\sigma_z \to \infty$, the results cannot be used in a failure criterion without further consideration. A numerical approximation of σ_{xz} for a $[\pm 45]_S$ laminate is plotted in Figure 5.9 in terms of the distance y' from the free edge.

Example 5.3 *Compute F_{xz} at all interfaces of a $[30_2/-30_2]_s$ balanced symmetric laminate (Figure 5.1) loaded with $N_x = 175$ KN/m. The material properties are given in Example 5.1. The lamina thickness is $t_k = 0.127$ mm.*

Solution to Example 5.3 *In-plane shear stress σ_{xy} through the thickness of the laminate can be obtained following the same procedure used to obtain σ_y in Example 5.1.*

For a symmetric balanced laminate under in-plane loads, use (5.19). For a general laminate under general load, use (5.18) or approximate F_{xz} by (5.19) taking the average of σ_{xy} in each lamina.

The results are obtained with a spreadsheet and shown in Table 5.2 and Figure 5.8.

Table 5.2: Interlaminar force F_{xz} due to mutual influence

k	Pos	σ_{xy} [MPa]	t_k [mm]	z [mm]	F_{xz} [kN/m]
8	TOP	78.6 10^{-3}		0.508	0.000
8	BOT	78.6 10^{-3}	0.127	0.381	-9.982
7	TOP	78.6 10^{-3}		0.381	-9.982
7	BOT	78.6 10^{-3}	0.127	0.254	-19.964
6	TOP	-78.6 10^{-3}		0.254	-19.964
6	BOT	-78.6 10^{-3}	0.127	0.127	-9.982
5	TOP	-78.6 10^{-3}		0.127	-9.982
5	BOT	-78.6 10^{-3}	0.127	0.000	0.000
4	TOP	-78.6 10^{-3}		0.000	0.000
4	BOT	-78.6 10^{-3}	0.127	-0.127	9.982
3	TOP	-78.6 10^{-3}		-0.127	9.982
3	BOT	-78.6 10^{-3}	0.127	-0.254	19.964
2	TOP	78.6 10^{-3}		-0.254	19.964
2	BOT	78.6 10^{-3}	0.127	-0.381	9.982
1	TOP	78.6 10^{-3}		-0.381	9.982
1	BOT	78.6 10^{-3}	0.127	-0.508	0.000

Example 5.4 *Plot σ_{xz} at the interface above the middle surface of a $[\pm 45]_S$ laminate using the material properties, geometry, and loading of Example 5.2.*

Solution to Example 5.4 *Note that in this case it is not possible to use the same symmetry conditions used in Example 5.2. Since the LSS is symmetric, it is possible to model half of the laminate ($z > 0$). Since the LSS contains laminas at angles other than 0 and 90, the plane $x = 0$ is not a symmetry plane, but rather a plane with $\epsilon_x = 0$. Also, the edge effects at the ends of the model in $x = 0$ and in $x = L\star$ are now important, so the results must be plotted at $x = L\star/2$ to avoid free edge effects at the loaded ends. The solution is shown in Figure 5.9.*

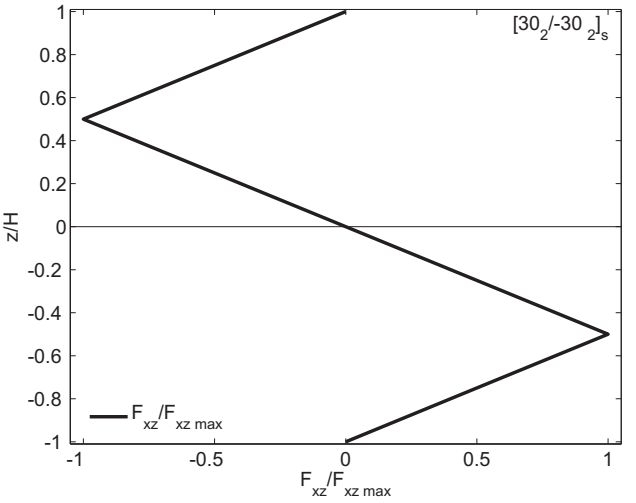

Figure 5.8: Interlaminar shear force due to mutual influence F_{xz}.

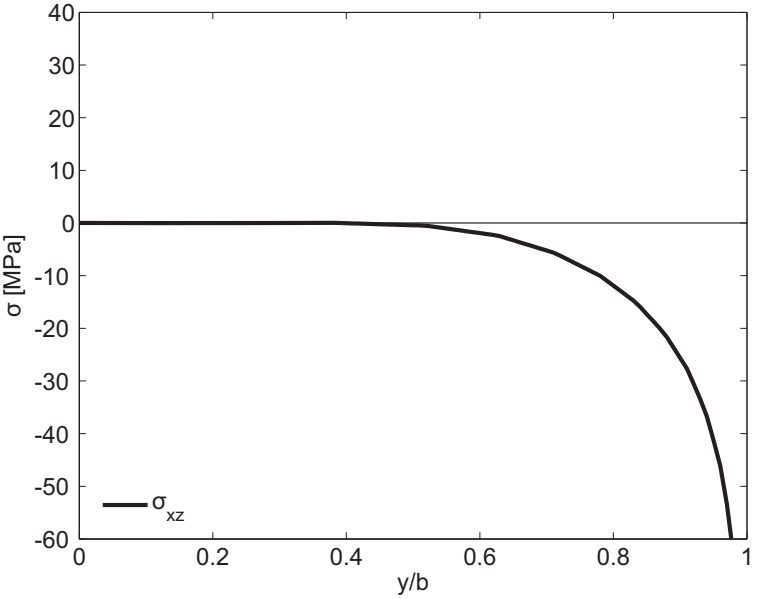

Figure 5.9: Interlaminar shear stress σ_{xz} at the interface above the middle-surface of a carbon/epoxy $[\pm 45]_S$ laminate (FEA).

```
/TITLE,Free Edge Analysis [45/-45]s laminate
/PREP7                  ! Pre-processor module
*SET,THZ,1.25           ! thickness of lamina in mm
*SET,LX,8*THZ           ! 1/2 length of laminate in mm
*SET,BY,10.0            ! 1/2 width of laminate in mm
*SET,NEX,8              ! number of elements in x/z direction
*SET,NEY,14             ! number of elements in y direction
*SET,EPSX,0.01          ! uniform strain in x direction

! Equivalent Material properties
UIMP,1,EX,EY,EZ,139E3,14.5E3,14.5E3
UIMP,1,GXY,GYZ,GXZ,5.86E3,5.25E3,5.86E3
UIMP,1,PRXY,PRYZ,PRXZ,0.21,0.38,0.21

ET,1,SOLID186               ! Chooses SOLID186 element for analysis
KEYOPT,1,2,1                ! KEYOPT(2) = 1 Enables Full Integration

! Define material orientation by local Coordinate
LOCAL,11,,0,0,0,-45         ! defines -45 degree local cs
LOCAL,12,,0,0,0,45          ! defines +45 degree local cs
CSYS,0                      ! set active cs to cart. system

! Generate Geometry
BLOCK,0,LX,0,BY,0,THZ       ! -45 degrees lamina
BLOCK,0,LX,0,BY,THZ,2*THZ   ! +45 degress lamina
VSYMM,Y,ALL
VGLUE,ALL                   ! Glue volumes

! Mesh Control and Mesh
LESIZE,ALL,,,NEX            ! line number divisions = nex
LSEL,S,LOC,Z,0              ! selects lines z=0
LSEL,A,LOC,Z,THZ            ! add lines z=thz to selection
LSEL,A,LOC,Z,2*THZ          ! add lines z=2thz to selection
LSEL,R,LOC,X,0              ! reselects lines x=0
LSEL,R,LOC,Y,0,2*BY
LESIZE,ALL,,,NEY,20,1,,,1   ! define element size in selected lines
LESIZE,ALL,,,NEX            ! line number divisions = nex
LSEL,S,LOC,Z,0              ! selects lines z=0
LSEL,A,LOC,Z,THZ            ! add lines z=thz to selection
LSEL,A,LOC,Z,2*THZ          ! add lines z=2thz to selection
LSEL,R,LOC,X,0              ! reselects lines x=0
LSEL,R,LOC,Y,-2*BY,0
LESIZE,ALL,,,NEY,(1/20),1,,,1   ! define element size in selected lines
LSEL,S,LOC,Z,0              ! selects lines z=0
LSEL,A,LOC,Z,THZ            ! add lines z=thz to selection
LSEL,A,LOC,Z,2*THZ          ! add lines z=2thz to selection
LSEL,R,LOC,X,LX             ! reselects lines x=lx
LESIZE,ALL,,,NEY,(1/20),1,,,1  ! define ele. size in selected lines
LSEL,ALL                    ! select all lines
MSHKEY,1                    ! Specifies mapped meshing
ESYS,11                     ! Selects -45 degrees material orientation
```

```
VMESH,1                     ! Meshes -45 degrees lamina
VMESH,6                     ! Meshes -45 degrees lamina
ESYS,12                     ! Selects 45 degrees material orientation
VMESH,5                     ! Meshes 45 degree lamina
VMESH,7                     ! Meshes 45 degree lamina
FINISH                      ! Exit pre-processor module

/SOLU                   ! Solution module,
ANTYPE,STATIC           ! Set static analysis
ASEL,S,LOC,X,0
ASEL,A,LOC,Z,0
DA,ALL,SYMM             ! Impose Symmetry BC
ASEL,S,LOC,X,LX
DA,ALL,UX,(EPSX*LX)     ! Impose displacement on the end = epsX*LX
ALLSEL,ALL              ! Selects all areas
DK,2,ALL
SOLVE                   ! Solve current load state
FINISH                  ! Exit solution module

/POST1                  ! Post-processor module
RSYS,0                  ! Set results in global coordinates system
PATH,INTERFACE,2,,100   ! Define a path between two points, compute 100 values
PPATH,1,0,LX/2,0,THZ,0  ! 1st point of the path location
PPATH,2,0,LX/2,BY,THZ,0 ! 2nd point of the path location
PDEF,SXZ,S,XZ,!AVG      ! Compute Sxz
PDEF,zero,EPSW,,!AVG    ! Compute zero axis (optional)
PLPATH,SXZ,ZERO         ! Plot Sxz
/PAGE,1000,,1000        ! Define print list without skips between pages
PRPATH,SXZ              ! Print Sxz
FINISH                  ! Exit post-processor module
```

Suggested Problems

Problem 5.1 *Write a computer program to use tabulated data of σ_y and σ_{xy} (at the top and bottom of every lamina) to compute F_{yz}, F_{xz}, and M_z, for all locations through the thickness of a laminate with any number of laminas. Using the program, plot F_{yz}, F_{xz}, and M_z, through the thickness $-4t < z < 4t$ of a $[\pm 45/0/90]_s$ laminate with lamina thickness $t = 0.125$ mm, loaded with $N_x = 100$ kN/m. Use carbon/epoxy properties E_1=139 GPa, E_2=14.5 GPa, $G_{12} = G_{13} = 5.86$ GPa, $G_{23} = 5.25$ GPa, $\nu_{12} = \nu_{13} = 0.21$, $\nu_{23} = 0.38$. Submit a report including the source code of the program.*

Problem 5.2 *Repeat Problem 5.1 for $M_x = 1$ Nm/m. Submit a report including the source code of the program.*

Problem 5.3 *Plot σ_z/σ_{x0} and σ_{yz}/σ_{x0} vs. y/b $(0 < y/b < 1)$ at $x = L/2$, at the first interface above the mid-surface for laminates, $[0/90]_s$ and with lamina thickness $t = 0.512$ mm, loaded with $\epsilon_x = 0.01$. Compute the far-field uniform stress σ_{x0} in terms of the applied strain. Use quadratic solid elements and a mesh biased toward the free edge (bias 0.1) to model 1/8 of a tensile specimen (see Example 5.2), of width $2b = 25.4$ mm and length $2L =$ 20 mm. Use carbon/epoxy properties $E_1 = 139$ GPa, $E_2 = 14.5$ GPa, $G_{12} = G_{13} = 5.86$*

GPa, $G_{23} = 5.25$ *GPa*, $\nu_{12} = \nu_{13} = 0.21$, $\nu_{23} = 0.38$. *Attempt to keep the aspect ratio of the elements near the free edge close to one. Submit the input command file to obtain the solution and the plot. In addition, submit the plot.*

Problem 5.4 *For the laminate and loading described in Problem 5.3, plot* σ_z/σ_{x0} *and* σ_{yz}/σ_{x0} *versus* z/t_k $(0 < z/t_k < 2)$ *above the mid-surface, at a distance* $0.1t_k$ *from the free edge and* $x = L/2$. *Study the effect of mesh refinement by providing four curves with different number of divisions along the* z*-direction. Attempt to keep the aspect ratio of the elements near the free edge close to one. Submit the input command file to obtain the solution and the plot. In addition, submit the plot.*

Problem 5.5 *Plot* σ_{xz}/σ_{x0} *as in Problem 5.3 for all the interfaces above the middle surface of a* $[\pm 10_2]_S$ *laminate.*

Problem 5.6 *Plot* σ_{xz}/σ_{x0} *as in Problem 5.4 for a* $[\pm 10_2]_S$ *laminate.*

Problem 5.7 *Use solid elements and a biased mesh to model 1/8 of a tensile specimen (see Example 5.2), of width* $2b = 24$ *mm and length* $2L = 20$ *mm. The laminate is* $[\pm 45/0/90]_s$ *with lamina thickness* $t = 0.125$ *mm, loaded with* $N_x = 175$ *KN/m. Use carbon/epoxy properties* $E_1 = 139$ *GPa*, $E_2 = 14.5$ *GPa*, $G_{12} = G_{13} = 5.25$ *GPa*, $G_{23} = 5.86$ *GPa*, $\nu_{12} = \nu_{13} = 0.21$, $\nu_{23} = 0.38$. *Plot the three interlaminar stress components, from the edge to the center line of the specimen, at the mid-surface of each lamina. Lump all four plots of the same stress into a single plot. Submit the input command file to obtain the solution and the three plots. In addition, submit the three plots.*

Problem 5.8 *Plot* E_x/E_2, G_{xy}/G_{12}, $10\nu_{xy}$, $-\eta_{xy,x}$ *and* $-\eta_{x,xy}$ *in the same plot vs* θ *in the range* $-\pi/2 < \theta < \pi/2$ *for a unidirectional single lamina oriented at an angle* θ. *The material is S-glass/epoxy [1, Tables 1.3–1.4].*

Problem 5.9 *Using the plot from Problem 5.8 and considering a* $[\theta_1/\theta_2]_S$ *laminate, what are the worst combinations of values* θ_1, θ_2 *for (a) Poisson's mismatch and (b) shear mismatch.*

Problem 5.10 *In a single plot, compare -*$\eta_{xy,x}$ *of E-glass/epoxy, Kevlar49/epoxy, and T800/3900-2 in the range -*$\pi/2 < \theta < \pi/2$ *([1, Tables 1.3–1.4]).*

Problem 5.11 *Obtain contour plots of the three deformations* u_x, u_y, u_z *(independently) on the top surface of a* $[\pm 45]_s$ *laminate. Use dimensions, load, and material properties of Problem 5.7. Explain your findings.*

Problem 5.12 *Repeat Problem 5.11 for a* $[0/90]_s$ *laminate. Explain your findings.*

Problem 5.13 *Use solid elements and a biased mesh to model 1/4 of a tensile specimen (Figure 5.1) of a total width* $2b = 12$ *mm and length* $2L = 24$ *mm. Compare in the same plot* σ_z *vs* z/H *for* $[\pm 15/\pm 45]_s$ *and [*$\pm(15/45)$*] of SCS-6/aluminum with 50% fiber volume. Use micromechanics (6.8) to predict the unidirectional composite properties. The lamina thickness* $t_k = 0.25$ *mm. The laminate is loaded with* $\epsilon_x = 0.01$.

	Al-2014-T6 *([28, App. B])*	*SCS-6* *([1, Tables 2.1–2.2])*
E [GPa]	*75.0*	*427.0*
G [GPa]	*27.0*	*177.9*

Problem 5.14 *Use a FEA model similar to Problem 5.13 to plot* $\sigma_{xz}/\sigma_{zx_{\max}}$ *vs* θ *(*$0 < \theta < \pi/2$*) for a* $[\pm\theta]_s$ *SCS-6/ Al laminate with* $\epsilon_x = 0.01$.

Problem 5.15 *Use the FEA model of Problem 5.13 to plot* σ_z *vs* y/b *(*$0 < y < 0.95b$*) at the mid-surface of the* $[\pm 15/\pm 45]_s$ *laminate. Note* $\sigma_z \to \infty$ *near* $y = b$*, so the actual value from FEA at* $y = b$ *is mesh dependent. Investigate mesh dependency at* $y = 0.95b$ *by tabulating the result using different mesh densities.*

Problem 5.16 *Use an FEA model similar to Problem 5.13 to plot* σ_x*,* σ_{xy} *and* σ_{xz} *vs* y/b *(*$0 < y < b$*) when a* $[\pm\theta]_s$ *SCS-6/Al laminate is subjected to 1% axial strain (*$\epsilon_x = 0.01$).

Problem 5.17 *A* $[0/90]_s$ *laminate with properties* $E_1 = 139$ *GPa,* $E_2 = 14.5$ *GPa,* $G_{12} = G_{13} = 5.86$ *GPa,* $G_{23} = 5.25$ *GPa,* $\nu_{12} = \nu_{13} = 0.21$*,* $\nu_{23} = 0.38$ *is shown in Figure 5.1. The strength properties of the lamina are* $F_{1t} = 1550$ *MPa,* $F_{1c} = 1090$ *MPa,* $F_{2t} = F_{2c} = 59$ *MPa, and* $F_6 = 75$ *MPa. Take* $2b = 20$ *mm, length of the sample* $2L = 200$ *mm, thickness of each lamina* $t_k = 1.25$ *mm. Load the sample with a uniform strain* $\epsilon_x = 0.01$ *by applying a uniform displacement. Use symmetry to model only the quadrant with* $x > 0$*,* $y > 0$*,* $z > 0$*. Use orthotropic solid elements on each lamina, with at least two quadratic elements through the thickness of each lamina. Compute the 3D Tsai-Wu failure index* I_F *using a USERMAT subroutine for solid elements. Obtain the contour plot of* I_F *in each lamina (do not use results averaging). Show all work in a report.*

Chapter 6

Computational Micromechanics

In Chapter 1, the elastic properties of composite materials were assumed to be available in the form of elastic modulus E, shear modulus G, Poisson's ratio ν, and so on. For heterogeneous materials such as composites, a large number of material properties are needed, and experimental determination of these many properties is a tedious and expensive process. Furthermore, the values of these properties change as a function of the volume fraction of reinforcement and so on. An alternative, or at least a complement to experimentation, is to use homogenization techniques to predict the elastic properties of the composite in terms of the elastic properties of the constituents (matrix and reinforcements). Since homogenization models are based on more or less accurate modeling of the microstructure, these models are also called micromechanics models, and the techniques used to obtain approximate values of the composite's properties are called micromechanics methods or techniques [1]. Micromechanics models can be classified into empirical, semiempirical, analytical, and numerical. Accurate semiempirical models are described in [1].

This book deals only with strictly analytical or numerical models that do not require empirical adjusting factors, so that no experimentation is required. Since most of this book deals with 3D analysis, emphasis is placed on micromechanics models that can estimate the whole set of elastic properties using a single model, rather than using a disjoint collection of models based on different assumptions to assemble the set of properties needed. Many analytical techniques of homogenization are based on the equivalent eigenstrain method [29, 30], which considers the problem of a single ellipsoidal inclusion embedded in an infinite elastic medium. The Eshelby solution is used in [31] to develop a method that takes into account, approximately, the interactions among the inclusions. One of the more used homogenization techniques is the self-consistent method [32], which considers a random distribution of inclusions in an infinite medium. The infinite medium is assumed to have properties equal to the unknown properties sought. Therefore, an iterative procedure is used to obtain the overall moduli. Homogenization of composites with periodic microstructure has been accomplished by using various techniques including an extension of the Eshelby inclusion problem [29, 30], the Fourier series technique (see Section 6.1.3 and [33, 34]), and variational principles. The periodic eigenstrain method was further developed to determine the overall relaxation moduli of linear

viscoelastic composite materials (see Section 7.6 and [35,36]). A particular case, the cell method for periodic media, considers a unit cell with a square inclusion [37].

The analytical procedures mentioned so far yield approximate estimates of the exact solution of the micromechanics problem. These estimates must lie between lower and upper bounds for the solution. Several variational principles were developed to evaluate bounds on the homogenized elastic properties of macroscopically isotropic heterogeneous materials [38]. Those bounds depend only on the volume fractions and the physical properties of the constituents.

In order to study the nonlinear material behavior of composites with periodic microstructure, numerical methods, mainly the finite element method, are employed. Nonlinear finite element analysis of metal matrix composites has been studied by looking at the behavior of the microstructure subjected to an assigned load history [39]. Bounds on overall instantaneous elastoplastic properties of composites have been derived by using the finite element method [40].

6.1 Analytical Homogenization

As discussed in the introduction, estimates of the average properties of heterogeneous media can be obtained by various analytical methods. Detailed derivations of the equations fall outside the scope of this book.

Available analytical models vary greatly in complexity and accuracy. Simple analytical models yield formulas for the stiffness $\mathbf{C}$ and compliance $\mathbf{S}$ tensors of the composite [37, (2.9) and (2.12)], such as

$$\begin{aligned} \mathbf{C} &= \sum V_i \; \mathbf{C}^i \mathbf{A}^i \quad ; \quad \sum V_i \mathbf{A}^i = \mathbf{I} \\ \mathbf{S} &= \sum V_i \; \mathbf{S}^i \mathbf{B}^i \quad ; \quad \sum V_i \mathbf{B}^i = \mathbf{I} \end{aligned} \tag{6.1}$$

where $V_i, \mathbf{C}^i, \mathbf{S}^i$, are the volume fraction, stiffness, and compliance tensors (in contracted notation)[1] of the i-th phase in the composite, respectively, and $\mathbf{I}$ is the 6×6 identity matrix. Furthermore, $\mathbf{A}^i, \mathbf{B}^i$, are the strain and stress concentration tensors (in contracted notation) of the i-th phase [37]. For fiber reinforced composites, $i = f, m$, represent the fiber and matrix phases, respectively.

6.1.1 Reuss Model

The *Reuss model* (also called rule of mixtures), assumes that the strain tensors[2] in the fiber, matrix, and composite are the same $\boldsymbol{\varepsilon} = \boldsymbol{\varepsilon}^f = \boldsymbol{\varepsilon}^m$, so, the strain concentration tensors are all equal to the 6×6 identity matrix $\mathbf{A}^i = \mathbf{I}$. The rule of mixtures (ROM) formulas for E_1 and ν_{12} are derived and computed in this way.

[1] Fourth-order tensors with minor symmetry are represented by a 6×6 matrix taking advantage of contracted notation.

[2] Tensors are indicated by boldface type, or by their components using index notation.

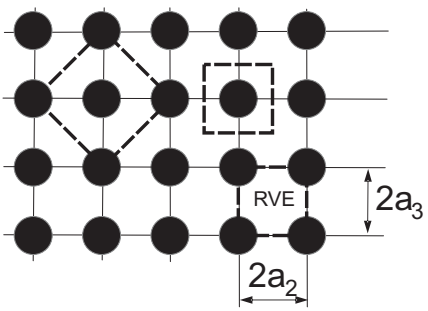

Figure 6.1: Three possible representative volume elements (RVE) for a composite material with a periodic, square fiber array.

6.1.2 Voigt Model

The *Voigt model* (also called inverse rule of mixtures), assumes that the stress tensors in the fiber, matrix, and composite are the same $\boldsymbol{\sigma} = \boldsymbol{\sigma}^f = \boldsymbol{\sigma}^m$, so, the stress concentration tensors are all equal to the 6×6 identity matrix $\mathbf{B}^i = \mathbf{I}$. The inverse rule of mixtures (IROM) formulas for E_2 and G_{12} are derived and computed in this way. More realistic concentration tensors are given in [41, Appendix B].

6.1.3 Periodic Microstructure Model

If the composite has a periodic microstructure, or if it can be approximated as having such a microstructure (see Section 6.1.4), then the Fourier series can be used to estimate all the components of the stiffness tensor of a composite. Explicit formulas for a composite reinforced by isotropic, circular-cylindrical fibers, which are periodically arranged in a square array (Figure 6.1), were developed by [34] and they are presented here. The fibers are aligned with the x_1 axis, and they are equally spaced ($2a_2 = 2a_3$). If the fibers are randomly distributed in the cross-section, the resulting composite has transversely isotropic properties, as explained in Section 6.1.4. The case of a composite reinforced with transversely isotropic fibers is presented in [36], and the resulting equations are implemented in [9].

Because the microstructure has a square symmetry, the stiffness tensor has six unique coefficients given by

$$C^*_{11} = \lambda_m + 2\,\mu_m - \frac{V_f}{D}\left[\frac{S_3^2}{\mu_m^2} - \frac{2S_6S_3}{\mu_m^2 g} - \frac{aS_3}{\mu_m\, c} + \frac{S_6^2 - S_7^2}{\mu_m^2 g^2} + \frac{aS_6 + bS_7}{\mu_m\, gc} + \frac{a^2 - b^2}{4\,c^2}\right]$$

$$C^*_{12} = \lambda_m + \frac{V_f}{D} b\left[\frac{S_3}{2c\mu_m} - \frac{S_6 - S_7}{2c\mu_m\, g} - \frac{a+b}{4\,c^2}\right]$$

$$C^*_{23} = \lambda_m + \frac{V_f}{D}\left[\frac{aS_7}{2\,\mu_m\, gc} - \frac{ba + b^2}{4\,c^2}\right]$$

$$C^*_{22} = \lambda_m + 2\,\mu_m - \frac{V_f}{D}\left[-\frac{aS_3}{2\,\mu_m\, c} + \frac{aS_6}{2\,\mu_m\, gc} + \frac{a^2 - b^2}{4\,c^2}\right]$$

$$C_{44}^{*} = \mu_m - V_f \left[-\frac{2\,S_3}{\mu_m} + (\mu_m - \mu_f)^{-1} + \frac{4\,S_7}{\mu_m(2-2\nu_m)} \right]^{-1}$$

$$C_{66}^{*} = \mu_m - V_f \left[-\frac{S_3}{\mu_m} + (\mu_m - \mu_f)^{-1} \right]^{-1} \tag{6.2}$$

where

$$D = \frac{aS_3^2}{2\,\mu_m^2 c} - \frac{aS_6S_3}{\mu_m^2 gc} + \frac{a(S_6^2 - S_7^2)}{2\mu_m^2 g^2 c} + \\ + \frac{S_3(b^2-a^2)}{2\,\mu_m\,c^2} + \frac{S_6(a^2-b^2) + S_7(ab+b^2)}{2\,\mu_m g c^2} + \frac{(a^3 - 2b^3 - 3\,ab^2)}{8\,c^3} \tag{6.3}$$

and

$$\begin{aligned} a &= \mu_f - \mu_m - 2\,\mu_f\,\nu_m + 2\,\mu_m\,\nu_f \\ b &= -\mu_m\,\nu_m + \mu_f\,\nu_f + 2\,\mu_m\,\nu_m\,\nu_f - 2\,\mu_1\,\nu_m\,\nu_f \\ c &= (\mu_m - \mu_f)(\mu_f - \mu_m + \mu_f\,\nu_f - \mu_m\,\nu_m + 2\,\mu_m\,\nu_f - 2\,\mu_f\,\nu_m + \\ &\quad + 2\,\mu_m\,\nu_m\,\nu_f - 2\,\mu_f\,\nu_m\,\nu_f) \\ g &= (2 - 2\nu_m) \end{aligned} \tag{6.4}$$

The subscripts $()_m$, $()_f$ refer to matrix and fiber, respectively. Assuming the fiber and matrix are both isotropic (Section 1.12.5), Lamé constants of both materials are obtained by using (1.75) in terms of the Young's modulus E, the Poisson's ratio ν, and the shear modulus $G = \mu$.

For a composite reinforced by long circular cylindrical fibers, periodically arranged in a square array (Figure 6.1), aligned with x_1-axis, with $a_2 = a_3$, the constants S_3, S_6, S_7 are given as follows [34]

$$\begin{aligned} S_3 &= 0.49247 - 0.47603V_f - 0.02748V_f^2 \\ S_6 &= 0.36844 - 0.14944V_f - 0.27152V_f^2 \\ S_7 &= 0.12346 - 0.32035V_f + 0.23517V_f^2 \end{aligned} \tag{6.5}$$

The resulting tensor $\mathbf{C}^*$ has a square symmetry (not transverse isotropy) due to the microstructural periodic arrangement in the form of a square array. The tensor $\mathbf{C}^*$ is therefore described by six constants. However, most composites have random arrangement of the fibers (see Figure 1.12), resulting in a transversely isotropic stiffness tensor, with only five independent constants. Therefore, the tensor $\mathbf{C}$ for a transversely isotropic material is derived from the tensor $\mathbf{C}^*$ in Section 6.1.4, next.

6.1.4 Transversely Isotropic Averaging

In order to obtain a transversely isotropic stiffness tensor (Section 1.12.4), equivalent in the average sense to the stiffness tensor with square symmetry, the following averaging procedure is used. A rotation θ of the tensor $\mathbf{C}^*$ about the x_1-axis produces

$$\mathbf{B}(\theta) = \overline{T}^T(\theta)\mathbf{C}^*\overline{T}(\theta) \tag{6.6}$$

where $\overline{T}(\theta)$ is the coordinate transformation matrix (see (1.50)). Then the equivalent transversely isotropic tensor is obtained by averaging as follows

$$\overline{\mathbf{B}} = \frac{1}{\pi}\int_0^{\pi} \mathbf{B}(\theta)d\theta \tag{6.7}$$

Then, using the relations between the engineering constants and the components of the $\overline{\mathbf{B}}$ tensor, the following expressions are obtained explicitly in terms of the coefficients (6.2–6.5) of the tensor $\mathbf{C}^*$

$$\begin{aligned}
E_1 &= C^*_{11} - \frac{2\,C^{*2}_{12}}{C^*_{22}+C^*_{23}}\\
E_2 &= \frac{\left(2\,C^*_{11}\,C^*_{22}+2\,C^*_{11}\,C^*_{23}-4\,C^{*2}_{12}\right)\left(C^*_{22}-C^*_{23}+2\,C^*_{44}\right)}{3\,C^*_{11}\,C^*_{22}+C^*_{11}\,C^*_{23}+2\,C^*_{11}\,C^*_{44}-4\,C^{*2}_{12}}\\
G_{12} &= G_{13} = C^*_{66}\\
\nu_{12} &= \nu_{13} = \frac{C^*_{12}}{C^*_{22}+C^*_{23}}\\
\nu_{23} &= \frac{C^*_{11}\,C^*_{22}+3\,C^*_{11}\,C^*_{23}-2\,C^*_{11}\,C^*_{44}-4\,C^{*2}_{12}}{3\,C^*_{11}\,C^*_{22}+C^*_{11}\,C^*_{23}+2\,C^*_{11}\,C^*_{44}-4\,C^{*2}_{12}}
\end{aligned} \tag{6.8}$$

Note that the transverse shear modulus G_{23} can be written in terms of the other engineering constants as

$$G_{23} = \frac{C^*_{22}}{4} - \frac{C^*_{23}}{4} + \frac{C^*_{44}}{2} = \frac{E_2}{2(1+\nu_{23})}$$

or directly in terms of μ_m, μ_f as

$$\begin{aligned}
G_{23} = \mu_m - \frac{f}{4D}\,[&(-\frac{aS_3}{2\,\mu_m\,c} + \frac{a(S_7+S_6)}{2\,\mu_m\,gc} - \frac{ba+2b^2-a^2}{4\,c^2})\\
&+2(-\frac{2\,S_3}{\mu_m} + (\mu_m-\mu_f)^{-1} + \frac{4\,S_7}{\mu_m(2-2\nu_m)})^{-1}]
\end{aligned} \tag{6.9}$$

where D is given by (6.3), a, b, c and g are given by (6.4) and S_3, S_6, and S_7 can be evaluated by (6.5). These equations are implemented in `PMMIE.m` and `PMMIE.xls`, available in [5, /Examples/Ch6Ex/]. For the case of transversely isotropic fibers, they are implemented in [9].

Example 6.1 *Compute the elastic properties of a composite material reinforced with parallel cylindrical fibers randomly distributed in the cross-section. The constituent properties are $E_f = 241\ GPa$, $\nu_f = 0.2$, $E_m = 3.12\ GPa$, $\nu_m = 0.38$, fiber volume fraction $V_f = 0.4$.*

Solution to Example 6.1 *The results shown in Table 6.1 are obtained using [9], which implements the periodic microstructure model (PMM) equations for the case of transversely isotropic fibers.*

Table 6.1: Lamina elastic properties for $V_f = 0.4$

Young's Moduli	**Poisson's Ratio**	**Shear Moduli**
$E_1 = 98,306\ MPa$	$\nu_{12} = \nu_{13} = 0.298$	$G_{12} = G_{13} = 2,594\ MPa$
$E_2 = E_3 = 6,552\ MPa$	$\nu_{23} = 0.600$	

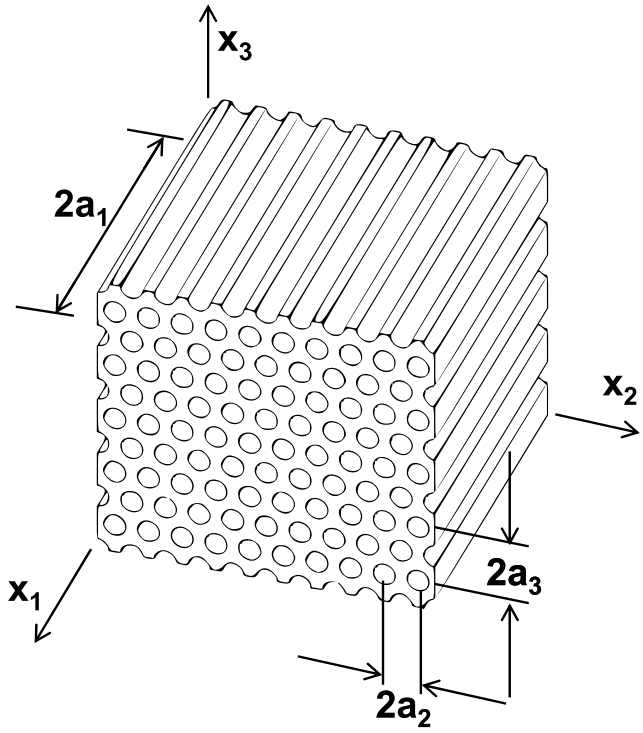

Figure 6.2: Composite material with hexagonal array.

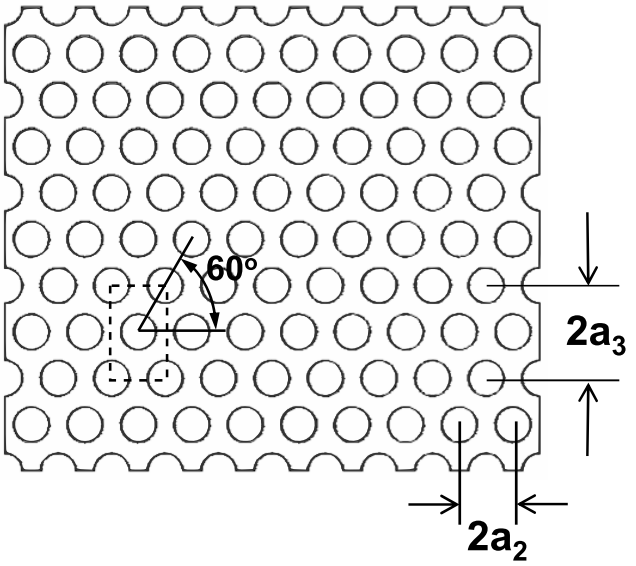

Figure 6.3: Cross-section of the composite material.

6.2 Numerical Homogenization

The composite material considered in this section has cylindrical fibers of infinite length, embedded in an elastic matrix, as shown in Figure 6.2. The cross-section of the composite obtained by intersecting with a plane orthogonal to the fiber axis is shown in Figure 6.3, which clearly shows a periodic microstructure. Because of the periodicity, the three-dimensional representative volume element (RVE) shown in Figure 6.4 can be used for finite element analysis.

In general, composites reinforced with parallel fibers display orthotropic material properties (Section 1.12.3) at the mesoscale (lamina level). In special cases, such as the hexagonal array shown in Figures 6.2 and 6.3, the properties become transversely isotropic (Section 1.12.4). In most commercially fabricated composites, it is impossible to control the placement of the fibers so precisely and most of the time the resulting microstructure is random, as shown in Figure 1.12. A random microstructure results in transversely isotropic properties at the mesoscale. The analysis of composites with random microstructure still can be done using a fictitious periodic microstructure, such as that shown in Figure 6.1, then averaging the stiffness tensor $\mathbf{C}$ as in Section 6.1.4 to obtain the stiffness tensor of a transversely isotropic material. A simpler alternative is to assume that the random microstructure is well approximated by the hexagonal microstructure displayed in Figure 6.3. Analysis of such microstructure directly yields a transversely isotropic stiffness tensor, represented by (1.70), which is reproduced here for convenience

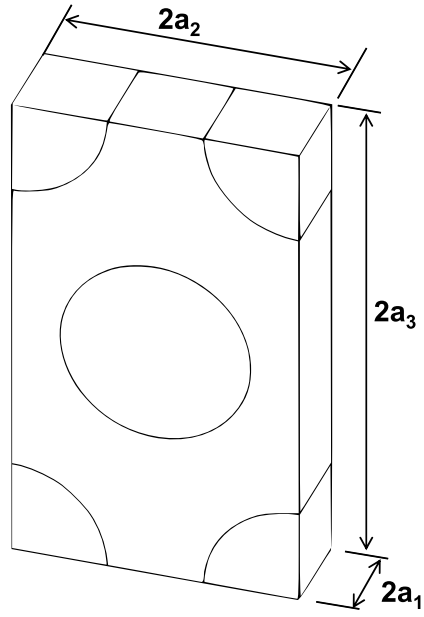

Figure 6.4: Representative volume element (RVE).

$$\begin{Bmatrix} \overline{\sigma}_1 \\ \overline{\sigma}_2 \\ \overline{\sigma}_3 \\ \overline{\sigma}_4 \\ \overline{\sigma}_5 \\ \overline{\sigma}_6 \end{Bmatrix} = \begin{bmatrix} C_{11} & C_{12} & C_{12} & 0 & 0 & 0 \\ C_{12} & C_{22} & C_{23} & 0 & 0 & 0 \\ C_{12} & C_{23} & C_{22} & 0 & 0 & 0 \\ 0 & 0 & 0 & \frac{1}{2}(C_{22} - C_{23}) & 0 & 0 \\ 0 & 0 & 0 & 0 & C_{66} & 0 \\ 0 & 0 & 0 & 0 & 0 & C_{66} \end{bmatrix} \begin{Bmatrix} \overline{\epsilon}_1 \\ \overline{\epsilon}_2 \\ \overline{\epsilon}_3 \\ \overline{\gamma}_4 \\ \overline{\gamma}_5 \\ \overline{\gamma}_6 \end{Bmatrix} \tag{6.10}$$

where the *1*-axis aligned with the fiber direction and an over-bar indicates the average computed over the volume of the RVE. Once the components of the transversely isotropic tensor $\mathbf{C}$ are known, the five elastic properties of the homogenized material can be computed by (6.11), i.e., the longitudinal and transversal Young's moduli E_1 and E_2, the longitudinal and transversal Poisson's ratios ν_{12} and ν_{23}, and the longitudinal shear modulus G_{12}, as follows

$$\begin{aligned} E_1 &= C_{11} - 2C_{12}^2/(C_{22} + C_{23}) \\ \nu_{12} &= C_{12}/(C_{22} + C_{23}) \\ E_2 &= \left[C_{11}\left(C_{22} + C_{23}\right) - 2C_{12}^2\right]\left(C_{22} - C_{23}\right)/\left(C_{11}C_{22} - C_{12}^2\right) \\ \nu_{23} &= \left[C_{11}C_{23} - C_{12}^2\right]/\left(C_{11}C_{22} - C_{12}^2\right) \\ G_{12} &= C_{66} \end{aligned} \tag{6.11}$$

The shear modulus G_{23} in the transversal plane can be obtained by the classical relation (1.74) or directly as follows

$$G_{23} = C_{44} = \frac{1}{2}\left(C_{22} - C_{23}\right) = \frac{E_2}{2\left(1 + \nu_{23}\right)} \tag{6.12}$$

In order to evaluate the overall elastic matrix $\mathbf{C}$ of the composite, the RVE is subjected to an average strain $\overline{\epsilon}_\beta$ [42]. The six components of strain ε^0_{ij} are applied by enforcing the following boundary conditions on the displacement components

$$u_i\left(a_1, x_2, x_3\right) - u_i\left(-a_1, x_2, x_3\right) = 2a_1\varepsilon^0_{i1} \qquad \begin{matrix} -a_2 \le x_2 \le a_2 \\ -a_3 \le x_3 \le a_3 \end{matrix} \tag{6.13}$$

$$u_i\left(x_1, a_2, x_3\right) - u_i\left(x_1, -a_2, x_3\right) = 2a_2\varepsilon^0_{i2} \qquad \begin{matrix} -a_1 \le x_1 \le a_1 \\ -a_3 \le x_3 \le a_3 \end{matrix} \tag{6.14}$$

$$u_i\left(x_1, x_2, a_3\right) - u_i\left(x_1, x_2, -a_3\right) = 2a_3\varepsilon^0_{i3} \qquad \begin{matrix} -a_1 \le x_1 \le a_1 \\ -a_2 \le x_2 \le a_2 \end{matrix} \tag{6.15}$$

Note that tensor components of strain, defined in (1.5) are used in (6.13-6.15). Also, note that a superscript $()^0$ indicates an *applied* strain, while a bar indicates a volume average. Furthermore, $2a_j\ \varepsilon^0_{ij}$ is the displacement necessary to enforce a strain ε^0_{ij} over a distance $2a_j$ (Figure 6.4).

The strain ε^0_{ij} applied on the boundary by using (6.13–6.15) results in a complex state of strain inside the RVE. However, the volume average of the strain in the RVE equals the applied strain,[3] i.e.,

$$\overline{\varepsilon}_{ij} = \frac{1}{V}\int_V \varepsilon_{ij} dV = \varepsilon^0_{ij} \tag{6.16}$$

For the homogeneous composite material, the relationship between average stress and strain is

$$\overline{\sigma}_\alpha = C_{\alpha\beta}\,\overline{\epsilon}_\beta \tag{6.17}$$

where the relationship between $i, j = 1..3$ and $\beta = 1..6$ is given by the definition of contracted notation in (1.9). Thus, the components of the tensor $\mathbf{C}$ are determined solving six elastic models of the RVE subjected to the boundary conditions (6.13–6.15), where only one component of the strain ϵ^0_β is different from zero for each of the six problems.

By choosing a unit value of applied strain, and once the problem defined by the boundary conditions (6.13–6.15) is solved, it is possible to compute the stress field σ_α, whose average gives the required components of the elastic matrix, one column at a time, as

$$C_{\alpha\beta} = \overline{\sigma}_\alpha = \frac{1}{V}\int_V \sigma_\alpha\left(x_1, x_2, x_3\right)\ dV \quad \text{with } \epsilon^0_\beta = 1 \tag{6.18}$$

where $\alpha, \beta = 1 \ldots 6$ (see Section 1.5). The integrals (6.18) are evaluated within each finite element using the Gauss-Legendre quadrature. Commercial programs, such as ANSYS®, have the capability to compute the average stress and volume, element by element. Therefore, computation of the integral (6.18) is a trivial matter. For more details see Example 6.2.

The coefficients in $\mathbf{C}$ are found by setting a different problem for each column in (6.10), as follows.

[3] As long as there are no discontinuities, such as voids or cracks, inside the RVE.

First Column of C

In order to determine the components C_{i1}, with $i = 1, 2, 3$, the following strain is applied to stretch the RVE in the fiber direction (x_1-direction)

$$\epsilon_1^o = 1 \qquad \epsilon_2^o = \epsilon_3^o = \gamma_4^o = \gamma_5^o = \gamma_6^o = 0 \tag{6.19}$$

Thus, the displacement boundary conditions (6.13–6.15) for the RVE in Figure 6.4 become

$$\begin{array}{rcll}
u_1(+a_1, x_2, x_3) - u_1(-a_1, x_2, x_3) &=& 2a_1 & \\
u_2(+a_1, x_2, x_3) - u_2(-a_1, x_2, x_3) &=& 0 & -a_2 \le x_2 \le a_2 \\
u_3(+a_1, x_2, x_3) - u_3(-a_1, x_2, x_3) &=& 0 & -a_3 \le x_3 \le a_3 \\
\\
u_i(x_1, +a_2, x_3) - u_i(x_1, -a_2, x_3) &=& 0 & -a_1 \le x_1 \le a_1 \\
& & & -a_3 \le x_3 \le a_3 \\
\\
u_i(x_1, x_2, +a_3) - u_i(x_1, x_2, -a_3) &=& 0 & -a_1 \le x_1 \le a_1 \\
& & & -a_2 \le x_2 \le a_2
\end{array} \tag{6.20}$$

The conditions (6.20) are constraints on the relative displacements between opposite faces of the RVE. Because of the symmetries of the RVE and symmetry of the constraints (6.20), only one-eighth of the RVE needs to be modeled in finite element analysis (FEA). Assuming the top-right-front portion is modeled (Figure 6.5), the following equivalent external boundary conditions, i.e., boundary conditions on components of displacements and stresses, can be used

$$\begin{array}{rcll}
u_1(a_1, x_2, x_3) &=& a_1 & \\
u_1(0, x_2, x_3) &=& 0 & \\
\sigma_{12}(a_1, x_2, x_3) &=& 0 & 0 \le x_2 \le a_2 \\
\sigma_{12}(0, x_2, x_3) &=& 0 & 0 \le x_3 \le a_3 \\
\sigma_{13}(a_1, x_2, x_3) &=& 0 & \\
\sigma_{13}(0, x_2, x_3) &=& 0 & \\
\\
u_2(x_1, a_2, x_3) &=& 0 & \\
u_2(x_1, 0, x_3) &=& 0 & \\
\sigma_{21}(x_1, a_2, x_3) &=& 0 & 0 \le x_1 \le a_1 \\
\sigma_{21}(x_1, 0, x_3) &=& 0 & 0 \le x_3 \le a_3 \\
\sigma_{23}(x_1, a_2, x_3) &=& 0 & \\
\sigma_{23}(x_1, 0, x_3) &=& 0 & \\
\\
u_3(x_1, x_2, a_3) &=& 0 & \\
u_3(x_1, x_2, 0) &=& 0 & \\
\sigma_{31}(x_1, x_2, a_3) &=& 0 & 0 \le x_1 \le a_1 \\
\sigma_{31}(x_1, x_2, 0) &=& 0 & 0 \le x_2 \le a_2 \\
\sigma_{32}(x_1, x_2, a_3) &=& 0 & \\
\sigma_{32}(x_1, x_2, 0) &=& 0 &
\end{array} \tag{6.21}$$

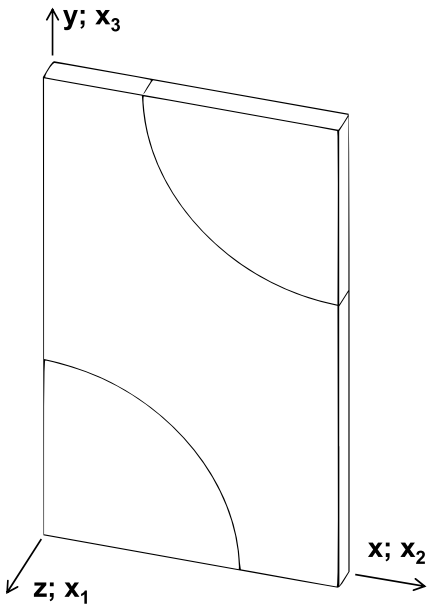

Figure 6.5: One-eighth model of the RVE. Note that the model is set up with the fiber along the z-axis, which corresponds to the x_1-direction in the equations.

These boundary conditions are very easy to apply. Symmetry boundary conditions are applied on the planes $x_1 = 0$, $x_2 = 0$, $x_3 = 0$. Then, a uniform displacement is applied on the plane $x_1 = a_1$. The stress boundary conditions do not need to be applied explicitly in a displacement-based formulation. The displacement components in (6.21) represent strains that are not zero along the x_1-direction and zero along the other two directions. The stress boundary conditions listed in (6.21) reflect the fact that, in the coordinate system used, the composite material is macroscopically orthotropic and that the constituent materials are orthotropic too. Therefore, there is no coupling between extension and shear strains. This is evidenced by the zero coefficients above the diagonal in columns 4 to 6 in (6.10).

The coefficients in column one of (6.10) are found by using (6.18), as follows

$$C_{\alpha 1} = \overline{\sigma}_\alpha = \frac{1}{V} \int_V \sigma_\alpha \left(x_1, x_2, x_3\right) \, dV \tag{6.22}$$

Second Column of C

The components $C_{\alpha 2}$, with $\alpha = 1, 2, 3$, are determined by setting

$$\epsilon_2^o = 1 \qquad \epsilon_1^o = \epsilon_3^o = \gamma_4^o = \gamma_5^o = \gamma_6^o = 0 \tag{6.23}$$

Thus, the following boundary conditions on displacements can be used

$$\begin{array}{rcl} u_1(a_1, x_2, x_3) &=& 0 \\ u_1(0, x_2, x_3) &=& 0 \\ u_2(x_1, a_2, x_3) &=& a_2 \\ u_2(x_1, 0, x_3) &=& 0 \\ u_3(x_1, x_2, a_3) &=& 0 \\ u_3(x_1, x_2, 0) &=& 0 \end{array} \tag{6.24}$$

The trivial stress boundary conditions have not been listed because they are automatically enforced by the displacement-based FEA formulation. Using (6.18), the stiffness terms in the second column of $\mathbf{C}$ are computed as

$$C_{\alpha 2} = \overline{\sigma}_\alpha = \frac{1}{V}\int_V \sigma_{\alpha 2}(x_1, x_2, x_3)\ dV \tag{6.25}$$

Third Column of C

Because of the transverse isotropy of the material (6.10), the components of the third column of the matrix $\mathbf{C}$ can be determined from the first and the second column, so no further computation is required. However, if desired, the components $C_{\alpha 3}$, with $\alpha = 1, 2, 3$, can be found by applying the following strain

$$\epsilon_3^o = 1 \qquad \epsilon_1^o = \epsilon_2^o = \gamma_4^o = \gamma_4^o = \gamma_5^o = 0 \tag{6.26}$$

Thus, the following boundary conditions on displacement can be used

$$\begin{array}{rcl} u_1(a_1, x_2, x_3) &=& 0 \\ u_1(0, x_2, x_3) &=& 0 \\ u_2(x_1, a_2, x_3) &=& 0 \\ u_2(x_1, 0, x_3) &=& 0 \\ u_3(x_1, x_2, a_3) &=& a_3 \\ u_3(x_1, x_2, 0) &=& 0 \end{array} \tag{6.27}$$

The required components of $\mathbf{C}$ are determined by averaging the stress field as in (6.18).

Example 6.2 *Compute E_1, E_2, ν_{12}, and ν_{23} for a unidirectional composite with isotropic fibers $E_f = 241$ GPa, $\nu_f = 0.2$, and isotropic matrix $E_m = 3.12$ GPa, $\nu_m = 0.38$ with fiber volume fraction $V_f = 0.4$. The fiber diameter is $d_f = 7$ μm, placed in a hexagonal array as shown in Figure 6.3.*

Solution to Example 6.2 *The dimensions a_2 and a_3 of the RVE, as shown in Figure 6.4, are chosen to obtain $V_f = 0.4$ with a hexagonal array microstructure. The fiber volume and the total volume of the RVE are*

$$v_f = 4a_1\pi\left(\frac{d_f}{2}\right)^2 \quad ; \qquad v_t = 2a_1\ 2a_2\ 2a_3$$

The ratio between both is the volume fraction. Therefore,

$$V_f = \pi\frac{(d_f/2)^2}{2\ a_2\ a_3} = 0.4$$

Additionally, the relation between a_2 and a_3 is established by the hexagonal array pattern

$$a_3 = a_2 \tan(60^\circ)$$

These two relations yield a_2 and a_3, while the a_1 dimension can be chosen arbitrarily. In this case, the RVE dimensions are

$$a_1 = a_2/4 \quad ; \qquad a_2 = 5.2701\ \mu m \quad ; \qquad a_3 = 9.1281\ \mu m$$

Since this RVE is symmetric, it is possible to model one-eighth of the RVE, as shown in Figure 6.5. The ANSYS® command list below is used to model one-eighth of the RVE.

```
/TITLE,ONE-EIGHT Symmetric Model of RVE hexagonal array
!Define variables for parametric modeling
rf=3.5      ! Radius fiber in microns
a2=5.2701   ! x2 length in microns
a3=9.1281   ! x3 length in microns
a1=a2/4     ! x1 length in microns

/PREP7              ! Pre-processor module
MP,EX,1,0.241       ! Fiber material properties in TeraPascals [TPa]
MP,PRXY,1,0.2
MP,EX,2,3.12e-3     ! Matrix material properties in TeraPascals [TPa]
MP,PRXY,2,0.38

ET,1,SOLID186       ! Choose SOLID186 element type

BLOCK,0,a2,0,a3,0,a1    ! Geometry definition
CYLIND,rf,,0,a1,0,90
WPOFF,a2,a3
CYLIND,rf,,0,a1,180,270
VOVLAP,all          ! Overlap volumes
NUMCMP,all          ! Renumbering volumes
/DEVICE,VECTOR,1
/VIEW,1,1,2,3
/ANG,1
/PNUM,VOLU,1
/PNUM,MAT,1
/REPLOT

LSEL,U,LOC,Z,A1     ! MESHING CONTROL
LSEL,U,LOC,Z,0
LESIZE,ALL,,,2      ! NUMBER OF DIVISIONS TROUGTH THE THICKNESS
VSEL,S,,,1,2
ASLV,S
LSLA,S
LESIZE,ALL,,,6      ! NUMBER OF DIVISIONS ON THE FIBER
LSEL,S,LOC,Y,A3
LSEL,A,LOC,Y,0
LESIZE,ALL,,,3      ! NUMBER OF DIVISIONS ON THE MATRIX
ALLSEL,ALL
LESIZE,ALL,,,8      ! NUMBER OF DIVISIONS ON THE MATRIX
```

```
MAT,1           ! ASSOCIATE MATERIAL #1 WITH VOLUMES 1 AND 2
VMESH,1,2       ! MESH VOLUME 1 AND 2
MAT,2           ! ASSOCIATE MATERIAL #2 WITH VOLUME 3
VSWEEP,3        ! MESH BY SWEEP PROCEDURE VOLUME 3
EPLOT
FINISH                  ! EXIT PRE-PROCESSOR MODULE
```

The boundary conditions are defined in three load steps, which are then used to obtain the coefficients $C_{\alpha\beta}$ in columns one, two, and three. A unit strain is applied along each direction, each time. Equation (6.18) is then used to obtain the stiffness coefficients.

```
/SOLU                   ! SOLUTION MODULE
ANTYPE,STATIC           ! SET STATIC ANALYSIS

LSCLEAR,ALL             ! BOUNDARY CONDITIONS COLUMN 1
ASEL,S,LOC,X,0          ! MODEL X DIRECTION = 2 MATERIAL DIRECTION
ASEL,A,LOC,X,A2
DA,ALL,UX,0
ASEL,S,LOC,Y,0          ! MODEL Y DIRECTION = 3 MATERIAL DIRECTION
ASEL,A,LOC,Y,A3
DA,ALL,UY,0
ASEL,S,LOC,Z,0          ! MODEL Z DIRECTION = 1 MATERIAL DIRECTION
DA,ALL,UZ,0
ASEL,S,LOC,Z,A1
DA,ALL,UZ,A1
ASEL,ALL
LSWRITE,1

LSCLEAR,ALL             ! boundary conditions column 2
ASEL,S,LOC,X,0          ! model x direction = 2 material direction
DA,ALL,UX,0
ASEL,S,LOC,X,A2
DA,ALL,UX,A2
ASEL,S,LOC,Y,0          ! model y direction = 3 material direction
ASEL,A,LOC,Y,A3
DA,ALL,UY,0
ASEL,S,LOC,Z,0          ! model z direction = 1 material direction
ASEL,A,LOC,Z,A1
DA,ALL,UZ,0
ASEL,ALL
LSWRITE,2

LSCLEAR,ALL             ! boundary conditions column 3
ASEL,S,LOC,X,0          ! model x direction = 2 material direction
ASEL,A,LOC,X,A2
DA,ALL,UX,0
ASEL,S,LOC,Y,0          ! model y direction = 3 material direction
DA,ALL,UY,0
ASEL,S,LOC,Y,A3
DA,ALL,UY,A3
```

```
ASEL,S,LOC,Z,0          ! model z direction = 1 material direction
ASEL,A,LOC,Z,A1
DA,ALL,UZ,0
ASEL,ALL
LSWRITE,3

LSSOLVE,1,3             ! Solve all load sets
FINISH                  ! Exit solution module
```

The APDL language macro `srecover`*, shown below, is defined in order to compute the average stress in the RVE.*

```
*CREATE,SRECOVER !,mac  ! macro to calculate average stress
/NOPR
ETABLE, ,VOLU,          ! Get element volume
ETABLE, ,S,X            ! Get element stress
ETABLE, ,S,Y
ETABLE, ,S,Z
ETABLE, ,S,XY
ETABLE, ,S,XZ
ETABLE, ,S,YZ
ETABLE, ,S,YZ
SMULT,SXV,VOLU,SX,1,1,  ! Stress by element volume
SMULT,SYV,VOLU,SY,1,1,
SMULT,SZV,VOLU,SZ,1,1,
SMULT,SXYV,VOLU,SXY,1,1,
SMULT,SXZV,VOLU,SXZ,1,1,
SMULT,SYZV,VOLU,SYZ,1,1,
SSUM
*GET,TOTVOL,SSUM,,ITEM,VOLU ! integrate stress
*GET,TOTSX ,SSUM,,ITEM,SXV
*GET,TOTSY ,SSUM,,ITEM,SYV
*GET,TOTSZ ,SSUM,,ITEM,SZV
*GET,TOTSXY ,SSUM,,ITEM,SXYV
*GET,TOTSXZ ,SSUM,,ITEM,SXZV
*GET,TOTSYZ ,SSUM,,ITEM,SYZV

SXX0 = TOTSX/TOTVOL         ! compute average stress
SYY0 = TOTSY/TOTVOL
SZZ0 = TOTSZ/TOTVOL
SXY0 = TOTSXY/TOTVOL
SXZ0 = TOTSXZ/TOTVOL
SYZ0 = TOTSYZ/TOTVOL
/GOPR
*END !SRECOVER
```

The coefficients $C_{\alpha\beta}$ *and the equivalent engineering elastic constants are computed using the previous macro, as follows.*

```
/POST1                      ! Post-processor module
/DEVICE,VECTOR,0
```

Table 6.2: Calculated elastic properties of the unidirectional lamina.

Property	PMM	FEA
E_1 [MPa]	98,306	98,302
E_2 [MPa]	6,552	7,479
$\nu_{12} = \nu_{13}$	0.298	0.298
ν_{23}	0.6	0.540
G_{12}	2,594	(*)

(*) Not possible with the boundary conditions used in this example.

```
PLESOL,S,Z,1

SET,1                        ! First column coefficients
*USE,SRECOVER
C11 = Szz0
C21 = Sxx0
C31 = Syy0

SET,2                        ! Second column coefficients
*USE,SRECOVER
C12 = Szz0
C22 = Sxx0
C32 = Syy0

SET,3                        ! Third column coefficients
*USE,SRECOVER
C13 = Szz0
C23 = Sxx0
C33 = Syy0

EL=C11-2*C12*C21/(C22+C23)              ! Longitudinal E1 modulus
nuL=C12/(C22+C23)                       ! 12 Poisson coefficient
ET=(C11*(C22+C23)-2*C12*C12)*(C22-C23)/(C11*C22-C12*C21)
                                        ! Transversal E2 modulus
nuT=(C11*C23-C12*C21)/(C11*C22-C12*C21) ! 23 Poisson coefficient
GT=(C22-C23)/2 ! or GT=ET/2/(1+nuT)     ! 23 Shear stiffness
FINISH                       ! Exit post-processor module
```

You need to look for the results in the ANSYS output window, which is minimized in the Windows Taskbar. The results are in the same units as the elastic properties, i.e., `TPa`; then converted to `MPa` to be displayed in Table 6.2.

Fourth Column of C

If the material is orthotropic, a procedure similar to that used for column number six must be used. But for a transversally isotropic material, only the term C_{44} is nonzero in column 4 of (6.10) and it can be determined as a function of the other

components as

$$C_{44} = \frac{1}{2}(C_{22} - C_{23}) \tag{6.28}$$

Fifth Column of C

If the material is orthotropic, a procedure similar to that used for column number six must be used. But for a transversally isotropic material, only the term $C_{55} = C_{66}$ is nonzero in column 5 of (6.10) and it can be found from column number six.

Sixth Column of C

Because of the lack of symmetry of the loads, in this case it is not possible to use boundary conditions as was done for the first three columns. Thus, the boundary conditions must be enforced by using coupling constraint equations (called CE in most FEA commercial packages).

According to (6.10), only the term C_{66} is different from zero. The components $C_{\alpha 6}$ are determined by setting

$$\gamma_6^0 = \varepsilon_{12}^0 + \varepsilon_{21}^0 = 1.0 \qquad \epsilon_1^0 = \epsilon_2^0 = \epsilon_3^0 = \gamma_4^0 = \gamma_5^0 = 0 \tag{6.29}$$

Note that $\varepsilon_{12}^0 = 1/2$ is applied between $x_1 = \pm a_1$ and another one-half is applied between $x_2 = \pm a_2$. In this case, the CE applied between two periodic faces (except points in the edges and vertices) are given as a particular case of (6.13–6.15) as follows

$$\begin{array}{rcll}
u_1(a_1, x_2, x_3) - u_1(-a_1, x_2, x_3) &=& 0 & \\
u_2(a_1, x_2, x_3) - u_2(-a_1, x_2, x_3) &=& a_1 & -a_2 < x_2 < a_2 \\
u_3(a_1, x_2, x_3) - u_3(-a_1, x_2, x_3) &=& 0 & -a_3 < x_3 < a_3 \\
u_1(x_1, a_2, x_3) - u_1(x_1, -a_2, x_3) &=& a_2 & \\
u_2(x_1, a_2, x_3) - u_2(x_1, -a_2, x_3) &=& 0 & -a_1 < x_1 < a_1 \\
u_3(x_1, a_2, x_3) - u_3(x_1, -a_2, x_3) &=& 0 & -a_3 < x_3 < a_3 \\
u_1(x_1, x_2, a_3) - u_1(x_1, x_2, -a_3) &=& 0 & \\
u_2(x_1, x_2, a_3) - u_2(x_1, x_2, -a_3) &=& 0 & -a_1 < x_1 < a_1 \\
u_3(x_1, x_2, a_3) - u_3(x_1, x_2, -a_3) &=& 0 & -a_2 < x_2 < a_2
\end{array} \tag{6.30}$$

Note that (6.30) are applied between opposite points on the faces of the RVE but not on edges and vertices. In FEA, CE are applied between degrees of freedom (DOF). Once a DOF has been used in a CE, it cannot be used in another CE. For example, the first of (6.30) for $x_2 = a_2$ becomes

$$u_1(a_1, a_2, x_3) - u_1(-a_1, a_2, x_3) = 0 \tag{6.31}$$

The DOF associated to $u_1(a_1, a_2, x_3)$ (for all $-a_3 < x_3 < a_3$) are eliminated because they are identical to $u_1(-a_1, a_2, x_3)$, as required by (6.31) and enforced by a CE based on the same. Once the DOF are eliminated, they cannot be used in another CE. For example, the fourth of (6.30) at $x_1 = a_1$ is

$$u_1(a_1, a_2, x_3) - u_1(a_1, -a_2, x_3) = 0 \tag{6.32}$$

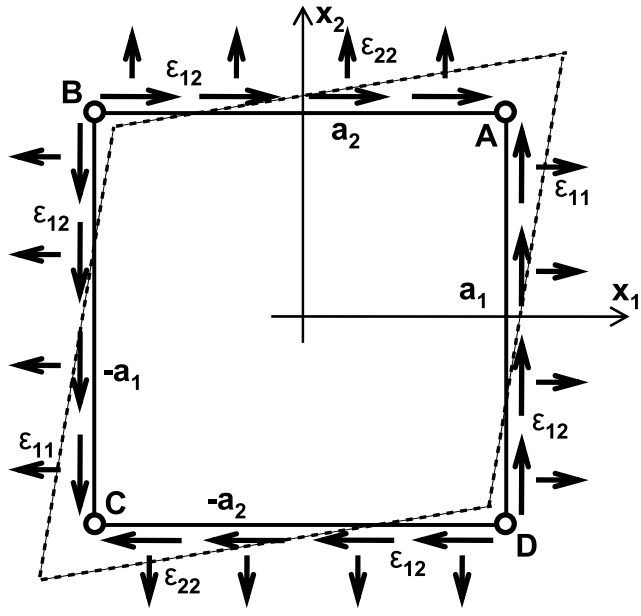

Figure 6.6: Top view of the RVE showing that two displacements (vertical and horizontal) must be applied at edges to impose shear strain (shown as points A, B, C, and D in the figure).

but this CE cannot be enforced because the DOF associated to $u_1(a_1, a_2, x_3)$ have been eliminated by the CE associated to (6.31). As a corollary, constraint equations on the edges and vertices of the RVE must be written separately from (6.30). Furthermore, only three equations, one for each component of displacement u_i can be written between a pair of edges or pair of vertices. Simply put, there are only three displacements that can be used to enforce periodicity conditions.

For pairs of edges, the task at hand is to reduce the first six equations of (6.30) to three equations that can be applied between pairs of edges for the interval $-a_3 < x_3 < a_3$. Note that the new equations will not be applied at $x_3 = \pm a_3$ because those are vertices, which will be dealt with separately. Therefore, the last three equations of (6.30) are inconsequential at this point.

The only way to reduce six equations to three, in terms of six unique DOF, is to add the equations for diagonally opposite edges. Figure 6.6 is a top view of the RVE looking from the positive x_3 axis. Point A in Figure 6.6 represents the edge formed by the planes $x_1 = a_1$ and $x_2 = a_2$. This location is constrained by the first of (6.30) at that location, which is precisely (6.31). Point C in Figure 6.6 represents the edge formed by the planes $x_1 = -a_1$ and $x_2 = -a_2$. This location is constrained by the fourth of (6.30), which at that location reduces to

$$u_1(-a_1, a_2, x_3) - u_1(-a_1, -a_2, x_3) = a_2 \tag{6.33}$$

Adding (6.31) and (6.33) yields a single equation as follows

$$u_1(a_1, a_2, x_3) - u_1(-a_1, -a_2, x_3) = a_2 \tag{6.34}$$

Repeating the procedure for the components u_2 and u_3, and grouping the resulting equations with (6.34) results in

$$\begin{array}{rcll} u_1\left(a_1, a_2, x_3\right) - u_1\left(-a_1, -a_2, x_3\right) & = & a_2 & \\ u_2\left(a_1, a_2, x_3\right) - u_2\left(-a_1, -a_2, x_3\right) & = & a_1 & -a_3 < x_3 < a_3 \\ u_3\left(a_1, a_2, x_3\right) - u_3\left(-a_1, -a_2, x_3\right) & = & 0 & \end{array} \tag{6.35}$$

Considering (6.30) between edges B and D in Figure 6.6 results in

$$\begin{array}{rcll} u_1\left(a_1, -a_2, x_3\right) - u_1\left(-a_1, a_2, x_3\right) & = & -a_2 & \\ u_2\left(a_1, -a_2, x_3\right) - u_2\left(-a_1, a_2, x_3\right) & = & a_1 & -a_3 < x_3 < a_3 \\ u_3\left(a_1, -a_2, x_3\right) - u_3\left(-a_1, a_2, x_3\right) & = & 0 & \end{array} \tag{6.36}$$

The planes $x_1 = \pm a_1$ and $x_3 = \pm a_3$ define two pairs of edges restrained by the following six CE

$$\begin{array}{rcll} u_1\left(+a_1, x_2, +a_3\right) - u_1\left(-a_1, x_2, -a_3\right) & = & 0 & \\ u_2\left(+a_1, x_2, +a_3\right) - u_2\left(-a_1, x_2, -a_3\right) & = & a_1 & -a_2 < x_2 < a_2 \\ u_3\left(+a_1, x_2, +a_3\right) - u_3\left(-a_1, x_2, -a_3\right) & = & 0 & \\ u_1\left(+a_1, x_2, -a_3\right) - u_1\left(-a_1, x_2, +a_3\right) & = & 0 & \\ u_2\left(+a_1, x_2, -a_3\right) - u_2\left(-a_1, x_2, +a_3\right) & = & a_1 & -a_2 < x_2 < a_2 \\ u_3\left(+a_1, x_2, -a_3\right) - u_3\left(-a_1, x_2, +a_3\right) & = & 0 & \end{array} \tag{6.37}$$

The six CE for the two pairs of edges defined by the planes $x_2 = \pm a_2$ and $x_3 = \pm a_3$ are

$$\begin{array}{rcll} u_1\left(x_1, +a_2, +a_3\right) - u_1\left(x_1, -a_2, -a_3\right) & = & a_2 & \\ u_2\left(x_1, +a_2, +a_3\right) - u_2\left(x_1, -a_2, -a_3\right) & = & 0 & -a_1 < x_1 < a_1 \\ u_3\left(x_1, +a_2, +a_3\right) - u_3\left(x_1, -a_2, -a_3\right) & = & 0 & \\ u_1\left(x_1, +a_2, -a_3\right) - u_1\left(x_1, -a_2, +a_3\right) & = & a_2 & \\ u_2\left(x_1, +a_2, -a_3\right) - u_2\left(x_1, -a_2, +a_3\right) & = & 0 & -a_1 < x_1 < a_1 \\ u_3\left(x_1, +a_2, -a_3\right) - u_3\left(x_1, -a_2, +a_3\right) & = & 0 & \end{array} \tag{6.38}$$

Note that (6.35–6.38) are not applied at the vertices because redundant CE would appear among pairs of vertices that are located symmetrically with respect to the center of the RVE's volume. Therefore, each of the four pairs of vertices need

to be constrained one at a time. The resulting CE are as follows

$$\begin{aligned}
u_1(+a_1,+a_2,+a_3) - u_1(-a_1,-a_2,-a_3) &= a_2 \\
u_2(+a_1,+a_2,+a_3) - u_2(-a_1,-a_2,-a_3) &= a_1 \\
u_3(+a_1,+a_2,+a_3) - u_3(-a_1,-a_2,-a_3) &= 0 \\
u_1(+a_1,+a_2,-a_3) - u_1(-a_1,-a_2,+a_3) &= a_2 \\
u_2(+a_1,+a_2,-a_3) - u_2(-a_1,-a_2,+a_3) &= a_1 \\
u_3(+a_1,+a_2,-a_3) - u_3(-a_1,-a_2,+a_3) &= 0 \\
u_1(-a_1,+a_2,+a_3) - u_1(+a_1,-a_2,-a_3) &= a_2 \\
u_2(-a_1,+a_2,+a_3) - u_2(+a_1,-a_2,-a_3) &= -a_1 \\
u_3(-a_1,+a_2,+a_3) - u_3(+a_1,-a_2,-a_3) &= 0 \\
u_1(+a_1,-a_2,+a_3) - u_1(-a_1,+a_2,-a_3) &= -a_2 \\
u_2(+a_1,-a_2,+a_3) - u_2(-a_1,+a_2,-a_3) &= a_1 \\
u_3(+a_1,-a_2,+a_3) - u_3(-a_1,+a_2,-a_3) &= 0
\end{aligned} \tag{6.39}$$

Equations (6.30–6.39) constrain the volume of the RVE with a unit strain given by (6.29). The FEA of this model yields all the component of stress. As discussed previously, element by element averages of these components of stress are available from the FEA (see macro `srecover` in Example 6.1) or they can be easily computed by post-processing. Therefore, the coefficient C_{66}, for this case is found using (6.18) written as

$$C_{66} = \overline{\sigma}_6 = \frac{1}{V}\int_V \sigma_6\left(x_1, x_2, x_3\right)\ dV \quad \text{with } \gamma_6^0 = 1 \tag{6.40}$$

Finally, the elastic properties of the composite are determined using (6.11).

Example 6.3 *Compute G_{12} for the composite in Example 6.2.*

Solution to Example 6.3 *To compute $G_{12} = C_{66}$, the RVE shown in Figure 6.4 must be used along with the CE explained in (6.30–6.39). The dimensions to define the RVE are the same used in Example 6.1. Therefore, the fiber diameter is $d_f = 7\ \mu m$ and the RVE dimensions are*

$$a_1 = a_2/4 \quad ; \qquad a_2 = 5.2701\ \mu m \quad ; \qquad a_3 = 9.1281\ \mu m$$

See the ANSYS command list below to model the whole RVE.

```
/TITLE, Full Model of RVE, hexagonal array

rf=3.5      ! Radius fiber in microns
a2=5.2701   ! x2 length in microns
a3=9.1281   ! x3 length in microns
a1=a2/4     ! x1 length in microns

/PREP7              ! Pre-processor module
MP,EX,1,0.241       ! Fiber material properties in TeraPascals [TPa]
MP,PRXY,1,0.2
MP,EX,2,3.12e-3     ! Matrix material properties in TeraPascals [TPa]
```

```
MP,PRXY,2,0.38

ET,1,SOLID186       ! Choose SOLID186 element type

BLOCK,-A2,A2,-A3,A3,-A1,A1,
CYLIND,RF, ,-A1,A1,  0, 90,
CYLIND,RF, ,-A1,A1, 90,180,
CYLIND,RF, ,-A1,A1,180,270,
CYLIND,RF, ,-A1,A1,270,360,
CYLIND,RF, ,-A1,A1,  0, 90,
CYLIND,RF, ,-A1,A1, 90,180,
CYLIND,RF, ,-A1,A1,180,270,
CYLIND,RF, ,-A1,A1,270,360,
VGEN,1,6,,,-A2,-A3,,,,1
VGEN,1,7,,, A2,-A3,,,,1
VGEN,1,8,,, A2, A3,,,,1
VGEN,1,9,,,-A2, A3,,,,1
ALLSEL,ALL
VOVLAP,all        ! Overlap volumes
NUMCMP,all        !  Renumbering all volumes, volume 9 is the matrix
/DEVICE,VECTOR,1
/VIEW,1,1,2,3
/ANG,1
/PNUM,VOLU,1
/PNUM,MAT,1
/REPLOT

LSEL,U,LOC,Z,A1     ! meshing control
LSEL,U,LOC,Z,-A1
LESIZE,ALL,,,4      ! number of divisions trougth the thickness
VSEL,S,,,1,8
ASLV,S
LSLA,S
LESIZE,ALL,,,6      ! number of divisions on the fiber
LSEL,S,LOC,Y,A3
LSEL,A,LOC,Y,-A3
LESIZE,ALL,,,6      ! number of divisions on the matrix
ALLSEL,ALL
LESIZE,ALL,,,16     ! number of divisions on the matrix

MAT,1               ! Associate material #1 with volumes 1 and 2
VMESH,1,8           ! Mesh volume 1 and 2
MAT,2               ! Associate material #2 with volume 3
VSWEEP,9            ! Mesh by sweep procedure volume 3
EPLOT
FINISH              ! Exit pre-processor module
```

The APDL macro `ceRVE.mac`*, available in [5], is used to define the CE and to implement (6.30–6.39). The macro is made available on the Web site because it is too long to be printed here. The RVE dimensions and the applied strain are input arguments to the macro. In this example, only a strain* $\gamma_6 = 1.0$ *is applied.*

Table 6.3: In-plane shear modulus of the unidirectional lamina

Property	PMM	FEA
G_{12} $[MPa]$	2,594	2,583

```
/SOLU               ! Solution module
! ceRVe arguments:
! a1,a2,a3,eps1,eps2,eps3,eps4,eps5,eps6
    *use,ceRVE,a1,a2,a3,0,0,0,0,0,0.5
    SOLVE           ! Solve analysis
FINISH              ! Exit solution module
```

To compute the average stress in the RVE, it is possible to use the macro `srecover`*, shown in Example 6.1. On account of the applied strain being equal to unity, the computed average stress is equal to* C_{66}*. Therefore,* $G_{12} = C_{66} = 2,583$ *MPa (Table 6.3).*

```
/POST1 ! Post-processor module
    *use,srecover
    C66 = Sxz0
FINISH                  ! Exit post-processor module
```

6.3 Global-Local Analysis

In global-local analysis (Figure 6.7), an RVE is used to to perform a refined computation at each Gauss integration point of the *global model*. The global model is used to compute the displacements and resulting strains, assuming that the material is homogeneous. The *local model* takes the inhomogeneities into account by modeling them with an RVE and thus providing a better computation of stress, state variables, as well as secant and tangent constitutive tensors. In a way, the local analysis is a surrogate for a constitutive equation that might be unknown due to the complexity of the material behavior inside the RVE. Also, the computational cost may be too high to model the entire structure with the refinement that can be afforded inside the RVE.

Equations (6.13–6.15) are used in Section 6.2 to enforce one component of strain at a time, with the objective of finding the equivalent elastic properties of the material. Equations (6.13–6.15) are still valid for a general state of strain applied to the RVE but care must be taken with the specification of periodic boundary conditions at the edges and vertices, as discussed on page 167. Equations (6.13–6.15) are nine constraint equations that can be imposed between all the pairs of periodic points on the faces of the RVE except on the edges and vertices.

On the faces $x_1 = \pm a_1$, u_1 is used to impose ε^0_{11}, u_2 is used to impose $\varepsilon^0_{21} = \gamma_6/2$, and u_3 is used to impose $\varepsilon^0_{31} = \gamma_5/2$. To achieve this, (6.13) is expanded into its three components, using tensor notation for strains, as follows

$$\begin{aligned} u_1(a_1, x_2, x_3) - u_1(-a_1, x_2, x_3) &= 2a_1\varepsilon^0_{11} \\ u_2(a_1, x_2, x_3) - u_2(-a_1, x_2, x_3) &= 2a_1\varepsilon^0_{21} \\ u_3(a_1, x_2, x_3) - u_3(-a_1, x_2, x_3) &= 2a_1\varepsilon^0_{31} \end{aligned} \tag{6.41}$$

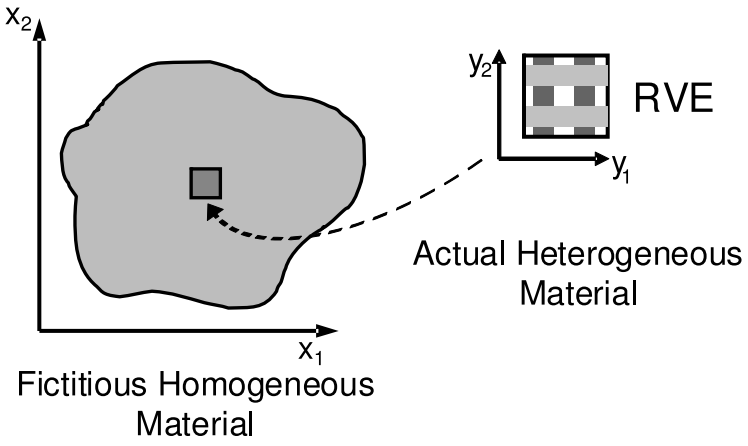

Figure 6.7: Global-local analysis using RVE.

On the faces $x_2 = \pm a_2$, u_1 is used to impose $\varepsilon^0_{12} = \gamma_6/2$, u_2 is used to impose ε^0_{22}, and u_3 is used to impose $\varepsilon^0_{32} = \gamma_4/2$. Therefore, (6.14) is expanded into its three components, using tensor notation for strains, as follows

$$\begin{aligned} u_1(x_1, a_2, x_3) - u_1(x_1, -a_2, x_3) &= 2a_2\varepsilon_{12} \\ u_2(x_1, a_2, x_3) - u_2(x_1, -a_2, x_3) &= 2a_2\varepsilon_{22} \\ u_3(x_1, a_2, x_3) - u_3(x_1, -a_2, x_3) &= 2a_2\varepsilon_{32} \end{aligned} \tag{6.42}$$

On the faces $x_3 = \pm a_3$, u_1 is used to impose $\varepsilon^0_{13} = \gamma_5/2$, u_2 is used to impose $\varepsilon^0_{23} = \gamma_4/2$, and u_3 is used to impose ε^0_{33}. Therefore, (6.15) is expanded into its three components, using tensor notation for strains, as follows

$$\begin{aligned} u_1(x_1, x_2, a_3) - u_1(x_1, x_2, -a_3) &= 2a_3\varepsilon_{13} \\ u_2(x_1, x_2, a_3) - u_2(x_1, x_2, -a_3) &= 2a_3\varepsilon_{23} \\ u_3(x_1, x_2, a_3) - u_3(x_1, x_2, -a_3) &= 2a_3\varepsilon_{33} \end{aligned} \tag{6.43}$$

Since each edge belongs to two faces, on every edge, it would seem that each component of displacement would be used to impose two CE, one from each face, as given by (6.41–6.43). However, as discussed on page 167, only one CE can be written for each component of displacement. Therefore, edges must be dealt with separately. Similarly, since three faces converge at a vertex, three periodic CE, one from each face, need to be imposed using a single component of displacement. Following a derivation similar to that presented on page 167, the following is obtained.

The planes $x_1 = \pm a_1$ and $x_2 = \pm a_2$ define two pairs of edges, for which (6.41–6.43) reduce to the following six equations (with $i = 1, 2, 3$), as follows

$$\begin{aligned} u_i(+a_1, +a_2, x_3) - u_i(-a_1, -a_2, x_3) - 2a_1\varepsilon_{i1} - 2a_2\varepsilon_{i2} &= 0 \\ u_i(+a_1, -a_2, x_3) - u_i(-a_1, +a_2, x_3) - 2a_1\varepsilon_{i1} + 2a_2\varepsilon_{i2} &= 0 \end{aligned} \tag{6.44}$$

The planes $x_1 = \pm a_1$ and $x_3 = \pm a_3$ define two pairs of edges, for which (6.41–6.43) reduce to the following six equations (with $i = 1, 2, 3$), as follows

$$\begin{aligned} u_i(+a_1, x_2, +a_3) - u_i(-a_1, x_2, -a_3) - 2a_1\varepsilon_{i1} - 2a_3\varepsilon_{i3} &= 0 \\ u_i(+a_1, x_2, -a_3) - u_i(-a_1, x_2, +a_3) - 2a_1\varepsilon_{i1} + 2a_3\varepsilon_{i3} &= 0 \end{aligned} \tag{6.45}$$

The planes $x_2 = \pm a_2$ and $x_3 = \pm a_3$ define two pairs of edges, for which (6.41–6.43) reduce to the following six equations (with $i = 1, 2, 3$), as follows

$$\begin{aligned} u_i(x_1, +a_2, +a_3) - u_i(x_1, -a_2, -a_3) - 2a_2\varepsilon_{i2} - 2a_3\varepsilon_{i3} &= 0 \\ u_i(x_1, +a_2, -a_3) - u_i(x_1, -a_2, +a_3) - 2a_2\varepsilon_{i2} + 2a_3\varepsilon_{i3} &= 0 \end{aligned} \tag{6.46}$$

Four pairs of corners need to be analyzed one at a time. For each pair, the corners are located symmetrically with respect to the center of the RVE located at coordinates $(0, 0, 0)$. The resulting CE are as follows

$$\begin{aligned} u_i(+a_1, +a_2, +a_3) - u_i(-a_1, -a_2, -a_3) - 2a_1\varepsilon_{i1} - 2a_2\varepsilon_{i2} - 2a_3\varepsilon_{i3} &= 0 \\ u_i(+a_1, +a_2, -a_3) - u_i(-a_1, -a_2, +a_3) - 2a_1\varepsilon_{i1} - 2a_2\varepsilon_{i2} + 2a_3\varepsilon_{i3} &= 0 \\ u_i(-a_1, +a_2, +a_3) - u_i(+a_1, -a_2, -a_3) + 2a_1\varepsilon_{i1} - 2a_2\varepsilon_{i2} - 2a_3\varepsilon_{i3} &= 0 \\ u_i(+a_1, -a_2, +a_3) - u_i(-a_1, +a_2, -a_3) - 2a_1\varepsilon_{i1} + 2a_2\varepsilon_{i2} - 2a_3\varepsilon_{i3} &= 0 \end{aligned} \tag{6.47}$$

Example 6.4 *Apply $\epsilon_2^0 = 0.2\%$ and $\gamma_4^0 = 0.1\%$ simultaneously to the composite in Example 6.2. Compute the average $\overline{\sigma}_2$ and $\overline{\sigma}_{12}$ in the RVE and the maximum stress σ_2 and σ_{12} anywhere in the RVE.*

Solution to Example 6.4 *The same procedure used in Example 6.3 is used to define the model. The APDL macro* `ceRVE.mac` *available in [5] is used to define the CE. The macro needs the RVE dimensions and the applied strain as input arguments. In this example, components of strain $\epsilon_2 = 0.2\%$ and $\gamma_4 = 0.1\%$ are applied, as follows*

```
/SOLU               ! Solution module
! units: TeraPascals, and microns, eps non-dimensional
! ceRVe arguments:
! a1,a2,a3,eps1,eps2,eps3,eps4,eps5,eps6
    *use,ceRVE,a1,a2,a3,0,2e-3,0,1e-3,0,0
    SOLVE           ! Solve analysis
FINISH              ! Exit solution module
```

The macro `srecover` *is used to compute the average stress of the RVE. The maximum stress in the RVE can be computed using the commands* `PLESOL,S,1` *or* `PRESOL,S,PRIN`*.*

```
/POST1              ! Post-processor module
*use,srecover       ! Compute average properties
    S_1 = Szz0
    S_2 = Sxx0
    S_3 = Syy0
    S_4 = Sxy0
    S_5 = Syz0
```

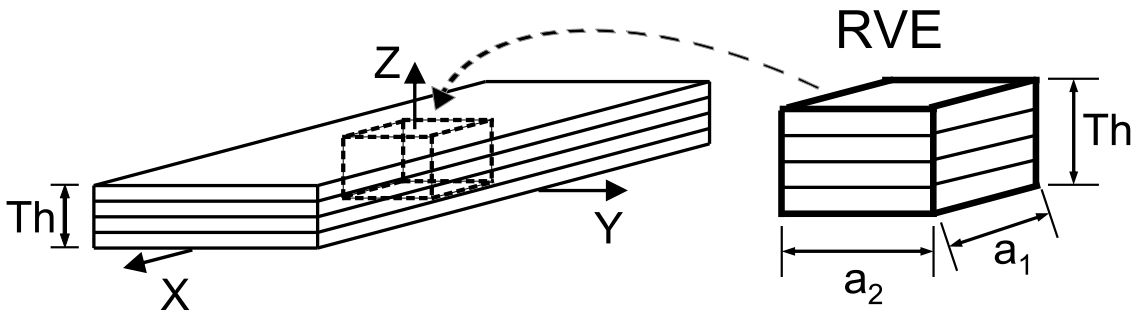

Figure 6.8: Laminated RVE.

```
    S_6 = Sxz0
VSEL,s,,,9
ESLV,S
plesol,s,x,1        ! Contour plot of S2 on matrix
plesol,s,xy,1       ! Contour plot of S23 on matrix
FINISH              ! Exit post-processor module
```

Taking into account the relation between the lamina coordinate system (c.s. 1,2,3) and ANSYS global c.s. X,Y,Z on which the mesh is defined, the results are transformed and shown in Table 6.4.

Table 6.4: Maximum stress on the matrix and average stress in the RVE

Average Results	**Maximum on the Matrix**
$\sigma_2 = 10.0$ MPa	$\overline{\sigma}_2 = 29.5$ MPa
$\sigma_{12} = 2.42$ MPa	$\overline{\sigma}_{12} = 6.07$ MPa

6.4 Laminated RVE

A similar procedure to that used to obtain the RVE at the microscale can be used to analyze laminates on the mesoscale. In this case the RVE represents a laminate. Therefore, the through-thickness direction should remain free to expand along the thickness. For example, with laminas parallel to the x-y plane, then $\sigma_z = 0$ and (6.15) is not enforced, so that the thickness coordinate is free to contract (see Figure 6.8). In general, the RVE must include the whole thickness. For symmetrical laminates subjected to in-plane loads, the RVE can be defined with half the thickness using symmetry boundary conditions (see Example 6.5).

The CE for a laminated RVE are simpler. Only (6.13) and (6.14) must be enforced. In an hexahedral RVE, such as shown in Figure 6.8, only four faces ($x_1 = \pm a_1$ and $x_2 = \pm a_2$) and the four edges defined by these faces need to be considered.

Therefore, in a laminated RVE the constraint equations (6.13) and (6.14) become the following. On the periodic pair of faces $x_1 = \pm a_1$, the CE are derived from (6.13)

as

$$\begin{aligned} u_1(a_1, x_2, x_3) - u_1(-a_1, x_2, x_3) - 2a_1\varepsilon_{11} &= 0 \\ u_2(a_1, x_2, x_3) - u_2(-a_1, x_2, x_3) - 2a_1\varepsilon_{21} &= 0 \\ u_3(a_1, x_2, x_3) - u_3(-a_1, x_2, x_3) - 2a_1\varepsilon_{31} &= 0 \end{aligned} \tag{6.48}$$

and on the pair of faces $x_2 = \pm a_2$, the CE are are derived from (6.14)

$$\begin{aligned} u_1(x_1, a_2, x_3) - u_1(x_1, -a_2, x_3) - 2a_2\varepsilon_{12} &= 0 \\ u_2(x_1, a_2, x_3) - u_2(x_1, -a_2, x_3) - 2a_2\varepsilon_{22} &= 0 \\ u_3(x_1, a_2, x_3) - u_3(x_1, -a_2, x_3) - 2a_2\varepsilon_{32} &= 0 \end{aligned} \tag{6.49}$$

The planes $x_1 = \pm a_1$ and $x_2 = \pm a_2$ define two pairs of periodic edges, for which (6.13–6.14) reduce to the following equations

$$\begin{aligned} u_1(+a_1, +a_2, x_3) - u_1(-a_1, -a_2, x_3) - 2a_1\varepsilon_{11} - 2a_2\varepsilon_{12} &= 0 \\ u_2(+a_1, +a_2, x_3) - u_2(-a_1, -a_2, x_3) - 2a_1\varepsilon_{21} - 2a_2\varepsilon_{22} &= 0 \\ u_3(+a_1, +a_2, x_3) - u_3(-a_1, -a_2, x_3) - 2a_3\varepsilon_{31} &= 0 \end{aligned} \tag{6.50}$$

and

$$\begin{aligned} u_1(+a_1, -a_2, x_3) - u_1(-a_1, +a_2, x_3) - 2a_1\varepsilon_{11} + 2a_2\varepsilon_{12} &= 0 \\ u_2(+a_1, -a_2, x_3) - u_2(-a_1, +a_2, x_3) - 2a_1\varepsilon_{21} + 2a_2\varepsilon_{22} &= 0 \\ u_3(+a_1, -a_2, x_3) - u_3(-a_1, +a_2, x_3) - 2a_3\varepsilon_{32} &= 0 \end{aligned} \tag{6.51}$$

For in-plane analysis, $\varepsilon_{31} = \varepsilon_{32} = 0$ and the third equation in (6.48)–(6.51) are automatically satisfied.

Example 6.5 *Compute G_{xy} for a $[0/90/-45/45]_S$ laminate with properties $E_1 = 139$ GPa, $E_2 = 14.5$ GPa, $G_{12} = G_{13} = 5.86$ GPa, $G_{23} = 2.93$ GPa, $\nu_{12} = \nu_{13} = 0.21$, $\nu_{23} = 0.38$ and lamina thickness $t_k = 1.25$ mm.*

Solution to Example 6.5 *A shear strain $\gamma^0_{xy} = 1$ is applied to the RVE. The laminate shear stiffness G_{xy} is obtained directly by computing the average stress in the RVE. As a result of laminate symmetry and in-plane load, an RVE of half thickness with symmetry boundary conditions in $z = 0$ can be used. The following APDL commands define the model and the laminate.*

```
/TITLE,RVE of [0/90/-45/45]s laminate
/PREP7                  ! Pre-processor module

TH =1.25            ! Thickness of lamina in mm
A1 =1               ! Half length of RVE in x direction
A2 =1               ! Half length of RVE in y direction

! Equivalent Material properties
UIMP,1,EX,EY,EZ,139E3,14.5E3,14.5E3
UIMP,1,GXY,GYZ,GXZ,5.86E3,2.93E3,5.86E3
UIMP,1,PRXY,PRYZ,PRXZ,0.21,0.38,0.21

ET,1,SOLID186               ! Chooses SOLID186 element for analysis
```

```
! Define material orientation by local Coordinate
LOCAL,11,,0,0,0,45          ! defines 45 degree local cs
LOCAL,12,,0,0,0,-45         ! defines -45 degree local cs
LOCAL,13,,0,0,0,0           ! defines 0 degree local cs
LOCAL,14,,0,0,0,90          ! defines 90 degree local cs
CSYS,0                      ! set active cs to cart. system

! Generate Geometry
BLOCK,-A1,A1,-A2,A2,0,TH        !  45 degrees layer
BLOCK,-A1,A1,-A2,A2,1*TH,2*TH   ! -45 degrees layer
BLOCK,-A1,A1,-A2,A2,2*TH,3*TH   !  90 degrees layer
BLOCK,-A1,A1,-A2,A2,3*TH,4*TH   !   0 degrees layer
VGLUE,ALL                       ! Glue volumes

! Mesh Control and Mesh
NUMCMP,ALL
LESIZE,ALL,,,2
ESYS,11                     ! Selects 45 degrees material orientation
VMESH,1                     ! Meshes 45 degrees layer
ESYS,12                     ! Selects -45 degrees material orientation
VMESH,2                     ! Meshes -45 degree layer
ESYS,13                     ! Selects 0 degrees material orientation
VMESH,3                     ! Meshes 0 degree layer
ESYS,14                     ! Selects 90 degrees material orientation
VMESH,4                     ! Meshes 90 degree layer
FINISH                      ! Exit pre-processor module
```

The APDL macro `ceRVElaminate.mac` *available in [5] is used to define the CE, thus implementing* (6.48)–(6.51)*. The macro needs the RVE dimensions and the applied strain as input arguments. In this example, only a strain* $\gamma_{xy}^0 = 1.0$ *is applied.*

```
/SOLU           ! Solution module
ANTYPE,STATIC   ! Set static analysis
NSEL,S,LOC,Z,0
D,ALL,UZ        ! Symmetry z=0
NSEL,R,LOC,Y,0
NSEL,R,LOC,X,0
D,ALL,ALL
NSEL,ALL

! ceRVElaminate arguments:
! a1,a2,epsX,epsY,epsXY

*use,ceRVElaminate,a1,a2,0,0,1
SOLVE            ! Solve analysis
FINISH           ! Exit solution module
```

To compute the average stress along the RVE, it is possible to use the macro `srecover`*, used in Example 6.1.*

```
/POST1              ! Post-processor module
/DEVICE,VECTOR,0
/PNUM,MAT,0
*USE,SRECOVER
G_XY =  SXY0
PLESOL,S,XY,1
FINISH              ! Exit post-processor module
```

The result `G_XY` is shown in the ANSYS output window, which is minimized in the Taskbar. On account of the applied strain being equal to unity, the computed average stress is equal to C_{66}. Therefore, $G_{12} = 21,441$ MPa.

Suggested Problems

Problem 6.1 *Consider a unidirectional composite with isotropic fibers $E_f = 241\ GPa$, $\nu_f = 0.2$, and isotropic matrix $E_m = 3.12\ GPa$, $\nu_m = 0.38$ with fiber volume fraction $V_f = 0.4$. The fiber diameter is $d_f = 7\ \mu m$, placed in a square array as shown in Figure 6.1. Choose an RVE including one full fiber in the center, with vertical faces spaced $2\ a_2$ and horizontal faces spaced $2\ a_3$.*

i. compute the first 3 columns of the stiffness matrix in (6.10).

ii. compute C_{66}.

Problem 6.2 *Consider the same material and fiber distribution of Problem 6.1, but choose an RVE with faces rotated 45° with respect to the horizontal and vertical direction in Figure 6.1. Therefore, the RVE size will be $2\sqrt{2}\ a_2$ by $2\sqrt{2}\ a_3$ and it will include two fibers (one full and four quarters). Be careful to select a correct RVE that is periodic.*

i. compute the first 3 columns of the stiffness matrix in (6.10).

ii. compute C_{66}.

Problem 6.3 *Compute $E_1, E_2, \nu_{12}, \nu_{23}, G_{12}, G_{23}$, using the stiffness matrices calculated in Problems 6.1 and 6.2. Compare and explain the results.*

Problem 6.4 *Perform the averaging (6.8) of the stiffness matrices calculated in Problems 6.1 and 6.2. Then, compute $E_1, E_2, \nu_{12}, \nu_{23}, G_{12}, G_{23}$, using the averaged matrices. Compare and explain the results.*

Problem 6.5 *Compute G_{12} as in Example 6.3 but using symmetry boundary conditions to discretize only one quarter of the RVE.*

Problem 6.6 *Compute G_{23} by using Example 6.4 as a guide.*

Chapter 7

Viscoelasticity

Our interest in viscoelasticity is motivated by observed creep behavior of polymer matrix composites (PMC), which is a manifestation of viscoelasticity. The time-dependent response of materials can be classified as elastic, viscous, and viscoelastic. On application of a sudden load, which is then held constant, an elastic material undergoes instantaneous deformation. In a *one-dimensional state of stress*, the elastic strain is $\varepsilon = D\sigma$, where $D = 1/E$ is the compliance or inverse of the modulus E. The deformation then remains constant. Upon unloading, the elastic strain reverses to its original value, thus all elastic deformation is recovered.

The viscous material flows at a constant rate $\dot{\varepsilon} = \sigma/\eta$ where $\eta = \tau E_0$ is the Newton viscosity, E_0 is the initial modulus, and τ is the time constant of the material. The accumulated strain $\varepsilon = \int \dot{\varepsilon} dt$ cannot be recovered by unloading.

A viscoelastic material combines the behavior of the elastic and viscous material in one, but the response is more complex than just adding the viscous strain to the elastic strain. Let H be the Heaviside function defined as

$$\begin{aligned} H(t - t_0) &= 0 \text{ when } t < t_0 \\ H(t - t_0) &= 1 \text{ when } t \geq t_0 \end{aligned} \tag{7.1}$$

Upon step loading $\sigma = H(t - t_0)\ \sigma_0$, with a constant load σ_0, the viscoelastic material experiences a sudden elastic deformation, just like the elastic material. After that, the deformation grows by a combination of recoverable and unrecoverable viscous flow.

A simple series addition of viscous flow and elastic strain (*Maxwell model*, Figure 7.1(a), with $\eta = \tau E_0$) yields totally unrecoverable viscous flow plus recoverable elastic deformation

$$\dot{\varepsilon}(t) = \frac{\sigma(t)}{\tau E_0} + \frac{\dot{\sigma}(t)}{E_0} \tag{7.2}$$

A simple parallel combination of elastic and viscous flow (*Kelvin model*, Figure 7.1(b), with $\eta = \tau E$) yields totally recoverable deformation with no unrecoverable viscous flow

$$\sigma(t) = \tau E \dot{\varepsilon}(t) + E\varepsilon(t) \tag{7.3}$$

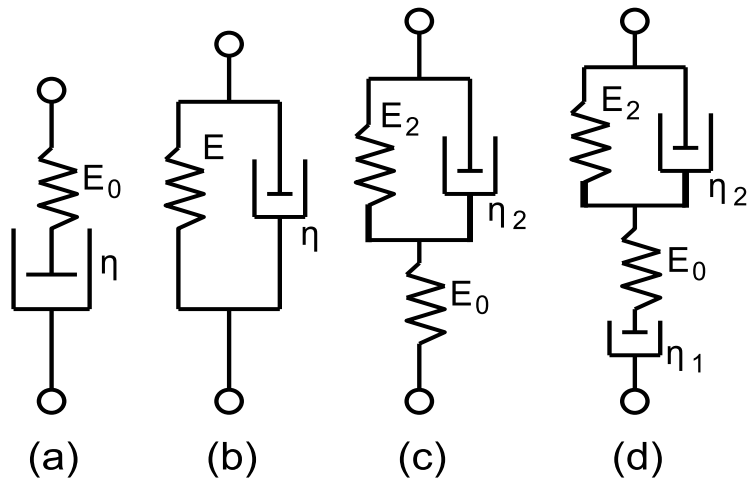

Figure 7.1: Viscoelastic models: (a) Maxwell, (b) Kelvin, (c) standard solid, (d) Maxwell-Kelvin.

but the deformation does not recover instantaneously.

Materials with unrecoverable viscous flow, such as (7.2), are called *liquids* even though the flow may occur very slowly. Glass is a liquid material over the time span of centuries; the thickness of window panes in medieval cathedrals is thicker at the bottom and thinner at the top, thus revealing the flow that took place over the centuries under the load imposed by gravity. Materials with fully recoverable viscous deformations, such as (7.3), are called *solids*. We shall see that structural design is much easier with solid materials than with liquid materials.

Please take heed of the common misconception introduced in early mechanics of materials courses that most structural materials are elastic. Only perfectly crystalline materials are elastic. Most materials are viscoelastic if observed for sufficiently long periods of time, or at a sufficiently high temperature. In other words, most real materials are viscoelastic.

For elastic materials, the compliance D is the inverse of the modulus E, both of which are constants, and they are related by

$$DE = 1 \tag{7.4}$$

For viscoelastic materials in the time domain, the compliance is called $D(t)$ and it is related to the time-varying relaxation $E(t)$ in a similar but not so simple way, as it will be shown in Section 7.3. Note that the relaxation $E(t)$ takes the place of the modulus E. A brief derivation of the relationship between compliance and relaxation is presented next, in order to facilitate the presentation of viscoelastic models in Section 7.1. When both the compliance D and the relaxation E are functions of time, (7.4) simply becomes

$$D(t)E(t) = 1 \tag{7.5}$$

Both $D(t)$ and $E(t)$ are functions of time and thus it is not possible to operate algebraically on (7.5) to get either function explicitly in terms of the other. To find

one from the other, take the Laplace transform (see Section 7.3) to get

$$s^2 D(s) E(s) = 1 \tag{7.6}$$

Since both $D(s)$ and $E(s)$ are algebraic functions of s, and the time t is not involved, it is possible to operate algebraically to get

$$E(s) = \frac{1}{s^2 D(s)} \tag{7.7}$$

Finally, the relaxation in the time domain is the inverse Laplace of (7.7) or

$$E(t) = L^{-1}[E(s)] \tag{7.8}$$

Similarly, the compliance $D(t)$ can be obtained from the relaxation $E(t)$ as

$$D(t) = L^{-1}\left[\frac{1}{s^2 L[E(t)]}\right] \tag{7.9}$$

where $L[\,]$ indicates the Laplace transform and $L^{-1}[\,]$ indicates the inverse Laplace transform.

7.1 Viscoelastic Models

The viscoelastic material models presented in this section are convenient curve fits of experimental data. In the time domain, the usual experiments are the creep and relaxation tests. In the *creep test*, a constant stress σ_0 is applied and the ensuing strain is measured. The ratio of measured strain to applied stress is the compliance $D(t) = \varepsilon(t)/\sigma_0$. In the *relaxation test*, a constant strain ε_0 is applied and the stress needed to maintain that strain is measured. The ratio of measured stress to applied strain is the relaxation $E(t) = \sigma(t)/\varepsilon_0$.

7.1.1 Maxwell Model

To derive the compliance of the *Maxwell* model [43], a creep test is performed under constant stress σ_0 applied at the ends of the model shown in Figure 7.1(a). The rate of strain is given by (7.2). Integrating with respect to time we get

$$\varepsilon(t) = \frac{1}{\tau E_0}\int_0^t \sigma_0 dt + \frac{\sigma_0}{E_0} \tag{7.10}$$

where E_0 is the elastic constant of the spring, τ is the time constant of the material, and $\eta_0 = \tau E_0$ in Figure 7.1(a). The spring and dashpot are subject to the same load and to the same constant stress σ_0, so evaluating the integral yields

$$\varepsilon(t) = \frac{\sigma_0\, t}{\tau E_0} + \frac{\sigma_0}{E_0} \tag{7.11}$$

Then, the compliance is

$$D(t) = \frac{1}{E_0} + \frac{t}{\tau E_0} \tag{7.12}$$

Table 7.1: Some common Laplace transforms

Function	**f(t)=L^{-1}{f(s)}**	**f(s)=L{f(t)}**
constant	a	a/s
linear	at	a/s^2
derivative	df/dt	sf(s)-f(0)
exponential	$\exp(at)$	$1/(s-a)$
convolution integral	$\int_0^t f(t-\tau)g(\tau)d\tau$	$L\{f\}L\{g\}$

To derive the relaxation of the Maxwell model, take the Laplace transform of (7.12), using Table 7.1 or MATLAB®, to get

$$D(s) = \frac{1}{sE_0} + \frac{1}{s^2\tau E_0} = \frac{s\tau + 1}{s^2\tau E_0} \tag{7.13}$$

At $t = 0$, the dashpot does not move, so E_0 is also the initial elastic modulus of the material. Now, the relaxation in the Laplace domain is

$$E(s) = \frac{1}{s^2 D(s)} = \frac{\tau E_0}{s\tau + 1} \tag{7.14}$$

and the relaxation in the time domain is obtained by taking the inverse Laplace transform (using Table 7.1 or MATLAB) to get

$$E(t) = E_0 \exp(-t/\tau) \tag{7.15}$$

Note that at $t = \tau$, the relaxation decays to 36.8% of its initial value, and thus τ is called the *time constant* of the material.

7.1.2 Kelvin Model

For the *Kelvin* model, only the creep test is possible, since a relaxation test would require an infinitely large stress to stretch the dashpot in Figure 7.1(b) to a constant value in no time. For a creep test, a constant stress $\sigma = \sigma_0$ is applied. Then, (7.3) is an ordinary differential equation (ODE) in $\varepsilon(t)$, which is satisfied by $\varepsilon(t) = (\sigma_0/E)\,[1 - exp(-t/\tau)]$. Therefore, the compliance $D(t) = \varepsilon(t)/\sigma_0$ is

$$D(t) = 1/E_0[1 - \exp(-t/\tau)] \tag{7.16}$$

Using (7.8), the relaxation function can be written with the aid of the Heaviside step function $H(t)$ and the Dirac delta function $\delta(t)$ as follows

$$E(t) = EH(t) + E\tau\delta(t) \tag{7.17}$$

where $\delta(t-t_0) = \infty \; if \;\; t = t_0$ and zero for any other time. The following MATLAB code yields (7.17):

```
syms s complex; syms Dt Et t E tau real;
Dt=expand((1-exp(-t/tau))/E)
Ds=laplace(Dt)
Es=1/Ds/s^2
Et=ilaplace(Es)
```

7.1.3 Standard Linear Solid

To have an initial compliance $1/E_0$, a spring is added to the Kelvin model (Figure 7.1.c). Then, the compliance is

$$D(t) = 1/E_0 + 1/E_2 \left[1 - \exp\left(\frac{-t}{\tau_2}\right)\right] \tag{7.18}$$

and

$$E(t) = E_\infty + (E_0 - E_\infty) \exp\left(\frac{-t\,(E_0 + E_2)}{\tau_2 E_2}\right) \tag{7.19}$$

where $E_\infty = (E_0^{-1} + E_2^{-1})^{-1}$ is the equilibrium modulus as time goes to infinity.

To obtain a better correlation, more spring-dashpot elements are added in series, as in

$$D(t) = D_0 + \sum_{j=1}^{n} D_j \left[1 - exp\left(-t/\tau_j\right)\right] \tag{7.20}$$

where τ_j are the retardation times [44]. When $n \to \infty$,

$$D(t) = \int_0^\infty \Delta(\tau) \left[1 - exp\left(-t/\tau\right) d\tau\right] \tag{7.21}$$

where $\Delta(\tau)$ is the compliance spectrum [44].

7.1.4 Maxwell-Kelvin Model

A crude approximation of a liquid material is the *Maxwell-Kelvin* model, also called the four-parameter model, described by Figure 7.1(d). Since the Maxwell and Kelvin elements are placed in series, the compliance is found by adding the compliances of the two individual modes, as

$$D\,(t) = \frac{1}{E_0} + \frac{t}{\tau_1 E_0} + \frac{1}{E_2} \left[1 - exp\left(-t/\tau 2\right)\right] \tag{7.22}$$

where E_0 is the elastic modulus, τ_1 takes the place of τ in (7.12), and E_2, τ_2, take the place of E, τ, in (7.16). The relaxation modulus is given by [43, page 28]

$$
\begin{aligned}
E(t) &= \left(P_1^2 - 4P_2\right)^{-1/2} \left[\left(q_1 - \frac{q_2}{T_1}\right) exp\left(-t/T_1\right) - \left(q_1 - \frac{q_2}{T_2}\right) exp\left(-t/T_2\right)\right] \\
\eta_1 &= E_0\tau_1 \quad ; \quad \eta_2 = E_0\tau_2 \\
q_1 &= \eta_1 \quad ; \quad q_2 = \frac{\eta_1\,\eta_2}{E_2} \\
T_1 &= \frac{1}{2P_2}\left[P_1 + \sqrt{P_1^2 - 4P_2}\right] \quad ; \quad T_2 = \frac{1}{2P_2}\left[P_1 - \sqrt{P_1^2 - 4P_2}\right] \\
P_1 &= \frac{\eta_1}{E_0} + \frac{\eta_1}{E_2} + \frac{\eta_2}{E_2} \quad ; \quad P_2 = \frac{\eta_1\,\eta_2}{E_0 E_2}
\end{aligned} \tag{7.23}
$$

Another way to determine if a material is a liquid or a solid is to look at its long-term deformation. If the deformation is unbounded, then it is a liquid. If the deformation eventually stops, then it is a solid.

7.1.5 Power Law

Another model, which is popular to represent the short-term deformation of polymers is the *power law*

$$E(t) = At^{-n} \tag{7.24}$$

The parameters A and n are adjusted with experimental data. The power law is popular because it fits well the short-time behavior of polymers and because fitting the data is very easy; just take a logarithm on both sides of (7.24) so that the equation becomes that of a line, then fit the parameters using linear regression. The compliance is obtained by using (7.9) as

$$
\begin{aligned}
D(t) &= D_0 + D_c(t) \\
D_c(t) &= [A\Gamma(1-n)\Gamma(1+n)]^{-1} t^n
\end{aligned} \tag{7.25}
$$

where Γ is the Gamma function [45], $D_0 = 1/E_0$ is the elastic compliance and the subscript $()_c$ indicates the creep component of the relaxation and compliance functions.

7.1.6 Prony Series

Although the short-term creep and relaxation of polymers can be described well by the power law, as the time range becomes longer, a more refined model becomes necessary. One such model is the *Prony series*, which consists of a number n of decaying exponentials

$$E(t) = E_\infty + \sum_{i=1}^{n} E_i \exp(-t/\tau_i) \tag{7.26}$$

where τ_i are the relaxation times, E_i are the relaxation moduli, and E_∞ is the equilibrium modulus, if any exists. For example, a Maxwell material is a "liquid"

and thus $E_\infty = 0$. The larger the τ_i the slower the decay is. Note that at $t = 0$, $E_0 = E_\infty + \sum E_i$. Equation (7.26) can be rewritten as

$$E(t) = E_\infty + \sum_1^n m_i \; E_0 \exp(-t/\tau_i) \tag{7.27}$$

where $m_i = E_i/E_0$ are the dimensionless moduli.

The Prony series can be written in terms of the shear modulus and bulk modulus (G, K, see Section 1.12.5) as follows

$$\begin{aligned} G(t) &= G_\infty + \sum_1^n g_i \; G_0 \exp(-t/\tau_i) \\ K(t) &= K_\infty + \sum_1^n k_i \; K_0 \exp(-t/\tau_i) \end{aligned} \tag{7.28}$$

where G_0, K_0 are the initial values of shear and bulk modulus, respectively; G_i, K_i are shear and bulk moduli of the i-th term; $g_i = G_i/G_0$ and $k_i = K_i/K_0$ are dimensionless shear/bulk moduli.

Noting that at $t = 0$, $G_\infty = G_0(1 - \sum_1^n g_i)$, and $K_\infty = K_0(1 - \sum_1^n k_i)$, the Prony series can be rewritten as

$$\begin{aligned} G(t) &= G_0 \left(1 - \sum_1^n g_i\right) + \sum_1^n g_i \; G_0 \exp(-t/\tau_i) \\ k(t) &= k_0 \left(1 - \sum_1^n k_i\right) + \sum_1^n k_i \; K_0 \exp(-t/\tau_i) \end{aligned} \tag{7.29}$$

For most polymers and composites it is usual to assume that the Poisson's ratio does not change with time, which according to (1.74) and (1.76) is achieved by setting $k_i = g_i$. Also, if ν is constant over time, $m_i = g_i$ in (7.27).

7.1.7 Standard Nonlinear Solid

While the Prony series can fit any material behavior if a large number of terms are used, other models are more efficient for fitting purposes, if harder to manipulate mathematically. For example the *Standard Nonlinear Solid* model

$$D(t) = D_0 + D_1'[1 - \exp(-t/\tau)^m] \tag{7.30}$$

can approximate well the long-term compliance in the α-region of polymer creep [46]. At room temperature, this is the region of interest to structural engineers since it spans the range of time from seconds to years. In contrast the β-region [46], is

of interest to sound and vibration experts, among others, since it spans the sub-second range of times. In other words, for long-term modeling, all compliance occurring in the β-region can be lumped in the term D_0, with D_1' representing all the compliance that could ever be accumulated in the α-region. Equation (7.30) has four parameters. When the data spans short times, it may be impossible to determine all four parameters because the material behavior cannot be distinguished from a 3-parameter power law (7.31). This can be easily understood if (7.30) is expanded in a power series, truncated after the first term as follows [46]

$$D(t) = D_0 + D_1'(t/\tau)^m[1 - (t/\tau)^m + ...] \approx D_0 + D_1 t^m \; ; \; D_1 = D_1'/\tau \tag{7.31}$$

For short times, all higher order powers of t can be neglected. What remains is a modified power law with only three parameters. Note that for short times, the parameter τ is combined with D_1' to form D_1. If the data cover a short time, the fitting algorithm will not be able to adjust both τ and D_1' in (7.31); virtually any combination of τ and D_1' will work. That means that short-term data must be modeled by a smaller number of parameters, in this case three.

7.1.8 Nonlinear Power Law

All models described so far represent linear viscoelastic materials. In the context of viscoelasticity, linear means that the parameters in the model are not a function of stress (see Section (7.2.1)). That means that the deformation at any fixed time can be made proportionally larger by increasing the stress. If any of the parameters are a function of stress, the material is nonlinear viscoelastic. For example a *nonlinear power law* takes the form

$$\dot{\varepsilon} = At^B\sigma^D \tag{7.32}$$

Take a logarithm to both sides of (7.32) to get a linear equation in two variables

$$y = \bar{A} + BX_1 + DX_2 \; ; \; \bar{A} = \log(A), X_1 = \log(t), X_2 = \log(\sigma) \tag{7.33}$$

that can be fitted with a multiple linear regression algorithm in MATLAB.

Although most materials are not linearly viscoelastic, they can be approximated as linear viscoelastic if the range of stress at which the structure operates is narrow.

Example 7.1 *Fit the creep data in Table 7.2 with (a) Maxwell (7.12), (b) Power Law* (7.31)*, and (c) Standard Nonlinear Solid* (7.30)*.*

Table 7.2: Creep data for Example 7.1

time [sec]	1	21	42	62	82	102	123	143	163	184	204
D(t) [GPa^{-1}]	1.49	1.99	2.21	2.35	2.56	2.66	2.75	2.85	2.92	2.96	3.01

Solution to Example 7.1 *To fit the Maxwell model, fit a line to the secondary creep data; that is, ignore the curvy portion for short times to get* $E_0 = 0.460$ *GPa,* $\tau = 495$ *s.*

To fit the Power Law, write (7.19) as

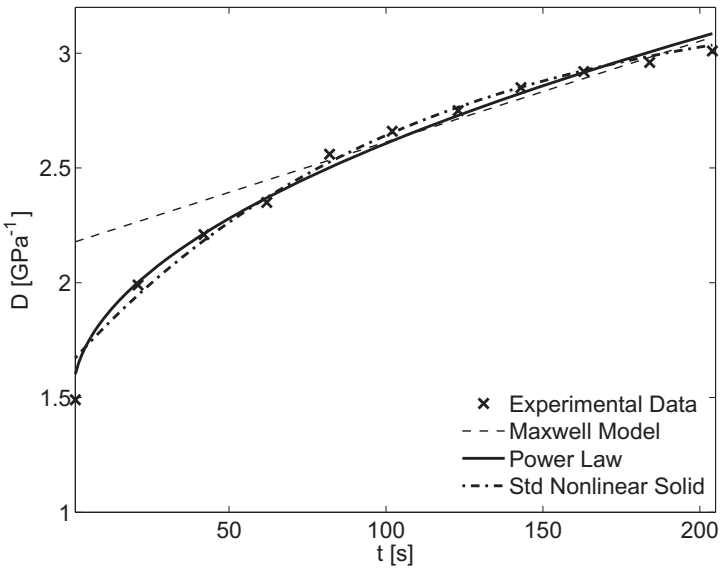

Figure 7.2: Viscoelastic fit: Maxwell Model, Power Law, and Standard Nonlinear Solid.

$$D(t) - D_0 = D_1 t^m$$

where $D_0 = 1.49\ GPa^{-1}$ *is the first datum in Table 7.2 (see also (7.31)). Take a logarithm to both sides of the above equation and adjust a line using linear regression to get* $D_0 = 1.49\ GPa^{-1}$, $D_1 = 0.1117\ (GPa\ sec)^{-1}$, *and* $m = 0.5$.

To fit the Standard Nonlinear Solid you need to use a nonlinear solver to minimize the error between the predicted (expected) values e_i *and the experimental (observed) values* o_i. *Such an error is defined as the sum over all the available data points:* $\chi^2 = \sum (e_i - o_i)^2 / o_i^2$. *In this way, the following are obtained:* $D_0 = 1.657\ GPa^{-1}$, $D_1' = 1.617\ GPa^{-1}$, $\tau = 0.273$ *sec, and* $m = 0.0026$.

The experimental data and the fit functions are shown in Figure 7.2.

7.2 Boltzmann Superposition

7.2.1 Linear Viscoelastic Material

A viscoelastic material is linear if superposition applies. That is, given a stress history

$$\sigma(t) = \sigma_1(t) + \sigma_2(t) \tag{7.34}$$

the strain is given by

$$\varepsilon(t) = \varepsilon_1(t) + \varepsilon_2(t) \tag{7.35}$$

where $\varepsilon_1(t)$, $\varepsilon_2(t)$ are the strain histories corresponding to $\sigma_1(t)$ and $\sigma_2(t)$, respectively. For linear materials, the creep compliance and relaxation modulus are independent of stress

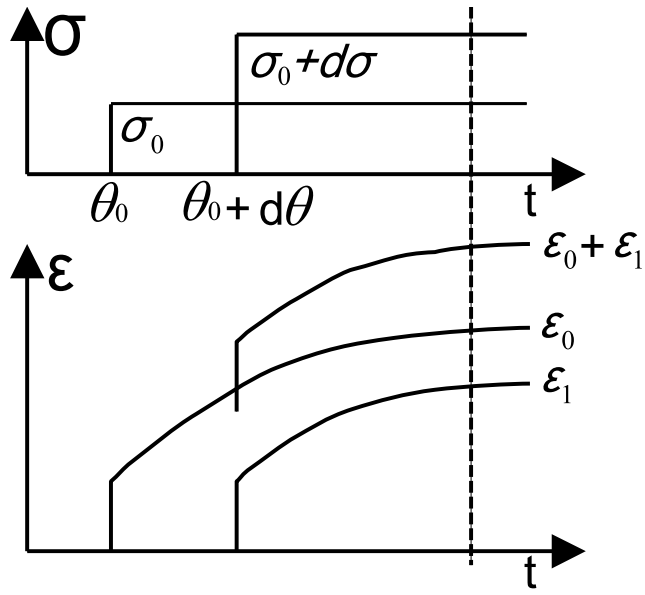

Figure 7.3: Boltzmann superposition of strains.

$$D(t) = \frac{\varepsilon(t)}{\sigma_0}$$
$$E(t) = \frac{\sigma(t)}{\varepsilon_0} \tag{7.36}$$

For nonlinear materials, $D(t, \sigma)$ is a function of stress and $E(t, \varepsilon)$ is a function of strain.

For a linear material subjected to a stress σ_0 applied at time $t = \theta_0$ (Figure 7.3) we have

$$\varepsilon(t) = \sigma_0 \; D(t, \theta_0) \quad ; \quad t > \theta_0 \tag{7.37}$$

Adding an infinitesimal load step $d\sigma$ at time $\theta_0 + d\theta$ results in

$$\varepsilon(t) = \sigma_0 \; D(t, \theta_0) + d\sigma \; D(t, \theta_0 + d\theta) \quad ; \quad t > \theta_0 + d\theta \tag{7.38}$$

If stress changes continuously by $d\sigma$ over intervals $d\theta$, the summation (7.38) can be replaced by an integral to yield the accumulated strain as

$$\varepsilon(t) = \sigma_0 \; D(t, \theta_0) + \int_{\theta_0}^{t} D(t, \theta) d\sigma = \sigma_0 \; D(t, \theta_0) + \int_{\theta_0}^{t} D(t, \theta) \frac{d\sigma}{d\theta} d\theta \tag{7.39}$$

where the discrete times θ_0, $\theta_0 + d\theta$, etc., are represented by the continuous function θ. Although aging effects are negligible over each infinitesimal $d\theta$, they are significant over time. Therefore, the compliance $D(t, \theta)$ is a function of the current time t and all the time-history represented by θ in $D(t, \theta)$.

7.2.2 Unaging Viscoelastic Material

If the $\varepsilon_1(t,\theta)$ curve has the same shape as the $\varepsilon_1(t,\theta_0)$ curve, only translated horizontally, any curve can be shifted to the origin (Figure 7.3)

$$D(t,\theta) = D(t-\theta) \tag{7.40}$$

Equation (7.40) is the definition of unaging material. For a discussion of aging materials see [43, 47–49]. Equation (7.40) means that all the curves have the same shape regardless of age θ, only shifted. Note θ in (7.40) is a continuous function $\theta < t$ that denotes the time of application of each load (σ_0, $d\sigma$, etc.).

The response $\varepsilon(t,\theta)$ at a fixed time t is a function of the response at all times $\theta < t$. Therefore, it is said that the response is hereditary. If the material is aging, t and θ are independent variables in $D(t,\theta)$. For unaging materials, only one variable, $t-\theta$, is independent, so it does not matter how old the material is (t), it only matters for how long $(t-\theta)$ it has been loaded with $d\sigma(\theta)$.

The creep compliance is the response of the material to stress and always starts when the stress is applied. If the change is gradual, from (7.39) we have

$$\varepsilon(t) = \int_0^t D(t-\theta)\ \dot{\sigma}(\theta)\ d\theta \tag{7.41}$$

The relaxation is

$$\sigma(t) = \int_0^t E(t-\theta)\ \dot{\varepsilon}(\theta)\ d\theta \tag{7.42}$$

The time-dependent behavior of linear viscoelastic materials is hereditary, meaning that the behavior at time t depends on what happened to the material since the beginning of loading at $t = 0$.

Example 7.2 *Consider an unaging material represented by $D(t-\theta) = 1/E + (t-\theta)/\eta$ and loaded with (a) $\sigma_0 H(\theta)$ and (b) $\sigma_0 H(\theta-1)$. Find $\varepsilon(t)$ in both cases and comment on the results.*

Solution to Example 7.2

$$\begin{aligned}
&(\mathbf{a}) \quad \sigma = \sigma_0 H(\theta) \ \Rightarrow\ d\sigma/dt = \sigma_0\delta(0)\\
&\varepsilon(t) = \textstyle\int_0^t \left[\frac{1}{E} + \frac{(t-\theta)}{\eta}\right]\sigma_0\delta(0)d\theta\\
&\varepsilon(t) = \left[\frac{1}{E} + \frac{t}{\eta}\right]\sigma_0\ ;\ t > 0
\end{aligned}$$

$$\begin{aligned}
&(\mathbf{b}) \quad \sigma = \sigma_0 H(\theta-1) \ \Rightarrow\ d\sigma/dt = \sigma_0\delta(1)\\
&\varepsilon(t) = \textstyle\int_0^t \left[\frac{1}{E} + \frac{(t-\theta)}{\eta}\right]\sigma_0\delta(1)d\theta\\
&\varepsilon(t) = \left[\frac{1}{E} + \frac{(t-1)}{\eta}\right]\sigma_0;\ t > 1
\end{aligned}$$

It can be seen that (b) is identical to (a), only shifted; meaning that there is no aging.

7.3 Correspondence Principle

The Laplace transform of a function $f(t)$ in the time domain (t-domain) maps to the Laplace domain (s-domain) as $f(s)$. The Laplace transform is defined as

$$L[f(t)] = f(s) = \int_0^\infty \exp(-st) f(t) dt \tag{7.43}$$

Most of the time, the Laplace transform can be obtained analytically, just using a table of transforms, such as Table 7.1. Taking the Laplace transform of (7.41, 7.42), yields

$$\varepsilon(s) = L[D(t)]\ L[\dot{\sigma}(t)] = sD(s)\sigma(s) \tag{7.44}$$

$$\sigma(s) = L[E(t)]\ L[\dot{\varepsilon}(t)] = sE(s)\varepsilon(s) \tag{7.45}$$

Multiplying (7.44) times (7.45) yields

$$s^2\ D(s)E(s) = 1 \tag{7.46}$$

or

$$s\ D(s) = [s\ E(s)]^{-1} \tag{7.47}$$

where it can be seen that $sD(s)$ is the inverse of $sE(s)$. This is analogous to (7.4) for elastic materials.

The correspondence principle states that all the equations of elasticity, available for elastic materials, are valid for linearly viscoelastic materials in the Laplace domain. This principle is the basis, for example, of the determination of creep and relaxation of polymer matrix composites in terms of fiber and matrix properties using standard micromechanics methods, as shown in Section 7.6.

The inverse mapping from the Laplace domain to the time domain

$$f(t) = L^{-1}(f(s)) \tag{7.48}$$

is more difficult to compute. Decomposition in partial fractions [50] is a useful technique to break up $f(s)$ into simpler component functions for which the inverse Laplace can be found analytically. Another useful technique is the convolution theorem defined in Table 7.1. Also, the limiting value theorems

$$\begin{aligned} f(0) &= \lim_{s\to\infty} [sF(s)] \\ f(\infty) &= \lim_{s\to 0} [sF(s)] \end{aligned} \tag{7.49}$$

can be used to evaluate the initial and final response of a material in the time domain directly in the Laplace domain. Otherwise, the inverse Laplace can be found numerically using [51] or by the collocation method described in [41, Appendix D].

The Carson transform is defined as

$$\hat{f}(s) = sf(s) \tag{7.50}$$

In the Carson domain, the constitutive equations (7.41–7.42) become

$$\begin{aligned} \varepsilon(s) &= \hat{D}(s)\sigma(s) \\ \sigma(t) &= \hat{E}(s)\varepsilon(s) \end{aligned} \tag{7.51}$$

which are analogous, in the Carson domain, to the stress-strain equations of elastic materials in the time domain. Furthermore, the relationship between compliance and relaxation becomes

$$\hat{D}(s) = 1/\hat{E}(s) \tag{7.52}$$

7.4 Frequency Domain

The Fourier transform maps the time domain into the frequency domain. It is defined as

$$F[f(t)] = f(\omega) = \int_{-\infty}^{\infty} \exp(-i\omega t) f(t)\ dt \tag{7.53}$$

and its inverse

$$f(t) = \frac{1}{\sqrt{2\pi}} \int_{-\infty}^{\infty} \exp(i\omega t) f(w) d\omega \tag{7.54}$$

Applying the Fourier transform to (7.41–7.42) yields

$$\begin{aligned} \varepsilon(\omega) &= D(\omega)\dot{\sigma}(\omega) \\ \sigma(\omega) &= E(\omega)\dot{\varepsilon}(\omega) \end{aligned} \tag{7.55}$$

and

$$D(\omega) = -\frac{1}{\omega^2 E(\omega)} \tag{7.56}$$

where $D(\omega) = D' + iD''$ and $E(\omega) = E' + iE''$ are complex numbers. Here D', D'' are the storage and loss compliances, and E', E'' are the storage and loss moduli.

Using standard complex analysis we get

$$\begin{aligned} D' &= \frac{E'}{E'^2 + E''^2} \\ D'' &= \frac{E''}{E'^2 + E''^2} \end{aligned} \tag{7.57}$$

The frequency domain has a clear physical meaning. If a sinusoidal stress $\sigma(\omega, t) = \sigma_0 \exp(-i\omega t)$ is applied to a viscoelastic material, it responds with an out-of-phase sinusoidal strain $\varepsilon(\omega, t) = \varepsilon_0 \exp(-i\omega t + \phi)$. Furthermore, the complex compliance is $D(\omega) = \varepsilon(\omega, t)/\sigma(\omega, t)$ and the complex relaxation is simply the inverse of the complex compliance, $E(\omega) = \sigma(\omega, t)/\varepsilon(\omega, t)$.

7.5 Spectrum Representation

The Prony series (7.26) provides a physical interpretation of polymer behavior as a series of Maxwell models, each with its own decay time. In the limit, a real polymer has an infinite number of such models [52], so that

$$E(t) - E_\infty = \int_{-\infty}^{\infty} H(\theta) \exp(-t/\theta) d \ln \theta = \int_0^{\infty} \frac{H(\theta)}{\theta} \exp(-t/\theta) d\theta \tag{7.58}$$

where $H(\theta)$ is the relaxation spectrum [53]. In terms of compliance, we have

$$D(t) - D_0 = \frac{t}{\eta} + \int_{-\infty}^{\infty} \frac{L(\theta)}{\theta} [1 - \exp(-t/\theta)] d\theta \tag{7.59}$$

where $L(\theta)$ is the retardation spectrum [53], D_0 is the elastic compliance, η is the asymptotic viscosity of liquids, with $\eta \to \infty$ for solids (see also [54]).

7.6 Micromechanics of Viscoelastic Composites

7.6.1 One-Dimensional Case

Recall the constitutive equations (7.51) in the Carson domain. By the correspondence principle, all equations of micromechanics for elastic materials are valid in the Carson domain for linear viscoelastic materials. For example, the Reuss micromechanical model assumes uniform identical strain in the matrix and fiber (see discussion on page 152). Therefore, the stiffness of the composite $\mathbf{C}$ is a linear combination of the stiffness of the constituents (fiber and matrix) weighed by their respective volume fractions V_m, V_f

$$\mathbf{C} = V_m \mathbf{C}^m + V_f \mathbf{C}^f \tag{7.60}$$

with $\mathbf{A}^m = \mathbf{A}^f = \mathbf{I}$ in (6.1). Taking into account the correspondence principle for a viscoelastic material (Section 7.3), it is possible to write the stiffness tensor in the Carson domain by analogy with (7.60) simply as

$$\hat{\mathbf{C}}(s) = V_m \hat{\mathbf{C}}^m + V_f \hat{\mathbf{C}}^f \tag{7.61}$$

From it, the stiffness tensor in the Laplace domain is (see (7.47))

$$\mathbf{C}(s) = \frac{1}{s} \hat{\mathbf{C}}(s) \tag{7.62}$$

Finally, the stiffness tensor in the time domain is obtained by finding the inverse Laplace transform (7.48) as

$$\mathbf{C}(t) = L^{-1}[\mathbf{C}(s)] \tag{7.63}$$

Example 7.3 *Derive the transverse compliance $D_2(t)$ in the time domain for a unidirectional composite with elastic fibers and a viscoelastic matrix represented by $D_m = 1/E_m + t/\eta_m$. Plot D_f, $D_m(t)$, and $D_2(t)$ for $0 < t < 0.1$, $E_f = 10$, $V_f = 0.5$, $E_m = 5$, $\eta_m = 0.05$. Use the Reuss model and discuss the results.*

Solution to Example 7.3 *The elastic behavior of the fiber and viscoelastic behavior of the matrix are defined as follows:*

Fiber (elastic): $E_f = \text{constant} \rightarrow D_f = \dfrac{1}{E_f}$

Matrix (Maxwell model (7.12) with $E_m = E_0$, $\eta_m = \tau E_0$*):* $\dfrac{1}{E_m} = \dfrac{1}{E_m} + \dfrac{t}{\eta_m}$

Take the Laplace transform,

$D_f(s) = \dfrac{1}{sE_f}$ *because* $\dfrac{1}{E_f}$ *is constant.*

$D_m(s) = \dfrac{1}{sE_m} + \dfrac{1}{s^2\eta_m}$

Then, the Carson transform is

$\hat{D}_f(s) = s\ D_f(s) = \dfrac{1}{E_f}$

$\hat{D}_m(s) = s\ D_m(s) = \dfrac{1}{E_m} + \dfrac{t}{s\eta_m}$

Using the Reuss model (page 152) to compute the composite behavior

$\hat{D}_2 = V_f\hat{D}_f + V_m\hat{D}_m$

$\hat{D}_2 = V_f\dfrac{1}{E_f} + V_m\left(\dfrac{1}{E_m} + \dfrac{1}{s\eta_m}\right)$

Back to the Laplace domain

$D_2(s) = \dfrac{V_f}{sE_f} + \dfrac{V_m}{sE_m} + \dfrac{V_m}{s^2\eta_m}$

Back transform to the time domain (inverse Laplace)

$D_2(t) = L^{-1}(D_2(s)) = \dfrac{V_f}{E_f} + \dfrac{V_m(E_m t + \eta_m)}{E_m\eta_m}$

To make a plot, take $E_f = 10$, $V_f = 0.5$, $E_m = 5$, $\eta_m = 0.05$, *which results in*

$$D_f = 0.1 = 1/10$$
$$D_m(t) = 0.2 + 20t$$
$$D_2(t) = 0.15 + 10t$$

Since $V_f = 0.5$, *the initial compliance is halfway between those of the fiber and the matrix. The elastic fiber has a constant compliance. The creep rate of the composite* $1/\eta_c$ *is 1/2 of the creep rate of the matrix* $1/\eta_m$.

7.6.2 Three-Dimensional Case

The constitutive equation for an elastic, isotropic material (1.78) can be written in terms of just two material parameters λ and $\mu = G$ as

$$\boldsymbol{\sigma} = (\lambda\mathbf{I}^{(2)} \otimes \mathbf{I}^{(2)} + 2\mu\mathbf{I}^{(4)}) : \boldsymbol{\varepsilon} \tag{7.64}$$

where $\mathbf{I}^{(2)}$ and $\mathbf{I}^{(4)}$ are the second- and fourth-order identity tensors[1] (see Appendix A). The constitutive equation of isotropic viscoelastic materials can be written in terms of the viscoelastic Lamé constants $\lambda(s)$ and $\mu(s)$ as follows [54]

$$\boldsymbol{\sigma}(t) = \int_0^t \lambda(t-\theta)\mathbf{I}^{(2)} \otimes \mathbf{I}^{(2)} :\ \dot{\boldsymbol{\varepsilon}}(\theta)d\theta + \int_0^t 2\mu(t-\theta)\mathbf{I}^{(4)} : \dot{\boldsymbol{\varepsilon}}(\theta)d\theta \tag{7.65}$$

[1] Tensors are indicated by boldface type, or by their components using index notation.

Using the convolution theorem (Table 7.1), the Laplace transform of (7.65) is

$$\boldsymbol{\sigma}(s) = s\lambda(s)\mathbf{I}^{(2)} \otimes \mathbf{I}^{(2)} : \boldsymbol{\varepsilon}(s) + s\ 2\mu(s)\mathbf{I}^{(4)} : \boldsymbol{\varepsilon}(s) \tag{7.66}$$

or in terms of the Carson transform

$$\hat{\boldsymbol{\sigma}}(s) = \hat{\mathbf{C}}(s) : \hat{\boldsymbol{\varepsilon}}(s) \tag{7.67}$$

Assuming that the fiber is elastic, and the matrix is viscoelastic; the latter represented with a Maxwell model

$$D_m(t) = 1/E_m + t/\eta_m \tag{7.68}$$

the Carson transform is

$$\hat{D}_m = 1/E_m + 1/s\eta_m = \frac{E_m + s\eta_m}{s\eta_m E_m} \tag{7.69}$$

Using the correspondence principle yields

$$\hat{E}_m = 1/\hat{D}_m = \frac{s\eta_m E_m}{E_m + s\eta_m} = \frac{sE_m}{E_m/\eta_m + s} \tag{7.70}$$

Using (1.75) and assuming the Poisson's ratio ν_m of the matrix to be constant, the Lamé constant of the matrix in the Carson domain is

$$\hat{\lambda}_m = \frac{\hat{E}_m \nu_m}{(1+\nu_m)(1-2\nu_m)} \tag{7.71}$$

and the shear modulus of the matrix is

$$\hat{\mu}_m = \frac{\hat{E}_m}{2(1+\nu_m)} \tag{7.72}$$

Barbero and Luciano [36] used the the Fourier expansion method to get the components of the relaxation tensor in the Carson domain for a composite with cylindrical fibers arranged in a square array with fiber volume fraction V_f. The elastic, transversely isotropic fibers are represented by the transversely isotropic stiffness tensor $\mathbf{C}'$ defined by (1.70, 1.92) in terms of fiber properties in the axial and transverse (radial) directions E_A, E_T, G_A, G_T, and ν_T. Defining the matrix properties in the Laplace $\widetilde{\ }$ and Carson domain $\widehat{\ }$ as $\widehat{\lambda}_m = s\widetilde{\lambda}_m(s)$ and $\widehat{\mu}_m = s\widetilde{\mu}_m(s)$, the components of the relaxation tensor of the composite in the Carson domain $\widehat{\mathbf{L}}^*$ become [36]

$$\widehat{L}^*_{11}(s) = \widehat{\lambda}_m + 2\,\widehat{\mu}_m - V_f\ \left(\ -a_4^2 + a_3^2\right)$$
$$\left(-\frac{\left(2\,\widehat{\mu}_m + 2\,\widehat{\lambda}_m - C'_{33} - C'_{23}\right)\left(a_4^2 - a_3^2\right)}{a_1} + \frac{2\,(a_4 - a_3)\left(\widehat{\lambda}_m - C'_{12}\right)^2}{a_1^2}\right)^{-1}$$

$$\widehat{L}^*_{12}(s) = \widehat{\lambda}_m + V_f \left(\frac{\left(\widehat{\lambda}_m - C'_{12}\right)(a_4 - a_3)}{a_1} \right) \left(\frac{\left(2\,\widehat{\mu}_m + 2\,\widehat{\lambda}_m - C'_{33} - C'_{23}\right)(a_3^2 - a_4^2)}{a_1} + \frac{2\,(a_4 - a_3)\left(\widehat{\lambda}_m - C'_{12}\right)^2}{a_1^2} \right)^{-1}$$

$$\widehat{L}^*_{22}(s) = \widehat{\lambda}_m + 2\,\widehat{\mu}_m - V_f \left(\frac{\left(2\,\widehat{\mu}_m + 2\,\widehat{\lambda}_m - C'_{33} - C'_{23}\right) a_3}{a_1} - \frac{\left(\widehat{\lambda}_m - C'_{12}\right)^2}{a_1^2} \right) \left(\frac{\left(2\,\widehat{\mu}_m + 2\,\widehat{\lambda}_m - C'_{33} - C'_{23}\right)(a_3^2 - a_4^2)}{a_1} + \frac{2\,(a_4 - a_3)\left(\widehat{\lambda}_m - C'_{12}\right)^2}{a_1^2} \right)^{-1}$$

$$\widehat{L}^*_{23}(s) = \widehat{\lambda}_m + V_f \left(\frac{\left(2\,\widehat{\mu}_m + 2\,\widehat{\lambda}_m - C'_{33} - C'_{23}\right) a_4}{a_1} - \frac{\left(\widehat{\lambda}_m - C'_{12}\right)^2}{a_1^2} \right) \left(\frac{\left(2\,\widehat{\mu}_m + 2\,\widehat{\lambda}_m - C'_{33} - C'_{23}\right)(a_3^2 - a_4^2)}{a_1} + \frac{2\,(a_4 - a_3)\left(\widehat{\lambda}_m - C'_{12}\right)^2}{a_1^2} \right)^{-1}$$

$$\widehat{L}^*_{44}(s) = \widehat{\mu}_m - V_f \left(\frac{2}{2\,\widehat{\mu}_m - C'_{22} + C'_{23}} - \left(2\,S_3 - \frac{4\,S_7}{2 - 2\,\nu_m} \right) \widehat{\mu}_m^{-1} \right)^{-1}$$

$$\widehat{L}^*_{66}(s) = \widehat{\mu}_m - V_f \left(\left(\widehat{\mu}_m - C'_{66} \right)^{-1} - \frac{S_3}{\widehat{\mu}_m} \right)^{-1} \tag{7.73}$$

where

$$\begin{aligned} a_1 = {} & 4\,\widehat{\mu}_m^2 - 2\,\widehat{\mu}_m\,C'_{33} + 6\,\widehat{\lambda}_m\,\widehat{\mu}_m - 2\,C'_{11}\,\widehat{\mu}_m - 2\,\widehat{\mu}_m\,C'_{23} + C'_{23}\,C'_{11} + 4\,\widehat{\lambda}_m\,C'_{12} \\ & - 2\,C'^{\,2}_{12} - \widehat{\lambda}_m\,C'_{33} - 2\,C'_{11}\,\widehat{\lambda}_m + C'_{11}\,C'_{33} - \widehat{\lambda}_m\,C'_{23} \end{aligned}$$

$$\begin{aligned} a_2 = {} & 8\,\widehat{\mu}_m^3 - 8\,\widehat{\mu}_m^2 C'_{33} + 12\,\widehat{\mu}_m^2\widehat{\lambda}_m - 4\,\widehat{\mu}_m^2 C'_{11} \\ & - 2\,\widehat{\mu}_m\,C'^{\,2}_{23} + 4\,\widehat{\mu}_m\,\widehat{\lambda}_m\,C'_{23} + 4\,\widehat{\mu}_m\,C'_{11}\,C'_{33} \\ & - 8\,\widehat{\mu}_m\,\widehat{\lambda}_m\,C'_{33} - 4\,\widehat{\mu}_m\,C'^{\,2}_{12} + 2\,\widehat{\mu}_m\,C'^{\,2}_{33} - 4\,\widehat{\mu}_m\,C'_{11}\,\widehat{\lambda}_m + 8\,\widehat{\mu}_m\,\widehat{\lambda}_m\,C'_{12} \\ & + 2\,\widehat{\lambda}_m\,C'_{11}\,C'_{33} + 4\,C'_{12}\,C'_{23}\,\widehat{\lambda}_m - 4\,C'_{12}\,C'_{33}\,\widehat{\lambda}_m - 2\,\widehat{\lambda}_m\,C'_{11}\,C'_{23} \\ & - 2\,C'_{23}\,C'^{\,2}_{12} + C'^{\,2}_{23}C'_{11} + 2\,C'_{33}\,C'^{\,2}_{12} - C'_{11}\,C'^{\,2}_{33} + \widehat{\lambda}_m\,C'^{\,2}_{33} - \widehat{\lambda}_m\,C'^{\,2}_{23} \end{aligned}$$

$$a_3 = \frac{4\,\widehat{\mu}_m^2 + 4\,\widehat{\lambda}_m\,\widehat{\mu}_m - 2\,C'_{11}\,\widehat{\mu}_m - 2\,\widehat{\mu}_m\,C'_{33} - C'_{11}\,\widehat{\lambda}_m - \widehat{\lambda}_m\,C'_{33} - C'^{\,2}_{12}}{a_2}$$
$$+ \frac{C'_{11}\,C'_{33} + 2\,\widehat{\lambda}_m\,C'_{12}}{a_2} - \frac{S_3 - \dfrac{S_6}{2-2\nu_m}}{\widehat{\mu}_m}$$

$$a_4 = -\frac{-2\,\widehat{\mu}_m\,C'_{23} + 2\,\widehat{\lambda}_m\,\widehat{\mu}_m - \widehat{\lambda}_m\,C'_{23} - C'_{11}\,\widehat{\lambda}_m - C'^{\,2}_{12} + 2\,\widehat{\lambda}_m\,C'_{12} + C'_{11}\,C'_{23}}{a_2}$$
$$+ \frac{S_7}{\widehat{\mu}_m\,(2-2\,\nu_m)} \tag{7.74}$$

The coefficients S_3, S_6, S_7 account for the geometry of the microstructure, including the geometry of the inclusions and their geometrical arrangement [33]. For cylindrical fibers arranged in a square array [34] we have

$$\begin{aligned} S_3 &= 0.49247 - 0.47603V_f - 0.02748V_f^2 \\ S_6 &= 0.36844 - 0.14944V_f - 0.27152V_f^2 \\ S_7 &= 0.12346 - 0.32035V_f + 0.23517V_f^2 \end{aligned} \tag{7.75}$$

Note that (7.73) yield six independent components of the relaxation tensor. This is because (7.73) represent a composite with the microstructure arranged in a square array. If the microstructure is random (Figure 1.12), the composite is transversely isotropic (Section 1.12.4) and only five components of the relaxation tensor are independent. When the axis x_1 is the axis of transverse isotropy for the composite, the averaging procedure (6.7) yields the relaxation tensor with transverse isotropy as

$$\begin{aligned} \hat{C}_{11} &= \hat{L}^*_{11} \\ \hat{C}_{12} &= \hat{L}^*_{12} \\ \hat{C}_{22} &= \frac{3}{4}\hat{L}^*_{22} + \frac{1}{4}\hat{L}^*_{23} + \frac{1}{2}\hat{L}^*_{44} \\ \hat{C}_{23} &= \frac{1}{4}\hat{L}^*_{22} + \frac{3}{4}\hat{L}^*_{23} - \frac{1}{2}\hat{L}^*_{44} \\ \hat{C}_{66} &= \hat{L}^*_{66} \end{aligned} \tag{7.76}$$

where the remaining coefficients are found using (1.70) due to transverse isotropy of the material. For example, $\hat{C}_{44} = (\hat{C}_{22} - \hat{C}_{23})/2$. This completes the derivation of the relaxation tensor $\hat{\mathbf{C}}_{ij} = s\mathbf{C}_{ij}(s)$ in the Carson domain. Next, the inverse Laplace transform of each coefficient yields the coefficients of the stiffness tensor in the time domain as

$$\mathbf{C}_{ij}(t) = L^{-1}\left[\frac{1}{s}\hat{\mathbf{C}}_{ij}\right] \tag{7.77}$$

A MATLAB code based on [51] is available in [5, invlapFEAcomp.m] to perform the inverse Laplace numerically. Another algorithm is provided in [41, Appendix D].

Example 7.4 *Consider a composite made with 60% by volume of transversally isotropic fibers with axial properties $E_A = 168.4$ GPa, $G_A = 44.1$ GPa, $\nu_A = 0.443$, and transverse properties $E_T = 24.8$ GPa and $\nu_T = 0.005$. The epoxy matrix is represented by a Maxwell model (7.12) with $E_0 = 4.08$ GPa, $\tau = 39.17$ min and $\nu_m = 0.311$. Plot the relaxation $E_2(t)$ of the composite as a function of time for $0 < t < 100$ minutes, compared to the elastic value of the transverse modulus E_2.*

Solution to Example 7.4 *This example has been solved using MATLAB. The elastic and viscoelastic values of the transverse modulus E_2 are shown in Figure 7.4. The calculation procedure is explained next:*

- *Program the equations of Section 7.6.2 and use them to calculate the elastic values of the composite's elastic properties such as E_2. These equations have been implemented in* `PMMViscoMatrix.m`.
- *Replace the elastic modulus of the matrix E_0 by the Maxwell model for the matrix Eq. (7.15) in the Carson domain $\hat{E}_0$ (See* `PMMViscoMatrix.m`*), as follows:*
  - i. *The output from the portion of the code implementing (7.73–7.76) are equations for the relaxation moduli in terms of s in the Carson domain. Note that it is necessary to declare the variable s as symbolic.*
  - ii. *Divide them by s to go back to the Laplace domain.*
  - iii. *Back transform to the time domain using the function* `invlapFEAcomp`*, which is derived from [51].*
  - iv. *Finally, fit the numerical values of $E_2(t)$ with a viscoelastic model equation. Usually it is convenient to use the same model equation for the composite relaxation as that used for the matrix relaxation; in this case the Maxwell model. This step is implemented in* `fitfunFEAcomp.m`

The MATLAB codes `PMMViscoMatrix.m`*,* `invlapFEAcomp.m`*, and* `fitfunFEAcomp.m` *are available in [5]. The results are shown in Figure 7.4. The complete set of Maxwell parameters for the composite are calculated in Example 7.5.*

7.7 Macromechanics of Viscoelastic Composites

7.7.1 Balanced Symmetric Laminates

The in-plane viscoelastic behavior of a balanced symmetric laminate can be obtained using the procedure in Section 1.15 (Apparent Laminate Properties), but in the Carson domain. Start with the stiffness of the laminas (7.76) in lamina coordinates, in the Carson domain. Rotate each matrix to laminate coordinates. Then, average them using (1.102). Using (1.105), find the laminate engineering properties in the Carson domain and divide by s to go back to the Laplace domain. Finally, take the inverse Laplace transform to find the laminate stiffness in the time domain. Then, fit them with a model equation as is done in Example 7.4.

7.7.2 General Laminates

Thanks to the correspondence principle, the stress-resultant vs. strain-curvature equations from classical lamination theory (CLT, see Chapter 3) are valid for linearly

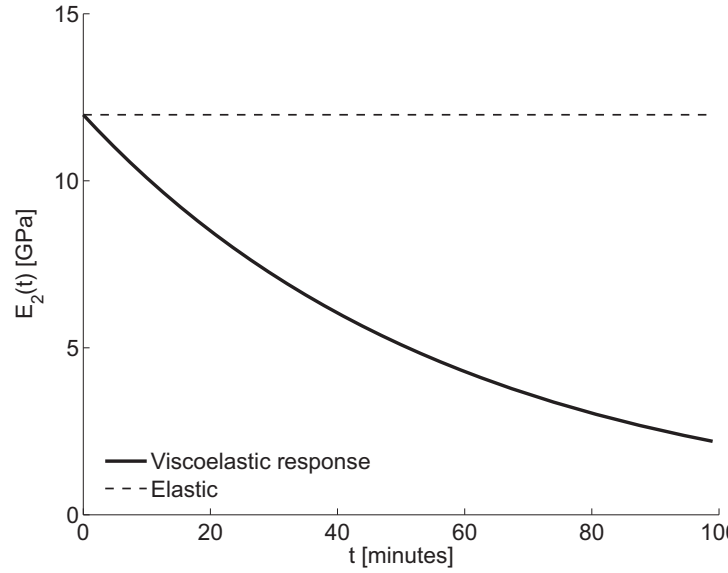

Figure 7.4: Elastic and viscoelastic values of the transverse modulus E_2.

Table 7.3: Lamina viscoelastic properties for Example 7.5

Young's Moduli	**Shear Moduli**	**Poisson's Ratio**
$(E_1)_0 = 102417$ MPa	$(G_{12})_0 = (G_{13})_0 = 5553.8$ MPa	$\nu_{12} = \nu_{13} = 0.4010$
$\tau_1 = 16551$ min	$\tau_{12} = \tau_{13} = 44.379$ min	
$(E_2)_0 = (E_3)_0 = 11975$ MPa	$(G_{23})_0 = 5037.3$ MPa	$\nu_{23} = 0.1886$
$\tau_2 = \tau_3 = 58.424$ min	$\tau_{23} = 54.445$ min	

viscoelastic laminated composites in the Carson domain. The A, B, D, H matrices of a laminate in the Carson domain can be computed by using the equations from first-order shear deformation theory (FSDT, Section 3.1.1). This methodology was used in [55].

7.8 FEA of Viscoelastic Composites

Most commercial codes have implemented viscoelasticity (creep) for isotropic materials. This is a severe limitation for users interested in the analysis of viscoelastic behavior of polymer matrix composites.

However, it is possible to take advantage of the user programmable features of commercial software in order to implement the formulations presented in this chapter. This is relatively easy because the approach used in this chapter is not stress dependent, but a linear viscoelastic approach, and its implementation is not complicated. A USERMAT subroutine is used in Example 7.5 to implement the viscoelastic formulation.

Example 7.5 *Compute the relaxation response of a* $[0/90_8]_s$ *laminate. The thickness of each lamina is* $t_k = 1.25$ *mm. The laminate width is* $2b = 20$ *mm and its length is*

$2L = 40$ *mm. Load the sample with a uniform strain* $\epsilon_x = 0.1$ *by applying a uniform displacement at* $x = L$. *Use solid elements on each lamina and symmetry conditions. Plot the laminate stiffness* $E_x(t)$ *for* $0 > t > 150$ *minutes. Use the lamina material properties given in Table 7.3, which were computed with the procedure used in Example 7.4.*

Solution to Example 7.5 *First, compute the viscoelastic engineering properties using the procedure described in Example 7.4. The resulting Maxwell parameters of the lamina are shown in Table 7.3.*

In ANSYS®, using an USERMAT subroutine for solid elements, it is possible to implement the constitutive equation of an orthotropic material with the following time-dependent properties:

$$E_1(t) = (E_1)_0 \exp(-t/\tau_1) \; ; \; E_2(t) = E_3(t) = (E_2)_0 \exp(-t/\tau_2)$$

$$G_{12}(t) = G_{13}(t) = (G_{12})_0 \exp(-t/\tau_{12}) \; ; \; G_{23}(t) = (G_{23})_0 \exp(-t/\tau_{23})$$

Such subroutine is available in [5, usermat3d_705.f90]. Next, the geometry can be modeled using a command file similar to that used in Example 5.2.

```
! FEAcomp. Solution of Example 7.5. USERMAT3D
/TITLE,Viscoelastic Analysis [0/90_8]s laminate
/PREP7                  ! Pre-processor module
*set,ThZ,1.25           ! Thickness of lamina in mm
*set,n90,8              ! 1/2 number 90 layers half laminate
*set,LX,25              ! 1/2 Length of laminate in mm
*set,bY,20.0            ! 1/2 width of laminate in mm
*set,neX,n90*2          ! Number of elements in x/z direction
*set,neY,10             ! Number of elements in y direction
*set,epsX,0.01          ! Uniform strain in x direction

! Equivalent Material properties

TB,USER,1,1,12, ! Material properties #1, Maxwell Model, 10 variables
TBTEMP,0
!    Variable descriptions fot the USERMAT sobroutine
!    ------------------------------------------------
!        E1     E2     nu12    nu23    G12     G23
!        Tau1   Tau2   Tau12   Tau13
TBDATA,,102417,11974.8,0.40096,0.18864,5553.8,5037.3
TBDATA,,16550.7243,58.4242,44.3791,54.4447

TB,STAT,1,,2,           ! NUMBER OF STAT VARIABLES

ET,1,SOLID186           ! Chooses SOLID186 element for analysis

! Define material orientation by local Coordinate
local,11,,0,0,0,90      ! defines 90 degree local cs
local,12,,0,0,0,0       ! defines 0 degree local cs
CSYS,0                  ! set active cs to cart. system

! Generate Geometry
BLOCK,0,LX,0,bY,0,n90*ThZ           ! 90 degrees layer
```

```
BLOCK,0,LX,0,bY,n90*ThZ,(n90+1)*ThZ ! 0 degress layer
VGLUE,ALL                           ! Glue volumes

! Mesh Control and Mesh
lesize,all,,,neX            ! line number divisions = neX
lsel,s,loc,y,0              ! selects lines y=0
lsel,a,loc,y,bY             ! add lines y=bY
lsel,r,loc,z,n90*ThZ,(n90+1)*ThZ    ! reselect lines volume 2
lsel,r,loc,x,LX                     ! reselects lines x=LX
lesize,all,,,neX/n90,,1,,,1         ! line number divisions = neX/n90
lsel,s,loc,y,0              ! selects lines y=0
lsel,a,loc,y,bY             ! add lines y=bY
lsel,r,loc,z,n90*ThZ,(n90+1)*ThZ    ! reselect lines volume 2
lsel,r,loc,x,0              ! reselects lines x=0
lesize,all,,,neX/n90,,1,,,1         ! line number divisions = neX/n90
lsel,s,loc,z,0              ! selects lines z=0
lsel,a,loc,z,n90*ThZ        ! add lines z=Thz to selection
lsel,a,loc,z,(n90+1)*ThZ    ! add lines z=2Thz to selection
lsel,r,loc,x,0              ! reselects lines x=0
LESIZE,ALL,,,neY,8,1,,,1    ! define element size in selected lines
lsel,s,loc,z,0              ! selects lines z=0
lsel,a,loc,z,n90*ThZ        ! add lines z=Thz to selection
lsel,a,loc,z,(n90+1)*ThZ    ! add lines z=2Thz to selection
lsel,r,loc,x,LX             ! reselects lines x=LX
LESIZE,ALL,,,NEy,(1/8),1,,,1    ! define ele. size in selected lines
lsel,all                    ! select all lines
MSHKEY,1                    ! Specifies mapped meshing
ESYS,11                     ! Selects 90 degrees material orientation
VMESH,1                     ! Meshes 90 degrees layer
ESYS,12                     ! Selects 0 degrees material orientation
VMESH,3                     ! Meshes 0 degree layer
FINISH                      ! Exit pre-processor module

/SOLU                   ! Solution module,
ANTYPE,STATIC           ! Set static analysis
OUTRES,ALL,1            ! STORE RESULTS FOR EVERY SUBSTEP
OUTRES,SVAR,1           ! STORE STATE VARIABLES

KBC,1           ! Specifies stepped loading within a load step
NSUBST,1        ! 1 = Number of substeps in this load step
TIME,1e-6       ! Define time near to zero

ASEL,S,LOC,X,0
ASEL,A,LOC,Y,0
ASEL,A,LOC,Z,0
DA,ALL,SYMM             ! Impose Symmetry BC
ASEL,S,LOC,X,LX
DA,ALL,UX,(epsX*LX)    ! Impose displacement on the end = epsX*LX
!SFA,ALL,,PRESS,-100     ! or could impose a load
NSLA,s,1
CP,1,UX,all
```

```
ALLSEL,ALL              ! Selects all areas
SOLVE                   ! Solve current load state

NSUBST,10,25,10         ! 10 = Number of substeps in this load step
TIME,300                ! Time at the end of load step
SOLVE                   ! Solve current load state
FINISH                  ! Exit solution module

/POST26                 ! Post-processor module
NUMVAR,200
ESOL,2,2721,12588,s,x,s0layer
ESOL,3,1,2,s,y,s90layer
NSOL,4,54,u,x,displacement

PLVAR,2,3
lines,1000
PRVAR,2,3,4
FINISH                  ! Exit post-processor module
```

The results are shown in Figures 7.5 and 7.6. The following APDL generates results to plot stress components along a user defined path.

```
/POST1                  ! Post-processor module
RSYS,0                  ! Set results in global coordinates system
PATH,INTERFACE,2,,100   ! Define a path between two points, compute 100 values
PPATH,1,0,0,0,ThZ,0     ! 1st point of the path location
PPATH,2,0,0,bY,ThZ,0    ! 2nd point of the path location
PDEF,zero,EPSW,,AVG     ! Compute zero axis (optional)
PLPATH,Sz,Sxz,Syz,zero  ! Plot Sz,Sxz,Syz
/page,1000,,1000        ! Define print list without skips between pages
PRPATH,Sz,Sxz,Syz       ! Print Sz,Sxz,Syz
FINISH                  ! Exit post-processor module

/POST1                  ! Post-processor module
RSYS,0                  ! Set results in global coordinates system
PATH,INTERFACE,2,,100   ! Define a path between two points, compute 100 values
PPATH,1,0,LX/2,0,ThZ,0  ! 1st point of the path location
PPATH,2,0,LX/2,bY,ThZ,0 ! 2nd point of the path location
PDEF,Sz ,S,Z,AVG        ! Compute Sz
PDEF,Syz,S,YZ,AVG       ! Compute Syz
PDEF,zero,EPSW,,!AVG    ! Compute zero axis (optional)
PLPATH,Sz,Syz,zero      ! Plot Sz,Syz
/page,1000,,1000        ! Define print list without skips between pages
PRPATH,Sz,Syz           ! Print Sz,Syz
FINISH                  ! Exit post-processor module
```

Example 7.6 *Consider a composite made with 40% by volume of isotropic graphite fibers with properties* $E_f = 168.4\ GPa$, $\nu_f = 0.443$ *and epoxy matrix represented by a Maxwell model with* $E_0 = 4.082\ GPa$, $\tau = 39.15\ min$ *and* $\nu_m = 0.311$ *(independent of time). Construct a finite element micromechanical model using a hexagonal microstructure (see Example 6.3), subject to shear strain* $\gamma_4 = 0.02$ *applied suddenly at* $t = 0$. *Tabulate the*

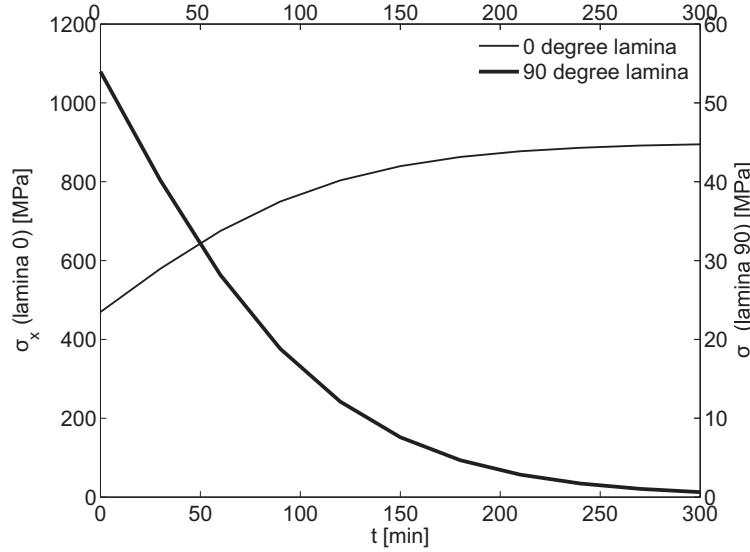

Figure 7.5: Time stress evolution in 0°-lamina, and 90°-lamina.

average stress σ_4 *over the representative volume element (RVE) at times* $t = 0, 20, 40, 60, 80,$ *and* 100 *minutes.*

Solution to Example 7.6 *The fiber can be represented using standard elastic properties in ANSYS. The matrix should be modeled using the USERMAT provided in Example 7.5 (`usermat3d_705.f90`). Therefore, the only part of the ANSYS model definition that changes with respect to Example 6.3 is the definition of the material, as follows*

```
MP,EX,1,168.4e-3    ! Fiber material properties in Tera Pascals [TPa]
MP,PRXY,1,0.443

TB,USER,2,1,12,     ! Material properties #2, Maxwell Model, 10 variables
TBTEMP,0            ! Matrix material properties in Tera Pascals [TPa]
!    Variable descriptions for the USERMAT subroutine
!    ------------------------------------------------
!        E1     E2     nu12    nu23    G12     G23
!        Tau1   Tau2   Tau12   Tau13
TBDATA,,4.082e-3,4.082e-3,0.311,0.311,1.556e-3,1.556e-3
TBDATA,,39.15,39.15,39.15,39.15
```

The APDL macro `ceRVE.mac` *available in [5] is used to define the constraint equations (CE) for the periodic model. The macro needs the RVE dimensions and the applied strain as input arguments. In this example, only a strain* $\gamma_4 = 0.04$ *is applied. The model is solved, using different substeps at times* $t = 0, 20, 40, 60, 80,$ *and* 100 *minutes.*

```
/SOLU           ! Solution module,
ANTYPE,STATIC   ! Set static analysis
OUTRES,ALL,1    ! STORE RESULTS FOR EVERY SUBSTEP
OUTRES,SVAR,1   ! STORE STATE VARIABLES
```

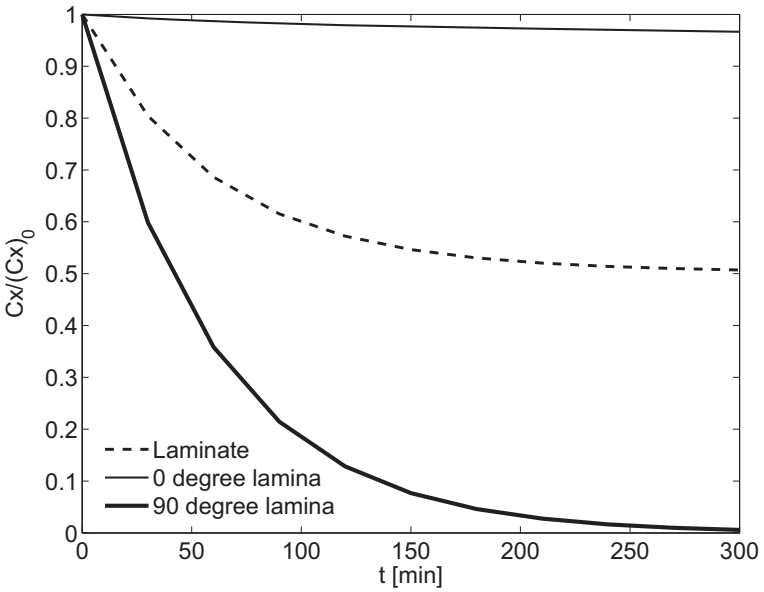

Figure 7.6: Normalized stiffness $C_{22}(t)/(C_{22})_o$ for global laminate, 0°-lamina, and 90°-lamina.

```
KBC,1            ! Specifies stepped loading within a load step
NSUBST,1         ! 1 = Number of substeps in this load step
TIME,1e-6        ! Define time near to zero
! ceRVe arguments:
! a1,a2,a3,eps1,eps2,eps3,eps4,eps5,eps6
*use,ceRVE,a1,a2,a3,0,0,0,20e-3,0,0
SOLVE            ! Solve analysis
NSUBST,5,10,5    ! 10 = Number of substeps in this load step
TIME,100         ! Time at the end of load step
SOLVE            ! Solve current load state
FINISH           ! Exit solution module
```

To compute the average stress in the RVE, it is possible to use the macro ***srecover****, described in Example 6.2. The average stress obtained is shown in Table 7.4. The* ***SET,LIST*** *command lists all the load steps and substeps, each of which can be selected inside POST1 with the command* ***SET,#loadstep,#substep****.*

```
/POST1               ! Post-processor module
/DEVICE,VECTOR,0
/PNUM,MAT,0
SET,1,1
*use,srecover
!S_1 = Szz0
!S_2 = Sxx0
!S_3 = Syy0
S_4 = Sxy0           !Average stress t = 0
!S_5 = Syz0
!S_6 = Sxz0
```

```
SET,2,1
*use,srecover
S_4 = Sxy0          !Average stress t = 20
SET,2,2
*use,srecover
S_4 = Sxy0          !Average stress t = 40
SET,2,3
*use,srecover
S_4 = Sxy0          !Average stress t = 60
SET,2,4
*use,srecover
S_4 = Sxy0          !Average stress t = 80
SET,2,5
*use,srecover
S_4 = Sxy0          !Average stress t = 100
VSEL,s,,,9
ESLV,S
plesol,s,x,1
plesol,s,xy,1
FINISH              !Exit post-processor module
```

Table 7.4: Average stress σ_4 along time

Time [min]	0	20	40	60	80	100
Average σ_4 [MPa]	62.6	38.1	23.1	13.9	8.4	5.04

Using an exponential regression it is possible to calculate the values of $(G_0)_{23} = 3.13$ *GPa and* $\tau = 39.97$ *min that represent the relaxation of the composite in the 23-shear direction using a Maxwell model (see Figure 7.7).*

Suggested Problems

Problem 7.1 *Consider a composite made with* 60% *by volume of isotropic fibers with properties* $E_f = 168.4$ *GPa and* $\nu_f = 0.443$*, and epoxy matrix represented by a power law model (7.24) with* $D_0 = 0.222$ GPa^{-1}*,* $D_1 = 0.0135$ $(GPa\ min)^{-1}$*,* $m = 0.17$ *and* $\nu_m = 0.311$*. Plot the relaxation* $C_{22}(t)$ *of the composite as a function of time for* $0 < t < 100$ *minutes. Compare it to the elastic value of the stiffness* C_{22} *of the composite and the elastic stiffness* C_{22} *of the matrix.*

Problem 7.2 *Consider a composite made with 60% by volume of transversely isotropic graphite fibers with properties* $E_A = 168.4$ *GPa,* $E_T = 24.82$ *GPa,* $\nu_A = 0.443$*,* $\nu_T = 0.005$*,* $G_A = 44.13$ *GPa and epoxy matrix represented by a Maxwell model (7.15) with* $E_0 = 4.082$ *GPa,* $\tau = 39.15$ *min and* $\nu_m = 0.311$*. Plot the relaxation tensor stiffness components* $C(t)$ *of the composite as a function of time for* $0 < t < 100$ *minutes, compared to the elastic stiffness* C *of the composite and the elastic stiffness* C_m *of the matrix.*

Problem 7.3 *Compute the parameters in the Maxwell model for unidirectional lamina (see Section 1.14) of carbon/epoxy material used in Problem 7.2. Plot and compare the elastic and viscoelastic properties:* $E_1(t)$*,* $E_2(t)$ *and* $G_{12}(t)$*. Show all work in a report.*

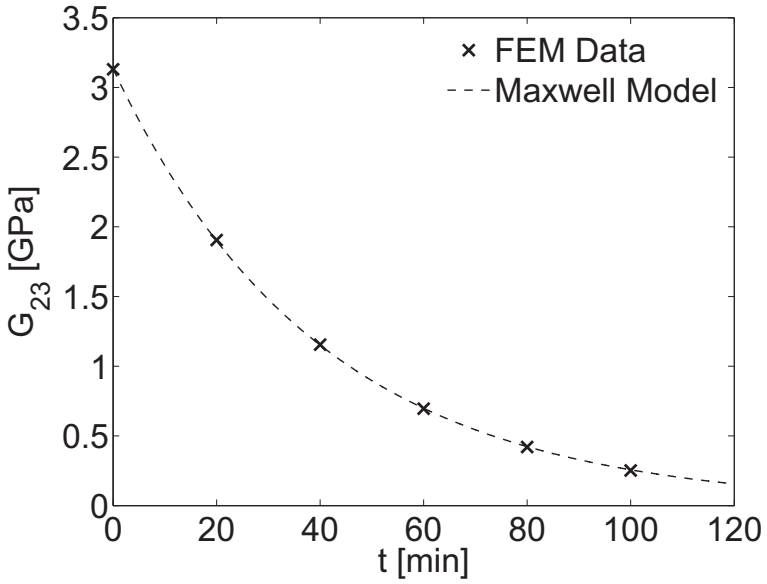

Figure 7.7: Average $(G_0)_{23}$ vs. time.

Problem 7.4 *Use the user programmable features to implement the Maxwell model constitutive equations for a transversally orthotropic lamina material under plane stress conditions. Using the viscoelastic materials properties obtained in Problem 7.3, compute the response of a* $[\pm 45/90_2]_s$ *laminate. The thickness of each lamina is* $t_k = 1.25$ *mm. Load the sample with uniform edge loads in the middle laminate surface* $N_x = N_y = 10$ *N/mm. Plot the laminate and the laminas relaxations, as well as the laminas stress* σ_x *as a function of time for* $0 > t > 300$ *minutes.*

Problem 7.5 *Compute the parameters in the Maxwell model for all the nine engineering properties of a* $[0/90]_S$ *laminate. Each lamina is* 1.25 *mm thick. The material is carbon T300 and Epoxy 934(NR) with* $V_f = 0.62$ *and lamina thickness 1.25 mm. Epoxy is represented by a Maxwell model (7.15) with* $E_0 = 4.082$ *GPa,* $\tau = 39.15$ *min and* $\nu_m = 0.311$*. Carbon T300 is transversely isotropic with axial modulus* $E_A = 202.8$ *GPa, transverse modulus* $E_T = 25.3$ *GPa,* $G_A = 44.1$ *GPa,* $\nu_A = 0.443$*, and* $\nu_T = 0.005$*, where the subscripts A and T indicate the axial and radial (transverse) directions of the fiber, respectively.*

Chapter 8

Continuum Damage Mechanics

Many modes of damage can be observed in composite materials, including matrix cracks, fiber breakage, fiber-matrix debonding, and so on. Much work has been done trying to quantify each of these damage modes, their evolution with respect to load, strain, time, number of cycles, etc., and their effect on stiffness, remaining life, etc. *Continuum Damage Mechanics* (CDM) represents all these failure modes by the effect they have on the mesoscale behavior (lamina level) of the material. That is, CDM calculates the degraded moduli of the laminas and laminate in terms of continuum damage variables. Then, either strength or fracture mechanics failure criteria are used to detect damage initiation. Finally, damage evolution is predicted in terms of empirical hardening/softening equations set up in terms of additional parameters, such as the hardening exponent used for metal plasticity. For example, a form of CDM is used in Chapter 10 to represent the degradation of the interface between laminas.

Hardening equations require non-standard experimentation to adjust the additional, empirical parameters. Since the parameters are adjusted to the model, some shortcomings of the model may be masked by the fitting of the additional parameters. From a thermodynamics point of view, damage variables are the state variables of the formulation, and they are not measurable. This is in contrast to the micromechanics of damage models (Chapter 9) and metal plasticity where the state variables, i.e., crack density and plastic strain, are measurable. From a practical point of view, CDM major shortcoming is the need for additional experimentation to determine parameters that are particular to each model. Furthermore, since the state variables are not measurable, the additional parameters need to be adjusted to the model through the loss of stiffness, which may not be sufficiently sensitive to damage [56].

One notable effect of damage is a reduction of stiffness, which can be used to define damage [57]. One-dimensional models are used in Section 8.1 to introduce the concepts. The theoretical formulation for the general three-dimensional case is developed in Sections 8.2–8.4.

8.1 One-Dimensional Damage Mechanics

The development of a one-dimensional damage mechanics solution involves the definition of three major entities: (1) a suitable damage variable, (2) an appropriate damage activation function, and (3) a convenient damage evolution, or kinetic equation.

8.1.1 Damage Variable

Consider a composite rod of nominal area $\widetilde{A}$, unloaded, and free of any damage (Figure 8.1.a). Upon application of a sufficiently large load P, damage appears (Figure 8.1.b). On a macroscopic level, damage can be detected by the loss of stiffness of the material. In CDM, damage is represented by a state variable, also called *damage variable* D, which represents the loss of stiffness [57]

$$D = 1 - E/\widetilde{E} \tag{8.1}$$

where $\widetilde{E}$ is the initial (virgin) Young's modulus, and E is the modulus after damage.[1] Earlier work [58] conceptualized damage as the reduction of area due to accumulation of microcracks having the same effect as the actual damage

$$D = 1 - A/\widetilde{A} \tag{8.2}$$

where $\widetilde{A}$, A, are the initial and remaining cross-sectional areas, respectively. The complement to damage is the integrity [59]

$$\Omega = 1 - D = A/\widetilde{A} \tag{8.3}$$

which can be interpreted as the remaining cross-sectional area ratio, using the original area as basis. It is noted that, in principle, damage is a measurable parameter, which could be determined by measuring the damaged area, remaining area, or more practically measuring the initial and remaining moduli. Therefore, in thermodynamic terms, damage is a measurable state variable, in the same sense as the temperature is a measurable state variable that quantifies in macroscopic terms the random agitation of atoms, molecules, and other elementary particles. While it is possible, but extremely difficult, to track the agitation of atoms and molecules, it is very easy to measure the temperature with a thermometer or other device. The same holds true for damage in composite materials.

The analysis of a structural component is done in terms of the nominal area $\widetilde{A}$, which is the only one known to the designer. The remaining area $A = (1-D)\widetilde{A}$ is not known *a priori*. The nominal stress is $\sigma = P/\widetilde{A}$. Neglecting stress concentrations at the tips of the fictitious cracks representing damage in the damaged configuration (Figure 8.1.b), the value of effective stress[2] acting on the remaining area A is $\widetilde{\sigma} = P/A > P/\widetilde{A}$.

[1] See also (8.10).

[2] Even taking into account the stress concentrations, the volume average of the distribution of *effective stress* in the representative volume element (RVE, see Chapter 6) is still $\widetilde{\sigma} = P/A$.

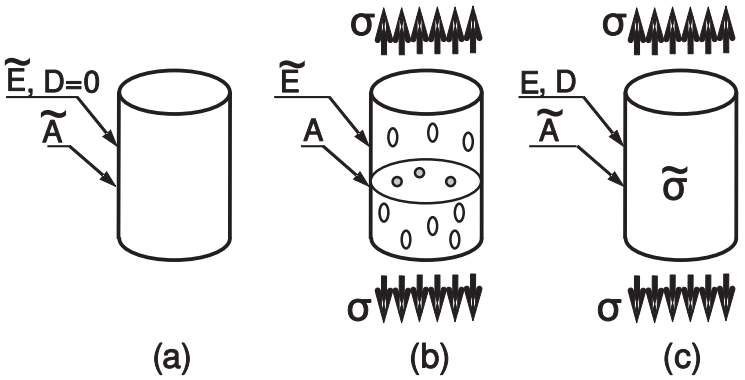

Figure 8.1: (a) Unstressed material configuration, (b) stressed material configuration with distributed damage, (c) effective configuration.

Therefore, we can envision a configuration (Figure 8.1.c) free of damage, with nominal area $\widetilde{A}$, loaded by nominal stress σ, but internally subjected to effective stress $\widetilde{\sigma}$ and degraded stiffness E. Thus, the effective configuration allows us to perform a structural analysis using the nominal geometry but effectively taking into account the increase of effective stress and the decrement of stiffness caused by damage.

In the undamaged configuration (a), $D = 0$, $\sigma = \widetilde{\sigma}$, $\varepsilon = \widetilde{\varepsilon}$, and Hooke's law is

$$\widetilde{\sigma} = \widetilde{E}\widetilde{\varepsilon} \tag{8.4}$$

In the effective configuration (c)

$$\sigma = E(D)\varepsilon \tag{8.5}$$

The *principle of strain equivalence* assumes that the strain is the same in the configurations (b) and (c), or $\varepsilon = \widetilde{\varepsilon}$. Starting with the nominal stress $\sigma = P/\widetilde{A}$, multiplying by A/A and using (8.3), the relationship between effective stress $\widetilde{\sigma}$ and nominal stress σ (under strain equivalence) is

$$\sigma = \widetilde{\sigma}\,(1 - D) \tag{8.6}$$

Using (8.6), (8.4) and $\varepsilon = \widetilde{\varepsilon}$ in (8.5), the apparent modulus is a function of the damage D given by

$$E(D) = \widetilde{E}(1 - D) \tag{8.7}$$

The *principle of energy equivalence* [60] states that the elastic strain energy is identical in the configurations (b) and (c). That is, $\sigma : \varepsilon = \widetilde{\sigma} : \widetilde{\varepsilon}$, which is satisfied by

$$\begin{aligned} \sigma &= \widetilde{\sigma}(1 - D) \\ \widetilde{\varepsilon} &= \varepsilon(1 - D) \end{aligned} \tag{8.8}$$

Substituting (8.8) in (8.5) yields

$$E(D) = \widetilde{E}(1-D)^2 \tag{8.9}$$

which redefines the damage variable as

$$D = 1 - \sqrt{E/\widetilde{E}} \tag{8.10}$$

Every state variable has a conjugate thermodynamic force driving its growth. In plasticity, the measurable state variable is the plastic strain tensor ε^p, which is driven to grow by its conjugate thermodynamic force, the stress tensor σ. The thermodynamic damage force Y is defined as conjugate to the state variable D.

A kinetic equation $\dot{D}(Y)$ governs the growth of the state variable D as a function of its conjugate thermodynamic force Y. In principle, any relevant variable can be chosen as independent variable Y to define the kinetic equation $\dot{D}(Y)$, as long as it is independent of its conjugate state variable. When the damage D is a scalar and it is used to analyze one-dimensional problems, various authors have chosen independent variables in the form of strain ε [61], effective stress $\widetilde{\sigma}$ [62, 63], excess energy release rate $G - 2\gamma_c$ [64], and so on. However, the choice is better based on the appropriate form of the thermodynamic principle governing the problem, as it is shown in Section 8.3.

8.1.2 Damage Threshold and Activation Function

The elastic domain is defined by a threshold value for the thermodynamic force; no damage occurs below the threshold. When the load state is in the elastic domain, damage does not grow. When the load state reaches the limit of the elastic domain, additional damage occurs. Furthermore, the elastic domain modifies its size or hardens. Typical one-dimensional responses of two materials are shown in Figure 8.2. Initially the elastic domain is defined by the initial threshold values, $\sigma \leq \sigma_0$ and $\varepsilon \leq \varepsilon_0$. While the load state is inside this domain, no damage occurs. When the load state is higher than the threshold, damage increases and the threshold changes. The elastic domain may evolve as hardening or softening. A stress threshold increases for materials with hardening (see Figure 8.2a), and it decreases for materials with softening (see Figure 8.2b). On the other hand, a strain or effective stress threshold always increases for hardening and softening behavior, as shown in Figure 8.2.

The elastic domain can be defined by the *damage activation function* g as

$$g = \hat{g} - \hat{\gamma} \leq 0 \tag{8.11}$$

where $\hat{g}$ is a positive function (norm) that depends on the independent variable (in a one-dimensional case a scalar Y) and $\hat{\gamma}$ is the updated damage threshold for isotropic hardening. According to the positive dissipation principle (see Section 8.3 and (8.82),(8.97)), the updated damage threshold $\hat{\gamma}$ can be written as

$$\hat{\gamma} = \gamma(\delta) + \gamma_0 \tag{8.12}$$

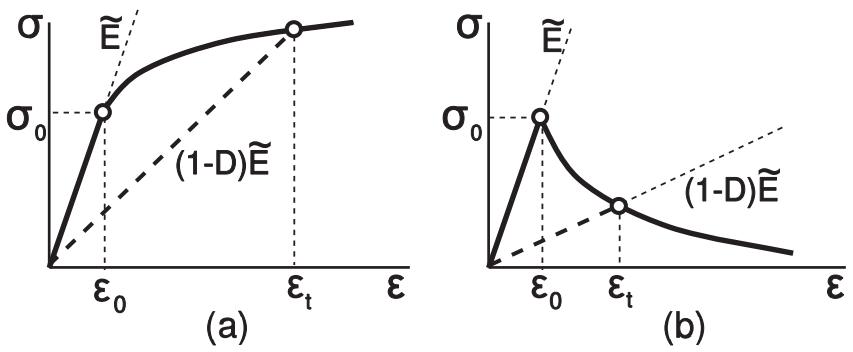

Figure 8.2: (a) Hardening behavior and (b) softening behavior. No damage occurs until the strain reaches a threshold value ε_0, and no damage occurs during unloading.

where γ_0 denotes the virgin damage threshold, and γ is a positive monotonic function, called the *hardening (or softening) function*, that depends on the internal variable δ, called the *damage hardening variable*.

8.1.3 Kinetic Equation

The rate of damage accumulation is represented by a kinetic equation. The evolution of damage and hardening are defined by

$$\dot{D} = \dot{\lambda}\frac{\partial g}{\partial Y} \quad ; \qquad \dot{\delta} = \dot{\lambda}\frac{\partial g}{\partial \gamma} \tag{8.13}$$

where Y is the independent variable and $\dot{\lambda} \geq 0$ is the damage multiplier that enforces consistency among the damage and hardening evolution as defined by (8.13). Furthermore, the values of $\dot{\lambda}$ and g allow us to distinguish among two possible situations, loading or unloading without damage growth, and loading with damage growth, according to the Kuhn-Tucker conditions [65]

$$\dot{\lambda} \geq 0 \quad ; \quad g \leq 0 \quad ; \quad \dot{\lambda} g = 0 \tag{8.14}$$

In other words, the Kuhn-Tucker conditions allow us to differentiate among two different cases:

i. Undamaging loading or unloading, in the elastic domain. The damage activation function is $g < 0$ and by condition (8.14.c) $\dot{\lambda} = 0$, and by (8.13.a) $\dot{D} = 0$.

ii. Damage loading. In this case $\dot{\lambda} > 0$ and condition (8.14.c) implies that $g = 0$. Then, the value of $\dot{\lambda}$ can be determined by the damage consistency condition

$$g = 0 \quad \text{and} \quad \dot{g} = 0 \tag{8.15}$$

Example 8.1 *Compute $\dot{\lambda}$ for a one-dimensional model under tensile load where the independent variable is the effective stress $Y = \widetilde{\sigma}$, the activation function is defined by $\hat{g} = \widetilde{\sigma}$, and the hardening function is defined by*

$$\hat{\gamma} = (F_0 - F_R)\delta + F_0$$

where F_0 and F_R are the initial threshold and the strength of the strongest microscopic element in the material, respectively.

Solution to Example 8.1 *The damage activation function g is defined as*

$$g = \hat{g} - \hat{\gamma} = \widetilde{\sigma} - [(F_0 - F_R)\delta + F_0] \leq 0$$

Therefore,

$$\frac{\partial g}{\partial \widetilde{\sigma}} = +1 \quad ; \qquad \frac{\partial g}{\partial \hat{\gamma}} = -1$$

Using (8.13), the kinetic equations can be written as

$$\dot{D} = \dot{\lambda}\frac{\partial g}{\partial \widetilde{\sigma}} = \dot{\lambda} \quad ; \qquad \dot{\delta} = \dot{\lambda}\frac{\partial g}{\partial \hat{\gamma}} = -\dot{\lambda}$$

When new damage appears, the consistency conditions (8.15) yield

$$g = 0 \quad \Rightarrow \quad \hat{\gamma} = \widetilde{\sigma}$$

and

$$\dot{g} = 0 \quad \Rightarrow \quad \dot{g} = \frac{\partial g}{\partial \widetilde{\sigma}}\dot{\widetilde{\sigma}} + \frac{\partial g}{\partial \hat{\gamma}}\dot{\hat{\gamma}} = \dot{\widetilde{\sigma}} - \dot{\hat{\gamma}} = 0$$

where

$$\dot{\hat{\gamma}} = \frac{\partial \hat{\gamma}}{\partial \delta}\dot{\delta} = (F_0 - F_R)(-\dot{\lambda}) = (F_R - F_0)\dot{\lambda}$$

Substituting into the second consistency condition (8.15) we obtain $\dot{\lambda}$ as

$$\dot{\lambda} = \frac{1}{F_R - F_0}\dot{\widetilde{\sigma}}$$

8.1.4 Statistical Interpretation of the Kinetic Equation

Let's assume that individual damaging events are caused by the failure of microscopic elements inside the material (e.g., fiber breaks, matrix cracks, fiber-matrix debond, etc.). Furthermore, assume each of these material points has a failure strength $\widetilde{\sigma}$ and that the collection of failure strengths for all these points, i.e., elements failing at a certain stress $\widetilde{\sigma}$ over the total number of elements available, is represented by a probability density $f(\widetilde{\sigma})$ (Figure 8.3.b). The fraction of elements broken during an effective stress excursion from zero to $\widetilde{\sigma}$ provides a measure of damage

$$D(\widetilde{\sigma}) = \int_0^{\widetilde{\sigma}} f(\sigma')d\sigma' = F(\widetilde{\sigma}) \tag{8.16}$$

where $F(\widetilde{\sigma})$ is the cumulative probability (Figure 8.3.b) corresponding to the probability density $f(\widetilde{\sigma})$, and σ' is a dummy integration variable. Then, the kinetic equation in terms of effective stress $\widetilde{\sigma}$ is

$$\dot{D} = \frac{dD}{d\widetilde{\sigma}}\dot{\widetilde{\sigma}} = f(\widetilde{\sigma})\dot{\widetilde{\sigma}} \tag{8.17}$$

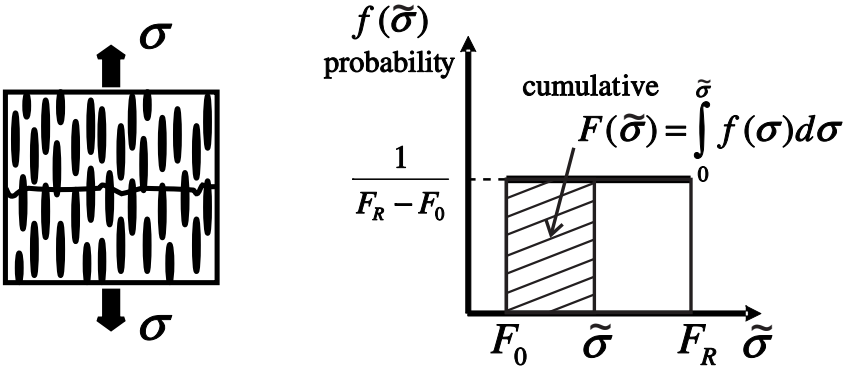

Figure 8.3: One-dimensional random-strength model.

8.1.5 One-Dimensional Random-Strength Model

As explained in Section 8.1.3, the rate of damage accumulation is represented by a kinetic equation. Equation (8.17) represents a generic kinetic equation, which becomes specific once a particular probability density of failure is adopted.

Consider a loose bundle of short fibers embedded in a matrix and subjected to a uniform stress. The fiber-matrix interfacial strength is assumed to be identical for all fibers but the embedment length is random. The fiber pull-out strength is therefore random. Random means that the probability of finding a fiber pulling out at any value of stress $F_0 < \widetilde{\sigma} < F_R$ is constant. In other words, there is no stress level at which more fibers or less fibers pull out because the probability of pull out is random. This is represented in Figure 8.3 and given by the equation $f(\widetilde{\sigma}) = 1/(F_R - F_0)$. Substituting $\widetilde{\varepsilon}$ for $\widetilde{\sigma}$ as the independent variable in (8.17), and assuming strain equivalence $\varepsilon = \widetilde{\varepsilon}$, we have

$$f(\widetilde{\varepsilon}) = \frac{\widetilde{E}}{F_R - F_0} \qquad ; \quad F_0 \leq \widetilde{\sigma} \leq F_R \tag{8.18}$$

Equation (8.18) yields the model proposed in [61], which represents well the damaging behavior of Haversian bone [66], concrete in tension [67], fiber composites when damage is controlled by fiber pull out [68], and transverse damage of unidirectional composites.

Damage Activation Function

For a one-dimensional problem, choosing strain as the independent variable, it is possible to write $\hat{g} = \varepsilon$. Therefore, the damage activation function can be written as

$$g = \varepsilon - \hat{\gamma} \leq 0 \tag{8.19}$$

where $\hat{\gamma}$ is the updated damage threshold. Assuming that no damage occurs until the strain reaches a threshold value $\varepsilon_0 = F_0/\widetilde{E}$, and applying the consistency

conditions (8.15) and using (8.19), the updated damage threshold $\hat{\gamma}$ is given by the highest value of strain seen by the material, or

$$\hat{\gamma} = \max(\varepsilon_0, \varepsilon) \tag{8.20}$$

Kinetic Equation

The kinetic equation (8.17) for the case of random strength (8.18) in terms of strains $\widetilde{\varepsilon} = \varepsilon$ can be expressed as

$$\dot{D} = \frac{dD}{d\varepsilon}\dot{\varepsilon} = \begin{cases} \widetilde{E}/(F_R - F_0)\dot{\varepsilon} & \text{when } ;\ \varepsilon > \hat{\gamma} \\ 0 & \text{otherwise} \end{cases} \tag{8.21}$$

In this case, the independent variable is ε, and using (8.19), the kinetic equation (8.13) reduces to

$$\dot{D} = \dot{\lambda} \tag{8.22}$$

Using the Kuhn-Tucker conditions and (8.21), the consistency condition (8.15) reduces to

$$\dot{\lambda} = \widetilde{E}/(F_R - F_0)\dot{\varepsilon} \tag{8.23}$$

when damage occurs and $\dot{\lambda} = 0$ otherwise. In this particular case, the kinetic equation is known explicitly (8.22)–(8.23). Therefore, it is not necessary to evaluate the evolution of hardening (8.12) because hardening is computed explicitly by (8.20). Note that (8.23) is identical to the solution of Example 8.1 because the hardening function was chosen deliberately to yield this result.

Secant Constitutive Equation

In this particular case, the damage variable is active when tensile load appears, and it can be obtained by integrating (8.21) as

$$D_t = \widetilde{E}\ \frac{\hat{\gamma} - \varepsilon_0}{F_R - F_0} \quad \text{when } \varepsilon > 0 \tag{8.24}$$

Note that the damage state does not depend on the actual load state ε, it only depends on the history of the load state $\hat{\gamma}$. In this example, crack closure is assumed in compression, damage becomes passive, and $D_c = 0$. Mathematically, damage under unilateral contact conditions can be defined by the following equation

$$D = D_t \frac{\langle \varepsilon \rangle}{|\varepsilon|} + D_c \frac{\langle -\varepsilon \rangle}{|\varepsilon|} \tag{8.25}$$

where the McCauley operator $\langle x \rangle$ is defined as $\langle x \rangle := \frac{1}{2}(x + |x|)$.

Substituting (8.24) into (8.5), and using strain equivalence, yields the following constitutive equation

$$\sigma = E(D)\,\varepsilon = \begin{cases} \left(1 - \widetilde{E}\ \dfrac{\hat{\gamma} - \varepsilon_0}{F_R - F_0}\right) \widetilde{E}\,\varepsilon & \text{when } \varepsilon > 0 \\ \widetilde{E}\,\varepsilon & \text{when } \varepsilon < 0 \end{cases} \tag{8.26}$$

Tangent Constitutive Equation

In a finite element formulation, it is necessary to provide the constitutive equation in rate form, where the rates of stress $\dot{\sigma}$ and strain $\dot{\varepsilon}$ are expressed as functions of pseudo-time. In this particular case, the tangent constitutive equation can be obtained by differentiation of the secant constitutive equation as

$$\dot{\sigma} = E(D)\dot{\varepsilon} + \dot{E}(D)\varepsilon \tag{8.27}$$

The term $\dot{E}(D)$ is zero when new damage does not appear, i.e., when there is elastic loading or unloading. When damaging behavior occurs (8.20) yields $\hat{\gamma} = \varepsilon$, and differentiating $E(D)$ in (8.26) we obtain

$$\dot{E}(D) = -\frac{\widetilde{E}^2}{F_R - F_0}\dot{\varepsilon} \tag{8.28}$$

Substituting (8.28) into (8.27) if damage occurs, or $\dot{E}(D) = 0$ if no damage occurs, the tangent constitutive equation can be written as

$$\dot{\sigma} = \begin{cases} \left(1 - \widetilde{E}\,\dfrac{2\hat{\gamma} - \varepsilon_0}{F_R - F_0}\right)\widetilde{E}\,\dot{\varepsilon} & \text{when } \varepsilon > \hat{\gamma} \\ E(D)\,\dot{\varepsilon} & \text{when } \varepsilon < \hat{\gamma} \end{cases} \tag{8.29}$$

Model Identification

The initial damage threshold ε_0 represents the minimum strain to initiate damage and it is proportional to F_0 as follows

$$F_0 = \widetilde{E}\varepsilon_0 \tag{8.30}$$

Under load control, a tensile specimen breaks at $\varepsilon = \hat{\gamma} = \varepsilon_{cr}$ when $d\sigma/d\varepsilon = 0$. Then, using (8.29.a), the only unknown parameter in the model can be computed as

$$F_R = 2\widetilde{E}\varepsilon_{cr} \tag{8.31}$$

The material parameters F_0 and F_R can be calculated from the experimental data using (8.30) and (8.31) with $\widetilde{E}$ being the undamaged modulus of the material. The measurable values ε_0 and ε_{cr} can be obtained easily from material testing at the macroscopic level.

For the particular case $\varepsilon_0 = 0$, using (8.24) and (8.31) at $\varepsilon = \varepsilon_{cr}$, the critical damage at failure under tensile load is

$$D_{cr} = 0.5 \tag{8.32}$$

Therefore, the critical effective stress is

$$\widetilde{\sigma}_{T\,cr} = \widetilde{E}\varepsilon_{cr} = 0.5F_R \tag{8.33}$$

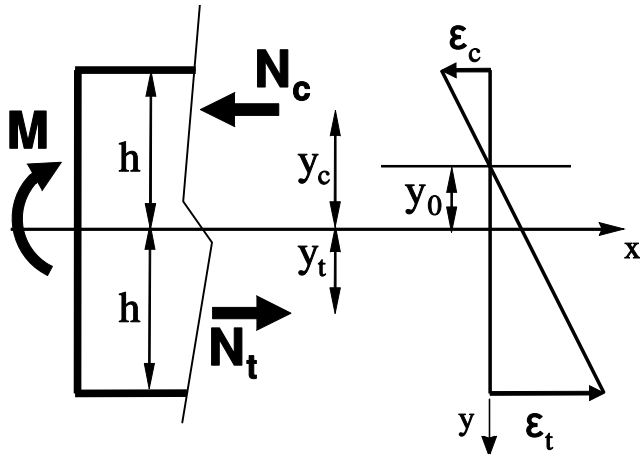

Figure 8.4: One-dimensional random-strength model for Example 8.2.[3]

and using (8.7) the critical applied stress is

$$\sigma_{T\,cr} = 0.25 F_R \tag{8.34}$$

Therefore, in a material with initial threshold $\varepsilon_0 = 0$, a tensile specimen under load control fails when $D = 1/2$ and applied stress $F_R/4$.

A conservative estimate of transverse tensile strength of a fiber-reinforced lamina can be obtained assuming that the fiber-matrix bond strength is negligible. In the limit, only the matrix between fibers carries the transverse load, with the fibers acting as holes. In this limit case, the matrix links can be assumed to have a random distribution of strength (8.18). Therefore, the random-strength model (8.29) applies, and the critical damage for transverse tensile loading of unidirectional fiber-reinforced lamina can be estimated by (8.32) as $D_{2t}^{cr} = 0.5$. At the present time, there is no model available to estimate the critical transverse-direction compression damage D_{2c}^{cr}.

Example 8.2 *A beam of rectangular cross-section, width $b = 100$ mm and height $2h = 200$ mm is subjected to pure bending. The bending moment at failure is $25.1\ MN\,mm$. The beam is made of carbon/epoxy composite with randomly oriented short fibers with undamaged Young's modulus $\widetilde{E} = 46\ GPa$. Find the bending moment at failure in terms of F_R in (8.21). Assume that the material does not damage in compression and it has a random distribution of strength in tension, with the strongest material element having unknown strength $F_R > 0$ and $F_0 = 0$. Determine F_R using the data given.*

Solution to Example 8.2 *This problem was solved in [68]. With reference to Figure 8.4, M is the applied bending moment, and y_c, y_t, are the distances from the neutral axis to the stress resultants N_c, N_t, on the tensile and compression portions of the beam.*

Denoting by ε_t and ε_c the tension and compression strain on the outer surfaces of the beam, y_0 the distance from the mid-plane to the neutral surface, and assuming linear strain

[3]Reprinted from *Mechanics of Materials*, vol. 8 (1998), D. Kracjcinovic, *Damage Mechanics*, Figure 2.11, p. 134, copyright (1998), with permission from Elsevier.

distribution through the thickness we have

$$\varepsilon(y) = \frac{y - y_0}{h - y_0}\varepsilon_t \quad or \quad \varepsilon(y) = \frac{-y + y_0}{h + y_0}\varepsilon_c$$

Since there is no damage in compression, the compression stress distribution is linear, and the resulting compression stress resultant is

$$N_c = \frac{1}{2}b(h + y_0)\widetilde{E}\varepsilon_c$$

and the distance y_c is

$$y_c = \frac{1}{3}(y_0 - 2h)$$

As the tensile side of the beam damages, the neutral axis moves away from the mid-surface. The tensile stress resultant is obtained using (8.26) and integrating the stress between y_0 and h as

$$N_t = \int_{y_0}^{h} dN_t = b\int_{y_0}^{h} E(D)\varepsilon(y)dy = \frac{1}{6}(h - y_0)b\left(3 - 2(\widetilde{E}/F_R)\varepsilon_t\right)\widetilde{E}\varepsilon_t$$

where $\widetilde{E}$ is the undamaged elastic moduli. The distance y_t is

$$y_t = \frac{1}{N_t}\int_{y_0}^{h} y dN_t = \frac{4h - 2y_0 - (\widetilde{E}/F_R)\varepsilon_t\,(3h + y_0)}{6 - 4(\widetilde{E}/F_R)\varepsilon_t}$$

The force and moment equations of equilibrium are

$$N_c + N_t = 0$$
$$N_c y_c + N_t y_t = M$$

Using the force equilibrium equation and assuming linear strain distribution through the thickness, it is possible to obtain the strains ε_t and ε_c in terms of y_0 as

$$\varepsilon_t = -\frac{6hy_0}{(h - y_0)^2}\frac{F_R}{\widetilde{E}} \quad ; \quad \varepsilon_c = \frac{6hy_0(h + y_0)}{(h - y_0)^3}\frac{F_R}{\widetilde{E}}$$

Using the above relation, it is possible to reduce the moment equilibrium equation to a single cubic equation in y_0

$$M = \frac{-y_0(4h^2 + 9hy_0 + 3y_0^2)}{(h - y_0)^3}\, bh^2 F_R$$

The ultimate bending moment can be determined by differentiation with respect to y_0

$$\frac{dM}{dy_0} = 0$$

that yields $y_{0\,cr} = -0.175\ h$ at beam failure. Therefore, the rupture bending moment is

$$M_{cr} = 0.2715\ bh^2\ F_R$$

A simple test (ASTM D790 or D6272) can be used to obtain the bending moment at failure; in this example $M_{cr} = 25.1\ 10^6 N\,mm$. Therefore, F_R can be estimated as $F_R = 92\ MPa$. As it is customary in structural engineering, the equivalent bending strength is defined as

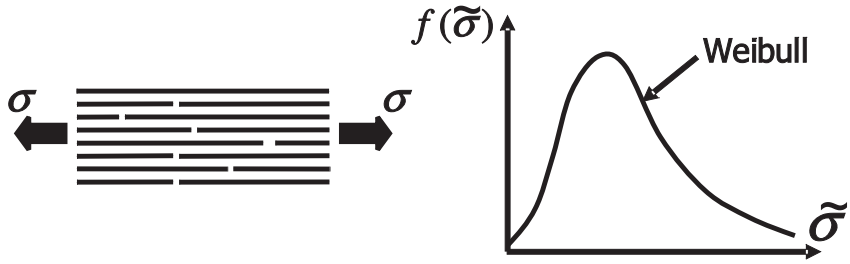

Figure 8.5: One-dimensional longitudinal tensile strength model.

$$\sigma_{Bcr} = \frac{M_{cr}}{S} = 0.407\ F_R$$

where S is the section modulus (for a rectangular beam $S = \frac{2}{3}bh^2$). Note that according to (8.34), the tensile strength of the same material assuming the same kinetic equation (8.26) would be $\sigma_{T\ cr} = 0.25\ F_R$. This gives a ratio of equivalent bending to tensile strength equal to $\sigma_{B\ cr}/\sigma_{T\ cr} = 1.63$, which is in good agreement with experimental data $\sigma_{B\ cr}/\sigma_{T\ cr} = 1.6$ [69] obtained for unreinforced concrete and also with the value $\sigma_{B\ cr}/\sigma_{T\ cr} = 1.5$ recommended by the ACI Code [70].

8.1.6 Fiber Direction, Tension Damage

If a lamina is subjected to tensile stress in the fiber direction, it is reasonable to assume that the matrix carries only a small portion of the applied load and no damage is expected in the matrix during loading. Then, the ultimate tensile strength of the composite lamina can be accurately predicted by computing the strength of a bundle of fibers.

Fiber strength is a function of the gauge length used during fiber strength tests. The length scale that determines how much of the fiber strength is actually used in a composite is the ineffective length δ. Starting at a fiber break point, the ineffective length is that length over which a fiber recovers a large percentage of its load (say, 90%). Rosen [71] recognized this fact and proposed that the longitudinal ultimate strength of fibers embedded in a ductile-matrix can be accurately predicted by the strength of a dry bundle of fibers with length δ.

A dry bundle is defined as a number of parallel fibers of some given length and diameter which, if unbroken, carry the same load (Figure 8.5). After a fiber within a dry bundle fails, the load is shared equally by the remaining unbroken fibers. A dry bundle typically refers to fibers which have not yet been combined with the matrix. As tensile load is slowly applied to a dry bundle of fibers, the weaker fibers (with large flaw sizes) begin to fail and the stress on the remaining unbroken fibers increases accordingly. The Weibull expression [72]

$$F(\widetilde{\sigma}) = 1 - \exp\left(-\frac{\delta}{L_0}\left(\frac{\widetilde{\sigma}}{\widetilde{\sigma}_0}\right)^m\right) \tag{8.35}$$

is often used to describe the cumulative probability $F(\widetilde{\sigma})$ that a fiber of length δ will fail at or below an effective stress $\widetilde{\sigma}$. The values of $\widetilde{\sigma}_0$ and m, which represent the

characteristic strength of the fiber, and the dispersion of fiber strength, respectively, can be determined from fiber strength experiments performed with a gauge length L_0. Equation (8.35) can be simplified as

$$F(\widetilde{\sigma}) = 1 - \exp\left(-\delta\alpha\widetilde{\sigma}^m\right) \tag{8.36}$$

where

$$\alpha = \frac{1}{L_0\widetilde{\sigma}_0^m} = \left[\frac{\Gamma(1+1/m)}{\widetilde{\sigma}_{av}}\right]^m \frac{1}{L_0} \tag{8.37}$$

where $\Gamma(x)$ is the Gamma function [45], $\widetilde{\sigma}_{av}$ is the average strength for a gauge length L_0. Equation (8.36) provides the percentage of fibers in a bundle which are broken as a function of the actual (or apparent) stress in the unbroken fibers. The percentage of fibers which are unbroken is $1 - F(\widetilde{\sigma})$. The apparent stress or bundle stress $\sigma = \sigma_b$ is equal to the applied load divided by the total fiber cross-sectional area. It is also equal to the product of the stress in unbroken fibers and the percentage of fibers which are unbroken

$$\sigma = \sigma_b = \widetilde{\sigma}\exp(-\delta\alpha\widetilde{\sigma}^m) \tag{8.38}$$

The value $\widetilde{\sigma}_{\max}$ which maximizes (8.38), can be easily determined and is given by

$$\widetilde{\sigma}_{\max} = (\delta\alpha m)^{-1/m} \tag{8.39}$$

The maximum (or critical) bundle strength σ_{cr} is determined by substituting (8.39) into (8.38)

$$\sigma_{cr} = (\delta\alpha m)^{-1/m}\exp(-1/m) = (\delta\alpha me)^{-1/m} \tag{8.40}$$

where e is the basis of the natural logarithms. The composite longitudinal tensile strength is [1, (4.82)]

$$F_{1t} = \left[V_f + \frac{E_m}{E_f}(1 - V_f)\right]\sigma_{cr} \tag{8.41}$$

where V_f is the fiber volume fraction, and E_f and E_m are the fiber and matrix elastic Young's moduli, respectively.

Combining (8.36) and (8.39), we get

$$D_{1t}^{cr} = 1 - \exp(-1/m) \tag{8.42}$$

Therefore, the critical or maximum damage D_{1t}^{cr} for longitudinal tensile loading can be computed as the area fraction of broken fibers in the lamina prior to catastrophic failure [62, 63], which turns out to be a function of the Weibull shape modulus m only.

Example 8.3 *The data sheet of carbon fiber T300 from Toray^{TM} Carbon Fibers, Inc. gives average tensile strength of the fiber $\sigma_{av} = 3.53\ GPa$, and tensile modulus $E_f = 230\ GPa$. Also, the same data sheet provides results of tensile tests of a unidirectional (UD) composite with epoxy $E_m = 4.5\ GPa$ and fiber volume fraction $V_f = 0.6$. The tensile strength reported is $F_{1t} = 1860\ MPa$. Using this experimental data, and assuming a Weibull shape parameter $m = 8.9$, identify the damage model under tensile load. Then, formulate the damage model and implement it in ANSYS® for a one-dimensional bar element. Finally, obtain the strain vs. stress response of the UD composite.*

Solution to Example 8.3

MODEL IDENTIFICATION *From (8.41) and using the experimental data available, it is possible to obtain σ_{cr} as*

$$\sigma_{cr} = \frac{F_{1t}}{V_f + \frac{E_m}{E_f}(1 - V_f)} = 3060\ MPa$$

Then, the product $\delta\alpha$ can be obtained using (8.40) as

$$\delta\alpha = \frac{(\sigma_{cr})^{-m}}{me} = 3.92\ 10^{-33}$$

The properties $E_f = 230\ GPa$, $m = 8.9$, and $\delta\alpha = 3.92 \times 10^{-33}$ are sufficient for the identification of the model.

MODEL FORMULATION *Following a procedure similar to that shown in Section 8.1.5 to implement a damage model, the following items are needed*

Damage Activation Function *In this example, the effective stress is chosen as the independent variable. Therefore, the damage activation function can be written as*

$$g = \widetilde{\sigma} - \hat{\gamma} \leq 0 \tag{8.43}$$

where $\hat{\gamma}$ is the updated damage threshold. Assuming an initial threshold value $\sigma_0 = 0$, from the consistency conditions (8.15) and (8.19), $\hat{\gamma}$ is given by the highest value of effective stress seen by the material

$$\hat{\gamma} = \max(0, \widetilde{\sigma}) \tag{8.44}$$

Secant Constitutive Equation *In this example, the kinetic equation (8.1.3) is available in integral form and given explicitly by (8.36) as*

$$D = 1 - \exp\left(-\delta\alpha\hat{\gamma}^m\right) \quad when\ \widetilde{\sigma} > 0;\ \varepsilon > 0 \tag{8.45}$$

where the damage state does not depend on the actual load state $\widetilde{\sigma}$; it only depends on the load history state $\hat{\gamma}$.

Substituting (8.45) into (8.5) and (8.7), and using strain equivalence, yields the constitutive equation

$$\sigma = E(D)\,\varepsilon = \exp\left(-\delta\alpha\hat{\gamma}^m\right)\,\widetilde{E}\,\varepsilon \quad when \quad \varepsilon > 0 \tag{8.46}$$

Tangent Constitutive Equation *The tangent constitutive equation can be obtained by differentiating the secant constitutive equation as*

$$\dot{\sigma} = E(D)\dot{\varepsilon} + \dot{E}(D)\varepsilon \tag{8.47}$$

The factor $\dot{E}(D)$ is zero when no new damage appears, i.e., during elastic loading or unloading. When damage occurs, (8.44) yields $\hat{\gamma} = \widetilde{E}\varepsilon$, and differentiating $E(D)$ in (8.46) we obtain

$$\dot{E}(D) = -\delta\alpha m\hat{\gamma}^{m-1}\exp\left(-\delta\alpha\hat{\gamma}^{m}\right)\widetilde{E}^{2}\dot{\varepsilon} \tag{8.48}$$

The tangent constitutive equation is obtained by substituting (8.48) into (8.47) when damage occurs, or $\dot{E}(D) = 0$ when no new damage appears. Therefore, the tangent constitutive equation can be written as

$$\dot{\sigma} = \begin{cases} (1-\delta\alpha m\hat{\gamma}^{m})\exp\left(-\delta\alpha\hat{\gamma}^{m}\right)\widetilde{E}\,\dot{\varepsilon} & when \quad \varepsilon > \hat{\gamma}/\widetilde{E} \\ E(D)\,\dot{\varepsilon} & when \quad \varepsilon < \hat{\gamma}/\widetilde{E} \end{cases} \tag{8.49}$$

NUMERICAL ALGORITHM *The one-dimensional damage model is implemented in ANSYS using the subroutine* `usermat1d_803.f90`*, available in [5]. The following items describe the procedure used to explicitly evaluate the damage constitutive equation.*[4]

i. Read the strain at time t

$$\varepsilon_t$$

ii. Compute the effective stress (assuming strain equivalence)

$$\widetilde{\sigma}_t = \widetilde{E}\varepsilon_t$$

iii. Update the threshold value

$$\hat{\gamma}_t = \max(\hat{\gamma}_{t-1}, \widetilde{\sigma}_t)$$

iv. Compute the damage variable

$$D_t = 1 - \exp\left(-\delta\alpha(\hat{\gamma}_t)^{m}\right)$$

v. Compute the nominal stress

$$\sigma_t = (1-D_t)\,\widetilde{E}\,\varepsilon_t$$

vi. Compute the tangent stiffness

$$E_t^{dam} = \begin{cases} (1-\delta\alpha m(\hat{\gamma}_t)^{m})\exp\left(-\delta\alpha(\hat{\gamma}_t)^{m}\right)\widetilde{E} & when\ \hat{\gamma}_t > \hat{\gamma}_{t-1} \\ (1-D_t)\,\widetilde{E} & when\ \hat{\gamma}_t = \hat{\gamma}_{t-1} \end{cases}$$

[4] See Section 8.4.1 for those cases for which it is not possible to integrate the constitutive equation explicitly.

MODEL RESPONSE *The APDL code below and user subroutine* `usermat1d_803.f90`*, available in [5], are used to model a one-dimensional bar representative of a carbon fiber UD composite. The nominal stress-strain response is shown with a solid line in Figure 8.6. The UD composite fails at* $\varepsilon_{cr} = 1.5\%$*, in good agreement with the strain to failure reported by Toray. Your results must be similar to those shown in Figure 8.6.*

```
/TITLE, Tensile response bundle Carbon Fiber T300, FEAcomp Ex. 8.3
/PREP7              ! Start pre-processor module

!=== USER MATERIAL DECLARATION ==================
TB,USER,1,1,3,  ! DECLARES USERMAT 1, MAT 1, PROPERTIESS 3
TBTEMP,0
TBDATA,,230000,8.9,3.92e-033    ! PROPERTIES: E, m, delta_alpha
TB,STAT,1,,2,       ! NUMBER OF STATE VARIABLES 2
!================================================

ET,   1,  180       ! LINK180, link element for analysis
R,1,1               ! Real constant #1, Area = 1
N,1                 ! Define node 1, coordinates=0,0,0
NGEN,6,1,1,,,2      ! Generate 5 additional nodes
                    ! distance between adjacent nodes 2mm
E,1,2               ! Generate element 1 by node 1 to 2
EGEN,5,1,1          ! Generate element 2,3,4 and 5
FINISH              ! Exit pre-processor module

/SOLU               ! Start Solution module
ANTYPE,STATIC
OUTRES,ALL,1        ! Store results for each substep
D,1,all             ! Define b.c. on node 1, totally fixed
D,6,UX,0.25         ! Define horizontal displacement on node 6.
NSUBST,50,75,50     ! 50 = Number of substeps in this load step
SOLVE               ! Solve load step
FINISH              ! Exit solution module

/POST26         ! Start time-historic post-process
NSOL,2,6,U,X, UXnode6   ! Load displacements node 6
RFORCE,3,6,F,X, FXnode6 ! Load reaction force node 6
XVAR,2          ! displacement x-graph variable
PLVAR,3         ! plot reaction as y-graph variable
lines,1000      !
PRVAR,2,3       ! list displacements and reactions
FINISH          ! Exit post-process module
```

8.1.7 Fiber Direction, Compression Damage

Many models have been proposed trying to improve the prediction of compression strength of composites first introduced by Rosen [73]. The literature encompasses fiber buckling modes [17, 22, 74, 75], kink-band models [76], and kink-bands induced by buckling [77]. In fiber buckling models, it is assumed that buckling of

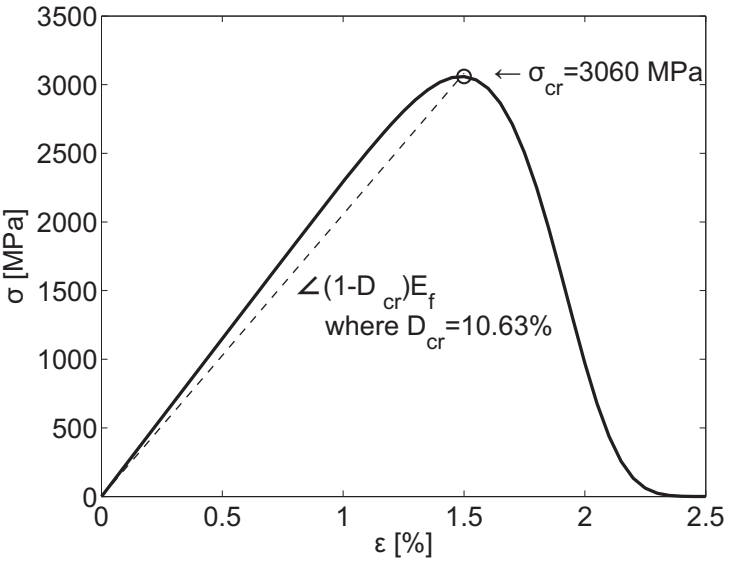

Figure 8.6: Fiber tensile damage model response.

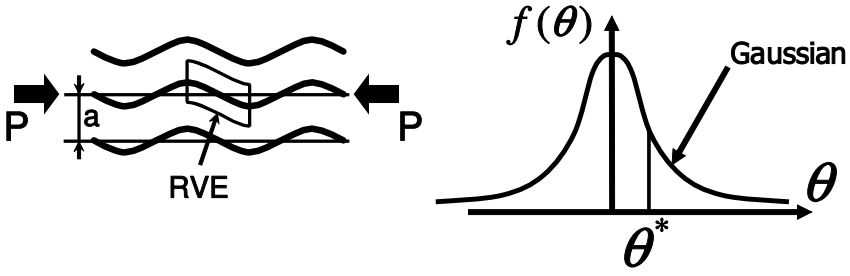

Figure 8.7: One-dimensional longitudinal compression strength model.

the fibers initiates a process that leads to the collapse of the material [73]. Rosen's model has been refined with the addition of initial fiber misalignment and non-linear shear stiffness [74]. Experimental evidence suggests that fiber buckling of perfectly aligned fibers (Rosen's model) is an imperfection sensitive problem (see Section 4.1.1). Therefore, small amounts of imperfection (misalignment) cause large reductions in the buckling load, thus the reduction of the compression strength with respect to Rosen's prediction. Each fiber has a different value of fiber misalignment. The probability of finding a fiber with misalignment angle α is given by a Gaussian distribution [22, 78].

An optical technique [13] can be used to measure the misalignment angle of each fiber in the cross-section. The resulting distribution of fiber misalignment was shown to be Gaussian (Figure 8.7) by using the cumulative distribution function (CDF) plot and the probability plot [22]. Therefore, the probability density is

$$f(z) = \frac{\exp(-z^2)}{\Lambda\sqrt{2\pi}} \quad ; \quad z = \frac{\alpha}{\Lambda\sqrt{2}} \tag{8.50}$$

where Λ is the standard deviation and α is the continuous random variable, in this case being equal to the misalignment angle. The CDF gives the probability of obtaining a value smaller than or equal to some value of α, as follows

$$F(z) = \text{erf}(z) = \frac{2}{\sqrt{\pi}} \int_0^z exp(-z'^2) dz' \tag{8.51}$$

where $erf(z)$ is the error function.

The relationship between the buckling stress and the imperfection (misalignment) is known in stability theory as the imperfection sensitivity curve. Several models from the literature can be used to develop this type of curve. The deterministic model, similar to the one presented by Wang [74] is developed in [17] but using the representation of the shear response given by Equation (8.52).

The shear stress-strain response of polymer-matrix composites can be represented [22, 77] by

$$\sigma_6 = F_6 \tanh\left(\frac{G_{12}}{F_6}\gamma_6\right) \tag{8.52}$$

where γ_6 is the in-plane shear strain. Furthermore, G_{12} is the initial shear stiffness and F_6 is the shear strength, which are obtained by fitting the stress-strain experimental data. Complete polynomial expansions [79] fit the experimental data well but they are not antisymmetric with respect to the origin. This introduces an artificial asymmetric bifurcation during the stability analysis [75]. Shear experimental data can be obtained by a variety of techniques including the ± 45 coupon, 10° off-axis, rail shear, Iosipescu, Arcan, and torsion tests [80]. The nonlinear shear stress-strain curve should be measured for the actual composite being tested in compression.

Barbero [17] derived the equilibrium stress σ_{eq} as a function of the shear strain and the misalignment angle as

$$\begin{aligned} \widetilde{\sigma}_{eq}(\alpha, \gamma_6) = & \frac{F_6}{2(\gamma_6 + \alpha)} \frac{(\sqrt{2}-1)a + (\sqrt{2}+1)(b-1)}{1 - a + b} \\ a = & \exp(\sqrt{2}g) - \exp(2g) \\ b = & \exp(2g + \sqrt{2}g) \\ g = & \frac{\gamma_6 G_{12}}{F_6} \end{aligned} \tag{8.53}$$

with G_{12} and F_6 as parameters. Note that if the shear behavior is assumed to be linear $\widetilde{\sigma}_6 = G_{12}\gamma_6$ [81], then (8.53) does not have a maximum with respect to γ_6 and thus misaligned fibers embedded in a linear elastic matrix do not buckle. On the contrary, by using the hyperbolic tangent representation of shear (8.52), a maximum with respect to γ_6 is shown in (8.53). The maxima of the curves $\widetilde{\sigma}(\gamma_6)$ as a function of the misalignment angle α is the imperfection sensitivity curve, which represents the compression strength of a fiber (and surrounding matrix) as a function of its misalignment. For negative values of misalignment, it suffices to assume that the function is symmetric $\widetilde{\sigma}(-\alpha) = \widetilde{\sigma}(\alpha)$.

The stress carried by a fiber reduces rapidly after reaching its maximum because the load-carrying capacity of a buckled fiber is much lower than the applied load. Several models can be constructed depending on the assumed load that a fiber carries after buckling. A lower bound can be found assuming that buckled fibers carry no more load because they have no post-buckling strength. According to the imperfection sensitivity equation (8.53), fibers with large misalignment buckle under low applied stress. If the post-buckling strength is assumed to be zero, the applied stress is redistributed onto the remaining, unbuckled fibers, which then carry a higher effective stress $\widetilde{\sigma}(\alpha)$. At any time during loading of the specimen, the applied load σ (applied stress times initial fiber area) is equal to the effective stress times the area of fibers that remain unbuckled

$$\sigma = \bar{\sigma}(\alpha)[1 - D(\alpha)] \tag{8.54}$$

where $0 \leq D(\alpha) \leq 1$ is the area of the buckled fibers per unit of initial fiber area. For any value of effective stress, all fibers having more than the corresponding value of misalignment have buckled. The area of buckled fibers $D(\alpha)$ is proportional to the area under the normal distribution located beyond the misalignment angle $\pm\alpha$.

Equation (8.54) has a maximum that corresponds to the maximum stress that can be applied to the composite. Therefore, the compression strength of the composite is found as

$$\sigma_c = \max \left[\bar{\sigma}(\alpha) \int_{-\alpha}^{\alpha} f(\alpha') d\alpha' \right] \tag{8.55}$$

where $\bar{\sigma}(\alpha)$ is given by Equation (8.53) and $f(\alpha')$ is given by (8.50). The maximum of (8.54), given by Equation (8.55) is a unique value for the compression strength of the composite that incorporates both the imperfection sensitivity and the distribution of fiber misalignment. Note that the standard deviation Λ is a parameter that describes the actual, measured, distribution of fiber misalignment, and it is not to be chosen arbitrarily as a representative value of fiber misalignment for all the fibers.

Since the distribution given in (8.50) cannot be integrated in closed form, (8.55) is evaluated numerically. However, it is advantageous to develop an explicit formula so that the compression strength can be easily predicted. Following the explicit formulation in [17], the compression strength of the unidirectional composite, explicitly in terms of the standard deviation of fiber misalignment Λ, the in-plane shear stiffness G_{12}, and the shear strength F_6 is

$$\frac{F_{1c}}{G_{12}} = (1 + 4.76 B_a)^{-0.69} \tag{8.56}$$

where 4.76 and -0.69 are two constants chosen to fit the numerical solution to the exact problem [17], with the dimensionless group B_a given by

$$B_a = \frac{G_{12}\Lambda}{F_6} \tag{8.57}$$

The misalignment angle of the fibers that buckle just prior to compression failure is given by [17, (23)]

$$\begin{aligned}
\alpha_{cr} &= a/b \\
a &= 1019.011 G_{12} C_2^2 \Lambda^3 - 375.3162 C_2^3 \Lambda^4 - 845.7457 G_{12}^2 C_2 \Lambda^2 \\
&\quad + g\left(282.1113 G_{12} C_2 \Lambda^2 - 148.1863 G_{12}^2 \Lambda - 132.6943 C_2^2 \Lambda^3\right) \\
b &= 457.3229 C_2^3 \Lambda^3 - 660.77 G_{12} C_2^2 \Lambda^2 - 22.43143 G_{12}^2 C_2 \Lambda \\
&\quad + g\left(161.6881 C_2^2 \Lambda^2 - 138.3753 G_{12} C_2 \Lambda - 61.38939 G_{12}^2\right) \\
g &= \sqrt{C_2 \Lambda \left(8.0 C_2 \Lambda - 9.424778 G_{12}\right)} \\
C_2 &= -G_{12}^2 / \left(4 F_6\right)
\end{aligned} \tag{8.58}$$

Additionally, the shear strain at failure is

$$\gamma_{cr} = -\alpha_{cr} + \sqrt{\alpha_{cr}^2 + \frac{3}{2}\frac{\pi F_6 \alpha_{cr}}{G_{12}}} \tag{8.59}$$

In summary, when a fiber-reinforced lamina is compressed, the predominant damage mode is fiber buckling. However, the buckling load of the fibers is lower than that of the perfect system because of fiber misalignment, so much that a small amount of fiber misalignment could cause a large reduction in the buckling load. For each misalignment angle α, the composite area-fraction with buckled fibers $D(\alpha)$, corresponding to fibers with misalignment angle greater than α, can be taken as a measure of damage. If the fibers are assumed to have no post-buckling strength, then the applied stress is redistributed onto the remaining unbuckled fibers, which will be carrying a higher effective stress. The applied stress, which is lower than the effective stress by the factor $(1 - D)$, has a maximum, which corresponds to the compressive strength of the composite. Therefore, it is possible to compute the critical damage D_{1c} for longitudinal compressive loading as

$$D_{1c}^{cr} = 1 - \Omega_{1c} = 1 - erf\left(\frac{\alpha_{cr}}{\Lambda\sqrt{2}}\right) \tag{8.60}$$

where erf is the error function, Λ is the standard deviation of the actual Gaussian distribution of fiber misalignment (obtained experimentally [78]), and α_{cr} is the critical misalignment angle at failure. The three-dimensional theoretical formulation is developed in the next three sections.

8.2 Multidimensional Damage and Effective Spaces

The first step in the formulation of a general multidimensional damage model is to define the damage variable as well as the effective stress and strain spaces, as shown in this section. The second step is to define the form of either the Helmholtz free energy or the Gibbs energy and from them derive the thermodynamic forces conjugate to the state variables representing damage and hardening, as shown in Section 8.3. The third step is to derive the kinetic laws governing the rate of damage

hardening, which are functions of the damage and hardening potentials, as shown in Section 8.4.

Experimental knowledge of the degradation and subsequent material response is used to guide the selection on the variable used to represent damage. A second-order damage tensor $\mathbf{D}$ can be used to represent damage of orthotropic fiber-reinforced composite materials, following Kachanov-Rabotnov's approach [59, 82]. For composite materials reinforced with stiff and strong fibers, damage can be accurately represented by a second-order tensor[5] with principal directions aligned with the material directions $(1, 2, 3)$ [83, 84]. This is due to the fact that the dominant modes of damage are microcracks, fiber breaks, and fiber-matrix debond, all of which can be conceptualized as cracks either parallel or perpendicular to the fiber direction.[6] Therefore, the damage tensor can be written as

$$\mathbf{D} = D_{ij} = D_i \delta_{ij} \quad \text{no sum on i} \tag{8.61}$$

where D_i are the eigenvalues of $\mathbf{D}$, which represent the net stiffness reduction along the principal material directions n_i, and δ_{ij} is the Kronecker delta ($\delta_{ij} = 1$ if $i = j$, or zero otherwise). The integrity tensor is also diagonal, and using energy equivalence (8.8),we have

$$\mathbf{\Omega} = \Omega_{ij} = \sqrt{1 - D_i}\delta_{ij} \quad \text{no sum on i} \tag{8.62}$$

The integrity tensor is always symmetric and positive, because the net area reduction must be positive definite during damage evolution [85]. Both tensors are diagonal when represented in the principal system. Introducing a symmetric fourth-order tensor, $\mathbf{M}$, called the *damage effect tensor*, as

$$\mathbf{M} = M_{ijkl} = \frac{1}{2}\left(\Omega_{ik}\Omega_{jl} + \Omega_{il}\Omega_{jk}\right) \tag{8.63}$$

The transformation of stress and strain between the effective and damaged configurations is accomplished as follows

$$\widetilde{\boldsymbol{\sigma}} = \mathbf{M}^{-1} : \boldsymbol{\sigma} \qquad \begin{aligned} \widetilde{\boldsymbol{\varepsilon}} &= \mathbf{M} : \boldsymbol{\varepsilon} \\ \widetilde{\boldsymbol{\varepsilon}}^e &= \mathbf{M} : \boldsymbol{\varepsilon}^e \\ \widetilde{\boldsymbol{\varepsilon}}^p &= \mathbf{M} : \boldsymbol{\varepsilon}^p \end{aligned} \tag{8.64}$$

where an over-bar indicates that the quantity is evaluated in the effective configuration and the superscripts e, p, denote quantities in the elastic and plastic domains, respectively.

By the energy equivalence hypothesis [60], it is possible to define the constitutive equation in the effective configuration (Figure 8.1.c) as

[5] Tensors are denoted by boldface type, or by their components with index notation.

[6] Strictly speaking, damage is transversely isotropic since cracks can also be aligned along any direction in the 2-3 plane.

$$\widetilde{\boldsymbol{\sigma}} = \widetilde{\mathbf{C}} : \widetilde{\boldsymbol{\varepsilon}}^e \quad ; \qquad \widetilde{\boldsymbol{\varepsilon}}^e = \widetilde{\mathbf{C}}^{-1} : \widetilde{\boldsymbol{\sigma}} = \widetilde{\mathbf{S}} : \widetilde{\boldsymbol{\sigma}} \tag{8.65}$$

where the fourth-order tensors $\mathbf{C}$ and $\mathbf{S}$ denote the secant stiffness tensor and compliance tensor, respectively. The stress-strain equations in the damaged configuration (Figure 8.1.b) are obtained by substituting (8.65) into (8.64),

$$\begin{aligned} &\boldsymbol{\sigma} = \mathbf{M} : \widetilde{\boldsymbol{\sigma}} = \mathbf{M} : \widetilde{\mathbf{C}} : \widetilde{\boldsymbol{\varepsilon}}^e, && \boldsymbol{\varepsilon}^e = \mathbf{M}^{-1} : \widetilde{\boldsymbol{\varepsilon}}^e = \mathbf{M}^{-1} : \widetilde{\mathbf{S}} : \widetilde{\boldsymbol{\sigma}}, \\ &\boldsymbol{\sigma} = \mathbf{M} : \widetilde{\mathbf{C}} : \mathbf{M} : \boldsymbol{\varepsilon}^e, && \boldsymbol{\varepsilon}^e = \mathbf{M}^{-1} : \widetilde{\mathbf{S}} : \mathbf{M}^{-1} : \boldsymbol{\sigma}, \\ &\boldsymbol{\sigma} = \mathbf{C} : \boldsymbol{\varepsilon}^e && \boldsymbol{\varepsilon}^e = \mathbf{S} : \boldsymbol{\sigma} \end{aligned} \tag{8.66}$$

with

$$\mathbf{C} = \mathbf{M} : \widetilde{\mathbf{C}} : \mathbf{M} \qquad \mathbf{S} = \mathbf{M}^{-1} : \widetilde{\mathbf{S}} : \mathbf{M}^{-1} \tag{8.67}$$

The explicit form of these tensors are presented in Appendix B. Given that the tensor $\mathbf{M}$ is symmetric, the secant stiffness and compliance tensors are also symmetric.

8.3 Thermodynamics Formulation

The damage processes considered in this chapter can be described by a series of equilibrium states reached while the system traverses a nonequilibrium path due to the irreversibility of damage and plasticity. In general, the current state of a system (e.g., stress, stiffness, compliance) depends on the current state (e.g., strain) as well as on the history experienced by the system. This is the case for viscoelastic materials discussed in Chapter 7. However, for damaging and elastoplastic materials, the current state can be described in terms of the current strain and the *effects of history* on the material, which in this chapter are characterized by the damage tensor $\mathbf{D}$ and the plastic strain tensor $\boldsymbol{\varepsilon}^{\mathbf{p}}$.

8.3.1 First Law

The *first law* of thermodynamics states that any increment of internal energy of the system is equal to the heat added to the system minus the work done by the system on its surroundings

$$\delta U = \delta Q - \delta W \tag{8.68}$$

The system under consideration in this section is a representative volume element (RVE), which is the smallest volume element that contains sufficient features of the microstructure and irreversible processes, such as damage and plasticity, to be representative of the material as a whole. Further discussions about the RVE can be found in Chapter 6.

In rate form, (8.68) is

$$\dot{U} = \dot{Q} - \dot{W} \tag{8.69}$$

where

$$\dot{U} = \frac{d}{dt}\int_{\Omega} \rho u dV \tag{8.70}$$

Here ρ is the density, Ω is the volume of the RVE, and u is the *internal energy density*, which is an internal variable and a potential function.[7]

For a deformable solid, the rate of work done *by* the system is minus the product of the stress *applied* on the system times the rate of strain

$$\dot{W} = -\int_{\Omega} \boldsymbol{\sigma} : \dot{\boldsymbol{\varepsilon}}\, dV \tag{8.71}$$

where $\boldsymbol{\varepsilon}$ is the *total* strain (see (8.125)).

The heat flow into the RVE is given by

$$\dot{Q} = \int_{\Omega} \rho r dV - \int_{\partial\Omega} \mathbf{q}\cdot\mathbf{n} d\mathbf{A} \tag{8.72}$$

where r is the radiation heat per unit mass, $\mathbf{q}$ is the heat flow vector per unit area, and $\mathbf{n}$ is the outward normal vector to the surface $\partial\Omega$ enclosing the volume Ω. Since the volume Ω of the RVE does not change with time, and using the divergence theorem,[8] the *first law at the local level* becomes

$$\rho\dot{u} = \boldsymbol{\sigma} : \dot{\boldsymbol{\varepsilon}} + \rho r - \nabla\cdot\mathbf{q} \tag{8.73}$$

The internal energy accounts for all the energy stored into the system. For example, a system undergoing elastic deformation $\delta\boldsymbol{\varepsilon}^e$, raising temperature δT, and damage in the form of cracks of area growing by δA_c, undergoes a change of internal energy u given[9] by

$$\delta u = \boldsymbol{\sigma} : \delta\boldsymbol{\varepsilon}^e + C_p\delta T - (G - G_c)\delta A_c \tag{8.74}$$

where G is the strain energy release rate, G_c is the surface energy needed to create the increment of the two surfaces of an advancing crack, and $C_p = C_v$ is the specific heat capacity of the solid.

In general $\boldsymbol{\varepsilon} = \boldsymbol{\varepsilon}(\boldsymbol{\sigma}, u, s_\alpha)$ where s_α are internal variables. Let's assume for the time being that the system is adiabatic, i.e., $\rho r - \nabla\cdot\mathbf{q} = 0$. Further, if there are no dissipative effects or heat transfer, then u is a function of $\boldsymbol{\varepsilon}$ only, $u = u(\boldsymbol{\varepsilon}^e)$, where $\boldsymbol{\varepsilon}^e$ is the elastic strain. In such a case, the internal energy density reduces to the strain energy density, which in rate form is

$$\dot{\varphi}(\boldsymbol{\varepsilon}) = \boldsymbol{\sigma} : \dot{\boldsymbol{\varepsilon}}^e \tag{8.75}$$

and the complementary strain energy density is

$$\dot{\varphi}^*(\boldsymbol{\varepsilon}) = \boldsymbol{\sigma} : \dot{\boldsymbol{\varepsilon}}^e - \dot{\varphi} = \dot{\boldsymbol{\sigma}} : \boldsymbol{\varepsilon}^e \tag{8.76}$$

[7]The values of the potential functions depend on the state and not on the path or process followed by the system to reach such a state [86].

[8]$(\int_{\partial\Omega} \mathbf{q}\cdot\mathbf{n} dA = \int_{\Omega} \nabla\cdot\mathbf{q} dV)$; $div(\mathbf{q}) = \nabla\cdot\mathbf{q} = \partial\mathbf{q}_i/\partial x_i$.

[9]Thermodynamics custom and [87] are followed here in representing the internal energy with the letter u, not to be confused with the displacement vector $\mathbf{u}$ used elsewhere.

8.3.2 Second Law

The *second law* of thermodynamics formalizes the fact that heat flows from hot to cold. Mathematically, the heat flow $\mathbf{q}$ has the opposite direction to the gradient[10] of temperature T, which is formally written as

$$\mathbf{q} \cdot \nabla T \leq 0 \tag{8.77}$$

where the equal sign holds true only for adiabatic processes, i.e., when there is no heat exchange and thus no thermal irreversibility.

Let's visualize a process of heat transfer from a hot reservoir to a cold reservoir, happening in such a way that no heat is lost to, and no work is exchanged with the environment. Once heat has flowed to the cold reservoir, it is impossible to transfer it back to the hot reservoir without adding external work. That is, the process of heat transfer is irreversible even though, on account of the first law energy balance (8.73), no energy has been lost. For future use (8.77) can be written[11] as

$$\mathbf{q} \cdot \nabla T^{-1} \geq 0 \tag{8.78}$$

The second law justifies the introduction of a new internal variable, the entropy density $s = s(u, \varepsilon)$, which is also a potential function [88]. According to the second law, the entropy density rate is $\dot{s} \geq 0$, where the equal sign holds true only for adiabatic processes.

Assume the specific entropy $s = s(u, \varepsilon)$ is a potential function such that for a reversible process [88]

$$ds = \left(\frac{\delta q}{T}\right)_{rev} \tag{8.79}$$

with $\delta Q = \int_\Omega \rho \ \delta q \ d\Omega$, where $\delta q = r - \rho^{-1} \nabla \cdot \mathbf{q}$ is the heat input per unit mass, and $S = \int_\Omega s \ \rho \ d\Omega$ is the entropy. We use δ, not d, to emphasize that δq is not the differential (perfect or total) of any (potential) function.

As a preamble to the definition of conjugate variables (see (8.86, 8.92, 8.99)), note that using (8.79), the first law can be rewritten for a *reversible* process on an ideal gas ($pv = RT$), as the *Gibbs* equation for an ideal gas,

$$du = T \ ds - p \ dv \tag{8.80}$$

where v is the specific volume (volume per unit mass). It can be seen in (8.80) that v is conjugate to $-p$ for calculating work input for an ideal gas and s is conjugate to T for calculating thermal energy input.

For a *cyclic reversible* process returning to its initial state characterized by state variables (e.g., u, T, ε), by virtue of (8.79) we have $\oint ds = \oint \left(\frac{\delta \mathbf{q}}{T}\right)_{rev} = 0$. Since s is a potential function but q is not, for an *irreversible* process we have $\oint ds = 0$ but $\oint \left(\frac{\delta q}{T}\right)_{irrev} < 0$, as corroborated by experiments. The heat δq entering at

[10] The gradient of a scalar yields a vector, $\nabla T = \partial T / \partial x_i$.

[11] $\nabla T^{-1} = -T^{-2} \nabla T$.

temperature T_i provides less entropy input $\delta q/T_i$ than the entropy output $\delta q/T_o$ leaving the same cycle at temperature $T_o < T_i$ (see also [89, Example 6.2]). Since entropy is a potential function, and therefore a state variable, it always satisfies $\oint ds = 0$. Therefore, a negative net entropy supply must be compensated by internal entropy production. The entropy of a system can be raised or lowered by adding or extracting heat (in the form of $\delta q/T$) *but it is always raised by internal irreversible processes such as crack formation and so on* (positive dissipation principle).

Adiabatic systems do not exchange heat with the surroundings ($\delta q = 0$), so the only change in entropy is due to internal irreversibility $\dot{s} \geq 0$, where the equal sign holds for reversible processes only. Note that any system and its surroundings can be made adiabatic by choosing sufficiently large surroundings, e.g., the universe. For an arbitrary system, the total entropy rate is greater than (or equal to) the net entropy input due to heat

$$\dot{s} \geq \frac{r}{T} - \frac{1}{\rho}\nabla \cdot \left(\frac{\mathbf{q}}{T}\right) \tag{8.81}$$

The left-hand side of (8.81) represents the total entropy rate of the system. The right-hand side of (8.81) represents the external entropy supply rate. The difference is the internal entropy production rate

$$\dot{\gamma}_s = \dot{s} - \frac{r}{T} + \frac{1}{\rho}\nabla \cdot \left(\frac{\mathbf{q}}{T}\right) \geq 0 \tag{8.82}$$

Equation 8.82 is called the *local Clausius-Duhem inequality*. Noting that $\nabla \cdot \left(T^{-1}\mathbf{q}\right) = T^{-1}\nabla \cdot \mathbf{q} + \mathbf{q}\nabla\, T^{-1}$ results in

$$\dot{\gamma}_s = \dot{s} - \frac{1}{\rho T}\left(\rho r - \nabla \cdot \mathbf{q}\right) + \frac{1}{\rho}\,\mathbf{q} \cdot \nabla\, T^{-1} \geq 0 \tag{8.83}$$

where the first two terms represent the local entropy production due to local dissipative phenomena, and the last term represents the entropy production due to heat conduction[12] [88]. Assuming it is possible to identify all local dissipative phenomena, their contributions can be written as products of conjugate variables $p_\alpha \dot{s_\alpha} \geq 0$, and (8.83) can be written as

$$\rho T \dot{\gamma}_s = p_\alpha \dot{s_\alpha} + T\mathbf{q} \cdot \nabla T^{-1} \geq 0 \tag{8.84}$$

where $\alpha = 1 \ldots n$, spans the total number of dissipative phenomena considered. Note that the dissipation is a scalar given by the contracted product of a thermodynamic force p_α times the increment of a measurable state variable s_α. The state variable, also called thermodynamic flux, describes univocally the effects of history (e.g., yield, damage) on the material. Note that γ_s is defined as an entropy, not as a dissipation heat, so that it is a potential function, while q is not.

For the particular case of damage due to penny-shaped cracks growing self similarly [64], the state variable is the crack area A_c and the thermodynamic force is

[12] Even absent local dissipative phenomena, $\mathbf{q} \cdot \nabla T^{-1} \geq 0$ represents the well-known fact that heat flows opposite to the temperature gradient ∇T.

the energy available to grow the cracks $p_c = G - G_c$, which is equal to the difference between the energy release rate (ERR) G and the critical ERR $G_c = 2\gamma_c$, the latter being equal to twice the surface energy because two surfaces must be created every time a crack appears (see Chapter 10). In this case, the dissipation (heat) is $\rho T\dot{\gamma} = p_c\dot{A}_c$.

From the first law (8.73), considering an adiabatic process ($\rho r - \nabla \cdot \mathbf{q}$) and using the chain rule $\dot{u} = \partial u/\partial \boldsymbol{\varepsilon} : \dot{\boldsymbol{\varepsilon}}$ we have

$$\left[\boldsymbol{\sigma} - \rho\frac{\partial u}{\partial \boldsymbol{\varepsilon}}\right] : \dot{\boldsymbol{\varepsilon}} = 0 \tag{8.85}$$

Since $\dot{\boldsymbol{\varepsilon}} = 0$ would be a trivial solution, the stress tensor, conjugate to strain, is defined as

$$\boldsymbol{\sigma} = \rho\frac{\partial u}{\partial \boldsymbol{\varepsilon}} \tag{8.86}$$

The Clausius-Duhem inequality (8.83) for an *isothermal* ($\nabla T = 0$) system reduces to

$$\dot{\gamma}_s = \dot{s} - \frac{1}{\rho T}\left(\rho r - \nabla \cdot \mathbf{q}\right) \geq 0 \tag{8.87}$$

and using the first law we get

$$\rho T\dot{\gamma}_s = \rho T\dot{s} - \left(\rho\dot{u} - \boldsymbol{\sigma} : \boldsymbol{\varepsilon}\right) \geq 0 \tag{8.88}$$

The *Helmholtz free energy (HFE) density* is defined as

$$\psi(T, \boldsymbol{\varepsilon}, s_\alpha) = u - Ts \tag{8.89}$$

which is also a potential function. The corresponding extensive function is the Helmholtz free energy[13] $A = \int_\Omega \rho\psi dV$. The rate of change of HFE density is

$$\dot{\psi} = \dot{u} - \dot{T}s - T\dot{s} \tag{8.90}$$

and introducing (8.88), with $\dot{\gamma}_s = 0$ at an equilibrium state, we get

$$\rho\dot{\psi} = -\rho s\dot{T} + \boldsymbol{\sigma} : \dot{\boldsymbol{\varepsilon}} \tag{8.91}$$

from which an alternative definition of stress, conjugate to strain, is found as

$$\boldsymbol{\sigma} = \rho\frac{\partial \psi}{\partial \boldsymbol{\varepsilon}} = \mathbf{C} : \varepsilon \tag{8.92}$$

where the secant elastic stiffness, which is affected by dissipative phenomena, including damage, is defined as

$$\mathbf{C}(s_\alpha) = \rho\frac{\partial^2 \psi}{\partial \boldsymbol{\varepsilon}^2} \tag{8.93}$$

[13]The nomenclature of [87] has been used.

Using the first law (8.73) in the internal entropy production per unit volume, or local Clausius-Duhem inequality (8.83), and expanding $\nabla \cdot (\mathbf{q}T^{-1}) = T^{-1}\nabla \cdot \mathbf{q} + \mathbf{q} \cdot \nabla T^{-1}$, we get

$$\rho T \dot{\gamma}_s = \frac{\mathbf{q}}{T} \cdot \nabla T^{-1} - \rho \left(\dot{\psi} + s\dot{T} - \rho^{-1} \boldsymbol{\sigma} : \dot{\boldsymbol{\varepsilon}} \right) \geq 0 \tag{8.94}$$

Realizing that $\nabla T^{-1} = -\nabla T / T^2$, the Clausius-Duhem inequality becomes

$$T\rho \dot{\gamma}_s = \boldsymbol{\sigma} : \dot{\boldsymbol{\varepsilon}} - \rho \left(\dot{\psi} + s\dot{T} \right) - \frac{\mathbf{q}}{T} \cdot \nabla T \geq 0 \tag{8.95}$$

Since the HFE density is a function of the internal variables $\boldsymbol{\varepsilon}, T, s_\alpha$, we have

$$\dot{\psi} = \left. \frac{\partial \psi}{\partial \boldsymbol{\varepsilon}} \right|_{T, s_\alpha} : \dot{\boldsymbol{\varepsilon}} \; + \; \left. \frac{\partial \psi}{\partial T} \right|_{\boldsymbol{\varepsilon}, s_\alpha} \dot{T} \; + \; \left. \frac{\partial \psi}{\partial s_\alpha} \right|_{\boldsymbol{\varepsilon}, T} \dot{s}_\alpha \quad ; \quad \alpha = 1 \ldots n \tag{8.96}$$

where $\left. \dfrac{\partial}{\partial y} \right|_x$ represents the partial derivative with respect to y at constant x.

Inserting (8.96) into (8.95), using (8.89), (8.92), and $\nabla T^{-1} = -\nabla T / T^2$, the second law can be written as follows

$$\dot{\gamma} = \rho T \dot{\gamma}_s = -\rho \frac{\partial \psi}{\partial s_\alpha} s_\alpha + T \mathbf{q} \cdot \nabla T^{-1} \geq 0 \tag{8.97}$$

where $\dot{\gamma}$ is the heat dissipation rate per unit volume. Comparing (8.97) to (8.84) it becomes clear that $-\rho \partial \psi / \partial s_\alpha = p_\alpha$ are the thermodynamic forces conjugated to s_α, which provides a definition for the thermodynamic forces.

The complementary free-energy density, or *Gibbs energy density*, is defined as

$$\chi = \rho^{-1} \boldsymbol{\sigma} : \boldsymbol{\varepsilon} - \psi \tag{8.98}$$

which is also a potential function. The corresponding extensive function is the Gibbs energy[14] $G = \int_\Omega \rho \chi dV$. From (8.98) it follows the definition of strain, conjugate to stress, and the definition of the thermodynamic forces, conjugate to the state variables s_α, as

$$\varepsilon = \rho \frac{\partial \chi}{\partial \boldsymbol{\sigma}} \quad ; \quad p_\alpha = \rho \frac{\partial \chi}{\partial s_\alpha} = -\rho \frac{\partial \psi}{\partial s_\alpha} \tag{8.99}$$

where s_α includes the damage variables and consequently p_α includes the thermodynamic damage forces (see Example 8.4).

The secant elastic compliance, which is affected by dissipative phenomena, including damage, is defined by

$$S(s_\alpha) = \rho \frac{\partial^2 \chi}{\partial \boldsymbol{\sigma}^2} \tag{8.100}$$

[14] The nomenclature of [87] has been used.

Example 8.4 *The following Gibbs free energy is proposed to represent the onset and accumulation of transverse matrix cracks resulting from transverse tension and in-plane shear loads:*

$$\chi = \frac{1}{2\,\rho}\left[\frac{\sigma_1^2}{\widetilde{E}_1} + \frac{\sigma_2^2}{(1-D_2)^2\,\widetilde{E}_2} + \frac{\sigma_6^2}{(1-D_6)^2\,2G_{12}} - \left(\frac{\widetilde{\nu}_{21}}{\widetilde{E}_2} + \frac{\widetilde{\nu}_{12}}{\widetilde{E}_1}\right)\frac{\sigma_1\sigma_2}{1-D_2}\right]$$

where $\widetilde{E}_1$, $\widetilde{E}_2$, $\widetilde{\nu}_{12}$, $\widetilde{\nu}_{21}$ and $\widetilde{G}_{12}$ are the undamaged in-plane elastic orthotropic properties of a unidirectional lamina where the subscript $()_1$ denotes the fiber direction and $()_2$ denotes the transverse direction. The damage variables D_2 and D_6 represent the effect of matrix cracks. The proposed distinguishes between active (D_{2+}) and passive damage (D_{2-}), corresponding to the opening or closure of transverse matrix cracks, respectively. The determination of the active damage variable is based on the following equation:

$$D_2 = D_{2+}\frac{\langle\sigma_2\rangle}{|\sigma_2|} + D_{2-}\frac{\langle-\sigma_2\rangle}{|\sigma_2|}$$

where $\langle x\rangle$ is defined as $\langle x\rangle = \frac{1}{2}(x+|x|)$.

For a lamina in a state of plane stress, subjected to in-plane stress only, without fiber damage ($D_1 = 0$), and using the energy equivalence principle (8.8), derive expressions for (a) the secant stiffness tensor, (b) the effective stress, and (c) the thermodynamic forces associated to the model. Use tensor components of strain $(\varepsilon_1, \varepsilon_2, \varepsilon_6)$.

Solution to Example 8.4 *The constitutive model is defined as the derivative of the Gibbs free energy with respect to the stress tensor*

$$\boldsymbol{\varepsilon} = \rho\frac{\partial\chi}{\partial\boldsymbol{\sigma}} = \mathbf{S} : \boldsymbol{\sigma}$$

where the compliance tensor $\mathbf{S}$ is defined as:

$$\mathbf{S} = \rho\frac{\partial^2\chi}{\partial\boldsymbol{\sigma}^2}$$

The compliance tensor for plane stress $\mathbf{S}$ in Voigt contracted notation is

$$\mathbf{S} = \begin{bmatrix} \dfrac{1}{\widetilde{E}_1} & -\dfrac{\widetilde{\nu}_{21}}{\widetilde{E}_2\,(1-D_2)} & 0 \\ -\dfrac{\widetilde{\nu}_{12}}{\widetilde{E}_1\,(1-D_2)} & \dfrac{1}{\widetilde{E}_2\,(1-D_2)^2} & 0 \\ 0 & 0 & \dfrac{1}{2\widetilde{G}_{12}\,(1-D_6)^2} \end{bmatrix}$$

The damage variables appear in S_{12}, S_{21}, S_{22} and S_{66} and $\epsilon_6 = \gamma_6/2$. To perform tensor products using matrix multiplications, see (A.14) and (A.20). Using the energy equivalence principle and (8.67), the compliance matrix can be written as

$$\mathbf{S} = \mathbf{M}^{-1} : \widetilde{\mathbf{S}} : \mathbf{M}^{-1}$$

where the undamaged compliance is

$$\widetilde{\mathbf{S}} = \begin{bmatrix} \dfrac{1}{\widetilde{E}_1} & -\dfrac{\widetilde{\nu}_{21}}{\widetilde{E}_2} & 0 \\ -\dfrac{\widetilde{\nu}_{12}}{\widetilde{E}_1} & \dfrac{1}{\widetilde{E}_2} & 0 \\ 0 & 0 & \dfrac{1}{2\widetilde{G}_{12}} \end{bmatrix}$$

and where the effective damage tensor $\mathbf{M}$*, written in contracted notation, multiplied by the 3×3 version of the Reuter matrix (A.13) is*

$$\mathbf{M} = \begin{bmatrix} 1 & 0 & 0 \\ 0 & (1-D_2) & 0 \\ 0 & 0 & (1-D_6) \end{bmatrix}$$

The stiffness tensor $\mathbf{C}$ *is obtained by*

$$\mathbf{C} = \mathbf{M} : \widetilde{\mathbf{C}} : \mathbf{M}$$

where, for this particular example, the secant stiffness tensor is

$$\mathbf{C} = \begin{bmatrix} \dfrac{\widetilde{E}_1}{1-\widetilde{\nu}_{21}\widetilde{\nu}_{12}} & \dfrac{\widetilde{\nu}_{12}\widetilde{E}_2\,(1-D_2)}{1-\widetilde{\nu}_{21}\widetilde{\nu}_{12}} & 0 \\ \dfrac{\widetilde{\nu}_{21}\widetilde{E}_1\,(1-D_2)}{1-\widetilde{\nu}_{21}\widetilde{\nu}_{12}} & \dfrac{\widetilde{E}_2\,(1-D_2)^2}{1-\widetilde{\nu}_{21}\widetilde{\nu}_{12}} & 0 \\ 0 & 0 & 2\widetilde{G}_{12}\,(1-D_6)^2 \end{bmatrix}$$

The effective stress $\widetilde{\boldsymbol{\sigma}}$ *is related to the nominal stress* $\boldsymbol{\sigma}$ *by the effective damage tensor* $\mathbf{M}$ *using* $\widetilde{\boldsymbol{\sigma}} = \mathbf{M}^{-1} : \boldsymbol{\sigma}$*, which yields*

$$\widetilde{\boldsymbol{\sigma}}^T = \left\{ \sigma_1, \frac{\sigma_2}{1-D_2}, \frac{\sigma_6}{1-D_6} \right\}$$

The thermodynamic forces are obtained by using $Y = \rho \partial \chi / \partial D$*, which for this particular example yield*

$$\mathbf{Y} = \left\{ \begin{array}{c} Y_1 \\ Y_2 \\ Y_6 \end{array} \right\} = \left\{ \begin{array}{c} 0 \\ \dfrac{{\sigma_2}^2}{(1-D_2)^3\,\widetilde{E}_2} - \dfrac{\sigma_1\sigma_2\widetilde{\nu}_{12}}{(1-D_2)^2\,\widetilde{E}_1} \\ \dfrac{{\sigma_6}^2}{(1-D_6)^3\,2\widetilde{G}_{12}} \end{array} \right\}$$

8.4 Kinetic Law in Three-Dimensional Space

The damage variable $\mathbf{D}$ introduced in Section 8.2 is a state variable that represents the history of what happened to the material. Next, a kinetic equation is needed to predict the evolution of damage in terms of the thermodynamic forces. Kinetic equations can be written directly in terms of internal variables as in (8.21) or as derivatives of potential functions. For three-dimensional problems, it is convenient to derive the kinetic law from a potential function, similar to the flow potential used in plasticity theory.

Two functions are needed. A damage surface $g(\mathbf{Y}(\mathbf{D}), \gamma(\delta)) = 0$ and a convex damage potential $f(\mathbf{Y}(\mathbf{D}), \gamma(\delta)) = 0$ are postulated. The damage surface delimits a region in the space of thermodynamic forces $\mathbf{Y}$ where damage does not occur because the thermodynamic force $\mathbf{Y}$ is inside the g-surface. The function $\gamma(\delta)$ accomplishes the expansion of g and f needed to model hardening. The damage potential controls the direction of damage evolution (8.102).

If the damage surface and the damage potential are identical ($g = f$), the model is said to be associated and the computational implementation is simplified significantly. For convenience, the damage surface is assumed to be separable in the variables $\mathbf{Y}$ and γ, and written as the sum (see (8.11)–(8.12))

$$g(\mathbf{Y}(\mathbf{D}), \gamma(\delta)) = \hat{g}(\mathbf{Y}(\mathbf{D})) - (\gamma(\delta) + \gamma_0) \tag{8.101}$$

where $\mathbf{Y}$ is the thermodynamic force tensor, $\gamma(\delta)$ is the hardening function, γ_0 is the damage threshold, and δ is the hardening variable.

As a result of damage, $\hat{g}$ may grow but the condition $g < 0$ must be satisfied. This is possible by *increasing* the value of the hardening function $\gamma(\delta)$, effectively allowing $\hat{g}(\mathbf{Y}(\mathbf{D}))$ to grow. Formally, the hardening function $\gamma(\delta)$ can be derived from the dissipation potential as per (8.99), (8.124), provided the form of the potential can be inferred from knowledge about the hardening process. Alternatively, the form of the function (e.g., polynomial, Prony series, etc.) can be chosen so that the complete model fits adequately the experimental data available. The latter approach is more often followed in the literature.

When $g = 0$, damage occurs, and a kinetic equation is needed to determine the magnitude and components of the damage $\dot{\mathbf{D}}$. This is accomplished by

$$\dot{\mathbf{D}} = \frac{\partial \mathbf{D}}{\partial \mathbf{Y}} = \dot{\lambda} \frac{\partial f}{\partial \mathbf{Y}} \tag{8.102}$$

where $\dot{\lambda}$ yields the magnitude of the damage increment and $\partial f / \partial \mathbf{Y}$ is a direction in $\mathbf{Y}$-space. To find the damage multiplier $\dot{\lambda}$, it is postulated that $\dot{\lambda}$ is also involved in the determination of the rate of change of the hardening variable as follows

$$\dot{\delta} = \dot{\lambda} \frac{\partial g}{\partial \gamma} \tag{8.103}$$

There are two possible situations regarding g and $\dot{\lambda}$:

i. If $g < 0$, damage is not growing and $\dot{\lambda} = 0$, so $\dot{\mathbf{D}} = 0$.

ii. If $g = 0$, damage occurs and $\dot{\lambda} > 0$, so $\dot{\mathbf{D}} > 0$.

These are summarized by the Kuhn-Tucker conditions

$$\dot{\lambda} \geq 0 \quad ; \quad g \leq 0 \quad ; \quad \dot{\lambda} g = 0 \tag{8.104}$$

The value of $\dot{\lambda}$ can be determined by the consistency condition, which leads to

$$\dot{g} = \frac{\partial g}{\partial \mathbf{Y}} : \dot{\mathbf{Y}} + \frac{\partial g}{\partial \gamma} \dot{\gamma} = 0 \; ; \quad g = 0 \tag{8.105}$$

On the other hand, the rates of thermodynamic forces and hardening function can be written as

$$\begin{aligned} \dot{\mathbf{Y}} &= \frac{\partial \mathbf{Y}}{\partial \boldsymbol{\varepsilon}} : \dot{\boldsymbol{\varepsilon}} + \frac{\partial \mathbf{Y}}{\partial \mathbf{D}} : \dot{\mathbf{D}} \\ \dot{\gamma} &= \frac{\partial \gamma}{\partial \delta} \dot{\delta} \end{aligned} \tag{8.106}$$

or in function of $\dot{\lambda}$, introducing (8.103) and (8.104) into (8.106) as follows

$$\begin{aligned} \dot{\mathbf{Y}} &= \frac{\partial \mathbf{Y}}{\partial \boldsymbol{\varepsilon}} : \dot{\boldsymbol{\varepsilon}} + \dot{\lambda} \frac{\partial \mathbf{Y}}{\partial \mathbf{D}} : \frac{\partial f}{\partial \mathbf{Y}} \\ \dot{\gamma} &= \frac{\partial \gamma}{\partial \delta} \dot{\lambda} \frac{\partial g}{\partial \gamma} \end{aligned} \tag{8.107}$$

Introducing (8.107) into (8.105) we obtain the following equation

$$\dot{g} = \frac{\partial g}{\partial \mathbf{Y}} : \left[\frac{\partial \mathbf{Y}}{\partial \boldsymbol{\varepsilon}} : \dot{\boldsymbol{\varepsilon}} + \dot{\lambda} \frac{\partial \mathbf{Y}}{\partial \mathbf{D}} : \frac{\partial f}{\partial \mathbf{Y}} \right] + \frac{\partial g}{\partial \gamma} \frac{\partial \gamma}{\partial \delta} \dot{\lambda} \frac{\partial g}{\partial \gamma} = 0 \tag{8.108}$$

Next, $\partial f / \partial \gamma = \partial g / \partial \gamma = -1$, (8.108) can be written as

$$\dot{g} = \frac{\partial g}{\partial \mathbf{Y}} : \frac{\partial \mathbf{Y}}{\partial \boldsymbol{\varepsilon}} : \dot{\boldsymbol{\varepsilon}} + \left[\frac{\partial g}{\partial \mathbf{Y}} : \frac{\partial \mathbf{Y}}{\partial \mathbf{D}} : \frac{\partial f}{\partial \mathbf{Y}} + \frac{\partial \gamma}{\partial \delta} \right] \dot{\lambda} = 0 \tag{8.109}$$

Therefore, the damage multiplier $\dot{\lambda}$ can be obtained as

$$\dot{\lambda} = \begin{cases} \mathbf{L}^d : \dot{\boldsymbol{\varepsilon}} & \text{when} \quad g = 0 \\ 0 & \text{when} \quad g < 0 \end{cases} \tag{8.110}$$

where

$$\mathbf{L}^d = - \frac{\dfrac{\partial g}{\partial \mathbf{Y}} : \dfrac{\partial \mathbf{Y}}{\partial \boldsymbol{\varepsilon}}}{\dfrac{\partial g}{\partial \mathbf{Y}} : \dfrac{\partial \mathbf{Y}}{\partial \mathbf{D}} : \dfrac{\partial f}{\partial \mathbf{Y}} + \dfrac{\partial \gamma}{\partial \delta}} \tag{8.111}$$

Equations (8.103), (8.104), and (8.110) yield the pair $\mathbf{D}, \delta$, in rate form as

$$\dot{\mathbf{D}} = \mathbf{L}^d : \frac{\partial f}{\partial Y} : \dot{\boldsymbol{\varepsilon}} \quad ; \quad \dot{\delta} = -\dot{\lambda} \tag{8.112}$$

The tangent constitutive equation can be obtained by differentiation of the constitutive equation $\boldsymbol{\sigma} = \mathbf{C} : \boldsymbol{\varepsilon}$, which yields

$$\dot{\sigma} = \mathbf{C} : \dot{\boldsymbol{\varepsilon}} + \dot{\mathbf{C}} : \boldsymbol{\varepsilon} \tag{8.113}$$

where the last term represents the stiffness reduction. Next, the last term in (8.113) can be written as

$$\dot{C} : \boldsymbol{\varepsilon} = \frac{\partial \mathbf{C}}{\partial \mathbf{D}} : \dot{\mathbf{D}} : \boldsymbol{\varepsilon} \tag{8.114}$$

Introduce (8.112) and rearrange

$$\dot{C} : \boldsymbol{\varepsilon} = \frac{\partial \mathbf{C}}{\partial \mathbf{D}} : \boldsymbol{\varepsilon} : \mathbf{L}^d : \frac{\partial f}{\partial \mathbf{Y}} : \dot{\boldsymbol{\varepsilon}} \tag{8.115}$$

Since $(\boldsymbol{\varepsilon}, \mathbf{D})$ are state variables, and thus independent variables,

$$\frac{\partial \boldsymbol{\varepsilon}}{\partial \mathbf{D}} = 0 \tag{8.116}$$

Therefore,

$$\dot{\mathbf{C}} : \boldsymbol{\varepsilon} = \frac{\partial \boldsymbol{\sigma}}{\partial \mathbf{D}} : \mathbf{L}^d : \frac{\partial f}{\partial \mathbf{Y}} : \dot{\boldsymbol{\varepsilon}} \tag{8.117}$$

Finally, reintroduce the above into (8.113) to get

$$\dot{\boldsymbol{\sigma}} = \mathbf{C}^{ed} : \dot{\boldsymbol{\varepsilon}} \tag{8.118}$$

where the *damaged tangent constitutive tensor*, $\mathbf{C}^{ed}$, can be written as follows

$$\mathbf{C}^{ed} = \begin{cases} \mathbf{C} & \text{if } \dot{\mathbf{D}} \leq 0 \\ \mathbf{C} + \dfrac{\partial \boldsymbol{\sigma}}{\partial \mathbf{D}} : \mathbf{L}^d : \dfrac{\partial f}{\partial \mathbf{Y}} & \text{if } \dot{\mathbf{D}} \geq 0 \end{cases} \tag{8.119}$$

The internal variables $\mathbf{D}, \delta$, and related variables, are found using numerical integration, usually using a return-mapping algorithm as explained in Section 8.4.1.

As explained in Sections 8.1.3 and 8.4, a number of internal material parameters are needed to define the damage surface, damage potential, and hardening functions. These parameters cannot be obtained directly from simple tests, but rather the model is *identified* by adjusting the internal parameters in such a way that model predictions fit well some observed behavior that can be quantified experimentally. Model identification is very specific to the particular model formulation, material, availability of experiments, and feasibility of conducting relevant experiments. Therefore, model identification can be explained only on a case-by-case basis, as is done in Example 8.3.

8.4.1 Return-Mapping Algorithm

A return-mapping algorithm [90–92] is used to solve for the variables $\dot{\lambda}, \dot{\delta}, \dot{\mathbf{D}}, \delta$, and $\mathbf{D}$, in numerically approximated form.

The internal variables are updated by a linearized procedure between two consecutive iterations ($k-1$ and k). The first-order linearization of (8.109) yields

$$(g)_k - (g)_{k-1} = \left(\frac{\partial g}{\partial \mathbf{Y}} : \frac{\partial \mathbf{Y}}{\partial \mathbf{D}} : \frac{\partial f}{\partial \mathbf{Y}} + \frac{\partial \gamma}{\partial \delta} \right)_{k-1} \Delta\lambda_k = 0 \tag{8.120}$$

Successful iterations yield $[g]_k = 0$ and

$$\Delta\lambda_k = \frac{-(g)_{k-1}}{\left(\dfrac{\partial g}{\partial \mathbf{Y}} : \dfrac{\partial \mathbf{Y}}{\partial \mathbf{D}} : \dfrac{\partial f}{\partial \mathbf{Y}} + \dfrac{\partial \gamma}{\partial \delta} \right)_{k-1}} \tag{8.121}$$

The complete algorithm used for a typical integration of constitutive equations is shown next:

i. Retrieve the strain $(\boldsymbol{\varepsilon})^{n-1}$ from the previous increment and the strain increment $(\Delta\boldsymbol{\varepsilon})^{n}$ for the current increment from the finite element method (FEM) code. The updated strain is calculated as

$$(\boldsymbol{\varepsilon})^{n} = (\boldsymbol{\varepsilon})^{n-1} + (\Delta\varepsilon)^{n}$$

ii. Retrieve the state variables from the previous step and start the return-mapping algorithm by setting the predictor iteration $k = 0$

$$(\mathbf{D})_0^n = (\mathbf{D})^{n-1}\,; \quad (\delta)_0^n = (\delta)^{n-1}$$

iii. Update the secant stiffness and Cauchy stress, which are used to calculate the thermodynamic forces and damage hardening at this point

$$\begin{array}{l}(\mathbf{C})_k^n = (\mathbf{M})_k^n : \widetilde{\mathbf{C}} : (\mathbf{M})_k^n \\ (\sigma)_k^n = (\mathbf{C})_k^n : (\epsilon)^n \\ (\mathbf{Y})_k^n \quad ; \quad (\gamma)_k^n\end{array}$$

iv. The damage threshold is evaluated at this point

$$(g)_k = g\left((\mathbf{Y})_k^n, (\gamma(\delta))_k^n, \gamma_0\right)$$

There are two possible cases:

(a) If $(g)_k \leq 0$, there is no damage, then $\Delta\lambda_k = 0$. Go to (viii).

(b) If $(g)_k > 0$, there is damage evolution, then $\Delta\lambda_k > 0$. Go to (v).

v. Damage evolution. Starting at iteration k, the damage multiplier is found from $(g)_k = 0$ as

$$\Delta\lambda_k = \frac{-(g)_{k-1}}{\left(\dfrac{\partial g}{\partial \mathbf{Y}}\right)_{k-1} : \left(\dfrac{\partial \mathbf{Y}}{\partial \mathbf{D}}\right)_{k-1} : \left(\dfrac{\partial f}{\partial \mathbf{Y}}\right)_{k-1} + \left(\dfrac{\partial \gamma}{\partial \delta}\right)_{k-1}}$$

vi. Update the state variables using $\Delta\lambda_k$

$$\left(D_{ij}\right)_k^n = \left(D_{ij}\right)_{k-1}^n + \Delta\lambda_k \left(\frac{\partial f}{\partial \mathbf{Y}}\right)_{k-1}$$

$$(\delta)_k^n = (\delta)_{k-1}^n + \Delta\lambda_k \left(\frac{\partial f}{\partial \gamma}\right)_{k-1} = (\delta)_{k-1}^n - \Delta\lambda_k$$

vii. End of linearized damage process. Go to (iii).

viii. Compute the tangent stiffness tensor

$$\left(\mathbf{C}^{ed}\right)^n = (\mathbf{C})^n + \left(\frac{\partial \sigma}{\partial \mathbf{D}}\right)^n : \left(\mathbf{L}^d\right)^n : \left(\frac{\partial f}{\partial \mathbf{Y}}\right)^n$$

ix. Store the stress and state variables to be used on the next load increment

$$(\boldsymbol{\sigma})^n = (\boldsymbol{\sigma})_k^n\,; \quad (\mathbf{D})^n = (\mathbf{D})_k^n\,; \quad (\delta)^n = (\delta)_k^n$$

x. End of the integration algorithm.

Example 8.5 *Implement the damage model developed in Example 8.4 into a user material subroutine for a 2-D plane stress element with damage in the directions 2 (transverse) and 6 (shear). Use a return-mapping algorithm as shown in Section 8.4.1. Furthermore, use the following damage activation function*

$$g = \hat{g} - \hat{\gamma} = \sqrt{\left(1 - \frac{G_{Ic}}{G_{IIc}}\right)\frac{Y_2 \widetilde{E}_2}{{F_{2t}}^2} + \frac{G_{Ic}}{G_{IIc}}\left(\frac{Y_2 \widetilde{E}_2}{{F_{2t}}^2}\right)^2 + \left(\frac{Y_6 \widetilde{G}_{12}}{{F_6}^2}\right)^2} - \hat{\gamma} \leq 0$$

where G_{Ic} and G_{IIc} are the critical energy release in mode I and in mode II, respectively, F_{2t} and F_6 are the transverse tensile strength and the shear strength, respectively. Also, use the following damage hardening function

$$\hat{\gamma} = \gamma + \gamma_0 = c_1\left[\exp\left(\frac{\delta}{c_2}\right) - 1\right] + \gamma_0 \quad ; \quad \gamma_0 - c_1 \leq \widehat{\gamma} \leq \gamma_0$$

where γ_0 defines the initial threshold value, c_1 and c_2 are material parameters. For this particular damage model, the model parameters for AS4/8852 carbon/epoxy are given Tables 8.1 and 8.2.

Table 8.1: Elastic and strength properties for AS4/8852 unidirectional lamina

$\widetilde{\mathbf{E}}_\mathbf{1}$	$\widetilde{\mathbf{E}}_\mathbf{2}$	$\widetilde{\mathbf{G}}_\mathbf{12}$	$\widetilde{\boldsymbol{\nu}}_\mathbf{12}$	$\mathbf{F_{2t}}$	$\mathbf{F_6}$
171.4 GPa	9.08 GPa	5.29 GPa	0.32	62.29 MPa	92.34 MPa

Table 8.2: Critical energy release, and hardening parameters for AS4/8852 unidirectional lamina

$\mathbf{G_{Ic}}$	$\mathbf{G_{IIc}}$	$\boldsymbol{\gamma_0}$	$\mathbf{c_1}$	$\mathbf{c_2}$
170 J/m^2	230 J/m^2	1.0	0.5	-1.8

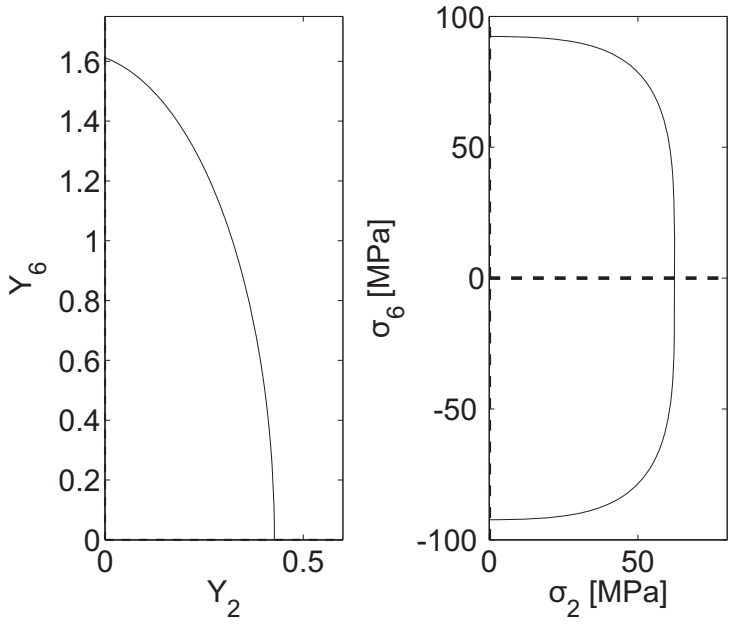

Figure 8.8: Initial damage surface in thermodynamic and stress spaces.

Solution to Example 8.5 *This model represents damage caused by transverse-tensile and in-plane-shear stress. Longitudinal tension/compression have no effect. Therefore, the model is defined in the thermodynamic force space Y_2, Y_6. The shape of the damage surface for AS4/8852 lamina is shown in Figure 8.8.*

To implement the return mapping algorithm shown in Section 8.4.1, expressions for $\partial f/\partial \mathbf{Y}$, $\partial g/\partial \mathbf{Y}$, $\partial f/\partial \gamma$, $\partial g/\partial \gamma$,$\partial \gamma/\partial \delta$, and $\partial \mathbf{Y}/\partial \mathbf{D}$ are needed.

Assuming $f = g$, the derivative of the potential function and the damage surface with respect to the thermodynamic forces is given by

$$\frac{\partial g}{\partial \mathbf{Y}} = \frac{\partial f}{\partial \mathbf{Y}} = \left\{ \begin{array}{c} 0 \\ \frac{1}{\hat{g}} \left(\left(1 - \frac{G_{Ic}}{G_{IIc}} \right) \frac{1}{4F_{2t}} \sqrt{\frac{2E_2}{Y_2}} + \frac{G_{Ic}}{G_{IIc}} \frac{E_2}{(F_{2t})^2} \right) \\ \frac{1}{\hat{g}} G_{12} \end{array} \right\}$$

and the derivative of the damage surface with respect to the damage hardening function is

$$\frac{\partial g}{\partial \gamma} = \frac{\partial f}{\partial \gamma} = -1$$

Also, the derivative of the hardening function γ with respect to conjugate variable δ is needed

$$\frac{\partial \gamma}{\partial \delta} = \frac{c_1}{c_2} \exp\left(\frac{\delta}{c_2} \right)$$

Next, the derivative of the thermodynamic forces w.r.t the internal damage variables is written as

$$\frac{\partial \mathbf{Y}}{\partial \mathbf{D}} = \left. \frac{\partial \mathbf{Y}}{\partial \mathbf{D}} \right|_{\sigma = const} + \frac{\partial \mathbf{Y}}{\partial \boldsymbol{\sigma}} : \frac{\partial \boldsymbol{\sigma}}{\partial \mathbf{D}}$$

Furthermore, the derivative of the thermodynamic forces w.r.t strain is written as

$$\frac{\partial \mathbf{Y}}{\partial \boldsymbol{\varepsilon}} = \frac{\partial \mathbf{Y}}{\partial \boldsymbol{\sigma}} : \frac{\partial \boldsymbol{\sigma}}{\partial \boldsymbol{\varepsilon}} = \frac{\partial \mathbf{Y}}{\partial \boldsymbol{\sigma}} : \mathbf{C}$$

The following are written in contracted notation as

$$\frac{\partial \mathbf{Y}}{\partial \boldsymbol{\sigma}} = \begin{bmatrix} 0 & 0 & 0 \\ \dfrac{-\sigma_2 \widetilde{\nu}_{12}}{(1-D_2)^2 \widetilde{E}_1} & \dfrac{2\sigma_2}{(1-D_2)^3 \widetilde{E}_2} - \dfrac{\sigma_1 \widetilde{\nu}_{12}}{(1-D_2)^2 \widetilde{E}_1} & 0 \\ 0 & 0 & \dfrac{2\sigma_6}{(1-D_6)^3 \widetilde{G}_{12}} \end{bmatrix}$$

and

$$\frac{\partial \boldsymbol{\sigma}}{\partial \mathbf{D}} = \begin{bmatrix} 0 & -\dfrac{\widetilde{E}_2 \widetilde{\nu}_{12}}{1-\widetilde{\nu}_{12}\widetilde{\nu}_{21}}\varepsilon_2 & 0 \\ 0 & -\dfrac{\widetilde{E}_1 \widetilde{\nu}_{21}}{1-\widetilde{\nu}_{12}\widetilde{\nu}_{21}}\varepsilon_1 - \dfrac{2\,(1-D_2)\widetilde{E}_2}{1-\widetilde{\nu}_{12}\widetilde{\nu}_{21}}\varepsilon_2 & 0 \\ 0 & 0 & -4(1-D_6)\,\widetilde{G}_{12}\varepsilon_6 \end{bmatrix}$$

The damage model is implemented in ANSYS using subroutine ***usermatps_805.f90****, available in [5], which can be used in conjunction with plain stress element (*`PLANE182` *or* `PLANE183`*) and laminate shells (*`SHELL181` *or* `SHELL281`*).*

First, follow the instructions in Appendix C.1.1 to make a dynamic link library (DLL) with ***usermatps_805.f90****, which you have to copy as* ***usermatps.f90*** *in your work directory before making the new* `DLL` *with* ***AnsUserMatEjb.bat****.*

Next, use the APDL commands shown below and available in [5] for this example:

```
/TITLE, Matrix cracking Carbon/Epoxy, FEAcomp Ex. 8.5
/PREP7              ! Start pre-processor module

!=== USERMAT DECLARATION SECTION ================================
TB,USER,1,1,13,     ! DECLARES USAGE OF USERMAT 1, MAT 1, PROPERTIES 13
TBTEMP,0
TBDATA,,171.4e3,9.08e3,0.32,,5.29e3,     ! E1,E2,nu12,nu23,G12,G23
TBDATA,,62.29,92.34,170e-3,230e-3,0.5,-1.8  ! F2t,F6,GIc,GIIc,c1,c2
TBDATA,,1           ! gamma0
TB,STAT,1,,3        ! NUMBER OF STATE VARIABLES 3
!================================================================

ET,1,182,,,3        ! PLANE182, plane elements with plane stress
R,1,1               ! Real constant #1, thickness = 1
N,1                 ! Define node 1, coordinates=0,0,0
N,2,1,0             ! Define node 2,
N,3,1,1
N,4,0,1
E,1,2,3,4           ! Generate element 1 by node 1 to 4
FINISH              ! Exit pre-processor module

/SOLU               ! Start Solution module
```

```
ANTYPE,STATIC
OUTRES,ALL,1        ! Store results for each substep
OUTRES,STAT,1       ! Store results of damage variables

D,1,all             ! Define b.c. on node 1, totally fixed

! case 1
! apply one-dimensional strain in x-direction
!D,2,UX,0.02
!D,3,UX,0.02
!D,4,UX

! case 2
! apply one-dimensional strain in y-direction
!D,2,UY
!D,3,UY,0.02
!D,4,UY,0.02

! case 3
! apply in-plane shear stress
D,2,UY
D,3,UX,0.04
D,4,UX,0.04
D,3,UY,0.0
D,4,UY,0.0

NSUBST,50,75,50     ! 50 = Number of substeps in this load step
SOLVE               ! Solve load step
FINISH              ! Exit solution module

/POST26             ! Start time-history post-process

! Stress X vs strain X
!ANSOL,2,3,S,X, UXnode     ! stress-x
!ANSOL,3,3,EPEL,X, FXnode  ! strain-x

! Stress Y vs strain Y
!ANSOL,2,3,S,Y, UXnode      ! stress-y
!ANSOL,3,3,EPEL,Y, FXnode   ! strain-y

! Stress XY vs strain XY
ANSOL,2,3,S,XY, UXnode    ! stress-xy
ANSOL,3,3,EPEL,XY, FXnode ! strain-xy

XVAR,3          ! x-graph variable: strain
PLVAR,2         ! plot, y-graph variable: stress

LINES,1000      !
PRVAR,2,3       ! list stress and strain
!FINISH         ! Exit post-process module
```

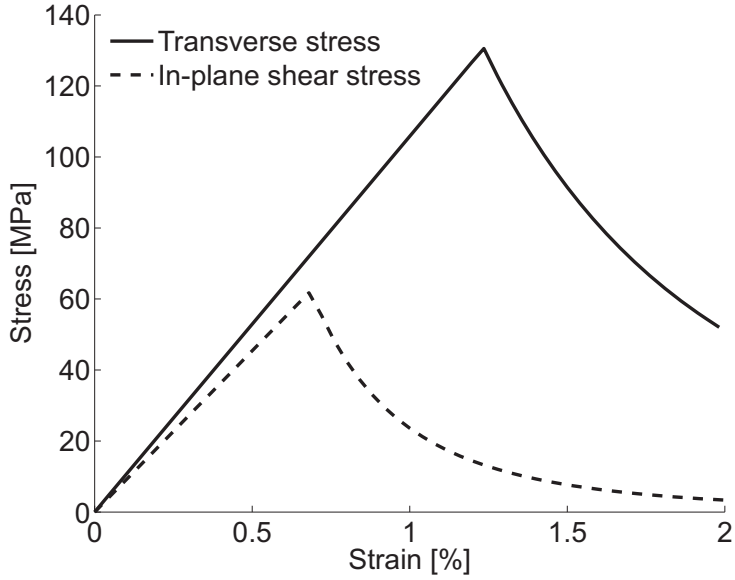

Figure 8.9: Response to in-plane shear stress and to transverse tensile stress.

The model response under one-dimensional transverse stress and under only in-plane shear stress is shown in Figure 8.9.

8.5 Damage and Plasticity

For polymer matrix composites reinforced by strong and stiff fibers, damage and its conjugate thermodynamic force can be described by second-order tensors $\mathbf{D}$ and $\mathbf{Y}$. Furthermore, the hardening processes that take place during plasticity and damage imply additional *dissipation*, so that

$$\rho\pi = T\rho\pi_s = \boldsymbol{\sigma} : \dot{\boldsymbol{\varepsilon}}^p + R\,\dot{p} + \mathbf{Y} : \dot{\mathbf{D}} + \gamma\dot{\delta} \tag{8.122}$$

where (R, p) is the thermodynamic force-flux pair associated to plastic hardening, and (γ, δ) is the thermodynamic force-flux pair associated to damage hardening, and $\rho\pi$ is the dissipation heat due to irreversible phenomena.

For the particular case of (8.122), from (8.92) and (8.99), the following definitions for the thermodynamic forces are obtained

$$\boldsymbol{\sigma} = \rho\frac{\partial\psi}{\partial\boldsymbol{\varepsilon}} = -\rho\frac{\partial\psi}{\partial\boldsymbol{\varepsilon}^p} \quad \boldsymbol{\varepsilon} = \rho\frac{\partial\chi}{\partial\boldsymbol{\sigma}} \quad \mathbf{Y} = -\rho\frac{\partial\psi}{\partial\mathbf{D}} = \rho\frac{\partial\chi}{\partial\mathbf{D}} \tag{8.123}$$

as well as definitions for the hardening equations

$$\gamma = \rho\frac{\partial\chi}{\partial\delta} = -\rho\frac{\partial\psi}{\partial\delta} = \rho\frac{\partial\pi}{\partial\delta} \qquad R = \rho\frac{\partial\chi}{\partial p} = -\rho\frac{\partial\psi}{\partial p} = \rho\frac{\partial\pi}{\partial p} \tag{8.124}$$

The additive decomposition [64]

$$\boldsymbol{\varepsilon} = \boldsymbol{\varepsilon}^e + \boldsymbol{\varepsilon}^p \tag{8.125}$$

can be rewritten taking into account that the elastic component of strain can be calculated from stress and compliance, so that

$$\boldsymbol{\varepsilon} = \mathbf{S} : \boldsymbol{\sigma} + \varepsilon^p \tag{8.126}$$

Therefore, the strain-stress law in incremental and rate form are

$$\begin{aligned} \delta\boldsymbol{\varepsilon} &= \mathbf{S} : \delta\boldsymbol{\sigma} + \delta\mathbf{S} : \boldsymbol{\sigma} + \delta\boldsymbol{\varepsilon}^p \\ \dot{\boldsymbol{\varepsilon}} &= \mathbf{S} : \dot{\boldsymbol{\sigma}} + \dot{\mathbf{S}} : \boldsymbol{\sigma} + \dot{\boldsymbol{\varepsilon}^p} \end{aligned} \tag{8.127}$$

showing that an increment of strain has three contributions: elastic, damage, and plastic. The elastic strain occurs as a direct result of an increment in stress, the damage strain is caused by the increment in compliance as the material damages, and the plastic strain occurs at constant compliance. The elastic unloading stiffness does not change due to plasticity but it reduces due to damage. Following this argument, it is customary [93] to assume that the free energy and complementary free energy can be separated as follows

$$\begin{aligned} \psi(\boldsymbol{\varepsilon}, \boldsymbol{\varepsilon}^p, p, \mathbf{D}, \delta) &= \psi^e(\boldsymbol{\varepsilon}^e, \mathbf{D}, \delta) + \psi^p(\boldsymbol{\varepsilon}^p, p) \\ \chi(\boldsymbol{\sigma}, \boldsymbol{\varepsilon}^p, p, \mathbf{D}, \delta) &= \chi^e(\boldsymbol{\sigma}, \mathbf{D}, \delta) + \chi^p(\boldsymbol{\varepsilon}^p, p) \end{aligned} \tag{8.128}$$

Suggested Problems

Problem 8.1 *Using the formulation and properties of Example 8.2, obtain a graphical representation of the evolution of strain vs. nominal stress (ε vs. σ) and the evolution of strain vs. effective stress (ε vs. $\widetilde{\sigma}$) for a point on the top surface of the beam and for another point on the bottom surface of the beam. Comment on the graphs obtained.*

Problem 8.2 *Implement a USERMAT for a one-dimensional CDM model active in the x_1-direction only. Use 2D plane stress constitutive equations. Leave the x_2-direction, Poisson's, and shear terms as linear elastic with no damage. Verify the program by recomputing Example 8.2 and the plots obtained in Problem 8.1. Note that to obtain the same values, the Poisson's ratio should be set to zero.*

Problem 8.3 *The Gibbs free energy is defined in expanded form and using Voigt contracted notation, as:*

$$\chi = \frac{1}{2\,\rho} \left[\frac{\sigma_1^2}{(1-D_1)^2\,\widetilde{E}_1} + \frac{\sigma_2^2}{(1-D_2)^2\,\widetilde{E}_2} + \frac{\sigma_6^2}{(1-D_1)\,(1-D_2)\,\widetilde{G}_{12}} - \right.$$
$$\left. - \left(\frac{\widetilde{\nu}_{21}}{\widetilde{E}_2} + \frac{\widetilde{\nu}_{12}}{\widetilde{E}_1} \right) \frac{\sigma_1 \sigma_2}{(1-D_1)\,(1-D_2)} \right]$$

Table 8.3: Elastic properties for composite material lamina

$\widetilde{E}_1$	$\widetilde{E}_2$	$\widetilde{G}_{12}$	$\widetilde{\nu}_{12}$
171.4 GPa	9.08 GPa	5.29 GPa	0.32

Table 8.4: Identification model parameters for composite material lamina

H_1	H_2	γ_0	c_1	c_2
0.024	8.36	1.0	1.5	-2.8

where $\widetilde{E}_1, \widetilde{E}_2, \widetilde{\nu}_{12}, \widetilde{\nu}_{21}$, *and* $\widetilde{G}_{12}$ *are the undamaged in-plane elastic orthotropic properties of a unidirectional lamina where the subindex* $()_1$ *denotes the fiber direction and* $()_2$ *denotes the transverse direction. (a) Obtain the secant constitutive equations,* $\mathbf{C}$ *and* $\mathbf{S}$*, using the given Gibbs free energy. (b) Obtain the thermodynamic forces* Y_1 *and* Y_2 *associated to* D_1 *and* D_2*. (c)If* $\mathbf{M}$ *is represented using Voigt contracted notation and multiplied by a Reuter matrix as*

$$\mathbf{M} = \begin{bmatrix} (1-D_1) & 0 & 0 \\ 0 & (1-D_2) & 0 \\ 0 & 0 & \sqrt{1-D_1}\sqrt{1-D_2} \end{bmatrix}$$

check if this definition of $\mathbf{M}$ *can be used as the damage effect tensor in a damage model using the principle of energy equivalence. Justify and comment on your conclusion.*

Problem 8.4 *The damage activation function, for the model shown in Problem 8.3, is defined as*

$$g := \hat{g} - \hat{\gamma} = \sqrt{{Y_1}^2 H_1 + {Y_2}^2 H_2} - (\gamma + \gamma_0)$$

where H_1 *and* H_2 *are model parameters that depend on elastic and strength material properties, and* Y_1 *and* Y_2 *are the thermodynamic forces associated to the damage variables* D_1 *and* D_2*, respectively. The damage hardening depends on* δ *according to*

$$\hat{\gamma} = \gamma + \gamma_0 = c_1 \left[\exp\left(\frac{\delta}{c_2}\right) - 1 \right] + \gamma_0$$

where γ_0 *defines the initial threshold value,* c_1 *and* c_2 *are material parameters. All necessary material parameters are shown in Tables 8.3 and 8.4.*

a) Using a flowchart diagram, describe the algorithm, with all necessary steps to implement it as a constitutive subroutine in a finite element package.

b) Compute the analytic expressions necessary to implement the model in a USERMAT.

c) Program the algorithm using the USERMAT capability for a plane stress constitutive equation.

d) Finally, using ANSYS, plot a single curve of apparent stress σ_2 *vs. apparent strain* ε_2 *for a RVE loaded only with* ε_2*.*

e) Using APDL code, describe the process used to solve the problem in ANSYS.

Chapter 9

Discrete Damage Mechanics

Prediction of damage initiation and propagation is tackled in Chapter 8 using continuum damage mechanics (CDM). Then, a particular CDM approach, called cohesive zone model (CZM), is explained in Chapter 10. Application of CZM methodology to the problem of intralaminar damage is made in *Abaqus*' progressive damage approach (PDA). A methodology to determine the critical energy release rates for transverse tension and shear using *Abaqus*' PDA is available in [56]. Also, a progressive CDM model for intralaminar damage is announced for ANSYS® 15.

Alternatives to CDM include: micromechanics of damage, crack opening displacement methods, computational micromechanics, and synergistic methods. While CDM (Chapter 8) homogenizes the damage and treats it phenomenologically, the alternative methods attempt to represent the actual geometry and characteristics of damage. *Accurate physical representation of the fracture phenomena is the most salient feature of alternative models, thus motivating their inclusion in this chapter.*

Prediction of transverse matrix cracking in laminated composites has been extensively studied for the particular case of symmetric $[0_m/90_n]_S$ laminates under membrane loads, for which matrix cracking is found in the 90° laminas (transverse laminas). Extensions to other laminate configurations such as $[0/\pm\theta/0]_S$ and $[0/\theta_1/\theta_2]_S$, models featuring cracks in the off-axis θ laminas have been developed, but they are still limited to symmetric laminates subjected to in-plane loading.

Micromechanics of Damage Models (MMD) find an approximate elasticity solution for a laminate with a discrete crack or cracks [94–115]. The solutions are approximate because kinematic assumptions are made, such as a linear [116] or bilinear [117] distribution of interlaminar shear stress through the thickness of each lamina, as well as particular spatial distributions of in-plane displacement functions [114], stresses, and so on. The state variable is the crack density in the cracking lamina, defined as the number of cracks per unit distance perpendicular to the crack surface. Therefore, the state variable is measurable. One advantage of MMD is that the reduction of laminate moduli as a function of crack density is calculated without resorting to *adjustable* parameters as in the case of CDM. In CDM, those parameters have to be found from often numerous and difficult physical experiments, thus invalidating the main premise of virtual testing.

The main disadvantage of MMD is that most of the solutions available are

limited to symmetric laminates under membrane loads with only one or two laminas cracking. A generalization to the case of multiple cracking laminas is presented in this chapter by resorting to the concept of synergistic methods, explained below.

Crack Opening Displacement (COD) methods [118–125] are based on the theory of elastic bodies with voids [126]. The distinct advantage of COD models is that the laminate stiffness can be calculated for any laminate configuration, even non-symmetric laminate stacking sequence (LSS), subject to any deformation, including bending, featuring matrix cracking in any of its laminas [127]. The main disadvantage of COD methods is that they often rely on parametric finite element analysis (FEA), and thus their applicability is limited to the range of materials, LSS, loads, and boundary conditions used in the underlying parametric/verification studies.

Numerical solutions, such as FEA, provide 3D solutions without the kinematic simplifications of MMD and COD models [105, 121, 124, 128–131]. However, FEA solutions require a new mesh and boundary conditions for each LSS, crack orientation, and so on, making them too cumbersome for practical application. Another numerical approach is Monte Carlo simulation, where the probabilistic distribution of flaws in material is considered [132–134]. Unfortunately, Monte Carlo simulations require additional parameters that have to be adjusted by fitting the results of the model to experimental damage evolution data. Such data is scarce.

Synergistic Damage Mechanics (SDM) methods combine elements of different modeling strategies such as CDM and MMD [132, 133, 135–139], bringing the best features of each of the models involved. For example, in this chapter the laminate stiffness reduction is computed via MMD methods and the generalization to multiple cracking laminas is made via CDM concepts, but unlike CDM models, no adjustable parameters are needed.

9.1 Overview

In the following we describe how to use two material properties, the fracture toughness in modes I and II, G_{Ic}, G_{IIc}, to predict the damaging behavior and transverse tensile and in-plane shear failure of a unidirectional fiber reinforced lamina embedded in a laminate. The constraining effect of adjacent laminas is taken into account, leading to apparent transverse strength F_{2t} being a function of ply thickness. The crack initiation strain, crack density evolution as a function of stress (strain) up to crack saturation, and stress redistribution to adjacent laminas is predicted accurately.

The physics of matrix cracking under transverse tension and in-plane shear is as follows. No matter how much care is taken during the production process, there are always defects in the material. These defects may be voids, microcracks, fiber–matrix debonding, and so on, but all of them can be represented by a typical matrix crack of representative size $2a_0$, as shown in Figure 9.1.

When subject to load, matrix cracks grow parallel to the fiber orientation, as shown in Figure 9.2, where it can be seen that cracks are aligned with the fiber direction in the $\pm 55^\circ$ laminas. These sets of parallel cracks reduce the stiffness of the

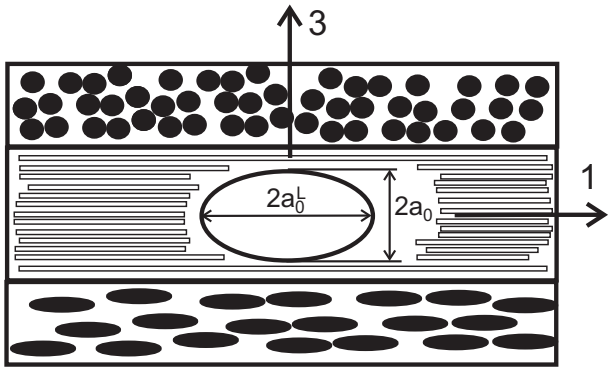

Figure 9.1: Representative crack geometry.

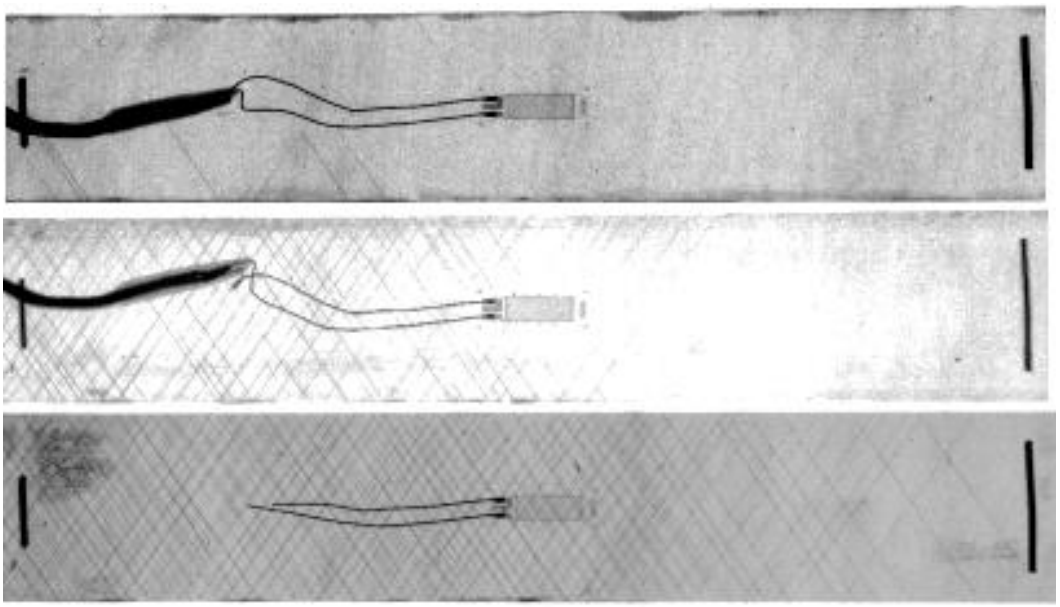

Figure 9.2: Matrix cracks in the ± 55 laminas of a $[0/\pm 55_4/0_{1/2}]_S$ laminate loaded by an increasing tensile strain (top to bottom) along the 0° direction [140].

cracked lamina, which then sheds its share of the load onto the remaining laminas. In each lamina, the damage caused by this set of parallel cracks is represented by the crack density, defined as the inverse of the distance between two adjacent cracks $\lambda = 1/(2l)$, as shown in Figure 9.3. Therefore, the crack density is the `only` state variable needed to represent the state of damage in the cracked lamina. Note that the actual, discrete cracks are modeled by the theory, which is thus named *discrete damage mechanics* (DDM).

The basic ingredients of the DDM model for transverse tension and in-plane shear damage are listed below:

i. In each lamina i, the state variable is the crack density λ_i. Two damage variables $D_2(\lambda_i)$ and $D_6(\lambda_i)$ are defined for convenience but they are not independent variables; instead, they are computed in terms of the crack density. The set of crack densities for the laminate is denoted by $\lambda = \lambda_i$ with $i = 1...N$, where N is the number of laminas in the laminate.

ii. The independent variable is the midsurface[1] strain $\epsilon = \{\epsilon_1, \epsilon_2, \gamma_{12}\}^T$.

iii. The damage activation function, which separates the damaging states from the undamaging states is written as follows

$$g = \max\left[\frac{G_I(\lambda, \epsilon, \Delta T)}{G_{Ic}}, \frac{G_{II}(\lambda, \epsilon, \Delta T)}{G_{IIc}}\right] - 1 \leq 0 \tag{9.1}$$

where $g \leq 0$ represents the undamaging domain. The critical energy release rates (ERR) are not easily found in the literature but they can be fit to available experimental data in the form of crack density vs. applied strain or laminate modulus vs. applied strain [56].

iv. The damage threshold is embedded into g, and represented by the (invariant) material properties G_{Ic}, G_{IIc}. Before damage starts, $\lambda = 0$ and (9.1) is a damage initiation criterion, similar to [141] but without mode interaction. With $\lambda = 0$, the strain for which $g = 0$ is the strain for crack initiation. Once damage starts, (9.1) becomes a damage activation function by virtue of the automatic hardening described below.

v. The hardening function is embedded into the damage activation function g. For a given value of strain, the calculated values of energy release rate $G_I(\lambda), G_{II}(\lambda)$ are monotonically decreasing functions of λ. Therefore, as soon as λ grows, $G_I(\lambda), G_{II}(\lambda)$ decrease, making $g < 0$ and thus stopping further damage until the *driving thermodynamic force*, i.e., the strain, is increased by the application of additional load [83].

vi. No damage evolution function need to be postulated, with the advantage that no new empirical parameters are needed. Simply the crack density λ

[1]The analysis presented in this section is for symmetric laminates under membrane forces. A formulation for unsymmetric laminates and/or laminates under bending is being reported in [127].

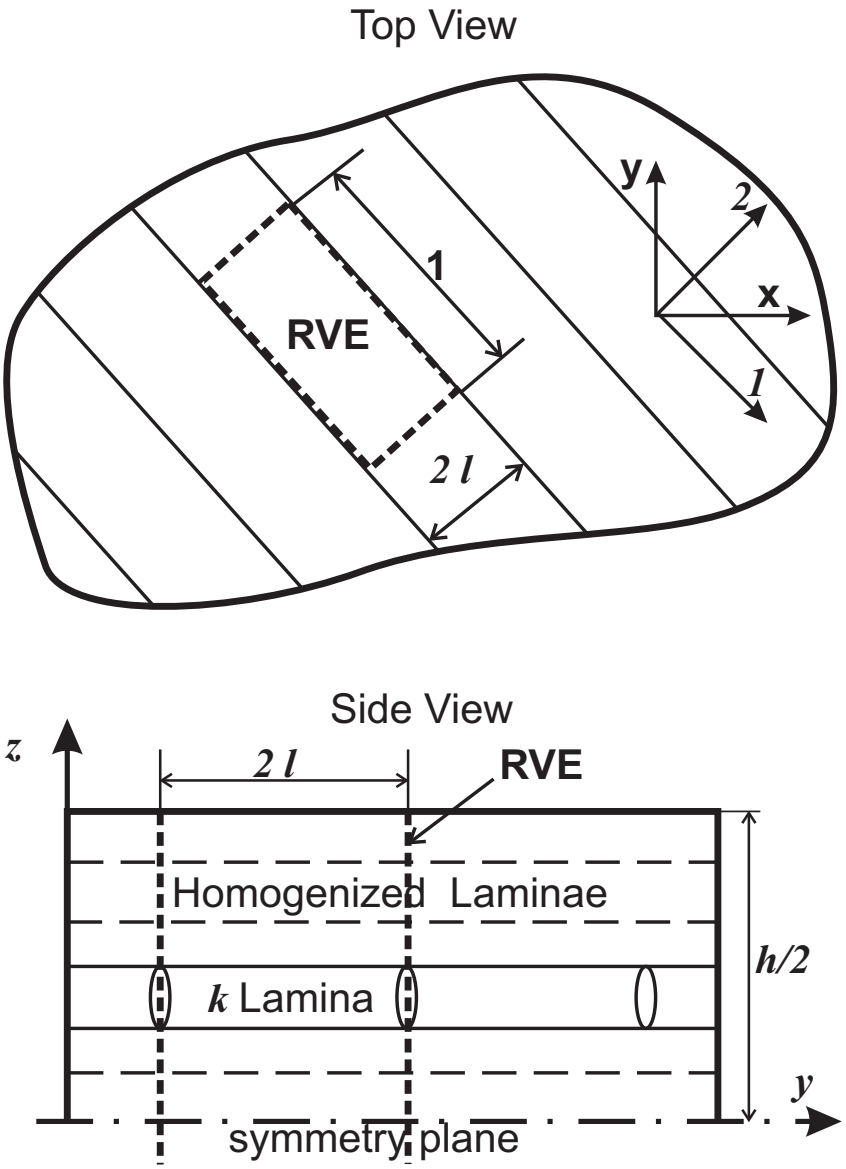

Figure 9.3: Representative unit cell used in discrete damage mechanics.

adjusts itself to a value that will set the laminate in equilibrium with the external loads for the current strain while satisfying $g = 0$. A return mapping algorithm (Section 8.4.1) achieves this by iterating until $g = 0$ and updating the crack density with iterative increments calculated as $\Delta\lambda = -g/\frac{\partial g}{\partial \lambda}$.

vii. The crack density grows until the lamina is saturated with cracks ($\lambda \to \infty$). At that point the lamina loses all of its transverse and shear stiffness ($D_2 \approx 1, D_6 \approx 1$), at which point all of the load is already transferred to the remaining laminas in the laminate. The analysis of the cracked lamina is stopped when the crack density reaches $\lambda_{lim} = 1/h_k$, where h_k is the thickness of lamina k; i.e., when cracks are closely spaced at a distance equal to the lamina thickness.

Having described the ingredients of the model, it now remains to show how to calculate the various quantities. The solution begins by calculating the degraded[2] stiffness of the laminate $Q = \mathbf{A}/h$ for a given crack density λ_k in a cracked lamina k, where $\mathbf{A}$ is the in-plane laminate stiffness matrix, and h is the thickness of the laminate.

The following conventions are used in this section:

- (i) denotes any lamina in the laminate.
- (k) denotes the cracking lamina.
- (m) denotes any lamina other than the cracking one ($m \neq k$).
- A superscript in parentheses (i) denotes the lamina number; not a power or order of differentiation.
- x_j with $j = 1, 2, 3$, denote the coordinates x_1, x_2, x_3, or $j = 1, 2, 6$ for quantities expressed in Voigt contracted notation.
- $u(x_j), v(x_j), w(x_j)$, with $j = 1, 2, 3$ are the three components of the displacement.
- *hat* $\hat{p}$ denotes the thickness average of quantity p, where the thickness is mentioned or it is obvious from context.
- *tilde* $\widetilde{p}$ denotes the virgin value of quantity p.
- *overline* $\overline{p}$ denotes the volume average of quantity p.

9.2 Approximations

Most practical laminates are symmetric and the most efficient use of them is by designing the structure to be loaded predominantly with membrane loads [1, Chapter 12]. Therefore, the solution presented here is for a symmetric laminate under membrane loads. In this case,

$$\frac{\partial w^{(i)}}{\partial x_1} = \frac{\partial w^{(i)}}{\partial x_2} = 0 \tag{9.2}$$

where $u(x_j), v(x_j), w(x_j)$, with $j = 1, 2, 3$ are the displacements of a point in lamina i as a function of the coordinates x_j with $j = 1, 2, 3$. Furthermore, the thickness

[2] Also called "damaged," "reduced," or "homogenized."

$h^{(i)}$ of the laminas are assumed to be small, so that the plane stress assumption holds

$$\sigma_3^{(i)} = 0 \tag{9.3}$$

Since all cracks are parallel to the fiber direction and practical designs avoid thick laminas, it can be expected that the cracks occupy the entire thickness of the lamina. Any crack smaller than the lamina thickness is unstable both through the lamina thickness and along the fiber direction [1, Section 7.2.1].

Since the objective is to calculate the laminate stiffness reduction due to cracks, it suffices to work with thickness averages of the variables. A thickness average is denoted by

$$\hat{\phi} = \frac{1}{h'} \int_{h'} \phi \; dx_3 \quad ; \quad h' = \int dx_3 \tag{9.4}$$

where h' can be the lamina or laminate thickness, denoted by $h^{(i)}, h$, respectively.

Specifically,

- $\hat{u}^{(i)}(x_j), \hat{v}^{(i)}(x_j), \hat{w}^{(i)}(x_j)$, are the thickness-average displacements in lamina i as a function of the in-plane coordinates x_j with $j = 1, 2$.
- $\hat{\epsilon}_1^{(i)}(x_j), \hat{\epsilon}_2^{(i)}(x_j), \hat{\gamma}_{12}^{(i)}(x_j)$, are the thickness-average strains in lamina i.
- $\hat{\sigma}_1^{(i)}(x_j), \hat{\sigma}_2^{(i)}(x_j), \hat{\tau}_{12}^{(i)}(x_j)$, are the thickness-average stress in lamina i.

Out-of-plane (intralaminar) shear stress components appear due to the the perturbation of the displacement field caused by the crack. These are approximated by linear functions through the thickness of the lamina i, as follows

$$\begin{aligned} \tau_{13}^{(i)}(x_3) &= \tau_{13}^{i-1,i} + \left(\tau_{13}^{i,i+1} - \tau_{13}^{i-1,i}\right) \frac{x_3 - x_3^{i-1,i}}{h^{(i)}} \\ \tau_{23}^{(i)}(x_3) &= \tau_{23}^{i-1,i} + \left(\tau_{23}^{i,i+1} - \tau_{23}^{i-1,i}\right) \frac{x_3 - x_3^{i-1,i}}{h^{(i)}} \end{aligned} \tag{9.5}$$

where x_3^{i-1} is the thickness coordinate at the bottom of lamina i, i.e., at the interface between lamina $i-1$ and lamina i, and $\tau_{13}^{i-1,i}$ is the shear stress at the interface between the $i-1$ and the i lamina. This assumption, which is common to several other analytical models, is called the *shear lag assumption*. The linear approximation has been shown to yield accurate results [131].

The shear lag equations are obtained from the constitutive equations for out-of-plane shear strains and stresses using weighted averages [137, Appendix A],

$$\begin{aligned} \left\{ \begin{array}{c} \hat{u}^{(i)} - \hat{u}^{(i-1)} \\ \hat{v}^{(i)} - \hat{v}^{(i-1)} \end{array} \right\} &= \frac{h^{(i-1)}}{6} \left[\begin{array}{cc} S_{45} & S_{55} \\ S_{44} & S_{45} \end{array} \right]^{(i-1)} \left\{ \begin{array}{c} \tau_{23}^{i-2,i-1} \\ \tau_{13}^{i-2,i-1} \end{array} \right\} \\ &+ \left[\frac{h^{(i-1)}}{3} \left[\begin{array}{cc} S_{45} & S_{55} \\ S_{44} & S_{45} \end{array} \right]^{(i-1)} + \frac{h^{(i)}}{3} \left[\begin{array}{cc} S_{45} & S_{55} \\ S_{44} & S_{45} \end{array} \right]^{(i)} \right] \left\{ \begin{array}{c} \tau_{23}^{i-1,i} \\ \tau_{13}^{i-1,i} \end{array} \right\} \\ &+ \frac{h^{(i)}}{6} \left[\begin{array}{cc} S_{45} & S_{55} \\ S_{44} & S_{45} \end{array} \right]^{(i)} \left\{ \begin{array}{c} \tau_{23}^{i,i+1} \\ \tau_{13}^{i,i+1} \end{array} \right\} \end{aligned} \tag{9.6}$$

Inverting (9.6), the intralaminar stresses are written in terms of displacements at the interfaces, as follows

$$\begin{aligned}\tau_{23}^{i,i+1}-\tau_{23}^{i-1,i}&=\sum_{j=1}^{n-1}\left[[H]^{-1}{}_{2i-1,2j-1}-[H]^{-1}{}_{2i-3,2j-1}\right]\left\{\hat{u}^{(j+1)}-\hat{u}^{(j)}\right\}\\&\quad+\left[[H]^{-1}{}_{2i-1,2j}-[H]^{-1}{}_{2i-3,2j}\right]\left\{\hat{v}^{(j+1)}-\hat{v}^{(j)}\right\}\\\tau_{13}^{i,i+1}-\tau_{13}^{i-1,i}&=\sum_{j=1}^{n-1}\left[[H]^{-1}{}_{2i,2j-1}-[H]^{-1}{}_{2i-2,2j-1}\right]\left\{\hat{u}^{(j+1)}-\hat{u}^{(j)}\right\}\\&\quad+\left[[H]^{-1}{}_{2i,2j}-[H]^{-1}{}_{2i-2,2j}\right]\left\{\hat{v}^{(j+1)}-\hat{v}^{(j)}\right\}\end{aligned}\tag{9.7}$$

in terms of the $2(N-1)$ by $2(N-1)$ coefficient matrix H.

9.3 Lamina Constitutive Equation

The stress-strain law for the cracking lamina k is that of an intact material, i.e.,

$$\hat{\sigma}_i^{(k)}=\widetilde{Q}_{ij}^{(k)}\left(\hat{\epsilon}_j^{(k)}-\alpha_j^{(k)}\Delta T\right)\tag{9.8}$$

where $\alpha^{(k)}$ is the coefficient of thermal expansion (CTE) of lamina k, $\sigma_i^{(k)}=\left\{\sigma_1^{(k)},\sigma_2^{(k)},\tau_{12}^{(k)}\right\}^T$, and *tilde* denotes a virgin property. The strain-displacement equations are

$$\epsilon^{(k)}=\left\{\begin{array}{l}\epsilon_1^{(k)}=u_{,1}^{(k)}\\\epsilon_2^{(k)}=v_{,2}^{(k)}\\\gamma_{12}^{(k)}=u_{,2}^{(k)}+v_{,1}^{(k)}\end{array}\right\}\tag{9.9}$$

For the remaining laminas ($m\neq k$), the constitutive equations can be obtained using (9.8) and the stiffness matrix $Q_{ij}^{(m)}$, written in terms of their previously calculated damage values $D_2^{(m)},D_6^{(m)}$, defined in (9.32), and rotated to the k coordinate system using the usual transformation equations [1, Section 5.4]

$$Q^{(m)}=[T(-\theta)]\left[\begin{array}{ccc}\widetilde{Q}_{11}^{(m)}&1-D_2^{(m)}\widetilde{Q}_{12}^{(m)}&0\\1-D_2^{(m)}\widetilde{Q}_{12}^{(m)}&\left(1-D_2^{(m)}\right)\widetilde{Q}_{22}^{(m)}&0\\0&0&\left(1-D_6^{(m)}\right)\widetilde{Q}_{66}^{(m)}\end{array}\right][T(-\theta)]^T\tag{9.10}$$

9.4 Displacement Field

The objective now is to solve for the average displacements $\hat{u}^{(i)}(x_j),\hat{v}^{(i)}(x_j);j=1,2$, in all laminas i for a given crack density set λ and applied strain ϵ. Taking into

account that the intralaminar shear stresses are assumed to vary linearly through the thickness of each lamina, the equilibrium equations (1.15) for each lamina can be written as follows

$$\hat{\sigma}^{(i)}_{1,1} + \hat{\tau}^{(i)}_{12,2} + \left(\hat{\tau}^{i,i+1}_{13} - \hat{\tau}^{i-1,i}_{13}\right)/h_i = 0 \tag{9.11}$$

$$\hat{\tau}^{(i)}_{12,1} + \hat{\sigma}^{(i)}_{2,2} + \left(\hat{\tau}^{i,i+1}_{23} - \hat{\tau}^{i-1,i}_{23}\right)/h_i = 0 \tag{9.12}$$

Using the the strain-displacement equations (9.9), the constitutive equations (9.8), and the shear lag equations (9.7) into the equilibrium equations (9.11)–(9.12) leads to a system of $2N$ partial differential equations (PDE) in $\hat{u}^{(i)}(x_j), \hat{v}^{(i)}(x_j)$. The PDE has particular solutions of the form

$$\begin{aligned} \hat{u}^{(i)} &= a_i \sinh \lambda_e x_2 + a\ x_1 + b\ x_2 \\ \hat{v}^{(i)} &= b_i \sinh \lambda_e x_2 + b\ x_1 + a^* x_2 \end{aligned} \tag{9.13}$$

where e is the eigenvalue number. The general solution can be written as

$$\begin{Bmatrix} \hat{u}^{(1)} \\ \hat{u}^{(2)} \\ . \\ . \\ . \\ \hat{u}^{(n)} \\ \hat{v}^{(1)} \\ \hat{v}^{(2)} \\ . \\ . \\ . \\ \hat{v}^{(n)} \end{Bmatrix} = \sum_{e=1}^{2N} A_e \begin{Bmatrix} a_1 \\ a_2 \\ . \\ . \\ . \\ a_n \\ b_1 \\ b_2 \\ . \\ . \\ . \\ b_n \end{Bmatrix}_e sinh\left(\eta_e x_2\right) + \begin{Bmatrix} a \\ a \\ . \\ . \\ . \\ a \\ b \\ b \\ . \\ . \\ . \\ b \end{Bmatrix} x_1 + \begin{Bmatrix} b \\ b \\ . \\ . \\ . \\ b \\ a^* \\ a^* \\ . \\ . \\ . \\ a^* \end{Bmatrix} x_2 \tag{9.14}$$

which substituted into the PDE leads to the eigenvalue problem

$$\begin{bmatrix} \alpha_1 & \beta_1 \\ \alpha_2 & \beta_2 \end{bmatrix} \begin{Bmatrix} a_j \\ b_j \end{Bmatrix} + \eta^2 \begin{bmatrix} \zeta_{26} & \zeta_{22} \\ \zeta_{66} & \zeta_{26} \end{bmatrix} \begin{Bmatrix} a_j \\ b_j \end{Bmatrix} = \begin{Bmatrix} 0 \\ 0 \end{Bmatrix} \tag{9.15}$$

where $j = 1...2N$; η are the $2N$ eigenvalues and $\{a_j, b_j\}^T$ are the $2N$ eigenvectors of (9.15).

It turns out that two of the eigenvalues are always zero (corresponding to the linear terms in (9.14)), which can be taken to be the last two in the set, thus remaining only $2N-2$ independent solutions. Then, the general solution of the PDE system is built as the linear combination of the $2N-2$ independent solutions as follows

$$\begin{Bmatrix} \hat{u}^{(i)} \\ \hat{v}^{(i)} \end{Bmatrix} = \sum_{e=1}^{2N-2} A_e \begin{Bmatrix} a_i \\ b_i \end{Bmatrix}_e \sinh\left(\eta_e x_2\right) + \begin{Bmatrix} a \\ b \end{Bmatrix} x_1 + \begin{Bmatrix} b \\ a^* \end{Bmatrix} x_2 \tag{9.16}$$

where A_e are unknown coefficients in the linear combination. It can be seen that the general solution contains $2N+1$ unknown coefficients, including the scalars a, b, a^*, and the sets A_e with $e = 1...2N-2$. To determine these coefficients, one needs $2N+1$ boundary conditions on the boundary of the representative volume element (RVE) in Figure 9.3. Note the that RVE spans a unit length along the fiber direction x_1, a distance $2l$ between successive cracks (along x_2) and the whole thickness h of the symmetric laminate.

Two very important parameters are introduced through the boundary conditions, namely the crack density λ and the stress $\hat{\sigma} = \mathbf{N}/h$ applied to the laminate, where $\mathbf{N}$ is the in-plane force per unit length.[3] The crack density enters through the dimension of the RVE, which has a width of $2l = 1/\lambda$. The applied stress (or strain) enters through the force equilibrium on the RVE. In summary, there are $2N+1$ boundary conditions that lead to a system of $2N+1$ algebraic equations that can be solved for the $2N+1$ coefficients in (9.16). Therefore, the average displacements in all laminas are now known from (9.16) for given values of crack density λ and applied load $\hat{\sigma} = \mathbf{N}/h$.

9.4.1 Boundary Conditions for $\Delta T = 0$

First consider the case of mechanical loads and no thermal loads. To find the values of $A_e, a, a*, b$, the following boundary conditions are enforced: (a) stress-free at the crack surfaces, (b) external loads, and (c) homogeneous displacements. The boundary conditions are then assembled into an algebraic system as follows

$$[B]\left\{A_e, a, a^*, b\right\}^T = \{F\} \tag{9.17}$$

where $[B]$ is the coefficient matrix of dimensions $2N+1$ by $2N+1$; $\left\{A_e, a, a^*, b\right\}^T$ represents the $2N+1$ unknown coefficients, and $\{F\}$ is the right hand side (RHS) or force vector, also of dimension $2N+1$.

(a) Stress-Free at the Crack Surfaces

The surfaces of the cracks are stress-free

$$\int_{-1/2}^{1/2} \hat{\sigma}_2^{(k)}(x_1, l)\,\mathrm{d}x_1 = 0 \tag{9.18}$$

$$\int_{-1/2}^{1/2} \hat{\tau}_{12}^{(k)}(x_1, l)\,\mathrm{d}x_1 = 0 \tag{9.19}$$

[3] Not to be confused with the number of laminas N.

(b) External Loads

In the direction parallel to the surface of the cracks (fiber direction x_1) the load is supported by all the laminas

$$\frac{1}{2l}\sum_{i=1}^{N} h_i \int_{-l}^{l} \hat{\sigma}_1^{(i)}(1/2, x_2)dx_2 = h\hat{\sigma}_1 \tag{9.20}$$

In the direction normal to the crack surface (x_2 direction) only the uncracking (homogenized) laminas carry load

$$\sum_{m\neq k} h_m \int_{1/2}^{1/2} \hat{\sigma}_2^{(m)}(x_1, l)\, dx_1 = h\hat{\sigma}_2 \tag{9.21}$$

$$\sum_{m\neq k} h_m \int_{1/2}^{1/2} \hat{\tau}_{12}^{(m)}(x_1, l)dx_1 = h\hat{\tau}_{12} \tag{9.22}$$

(c) Homogeneous Displacements

For a homogenized symmetric laminate, membrane loads produce a uniform displacement field through the thickness, i.e., all the uncracking laminas are subjected to the same displacement

$$\hat{u}^{(m)}(x_1, l) = \hat{u}^{(r)}(x_1, l) \quad ; \quad \forall m \neq k \tag{9.23}$$

$$\hat{v}^{(m)}(x_1, l) = \hat{v}^{(r)}(x_1, l) \quad ; \quad \forall m \neq k \tag{9.24}$$

where r is an uncracked lamina taken as the reference. In the computer implementation, lamina 1 is taken as the reference unless lamina 1 is cracking, in which case lamina 2 is taken as the reference lamina.

9.4.2 Boundary Conditions for $\Delta T \neq 0$

Next, consider the case of thermal loads, which add a constant term to the boundary conditions. Constant terms do not affer the matrix $[B]$, but rather subtract from

the forcing vector $\{F\}$, as follows

$$\{\Delta F\}_{\Delta T\neq 0} = \left\{ \begin{array}{c} \Delta T \sum\limits_{j=1,2,6} \bar{Q}_{1j}^{(k)} \bar{\alpha}_j^{(k)} \\ \Delta T \sum\limits_{j=1,2,6} \bar{Q}_{1j}^{(k)} \bar{\alpha}_j^{(k)} \\ \Delta T \sum\limits_{i\neq(k)} \sum\limits_{j=1,2,6} \bar{Q}_{1j}^{(i)} \bar{\alpha}_j^{(i)} \\ \Delta T \sum\limits_{i\neq k} \sum\limits_{j=1,2,6} \bar{Q}_{2j}^{(i)} \bar{\alpha}_j^{(i)} \\ \Delta T \sum\limits_{i\neq k} \sum\limits_{j=1,2,6} \bar{Q}_{6j}^{(i)} \bar{\alpha}_j^{(i)} \\ 0 \\ 0 \\ \cdots \\ \cdots \\ 0 \\ 0 \end{array} \right\} \tag{9.25}$$

In this way, the strain calculated for a unit thermal load ($\Delta T = 1$) is the degraded CTE of the laminate for the current crack density set λ.

9.5 Degraded Laminate Stiffness and CTE

In this section, we calculate the degraded stiffness of the laminate $Q = \mathbf{A}/h$ for a given crack density λ_k in a cracked lamina k, where $\mathbf{A}$ is the in-plane laminate stiffness matrix, and h is the thickness of the laminate. First, the thickness-averaged strain field in all laminas can be obtained by using the kinematic equations (9.9), namely by differentiating (9.16). Then, the compliance of the laminate S in the coordinate system of lamina k can be calculated one column at a time by solving for the strains (9.9) for three load cases, *a, b,* and *c,* all with $\Delta T = 0$, as follows

$${}^a\hat{\sigma} = \left\{ \begin{array}{c} 1 \\ 0 \\ 0 \end{array} \right\}; \quad {}^b\hat{\sigma} = \left\{ \begin{array}{c} 0 \\ 1 \\ 0 \end{array} \right\}; \quad {}^c\hat{\sigma} = \left\{ \begin{array}{c} 0 \\ 0 \\ 1 \end{array} \right\}; \quad \Delta\, T = 0 \tag{9.26}$$

Since the three applied stress states are unit values, for each case, *a, b, c,* the volume average of the strain (9.9) represents one column in the laminate compliance matrix

$$S = \begin{bmatrix} {}^a\epsilon_x & {}^b\epsilon_x & {}^c\epsilon_x \\ {}^a\epsilon_y & {}^b\epsilon_y & {}^c\epsilon_y \\ {}^a\gamma_{xy} & {}^b\gamma_{xy} & {}^c\gamma_{xy} \end{bmatrix} \tag{9.27}$$

where x, y, are the coordinates of lamina k (Figure 9.3). Next, the laminate stiffness in the coordinate system of lamina k is

$$Q = S^{-1} \tag{9.28}$$

To get the degraded CTE of the laminate, one sets $\hat{\sigma} = \{0, 0, 0\}^T$ and $\Delta T = 1$. The resulting strain is equal to the CTE of the laminate, i.e., $\{\alpha_x, \alpha_y, \alpha_{xy}\}^T = \{\epsilon_x, \epsilon_y, \gamma_{xy}\}^T$.

9.6 Degraded Lamina Stiffness

The stiffness of lamina m, with $m \neq k$, in the coordinate system of lamina k (see Figure 9.3) is given by (9.10) in terms of the previously calculated values $D_2^{(m)}, D_6^{(m)}$, given by (9.32). The stiffness of the cracking lamina $Q^{(k)}$ is yet unknown. Note that all quantities are expressed in the coordinate system of lamina k.

The laminate stiffness is defined by the contribution of the cracking lamina k plus the contribution of the remaining $N-1$ laminas, as follows

$$Q = Q^{(k)} \frac{h_k}{h} + \sum_{m=1}^{n} (1 - \delta_{mk}) Q^{(m)} \frac{h_m}{h} \tag{9.29}$$

where the *delta* Dirac is defined as $\delta_{mk} = 1$ if $m = k$, otherwise 0. The left-hand side (LHS) of (9.29) is known from (9.28) and all values of $Q^{(m)}$ can be easily calculated since the m laminas are not cracking at the moment. Therefore, one can calculate the degraded stiffness $Q^{(k)}$ of lamina k as follows

$$Q^{(k)} = \frac{h}{h_k} \left[Q - \sum_{m=1}^{n} (1 - \delta_{mk}) Q^{(m)} \frac{h_m}{h} \right] \tag{9.30}$$

where Q without a superscript is the stiffness of the laminate.

To facilitate later calculations, the stiffness $Q^{(k)}$ can be written using concepts of continuum damage mechanics (Section 8.2) in terms of the stiffness of the undamaged lamina and damage variables $D_2^{(k)}, D_6^{(k)}$, as follows

$$Q^{(k)} = \begin{bmatrix} \widetilde{Q}_{11}^{(k)} & (1 - D_2)\, \widetilde{Q}_{12}^{(k)} & 0 \\ (1 - D_2)\, \widetilde{Q}_{12}^{(k)} & (1 - D_2)\, \widetilde{Q}_{22}^{(k)} & 0 \\ 0 & 0 & (1 - D_6)\, \widetilde{Q}_{66}^{(k)} \end{bmatrix} \tag{9.31}$$

with $D_j^{(k)}$ calculated for a given crack density λ_k and applied strain ϵ^0, as follows

$$D_j^{(k)}(\lambda_k, \epsilon^0) = 1 - Q_{jj}^{(k)} / \widetilde{Q}_{jj}^{(k)} \quad ; \quad j = 2, 6; \text{ no sum on } j \tag{9.32}$$

where $\widetilde{Q}^{(k)}$ is the original value of the undamaged property and $Q^{(k)}$ is the degraded[4] value computed in (9.30), both expressed in the coordinate system of lamina k.

[4]Homogenized.

The coefficient of thermal expansion of the cracking lamina k is calculated in a similar fashion, as follows

$$\alpha^{(k)} = \frac{1}{t^{(k)}} S^{(k)} \left(hQ\alpha - \sum_{m \neq k} h^{(m)} Q^{(m)} \alpha^{(m)} \right) \tag{9.33}$$

with $S = \left[Q^{(k)} \right]^{-1}$. The corresponding thermal damage is calculated as

$$D_j^{\alpha(k)} = 1 - {\alpha_j}^{(k)} / \widetilde{\alpha}_j^{(k)} \quad ; \quad j = 2, 6 \tag{9.34}$$

9.7 Fracture Energy

Under displacement control, the energy release rate (ERR) is defined as the partial derivative of the strain energy U with respect to the crack area A (see (10.1)). According to experimental observations on laminated, brittle matrix composites (e.g., using most toughened epoxy matrices), cracks develop suddenly over a finite length, and thus are not infinitesimal. Then, Griffith's energy principle is applied on its discrete (finite) form in order to describe the observed, discrete (finite) behavior of crack growth, as follows

$$\begin{aligned} G_I &= -\frac{\Delta U_I}{\Delta A} \\ G_{II} &= -\frac{\Delta U_{II}}{\Delta A} \end{aligned} \tag{9.35}$$

where $\Delta U_I, \Delta U_{II}$, are the change in laminate strain energy during mode I and mode II finite crack growth, respectively; and ΔA is the is the newly created (finite) crack area, which is one half of the new crack surface. Counting crack area as one-half of crack surface is consistent with the classical fracture mechanics convention for which fracture toughness G_c is twice of Griffith's surface energy γ_c.

To calculate the ERR, it is convenient to use the laminate stiffness Q_{ij} in the coordinate system (c.s.) of the cracked lamina, because in this way, the ERR can be decomposed into opening and shear modes. Since the laminate stiffness is available from the analysis as a function of crack densityλ, the ERR can be calculated, for a fixed strain level (load), and using [111] and [142, Section 3.2.10], into (9.35), we arrive at

$$G_I = -\frac{V}{2\Delta A} \left(\epsilon_2 - \alpha_2 \Delta T \right) \Delta Q_{2j} \left(\epsilon_j - \alpha_j \Delta T \right) \quad ; \quad \text{opening mode} \tag{9.36}$$

$$G_{II} = -\frac{V}{2\Delta A} \left(\epsilon_6 - \alpha_6 \Delta T \right) \Delta Q_{6j} \left(\epsilon_j - \alpha_j \Delta T \right) \quad ; \quad \text{shear mode} \tag{9.37}$$

where $V, \Delta A$, are the volume of the RVE and the increment of crack area, respectively; ΔQ_{ij} is the change in laminate stiffness corresponding to the change in crack

area experienced; and all quantities are *laminate average* quantities expressed in the c.s of the cracked lamina in order to allow for ERR mode decomposition [111].

In the current implementation of the model, which is used in Example 9.1, $\Delta A = h_k$ is the area of one new crack appearing halfway between two existing cracks. In this case the crack density doubles and $\Delta Q = Q(2\lambda) - Q(\lambda) < 0$. Alternative crack propagation strategies are considered in [127].

It can be seen that the proposed methodology provides the key ingredients for the computation of the ERR; namely the degraded stiffness and degraded CTE of the laminate, both as a function of crack density.

The damage activation function (9.1) can now be calculated for any value of λ and applied strain $\epsilon_x, \epsilon_y, \gamma_{xy}$. Note that the computation of the ERR components derives directly from the displacement solution (9.16) for a discrete crack (Figure 9.3). When this formulation is used along with the finite element method (FEM), it does not display mesh dependency on the solution and does not require the arbitrary specification of a characteristic length [138], in contrast to formulations based on smeared crack approximations [56]. The effect of residual thermal stresses is incorporated into the formulation. The code is available as a user material for ANSYS [138], which is used in Example 9.1. Other implementations include a shell user element for ANSYS [139] and a user general section (UGENS) for *Abaqus*$^{\text{TM}}$.

9.8 Solution Algorithm

The solution algorithm consists of (a) strain steps, (b) laminate-iterations, and (c) lamina-iterations. The state variables for the laminate are the array of crack densities for all laminas i and the membrane strain ϵ. At each load (strain) step, the strain on the laminate is increased and the laminas are checked for damage.

9.8.1 Lamina Iterations

When matrix cracking is detected in lamina k, a return-mapping algorithm (RMA) (Section 8.4.1) is invoked to iterate and adjust the crack density λ_k in lamina k in such a way that g_k returns to zero while maintaining equilibrium between the external forces and the internal forces in the laminas. The iterative procedure works as follows. At a given strain level ϵ for the laminate and given λ_k for lamina k, calculate the value of the damage activation function g_k and the damage variables, which are both functions of λ_k. The RMA calculates the increment (decrement) of crack density as

$$\Delta\lambda_k = -g_k / \frac{\partial g_k}{\partial \lambda} \tag{9.38}$$

until $g_k = 0$ is satisfied within a given tolerance, for all $k = 1...n$, where n is the number of laminas in the laminate. The analysis starts with a negligible value of crack density present in all laminas ($\lambda = 0.02$ cracks/mm were used in the examples).

Table 9.1: Properties for Example 9.1

Property	Value
E_1 [GPa]	44.7
E_2 [GPa]	12.7
G_{12} [GPa]	5.8
ν_{12}	0.297
ν_{23}	0.41
Ply thickness [mm]	0.144
G_{Ic} $[kJ/m^2]$	0.254
G_{IIc} $[kJ/m^2]$	1.400
CTE_1 [1E-6/^circC]	3.7
CTE_2 [1E-6/°C]	30
ΔT[°C]	0

9.8.2 Laminate Iterations

To calculate the stiffness reduction of a cracked lamina (k-lamina), all of the other laminas (m-laminas) in the laminate are considered not damaging during the course of lamina-iterations in lamina k, but with damaged properties calculated according to the current values of their damage variables $D_i^{(m)}$. Given a trial value of λ_k, the analytical solution provides $g_k, D_i^{(k)}$, for lamina k assuming all other laminas do not damage while performing lamina iterations in lamina k. Since the solution for lamina k depends on the stiffness of the remaining laminas, a converged iteration for lamina k does not guarantee convergence for the same lamina once the damage in the remaining laminas is updated. In other words, within a given strain step, the stiffness and damage of all the laminas are interrelated and they must all converge. This can be accomplished by laminate-iterations; that is, looping over all laminas repeatedly until all laminas converge to $g = 0$ for all k.

Example 9.1 *Consider a* $[0/90_8/0/90_8/0]$ *laminate made of Glass/Epoxy with properties given in Table 9.1 subjected to a membrane strain* $\epsilon_x \neq 0, \epsilon_y = \gamma_{xy} = 0$. *Visualize the crack density in lamina* $k = 2$ *for an uniform applied strain* $\epsilon_x = 0.48\%$. *Also, plot the average laminate stress* $\sigma_x = N_x/h$, *where* N_x, h *are the stress resultant and the total laminate thickness, respectively.*

Solution to Example 9.1 *Since ANSYS does not have a built-in capability for calculating crack density, we have to use a plugin. In this case, we use a user material subroutine for a state of plane stress that implements Discrete Damage Mechanics. The DDM plugin is available in [5, USERMATLib.DLL] and the theory behind it is explained in this chapter.*

The DDM plugin employs $3+9N$ *parameters, and* $3N$ *state variables, as follows:*

- *The whole laminate thickness, which will be entered later as a REAL CONSTANT associated to the MESH. This is not really a requirement for the plugin, but ANSYS needs this value for plane stress elements, both PLANE and SHELL, so it is mentioned here as part of the requirements.*

– *The plugin requires an input of* $3 + 9 * N$ *material properties, where* N *is the number of laminas in the symmetric part of the laminate, i.e., in one half of the LSS. The properties are ordered as follows, starting with the first lamina,* $k = 1$ *(bottom surface), and continuing until the lamina* N *(middle surface):*

G_{Ic} *Critical value of ERR in mode I.*

G_{IIc} *Critical value of ERR in mode II. Use* $G_{IIc} > 4\ G_{Ic}$ *if data is not available.*

ΔT *Change in temperature from the temperature at which* G_{Ic}, G_{IIc}, *were measured to the operating temperature.*

E_1 *Longitudinal modulus.*

E_2 *Transverse modulus.*

G_{12} *In-plane shear modulus.*

ν_{12} *In-plane Poisson's ratio.*

ν_{23} *Intralaminar Poisson's ratio. Note;* $G_{23} = E_2/2/(1 + \nu_{23})$.

α_1 *Longitudinal coefficient of thermal expansion.*

α_2 *Transverse coefficient of thermal expansion.*

θ_k *Lamina orientation with respect to the laminate c.s.*

t_k *Lamina thickness.*

– *Next, the plugin calculates* $3 * N$ *state variables, starting with the first lamina,* $k = 1$ *(bottom surface), and continuing until the lamina* N *(middle surface):*

λ_k *Crack density in lamina* k.

D_2 *Transverse damage, lamina* k.

D_6 *Shear damage, lamina* k.

This example illustrates how to create a model using ANSYS/APDL, run the Job with the plugin, and visualize the results. Instructions on how to use a `.dll` *with ANSYS are given in Appendix C.1.1. The APDL input file is available in [5, FEAcomp_Ex901.inp] and it is fully explained next.*

i. Parametric modeling in APDL
First, the model is set parametrically, as follows. True parameters are:

– *The applied strain at the end of the time step,*
– *The initial crack density. Note that DDM requires a small amount of damage (material defects, etc.) to start the analysis.*
– *The shell dimensions, which in this case it is a square.*
– *The ply thickness. A lamina may use one or more plies to achieve the desired thickness.*
– *The number of laminas (call layers in the ANSYS documentation).*

– *The number of properties, which for DDM is calculated in terms of the number of laminas.*

The APDL code to set up the model parametrically is shown next.

```
/TITLE, FEAcomp Ex. 9.01, USERMATLib.DLL
/PREP7              ! Start pre-processor module
!=== PARAMETERS ================================================
appliedStrain = 2.      ! percent
L0 = 0.02               ! initial crack density
ShellDimensionX = 1.    ! model dimensions
ShellDimensionY = 1.    ! mm
tk =.144                ! ply thickness
NL = 3                  ! number layers half laminate
Nprops = 3+9*NL         ! # material properties
!=== NEXT VALUES GO IN TBDATA ==================================
GIc  = .254
GIIc = 1.E16
deltaT = 0.
E1 = 44700              ! MPa
E2 = 12700
G12= 5800
nu12 =.297
nu23 =.410
CTE1 =3.7
CTE2 =30.
!Angle      with TBDATA for each layer
!Thickness  with TBDATA for each layer
```

ii. TBDATA
The $3 + 9N$ required parameters are supplied via TBDATA line in the APDL file, as follows:

```
!=== USERMAT DECLARATION SECTION ================================
TB,USER,1,1,Nprops,     ! DECLARES USAGE OF USERMAT 1, MAT 1,
TBTEMP,0                ! ref. temperature
TBDATA,,GIc,GIIc,detaT,E1,E2,G12    ! 6 values per TBDATA line
TBDATA,,nu12,nu23,CTE1,CTE2,0,tk
TBDATA,,E1,E2,G12,nu12,nu23,CTE1
TBDATA,,CTE2,90,8*tk,E1,E2,G12
TBDATA,,nu12,nu23,CTE1,CTE2,0,tk/2
TB,STAT,1,,3*NL     ! NUMBER OF STATE VARIABLES
```

To complete the USERMAT declaration, the plugin requires the $3N$ state variables to be initialized to a small value, i.e.,

```
! INITIALIZE THE STATE VARIABLES
TBDATA,,L0,L0,L0,L0,L0,L0
TBDATA,,L0,L0,L0
```

iii. Creating the mesh
Since the strain field inside the shell is uniform (in x and y), we use only one PLANE182 element to model a unit cell with dimensions $a = 100 \times b = 100\ mm$, where a, b, are the dimensions of the model along the x, y, directions respectively.

```
!=== MESH ==========================================================
ET,1,182,,,3            ! PLANE182, plane elements with plane stress
R,1,2*NL*tk             ! Real const. #1, thickness of whole laminate
N,1                     ! Define node 1, coordinates=0,0,0
N,2,ShellDimensionX,0   ! Define node 2,
N,3,ShellDimensionX,ShellDimensionY
N,4,0,ShellDimensionY
E,1,2,3,4               ! Generate element 1 by node 1 to 4
FINISH                  ! Exit pre-processor module
```

iv. Solution
Use the OUTRES,SVAR,1 command to store the values of state variables for every substep.

```
/SOLU                   ! Start Solution module
ANTYPE,STATIC
OUTRES,ALL,1            ! Store results for each substep
OUTRES,SVAR,1           ! Store results of state variables
```

Then, set up a uniform deformation ϵ_x using displacement boundary conditions.

```
! Define one-dimensional stress in 1-axes direction
D,1,all                 ! Define b.c. on node 1, fixed
D,2,UY,0.00                                  ! Symmetry
D,4,UX,0.00                                  ! Symmetry
D,2,UX,appliedStrain*ShellDimensionX/100     ! applied displacement
D,3,UX,appliedStrain*ShellDimensionX/100     ! applied displacement
```

Since damage is a nonlinear problem, one has to choose some time of incrementation within the STEP. If `AUTOS,ON`*, the solution is obtained for optimum but uneven substep size. If* `AUTOS,OFF`*, the solution is obtained for equal substeps, which makes it easier to plot the solution.*

```
AUTOS, OFF           ! Automatic substeps OFF (min supstep=1/desired)
NSUBST,100,200,100   ! substeps: desired, max.#, min.#
SOLVE                ! Solve load step
FINISH               ! Exit solution module
```

v. Field Visualization
The filed postprocessor (/POST1) can be used to produce a contour plot of state variables, as shown in Figure 9.4 which in this case is not very interesting because the values are uniform over the x-y domain. The $TIME = 0.24$ was selected purposely to coincide with the initiation of damage at $\epsilon_x = 0.48\%$.

```
/POST1          ! POST-PROCESSOR MODULE
/GRA,FULL       ! NEEDED FOR PLOTTING SVARS
RSYS,SOLU       ! RSYS: ACTIVATE RESULTS IN SOLUTION COORD. SYSTEM
SET,,,,,0.24     ! SET,,,,,TIME          : SELECT TIME
PLESOL,SVAR,4   ! PLESOL: CONTOUR PLOT STATE VAR NUMBER
FINISH                ! EXIT POST-PROCESSOR MODULE
```

vi. Time Visualization
The time postprocessor (/POST26) can be used to produce a time plot of state variables, as shown in Figure 9.5.

```
/POST26             ! Start time-history post-process
ANSOL,2,3,EPEL,X,EpsXNod3   ! Var #2, Node 3, Strain, X-dir, label
ANSOL,4,3,S,X,SxNod3    ! Var #3, Node 3, Stress, X-dir, label
/AXLAB,X,STRAIN
/AXLAB,Y,STRESS
XVAR,2          ! plot #2 as abscissa
PLVAR,3         ! plot #3 as ordinate
```

and also a printout, that can be saved to a file for further use.

```
! list time(default), strain=2, reactions=3
PRVAR,2,3
FINISH          ! Exit post-process module
```

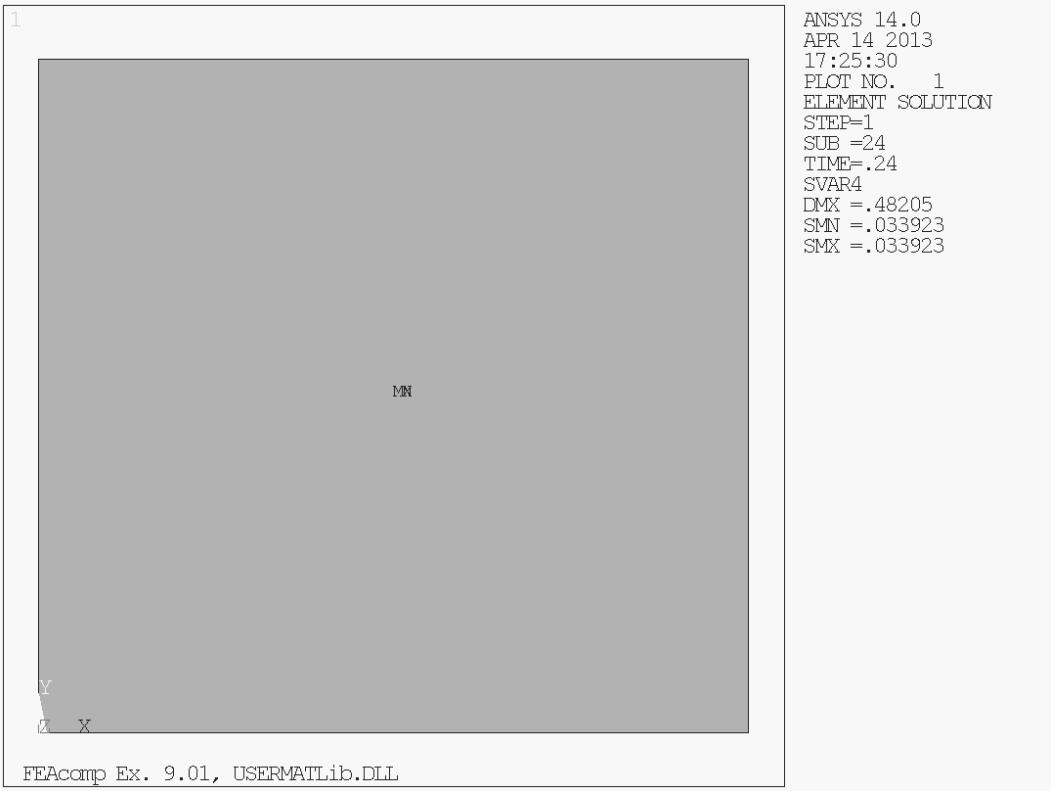

Figure 9.4: Uniform crack density $\lambda = 0.033923$ crack/mm, in layer 2 ($SVAR = 4$), shown for applied strain $\epsilon_x = 0.48205\%$, for Example 9.1.

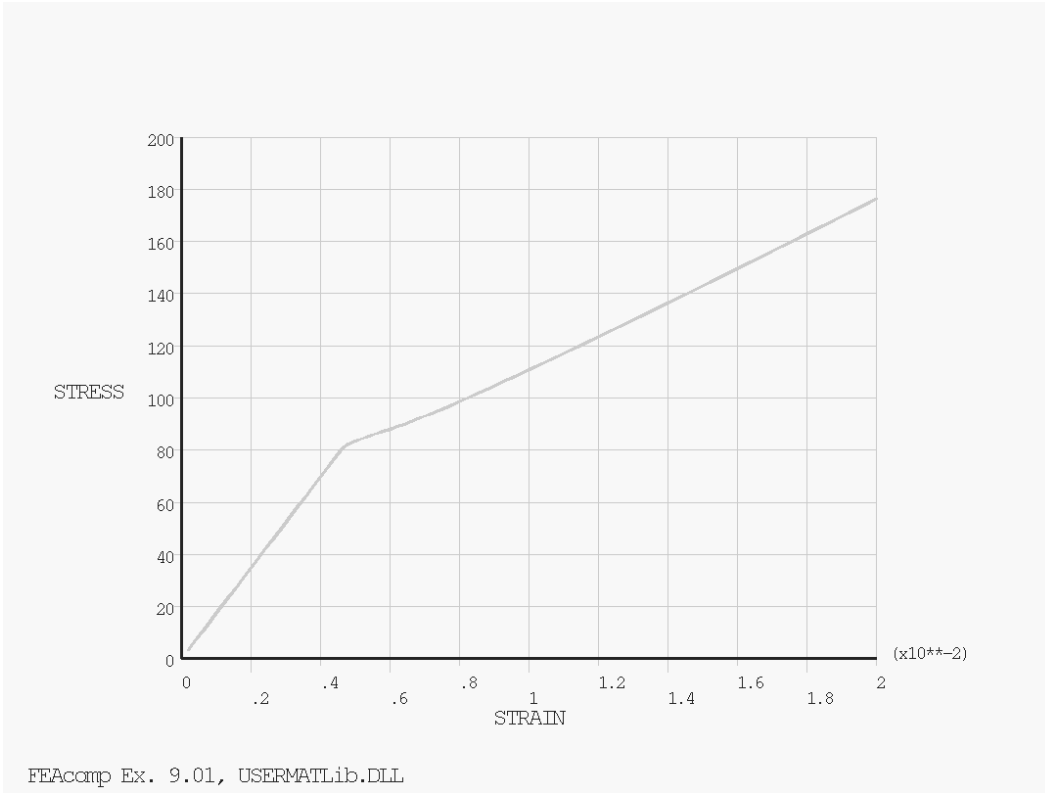

Figure 9.5: Average laminate stress $\sigma_x = N_x/h$ vs. applied strain ϵ_x, for Example 9.1.

Table 9.2: Laminates for Exercises 9.1–9.4

Laminate number	LSS
1	$[0/90_8/0/90_8/0]$
2	$[0/70_4/-70_4/0/-70_4/70_4/0]$
3	$[0/55_4/-55_4/0/-55_4/55_4/0]$
4	$[0_2/90_8/0_2]$
5	$[15/-15/90_8/-15/15]$
6	$[30/-30/90_8/-30/30]$
7	$[40/-40/90_8/-40/40]$

Suggested Problems

Problem 9.1 *Calculate the critical laminate strain ϵ_x^c for which the first crack appears in laminates 1 to 3 in Table 9.2, all made of Glass/Epoxy with properties given in Table 9.1 subjected to a membrane strain $\epsilon_x \neq 0, \epsilon_y = \gamma_{xy} = 0$. For each laminate, in what lamina the first crack appears?*

Problem 9.2 *Using the results from Exercise 9.1, calculate the the in-situ transverse strength F_{2t}^{is} of the laminas [1, Section 7.2.1].*

Problem 9.3 *Calculate the critical laminate strain ϵ_x^c for which the first crack appears in laminates 4 to 7 in Table 9.2, all made of Glass/Epoxy with properties given in Table 9.1 subjected to a membrane strain $\epsilon_x \neq 0, \epsilon_y = \gamma_{xy} = 0$. For each laminate, in what lamina the first crack appears?*

Problem 9.4 *Using the results from Exercise 9.3, calculate the the in-situ transverse strength F_{2t}^{is} of the laminas [1, Section 7.2.1].*

Chapter 10

Delaminations

Delamination is a frequent mode of failure affecting the structural performance of composite laminates. The interface between laminas offers a low-resistance path for crack growth because the bonding between two adjacent laminas depends only on matrix properties. Delamination may originate from manufacturing imperfections, cracks produced by fatigue or low velocity impact, stress concentration near geometrical/material discontinuity such as joints and free edges, or due to high interlaminar stresses.

In laminates loaded in compression, the delaminated laminas may buckle, and cracks propagate due to interaction between delamination growth and buckling. The presence of delaminations may reduce drastically the buckling load and the compressive strength of the composite laminates [143] (Figure 10.1). Delaminations may also be driven by buckling in laminates under transverse loading [144]. The analysis of delamination buckling requires the combination of geometrically nonlinear structural analysis with fracture mechanics.

According to its shape, delaminations are classified into through-the-width or strip [144–151], circular [151–157], elliptic [158], rectangular [159], or arbitrary [160, 161]. Depending on its location through the laminate thickness, delaminations are classified into thin film, symmetric split [143, 146, 147], and general [148, 151, 154, 155, 157]. In addition, analysis of combined buckling and growth for composite laminates containing multiple delaminations under in-plane compressive loading has been carried out [162, 163]. Experimental results on delamination buckling are presented in [164, 165].

Other delamination configurations that have been investigated in the literature are the beam-type delamination specimens subjected to bending, axial, and shear loading [164–170] which form the basis for experimental methods used to measure interlaminar fracture strength under pure mode I, mode II, and mixed mode conditions in composites, adhesive joints, and other laminated materials (Figure 10.2).

In plates with piezoelectric sensors or actuators, an imperfect bonding between the piezoelectric lamina and the base plate may grow under mechanical and/or electrical loading. As a consequence, the adaptive properties of the smart system can be significantly reduced since debonding results in significant changes to the static or dynamic response [171, 172]. Finally, delamination growth may be caused

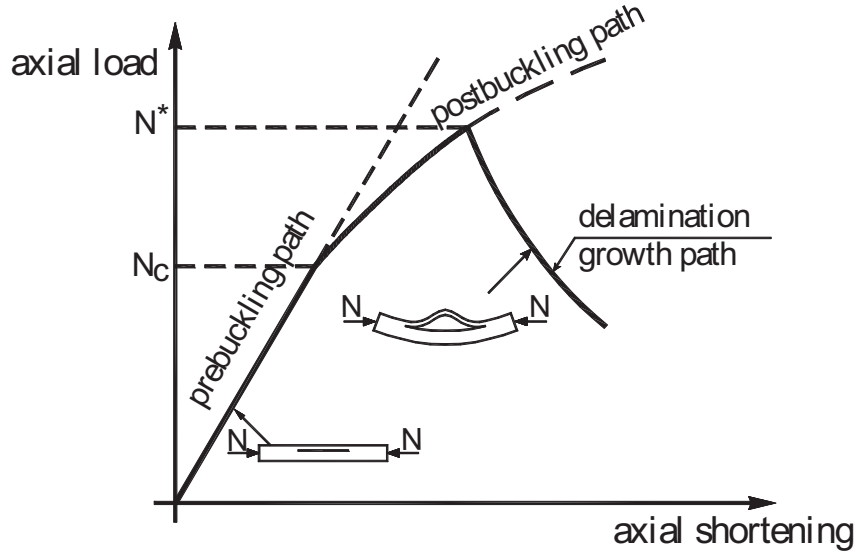

Figure 10.1: Delamination buckling in a compressed laminate.

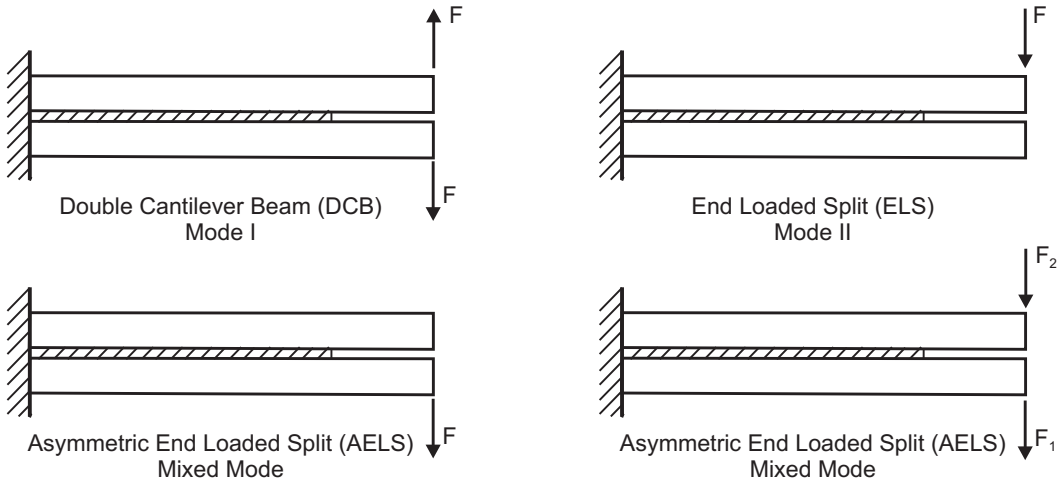

Figure 10.2: Beam-type delamination specimens.

by dynamic effects, such as vibration and impact. For instance, the dynamics effects resulting from the inertia of the laminate on the growth process resulting from the buckling of the delamination has been investigated for a circular delamination and time-dependent loadings [173].

Delaminations can be analyzed by using *cohesive damage models* (Section 10.1) and *fracture mechanics* (Section 10.2). A cohesive damage model implements interfacial constitutive laws defined in terms of damage variables and a damage evolution law. Cohesive damage elements are usually inserted between solid elements [174–177] or beam/shell elements [176].

In the fracture mechanics approach, the propagation of an existing delamination is analyzed by comparing the amount of energy release rate (ERR) with the fracture toughness of the interface. When mixed mode conditions are involved, the decomposition of the total ERR into mode I, mode II, and mode III components becomes necessary due to the mixed-mode dependency of interface toughness [168, 178]. A number of fracture mechanics-based models have been proposed in the literature to study delamination, including three-dimensional models [179–181] and simplified beam-like models [143, 145, 170, 182, 183].

Fracture mechanics allows us to predict the growth of a pre-existing crack or defect. In a homogeneous and isotropic body subjected to a generic loading condition, a crack tends to grow by kinking in a direction such that a pure mode I condition at its tip is maintained. On the contrary, delaminations in laminated composites are constrained to propagate in its own plane because the toughness of the interface is relatively low in comparison to that of the adjoining material. Since a delamination crack propagates with its advancing tip in mixed mode condition, the analysis requires a fracture criterion including all three mode components (Section 10.1.2).

The elastic strain energy per unit volume (density, in J/m^3) is defined as $U_0 = 1/2\sigma_{ij}\epsilon_{ij}$. The strain energy (in J) is defined as the volume integral $U = \int_V U_0 dV$. The energy required to form, or to propagate, a crack is equal to the elastic energy released by the solid during crack formation. The energy released is the difference between the elastic strain energy available before and after the crack is formed, i.e., $-\Delta U = U_{after} - U_{before}$. The rate of energy released per unit of crack area A is given, in J/m^2 by

$$G = -\frac{\Delta U}{\Delta A} \tag{10.1}$$

where A is one half the surface area created. The theory of crack growth may be developed by using one of two approaches due to Griffith and Irwin, respectively. The Griffith energy approach uses the concept of Energy Release Rate G as the (computable) energy available for fracture on one hand, and the material property G_c, which is the energy necessary for fracture, on the other hand. A crack grows when

$$G \geq G_c \tag{10.2}$$

where for completeness note that $G_c = 2\gamma_c$, where γ_c is the critical fracture energy per unit surface crack area, and A is one half of the crack area formed, i.e., the area

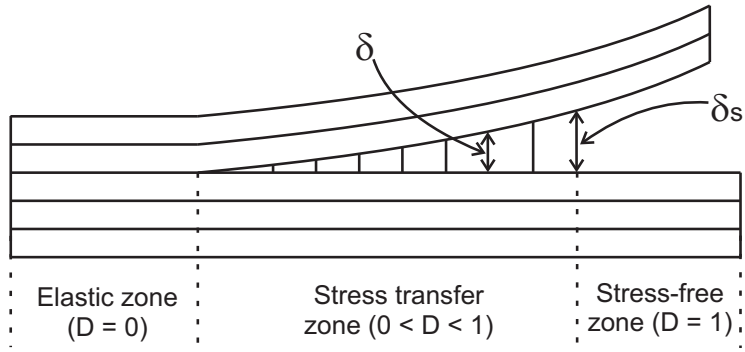

Figure 10.3: Cohesive zone model to simulate crack propagation.

of only one of the faces of the crack.

The Irwin (local) approach is based on the concept of stress intensity factor, which represents the stress field in the neighborhood of the crack tip. These two approaches are equivalent and, therefore, the energy criterion may be rewritten in terms of stress intensity factors. Further, a number of path independent integrals have been proposed to calculate the ERR, such as the J-integral [184].

The elastic strain energy released ΔU during crack propagation, and therefore used to create the new surface area, can be calculated as the work required to close the crack, i.e.,

$$\Delta U = W_{closure} \tag{10.3}$$

The crack closure method of computation provides the basis for the Virtual Crack Closure Technique (VCCT) described in Section 10.2.

10.1 Cohesive Zone Method

The cohesive zone method (CZM) is based on the assumption that the stress transfer capacity between the two separating faces of a delamination is not lost completely at damage initiation, but rather is a progressive event governed by progressive stiffness reduction of the interface between the two separating faces (Figure 10.3).

The interface between the two possible separating faces of the laminated material is modeled with *cohesive material behavior*, i.e., *cohesive zone method (CZM)*. There are two types of elements capable of using a CZM material model in ANSYS®:

Interface elements are based on a traction-separation ($\sigma - \delta$) constitutive behavior [13, Section 4.12.1]. They can occupy a finite thickness between the two surfaces that they join or they can have zero thickness. In any case, the contact between the two surfaces is known before the analysis and the surfaces are thus joined by the interface elements.

Contact elements have zero thickness and can detect contact, separation, penetration, and slip between a contact surface and a target surface [13, Sec-

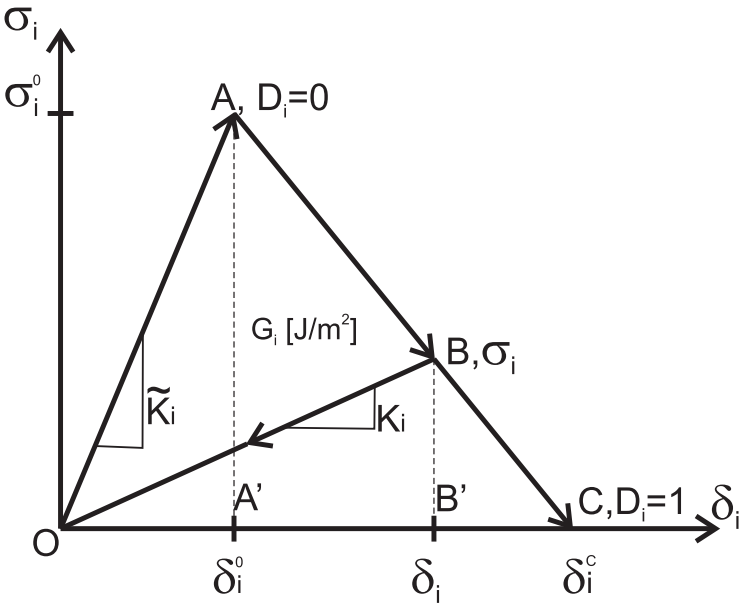

Figure 10.4: Stress transfer model for cohesive zone model.

tion 4.12.2], [13, Section 14.170.1]. The CZM model can be used only with bonded contact [13, Section 14.174.7].

The cohesive behavior is described in terms of a traction-separation equation (Figure 10.4). As the name implies, this approach replaces the engineering stress-strain ($\sigma - \epsilon$) equation with a traction-separation ($\sigma - \delta$) equation. The thickness of the element is set to zero by defining coincident opposite nodes of the cohesive element. However, even if the opposite nodes are initially coincident, they are still separate entities, and they separate during the deformation of the laminated composite. The separate faces of the laminated plies can be thought of as being connected to each other through the stiffness of the cohesive element. During the deformation, the resulting separation between the connected faces of the plies are proportional to the stiffness of the cohesive element.

Both, the interface element with finite thickness (Example 10.1) and the contact element with zero thickness (Example 10.2), can use the CZM traction-separation constitutive equation. The element stiffness matrix requires the stiffness $\widetilde{K}$ of the interface material, also called *penalty* stiffness, but the element stiffness matrix is not formulated as usual by integration over the volume of the element because the initial volume of the element is zero. The CZM can be visualized as a spring between the initially coincident nodes of the element. However, the stiffness of the element is part of the structural stiffness, and the element will undergo deformation during the loading of the laminate. The initially coincident nodes will open (mode I: opening) or slide (model II: shear and III: tearing) relative to each other (Figure 10.5). The nodal separation between the elements are always known by solving the discretized structure.

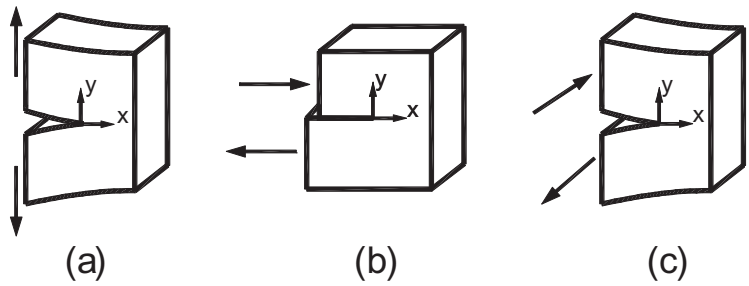

Figure 10.5: Crack propagation modes: (a) I-opening, (b) II-shear, (c) III: tearing.

If the initial thickness of the element is zero, the deformation state of the element can not be described by the classical definition of strain. Instead, the measure of the deformation becomes the separation δ between the faces connected through the element, and this makes possible the use of the $(\sigma - \delta)$ traction-separation equation instead of the classical engineering $(\sigma - \epsilon)$ equation.

10.1.1 Single Mode Cohesive Model

The CZM is formulated assuming the three crack propagation modes are uncoupled, even if multiple modes are active simultaneously, as described in Section 10.1.2. In this section we consider the case of a single mode deformation at an interface of the laminated material, either mode I, II, or III (Figure 10.5). The formulation is similar for any of the three modes. The surface tractions at the interface are σ_i with $i = I, II, III$ denoting the three modes of crack propagation. The corresponding separation between the opposite faces of the CZM element are denoted as δ_i, each related to the surface traction σ_i through the interface stiffness K_i, also called *penalty stiffness*. Therefore, material stiffness values are necessary for each of the loading modes, i.e., K_I, K_{II}, K_{III}. A discussion on how to choose numerical values for K_i is provided in [185].

The behavior of the material at the interface is assumed to be linear-elastic up to the onset of damage (OA in Figure 10.4) and damaging-elastic after that (OB in Figure 10.4). Consequently, the stress-separation is described by

$$\sigma_i = K_i \, \delta_i \tag{10.4}$$

and

$$K_i = (1 - D_i) \, \widetilde{K_i} \tag{10.5}$$

where D_i are the damage variables, and $\widetilde{K_i}$ in $[N/mm^3]$ are the stiffness values of the *undamaged* material at the interface, relating the stresses σ_i to the relative separation δ_i between the opposite faces of the element. The stiffness values $\widetilde{K_i}$ are additional material properties needed for CZM, which are different from the Young's modulus E for normal deformation, or G for shear deformation.

For each mode, there is a critical level of stress σ_i^0 and separation δ_i^0 when the damage at the interface starts (point A in Figure 10.4), called *damage onset*. At damage onset, the two laminas do not separate completely into a physical crack but rather the interface material starts losing its stiffness. Here, σ_i^0 represents the strength of the interface with one value of strength for each crack propagation mode: $\sigma_I^0, \sigma_{II}^0, \sigma_{III}^0$. In CZM, these modes are called *damage modes* because the CZM does not use fracture mechanics. Instead, CZM replaces the fracture mechanics problem by a continuum damage mechanics problem (Chapter 8). The interface strengths are therefore additional material parameters required by CZM.

Therefore, the *damage initiation criteria* are

$$\sigma_i = \sigma_i^0 \tag{10.6}$$

and the separations at damage onset are calculated as

$$\delta_i^0 = \sigma_i^0 / \widetilde{K_i} \tag{10.7}$$

After damage onset, the interface material starts losing its stiffness (OB in Figure 10.4), according to (10.5). Note that there are as many damage variables as damage modes: D_I, D_{II}, D_{III}, which are state variables (8.61) to be determined during the analysis. Their physical interpretation is given by (10.5) as measures of stiffness degradation (see also Section 8.2). The damage variables satisfy the following conditions:

- $D = 0$ up to damage onset (OA in Figure 10.4) while the interface material is undamaged, thus retaining its initial stiffness.
- $0 < D < 1$ during degradation of the interface material (AF in Figure 10.4), when the material is gradually loosing its stiffness.
- $D = 1$ at fracture (point C in Figure 10.4), when there is no remaining stiffness for the interface material, which means no stress transfer capacity is provided by the interface. This corresponds to the fracture of the cohesive connection between the two faces of the CZM element.

With reference to Figure 10.4 we have:

$$D_i = \begin{cases} 0, & \delta_i \leq \delta_i^0 \\ 1, & \delta_i = \delta_i^c \end{cases} \tag{10.8}$$

In stress-strain space, the cohesive behavior depicted in Figure 10.4 displays *stress softening*. That is, after damage onset the stresses σ_i in the damaged interface have lower values than the peak values σ_i^0.

The CZM uses the classical assumption of *elastic damage* typical of continuum damage mechanics (CDM, Chapter 8). Therefore, unloading from any point such as B on the line AF in Figure 10.4 will return to the origin without permanent deformation upon unloading.

Eventually, there will be total fracture of the cohesive bond (point C in Figure 10.4) when the stiffness of the interface reduces to zero. Due to the fact that total loss of stiffness, and thus total loss of cohesive stress transfer, does not take place until point C, the CZM is correlated with the Griffith crack propagation criterion (10.2) at point C. The correlation is made by considering that the area under the $(\sigma-\delta)$ curve in Figure 10.4 is equal to the critical ERR G_{ic} in Griffith's principle (10.2). In this way, the separation at fracture δ_i^c can be calculated as

$$\delta_i^c = \frac{2G_{ic}}{\sigma_i^0} \tag{10.9}$$

Since there is a critical ERR value for each damage mode, G_{ic}, with $i = I, II, III$, there will be three separations at fracture–one per mode. The three ERR values are material properties required by the CZM, in addition to the three values of strength σ_i^0 and the three values of interface stiffness $\widetilde{K_i}$. From the point of view of the amount of experimental data needed to perform an analysis, this is a disadvantage of CZM because it requires nine experimental values. On the other hand, discrete damage mechanics requires only the three values of ERR to predict both the onset and the evolution of damage (Chapter 9).

Substituting (10.4) into (10.5) and rearranging results in

$$D_i = 1 - \frac{\sigma_i \delta_i^0}{\sigma_i^0 \delta_i} \tag{10.10}$$

By similarity of triangles BB′C and AA′C, we have

$$\frac{\sigma_i}{\sigma_i^0} = \frac{\delta_i^c - \delta_i}{\delta_i^c - \delta_i^0} \tag{10.11}$$

which substituted into (10.10) yields

$$D_i = \frac{\delta_i^c(\delta_i - \delta_i^0)}{\delta_i(\delta_i^c - \delta_i^0)} \tag{10.12}$$

In this way, the damage variables D_i are calculated as a function of the relative separation between the faces of the laminate δ_i, which are provided by the finite element solution and the values δ_i^0, δ_i^c calculated previously.

In summary, there are four distinct stages in the material behavior described by Figure 10.4:

- linear elastic undamaged material behavior (line OA), with the associated constitutive equation (10.4).
- damage initiation (point A), with the associated criterion (10.6).
- damage evolution (line AF), with the associated damage evolution equation (10.5), (10.12).
- fracture (crack formation), with the associated crack formation criterion (10.2).

As previously stated, the formulation presented in this section works only for pure mode I, or II, or III. The general case of the mixed mode loading is presented in the following section.

10.1.2 Mixed Mode Cohesive Model

When the interface of the laminated material is under mixed modes, all three traction components $\sigma_I, \sigma_{II}, \sigma_{III}$ and all three separation components $\delta_I, \delta_{II}, \delta_{III}$ are active. In other words, mixed mode implies that two or more pairs (σ_i, δ_i) are non-vanishing, with $i = I, II, III$. However, to reduce the burden of experimentation, it is assumed[1] that the penalty stiffness (10.7) is the same for all modes $\widetilde{K} = \widetilde{K}_i$.

Mixed mode ratios can be defined between pairs of mode components. For example, in terms of separations

$$\beta_{\delta_{II}} = \frac{\delta_{II}}{\delta_I} \quad ; \quad \beta_{\delta_{III}} = \frac{\delta_{III}}{\delta_I} \tag{10.13}$$

or in terms of ERRs

$$\beta_{G_{II}} = \frac{G_{II}}{\sum_1^3 G_i} \quad ; \quad \beta_{G_{III}} = \frac{G_{III}}{\sum_1^3 G_i} \tag{10.14}$$

Regardless of the definition used, mixed mode ratios are just parameters characterizing the mixed mode state, which allow for a simplification of the analysis by assuming that decohesion progresses at constant mixed mode ratios. It is further assumed that the modes are uncoupled even though they occur simultaneously. That is, the stress-separation relationship for each uncoupled mode is again expressed by (10.4), separately for each mode.

Next, a mixed mode separation is defined by the L^2 norm of the mode separations, i.e.,

$$\delta_m = \sqrt{\sum_{i=1}^{M} \delta_i^2} \tag{10.15}$$

where M is the number of modes involved (i.e., 2 or 3 modes). Next, the single mode damage initiation criterion in (10.6) is replaced, for example, by a quadratic stress criterion

$$\sum_{i=1}^{M} \left(\frac{\sigma_i}{\sigma_i^0} \right)^2 = 1 \tag{10.16}$$

For the case of mode I and II only, $M = 2$ and the *equivalent mixed mode separation at damage onset* δ_m^0 is found as follows. First, rewrite the damage initiation criteria (10.16) in terms of separations using (10.7) and (10.4)–(10.5), taking into account that $D_i = 0$ up to damage initiation. Therefore, mixed mode damage initiation is predicted by

[1] As far as we know, there is no experimental evidence to support this simplification.

$$\left(\frac{\delta_I}{\delta_I^0}\right)^2 + \left(\frac{\delta_{II}}{\delta_{II}^0}\right)^2 = 1 \tag{10.17}$$

Next, rewrite (10.15) using the first of (10.13) to get

$$\delta_I = \frac{\delta_m}{\sqrt{1+\beta^2}} \tag{10.18}$$

and using (10.13) again

$$\delta_{II} = \beta \frac{\delta_m}{\sqrt{1+\beta^2}} \tag{10.19}$$

Now, substitute (10.18) and (10.19) into (10.17), taking into account that since (10.17) represents damage initiation, one should write δ_m^0 for δ_m. Therefore,

$$\delta_m^0 = \sqrt{(\delta_I^0)^2(\delta_{II}^0)^2 \frac{1+\beta^2}{(\delta_{II}^0)^2 + \beta^2(\delta_I^0)^2}} \tag{10.20}$$

The quantities δ_i^0 in (10.20) represent the separations at damage onset during single mode loading, calculated with (10.7) and β is the mixed mode ratio, which is assumed to be constant during the damage process.

A mixed mode crack propagation criterion is now needed to replace the single mode criterion (10.2). A possible choice is to use an ERR power criterion as follows

$$\sum_{i=1}^{3} \left(\frac{G_i}{G_{ic}}\right)^{\alpha_i} = 1 \tag{10.21}$$

which attempts to predict fracture under mixed mode conditions, similarly to point C in Figure 10.4 for the single mode situation. To reduce the burden of experimentation, it is customary to assume that the exponents are the same for all modes, i.e., $\alpha_i = \alpha$.

Each of the single mode component G_i can be calculated by one of two methodologies. Some authors [174, 176] calculate each single mode component ERR by considering the area OABB' in Figure 10.4, thus including the recoverable energy OBB' in the definition of G_i. This approach is indirectly related to linear elastic fracture mechanics (LEFM). Other authors [185] use a damage mechanics approach where each single mode component ERR is calculated by considering only the unrecoverable energy represented by the area OAB. Both approaches lead to the same results for a single mode delamination since loss of adhesion occurs at δ_i^c where both approaches predict the same values for G_i (point B reaches point C). However, different results are obtained for mixed mode delamination because the crack propagates when an interaction criterion is satisfied, the later involving the ratios G_i/G_{ic}.

In principle, the approach based on LEFM should lead to conservative predictions of the load-carrying capacity for mixed-mode delamination. On the other hand, since the total energy dissipated during the delamination at each point is not released instantaneously as assumed in LEFM, the damage mechanics based definition appears appropriate especially when the size of nonlinear fracture process zone ahead the delamination front is not negligible as it may occur in the case of laminated composite materials where the damage zone may be comparable to or larger than the single-ply thickness, which generally scales with the near-tip stress field.

In the sequel, the damage mechanics approach is used. That is, for each single mode component separation δ_i, the single mode component ERR G_i is calculated as the area OAB in Figure 10.4, which represents dissipated energy, i.e.,

$$A_{OAB} = A_{OAF} - A_{OBF} \tag{10.22}$$

where A_{OAF} is the single mode critical ERR G_{ic}, and A_{OBF} can be calculated based on the geometry in Figure 10.4 as

$$A_{OBF} = \frac{1}{2} BB' \times OF = \frac{1}{2}\ K_i \delta_i^0 \frac{\delta_i^c - \delta_i}{\delta_i^c - \delta_i^0}\ \delta_i^c \tag{10.23}$$

where $\delta_i^c = OF$, $k_i \delta_i^0 = \sigma_i^0$, and σ_i / σ_i^0 is given by (10.11). Based on (10.22), (10.23), the single mode component ERR at the moment of mixed mode fracture is calculated as

$$G_i = G_{ic} - \frac{1}{2} K_i \delta_i^0 \delta_i^c \frac{\delta_i^c - \delta_i}{\delta_i^c - \delta_i^0} \tag{10.24}$$

The assumed mode decomposition (10.24) is necessary so that each single mode component ERR G_i corresponding to mixed mode fracture can be expressed as a function of the single mode separation δ_i, i.e., $G_i = G_i(\delta_i)$. All other quantities in (10.24) are known, as follows:

- G_{ic} is the single mode critical ERR (material parameter).
- δ_i^0 is the separation at damage onset under single mode loading (point A in Figure 10.4), given by (10.7)
- δ_i^c is the separation at fracture under single mode loading (point C in Figure 10.4), given by (10.9).

The single mode ERR components of the mixed mode condition in (10.24) has to satisfy the energy criterion (10.21) at the moment of fracture (crack propagation). For the case of two modes, and assuming $\alpha_i = \alpha = 2$ in (10.21), the mixed mode separation at fracture (point C) is calculated in [185, (15)] as

$$\delta_m^c = \frac{\sqrt{1+\beta}}{\beta^2(\delta_I^{0F})^2 + (\delta_{II}^{0F})^2} \times \left\{ \delta_I^0(\delta_{II}^{0F})^2 + \beta\delta_{II}^0(\delta_I^{0F})^2 + \delta_I^{0F}\delta_{II}^{0F}\sqrt{(\delta_{II}^{0F})^2 - (\delta_{II}^0)^2 + 2\beta\delta_I^0\delta_{II}^0 - \beta^2(\delta_I^0)^2 + \beta^2(\delta_I^{0F})^2} \right\} \tag{10.25}$$

where $\delta_I^{0F} = \delta_I^c - \delta_I^0, \delta_{II}^{0F} = \delta_{II}^c - \delta_{II}^0$.

Once the mixed mode separation at fracture (10.25) is calculated based on the selected criterion, and the mixed mode separation at damage onset is known based on (10.20), the damage variable for mixed mode conditions can be expressed in a similar manner as for the case of the single mode condition (10.12) by satisfying the requirement in (10.8), i.e.,

$$D_m = \frac{\delta_m^c(\delta_m - \delta_m^0)}{\delta_m(\delta_m^c - \delta_m^0)} \tag{10.26}$$

where the onset and fracture separations δ_m^0 and δ_m^c are calculated based on (10.20) and (10.25) respectively; and δ_m is the current level of separation under mixed mode conditions obtained using (10.15) in terms of the single modes separations δ_i provided by the FE model. The stiffness degradation for the cohesive material is then calculated according with (10.5). The stress softening evolution of the cohesive material under mixed mode conditions is similar to the one depicted in Figure 10.4, by substituting δ_m^0, δ_m^c for δ^0, δ^c.

Example 10.1 *A laminated double cantilever beam (DCB)* 100 *mm long and* 20 *mm wide is made up of two laminas bonded by adhesive lamina of negligible thickness. Each lamina is* 1.5 *mm thick. Apply a loading system to induce delamination and mode I crack growth through the adhesive lamina. Assuming linear elastic behavior, create a 2D model of the DCB using interface elements* `INTER202` *to represent the adhesive lamina. Use the* `PLANE182` *for the two laminas. The lamina material properties are:* $E_1 = 135.3\ GPa, E_2 = E3 = 9\ GPa, \nu_{12} = \nu_{13} = 0.24, \nu_{23} = 0.46, G_{12} = G_{23} = 4.5\ GPa; G_{13} = 3.3\ GPa$. *The adhesive properties are:* $\sigma_I^0 = \sigma_{II}^0 = 25.0\ MPa$ *and* $G_{Ic} = G_{IIc} = 280\ J/m^2$.

Solution to Example 10.1 *Using* (10.9) *to calculate the separation at fracture (Figure 10.4), with a bilinear (BILI) model [186, Section 3.22.2], [13, Section 4.12.1.2], we have*

$$\delta_I^c = \delta_{II}^c = \frac{2 \times 280 Nm/m^2}{25 \times 10^6 N/M^2} = 0.0224\ mm$$

The APDL file, which is available in [5, Ex101bili.log], is as follows

```
/TITLE,Example 10.1: DCB specimen under mode I loading
/UNITS,MPa                  ! Units are in mm, N and MPa

/PREP7
ET,1,PLANE182               !DEFINE PLANE STRESS/STRAIN ELEMENT - 2D
KEYOPT,1,1,2                !ENHANCE STRAIN FORMULATION
KEYOPT,1,3,2                !PLANE STRAIN
```

```
ET,2,PLANE182
KEYOPT,2,1,2
KEYOPT,2,3,2
ET,3,INTER202                !DEFINE INTERFACE ELEMENT - 2D
KEYOPT,3,3,2                 !PLANE STRAIN

MP,EX,1,135.3E3              !MATERIAL PROPERTIES LAMINA
MP,EY,1,9.0E3
MP,EZ,1,9.0E3
MP,GXY,1,4.5E3
MP,GYZ,1,4.5E3
MP,GXZ,1,3.3E3
MP,PRXY,1,0.24
MP,PRXZ,1,0.24
MP,PRYZ,1,0.46

TB,CZM,2,,,BILI              !MATERIAL PROPERTIES ADHESIVE
TBDATA,1,25.0,0.0224,-25.0,0.0224,1.0,1.0

RECTNG,0,100,0,1.5           !DEFINE AREA 1.5x100 mm
RECTNG,0,100,0,-1.5          !DEFINE AREA 1.5x100 mm

LSEL,S,LINE,,2,8,2
LESIZE,ALL, , ,2             !NUMBER ELEMENTS VERTICAL
LSEL,INVE
LESIZE,ALL, , ,400           !NUMBER ELEMENTS HORIZONTAL
ALLSEL,ALL
TYPE,1
MAT,1
LOCAL,11,0,0,0,0
ESYS,11
AMESH,2                      !MESH
CSYS,0
TYPE,2
ESYS,11
AMESH,1                      !MESH
CSYS,0
NSEL,S,LOC,X,30,100
NUMMRG,NODES
ESLN
TYPE,3
MAT,2
CZMESH,,,1,Y,0,              !MESH INTERFACE ELEMENTS
ALLSEL,ALL
NSEL,S,LOC,X,100             !CONSTRAINTS
D,ALL,ALL
NSEL,ALL
FINISH

/SOLU
ESEL,S,TYPE,,2
```

```
NSLE,S
NSEL,R,LOC,X
NSEL,R,LOC,Y,1.5            !DISPLACEMENT ON TOP
D,ALL,UY,6
NSEL,ALL
ESEL,ALL
ESEL,S,TYPE,,1
NSLE,S
NSEL,R,LOC,X
NSEL,R,LOC,Y,-1.5           !DISPLACEMENT ON BOTTOM
D,ALL,UY,-6
NSEL,ALL
ESEL,ALL
NLGEOM,ON
AUTOTS,ON
TIME,1
NSUBST,500,500,500          !LOAD STEPS
OUTRES,ALL,ALL
SOLVE
FINISH

/POST26
NSEL,S,LOC,Y,1.5
NSEL,R,LOC,X,0
*GET,NTOP,NODE,0,NUM,MAX
NSEL,ALL
NSOL,2,NTOP,U,Y,UY
RFORCE,3,NTOP,F,Y,FY
PROD,4,3, , ,RF, , ,20 !width=20
/AXLAB,X,DISPLACEMENT [mm]
/AXLAB,Y,REACTION FORCE [N]
/XRANGE,0,6
/YRANGE,0,65
XVAR,2
PLVAR,4                     !PLOT FORCE vs DISPLACEMENT
PRVAR,UY,RF                 !LIST FORCE & DISPLACEMENT vs TIME
FINISH

/POST1
PLDISP                      !PLOT DEFORMED PLATE
FINISH
```

The deformed shape is illustrated in Figure 10.6. Instead of bilinear material model `BILI`*, an exponential material model* `EXPO` *could be used [5, Ex101expo.log]. The required data [186, Section 3.22.1] includes the maximum normal and shear separations (point C in Figure 10.4). Taking into account that* $\phi_n = J$ *in [177], and* $J = G$ *for a linear elastic material [187], and using [13, (4-368),(4-369)], we have*

$$\delta_n^c = \frac{G_{Ic}}{e\,\sigma_I^0} = 0.004\ mm \quad ; \quad \delta_t^c = \frac{G_{Ic}}{\sqrt{2e}\,\sigma_I^0} = 0.005\ mm$$

where $e = 2.7182818$ *is the base of the natural logarithms.*

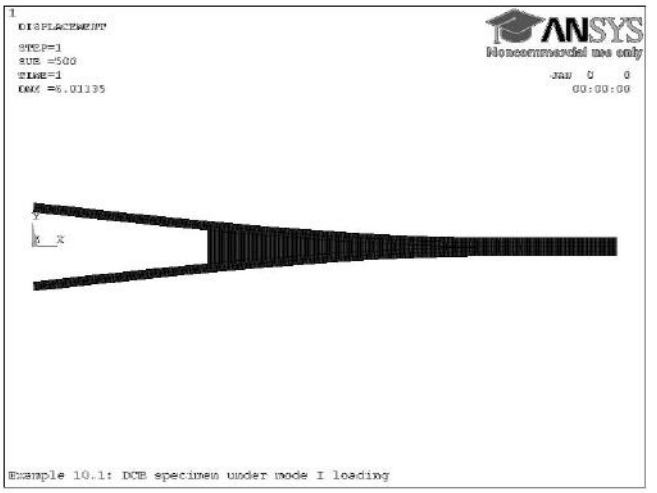

Figure 10.6: Deformed DCB using interface elements (Example 10.1).

The APDL code to define the exponential material model is

```
TB,CZM,2,,,EXPO     !MATERIAL PROPERTIES ADHESIVE
TBDATA,1,25.0,0.004,0.005
```

The resulting force-separation plot should look like the dash line in Figure 10.7. The drop of the reaction force occurs when the cohesive elements start to degrade (damage). As the cohesive elements degrade, the reaction force reduces.

Example 10.2 *Solve Example 10.1 using contact elements* `TARGE169` *and* `CONTA171`*.*

Solution to Example 10.2 *Using a cohesive zone material model in terms of critical fracture energies [186, CBDE, Section 3.22.3],* $\sigma_I^0 = 25.0\ MPa$ *and* $G_{Ic} = 0.28\ N\ mm$*. The artificial damping was chosen as* $\eta = 10^{-4}$ *to obtain a smooth force-separation plot. The APDL file, which is available in [5, EX102.inp], is as follows*

```
/TITLE,Example 10.2: DCB specimen under mode I loading
/UNITS,MPa                  ! Units are in mm, N, and MPa

/PREP7
ET,1,PLANE182               !DEFINE PLANE182 ELEMENT - 2D
ET,2,PLANE182               !DEFINE PLANE182 ELEMENT - 2D
ET,3,TARGE169               !DEFINE TARGE169 ELEMENT - 2D
ET,4,CONTA171               !DEFINE CONTA171 ELEMENT - 2D
KEYOPT,4,12,5               !BONDED (ALWAYS)

MP,EX,1,135.3E3             !MATERIAL PROPERTIES LAMINA
MP,EY,1,9.0E3
MP,EZ,1,9.0E3
MP,GXY,1,4.5E3
MP,GYZ,1,4.5E3
```

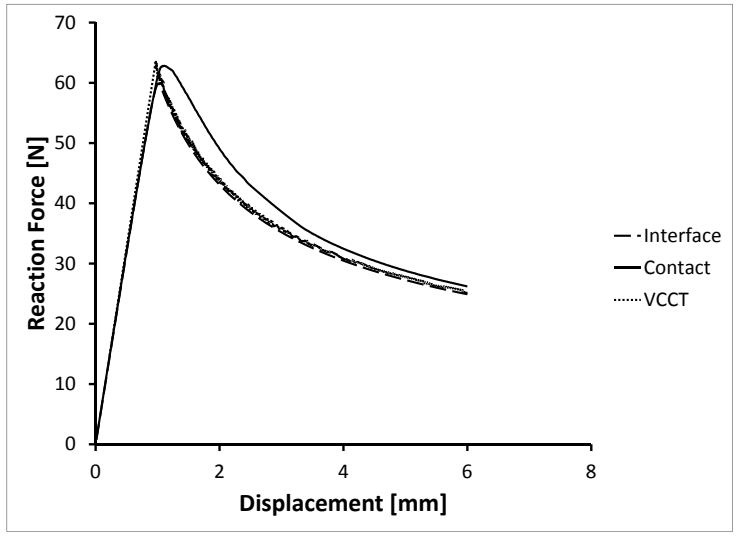

Figure 10.7: Force-separation plot using interface elements (Example 10.1), contact elements (Example 10.2), and VCCT (Example 10.3).

```
MP,GXZ,1,3.3E3
MP,PRXY,1,0.24
MP,PRXZ,1,0.24
MP,PRYZ,1,0.46

TB,CZM,2,,,CBDE              !MATERIAL PROPERTIES ADHESIVE
TBDATA,1,25.0,0.28,,,1.0E-4

RECTNG,0,100,0,1.5           !DEFINE AREA 1.5x100 mm
RECTNG,0,100,0,-1.5          !DEFINE AREA 1.5x100 mm

LSEL,S,LINE,,2,8,2
LESIZE,ALL, , ,2             !NUMBER ELEMENTS VERTICAL
LSEL,INVE
LESIZE,ALL, , ,400           !NUMBER ELEMENTS HORIZONTAL
ALLSEL,ALL
TYPE,1                       !MESH
MAT,1
LOCAL,11,0,0,0,0
ESYS,11
AMESH,2
CSYS,0
TYPE,2                       !MESH
ESYS,11
AMESH,1
```

```
CSYS,0
NSEL,S,LOC,X,30,100
TYPE,3
MAT,2
ESEL,S,TYPE,,2
NSLE,S
NSEL,R,LOC,Y
ESURF                          !TARGET ELEMENTS
TYPE,4
ESEL,S,TYPE,,1
NSLE,S
NSEL,R,LOC,Y
NSEL,R,LOC,X,30,100
ESURF                          !CONTACT ELEMENTS
ALLSEL,ALL
NSEL,S,LOC,X,100               !CONSTRAINTS
D,ALL,ALL
NSEL,ALL
FINISH

/SOLU
ESEL,S,TYPE,,2
NSLE,S
NSEL,R,LOC,X
NSEL,R,LOC,Y,1.5               !DISPLACEMENT ON TOP
D,ALL,UY,6
NSEL,ALL
ESEL,ALL
ESEL,S,TYPE,,1
NSLE,S
NSEL,R,LOC,X
NSEL,R,LOC,Y,-1.5              !DISPLACEMENT ON BOTTOM
D,ALL,UY,-6
NSEL,ALL
ESEL,ALL
NLGEOM,ON
TIME,1

NSUBST,500,500,500             !LOAD STEPS
OUTRES,ALL,ALL
SOLVE
FINISH

/POST26
NSEL,S,LOC,Y,1.5
NSEL,R,LOC,X,0
*GET,NTOP,NODE,0,NUM,MAX
NSEL,ALL
NSOL,2,NTOP,U,Y,UY
RFORCE,3,NTOP,F,Y,FY
PROD,4,3, , ,RF, , ,20 !width=20
```

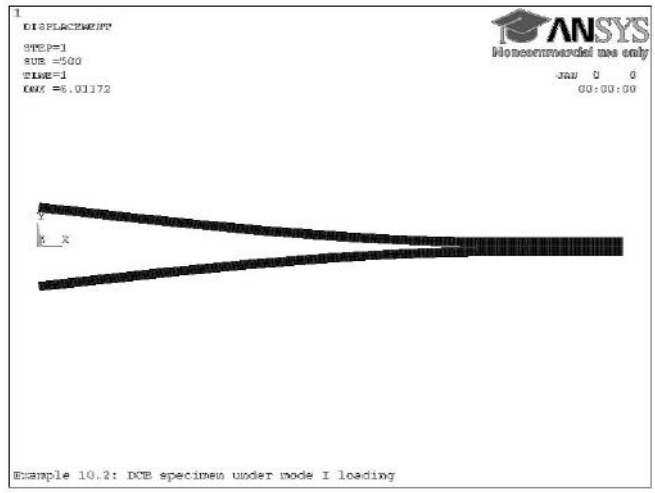

Figure 10.8: Deformed DCB using contact elements (Example 10.2).

```
/AXLAB,X,DISPLACEMENT [mm]
/AXLAB,Y,REACTION FORCE [N]
/XRANGE,0,6
/YRANGE,0,65
XVAR,2
PLVAR,4                    !PLOT FORCE vs DISPLACEMENT
PRVAR,UY,RF                !LIST FORCE & DISPLACEMENT vs TIME
FINISH

/POST1
PLDISP                     !PLOTS DEFORMED PLATE
FINISH
```

The deformed shape is illustrated in Figure 10.8. The resulting force-separation plot should look like the solid line in Figure 10.7.

10.2 Virtual Crack Closure Technique

The virtual crack closure technique (VCCT) can be used analyze delaminations in laminated materials using a fracture mechanics approach. The method implements Linear Elastic Fracture Mechanics (LEFM). Only brittle crack propagation is modeled. The energy dissipated by the formation of plastic zones at the crack tip is not considered.

The condition for crack propagation is based on the Griffith principle (10.2). For the case of single mode deformation under mode I conditions, the crack grows when

$$\frac{G_I}{G_{Ic}} \geq 1 \tag{10.27}$$

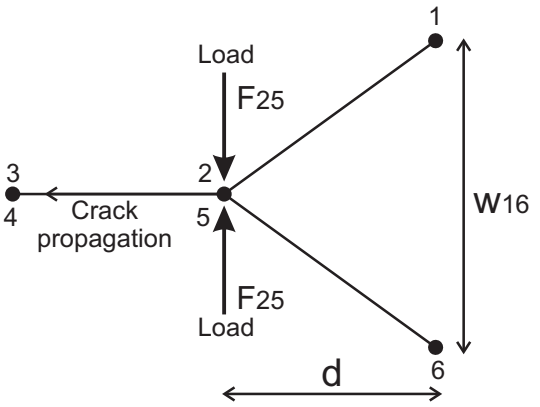

Figure 10.9: Virtual crack closure technique (VCCT).

where G_I is the ERR for mode I crack formation and G_{Ic} a material property representing the critical ERR for mode I crack formation.

The definition of ERR is given by (10.1). In VCCT, the Irwin principle (10.3) is used to calculate the change in strain energy ΔU, which is considered to be equal to the work required for crack closure $W_{closure}$.

By substituting (10.3) and (10.1) into (10.27), the condition for crack propagation under mode I loading becomes

$$\frac{W_{closure}/\Delta A}{G_{Ic}} \geq 1 \tag{10.28}$$

The crack closure work $W_{closure}$ is calculated from the FE nodal separations and forces as illustrated in Figure 10.9. Initially the crack surfaces are rigidly bonded. The nodal forces at the coincident nodes $2-5$ are calculated from the FE solution. The hypothesis of *self-similar crack propagation* is used, which says that during crack propagation, the crack configuration between nodes $2-3-4-5$ will be similar to the crack configuration between nodes $1-2-5-6$. This implies that the separation between nodes $2-5$ after crack propagation will be equal to the separation between nodes $1-6$ before crack propagation: $v_{2,5} = v_{1,6}$. If the nodes $2-5$ open (crack propagation), the elastic work required to close the crack is

$$W_{closure} = \frac{1}{2} F_{2,5}\ v_{2,5} = \frac{1}{2} F_{2,5}\ v_{1,6} \tag{10.29}$$

By substituting (10.29) in (10.28), the condition for crack propagation becomes

$$\frac{F_{2,5}\ v_{1,6}}{2\Delta A} \frac{1}{G_{Ic}} \geq 1 \tag{10.30}$$

The area ΔA of the newly formed crack is $\Delta A = d \times b$, where d is the length of the finite element undergoing crack propagation, and b is the width of the crack.

The VCCT method works similarly for the modes II or III, by considering the corresponding components of the separations and nodal forces. A refined formulation called the *Jacobian Derivative Method (JDM)* is available in [188].

The crack propagation criterion (10.30) applies for single mode loading only, as it is derived from the single mode criterion in (10.2). For mixed mode loading, the single mode crack propagation criterion (10.2) has to be replaced with a mixed mode criterion. For example, one could use the power equation (10.21), where the critical ERRs G_{ic}, with $i = I, II, III$, are material properties and the ERRs G_i are calculated similarly to (10.30) by using VCCT. Alternatively, one could use the Benzeggagh-Kenane (BK) equation [189] or the Reeder equation [178, 190].

Example 10.3 *Solve Example 10.1 using the virtual crack closure technique (VCCT).*

Solution to Example 10.3 *In this example, a VCCT model [8, Section 12.1.1] is implemented using* `INTER202` *elements. The fracture energy of the adhesive is* $G_{Ic} = 0.28\ N\ mm$. *The APDL file, which is available in [5, EX103.inp], is as follows*

```
/TITLE,Example 10.3: DCB specimen under mode I loading using VCCT
/UNITS,MPa                  ! Units: [mm, N, MPa]

/PREP7
ET,1,PLANE182               !DEFINE PLANE182 ELEMENT - 2D
KEYOPT,1,1,2                !ENHANCE STRAIN FORMULATION
KEYOPT,1,3,2                !PLANE STRAIN
ET,2,PLANE182
KEYOPT,2,1,2
KEYOPT,2,3,2
ET,3,INTER202               !DEFINE INTER202 ELEMENT - 2D
KEYOPT,3,3,2                !PLANE STRAIN

MP,EX,1,135.3E3             !MATERIAL PROPERTIES LAMINA
MP,EY,1,9.0E3
MP,EZ,1,9.0E3
MP,GXY,1,4.5E3
MP,GYZ,1,4.5E3
MP,GXZ,1,3.3E3
MP,PRXY,1,0.24
MP,PRXZ,1,0.24
MP,PRYZ,1,0.46

TB,CGCR,1,,3,LINEAR         !MATERIAL PROPERTIES ADHESIVE
TBDATA,1,0.28,0.28,0.28

RECTNG,0,100,0,1.5          !DEFINE AREA 1.5x100 mm
RECTNG,0,100,0,-1.5         !DEFINE AREA 1.5x100 mm

LSEL,S,LINE,,2,8,2
LESIZE,ALL, , ,2            !NUMBER ELEMENTS VERTICAL
LSEL,INVE
LESIZE,ALL, , ,400          !NUMBER ELEMENTS HORIZONTAL
ALLSEL,ALL
TYPE,1
```

```
MAT,1
LOCAL,11,0,0,0,0
ESYS,11
AMESH,2                    !MESH
CSYS,0
TYPE,2
ESYS,11
AMESH,1                    !MESH
CSYS,0
NSEL,S,LOC,X,30,100
NUMMRG,NODES
ESLN
TYPE,3
MAT,1
CZMESH,,,1,Y,0,            !MESH INTERFACE ELEMENTS
ALLSEL,ALL
NSEL,S,LOC,X,100           !CONSTRAINTS
D,ALL,ALL
NSEL,ALL

ESEL,S,ENAME,,INTER202     !SELECT INTERFACE ELEMENTS
CM,CPATH,ELEM              !DEFINE CRACK GROWTH PATH
NSEL,ALL

NSEL,S,LOC,X,30
NSEL,R,LOC,Y,0
CM,CRACK1,NODE
ALLS
FINISH

/SOLU
RESC,,NONE
ESEL,S,TYPE,,2
NSLE,S
NSEL,R,LOC,X
NSEL,R,LOC,Y,1.5           !DISPLACEMENT ON TOP
D,ALL,UY,0.9
NSEL,ALL
ESEL,ALL
ESEL,S,TYPE,,1
NSLE,S
NSEL,R,LOC,X
NSEL,R,LOC,Y,-1.5          !DISPLACEMENT ON BOTTOM
D,ALL,UY,-0.9
NSEL,ALL
ESEL,ALL

AUTOTS,ON
TIME,1
CINT,NEW,1                 !DEFINE CRACK ID
CINT,TYPE,VCCT
```

```
CINT,CTNC,CRACK1            !DEFINE CRACK TIP NODE COMPONENT
CINT,SYMM,OFF               !SYMMETRY OFF
CINT,NORM,0,2               !DEFINE CRACK PLANE NORMAL

CGROW,NEW,1                 !DEFINE CRACK-GROWTH INFORMATION
CGROW,CID,1
CGROW,FCOPTION,MTAB,1       !DEFINE FRACTURE CRITERION FOR CRACK-GROWTH
CGROW,CPATH,CPATH
CGROW,DTIME,1.0e-4
CGROW,DTMIN,1.0e-4
CGROW,DTMAX,1.0e-4
NSUB,4,4,4
ALLSEL,ALL
OUTRES,ALL,ALL
SOLVE

TIME,2
ESEL,S,TYPE,,2
NSLE,S
NSEL,R,LOC,X
NSEL,R,LOC,Y,1.5            !DISPLACEMENT ON TOP
D,ALL,UY,6
NSEL,ALL
ESEL,ALL
ESEL,S,TYPE,,1
NSLE,S
NSEL,R,LOC,X
NSEL,R,LOC,Y,-1.5           !DISPLACEMENT ON BOTTOM
D,ALL,UY,-6
NSEL,ALL
ESEL,ALL
NSUBST,500,500,500
OUTRES,ALL,ALL
SOLVE
FINISH

/POST26
NSEL,S,LOC,Y,1.5
NSEL,R,LOC,X,0
*GET,NTOP,NODE,0,NUM,MAX
NSEL,ALL
NSOL,2,NTOP,U,Y,UY
RFORCE,3,NTOP,F,Y,FY
PROD,4,3, , ,RF, , ,20 !width=20
/AXLAB,X,DISPLACEMENT [mm]
/AXLAB,Y,REACTION FORCE [N]
/XRANGE,0,6
/YRANGE,0,65
XVAR,2
PLVAR,4                     !PLOT FORCE vs DISPLACEMENT
PRVAR,UY,RF                 !LIST FORCE & DISPLACEMENT vs TIME
```

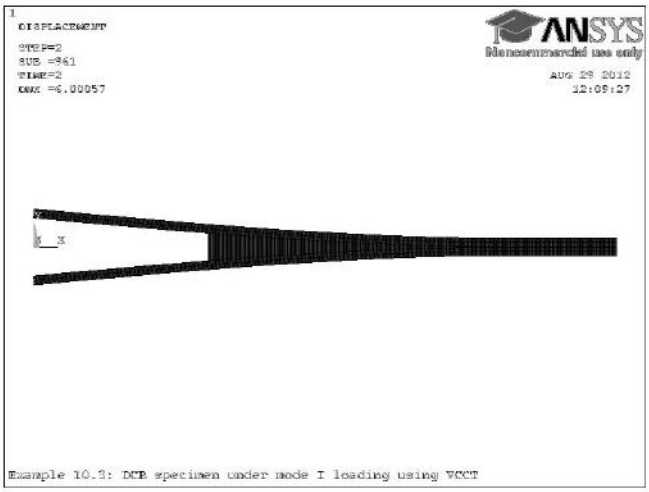

Figure 10.10: Deformed DCB using VCCT (Example 10.3).

```
FINISH

/POST1
PLDISP                          !PLOT DEFORMED PLATE
FINISH
```

The deformed shape is illustrated in Figure 10.10. The resulting force-separation plot should look like the dotted line in Figure 10.7.

Suggested Problems

Problem 10.1 *Retrieve the values of reaction force vs. separation for Examples 10.1 and 10.2. Plot them together and discuss the difference. Your plot should be similar to the one shown in Figure 10.7.*

Problem 10.2 *Retrieve the values of reaction force vs. separation for Example 10.3 and plot them along those of Examples 10.1 and 10.2. Discuss the differences. The comparative plot should be similar to the one shown in Figure 10.7.*

Appendix A

Tensor Algebra

Tensor operations are needed for the derivation of some of the equations in this textbook. Since most of these operations are not easily found in textbooks, they are presented here for reference [191].

A.1 Principal Directions of Stress and Strain

Since stress and strain tensors are symmetric and of second order, they have three real principal values and three orthogonal principal directions. The principal values λ^q and directions n_i^q of the stress tensor σ_{ij} satisfy the following

$$[\sigma_{ij} - \lambda^q \delta_{ij}] n_i^q = 0 \tag{A.1}$$

$$n_i^q n_j^q = 1 \tag{A.2}$$

where δ_{ij} is the Kronecker delta ($\delta_{ij} = 1$ if $i = j$, zero otherwise). Each of the principal directions is described by its direction cosines with respect to the original coordinate system.

The principal directions are arranged by rows into a matrix $[A]$. Then, the diagonal matrix $[A^*]$ of the principal values is

$$[A^*] = [a][A][a]^T \tag{A.3}$$

It can be shown that $[a]^{-1} = [a]^T$, where $[a]$ is the transformation matrix given by (1.21)

A.2 Tensor Symmetry

Minor symmetry provides justification for using contracted notation (Section 1.5). Minor symmetry refers to identical values of tensor components when adjacent subscripts are swapped. For example, minor symmetry of the stiffness tensor $\mathbf{C}$ means

$$A_{ijkl} = A_{jilk} = A_{\alpha\beta} \tag{A.4}$$

Major symmetry refers to identical values when adjacent pairs of subscripts are swapped, or when contracted subscripts are swapped. For example,

$$\begin{aligned} A_{ijkl} &= A_{klij} \\ A_{\alpha\beta} &= A_{\beta\alpha} \end{aligned} \tag{A.5}$$

A.3 Matrix Representation of a Tensor

A tensor A_{ijkl} with a minor symmetry has only 36 independent constants. Therefore, it can be represented in contracted notation by a 6×6 matrix. Let $[a]$ be the contracted form of the tensor A. Each element of $[a]$ corresponds to an element in the tensor A according to the following transformation

$$a_{\alpha\beta} = A_{ijkl} \tag{A.6}$$

with

$$\begin{aligned} \alpha &= i \text{ when } i = j \\ \alpha &= 9 - (i + j) \text{ when } i \neq j \end{aligned} \tag{A.7}$$

The same transformations apply between β and k and l, or in matrix representation, as

$$[a] = \begin{bmatrix} A_{1111} & A_{1122} & A_{1133} & A_{1123} & A_{1113} & A_{1112} \\ A_{2211} & A_{2222} & A_{2233} & A_{2223} & A_{2213} & A_{2212} \\ A_{3311} & A_{3322} & A_{3333} & A_{3323} & A_{3313} & A_{3312} \\ A_{2311} & A_{2322} & A_{2333} & A_{2323} & A_{2313} & A_{2312} \\ A_{1311} & A_{1322} & A_{1333} & A_{1323} & A_{1313} & A_{1312} \\ A_{1211} & A_{1222} & A_{1233} & A_{1223} & A_{1213} & A_{1212} \end{bmatrix} \tag{A.8}$$

It is convenient to perform tensor operations using the contracted form, especially if the result can be represented also in the contracted form. This saves memory and time since it is faster to operate on 36 elements than on 81 elements. Examples of these operations are the inner product of two fourth-order tensors and the inverse of a fourth-order tensor. However, tensor operations in index notation do not translate directly into matrix operations in a contracted form. For example, the double contraction of two fourth-order tensors is

$$\begin{aligned} \mathbf{C} &= \mathbf{A} : \mathbf{B} \\ C_{ijkl} &= A_{ijmn} B_{mnkl} \end{aligned} \tag{A.9}$$

Let $[a]$, $[b]$, and $[c]$ the 6×6 matrix representations of the above tensors. Then, it can be shown that

$$\begin{aligned} [a]\,[b] &\neq [c] \text{ or} \\ a_{\alpha\beta} b_{\beta\gamma} &\neq c_{\alpha\gamma} \text{ (matrix multiplication)} \end{aligned} \tag{A.10}$$

The rest of this appendix presents formulas for adequate representation of tensor operations in their contracted form.

A.4 Double Contraction

In (A.9), an element like C_{1211} can be expanded as

$$\begin{aligned} C_{1211} &= A_{1211}B_{1111} + A_{1222}B_{2211} + A_{1233}B_{3311} \\ &\quad +2A_{1212}B_{1211} + 2A_{1213}B_{1311} + 2A_{1223}B_{2311} \end{aligned} \tag{A.11}$$

In order to achieve the same result by matrix multiplication, multiply the last three columns of the matrix $[a]$ by 2, and then perform the multiplication

$$\begin{aligned} [c] = & \begin{bmatrix} A_{1111} & A_{1122} & A_{1133} & 2A_{1123} & 2A_{1113} & 2A_{1112} \\ A_{2211} & A_{2222} & A_{2233} & 2A_{2223} & 2A_{2213} & 2A_{2212} \\ A_{3311} & A_{3322} & A_{3333} & 2A_{3323} & 2A_{3313} & 2A_{3312} \\ A_{2311} & A_{2322} & A_{2333} & 2A_{2323} & 2A_{2313} & 2A_{2312} \\ A_{1311} & A_{1322} & A_{1333} & 2A_{1323} & 2A_{1313} & 2A_{1312} \\ A_{1211} & A_{1222} & A_{1233} & 2A_{1223} & 2A_{1213} & 2A_{1212} \end{bmatrix} \\ & \begin{bmatrix} B_{1111} & B_{1122} & B_{1133} & B_{1123} & B_{1113} & B_{1112} \\ B_{2211} & B_{2222} & B_{2233} & B_{2223} & B_{2213} & B_{2212} \\ B_{3311} & B_{3322} & B_{3333} & B_{3323} & B_{3313} & B_{3312} \\ B_{2311} & B_{2322} & B_{2333} & B_{2323} & B_{2313} & B_{2312} \\ B_{1311} & B_{1322} & B_{1333} & B_{1323} & B_{1313} & B_{1312} \\ B_{1211} & B_{1222} & B_{1233} & B_{1223} & B_{1213} & B_{1212} \end{bmatrix} \end{aligned} \tag{A.12}$$

This transformation can be produced by using the Reuter matrix [R]

$$[R] = \begin{bmatrix} 1 & 0 & 0 & 0 & 0 & 0 \\ 0 & 1 & 0 & 0 & 0 & 0 \\ 0 & 0 & 1 & 0 & 0 & 0 \\ 0 & 0 & 0 & 2 & 0 & 0 \\ 0 & 0 & 0 & 0 & 2 & 0 \\ 0 & 0 & 0 & 0 & 0 & 2 \end{bmatrix} \tag{A.13}$$

Substituting in (A.12) we have

$$[c] = [a]\,[R]\,[b] \tag{A.14}$$

A.5 Tensor Inversion

First, it is convenient to define the fourth-order identity tensor I_{ijkl} as a tensor that multiplied innerly by another fourth-order tensor yields this same tensor, or

$$I_{ijmn}A_{mnkl} = A_{ijkl} \tag{A.15}$$

If A_{ijkl} has a minor symmetry, the following tensor achieves (A.15)

$$I_{ijkl} = \frac{1}{2}\left(\delta_{ik}\delta_{jl} + \delta_{il}\delta_{jk}\right) \tag{A.16}$$

where δ_{ij} is the Kronecker delta, defined as

$$\begin{array}{l} \delta_{ij} = 1 \quad \text{if } i = j \\ \delta_{ij} = 0 \quad \text{if } i \neq j \end{array} \tag{A.17}$$

In Voigt contracted notation, the fourth-order identity tensor is denoted as $[i]$, which is equal to the inverse of the Reuter matrix

$$[i] = \begin{bmatrix} 1 & 0 & 0 & 0 & 0 & 0 \\ 0 & 1 & 0 & 0 & 0 & 0 \\ 0 & 0 & 1 & 0 & 0 & 0 \\ 0 & 0 & 0 & 1/2 & 0 & 0 \\ 0 & 0 & 0 & 0 & 1/2 & 0 \\ 0 & 0 & 0 & 0 & 0 & 1/2 \end{bmatrix} = [R]^{-1} \tag{A.18}$$

Now, the inverse of a tensor is a tensor that multiplied by the original tensor yields the identity tensor, as follows:

$$A_{ijmn}A^{-1}_{mnkl} = I_{ijkl} \tag{A.19}$$

Let us introduce the following notation:

$[a]^{-1}$ = inverse of the contracted form of A_{ijkl}

$\left[a^{-1}\right]$ = contracted form of the inverse of A_{ijkl}

If A_{ijkl} has a minor symmetry, the components of $a^{-1}_{\alpha\beta}$ are:

i. Multiply the last three columns of $[a]$ by 2 by using the matrix $[R]$

ii. Invert the obtained matrix.

iii. Multiply the matrix by $[i]$

In order words, the matrix $\left[a^{-1}\right]$ is computed as

$$\left[a^{-1}\right] = \left[[a]\,[R]\right]^{-1}[i] = [i]\,[a]^{-1}\,[i] \tag{A.20}$$

A.6 Tensor Differentiation

A.6.1 Derivative of a Tensor with Respect to Itself

Any symmetric second-order tensor Φ_{ij} satisfies the following:

$$d\Phi_{ij} = d\Phi_{ji} \tag{A.21}$$

Therefore, differentiating a second-order symmetric tensor with respect to itself is accomplished as follows

$$\frac{\partial \Phi_{ij}}{\partial \Phi_{kl}} = J_{ijkl} \tag{A.22}$$

where J_{ijkl} is a fourth-order tensor defined as

$$\begin{array}{ll} J_{ijkl} = 1 & \text{if } i = k, \text{ and } j = l \\ J_{ijkl} = 1 & \text{if } i = l, \text{ and } j = k \\ J_{ijkl} = 0 & \text{otherwise} \end{array} \tag{A.23}$$

In contracted notation, the tensor J_{ijkl} is represented by

$$[j] = \begin{bmatrix} 1 & 0 & 0 & 0 & 0 & 0 \\ 0 & 1 & 0 & 0 & 0 & 0 \\ 0 & 0 & 1 & 0 & 0 & 0 \\ 0 & 0 & 0 & 1 & 0 & 0 \\ 0 & 0 & 0 & 0 & 1 & 0 \\ 0 & 0 & 0 & 0 & 0 & 1 \end{bmatrix} \tag{A.24}$$

A.6.2 Derivative of the Inverse of a Tensor with Respect to the Tensor

A second-order tensor contracted with its inverse yields the second-order identity tensor, or Kronecker delta

$$A_{ij} A^{-1}_{jk} = \delta_{ik} \tag{A.25}$$

Differentiating (A.25) with respect to A_{mn} and rearranging terms yields

$$A_{ij} \frac{\partial A^{-1}_{jk}}{\partial A_{mn}} = -\frac{\partial A_{ij}}{\partial A_{mn}} A^{-1}_{jk} \tag{A.26}$$

Pre-multiplying both sides by $A^{-1}_{li}$and rearranging yields

$$\frac{\partial A^{-1}_{ij}}{\partial A_{mn}} = -A^{-1}_{ik} \frac{\partial A_{kl}}{\partial A_{mn}} A^{-1}_{lj} \tag{A.27}$$

Finally, using (A.22) yields

$$\frac{\partial A^{-1}_{ij}}{\partial A_{mn}} = -A^{-1}_{ik} J_{klmn} A^{-1}_{lj} \tag{A.28}$$

Appendix B

Second-Order Diagonal Damage Models

Explicit expressions associated to second-order diagonal damage models are presented here for completeness.

B.1 Effective and Damaged Spaces

A *second-order damage tensor* can be represented as a diagonal tensor (see (8.61))

$$D_{ij} = d_i \, \delta_{ij} \quad ; \quad \text{no sum on } i \tag{B.1}$$

in a coordinate system coinciding with the principal directions of $\mathbf{D}$, which may coincide with the fiber, transverse, and thickness directions, and d_i are the eigenvalues of the damage tensor, which represent the damage ratio along these directions. The dual variable of the damage tensor is the *integrity tensor*, $\mathbf{\Omega} = \sqrt{\mathbf{I} - \mathbf{D}}$, which represents the undamaged ratio.

The *second-order damage tensor* $\mathbf{D}$ and the *integrity tensor* $\mathbf{\Omega}$ are diagonal and have the following explicit forms

$$D_{ij} = \begin{bmatrix} d_1 & 0 & 0 \\ 0 & d_2 & 0 \\ 0 & 0 & d_3 \end{bmatrix} \tag{B.2}$$

$$\Omega_{ij} = \begin{bmatrix} \sqrt{1-d_1} & 0 & 0 \\ 0 & \sqrt{1-d_2} & 0 \\ 0 & 0 & \sqrt{1-d_3} \end{bmatrix} = \begin{bmatrix} \Omega_1 & 0 & 0 \\ 0 & \Omega_2 & 0 \\ 0 & 0 & \Omega_3 \end{bmatrix} \tag{B.3}$$

A symmetric fourth-order tensor, $\mathbf{M}$, called the *damage effect tensor*, is defined (see (8.63)) as

$$M_{ijkl} = \frac{1}{2} \left(\Omega_{ik} \Omega_{jl} + \Omega_{il} \Omega_{jk} \right) \tag{B.4}$$

The *damage effect tensor* in contracted form multiplied by the Reuter matrix, takes the form of a 6×6 array as follows

$$\mathbf{M} = \mathbf{M}_{\alpha\beta} = \begin{bmatrix} \Omega_1^2 & 0 & 0 & 0 & 0 & 0 \\ 0 & \Omega_2^2 & 0 & 0 & 0 & 0 \\ 0 & 0 & \Omega_3^2 & 0 & 0 & 0 \\ 0 & 0 & 0 & \Omega_2\Omega_3 & 0 & 0 \\ 0 & 0 & 0 & 0 & \Omega_1\Omega_3 & 0 \\ 0 & 0 & 0 & 0 & 0 & \Omega_1\Omega_2 \end{bmatrix} \tag{B.5}$$

The damaged stiffness tensor $\mathbf{C}$ multiplied by the Reuter matrix can be written in explicit contracted notation for an orthotropic material by a 6×6 array as a function of the undamaged stiffness tensor $\overline{\mathbf{C}}$ as follows

$$\mathbf{C}_{\alpha\beta} = \begin{bmatrix} \overline{C}_{11}\Omega_1^4 & \overline{C}_{12}\Omega_1^2\Omega_2^2 & \overline{C}_{13}\Omega_1^2\Omega_3^2 & 0 & 0 & 0 \\ \overline{C}_{12}\Omega_1^2\Omega_2^2 & \overline{C}_{22}\Omega_2^4 & \overline{C}_{23}\Omega_2^2\Omega_3^2 & 0 & 0 & 0 \\ \overline{C}_{13}\Omega_1^2\Omega_3^2 & \overline{C}_{23}\Omega_2^2\Omega_3^2 & \overline{C}_{33}\Omega_3^4 & 0 & 0 & 0 \\ 0 & 0 & 0 & 2\overline{C}_{44}\Omega_2^2\Omega_3^2 & 0 & 0 \\ 0 & 0 & 0 & 0 & 2\overline{C}_{55}\Omega_1^2\Omega_3^2 & 0 \\ 0 & 0 & 0 & 0 & 0 & 2\overline{C}_{66}\Omega_1^2\Omega_2^2 \end{bmatrix} \tag{B.6}$$

where $\overline{C}_{44} = \overline{G}_{23}$, $\overline{C}_{55} = \overline{G}_{13}$ and $\overline{C}_{66} = \overline{G}_{12}$. The Voigt contracted notation for fourth-order elasticity tensors is used here: $C_{\alpha\beta}$ replaces C_{ijkl} where α, β take the values 1, 2, 3, 4, 5, 6, corresponding to the index pairs 11, 22, 33, 23, 13 and 12, respectively.

The relations between the effective and actual stress components assume the following expressions

$$\begin{aligned} \overline{\sigma}_1 &= \sigma_1\,\Omega_1^{-2}; & \overline{\sigma}_4 &= \sigma_4\,\Omega_2^{-1}\Omega_3^{-1}; \\ \overline{\sigma}_2 &= \sigma_2\,\Omega_2^{-2}; & \overline{\sigma}_5 &= \sigma_5\,\Omega_1^{-1}\Omega_3^{-1}; \\ \overline{\sigma}_3 &= \sigma_3\,\Omega_3^{-2}; & \overline{\sigma}_6 &= \sigma_6\,\Omega_1^{-1}\Omega_2^{-1}; \end{aligned} \tag{B.7}$$

and the strain components

$$\begin{aligned} \overline{\varepsilon}_1 &= \varepsilon_1\,\Omega_1^{2}; & \overline{\varepsilon}_4 &= \varepsilon_4\,\Omega_2\Omega_3; \\ \overline{\varepsilon}_2 &= \varepsilon_2\,\Omega_2^{2}; & \overline{\varepsilon}_5 &= \varepsilon_5\,\Omega_1\Omega_3; \\ \overline{\varepsilon}_3 &= \varepsilon_3\,\Omega_3^{2}; & \overline{\varepsilon}_6 &= \varepsilon_6\,\Omega_1\Omega_2; \end{aligned} \tag{B.8}$$

where the over-line indicates an effective property.

B.2 Thermodynamic Force Y

By satisfying the Clausius-Duhem inequality, thus assuring non-negative dissipation, the following thermodynamic forces (see (8.128)) are defined

$$Y_{ij} = -\frac{\partial\psi}{\partial D_{ij}} = -\frac{1}{2}\left(\varepsilon_{kl}-\varepsilon_{kl}^{p}\right)\frac{\partial C_{klpq}}{\partial D_{ij}}\left(\varepsilon_{pq}-\varepsilon_{pq}^{p}\right) = -\frac{1}{2}\varepsilon_{kl}^{e}\frac{\partial C_{klpq}}{\partial D_{ij}}\varepsilon_{pq}^{e} \tag{B.9}$$

The second-order tensor of the conjugate thermodynamic forces associated to the damage variables takes the following form

$$\mathbf{Y} = Y_{ij} = \begin{bmatrix} Y_{11} & 0 & 0 \\ 0 & Y_{22} & 0 \\ 0 & 0 & Y_{33} \end{bmatrix} \tag{B.10}$$

or in Voigt contracted notation as

$$\mathbf{Y} = Y_{\alpha} = \{Y_{11}, Y_{22}, Y_{33}, 0, 0, 0\}^T \tag{B.11}$$

Using (B.9), the explicit expressions for the thermodynamic forces written in terms of effective strain are found as

$$\begin{aligned} Y_{11} &= \frac{1}{\Omega_1^2}\left(\overline{C}_{11}\,\overline{\varepsilon}_1^{e\,2} + \overline{C}_{12}\,\overline{\varepsilon}_2^e\,\overline{\varepsilon}_1^e + \overline{C}_{13}\,\overline{\varepsilon}_3^e\,\overline{\varepsilon}_1^e + 2\overline{C}_{55}\,\overline{\varepsilon}_5^{e\,2} + 2\overline{C}_{66}\,\overline{\varepsilon}_6^{e\,2}\right) \\ Y_{22} &= \frac{1}{\Omega_2^2}\left(\overline{C}_{22}\,\overline{\varepsilon}_2^{e\,2} + \overline{C}_{12}\,\overline{\varepsilon}_2^e\,\overline{\varepsilon}_1^e + \overline{C}_{23}\,\overline{\varepsilon}_3^e\,\overline{\varepsilon}_2^e + 2\overline{C}_{44}\,\overline{\varepsilon}_4^{e\,2} + 2\overline{C}_{66}\,\overline{\varepsilon}_6^{e\,2}\right) \\ Y_{33} &= \frac{1}{\Omega_3^2}\left(\overline{C}_{33}\,\overline{\varepsilon}_3^{e\,2} + \overline{C}_{13}\,\overline{\varepsilon}_3^e\,\overline{\varepsilon}_1^e + \overline{C}_{23}\,\overline{\varepsilon}_3^e\,\overline{\varepsilon}_2^e + 2\overline{C}_{44}\,\overline{\varepsilon}_4^{e\,2} + 2\overline{C}_{55}\,\overline{\varepsilon}_5^{e\,2}\right) \end{aligned} \tag{B.12}$$

The thermodynamic forces written in terms of actual stress are

$$\begin{aligned} Y_{11} &= \frac{1}{\Omega_1^2}\left(\frac{\overline{S}_{11}}{\Omega_1^4}{\sigma_1}^2 + \frac{\overline{S}_{12}}{\Omega_1^2\Omega_2^2}\sigma_2\sigma_1 + \frac{\overline{S}_{13}}{\Omega_1^2\Omega_3^2}\sigma_3\sigma_1 + \frac{2\overline{S}_{55}}{\Omega_1^2\Omega_3^2}{\sigma_5}^2 + \frac{2\overline{S}_{66}}{\Omega_1^2\Omega_2^2}{\sigma_6}^2\right) \\ Y_{22} &= \frac{1}{\Omega_2^2}\left(\frac{\overline{S}_{22}}{\Omega_2^4}{\sigma_2}^2 + \frac{\overline{S}_{12}}{\Omega_2^2\Omega_1^2}\sigma_2\sigma_1 + \frac{\overline{S}_{23}}{\Omega_2^2\Omega_3^2}\sigma_3\sigma_2 + \frac{2\overline{S}_{44}}{\Omega_2^2\Omega_3^2}{\sigma_4}^2 + \frac{2\overline{S}_{66}}{\Omega_2^2\Omega_1^2}{\sigma_6}^2\right) \\ Y_{33} &= \frac{1}{\Omega_3^2}\left(\frac{\overline{S}_{33}}{\Omega_3^4}{\sigma_3}^2 + \frac{\overline{S}_{13}}{\Omega_3^2\Omega_1^2}\sigma_3\sigma_1 + \frac{\overline{S}_{23}}{\Omega_3^2\Omega_2^2}\sigma_3\sigma_2 + \frac{2\overline{S}_{44}}{\Omega_3^2\Omega_2^2}{\sigma_4}^2 + \frac{2\overline{S}_{55}}{\Omega_3^2\Omega_1^2}{\sigma_5}^2\right) \end{aligned} \tag{B.13}$$

The derivative of the thermodynamic forces with respect to the damage ($\partial\mathbf{Y}/\partial\mathbf{D}$) is given by

$$\frac{\partial\mathbf{Y}}{\partial\mathbf{D}} = \begin{bmatrix} \frac{Y_{11}}{\Omega_1^4} & 0 & 0 & 0 & 0 & 0 \\ 0 & \frac{Y_{22}}{\Omega_2^4} & 0 & 0 & 0 & 0 \\ 0 & 0 & \frac{Y_{33}}{\Omega_3^4} & 0 & 0 & 0 \\ 0 & 0 & 0 & 0 & 0 & 0 \\ 0 & 0 & 0 & 0 & 0 & 0 \\ 0 & 0 & 0 & 0 & 0 & 0 \end{bmatrix} \tag{B.14}$$

The derivative of the thermodynamic forces with respect to the actual strain is

given by

$$\frac{\partial \mathbf{Y}}{\partial \boldsymbol{\varepsilon}^e} = \begin{bmatrix} -\frac{P_{11}}{\Omega_1^2} & -\frac{\overline{C}_{12}\,\overline{\varepsilon}_1^e}{\Omega_1^2} & -\frac{\overline{C}_{13}\,\overline{\varepsilon}_1^e}{\Omega_1^2} & 0 & -2\,\frac{\overline{C}_{55}\,\overline{\varepsilon}_5^e}{\Omega_1^2} & -2\,\frac{\overline{C}_{66}\,\overline{\varepsilon}_6^e}{\Omega_1^2} \\ -\frac{\overline{C}_{12}\,\overline{\varepsilon}_2^e}{\Omega_2^2} & -\frac{P_{22}}{\Omega_2^2} & -\frac{\overline{C}_{23}\,\overline{\varepsilon}_2^e}{\Omega_2^2} & -2\,\frac{\overline{C}_{44}\,\overline{\varepsilon}_4^e}{\Omega_2^2} & 0 & -2\,\frac{\overline{C}_{66}\,\overline{\varepsilon}_6^e}{\Omega_2^2} \\ -\frac{\overline{C}_{13}\,\overline{\varepsilon}_3^e}{\Omega_3^2} & -\frac{\overline{C}_{23}\,\overline{\varepsilon}_3^e}{\Omega_3^2} & -\frac{P_{33}}{\Omega_3^2} & -2\,\frac{\overline{C}_{44}\,\overline{\varepsilon}_4^e}{\Omega_3^2} & -2\,\frac{\overline{C}_{55}\,\overline{\varepsilon}_5^e}{\Omega_3^2} & 0 \\ 0 & 0 & 0 & 0 & 0 & 0 \\ 0 & 0 & 0 & 0 & 0 & 0 \\ 0 & 0 & 0 & 0 & 0 & 0 \end{bmatrix} \tag{B.15}$$

where

$$\begin{aligned} P_{11} = &\ 2\,\overline{C}_{11}\,\overline{\varepsilon}_1^e + \overline{C}_{12}\,\overline{\varepsilon}_2^e + \overline{C}_{13}\,\overline{\varepsilon}_3^e \\ P_{22} = &\ \overline{C}_{12}\,\overline{\varepsilon}_1^e + 2\,\overline{C}_{22}\,\overline{\varepsilon}_2^e + \overline{C}_{23}\,\overline{\varepsilon}_3^e \\ P_{33} = &\ \overline{C}_{13}\,\overline{\varepsilon}_1^e + \overline{C}_{23}\,\overline{\varepsilon}_2^e + 2\,\overline{C}_{33}\,\overline{\varepsilon}_3^e \end{aligned} \tag{B.16}$$

The derivative of the thermodynamic forces with respect to the actual unrecoverable strain is given by

$$\frac{\partial \mathbf{Y}}{\partial \boldsymbol{\varepsilon}^p} = -\frac{\partial \mathbf{Y}}{\partial \boldsymbol{\varepsilon}^e} \tag{B.17}$$

The derivative of the actual stress with respect to damage is given by

$$\frac{\partial \boldsymbol{\sigma}}{\partial \mathbf{D}} = \begin{bmatrix} P'_{11} & 0 & 0 & 0 & 0 & 0 \\ 0 & P'_{22} & 0 & 0 & 0 & 0 \\ 0 & 0 & P'_{33} & 0 & 0 & 0 \\ 0 & -\frac{1}{2}\frac{\Omega_3 \overline{C}_{44}\,\overline{\varepsilon}_4^e}{\Omega_2} & -\frac{1}{2}\frac{\Omega_2 \overline{C}_{44}\,\overline{\varepsilon}_4^e}{\Omega_3} & 0 & 0 & 0 \\ -\frac{1}{2}\frac{\Omega_3 \overline{C}_{55}\,\overline{\varepsilon}_5^e}{\Omega_1} & 0 & -\frac{1}{2}\frac{\Omega_1 \overline{C}_{55}\,\overline{\varepsilon}_5^e}{\Omega_3} & 0 & 0 & 0 \\ -\frac{1}{2}\frac{\Omega_2 \overline{C}_{66}\,\overline{\varepsilon}_6^e}{\Omega_1} & -\frac{1}{2}\frac{\Omega_1 \overline{C}_{66}\,\overline{\varepsilon}_6^e}{\Omega_2} & 0 & 0 & 0 & 0 \end{bmatrix} \tag{B.18}$$

where

$$\begin{aligned} P'_{11} = &\ -\overline{C}_{11}\,\overline{\varepsilon}_1^e - \overline{C}_{12}\,\overline{\varepsilon}_2^e - \overline{C}_{13}\,\overline{\varepsilon}_3^e \\ P'_{22} = &\ -\overline{C}_{12}\,\overline{\varepsilon}_1^e - \overline{C}_{22}\,\overline{\varepsilon}_2^e - \overline{C}_{23}\,\overline{\varepsilon}_3^e \\ P'_{33} = &\ -\overline{C}_{13}\,\overline{\varepsilon}_1^e - \overline{C}_{23}\,\overline{\varepsilon}_2^e - \overline{C}_{33}\,\overline{\varepsilon}_3^e \end{aligned} \tag{B.19}$$

B.3 Damage Surface

An anisotropic damage criterion expressed in tensorial form, introducing two fourth-order tensors, **B** and **J** defines a multiaxial limit surface in the thermodynamic force space, **Y**, that bounds the damage domain. The damage evolution is defined by a damage potential associated to the damage surface and by an isotropic hardening function. The proposed damage surface g^d is given by

$$g^d = \left(\hat{Y}_{ij}^N J_{ijhk} \hat{Y}_{hk}^N\right)^{1/2} + \left(Y_{ij}^S B_{ijhk} Y_{hk}^S\right)^{1/2} - (\gamma(\delta) + \gamma_0) \tag{B.20}$$

where γ_0 is the initial damage threshold value and $\gamma(\delta)$ defines the hardening.

The derivative of the damage surface with respect to thermodynamic forces is given by

$$\frac{\partial g^d}{\partial \mathbf{Y}} = \begin{bmatrix} \dfrac{J_{11}\, Y_{11}^N}{\Phi^N} + \dfrac{B_{11}\, Y_{11}^S}{\Phi^S} \\ \dfrac{J_{22}\, Y_{22}^N}{\Phi^N} + \dfrac{B_{22}\, Y_{22}^S}{\Phi^S} \\ \dfrac{J_{33}\, Y_{33}^N}{\Phi^N} + \dfrac{B_{33}\, Y_{33}^S}{\Phi^S} \\ 0 \\ 0 \\ 0 \end{bmatrix} \tag{B.21}$$

where

$$\begin{aligned} \Phi^N = & \sqrt{J_{11}\,(Y_{11}^N)^2 + J_{22}\,(Y_{22}^N)^2 + J_{33}\,(Y_{33}^N)^2} \\ \Phi^S = & \sqrt{B_{11}\,(Y_{11}^S)^2 + B_{22}\,(Y_{22}^S)^2 + B_{33}\,(Y_{33}^S)^2} \end{aligned} \tag{B.22}$$

The derivative of the damage surface with respect to damage hardening is

$$\frac{\partial g^d}{\partial \gamma} = -1 \tag{B.23}$$

B.4 Unrecoverable-Strain Surface

The unrecoverable-strain (yield) surface g^p is a function of the thermodynamic forces in the effective configuration $(\overline{\sigma}, R)$. Therefore, the unrecoverable-strain surface is

$$g^p = \sqrt{f_{ij}\overline{\sigma}_i\overline{\sigma}_j + f_i\overline{\sigma}_i} - (R\,(p) + R_0) \tag{B.24}$$

where $(i = 1, 2...6)$, R_0 is the initial unrecoverable-strain threshold and R is the hardening function.

The derivative of the unrecoverable-strain surface with respect to effective stress is given by

$$\frac{\partial \mathbf{g^p}}{\partial \overline{\sigma}} = \begin{bmatrix} \dfrac{1}{2}\,\dfrac{f_1 + 2\,f_{11}\,\overline{\sigma}_1 + 2\,f_{12}\,\overline{\sigma}_2 + 2\,f_{13}\,\overline{\sigma}_3}{\Phi^p} \\ \dfrac{1}{2}\,\dfrac{f_2 + 2\,f_{22}\,\overline{\sigma}_2 + 2\,f_{12}\,\overline{\sigma}_1 + 2\,f_{23}\,\overline{\sigma}_3}{\Phi^p} \\ \dfrac{1}{2}\,\dfrac{f_3 + 2\,f_{33}\,\overline{\sigma}_3 + 2\,f_{13}\,\overline{\sigma}_1 + 2\,f_{23}\,\overline{\sigma}_2}{\Phi^p} \\ \dfrac{f_4\,\overline{\sigma}_4}{\Phi^p} \\ \dfrac{f_5\,\overline{\sigma}_5}{\Phi^p} \\ \dfrac{f_6\,\overline{\sigma}_6}{\Phi^p} \end{bmatrix} \tag{B.25}$$

where

$$\begin{aligned}\Phi^p &= (f_1\,\overline{\sigma}_1 + f_2\,\overline{\sigma}_2 + f_3\,\overline{\sigma}_3 + \\ &+ f_{11}\,\overline{\sigma}_1{}^2 + f_{22}\,\overline{\sigma}_2{}^2 + f_{33}\,\overline{\sigma}_3{}^2 + \\ &+ 2\,f_{12}\,\overline{\sigma}_1\,\overline{\sigma}_2 + 2\,f_{13}\,\overline{\sigma}_1\,\overline{\sigma}_3 + 2\,f_{23}\,\overline{\sigma}_2\,\overline{\sigma}_3 + \\ &+ f_6\,\overline{\sigma}_6{}^2 + f_5\,\overline{\sigma}_5{}^2 + f_4\,\overline{\sigma}_4{}^2\big)^{1/2}\end{aligned} \tag{B.26}$$

The derivative of the yield surface with respect to unrecoverable-strain hardening is

$$\frac{\partial g^p}{\partial R} = -1 \tag{B.27}$$

Appendix C

Software Used

Only four software applications are used throughout this textbook. By far the most used is ANSYS® Mechanical APDL (referred simply as ANSYS in this textbook). BMI3© is used only in Chapter 4. MATLAB® is used for symbolic as well as numerical computations. Finally, Intel Fortran must be available to compile and link ANSYS with user programmed material subroutines, but its usage is transparent to the user because it is called by a batch file requiring no user intervention. Of course, some knowledge of Fortran is required to program new user material subroutines, but programming is made easier by several example subroutines, which are provided and used in the examples.

The aim of this section is to present an introduction to the software used in this textbook, namely ANSYS and BMI3, as well as how to use Intel Fortran to compile and link user subroutines with ANSYS. It is assumed that the reader can use MATLAB without help besides that provided by the self-explanatory code included with the examples, either printed in this textbook or downloadable from the Web site [5].

Operation of the software is illustrated for a Windows 7 platform but operation in a Linux environment is very similar. For the sake of space, this section is very brief. The vendors of these applications have a wealth of information, training sessions, user groups, and so on, that the reader can use to get familiar with the software interface. One such source of information is the Web site for this textbook at `http://barbero.cadec-online.com/feacm-ansys/`. Another source of information is the book's user group at `http://tech.groups.yahoo.com/group/feacomposites/`.

C.1 ANSYS Mechanical APDL

ANSYS Mechanical APDL is a commercial finite element analysis (FEA) application. It has a friendly graphical user interface (GUI) and an extensive help system. Once started, the user should have no difficulty navigating menus and so on. Since all the mouse clicks in the GUI generate ANSYS command lines, which are saved in a `.log` file, it is easy to use the GUI to learn what the various commands do.

The ANSYS help can then be used to enhance the user's knowledge of the ANSYS command structure.

In this textbook, selected commands from a `.log` file created with the GUI are copied into a `.inp` file, which upon being read into ANSYS automatically performs all the tasks of model creation, execution, and post-processing. This methodology is recommended because the `.inp` file can be debugged, refined, adapted to similar situations, recalled later on, and it provides excellent documentation for project reporting to the client and even auditing by third parties. The `.inp` files provided with the examples in this textbook demonstrate their usefulness, even if the GUI was used to help generate most of them.

The examples in this textbook were produced using ANSYS version 14. They work identically in Windows and Linux platforms. On Windows, ANSYS is accessible from the START menu, through two icons: "Mechanical APDL (ANSYS)" and "Mechanical APDL Product Launcher." It is best to use at least once the later, as it allows us to set the default location for the model files.

In this Appendix, it is assumed that the user has created a folder `c:\ansys\user\`, where all the model files reside. Therefore, in "Product Launcher," under "File Management," the "Working Directory" should be set to `c:\ansys\user`. Clicking on `Run` invokes the GUI.

The ANSYS GUI has a command bar at the top and a menu list on the left. Below the command bar, there is single-line command window. ANSYS commands typed in this window are executed immediately and have the same effect as equivalent GUI operations.

Although the GUI is user friendly, it is very challenging to describe (in a textbook) all the mouse clicks one has to do in order to set up and solve a problem. It is also challenging to remember what one did during a previous session using the GUI. And there is no use trying to write down the myriad mouse clicks needed to accomplish a task. Fortunately, all GUI operations (mouse clicks, menu selections, data entry, and so on) are saved by ANSYS into a `.log` file in the current directory (`c:\ansys\user\`). The `.log` file is a text file that can be edited and cleaned up of the many commands that represent dead ends that one has reached during a session. Cleaned up `.log` files become `.inp` files, which can be recalled into ANSYS and executed to reproduce a prior session.

The `.inp` files can be recalled in three ways. First, each line in the `.inp` file can be typed in the command window and executed one at a time (by pressing `enter`, of course). This is very useful in order to learn the effect that each command line has on the model generation, execution, and so on. Second, a portion or the whole `.inp` file can be pasted into the command window and executed. Finally, once a `.inp` file is polished, the most computationally efficient way to enter a model is to type the following command `/input,file,inp`, in the command window. This will retrieve `file.inp` and execute it. The equivalent GUI mouse clicks are: `File, Read Input From, OK`.

As was mentioned before, this section is very brief. It has been my experience that students successfully teach themselves ANSYS by figuring out the commands used in the examples in this textbook, which are available on the Web site [5],

along with the help system and the documentation included with ANSYS. Video recordings illustrating the execution of the examples by using the ANSYS GUI are available on the Web site [5].

C.1.1 ANSYS USERMAT, Compilation and Execution

Compilation and execution of ANSYS user programmable features (UPF) can be accomplished following the procedure described in this section or as explained in [15]. In this section, it is assumed that ANSYS 14.0, Microsoft Visual Studio 2008, and Fortran Intel 11.1, are all available on a Windows system. Note that the path to software components will change with time as new versions and different platforms are released. Therefore, the paths given in this section may have to be adjusted. For example `v140` refers to version 14.0 and `intel` refers to the Intel^{TM} processor, which may have to be adjusted to reflect the software and hardware configuration available to you.

There are 3 methods in ANSYS 14.0 to access user programmable features:

- Custom dynamic link librariy (DLL, described and used in this book).
- Custom `.exe` (described in the first edition of this book). We no longer favor this method, but it is clearly explained in the ANSYS documentation in case the reader wants to use it.
- User programmable features /UPF command. We do not use this method because it cannot be used from the GUI, only in batch mode, but it is clearly explained in the ANSYS documentation in case the reader wants to use it.

ANSYS will look for a `USERMAT` in the form of a `USERMATLIB.DLL` provided two things happen:

- You have set up the environment variable `ANS_USER_PATH` in Windows, to point to the place where you want to store your DLLs. We recommend using the work directory, `c:\ANSYS\User`.
- A `TB,USER,` line appears in the `.inp` file.

One such DLL is available in `C:\Program Files\ANSYS Inc\v140\ansys\bin\winx64` containing some sample code. To bypass this DLL and use your own, you must do the following:

- Decide where you want to store your DLL. Our preference is to store them in our work directory, `c:\ANSYS\User`.
- Add the environment variable `ANS_USER_PATH` to Windows, to point to the place where you want to store your DLLs.

To add the environment variable, do this:

- Click Start, Control Panel, Advanced System Settings.
- Then, follow the steps illustrated in Figures C.1, where you click `Environment Variables`, and Figure C.2, where you can add/edit `ANS_USER_PATH`.

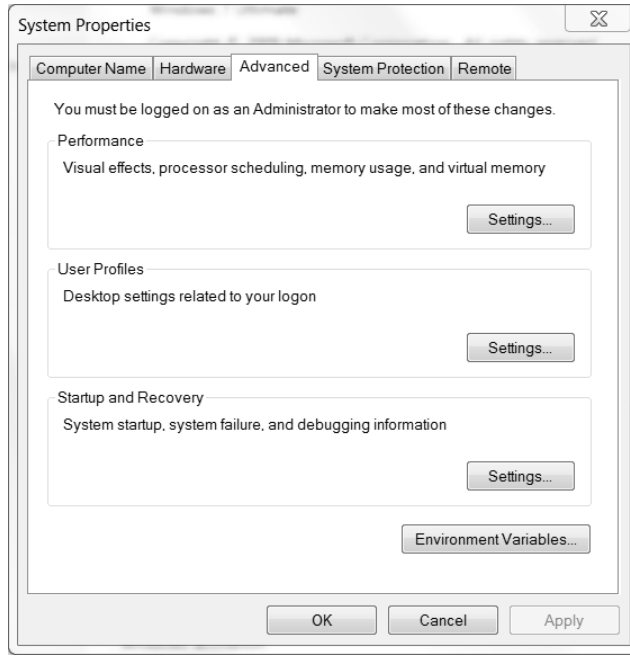

Figure C.1: Add environment variable. Step 1. Click `Environment Variables`.

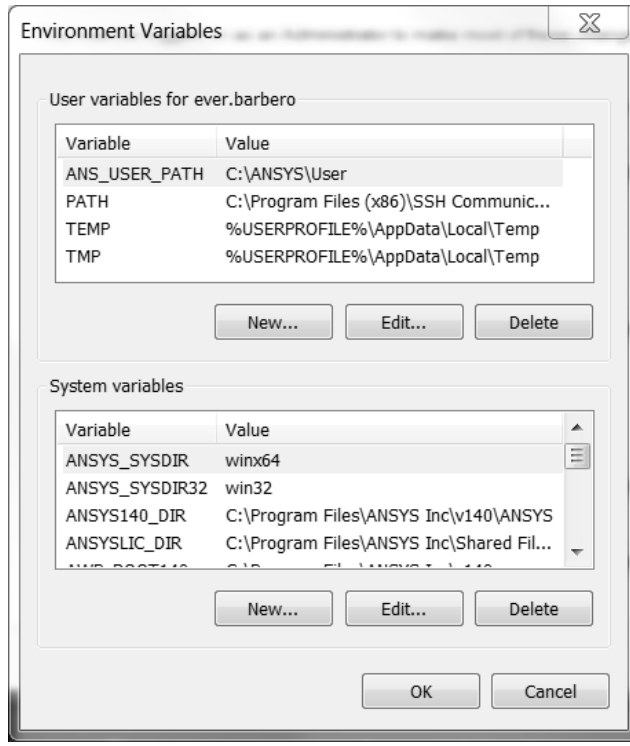

Figure C.2: Add environment variable. Step 2. Add/edit `ANS_USER_PATH`.

Making your own DLLs

In ANSYS, `USERMAT.F` calls four specific subroutines:

- `USERMAT1D` can be used for 1D elements such as bars and links, not beams.
- `USERMAT3D` is used for 3D solid elements.
- `USERMATBM` is used for BEAM elements.
- `USERMATPS` is used for PLANE STRESS elements such as PLANE and SHELL.

You should not modify `USERMAT.F`, but just the code in one or more of the specific routines listed above.

To make your own DLLs, copy the following from [5] to your work directory (folder):

- Copy `AnsUserMatEjb.bat` to your work directory. This is a modified version of `ANSUSERSHARED.BAT` provided by ANSYS. It has been modified to find the various files needed for compilation, as well as to allow you to write free formatted code (F90, F95).
- Copy `impcomEjb.inc` to your work directory. This is an interface to call ANSYS's `impcom.inc` from your own free formatted code. Note: `impcom.inc` is an include file called by ANSYS using a compiler directive.
- Copy the folder `\EJB` to your work directory. This folder contains templates for all five USERMAT routines, and a backup copy of `AnsUserMatEjb.bat` just in case. Do not modify anything in this folder. Just use it as a repository for templates that you may want to modify.

Then, copy all four specific routines from `\EJB` to your work directory. Modify one or more of them to suit your needs. The ones you do not modify will be there just to fill up a place when you build your DLL. The templates provided implement routines used in some of the examples. You can look at the source code to learn about them.

Once you have your own specific USERMATxx ready, you use `AnsUserMatEjb.bat` to make your DLL. `AnsUserMatEjb.bat` will look for a template `USERMAT.F` in the `\EJB` folder and needs the four `USERMATxx.F` and `impcom.inc` to be in your work directory. Double click on `AnsUserMatWvu.bat` to execute it. If the DLL is built correctly, it will be compiled and ANSYS will find it. If not, look at `compile.log` to see the errors.

Note that `.\usermat.F` residing in your work directory will be overwritten each time you use the batch file `AnsUserMatWvu.bat`, but it is not a problem because `AnsUserMatWvu.bat` looks for a fresh copy in `\EJB` and the four editable files will be automatically appended. You just edit any of the specific files listed above.

C.2 BMI3

Most users will run BMI3 within ANSYS as explained in Section C.2.2 but for troubleshooting it is useful to know how to operate it outside ANSYS, as explained in Section C.2.1 next.

C.2.1 Stand-Alone BMI3

Native BMI3 code accepts an input file in *Abaqus*™ format, as long as the input file is filtered by the program I2B [5]. Not all of the *Abaqus* commands are accepted by I2B. For example it only accepts models with concentrated forces on nodes.

Most commercial computer aided design (CAD) packages such as I-DEAS™ and FEMAP™ can output an *Abaqus* file. Then, it is easy to modify the file to make it comply with the restrictions of I2B. Run I2B to generate `DEMO.inp`, `ABAQUS.inp`, and `DEMO.dat`. If ABAQUS.inp were to be executed within *Abaqus*, it would give the bifurcation loads $\Lambda^{(cr)}$.

The material properties and perturbation parameters are in `DEMO.dat`. The last line contains *modenum*, *nodenum*, *component*. This is the mode, node, and component used as a perturbation parameter. If all are zeros, BMI3 picks the lowest mode and the node-component combination that yields the largest mode amplitude. The results are printed in `DEMO.out` and the mode shapes saved in `MODES` file.

C.2.2 BMI3 within ANSYS

It is possible to use the program BMI3 directly from ANSYS, with some restrictions:

- Use only element type `SHELL99`.
- Introduce the laminate properties using $ABDH$ matrices, with `KEYOPT(2)=2`.
- Only apply loads on nodes or keypoints using concentrated forces (do not use moments). If the model has distributed loads, calculate the equivalent nodal forces and apply them at the nodes.
- Use only one real constant set for all the models.

The procedure to compute the post-critical path parameters using BMI3 within ANSYS is described next.

- In the working directory (`c:\ansys`), copy the APDL macro `ans2i.mac`, and the programs `bmi3.exe` and `i2b_ans.exe` from [5].
- Define the model in ANSYS and solve it using the "Eigenvalue buckling analysis" procedure for obtaining the bifurcation loads $\Lambda^{(cr)}$ (e.g., Example 4.2).
- Run the APDL macro `ans2i` simply by entering `ans2i` in the ANSYS command line [5] to calculate parameters of the post-critical path.

- Look for the `c:\ANSYS 14.0 Output Window`, which is minimized in the Windows taskbar, and bring it to the foreground.
- In the `c:\ANSYS 14.0 Output Window`, respond to the two prompts: (i) activate or not sorting of the nodes in order to minimize the bandwidth of the system of equations (sorting along the longest dimension is recommended), (ii) introduce the *mode*, *node*, and *component* used as the perturbation parameter s or let BMI3 choose the default. By default, the lowest *mode* and the *node*, *component*, with the largest mode amplitude is used. If an error message of "INSUFFICIENT STORAGE" appears, try sorting along another direction. If that fails, BMI3 needs to be recompiled with larger arrays.
- In addition to the critical load $\Lambda^{(cr)}$, BMI3 computes the slope $L(1) = \Lambda^{(1)}$ and the curvature $L(2) = \Lambda^{(2)}$ of the bifurcation mode selected. These results are shown in the `c:\ANSYS 14.0 Output Window` and they are printed in `DEMO.out`
- Do not close the `c:\ANSYS 14.0 Output Window`, just minimize it. Otherwise, it will abort ANSYS. Instead, ANSYS should be closed from the GUI.

Note that the results (bifurcation loads, slopes, and curvatures) appear with a negative sign. This is usual in stability analysis. If a model is constructed with tensile loads (instead of the usual compression), one can type `REVERS=-1` in the ANSYS command line before executing the APDL macro `ANS2I`. Another peculiarity of the BMI3 software is that transverse deflections w (perpendicular to the plate) have an opposite sign to that used by ANSYS. Since transverse deflections w are often used as perturbation parameters, the change in sign must be taken into account during the interpretation of results.

References

[1] E. J. Barbero. *Introduction to Composite Materials Design–Second Edition.* `http://barbero.cadec-online.com/icmd`. CRC Press, Boca Raton, FL, 2010.

[2] D. Frederick and T.-S. Chang. *Continuum Mechanics.* Scientific Publishers, Cambridge, MA, 1972.

[3] F. P. Beer, E. R. Johnston Jr., and J. T. DeWolf. *Mechanics of Materials, 3rd Edition.* McGraw-Hill, Boston, MA, 2001.

[4] J. N. Reddy. *Energy and Variational Methods in Applied Mechanics.* Wiley, New York, 1984.

[5] E. J. Barbero. Web resource: `http://barbero.cadec-online.com/feacm-ansys`.

[6] S. S. Sonti, E. J. Barbero, and T. Winegardner. Mechanical properties of pultruded E-glass–vinyl ester composites. In *50th Annual Conference, Composites Institute, Society of the Plastics Industry (February) pp. 10-C/1-7*, 1995.

[7] E. J. Barbero. *Finite Element Analysis of Composite Materials Using Abaqus.* CRC Press, 2013.

[8] ANSYS Inc. ANSYS mechanical APDL structural analysis guide, release 14.0, 2011.

[9] E. J. Barbero. Computer aided design environment for composites. `http://www.cadec-online.com`, 2011.

[10] J. N. Reddy. *Mechanics of Laminated Composite Plates and Shells, 2nd Edition.* CRC Press, Boca Raton, FL, 2003.

[11] R. J. Roark and W. C. Young. *Roark's Formulas for Stress and Strain, 6th Edition.* McGraw-Hill, New York, NY, 1989.

[12] E. Hinton and D. R. J. Owen. *An Introduction to Finite Element Computations.* Pineridge Press, Swansea, UK, 1979.

[13] ANSYS Inc. ANSYS mechanical APDL theory reference, release 14.0, 2011.

[14] Simulia. Abaqus documentation. The default location for the HTML documentation is `http://HOME:2080/v6.10/` where `HOME` is the `url` of the server where the documentation is stored during installation. The default location for the PDF documentation is C:/SIMULIA/Documentation/docs/v6.10/pdf_books/index.pdf.

[15] ANSYS Inc. ANSYS mechanical APDL programmer's manual, release 14.0, 2011.

[16] E. J. Barbero and J. Trovillion. Prediction and measurement of post-critical behavior of fiber-reinforced composite columns. *Composites Science and Technology*, 58:1335–1341, 1998.

[17] E. J. Barbero. Prediction of compression strength of unidirectional polymer matrix composites. *Journal of Composite Materials*, 32(5)(5):483–502, 1998.

[18] A. Puck and H. Schurmann. Failure analysis of FRP laminates by means of physically based phenomenological models. *Composites Science and Technology*, 62:1633–1662, 2002.

[19] MIL17.org. The composite materials handbook, web resource, `http://www.mil17.org`.

[20] ANSYS Inc. ANSYS parametric design language guide, release 14.0, 2011.

[21] L. A. Godoy. *Theory of Stability-Analysis and Sensitivity.* Taylor and Francis, Philadelphia, PA, 2000.

[22] E. J. Barbero, L. A. Godoy, and I. G. Raftoyiannis. Finite elements for three-mode interaction in buckling analysis. *International Journal for Numerical Methods in Engineering*, 39(3):469–488, 1996.

[23] L. A. Godoy, E. J. Barbero, and I. G. Raftoyiannis. Finite elements for post-buckling analysis. I-The W-formulation. *Computers and Structures*, 56(6):1009–1017, 1995.

[24] E. J. Barbero, I. G. Raftoyiannis, and L. A. Godoy. Finite elements for post-buckling analysis. II-Application to composite plate assemblies. *Computers and Structures*, 56(6):1019–1028, 1995.

[25] I. G. Raftoyiannis, L. A. Godoy, and E. J. Barbero. Buckling mode interaction in composite plate assemblies. *Applied Mechanics Reviews*, 48(11/2):52–60, 1995.

[26] E. J. Barbero. Prediction of buckling-mode interaction in composite columns. *Mechanics of Composite Materials and Structures*, 7(3):269–284, 2000.

[27] S. Yamada and J. G. A. Croll. Buckling behavior pressure loaded cylindrical panels. *ASCE Journal of Engineering Mechanics*, 115(2):327–344, 1989.

[28] C. T. Herakovich. *Mechanics of Fibrous Composites.* Wiley, New York, 1998.

[29] J. D. Eshelby. The determination of the elastic field of an ellipsoidal inclusion and related problems. *Proceedings of the Royal Society*, A241:376–396, 1957.

[30] J. D. Eshelby. The elastic field outside an ellipsoidal inclusion. *Acta Metallurgica*, A252:561–569, 1959.

[31] T. Mori and K. Tanaka. The elastic field outside an ellipsoidal inclusion. *Acta Metallurgica*, 21:571–574, 1973.

[32] R. Hill. A self-consistent mechanics of composite materials. *Journal of Mechanics and Physics of Solids*, 13:213–222, 1965.

[33] S. Nemat-Nasser and M. Hori. *Micromechanics: Overall Properties of Heterogeneous Materials.* North-Holland, Amsterdam, 1993.

[34] R. Luciano and E. J. Barbero. Formulas for the stiffness of composites with periodic microstructure. *International Journal of Solids and Structures*, 31(21):2933–2944, 1995.

[35] R. Luciano and E. J. Barbero. Analytical expressions for the relaxation moduli of linear viscoelastic composites with periodic microstructure. *ASME J. Applied Mechanics*, 62(3):786–793, 1995.

[36] E. J. Barbero and R. Luciano. Micromechanical formulas for the relaxation tensor of linear viscoelastic composites with transversely isotropic fibers. *International Journal of Solids and Structures*, 32(13):1859–1872, 1995.

[37] J. Aboudi. *Mechanics of Composite Materials : A Unified Micromechanical Approach. Vol. 29 of Studies in Applied Mechanics*. Elsevier, New York, NY, 1991.

[38] Z. Hashin and S. Shtrikman. A variational approach to the elastic behavior of multiphase materials. *Journal of Mechanics and Physics of Solids*, 11:127–140, 1963.

[39] V. Tvergaard. Model studies of fibre breakage and debonding in a metal reinforced by short fibres. *Journal of Mechanics and Physics of Solids*, 41(8):1309–1326, 1993.

[40] J. L. Teply and G. J. Dvorak. Bound on overall instantaneous properties of elastic-plastic composites. *Journal of Mechanics and Physics of Solids*, 36(1):29–58, 1988.

[41] E. J. Barbero. *Finite Element Analysis of Composite Materials–First Edition*. CRC Press, Boca Raton, FL, 2007.

[42] R. Luciano and E. Sacco. Variational methods for the homogenization of periodic media. *European Journal of Mechanics A/Solids*, 17:599–617, 1998.

[43] G. J. Creus. *Viscoelasticity: Basic Theory and Applications to Concrete Structures*. Springer-Verlag, Berlin, 1986.

[44] E. J. Barbero. 3-D finite element for laminated composites with 2-d kinematic constraints. *Computers and Structures*, 45(2):263–271, 1992.

[45] Eric W. Weisstein. Gamma function. MathWorld–A Wolfram Web Resource. `http://mathworld.wolfram.com/GammaFunction.html`.

[46] G. D. Dean, B. E. Read, and P. E. Tomlins. A model for long-term creep and the effects of physical ageing in poly (butylene terephthalate). *Plastics and Rubber Processing and Applications*, 13(1):37–46, 1990.

[47] B. F. Oliveira and G. J. Creus. An analytical-numerical framework for the study of ageing in fibre reinforced polymer composites. *Composites B*, 65(3-4):443–457, 2004.

[48] E. J. Barbero. *Chapter 2: Time-Temperature-Age Superposition Principle for Predicting Long-Term Response of Linear Viscoelastic Materials, in Creep and Fatigue in Polymer Matrix Composites*. Woodhead, Cambridge, 2010.

[49] L. C. E. Struik. *Physical aging in amorphous polymers and other materials*. Elsevier Scientific Pub. Co. ; New York, 1978.

[50] K. Ogatha. *Discrete-Time Control System*. Prentice Hall, Englewood Cliffs, NJ, 1987.

[51] K. J. Hollenbeck. Invlap.m: A MATLAB function for numerical inversion of Laplace transforms by the de Hoog algorithm (1998), `http://www.mathworks.com/`.

[52] R. S. Lakes. *Viscoelastic Solids*. CRC Press, Boca Raton, FL, 1998.

[53] J. D. Ferry. *Viscoelastic Properties of Polymers. 3rd. Edition*. Wiley, New York, 1980.

[54] R. M. Christensen. *Theory of Viscoelasticity: Second Edition*. Dover, Mineola, NY, 2010.

[55] P. Qiao, E. J. Barbero, and J. F. Davalos. On the linear viscoelasticity of thin-walled laminated composite beams. *Journal of Composite Materials*, 34(1):39–68, 2000.

[56] E. J. Barbero, F. A. Cosso, R. Roman, and T. L. Weadon. Determination of material parameters for Abaqus progressive damage analysis of E-Glass Epoxy laminates, http://dx.doi.org/10.1016/j.compositesb.2012.09.069. *Composites Part B:Engineering*, 46(3):211–220, 2012.

[57] J. Lemaitre and A. Plumtree. Application of damage concepts to predict creep-fatigue failures. In *American Society of Mechanical Engineers, 78-PVP-26*, pages 10–26, 1978.

[58] I. N. Rabotnov. *Rabotnov: Selected Works - Problems of the Mechanics of a Deformable Solid Body.* Moscow Izdatel Nauka, 1991.

[59] L. M. Kachanov. On the creep fracture time. *Izv. Akad. Nauk USSR*, 8:26–31, 1958.

[60] N. R. Hansen and H. L. Schreyer. A thermodynamically consistent framework for theories of elastoplasticity coupled with damage. *International Journal of Solids and Structures*, 31(3):359–389, 1994.

[61] J. Janson and J. Hult. Fracture mechanics and damage mechanics: A combined approach. *Journal of Theoretical and Applied Mechanics*, 1:S18–28, 1977.

[62] E. J. Barbero and K. W. Kelly. Predicting high temperature ultimate strength of continuous fiber metal matrix composites. *Journal of Composite Materials*, 27(12):1214–1235, 1993.

[63] K. W. Kelly and E. Barbero. Effect of fiber damage on the longitudinal creep of a CFMMC. *International Journal of Solids and Structures*, 30(24):3417–3429, 1993.

[64] J. R. Rice. *Continuum Mechanics and Thermodynamics of Plasticity in Relation to Microscale Deformation Mechanisms*, chapter 2, pages 23–79. Constitutive Equations in Plasticity. MIT Press, Cambridge, MA, 1975.

[65] J. C. Simo and T. J. R. Hughes. *Computational Inelasticity.* Springer, Berlin, 1998.

[66] D. Krajcinovic, J. Trafimow, and D. Sumarac. Simple constitutive model for a cortical bone. *Journal of Biomechanics*, 20(8):779–784, 1987.

[67] D. Krajcinovic and D. Fanella. Micromechanical damage model for concrete. *Engineering Fracture Mechanics*, 25(5-6):585–596, 1985.

[68] D. Krajcinovic. Damage mechanics. *Mechanics of Materials*, 8(2-3):117–197, 1989.

[69] A. M. Neville. *Properties of Concrete, 2nd Edition.* Wiley, New York, NY, 1973.

[70] ACI, American Concrete Institute.

[71] B. W. Rosen. The tensile failure of fibrous composites. *AIAA Journal*, 2(11):1985–1991, 1964.

[72] W. Weibull. A statistical distribution function of wide applicability. *Journal of Applied Mechanics*, 18:293–296, 1951.

[73] B. W. Rosen. *Fiber Composite Materials*, chapter 3. American Society for Metals, Metals Park, OH, 1965.

[74] A. S. D. Wang. A non-linear microbuckling model predicting the compressive strength of unidirectional composites. In *ASME Winter Annual Meeting*, volume WA/Aero-1, 1978.

[75] J. S. Tomblin, E. J. Barbero, and L. A. Godoy. Imperfection sensitivity of fiber micro-buckling in elastic-nonlinear polymer-matrix composites. *International Journal of Solids and Structures*, 34(13):1667–1679, 1997.

[76] D. C. Lagoudas and A. M. Saleh. Compressive failure due to kinking of fibrous composites. *Journal of Composite Materials*, 27(1):83–106, 1993.

[77] P. Steif. A model for kinking in fiber composites. I. Fiber breakage via micro-buckling. *International Journal of Solids and Structures*, 26 (5-6):549–561, 1990.

[78] S. W. Yurgartis and S. S. Sternstein. *Experiments to Reveal the Role of Matrix Properties and Composite Microstructure in Longitudinal Compression Strength*, volume 1185 of *ASTM Special Technical Publication*, pages 193–204. ASTM, Philadelphia, PA, 1994.

[79] C. Sun and A. W. Jun. Effect of matrix nonlinear behavior on the compressive strength of fiber composites. In *AMD*, volume 162, pages 91–101, New York, NY, 1993. ASME, American Society of Mechanical Engineers, Applied Mechanics Division.

[80] D. Adams and E. Lewis. Current status of composite material shear test methods. *SAMPE Journal*, 31(1):32–41, 1995.

[81] A. Maewal. Postbuckling behavior of a periodically laminated medium in compression. *International Journal of Solids and Structures*, 17(3):335–344, 1981.

[82] L. M. Kachanov. Rupture time under creep conditions problems of continuum mechanics. *SIAM*, pages 202–218, 1958.

[83] E. J. Barbero and L. DeVivo. A constitutive model for elastic damage in fiber-reinforced PMC laminae. *Journal of Damage Mechanics*, 10(1):73–93, 2001.

[84] E. J. Barbero, F. Greco, and P. Lonetti. Continuum damage-healing mechanics with application to self-healing composites. *International Journal of Damage Mechanics*, 14(1):51–81, 2005.

[85] S. Murakami. Mechanical modeling of material damage. *Journal of Applied Mechanics*, 55:281–286, 1988.

[86] J. M. Smith and H. C. Van Ness. *Introduction to Chemical Engineering Thermodynamics, 3rd Edition.* McGraw-Hill, New York, NY, 1975.

[87] E. R. Cohen, T. Cvita, J. G. Frey, B. Holmstrm, K. Kuchitsu, R. Marquardt, I. Mills, F. Pavese, M. Quack, J. Stohner, H. L. Strauss, M. Takami, and A. J. Thor. *Quantities, Units and Symbols in Physical Chemistry : The IUPAC Green Book, 3rd Edition,* `http://old.iupac.org/publications/books/author/cohen.html`. RSC Publishing, 2007.

[88] L. E. Malvern. *Introduction to the Mechanics of a Continuous Medium.* Prentice Hall, Upper Saddle River, NJ, 1969.

[89] Y. A. Cengel and M. A. Boles. *Thermodynamics: An Engineering Approach, 3rd Edition.* McGraw-Hill, New York, NY, 1998.

[90] E. J. Barbero and P. Lonetti. Damage model for composites defined in terms of available data. *Mechanics of Composite Materials and Structures*, 8(4):299–315, 2001.

[91] P. Lonetti, R. Zinno, F. Greco, and E. J. Barbero. Interlaminar damage model for polymer matrix composites. *Journal of Composite Materials*, 37(16):1485–1504, 2003.

[92] P. Lonetti, E. J. Barbero, R. Zinno, and F. Greco. Erratum: Interlaminar damage model for polymer matrix composites. *Journal of Composite Materials*, 38(9):799–800, 2004.

[93] J. Lubliner. *Plasticity Theory.* Collier Macmillan, New York, NY, 1990.

[94] J. A. Nairn. The strain energy release rate of composite microcracking: A variational approach. *Journal of Composite Materials*, 23(11):1106–1129, 11 1989.

[95] J. A. Nairn, S. Hu, S. Liu, and J. S. Bark. The initiation, propagation, and effect of matrix microcracks in cross-ply and related laminates. In *Proceedings of the 1st NASA Advanced Composite Technical Conference*, pages 497–512, Oct. 29–Nov. 1, 1990.

[96] S. Liu and J. A. Nairn. The formation and propagation of matrix microcracks in cross-ply laminates during static loading. *Journal of Reinforced Plastics and Composites*, 11(2):158–178, Feb. 1992.

[97] J. A. Nairn. Microcracking, microcrack-induced delamination, and longitudinal splitting of advanced composite structures. Technical Report NASA Contractor Report 4472, 1992.

[98] J. A. Nairn and S. Hu. *Damage Mechanics of Composite Materials*, volume 9 of *Composite Materials Series*, chapter Matrix Microcracking, pages 187–244. Elsevier, 1994.

[99] J. A. Nairn. Applications of finite fracture mechanics for predicting fracture events in composites. In *5th International Conference on Deformation and Fracture of Composites*, 18–19 March 1999.

[100] J. A. Nairn. *Polymer Matrix Composites*, volume 2 of *Comprehensive Composite Materials*, chapter Matrix Microcracking in Composites, pages 403–432. Elsevier Science, 2000.

[101] J. A. Nairn. Fracture mechanics of composites with residual stresses, imperfect interfaces, and traction-loaded cracks. In *Recent Advances in Continuum Damage Mechanics for Composites Workshop*, volume 61, pages 2159–2167, UK, 20–22 Sept. 2000. Elsevier.

[102] J. A. Nairn and D. A. Mendels. On the use of planar shear-lag methods for stress-transfer analysis of multilayered composites. *Mechanics of Materials*, 33(6):335–362, 2001.

[103] J. A. Nairn. *Finite Fracture Mechanics of Matrix Microcracking in Composites*, pages 207–212. Application of Fracture Mechanics to Polymers, Adhesives and Composites. Elsevier, 2004.

[104] Y. M. Han, H. T. Hahn, and R. B. Croman. A simplified analysis of transverse ply cracking in cross-ply laminates. *Composites Science and Technology*, 31(3):165–177, 1988.

[105] C. T. Herakovich, J. Aboudi, S. W. Lee, and E. A. Strauss. Damage in composite laminates: Effects of transverse cracks. *Mechanics of Materials*, 7(2):91–107, 11 1988.

[106] J. Aboudi, S. W. Lee, and C. T. Herakovich. Three-dimensional analysis of laminates with cross cracks. *Journal of Applied Mechanics, Transactions ASME*, 55(2):389–397, 1988.

[107] F. W. Crossman, W. J. Warren, A. S. D. Wang, and G. E. Law. Initiation and growth of transverse cracks and edge delamination in composite laminates. II-Experimental correlation. *Journal of Composite Materials Supplement*, 14(1):88–108, 1980.

[108] D. L. Flaggs and M. H. Kural. Experimental determination of the in situ transverse lamina strength in graphite/epoxy laminates. *Journal of Composite Materials*, 16:103–116, 03 1982.

[109] S. H. Lim and S. Li. Energy release rates for transverse cracking and delaminations induced by transverse cracks in laminated composites. *Composites Part A*, 36(11):1467–1476, 2005.

[110] S. Li and F. Hafeez. Variation-based cracked laminate analysis revisited and fundamentally extended. *International Journal of Solids and Structures*, 46(20):3505–3515, 2009.

[111] J. L Rebiere and D. Gamby. A decomposition of the strain energy release rate associated with the initiation of transverse cracking, longitudinal cracking and delamination in cross-ply laminates. *Composite Structures*, 84(2):186–197, 2008.

[112] S. C. Tan and R. J. Nuismer. A theory for progressive matrix cracking in composite laminates. *Journal of Composite Materials*, 23:1029–1047, 1989.

[113] R. J. Nuismer and S. C. Tan. Constitutive relations of a cracked composite lamina. *Journal of Composite Materials*, 22:306–321, 1988.

[114] T. Yokozeki and T. Aoki. Stress analysis of symmetric laminates with obliquely-crossed matrix cracks. *Advanced Composite Materials*, 13(2):121–140, 2004.

[115] T. Yokozeki and T. Aoki. Overall thermoelastic properties of symmetric laminates containing obliquely crossed matrix cracks. *Composites Science and Technology*, 65(11-12):1647–1654, 2005.

[116] Z. Hashin. Analysis of cracked laminates: A variational approach. *Mechanics of Materials*, 4:121:136, 1985.

[117] J. Zhang, J. Fan, and C. Soutis. Analysis of multiple matrix cracking in $[\pm\theta/90_n]_s$ composite laminates, part I, inplane stiffness properties. *Composites*, 23(5):291–304, 1992.

[118] P. Gudmundson and S. Ostlund. First order analysis of stiffness reduction due to matrix cracking. *Journal of Composite Materials*, 26(7):1009–1030, 1992.

[119] P. Gudmundson and S. Ostlund. Prediction of thermoelastic properties of composite laminates with matrix cracks. *Composites Science and Technology*, 44(2):95–105, 1992.

[120] P. Gudmundson and W. Zang. An analytic model for thermoelastic properties of composite laminates containing transverse matrix cracks. *International Journal of Solids and Structures*, 30(23):3211–3231, 1993.

[121] E. Adolfsson and P. Gudmundson. Thermoelastic properties in combined bending and extension of thin composite laminates with transverse matrix cracks. *International Journal of Solids and Structures*, 34(16):2035–2060, 06 1997.

[122] E. Adolfsson and P. Gudmundson. Matrix crack initiation and progression in composite laminates subjected to bending and extension. *International Journal of Solids and Structures*, 36(21):3131–3169, 1999.

[123] W. Zang and P. Gudmundson. Damage evolution and thermoelastic properties of composite laminates. *International Journal of Damage Mechanics*, 2(3):290–308, 07 1993.

[124] E. Adolfsson and P. Gudmundson. Matrix crack induced stiffness reductions in [(0m/90n/+p/-q)s]m composite laminates. *Composites Engineering*, 5(1):107–123, 1995.

[125] P. Lundmark and J. Varna. Modeling thermo-mechanical properties of damaged laminates. In *3rd International Conference on Fracture and Damage Mechanics, FDM 2003*, volume 251–252 of *Advances in Fracture and Damage Mechanics*, pages 381–387, Switzerland, 2–4 Sept. 2003. Trans Tech Publications.

[126] M. Kachanov. *Elastic Solids with Many Cracks and Related Problems*, volume 30 of *Advances in Applied Mechanics*, chapter X, pages 260–445. Academic Press, Inc., 1993.

[127] A. Adumitroaie and E. J. Barbero. Intralaminar damage model for laminates subjected to membrane and flexural deformations. *Mechanics of Advanced Materials and Structures*, 2013.

[128] T. Yokozeki, T. Aoki, and T. Ishikawa. Transverse crack propagation in the specimen width direction of cfrp laminates under static tensile loadings. *Journal of Composite Materials*, 36(17):2085–2099, 2002.

[129] T. Yokozeki, T. Aoki, and T. Ishikawa. Consecutive matrix cracking in contiguous plies of composite laminates. *International Journal of Solids and Structures*, 42(9-10):2785–2802, 05 2005.

[130] T. Yokozeki, T. Aoki, T. Ogasawara, and T. Ishikawa. Effects of layup angle and ply thickness on matrix crack interaction in contiguous plies of composite laminates. *Composites Part A (Applied Science and Manufacturing)*, 36(9):1229–1235, 2005.

[131] E. J. Barbero, F. A. Cosso, and F. A. Campo. Benchmark solution for degradation of elastic properties due to transverse matrix cracking in laminated composites, `http://dx.doi.org/10.1016/j.compstruct.2012.11.009`. *Composite Structures*, 98(4):242–252, 2013.

[132] S. Li, S. R. Reid, and P. D. Soden. A continuum damage model for transverse matrix cracking in laminated fibre-reinforced composites. *Philosophical Transactions of the Royal Society London, Series A (Mathematical, Physical and Engineering Sciences)*, 356(1746):2379–2412, 10/15 1998.

[133] Janis Varna, Roberts Joffe, and Ramesh Talreja. A synergistic damage-mechanics analysis of transverse cracking $[\pm\theta/90_4]s$ laminates. *Composites Science and Technology*, 61(5):657–665, 2001.

[134] A. S. D. Wang, P. C. Chou, and S. C. Lei. A stochastic model for the growth of matrix cracks in composite laminates. *Journal of Composite Materials*, 18(3):239–254, 05 1984.

[135] S. Li, S. R. Reid, and P. D. Soden. Modelling the damage due to transverse matrix cracking in fiber-reinforced laminates. In *Proceedings 2nd International Conference on Nonlinear Mechanics (ICNP-2)*, pages 320–323. Peking University Press, 1993.

[136] D.H. Cortes and E.J. Barbero. Stiffness reduction and fracture evolution of oblique matrix cracks in composite laminates. `http://dx.doi.org/10.1007/s12356-009-0001-5`. *Annals of Solid and Structural Mechanics*, 1(1)(1):29–40, 2010.

[137] E. J. Barbero and D. H. Cortes. A mechanistic model for transverse damage initiation, evolution, and stiffness reduction in laminated composites. `http://dx.doi.org/10.1016/j.compositesb.2009.10.001`. *Composites Part B: Engineering*, 41(2):124–132, 2010.

[138] E. J. Barbero, G. Sgambitterra, A. Adumitroaie, and X. Martinez. A discrete constitutive model for transverse and shear damage of symmetric laminates with arbitrary stacking sequence. `http://dx.doi.org/10.1016/j.compstruct.2010.06.011`. *Composite Structures*, 93:1021–1030, 2011.

[139] G. Sgambitterra, A. Adumitroaie, E.J. Barbero, and A. Tessler. A robust three-node shell element for laminated composites with matrix damage. `http://dx.doi.org/10.1016/j.compositesb.2010.09.016`. *Composites Part B: Engineering*, 42(1):41–50, 2011.

[140] A. M. Abad Blazquez, M. Herraez Matesanz, Carlos Navarro Ugena, and E. J. Barbero. Acoustic emission characterization of intralaminar damage in composite laminates. In *Asociación Española de Materiales Compuestos MATCOMP 2013*, Algeciras, Spain, July 2–5, 2013.

[141] H. T. Hahn. A mixed-mode fracture criterion for composite materials. *Composites Technology Review*, 5:26–29, 1983.

[142] Allan F. Bower. *Mechanics of Solids*. CRC, 2010. Free at http://solidmechanics.org/.

[143] H. Chai, C. D. Babcock, and W. G. Knauss. One dimensional modeling of failure in laminated plates by delamination buckling. *International Journal of Solids and Structures*, 17(11):1069–1083, 1981.

[144] M.-K. Yeh and L.-B. Fang. Contact analysis and experiment of delaminated cantilever composite beam. *Composites: Part B*, 30(4):407–414, 1999.

[145] W. L. Yin, S. N. Sallam, and G. J. Simitses. Ultimate axial load capacity of a delaminated beam-plate. *AIAA Journal*, 24(1):123–128, 1986.

[146] D. Bruno. Delamination buckling in composite laminates with interlaminar defects. *Theoretical and Applied Fracture Mechanics*, 9(2):145–159, 1988.

[147] D. Bruno and A. Grimaldi. Delamination failure of layered composite plates loaded in compression. *International Journal of Solids and Structures*, 26(3):313–330, 1990.

[148] G. A. Kardomateas. The initial post-buckling and growth behaviour of internal delaminations in composite plates. *Journal of Applied Mechanics*, 60(4):903–910, 1993.

[149] G. A. Kardomateas and A. A. Pelegri. The stability of delamination growth in compressively loaded composite plates. *International Journal of Fracture*, 65(3):261–276, 1994.

[150] I. Sheinman, G. A. Kardomateas, and A. A. Pelegri. Delamination growth during pre- and post-buckling phases of delaminated composite laminates. *International Journal of Solids and Structures*, 35(1-2):19–31, 1998.

[151] D. Bruno and F. Greco. An asymptotic analysis of delamination buckling and growth in layered plates. *International Journal of Solids and Structures*, 37(43):6239–6276, 2000.

[152] H.-J. Kim. Postbuckling analysis of composite laminates with a delamination. *Computer and Structures*, 62(6):975–983, 1997.

[153] W. G. Bottega and A. Maewal. Delamination buckling and growth in laminates–closure. *Journal of Applied Mechanics*, 50(14):184–189, 1983.

[154] B. Cochelin and M. Potier-Ferry. A numerical model for buckling and growth of delaminations in composite laminates. *Computer Methods in Applied Mechanics*, 89(1-3):361–380, 1991.

[155] P.-L. Larsson. On delamination buckling and growth in circular and annular orthotropic plates. *International Journal of Solids and Structures*, 27(1):15–28, 1991.

[156] W.-L. Yin. Axisymmetric buckling and growth of a circular delamination in a compressed laminate. *International Journal of Solids and Structures*, 21(5):503–514, 1985.

[157] K.-F. Nilsson, L. E. Asp, J. E. Alpman, and L. Nystedt. Delamination buckling and growth for delaminations at different depths in a slender composite panel. *International Journal of Solids and Structures*, 38(17):3039–3071, 2001.

[158] H. Chai and C. D. Babcock. Two-dimensional modeling of compressive failure in delaminated laminates. *Journal of Composite Materials*, 19(1):67–98, 1985.

[159] J. D. Withcomb and K. N. Shivakumar. Strain-energy release rate analysis of plates with postbuckled delaminations. *Journal of Composite Materials*, 23(7):714–734, 1989.

[160] W. J. Bottega. A growth law for propagation of arbitrary shaped delaminations in layered plates. *International Journal of Solids and Structures*, 19(11):1009–1017, 1983.

[161] B. Storåkers and B. Andersson. Nonlinear plate theory applied to delamination in composites. *Journal of Mechanics and Physics of Solids*, 36(6):689–718, 1988.

[162] P.-L. Larsson. On multiple delamination buckling and growth in composite plates. *International Journal of Solids and Structures*, 27(13):1623–1637, 1991.

[163] M. A. Kouchakzadeh and H. Sekine. Compressive buckling analysis of rectangular composite laminates containing multiple delaminations. *Composite Structures*, 50(3):249–255, 2000.

[164] J. M. Comiez, A. M. Waas, and K. W. Shahwan. Delamination buckling: Experiment and analysis. *International Journal of Solids and Structures*, 32(6/7):767–782, 1995.

[165] G. A. Kardomateas. Postbuckling characteristics in delaminated kevlar/epoxy laminates: An experimental study. *Journal of Composites Technology and Research*, 12(2):85–90, 1990.

[166] O. Allix and A. Corigliano. Modeling and simulation of crack propagation in mixed-modes interlaminar fracture specimens. *International Journal of Fracture*, 77(2):111–140, 1996.

[167] D. Bruno and F. Greco. Delamination in composite plates: Influence of shear deformability on interfacial debonding. *Cement and Concrete Composites*, 23(1):33–45, 2001.

[168] J. W. Hutchinson and Z. Suo. Mixed mode cracking in layered materials. *Advances in Applied Mechanics*, 29:63–191, 1992.

[169] N. Point and E. Sacco. Delamination of beams: An application to the dcb specimen. *International Journal of Fracture*, 79(3):225–247, 1996.

[170] J. G. Williams. On the calculation of energy release rate for cracked laminates. *International Journal of Fracture*, 36(2):101–119, 1988.

[171] A. Tylikowsky. Effects of piezoactuator delamination on the transfer functions of vibration control systems. *International Journal of Solids and Structures*, 38(10-13):2189–2202, 2001.

[172] C. E. Seeley and A. Chattopadhyay. Modeling of adaptive composites including debonding. *International Journal Solids and Structures*, 36(12):1823–1843, 1999.

[173] W. J. Bottega and A. Maewal. Dynamics of delamination buckling. *International Journal of Non-Linear Mechanics*, 18(6):449–463, 1983.

[174] G. Alfano and M. A. Crisfield. Finite element interface models for the delamination analysis of laminated composites: Mechanical and computational issues. *International Journal for Numerical Methods in Engineering*, 50(7):1701–1736, 2001.

[175] P. P. Camanho, C. G. Dávila, and M. F. Moura. Numerical simulation of mixed-mode progressive delamination in composite materials. *Journal of Composite Materials*, 37(16):1415–1438, 2003.

[176] Z. Zou, S. R. Reid, and S. Li. A continuum damage model for delaminations in laminated composites. *Journal of Mechanics and Physics of Solids*, 51(2):333–356, 2003.

[177] X-P Xu and A. Needleman. Numerical simulations of fast crack growth in brittle solids. *Journal of Mechanics and Physics of Solids*, 42:1397–1434, 1994.

[178] J. R. Reeder. A bilinear failure criterion for mixed-mode delamination in composite materials. *ASTM STP 1206*, pages 303–322, 1993.

[179] H. Chai. Three-dimensional fracture analysis of thin-film debonding. *International Journal of Fracture*, 46(4):237–256, 1990.

[180] J. D. Withcomb. Three dimensional analysis of a post-buckled embedded delamination. *Journal of Composite Materials*, 23(9):862–889, 1989.

[181] D. Bruno, F. Greco, and P. Lonetti. A 3d delamination modelling technique based on plate and interface theories for laminated structures. *European Journal of Mechanics A/Solids*, 24:127–149, 2005.

[182] J. G. Williams. The fracture mechanics of delamination tests. *Journal of Strain Analysis*, 24(4):207–214, 1989.

[183] W.-L. Yin and J. T. S. Wang. The energy-release rate in the growth of a one-dimensional delamination. *Journal of Applied Mechanics*, 51(4):939–941, 1984.

[184] J. R. Rice. A path independent integral and the approximate analysis of strain concentrations by notches and cracks. *Journal of Applied Mechanics*, 35:379–386, 1968.

[185] C. G. Dávila, P. P. Camanho, and M. F. De Moura. Mixed-mode decohesion elements for analyses of progressive delamination. In *42nd AIAA/ASME/ASCE/AHS/ASC Structures, Structural Dynamics, and Materials Conference, April 16 - 19, 2001*, volume 3, pages 2277–2288, Seattle, WA, 2001. AIAA.

[186] ANSYS Inc. ANSYS mechanical APDL materials reference, release 14.0, 2011.

[187] T. L. Anderson. *Fracture Mechanics*. CRC, Boca Raton, FL, 1995.

[188] E.J. Barbero and J.N. Reddy. Jacobian derivative method for three-dimensional fracture mechanics. *Communications in Applied Numerical Methods*, 6(7):507–518, 1990.

[189] M. Benzeggagh and M. Kenane. Measurement of mixed-mode delamination fracture toughness of unidirectional glass/epoxy composites with mixed-mode bending apparatus. *Composite Science and Technology*, 56:439, 1996.

[190] J. Reeder, S. Kyongchan, P. B. Chunchu, and D. R.. Ambur. Postbuckling and growth of delaminations in composite plates subjected to axial compression. In *43rd AIAA/ASME/ASCE/AHS/ASC Structures, Structural Dynamics, and Materials Conference*, volume 1746, page 10, Denver, CO, 2002.

[191] A. Caceres. *Local Damage Analysis of Fiber Reinforced Polymer Matrix Composites, Ph.D. dissertation.* PhD thesis, West Virginia University, Morgantown, WV, 1998.

Materials Science/Mechanical Engineering/Civil Engineering

FINITE ELEMENT ANALYSIS OF COMPOSITE MATERIALS USING ANSYS®

SECOND EDITION

Ever J. Barbero

Designing structures using composite materials poses unique challenges, especially due to the need for concurrent design of both material and structure. Professors are faced with two options: textbooks that teach the theory of advanced mechanics of composites, but lack computational examples of advanced analysis, and books on finite element analysis that may or may not demonstrate very limited applications to composites. But there is a third option that makes the other two obsolete: Ever J. Barbero's **Finite Element Analysis of Composite Materials Using ANSYS®, Second Edition.**

The Only Finite Element Analysis Book on the Market Using ANSYS® to Analyze Composite Materials

By layering detailed theoretical and conceptual discussions with fully developed examples, this text supplies the missing link between theory and implementation. In-depth discussions cover all of the major aspects of advanced analysis, including three-dimensional effects, viscoelasticity, edge effects, elastic instability, damage, and delamination. This second edition of the bestseller has been completely revised to incorporate advances in the state of the art in such areas as modeling of damage in composites. In addition, all 50+ worked examples have been updated to reflect the newest version of ANSYS®. Including some use of MATLAB®, these examples demonstrate how to use the concepts to formulate and execute finite element analyses and how to interpret the results in engineering terms. In addition, the source code for each example is available to students for download online via a companion website featuring a special area reserved for instructors. A solutions manual is available upon qualifying course adoption.

Cementing applied computational and analytical experience to a firm foundation of basic concepts and theory, **Finite Element Analysis of Composite Materials Using ANSYS®, Second Edition** offers a modern, practical, and versatile classroom tool for today's engineering classroom.

K15077

CRC Press
Taylor & Francis Group
an informa business
www.crcpress.com

6000 Broken Sound Parkway, NW
Suite 300, Boca Raton, FL 33487
711 Third Avenue
New York, NY 10017
2 Park Square, Milton Park
Abingdon, Oxon OX14 4RN, UK

ISBN: 978-1-4665-1689-2
90000
9 781466 516892